Development of an equation of state for solution containing electrolytes

Lin, Yi

Publication date:
2007

Document Version
Publisher's PDF, also known as Version of record

Technical University of Denmark

Development of an equation of state for solutions containing electrolytes

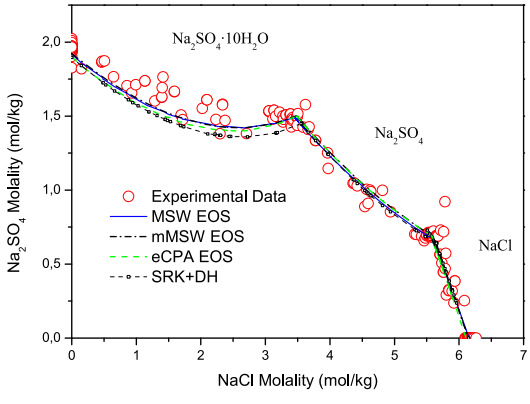

Yi Lin

2007

DTU Chemical Engineering
Department of Chemical and Biochemical Engineering

Development of an equation of state for solutions containing electrolytes

Yi Lin

Ph. D. Thesis

April 2007

Supervisor: Kaj Thomsen, Associate Professor

IVC-SEP
Department of Chemical and Biochemical Engineering
Technical University of Denmark
DK-2800 Kgs. Lyngby
Denmark

ISBN: 978-87-91435-77-3
Printed by Frydenberg A/S, Copenhagen, Denmark

Preface

This thesis as submitted as partial fulfillment of the requirements for the Ph. D. degree at the Technical University of Denmark.

This work was carried out at the Department of Chemical Engineering at the Technical University of Denmark (DTU) from September 2003 to January 2007. Associated Professor Kaj Thomsen has supervised this Ph. D. project. I wish to express my sincere gratitude to my supervisor for the time and effort he spent to direct me in my project. The discussions with Associated Professor Kaj Thomsen are always helpful and pleasant.

I would like to thank DTU for financial support for this Ph.D. project. I would like to thank Associated Professor Georgios Kontogeorgis for his useful discussion regarding to equation of state and cubic plus association (CPA) equation of state. Special mention has to be made for my fellow Ph. D. student Philip Loldrup Fosbøl, who provided constant help in programming and other scientific computation programs and discussion about electrolytes. I need t thank all staff working at IVC-SEP for their valuable contributions to this marvellous research group and its friendly working environment.

I am grateful to Dr Jean-Charles de Hemptinne for inviting me to work at Instiute Francais du Pétrole in Paris, France for my four-month external research period.

I want to thank my parents and my sister for their support, both financially and academically during my stay in Denmark.

Last, but not least, I would like to thank Mr. Li Hongzhi, who has introduced China Falun Gong to public worldwide to benefit people without any charge of money . This traditional Chinese Buddha school internal Kongfu (Qigong) completely healed my life-time-long chronological illnesses, such as viral myocarditis, insomnia, cervical spondylitis, shoulder periarthritis etc. after practicing it for one year. Were it not for Falun Gong, I would have to terminate my study for long-term hospital treatment in the end of the first year during my Master program study in DTU. At that time, the heart disease, viral myocarditis, from which I had suffered for over eighteen years since childhood, became server and threatened my life. I was even unable to continue the study for my master degree after my condition deteriorated. No words could be used to express my sinere gratitude to Falun Gong precisely. Falun Gong is wonderful. Its principle Truthfulness, Compassion, and Tolenrent is beneficial to all. “法輪大法好，真善忍好！”

Yi Lin 林益
Kgs. Lyngby, Denmark
March 2007

Summary

This thesis deals with equation of state (EOS) for aqueous electrolyte mixtures. Six electrolyte EOSs were developed from the residual Helmholtz free energy. Four out of the six electrolyte EOSs are selected for regression of ion-specific parameters of the test system consisting of six ions (Na^+, Ca^{2+}, H^+, Cl^-, OH^- SO_4^{2-}) and water. Both temperature independent and temperature dependent parameters have been obtained for the test system.

Chapter one is an introduction to the theories and models of electrolyte systems. The need for an electrolyte equation of state is stated.

In Chapter two, thermodynamic concepts pertinent to the rest of the thesis are derived or studied. The six electrolyte EOSs established in the work are presented.

Chapter three deals with the mathematic aspects of developing electrolyte EOS. The vector analysis and calculus of multi-variable functions have been applied here to derive derivatives. The composition, temperature and volume derivatives of the Helmholtz free energy terms are deducted and presented in Appendixes. They are fundamental to the electrolyte EOSs.

Chapter four deals with the experimental density data collection for IVC-SEP electrolyte databank and they are used for correlation of parameters for electrolyte EOSs in the later chapters. The IVC-SEP electrolyte databank is also briefly discussed in this chapter.

Chapter five deals with preliminary study of the six implemented electrolyte EOSs using salt-specific parameters for binary system. All electrolyte EOSs and their source codes are tested and checked thoroughly and programming errors are corrected. The comparison between EOSs and different terms are provided.

In chapter six, based on the studies of chapter five, four out of six EOSs are chosen for multi-component aqueous electrolyte systems at room temperature. The results are shown and temperature independent parameters are regressed. Phase diagrams for binary, ternary systems of ions are introduced. The abilities of electrolyte EOSs are illustrated and compared. A good representation of the experimental data is obtained.

Chapter seven deals with aqueous multi-component electrolyte systems at a wide temperature range. Temperature dependent ion-specific parameters and their temperature dependence function are presented. The four electrolyte EOSs can represent phase diagrams of the test system at a wide temperature range. Model extrapolation with respect to temperature is not very satisfactory.

Chapter eight is the conclusion part, summarising the results of this Ph. D. project.

Resumé på dansk

Denne afhandling omhandler tilstandsligninger for vandige elektrolytopløsninger. Seks elektrolytiske tilstandsligninger er blevet udviklet ved hjælp af den residuale Helmholtz-energi funktion. Fire af de seks tilstandsligninger blev valgt til regression af ionspecifikke parametre for testsystemet bestående af (Na^+, Ca^{2+}, H^+, Cl^-, OH^- SO_4^{2-}) og vand. Både temperaturuafhængige og temperaturafhængige parametre er blevet bestemt for testsystemet.

Kapitel et giver en introduktion til teorien og modellerne for elektrolytsystemer. Der bliver redegjort for behovet for en elektrolyt-tilstandsligning.

I kapitel to bliver de termodynamiske begreber af betydning for resten af afhandlingen udledt eller undersøgt. De seks elektrolyt-tilstandsligninger, der er opstillet under dette arbejde, bliver præsenteret.

Kapitel tre beskriver de matematiske aspekter ved udviklingen af elektrolyt-tilstandsligninger. Her anvendes vektoranalyse og multivariable funktions analyse for at bestmme de afledte af Helmholtz-energien. Ligningerne er fundamentale for elektrolyt-tilstandsligninger og de afledte med hensyn til sammensætning, temperatur og volumen udledes og præsenteres i appendiks.

Kapitel fire diskutterer IVC-SEP's elektrolytdatabase kort. Her præsenteres de indsamlede eksperimentelle litteratur densitetsdata. Data er lagt ind i IVC-SEP's elektrolytdatabase, og anvendes i senere kapitler til korrelation af tilstandsligningernes modelparametre.

Kapitel fem viser hvordan saltspecifikke parametre for binære systemer kan anvendes med de seks tilstandsligninger. Kildekoden for alle tilstandsligninger testes, kontrolleres og programmeringsfejl rettes. Desuden gives en sammenligning af forskellige tilstandsligninger og de forskellige bidrag i ligningerne undersøges.

I kapitel seks udvælges, på baggrund af undersøgelserne i kapitel 4, fire af de seks tilstandsligninger til at beskrive vandige multikomponent elektrolytsystemer ved stuetemperatur. Resultaterne vises og temperaturuafhængige parametre bestemmes. Fasediagrammer for binære og ternære systemer introduceres. Præcisionen af Elektrolyt-tilstandsligningerne illustreres og sammenlignes. En god gengivelse af de eksperimentelle data er opnået.

Kapitel syv omhandler vandige multikomponent elektrolytsystemer i et bredt temperaturinterval. Temperaturafhængige ionspecifikke parametre og deres temperaturafhængighedsfunktion præsenteres. De fire elektrolyt-tilstandsligninger kan reproducere fasediagrammer for testsystemet indenfor et større temperaturinterval. Ekstrapolation af modellerne til andre temperaturer er dog mindre tilfredsstillende.

Kapitel otte giver en konklusion, hvor resultaterne af dette Ph.D. projekt opsummeres.

Notation

Letters

A = Helmholtz free energy

a = van der Waals attraction parameter

a = activity

b = van der Waals excluded-volume parameter

c = volume translation parameter

C = concentration

d_0 = the density of the solvent in kg/m^3.

e = elementary charge

g = Gibbs free energy

$g(\rho)$ = the radial distribution function

G = Gibbs free energy

I = the molality based ionic strength

k = binary interaction parameter

k = Boltzmann constant

m = molality

M = molecular mass

n = number of moles

N = total number of moles in the system

N_A = Avogadro's number

P = pressure

R = gas constant

SI = the saturation index of a salt, equal to the activity product of the salt divided by its solubility product

T = absolute temperature

v = molar volume

V = total volume

V_Φ = apparent molar volume

w = the weight for the data

x = mole fraction

X = mole fraction

Z = compressibility factor

z_i = the valence of ionic species i and.

Z_i = ion charge number

Greek letters

Δ = the association strength between two association sites belonging in two different molecules

β = the association volume of interaction between two association sites

ε = the association energy of interaction between two association sites

ε = the relative permittivity of the medium

ε_0 = the vacuum permittivity

Φ = τhe osmotic coefficient

γ = the mole-fraction based activity coefficient of a mixture

Γ = the MSA screening parameters

γ^* = the mole-fraction based activity coefficient of ion *i* in a mixture

γ^m = the molality-based activity coefficient of ionic component *i* in a mixture

φ = the fugacity coefficient

$\hat{\varphi}$ = the fugacity coefficient of a component in mixture

κ = the Debye screening length

μ = the chemical potential of component *i*

ν = the sum of stoichoimetric coefficients of all ions in the solution

ρ = the molar density

σ_i = the diameter of ionic species

Subscripts

a = anion

c = cation

chg = charge

dis = discharge

Ex = explicit

i, j = species *i , j*; component *i, j*; Molecule *i,* j.

Im = implicit

MSA = mean spherical approximation

RPM = restricted primitive model

sMSA = simplified mean spherical approximation

Superscripts

0 = pure compound

∞ = infinite dilution

A = association site A of the molecule

assoc = association

B = association site B of the molecule

cal = calculated

exp = experimental

m = molality

r = residual property

CONTENTS

CHAPTER 1 Literature study of equation of state for electrolyte

1.1 *Introduction*

Electrolyte solutions are encountered in many industries. In geochemistry, electrolytes influence many processes such as seawater intrusion into fresh water aquifers, the flow of the pollution front of groundwater and the production of geothermal energy. In many chemical processes such as desalination, wastewater treatment, extractive distillation, fractional crystallization, scale formation in pipelines and gas scrubbing, the understanding of the phase equilibrium of systems containing electrolytes is crucial.[1] In biochemical industries, salt concentration is an important factor to purify protein products in protein precipitation processes. In the pharmaceutical industry, it is necessary to understand the behaviour of electrolytes in the human body to improve the transport of drugs in the body.[2] In oil- and gas production, equilibrium of systems containing electrolytes needs to be studied to avoid the formation of gas hydrates, in order to prevent corrosion, to avoid scaling problems, and to increase the oil recovery.
Electrolyte solutions are considerably more difficult to model than most other solutions encountered in engineering applications. Because in electrolyte solutions the ions are charged particles, the interaction between ions are on a much longer range than those of neutral molecules, which made the electrolyte solution more non-ideal than a non-electrolyte solution even at very low electrolyte concentrations.[1,3]
In the following sections, the theory of the electrolyte solution and engineering models will be considered in two separate parts. The present review focuses on the development of the theoretical and engineering model for ionic solutions at equilibrium. The non-equilibrium study will be mentioned very briefly.

1.2 *Electrolyte solution theory*

1.2.1 General

Many different models have been suggested for calculating the thermodynamic properties of electrolyte solutions. Quantum mechanics and statistical mechanics theories provide powerful theoretical tools for the development of the electrolyte theories. Modern electrolyte theories can be categorized in many different ways. From a physical perspective of the solvent, the electrolyte theories can be divided into theories based on a continuum-medium model and a discrete-medium model. Continuum-medium models view the solvent as a dielectric medium without structure. These models are described as primitive models too. Discrete-medium models include the presence of solvent molecules explicitly. Discrete-medium models are also described as the non-primitive models. They can also be categorized in a very simple way into the exact and approximate theories according to their accuracy and implicit assumptions. The exact theory available at present is the quantum theory: the exact solution of the N-particle time-independent Schrödinger equation describing the electrolyte solution system at equilibrium. While it is intellectually attractive to derive solution properties from the fundamental theory of Chemistry - the Schrödinger equation - the technical problems are formidable.[4] Due to the large amount of

particles and the available energy states involved in the system, different approximations have been made to simplify the procedure of solving the N-particle time-independent Schrödinger equation through mathematical treatment or reasonable physical assumption. These are the approximate theory at different accuracy levels. If we turn to classical mechanics and introduce some basic assumptions such as equal a priori probability, the quantum mechanical level properties of the electrolyte solution could be linked with the macroscopic level thermodynamic properties (e.g. Helmholtz free energy or entropy) through statistical mechanics.[5] According to the basic postulate of the statistical mechanics, the time average of a dynamic quantity is equal to the ensemble average of it. Further, the ensemble average of a mechanical quantity is equal to a thermodynamic quantity. The problem of solving a huge N-body system could be reduced to a few-body system or one-body system under the assumption of equal a priori probability and separability of the energy.[3,5]

For gases, the physical properties at molecular level have been linked to the macroscopic thermodynamic properties through partition function in a specific ensemble. If the Hamiltonian of particles is available, the thermodynamic properties of gas can be calculated through partition function.[3,5]

For liquid, partition function is related to another function described as the radial distribution function. The partition function of a real fluid is separated into two parts: one involving the intermolecular forces (i.e. the potential energy of the fluid) and is expressed in terms of the configuration integral and one involving the free motions of the molecules. A second assumption is proceeded, i.e. that of pairwise additivity, according to which the potential energies of the fluid can be approximate by the sum of interactions between all molecular pairs. This assumption allows us to determine the average thermodynamic properties of a real fluid in terms of the intermolecular potential energies and the radial distribution function. The radial distribution function is related to the average thermodynamic properties of a fluid through two equations: the pressure equation or the compressibility equation.[3,5, 6]

Unfortunately, the radial distribution function cannot be determined with sufficient accuracy at all densities in a simple analytical form. There are several equations from which the radial distribution function can be derived. The most commonly used equations are the Kirkwood, the Born-Green-Yvon (BGY), the Ornstein-Zernike (OZ) equations. [1,3] Once the radial distribution function is solved from these integral equations, either numerically or analytically, the thermodynamic properties of liquid can be calculated. The similar approach applies to the electronic solution.

The radial distribution function of the liquid constitutes a rigorous statistical mechanical theory, although some sort of approximations had to be introduced into the formalism eventually. Much evidence points to the fact that it can be depicted that the repulsive part of the potential as determining the structure of the liquid and the attractive part as holding the molecules together. This physical picture suggests that mathematically a fluid can be treated as a system of molecules governed by a repulsive potential with a small perturbation of an attractive potential. Perturbation theories have also been applied to electrolyte solutions, as they are special liquid systems. It constitutes a branch of the electrolyte theories too.

1.2.2 The level of the Hamiltonians

In the developing statistical mechanical theory of electrolyte solution, a general approach is to begin with the Hamiltonian of the particles which describes the forces or interactions among the particles of the system. Then the following step is to use

one of the available approximation methods to calculate the average properties of the real systems of interest. [3,5]

The general definition of the Hamiltonian function is the kinetic energy plus the potential energy of the system.

$$H = E_k + U \tag{1.1}$$

In the above equation, E_k is the kinetic energy and U denotes the potential energy.

The levels of the approximations in Hamiltonian describing the interactions between the particles in the solution, or in another word the types of different potential model for the electrolyte, determine the accuracy of the electrolyte model. They are classified into three levels consequently.[4] We start the discussion from the high accuracy level to low accuracy level.

Schrödinger level

As mentioned before, the most exact model available at present is the solution of the Schrödinger equation for N nuclei and M electrons in the electrolyte system. The Hamiltonian for the exact solution should include all interactions in the systems if possible. Due to the mathematical difficulties, some approximations have been introduced to avoid the formidable problem of directly solving the Schrödinger equation. Some approximate solutions of Schrödinger equation (models) with reasonable accuracy and physical meanings were archived in this way. In these Schrödinger level models, the particles studied are the nuclei and electrons. Few models describe the electrolyte systems in such details.[1,4,5]

Born-Oppenheimer level (BO)

In the BO level models, the particles studied are molecules, ions of the solute and the molecules of the solvent. In these models, the motion of the particles in the system is considered to be influenced by the electron-average interactions, i.e. the particles move on the Born-Oppenheimer electronic potential energy surface. In BO level models, not only the interactions between ions are counted for, but also the interactions between ions and solvent molecules and inter-molecular force have been considered. Usually pairwise additivity for the ions and solvent particles is assumed. [1,4,5]

McMillan-Mayer level (MM)

The McMillan Mayer level models consider the interaction between ions only. In these models, the smallest particles considered are the solute molecules (i.e. ions). The solvents are viewed as continuum-medium; consequently the interactions of the solvent molecules are taken into account by the dielectric constant. [1,3-5] Pairwise additivity for the N-ion potential is assumed. The potential function of the interactions between ions can be expressed in the following form:

$$u_{pij} = u_{pSR}(r) + \frac{z_i z_j e^2}{4\pi\varepsilon\varepsilon_0 r} \tag{1.2}$$

where $u_{pSR}(r)$ stand for the potential functions of the short range interaction between ions. $u_{pSR}(r)$ can be the potential functions of hard sphere $u_p^{HS}(r)$, square well $u_p^{SW}(r)$ or Lennard-Jones $u_p^{LJ}(r)$. If $u_{pSR}(r) = u_p^{HS}(r)$, the commonly used Primitive Model (PM) is obtained. In the Primitive Model the solvent is a dielectric continuum (characterized by its dielectric constant) and the ions are considered to be charged

spheres, as can be seen in the above equation. The majority of MM-level studies have proceeded from it. The model of an electrolyte solution as a mixture of ions in a dielectric continuum is not valid at very high ion concentrations. As a result the accuracy of the primitive model (short as PM) of electrolyte is decreasing rapidly when ion concentration increases.

The statistical mechanics models of electrolytes obtained from either the integral equation theories or the perturbation theories can be either MM level model or the BO level model. It depends on the interactions between the particles considered in the model. For the MM level the interactions between particles considered are relatively few while in the BO level models more interactions between particles are considered. They can be further grouped into five broad categories:

1) Those obtained from solving the Poisson-Boltzmann equation, such as the Debye-Hückel model[7], and the more complete model derived by Gronwall *et al*.[8]

2) Those obtained from perturbation theories using Taylor expansion of Helmholtz free energy such as the Barker-Henderson-Leonard method [9-11].

3) Those obtained from solving the Ornstein-Zernicke equation (OZ) using the integral-equation theories. Examples are the solution of the OZ equation with mean spherical approximation (MSA)[12 -14] closure and with Hypernetted Chain closure.[15]

4) Those focusing on the fluctuation of composition in an open system (fluctuation theory), such as the Kirkwood-Buff equation.[16]

5) The computer simulation results of the interacting particles from the Monte Carlo method and molecular dynamics method can also be converted into macroscopic thermodynamic properties for comparison with computational results from models or real electrolyte systems.[17, 18]

The first four categories will be explained one by one in the following sections.

1.2.3 Poisson-Boltzmann (PB) equation

Many models are derived from the approximate solution of Poisson-Boltzmann equation, such as Debye-Hückel equation and the Pitzer model etc.. In PB equation, the radial distribution function can be expressed in the following form:

$$g_{ij}(r) = e^{-\beta w_{ij}(r)} \tag{1.3}$$

where w_{ij} is the potential of mean force (PMF). It is assumed that the electrostatic potential energy of a given ion is equal to PMF, i.e. $w_{ij} = z_j e \psi_i(r)$. Equation (1.3) becomes:

$$g_{ij}(r) = \exp\left[-\beta z_i e \psi_i(r)\right] \tag{1.4}$$

$\psi_i(r)$ is the average electrostatic potential of the ion i as a function of distance from it. e is the charge of electron and $\beta = 1/k_B T$, where k_B is the Boltzmann's constant. Equation (1.4) has a form of Boltzmann distribution.

If equation (1.4) is substituted into Poisson equation

$$\nabla^2 \psi_i(r) = -\frac{1}{\varepsilon\varepsilon_0}\rho_i(r) = -\frac{1}{\varepsilon\varepsilon_0}\sum_j z_i e \rho_i g_{ij}(r) \tag{1.5}$$

The $\rho_i(r)$ in equation (1.5) is the charge density at the distance r from the central ion. ρ_i is the number of ions i per unit volume. Then we obtained the Poisson-Boltzmann equation[1,5,7]

$$\nabla^2\psi_i(r) = -\frac{1}{\varepsilon\varepsilon_0}\sum_j z_j e\rho_j \exp\left[-\beta z_j e\psi_j(r)\right] \tag{1.6}$$

for calculating the electrostatic potential $\psi_i(r)$.
Taylor expand the radial distribution function, i.e. the exponential term in the left hand side of the equation (1.4),

$$g_{ij}(r) = \exp\left[-\frac{z_j e\psi_i(r)}{kT}\right] = 1 - \frac{z_j e\psi_i(r)}{kT} + \frac{1}{2}\left[\frac{z_j e\psi_i(r)}{kT}\right]^2 - \cdots \tag{1.7}$$

Maintain different terms according to the accuracy requirement and solve equation (1.6), then different approximate models are obtained. Details about the derivation of Debye-Hückel theory will be explained, as it will be used to construct electrolyte EOS later in this project.

1.2.3.1 Debye-Hückel (DH) theory

The detailed derivation of the Debye-Hückel theory is given in Appendix I. Here we only show the main steps. In Debye-Hückel theory, [7] the radial distribution function has the form of

$$g_{ij}(r) = \exp\left[-\frac{z_j e\psi_i(r)}{kT}\right] \approx 1 - \frac{z_j e\psi_i(r)}{kT} \tag{1.8}$$

Taylor expand the exponential function, drop the higher order terms, substitute (1.8) into (1.5), the Poisson-Boltzmann equation becomes

$$\nabla^2\psi_i(r) = \frac{1}{\varepsilon\varepsilon_0}\sum_j z_j^2 e^2 \rho_j \frac{\psi_i(r)}{kT} \tag{1.9}$$

Solving the second order ordinary differential equation, we get the analytically expression for the electrical potential at distant *r*:

$$\psi_i(r) = \frac{e\,z_i}{4\pi\varepsilon\varepsilon_0(1+\kappa a_i)}\frac{\exp(\kappa a - \kappa r)}{r} \tag{1.10}$$

where κ^{-1} is called the Debye length and is calculated as

$$\kappa = \left(\frac{e^2 N_A^2}{\varepsilon\varepsilon_0 RTV}\sum_{ions} n_i Z_i^2\right)^{1/2} \tag{1.11}$$

Here Debye and Hückel[7] assume that the electrical potential of any point in the solution $\psi_i(r)$ is the sum of the electrical potential ϕ_i of the ion *i* at this point and the electrical potential of the ion atmosphere $\phi(r)$:

$$\psi_i(r) = \phi_i + \phi(r) = \frac{e\,z_i}{4\pi\varepsilon\varepsilon_0 r} + \phi(r) = \frac{e\,z_i}{4\pi\varepsilon\varepsilon_0(1+\kappa a_i)}\frac{\exp(\kappa a - \kappa r)}{r} \tag{1.12}$$

if $r = a_i$, and we get $\phi(a_i) = -\dfrac{e\,z_i\kappa}{4\pi\varepsilon\varepsilon_0(1+\kappa a_i)}$

and the charge of electric potential energy of a single ion is

$$u = -\frac{e^2 z_i^2 \kappa}{8\pi\varepsilon\varepsilon_0(1+\kappa a_i)} \tag{1.13}$$

From this point, there are two approaches to derive the expression for the activity coefficient for ion *i*. The approach Debye and Hückel[7] used in their paper is more cumbersome but accurate. From (1.13), they calculate the total electric potential

energy of the electrolyte solution with various ion species, then they obtained the internal energy of the system.

Complete Debye and Hückel term

Then they obtained the excess Helmholtz energy from the internal energy:

$$-\frac{A^E}{T}=\int\frac{U_e}{T^2}dT=\frac{kV}{4\pi\sum x_i z_i^2}\sum\int\frac{x_i z_i^2\kappa^2 d\kappa}{(1+\kappa a_i)}$$
$$=\frac{kV}{4\pi\sum x_i z_i^2}\sum\frac{x_i z_i^2}{a_i^3}\left(\frac{3}{2}+\ln(1+a_i\kappa)-2(1+a_i\kappa)+\frac{(1+a_i\kappa)^2}{2}\right) \tag{1.14}$$

Equation (1.14) is the original expression deduced by Debye and Hückel[7]. If we differentiate equation (1.14) with respect to mole composition, we get the complete expression for activity coefficient.[19]

Truncated Debye and Hückel term

The other simple and widely adopted approach, in most thermodynamic textbooks, made more assumptions to simplify the derivation.[3,20] It assumes that non-ideality of the electrolyte solution is caused by the electrostatic interactions between the ions. Assume the excess Helmholtz free energy is equal to the excess Gibbs free energy, it arrives at:

$$RT\ln\gamma_i=\Delta\mu_i\approx N_A u=-\frac{N_A e^2 z_i^2\kappa}{8\pi\varepsilon\varepsilon_0(1+\kappa a_i)}, \tag{1.15}$$

where N_A is the Avogadro number. Rearrange equation (1.15), we obtain the formula for the activity coefficient

$$\ln\gamma_i=-\frac{e^2 z_i^2\kappa}{8\pi\varepsilon\varepsilon_0 kT(1+\kappa a_i)} \tag{1.16}$$

Bearing in mind that the average activity coefficient is calculated by

$$\gamma_\pm^{\mathbf{v}}=\gamma_+^{\nu_+}\gamma_-^{\nu_-},\ \text{where}\ \mathbf{v}=\nu_++\nu_- \tag{1.17}$$

Combine equation (1.16) and (1.17), we reach to the equation for average activity coefficient

$$\ln\gamma_\pm=-\frac{e^2\kappa}{8\pi\varepsilon\varepsilon_0 kT(1+\kappa a_i)}\left(\frac{\nu_+z_+^2+\nu_-z_-^2}{\mathbf{v}}\right) \tag{1.18}$$

Note that $(\nu_+z_+^2+\nu_-z_-^2)/\mathbf{v}=\left|z_+z_-\right|=z^2$, rearrange equation (1.18), we get

$$\ln\gamma_\pm=-\frac{e^2\kappa z^2}{8\pi\varepsilon\varepsilon_0 kT(1+\kappa a_i)} \tag{1.19}$$

After some mathematical transformations, we get the familiar form of the Debye-Hückel equation on a molality base[3, 20, 21].

$$\ln\gamma_\pm=-\frac{Az^2\sqrt{I}}{1+Ba_i\sqrt{I}},\ \text{where}\ A=\frac{\sqrt{2\pi N_A d}}{(4\pi\varepsilon\varepsilon_0 kT)^{3/2}}e^3\ \text{and}\ B=\sqrt{\frac{2e^2N_A d}{4\pi\varepsilon\varepsilon_0{}^2kT}} \tag{1.20}$$

d is the solvent density in kg/m^3. where I is the molality based ionic strength, calculated as:

$$I=\frac{1}{2}\sum_{i=1}^{N}m_i z_i{}^2 \tag{1.21}$$

where m_i refers to the molality of ion *i*.

This term (1.20) is also described as in literature the truncated DH term. It can also be derived from the complete DH term by truncating the complete expression and omitting the higher order terms. The truncated DH term can be further simplified by letting $b \triangleq Ba_i$ in (1.20). Since the value of *b* does not vary much, the parameter *b* is often considered as a constant with a value of 1.50 $(kg/mol)^{1/2}$. Finally, we get another truncated DH term commonly seen in textbooks.

$$\ln \gamma_i^{DH} = -z_i^2 \frac{AI^{1/2}}{1+bI^{1/2}} \tag{1.22}$$

Based on table values of the relative permittivity and density of pure water, the *A* parameter can be approximate in the temperature range 273.15 K to 383.15 K according to Thomsen[21]:

$$A = 1.131 + 1.335\times10^{-3}\times(T-273.15) + 1.164\times10^{-5}\times(T-273.15)^2 \quad kg^{1/2}/mol^{1/2} \tag{1.23}$$

In this work, the Debye-Hückel *A* parameter was calculated from equation (1.23). This simplified DH term (1.22) is independent of pressure and volume. It does not give a contribution to the volume of the solution. The DH term in (1.22) with *A* parameter from equation (1.23) will be used in Chapter 2 for constructing electrolyte EOS.

The Debye-Hückel theory gave rise to a continuing series of more pragmatic and empirical extensions. The most remarkable are the Pitzer and Bromley theories.[1,3]

1.2.3.2 Pitzer theory

In 1973, Pitzer[22] developed a very useful extension of the DH theory where hard sphere effects are incorporated via a virial expansion including up to three virial coefficients.

It has been applied successfully to several geochemical systems and to systems of interest in the chemical industry.

In Pitzer's theory, the radial distribution function has been truncated to the second order to approximate the Boltzmann distribution:

$$g_{ij}(r) = \exp\left[-\frac{z_j e\psi_i(r)}{kT}\right] \approx 1 - \frac{z_j e\psi_i(r)}{kT} + \frac{z_j^2 e^2 \psi_i^2(r)}{2k^2T^2} \tag{1.24}$$

For an electrolyte solution containing w_s kilograms of solvent, with molalities m_i, m_j, …, of solute species *i*, *j*,…, the excess Gibbs energy in Pitzer Theory is expressed by

$$\frac{G^E}{RTw_s} = f(I) + \sum_i\sum_j m_i m_j \lambda_{ij}(I) + \sum_i\sum_j\sum_k m_i m_j m_k \Lambda_{ijk} + \cdots \tag{1.25}$$

Function $f(I)$ depends on ionic strength I , it represents long range electrostatic forces and includes the Debye-Hückel limiting law. $\lambda_{ij}(I)$ represents the short range interaction between two solute particles in the solvent; Λ_{ijk} terms account for three-body ion interactions, only important at high salt concentrations. $\lambda_{ij}(I)$ and Λ_{ijk} are analogous to second and third virial coefficients.

The mean activity coefficient, obtained from taking partial differentials of the above excess Gibbs energy, is a sum of an electrostatic (Debye-Hückel type) term and a virial expansion in electrolyte concentration. This agrees with the Guggenheim-Scatchard equation. On a molality base, the equation is:

$$\ln \gamma_{\pm} = \left|z_{+} z_{-}\right| f^{\gamma} + m(\frac{2\nu_{+}\nu_{-}}{\nu}) B^{\gamma}_{MX} + m\left[\frac{2(\nu_{+}\nu_{-})^{3/2}}{\nu}\right] C^{\gamma}_{MX} \tag{1.26}$$

Pitzer obtained these virial coefficients by applying the series expansion to the pressure equation of the solution and using an appropriate interaction potential for the ionic solution. The virial expansion provides very good representation of the properties of electrolyte solution. To fit the experimental data on mean ionic activity and osmotic coefficients, the viral coefficients are treated as adjustable parameters. Pitzer has generated a very useful set of the values of these fitting parameters. By using these values, it is possible to calculate the activity and osmotic coefficients for single and mixed electrolytes up to very high concentrations, i.e. usually >4 molal.

1.2.3.3 Bromley's model

L. A. Bromley has suggested a model in 1973 [23,24] based on the Guggenheim-Scatchard equation. He omitted the third virial coefficient and simplified the ionic strength dependence of the second virial coefficient on a molality base:

$$\ln \gamma_{\pm} = -\frac{A\left|z_{+} z_{-}\right| \sqrt{I}}{1+\sqrt{I}} + \mathrm{CI}, \text{ where } \frac{C}{\ln 10} = \frac{(0.06 + 0.6 B_{+-})\left|z_{+} z_{-}\right|}{\left(1 + \frac{1.5}{\left|z_{+} z_{-}\right|} I\right)^{2}} + B_{+-} \tag{1.27}$$

The Bromley equation can be used up to an ionic strength of about 6.0 molal.

1.2.4 Integral equation theory

Statistic mechanics have been applied to electrolyte systems.[1,4,5] The thermodynamic properties of liquid can be obtained once the radial distribution function has been determined. There are several integral equations established to calculate radial distribution function, Ornstein-Zernicke (OZ) equation is the most notable one of them. The OZ equation has the form as follows:

$$h_{12} = c_{12} + \rho \int c_{13} h_{13} dr_3 \tag{1.28}$$

where c_{ij} is the direct correlation function between particle *i* and *j*, $h_{ij} = g_{ij} - 1$ is the total correlation function and g_{ij} is the radial (pair) distribution function. This equation can be solved by providing different approximate closures. Most commonly seen solutions of OZ equation are the Percus-Yevick equation, Hypernetted Chain (HNC) integral equation and the mean spherical approximation (MSA). [1,2,4,5]

1.2.4.1 The hypernetted chain theory

The HNC integral equation was the most successful and accurate approach for electrolyte solutions among the above three. It based on a closure of the hierarchy of coupled correlation functions.[1,3,15]

$$c_{ij} = g_{ij} - 1 - \ln(g_{ij}) - \beta u_{ij} \tag{1.29}$$

It can accurately predict the structure of electrolytes solutions as well as their thermodynamic properties. One significant advantage of the HNC is its ability to supply accurate structural and thermodynamic properties of primitive electrolyte at low densities and high temperature, where the simpler MSA theories are not accurate.[1] Generally the HNC theory can give exact numerical simulation results for electrolytes up to 2 M. [25] However, HNC is not able to give an exact analytical solution and the computation involves numerically solving a complex system of highly nonlinear equations and thus limits its application.

1.2.4.2 The mean spherical approximation (MSA)

The solution of the OZ equation with MSA closure (short as MSA term) is based on the following closure:

$$\begin{aligned} g_{ij} &= 0 \qquad\qquad r_{ij} < \sigma_{ij} \\ c_{ij} &= -\beta u_{ij}(r) = -\frac{\beta z_i z_j e^2}{4\pi\varepsilon\varepsilon_0 r_{ij}} \qquad r_{ij} > \sigma_{ij} \end{aligned} \tag{1.30}$$

An analytical solution of MSA for the restricted primitive model (short as RPM) was first solved by Waisman and Lebowitz in the early 1970s using the perturbation theory.[1] Later Blum[12] and Blum and Hoye[13] solved the MSA for the primitive model and obtained analytical expression for excess thermodynamic properties including the Helmholtz free energy, activity coefficients, chemical potentials and osmotic coefficients. It was soon discovered that the equation for the activity coefficients in the dilute solution were closely analogous to those obtained from DH theory.[1,14] Blum[14] explained the MSA theory in relation to the DH and the integral equation theories.

a. The complete MSA

The complete solution of the OZ equation with MSA closure (short as the complete MSA)[12, 13, 26] yields the following equations:

$$\Omega = 1+\frac{\pi}{2\Theta}\sum_{ions}\frac{\rho_i\sigma_i^3}{1+\Gamma\sigma_i},\quad P_n = \frac{1}{\Omega}\sum_{ions}\frac{\rho_i\sigma_i z_i}{1+\Gamma\sigma_i},\quad \text{where } \Theta = 1-\frac{\pi}{6}\sum_{ions}\rho_i\sigma_i^3, \tag{1.31}$$

$$\Gamma = \frac{e}{2\sqrt{\varepsilon_0\varepsilon kT}}\left\{\sum_i \rho_i\left[\frac{z_i-\frac{\pi\sigma_i^2 P_n}{2\Theta}}{1+\Gamma\sigma_i}\right]^2\right\}^{1/2},\ \text{where } \rho_i = \frac{N_i}{V}\ \text{(number density of species } i) \tag{1.32}$$

The only restriction imposed is the electro-neutrality condition:

$$\sum_j \rho_j z_j = 0 \tag{1.33}$$

Γ is the MSA screening parameter and κ is the Debey screening length ($\Gamma \to \kappa/2$ at infinite dilution). e is the electronic charge, k is the Boltzmann's constant, ε is the relative permittivity of the medium, ε_0 is the vacuum permittivity, z_i is the valence and σ_i is the the diameter of species i, and the closest distance of the approach in MSA is $\sigma_{ij} = (\sigma_i + \sigma_j)/2$. T is the absolute temperature, ρ_i is the number density of species i. From the expression of the MSA screening parameter Γ, it can be seen that the explicit form of Γ cannot obtained from the complete MSA.

Expressions of the excess Helmholtz energy, the internal energy and the osmotic coefficient from the complete MSA are presented below.

$$A^E = -\frac{Ve^2}{4\pi\varepsilon_0\varepsilon}\left\{\Gamma\sum_{ions}\frac{\rho_i z_i^2}{1+\Gamma\sigma_i}+\frac{\pi}{2\Theta}\Omega P_n^2\right\}+\frac{V\Gamma^3}{3\pi}kT, \tag{1.34}$$

$$U = -\frac{Ve^2}{4\pi\varepsilon_0\varepsilon}\left\{\Gamma\sum_{ions}\frac{\rho_i z_i^2}{1+\Gamma\sigma_i}+\frac{\pi}{2\Theta}\Omega P_n^2\right\} \tag{1.35}$$

$$\Phi = -\frac{\Gamma^3}{3\pi\rho}-\frac{1}{8\rho}\left(\frac{4\pi e^2 P_n^2}{DkT\Theta^2}\right), \text{ where } \rho=\sum_{ions}\rho_i \tag{1.36}$$

Solution of the complete MSA requires an implicit solution for the screening parameter, i.e. a complicated set of equations which must be solved iteratively, this makes it particularly troublesome to use in iterative computations. Detailed algorithms are provided in Chapter 3.

b. The simplified implicit MSA

The analytic results of MSA have been modified and developed to other empirical but widely applicable models by many other persons. Planche and Renon[1,27] (1981) take into account the short range force between neutral solvent molecules in order to get a representation of electrolyte solution. They add a short range term to the Coulombic term in the potential energy:

$$\begin{aligned}\beta u_{ij}(r) &= \frac{\beta z_i z_j e^2}{4\pi\varepsilon\varepsilon_0 r}+\frac{W_{ij}}{2\pi r}\delta'(r-\sigma_{ij}) \quad & r_{ij}>\sigma_{ij}\\ u_{ij}(r) &= \infty & r_{ij}<\sigma_{ij}\end{aligned} \tag{1.37}$$

where δ' is the derivative of the Dirac delta function and W_{ij} is a parameter that characterizes the contact interaction in the fluid. By using the formalism of Blum, they solved the OZ equation and obtained the analytical solution. The resulting analytical expression for the Helmholtz energy of the mixture can be used to represent osmotic coefficients of a fully dissociated salt solution in water up to 6M within 1% error range. This approach was extended by Fürst and Renon (1993)[1,28] to develop a new equation of state(short as EOS) for electrolyte solution with a simplified implicit MSA term of Planche.

$$A^r(T,V,n) = -\frac{e^2 N_A}{4\pi\varepsilon_0\varepsilon}\left(\Gamma\sum_i\frac{n_i z_i^2}{1+\Gamma\sigma_i}\right)+\frac{V\Gamma^3}{3\pi}kT \tag{1.38}$$

where

$$4\Gamma^2 = \frac{e^2 {N_A}^2}{\varepsilon_0\varepsilon RT}\sum_i\frac{n_i}{V}\left[\frac{z_i}{1+\Gamma\sigma_i}\right]^2 \tag{1.39}$$

No mixing rule is needed for the ion diameter. Comparing with the complete MSA term in (1.31) and (1.34) from Blum and Harvey[13], it can be seen that if the term P_n in (1.31) and (1.34) is set to zero, equation (1.34) and (1.31) can be simplified into (1.39) and (1.38) respectively.

c. The simplified explicit MSA

Two simple and explicit approximations of the complete MSA have been shown to be accurate [26, 29]. First simplification is based on a linear mixing rule for a single

effective ion size. If all ions have the same diameter σ (common ion size), we have the following simplified expression (1.41) to (1.44) from the complete MSA of (1.31) to (1.36). Detailed deduction, see Appendix II. The above simplified implicit MSA in equation (1.38) and (1.39) from Fürst[28] can also be reduced to below simplified explicit MSA under the common ion size assumption.

$$P_n = \frac{1}{\Omega}\frac{\sigma}{1+\Gamma\sigma}\sum_{ions}\rho_i z_i = 0, \quad (1.40)$$

and

$$\Gamma = \frac{1}{2\sigma}\left[\sqrt{1+2\sigma\kappa}-1\right] \quad \text{and} \quad \kappa = \left(\frac{e^2 N_A^2}{\varepsilon\varepsilon_0 RTV}\sum_{ions} n_i Z_i^2\right)^{1/2} \quad (1.41)$$

The expressions of the excess Helmholtz energy, the internal energy and the osmotic coefficient from the MSA term turn to be the following simplified expressions:

$$A^E = -\frac{2\Gamma^3 RTV}{3\pi N_A}\left\{1+\frac{3}{2}\Gamma\sigma\right\} \quad (1.42)$$

$$U = -\frac{\Gamma^3(1+\Gamma\sigma)RTV}{\pi N_A} \quad (1.43)$$

$$\Phi = -\frac{\Gamma^3}{3\pi\rho}, \quad \text{where} \quad \rho = \sum_{ions}\rho_i \quad (1.44)$$

The second simplification from Copeman and Stein[26] is based on an extension of the Debye-Hückel radial distribution function, which is accurate at the low ion densities. The exact mathematical expression will not be given since it is not selected for the electrolyte EOS in this thesis; for details please refer to the relevant paper.

MSA term has been used to study the effects of ion association on the thermodynamics of electrolyte systems. It has also been used to study electrolyte-solution behaviour near the solution critical point due to its ability to model solvation effects in a simplified but useful way.[1]

1.2.4.3 Percus-Yevick (PY) theory

The PY closure of OZ equation is given by

$$\beta\frac{\partial\rho}{\partial P} = 1+\rho\int_0^\infty (g_{ij}-1)dr_{ij},$$
$$c_{ij} = g_{ij}\left[1-\exp(\beta u_{ij})\right]. \quad (1.45)$$

This closure has been used successfully to calculate thermodynamic and structural properties of fluids dominated by short range interactions.[1,30] However this approach has not been used widely.

1.2.5 Perturbation theory

Perturbation theories use a Taylor expansion of the Helmholtz free energy in inverses temperature around some known reference state.[1,5,20] The major advantages of this approach is that terms in the series expansion are written as functions of a reference system, whose properties are known and the possibility of associating term in the expansion with various interactions. [1] The disadvantages of perturbation theories when applied to mixtures of real fluids involve[15]: (1) The long and non-analytic calculations. (2) Numerical integrations are required for every temperature, density and composition.

However, with the increasingly efficient computers and with advances in molecular physics, perturbation theory has become one of the two non-PB theories widely adopted to the calculation of properties for real systems. The other theory is the MSA approach mentioned in the previous section. The two different methods for formulating expansions in perturbation theories have been applied successfully within this framework. [1,3] They differ in the way the pair potential is divided between the repulsive and attractive parts. One, due to Barker-Henderson-Leonard (BHL)[9,10] expands the Helmholtz free energy by writing the configuration integral as a double Taylor expansion in two perturbation parameters: a steepness parameter and well-depth parameter. The other is developed by Chandler, Weeks and Anderson (CWA) in 1971.[1,3] The CWA perturbation theory does not expand about the hard sphere fluid but rather about the restricted primitive model for electrolytes.

1.2.6 Fluctuation solution theory

Fluctuation solution theories, also known as the Kirkwood-Buff theories, relate concentration fluctuation in the statistical mechanical grand canonical ensemble to various observable partial derivatives of the thermodynamic functions. Fluctuation theory has been extended successfully to systems containing electrolytes by Perry et al 1988; Newman, 1989 and O'Connell, 1993.[1,3] A major disadvantage to this approach is that the thermodynamic properties which are easily calculated from the equations are not the properties useful for engineering application.

1.3 *Engineering models*

In the previous part, the major theories for electrolytes solution and the semi-empirical model developed from them have been explained. Many of these theories are only valid for electrolyte solutions with low concentration (below 1 M). Since the 1920s, significant advances have been made in combining theoretical and empirical approaches to develop engineering models being less rigorous and theoretical to describe electrolyte solutions. Many different engineering models, either empirical or semi-empirical, have been suggested in the passed three decays for calculating the thermodynamic properties of the concentrated electrolyte solutions (up to 6M or higher).

There are two kinds of approaches to establish an engineering model, i.e. the excess Gibbs free energy formalism and the residual Helmholtz free energy formalism. In excess Gibbs free energy formalism, excess Gibbs free energy is used to derive activity coefficients and the models established through this formalism are also described as activity coefficient models. Apart from classical activity coefficient models such as the well-known Debye-Hückel model, Bromley's model, Pitzer's model[22] and Meissner's model, other models in terms of the excess Gibbs free energy were also developed. Chen *et al.* developed the electrolyte NRTL activity coefficient model based on a modification of the NRTL local composition model[31,32]. Sander *et al.*[33] presented in 1986 an extension of the UNIQUAC model, later slightly modified by Thomsen *et al.*[21,34,35], and it has proven applicable for calculations of vapour-liquid-liquid-solid equilibria (VLLSE) and of thermal properties in aqueous electrolyte solutions.

There are some disadvantages by using g^E models. One disadvantage of the g^E model is that the density of the solution cannot be derived from the model itself. The pressure dependency of the activity coefficients cannot be calculated directly from a

g^E model too. To overcome these disadvantages another kind of models, the electrolyte EOS, has been developed. In spite of these disadvantages, g^E models have been applied successfully to geochemical systems and to systems of interest in the chemical industry, including multi-component mixed-solvent electrolytes.

1.3.1 Local composition models

Chen *et al.* first developed a local composition NRTL activity coefficient model for single, completely dissociated electrolytes in a single solvent. [31,32] The central idea is that the interaction between the ions and the solvent can be represented locally and generalized to the entire solution. This approach was excellent for reproducing experimental activity coefficients for dilute and moderately concentrated (up to 3m) solutions of strong electrolytes. Haghtalab and Vera (1988,1991) replace Chen's empirical expression for the non-random factors with an expression of the Wilson type.[36, 37] The fits are quite good with two binary parameters. Liu *et al.* (1989) include a modified Debye-Hückel term to account for the effect of long range electrostatic forces on the local composition and a short range term that differs significantly from Chen's short range term. [38,]

1.3.2 Hydration models

Hydration models are similar to local composition approaches, as they seek to compensate for the effect of ion-solvent association of the energy of the whole system. They differ from the local composition models, as rather often they contain specific expressions for the hydration energy and the hydration number. Recent studies in this area have combined hydration and ion-association concepts. Heyrovska (1989) explained an alternative view of electrolyte-solution modelling that considers the normal state of the electrolyte in aqueous solution to be hydrated and partially associated.[1] Schoenert has developed expression for the excess Gibbs free energy and excess enthalpy of hydrated and associated ions using a modified version of the hydration model of Robinson and Stockes.[1]

1.3.3 The extended UNIQUAC model

To represent phase equilibria in mixed-solvent (or aqueous) electrolyte systems, the excess Gibbs energy function is usually expressed as the sum of a DH and a short range term. The UNIQUAC model or the UNIFAC model was applied for the short range term. In 1986 Sander *et al.* [33] presented an extension of the UNIQUAC model by adding a DH term, allowing this Extended UNIQUAC model to be used for electrolyte solutions. The model has been slightly modified since then by Thomsen *et al.* [21,34,35].

Thomsen (1997) presented an excess Gibbs free energy model consisting of three terms [21]: a combinatorial or entropic term, a residual term and an electrostatic term:

$$G^E = G^E_{Combinatorial} + G^E_{\mathrm{Re}\,sidual} + G^E_{Debye\text{-}Hückel}$$

The combinatorial and the residual terms are identical to the terms used in the traditional UNIQUAC equation. The combinatorial term is

$$\frac{G^E_{Combinatorial}}{RT} = \sum_i x_i \ln\left(\frac{\phi_i}{x_i}\right) - \frac{z}{2}\sum_i q_i x_i \ln\left(\frac{\phi_i}{\theta_i}\right)$$

z is the co-ordination number, x_i is the mole fraction, ϕ_i is the volume fraction and θ_i is the surface area fraction of component i.
The residual term is

$$\frac{G^E_{\text{Residual}}}{RT} = -\sum_i q_i x_i \ln\left(\sum_k \theta_k \psi_{ki}\right), \quad \text{where } \psi_{ki} = \exp\left(-\frac{u_{ki} - u_{ii}}{T}\right)$$

u_{ki} and u_{ii} are interaction energy parameters.
The DH term however is expressed in terms of the rational, symmetrical convention for water and the rational, unsymmetrical convention for ions. The expression of the excess Gibbs energy for the DH suggested by Fowler and Guggenheim (1949) has been used:

$$\frac{G^E_{\text{Debye-Hückel}}}{RT} = -x_w M_w \frac{4A}{b^3}\left[\ln(I + bI^{1/2}) - bI^{1/2} + \frac{b^2 I}{2}\right]$$

The extended UNIQUAC model has been combined with the Soave-Redlich-Kwong (short as SRK) EOS to calculate vapour liquid equilibrium (VLE) in systems containing electrolytes. The model is applied under the circumstance with the assumption that all ions will remain in the liquid phase, while the volatile components are the following substances such as water, NH_3, carbon dioxide and SO_2 and various organic solvents. It is applicable for calculations of vapour-liquid-liquid-solid equilibria and of thermal properties in aqueous electrolyte solutions.

1.4 *Equation of state for electrolytes*

EOSs for electrolyte do not have the disadvantages which the excess Gibbs free energy models have and they can be established through the residual Helmholtz free energy formalism. Thermodynamic properties can be derived from the Helmholtz free energy by standard differentiation. However, electrolyte solutions are considerably more difficult to model than most other solutions encountered in engineering applications. Ions are charged particles, and the electrostatic interactions between ions and between ions and solvents are different from the dispersion and repulsive forces taken into account by most EOSs. These interactions make the electrolyte solution more non-ideal than a non-electrolyte solution even at very low concentrations. Thus additional Helmholtz free energy terms are needed to describe these interactions in electrolyte solutions. One of the first attempts to develop an EOS for electrolyte solutions was that of Planche and Renon (1981).[27] Several fundamental EOSs for electrolyte solutions have been published since, the most notable being the equations of Fürst and Renon, [28] Wu and Prausnitz [39] and Myers *et al.*[40] and electrolyte SAFT (statistical associated fluid theory) EOS.
In the following sections, the recently developed EOSs for electrolyte with relatively good performances will be considered. These electrolyte EOSs are used as engineering models for industrial application. The present review mainly focuses on electrolyte EOS (engineering model) development for ionic solutions at equilibrium. The theories for these electrolyte EOSs will be tackled very briefly.

1.4.1 Wu and Prausnitz electrolyte EOS

This EOS is mainly applied to the systems containing hydrocarbons, water and salt. In both Wu and Prausnitz's[39] and Myers, Sandler and Wood's[40] EOSs, a Peng-Robinson

(PR) term is selected to describe the interactions between uncharged species. They will be explained in details in below section.

Thermodynamic model

A path has to be considered to form an electrolyte solution from a mixture of ideal gases, i.e. the EOS is in terms of the Helmholtz free energy, and both temperature and volume remain constant on the path. The change in the Helmholtz free energy on forming an ionic solution from an ideal gas mixture is given by the sum of the increase in the Helmholtz free energy of each step on the path, as shown in the Figure. Thermodynamic properties can be derived from the sum of the Helmholtz free energy by standard differentiation.

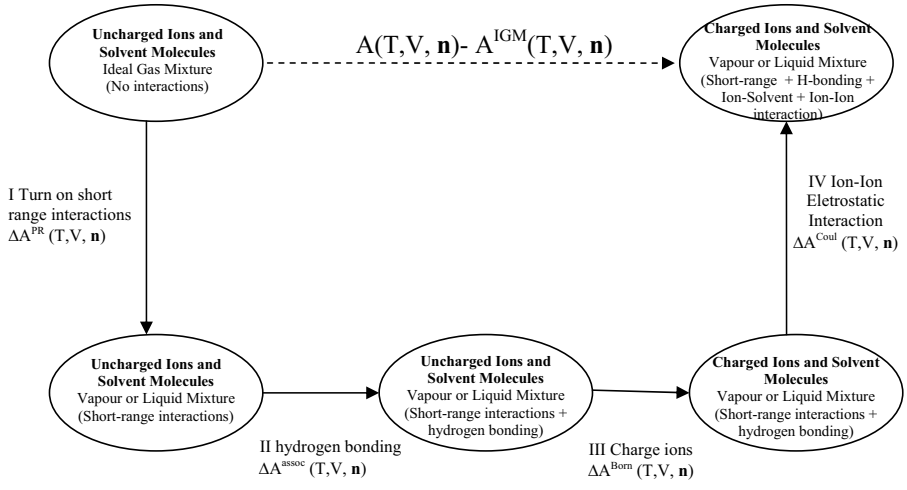

Figure 1.1. Path to the formation of an electrolyte solution at constant temperature and volume. This path is used for both the vapour and the liquid phase.

I. We start with a hypothetical ideal gas mixture containing uncharged ions and solvent molecules (water). There are no interactions between the particles in the mixture. For the first step, the excluded-volume repulsive forces and short range attractive forces between the neutral particles in the mixtures are added. The PR EOS is used to calculate the change in the Helmholtz free energy for this transition, ΔA^{PR}.

II. The hydrogen bondings between molecules are introduced. The additional Helmholtz energy is taken into account using the SAFT theory, ΔA^{assoc}.

III. The ions are charged, only taking into account the ion-solvent interaction. The contribution to the Helmholtz free energy of recharging the ions, ΔA^{Born}, is calculated from the Born equation for ions at infinite dilution in a dielectric solvent.

IV. Finally, the long range electrostatic interactions (Coulomb interaction) between the ions in the mixture are introduced. These interactions are accounted for by the mean spherical approximation (MSA). The change in the Helmholtz free energy is denoted as ΔA^{Coul}.

Using the property of a state function, we reach

$$A(T,V,\mathbf{n}) - A^{IGM}(T,V,\mathbf{n}) = \Delta A^{PR} + \Delta A^{assoc} + \Delta A^{Born} + \Delta A^{Coul}$$

where **n** is the vector of the number of moles of each component of the mixture, and A^{IGM} is the Helmholtz free energy of an ideal mixture.

The PR term is given by

$$\Delta A^{PR}(T,V,\mathbf{n}) = \frac{an}{2\sqrt{2}b}\ln\left(\frac{v+(1-\sqrt{2})b}{v+(1+\sqrt{2})b}\right) + nRT\ln\left(\frac{v}{v-b}\right) \tag{1.46}$$

The mixing rules used here are the van der Waals one-fluid mixing rules:

$$a = \sum_i \sum_j x_i x_j \sqrt{a_i a_j}(1-k_{ij}) \text{ and } b = \sum_i x_i b_i \tag{1.47}$$

where k_{ij} is the binary interaction parameter. It is the only adjustable parameter in the model.

Association contribution The hydrogen-bonding are counted for by the association term in SAFT model with the form of

$$\Delta A^{assoc}(T,V,\mathbf{n}) = nRT\sum_S\left(\ln X + \frac{1-X}{2}\right) \tag{1.48}$$

X stand for the monomer mole fraction. Details see the section of CPA EOS in later chapter.

Born contribution The free energy required to charge the ions in a medium with a relative permittivity of ε is calculated by the equation suggested by Born[41].

$$\Delta A^{Born}(T,V,\mathbf{n}) = \frac{N_A e^2}{4\pi\varepsilon_0\varepsilon}\sum_{ions}\frac{n_i Z_i^2}{\sigma_i} \tag{1.49}$$

Coulomb contribution The simplest description of long range ion-ion interactions in the electrolyte solution is achieved by the primitive model, where the ions are modelled as charged hard spheres in a medium of uniform relative permittivity. The additional Helmholtz free energy due to the Coulomb interaction between ions is calculated through the complete MSA by Wu and Prausnitz.[39].

$$\Delta A^{Coul} = -\frac{Ve^2}{4\pi\varepsilon_0\varepsilon}\left\{\Gamma\sum_{ions}\frac{\rho_i z_i^2}{1+\Gamma\sigma_i} + \frac{\pi}{2\Theta}\Omega P_n^2\right\} + \frac{V\Gamma}{3\pi}kT, \text{ where } \Theta = 1-\frac{\pi}{6}\sum_{ions}\rho_i\sigma_i^3, \tag{1.50}$$

The expression of the complete MSA term was introduced in details in previous section 1.2.4.2 from equation (1.31) to (1.34). Γ is the MSA screening parameter which is used in the computation of the excess thermodynamic properties due to ion-ion interactions. No mixing rules are needed for the complete MSA. For the mixing rules are incorporated in the expression in the form of the summation of different ion diameters.

Wu and Prausnitz[39] have used their EOS predicting solubilities of methane in salt-free water and in aqueous solution of 1 and 4 M sodium chloride from 100 to 600 bar at 125 °C. Agreement with experiment is good. Due to inconsistency of experimental data on the effect of temperature, calculations of the methane solubilities in NaCl solution at other temperatures have not been performed.

1.4.2 Myers, Sandler and Wood electrolyte EOS

Myers, Sandler and Wood [40] electrolyte EOS (MSW EOS) is intended to be developed for the systems more general than just containing hydrocarbons, water and salt and over wide ranges of temperature, pressure and composition.

Thermodynamic model

The path of constructing MSW EOS [40] is also starting from a mixture of ideal gases for an electrolyte solution, but slightly different than Wu and Prausnitz's. [39] Note that all the steps take place at constant temperature and volume along the path.

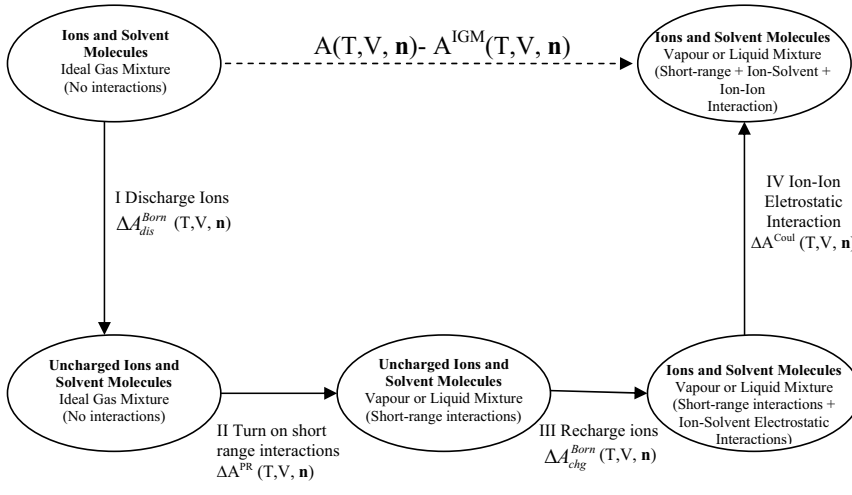

Figure 1.2. Path to the formation of an electrolyte solution at constant temperature and volume. This path is used for both the vapour and the liquid phase.

I. It is started with a hypothetical ideal gas mixture containing ions and solvent molecules at a temperature T and volume V. This is the reference state. There are no interactions between the particles in the mixture in ideal gas state. For the first step, the charges of the ions are removed. The Helmholtz free energy needed for discharging the ions, ΔA_{dis}^{Born}, is calculated from the Born equation for ions in a vacuum (ideal gas).

II. In ideal gas mixture of the neutral ions and solvent molecules, the excluded-volume repulsive forces and short range attractive forces between the neutral particles in the mixtures are added. The PR EOS is used to calculate the change in the Helmholtz free energy, ΔA^{PR}.

III. The ions are recharged, only taking into account the ion-solvent interaction. The contribution to the Helmholtz free energy of recharging the ions, ΔA_{chg}^{Born}, is calculated from the Born equation for ions at infinite dilution in a dielectric solvent.

IV. Finally, the long range electrostatic interactions between the ions are introduced. These interactions are explained by the simplified MSA

(sMSA) under the assumption of single effective ion diameter. The change in the Helmholtz free energy is denoted as ΔA^{Coul}.

We get the expression for the total change in Helmholtz free energy to form the electrolyte system:

$$A(T,V,\mathbf{n}) - A^{IGM}(T,V,\mathbf{n}) = \Delta A_{dis}^{Born} + \Delta A^{PR} + \Delta A_{chg}^{Born} + \Delta A^{Coul}$$

where **n** and A^{IGM} is the same as in previous section.

The PR term is given by

$$\Delta A^{PR}(T,V,\mathbf{n}) = \frac{an}{2\sqrt{2}b}\ln\left(\frac{v+c+(1-\sqrt{2})b}{v+c+(1+\sqrt{2})b}\right) + nRT\ln\left(\frac{v}{v+c-b}\right) \tag{1.51}$$

In this term, a volume translation parameter *c* suggested by Peneloux for the SRK EOS are introduced here for the PR EOS. This single parameter c can improve the volumetric predictions of PR EOS significantly.

The mixing rules used are the van der Waals one-fluid mixing rules:

$$a = \sum_i \sum_j x_i x_j \sqrt{a_i a_j}(1-k_{ij}),\ b = \sum_i x_i b_i \text{ and } c = \sum_i x_i c_i \tag{1.52}$$

where k_{ij} is the only binary interaction parameter in the model.

The parameters for pure water were fitted to volumetric and vapour-pressure data generated from the EOS of the International Association for the Properties of Water and Steam. The data used in the regression included vapour pressure from 10 °C to the critical temperature (374.15 °C) and the liquid densities from 10 °C to the critical temperature and pressure up to 250 bar. The following are the best-fit water parameters for PR EOS with volume translation parameter:

$$a_{H_2O} = 1.26944 - 0.89381T_r + 0.16937T_r^2 \qquad Pa\,m^6/mol \tag{1.53}$$

$$b_{H_2O} = 15.6345 + 6.14518T_r - 5.2795T_r^2 \qquad cm^3/mol \tag{1.54}$$

$$c_{H_2O} = -2.7227 + 11.4201T_r - 6.0157T_r^2 \qquad cm^3/mol \tag{1.55}$$

where $T_r = T/647.29\ K$.

Born contribution The free energy required to discharge ions in vacuum is calculated by the equation suggested by Born.

$$\Delta A_{dis}^{Born}(T,V,\mathbf{n}) = -\frac{N_A e^2}{4\pi\varepsilon_0}\sum_{ions}\frac{n_i Z_i^2}{\sigma_i} \tag{1.56}$$

The free energy required to charge the ions in a medium of electric constant ε is calculated by: .

$$\Delta A_{chg}^{Born}(T,V,\mathbf{n}) = \frac{N_A e^2}{4\pi\varepsilon_0\varepsilon}\sum_{ions}\frac{n_i Z_i^2}{\sigma_i} \tag{1.57}$$

The Born equation provides a means of calculating solvation free energies of ions in water. Born contribution has effect on the ion activity coefficients.

Coulomb contribution The additional Helmholtz free energy change due to the Coulomb interaction between ions is calculated through the solution of OZ equation with the MSA closure. The simplified explicit MSA term has been applied by Myers *et al.* [40]. It is derived under the assumption that all ions have the same average diameter σ. The expression of explicit MSA in terms of the Helmholtz free energy is

$$A^{Coul} = -\frac{2\Gamma^3 RTV}{3\pi N_A\varepsilon_0\varepsilon}\left\{1+\frac{3}{2}\Gamma\sigma\right\}, \qquad \text{where } \sigma = \frac{\sum_{ions} n_i\sigma_i}{\sum_{ions} n_i}, \tag{1.58}$$

The average diameter σ can be calculated through various mixing rules, and the conventional linear mixing rule has been adopted, see (1.58). This linear mixing rule is for ions with equal charges, however Myers *et al.*[40] also used it for ions with unequal charges. This might lead to some problems for the EOS and thus needs to be improved in the future. For unequal charges, the corollary to (1.58) is (1.59), where the diameters are weighted by the squares of the charges according to Blum[42] and Harvey *et al*.[26]. In this work, we used the linear mixing rule in (1.58) for MSW EOS in order to reproduce the publish results of Myers *et al.*[40]

$$\sigma = \frac{\sum_{ions} n_i z_i^2 \sigma_i}{\sum_{ions} n_i z_i^2} \tag{1.59}$$

It was described in details in equations (1.41) and (1.42) in section 1.2.4.2. The above simplified MSA reduces to the Debye-limiting law as σ approaches zero. However the MSA term gives more accurate predictions of the thermodynamic properties at high electrolyte concentrations.

The Uematsu and Franck[43] model has been used to calculate the relative permittivity of the medium ε for pure water. In this model the relative permittivity is given as a function of temperature and density over a temperature range of 238-1273 K and pressures up to 1200MPa.

The EOS was fitted to experimental data for 138 aqueous electrolyte solutions at 25 ºC and 1 bar to 300 ºC and from 1 to 120 bar. The equation does well in correlating activity coefficients, osmotic coefficients, densities and free energies of hydration over the wide range of conditions. The prediction of two aqueous mixed-salt systems of NaCl and LiCl at 25 ºC and 1 bar and NaCl and $CaCl_2$ at 110 ºC and 1.45 bar are also shown. The predicted osmotic coefficients of both mixed-salt solutions agree well with the experimental data. More comprehensive applications to mixed-salt systems were not given.

The limitations of MSW EOS [40] are mainly as follows. The PM of electrolyte solution is not valid at high ion concentrations. The authors suggest that their EOS should not be used for systems with salt concentrations greater than about 15 M. An improvement would be to adopt a model describing the solvent as discrete molecules, not as a continuum. But this would be at the cost of decreasing the simplicity of the suggested EOS.

1.4.3 Fürst and Renon's EOS

Fürst and Renon developed an EOS for electrolyte solutions around 1993.[28] The equation contains a non-electrolyte part and the electrolyte part. The non-electrolyte part is taken from the EOS of Schwartzentruber *et al.* (a modified SRK EOS). It is composed of a repulsive force term and an attractive short-arrange force term. The electrolyte part is composed of a simplified implicit MSA term to account for the long range electrostatic interactions and a short range interaction term specific to ions, denoted as SR2 term.

The model has three adjustable ion-specific parameters per ion. Using correlations between parameters and experimental ionic diameters, the model reduces to one-parameter model. This model has some predictive capability and has been tested against osmotic coefficients for single strong electrolytes and mixed two-electrolyte (ternary) system in water. The mean square deviations of the predicted values to the experimental data are within 2% to 6%.

The expression for the total change in Helmholtz free energy to form the electrolyte system is:

$$A(T,V,\mathbf{n}) - A^{IGM}(T,V,\mathbf{n}) = \Delta A^{Schwartzentruber} + \Delta A^{sMSA} + \Delta A^{SR2}$$

The Schwartzentruber non-electrolyte term is given by

$$\Delta A^{Schwartzentruber}(T,V,\mathbf{n}) = \sum_k x_k \ln\left(\frac{x_k RT}{P_0(v-b)}\right) + \frac{a^{SR}}{RT(b+c)}\ln\left(\frac{v+c}{v+2c+b}\right) \quad (1.60)$$

In this term, the mixing rules used are the van der Waals one-fluid mixing rules:

$$b = \sum_s x_s b_s + \sum_i x_i b_i, \text{ where } s = \text{molecular spiecies and } i = \text{ions} \quad (1.61)$$

and molecular species b_s is expressed in the usual way as a function of the critical properties:

$$b_s = \frac{\sqrt[3]{2}-1}{3}\frac{RT_c}{P_c} \quad (1.62)$$

The parameter a^{SR} and c for water is expressed as:

$$a^{SR} = x_w{}^2 a_w^{SR}, \qquad a_w^{SR} = \frac{1}{9(\sqrt[3]{2}-1)}\frac{RT_c}{P_c}\alpha(T_r) \quad (1.63)$$

where

$$\sqrt{\alpha(T_r)} = 1 + m(\omega)(1-\sqrt{T_r}) - p_1(1-\sqrt{T_r})(1+p_2T_r+p_3T_r{}^2)$$
$$\text{where } m(\omega) = 0.48508 + 1.55191\omega - 0.15613\omega^2 \quad (1.64)$$

$$c = x_w c_w \quad (1.65)$$

SR2 contribution The short range ionic term is given as

$$F_{SR2} = \frac{A_{SR2} - A^0}{RT} = -\sum_k \sum_l \frac{n_k n_l W_{kl}}{V(1-\varepsilon_3)} \triangleq \frac{W}{V(1-\varepsilon_3)} \quad (1.66)$$

and

$$\varepsilon_3 = \frac{N_A \pi}{6}\sum_k \frac{n_k \sigma_k^3}{V} \quad (1.67)$$

where k is over all ions. This term may be considered as a simplified form of the corresponding MSA term in Planche's model [27] (1981). The physical meaning of ε_3 is similar to packing fraction of various ions in the system. Two types of parameters appear in equation (1.66) and (1.67): they are interaction parameters W_{kl} and the ion diameters σ_k.

Coulomb contribution The additional Helmholtz free energy change due to the Coulomb interaction between ions is calculated through the simplified implicit MSA. The expression of Helmholtz free energy is given in previous section 1.2.4.2 as:

$$A^r(T,V,n) = -\frac{e^2 N_A}{4\pi\varepsilon_0\varepsilon}\left(\Gamma\sum_i \frac{n_i z_i^2}{1+\Gamma\sigma_i}\right) + \frac{V\Gamma^3}{3\pi}kT \quad (1.68)$$

The Pottel model has been used to calculate the relative permittivity of the electrolyte medium ε as follows

$$\varepsilon = 1 + (\varepsilon_s - 1)\frac{1-\varepsilon_3}{1+\varepsilon_3/2} \quad (1.69)$$

Where ε_3 is calculated by the same equation as in (1.67) and the solvent relative permittivity ε_s can be calculated according to the following equation:

$$\varepsilon_s = \frac{\sum_i n_i \varepsilon_i}{\sum_i n_i} \tag{1.70}$$

Only the relative permittivity of water is considered in equation (1.70). The relative permittivity of pure water ε_w is treated as a constant only changing with temperature .
The EOS was fitted to osmotic coefficients for 28 aqueous alkaline and alkaline-earth halide electrolyte solutions at 25 ºC and 1 bar. The equation gives a root mean square relative deviation of 2.9% in correlating activity coefficients osmotic coefficients using six parameters for all systems. The prediction of osmotic coefficients relative to six systems without any parameter adjustment deviates from 2.0% to 5.4%. The quality of the representation of mixed salts systems without mixing parameters was evaluated using experimental osmotic coefficients of 30 ternary systems.

1.4.4 Jin and Donohue's EOS

Jin and Donohue[44-46,] (1988) presented an EOS for mixtures containing electrolytes using perturbation theory for the short range interaction and long range Coulombic interactions. In the equation, short range interactions between molecules are calculated by using the Perturbed-Anisotropic-Chain theory (PACT) of Vimalchand and Donohue. A perturbation expansion based on Henderson's RPM is used for long range Columbic (charge-charge) interactions between ions. The solvation effects caused by charge-molecule interactions near ions are taken into account through the relative permittivity. Additional new expressions, a third-order perturbation expansion for charge-dipole interactions and a first-order perturbation expansion for charge-induced-dipole interactions, are derived for the interactions of ions with molecules in the bulk of the solution.
Jin and Donohue [44-46](1988 a, b; Jin 1991) introduced an extension of Henderson and Blum's temperature expansion for solution of primitive electrolytes around a hard-sphere fluid. This model requires one adjustable parameter (the ion size) per ion. This model works well in the prediction of mean ionic activity coefficients for solutions of single strong electrolytes, for mixtures of weak electrolytes, including those containing supercritical components and fairly well for mixture of strong electrolytes.
The PACT is a theoretically based equation which takes into account molecular motions that arise from rotational, vibrational and translational degrees of freedom. In the PACT, the Helmholtz free energy is calculated by corrections to ideal gas behaviour for molecular repulsions and molecular attractions; i.e.,

$$A_{PACT} = A^{IG} + A^{rep} + A^{att} \tag{1.71}$$

The first term in the equation is the contribution of the ideal gas law, the second term is a repulsive term and the last term, the attractive term, is given by

$$A^{att} = A^{LJ} + A^{DID} + A^{DD} + A^{QQ} + A^{DQ} \tag{1.72}$$

where the superscripts denote Lennard-Jones (LJ), dipole-induced-dipole (DID), dipole-dipole (DD), quadrupole-quadrupole (QQ) and dipole-quadrupole (DQ) interactions respectively.
Perturbation expansion for long range interactions is conducted in the following way for a RPMof electrolyte solutions. The ions in this model are considered as hard spheres with charges located at the centres of the particles. The long range charge-charge interactions are treated as a perturbation about a hard-sphere reference system

with the Columbic potential energy. A convergent form of perturbation expansion for the Helmholtz free energy can be written as:

$$A^{CC} = A^{cc}_{3/2} + A^{CC}_{2} + A^{cc}_{5/2} + A^{ccc}_{3} \tag{1.73}$$

Interactions between ions and molecules which are very near ions (solvation effects) are taken into account using the dielectric constant. In order to calculate interactions between molecules in the bulk of the solution and ions, the perturbation theory is used again.

The reference system for perturbation expansion for charge-molecule interactions is the particles interacting with hard-sphere potential.

The first order term for the charge-induced-dipole interactions is given by:

$$\frac{A^{CID}}{N_A kT} = -\frac{\kappa^2 W}{16\pi\rho\sigma} I^{c\mu} \tag{1.74}$$

with

$$W = 4\pi\rho\sum_i x_i\alpha_i \tag{1.75}$$

The result of the charge-dipole interaction is as follows:

$$A^{CD} = A^{c\mu}_{2} + A^{\mu\mu}_{5/2} + A^{cc\mu}_{3} + A^{c\mu\mu}_{3} \tag{1.76}$$

The detailed expressions for each terms in the above Helmholtz free energy are rather complicated and hereby we skip these expressions. Details are written clearly in the original papers. The complete form of the EOS for electrolyte is written as follows:

$$\mathrm{A_{PACT}} = \mathrm{A^{IG}} + \mathrm{A^{rep}} + \mathrm{A^{LJ}} + \mathrm{A^{DID}} + \mathrm{A^{DD}} + \mathrm{A^{QQ}} + \mathrm{A^{DQ}} + A^{CC} + A^{CID} + A^{CD} \tag{1.77}$$

To relax the assumption that all species are of equal size, it is necessary to introduce several mixing rules. A characteristic volume of the mixture is averaged by

$$\langle v^* \rangle \propto \langle d^3 \rangle = \sigma^3 \sum_i x_i s_i \tag{1.78}$$

The average Coulombic interaction energy of ionic mixture is given by

$$\langle E_c \rangle = \langle \varepsilon_c q \rangle = \sigma^3 \sum_i x_i \varepsilon_{c,i} q_i \tag{1.79}$$

The cross term $\varepsilon_{c,ij}$ and σ^3_{ij} are calculated by using the geometric mean mixing rule and the arithmetic mean mixing rule as

$$\varepsilon_{c,ij} = \sqrt{\varepsilon_{c,ii}\varepsilon_{c,jj}} \qquad \text{and} \quad \sigma^3_{ij} = \frac{\sigma^3_{jj} + \sigma^3_{ii}}{2} \tag{1.80}$$

.

Preliminary calculations involved mean ionic activity coefficients for 50 strong electrolytes in water specific volumes of several binary electrolyte solutions. In these calculations only one adjustable parameter C_s is used over a range of molarities from infinite dilution to 6M. Average absolute errors are less than 6% for activity coefficients for most binary systems, 2% for specific volumes of two binary systems and 5% for K factors for the ternary systems.

In the third articles of the series [46], Jin and Donohue used a single adjustable parameter for each ion. These parameters were determined from mean ionic activity coefficient data for a large number of single-salt aqueous systems. The values are then used in the calculations for multi-salt systems without any additional adjustable binary or ternary parameters. Preliminary calculations are conducted for several double-salt aqueous solutions and one triple-salt system, $CaSO_4$-$MgCl_2$-NaCl-H_2O.

1.4.5 Electrolyte SAFT EOS

Progress in developing a series of EOSs, the statistical associated fluid theory (SAFT), has been achieved since the 1980s [47]. SAFT was developed by Chapman, Gubbins, Radosz and co-workers at Cornell University and Exxon Research[0]. SAFT considers a molecule as a chain of tangent spherical segments starting from the reference system of hard sphere, with different perturbation contributions assumed to effect independently. The Helmholtz free energy is written as the sum of contributions due to hard-sphere repulsive interactions, due to chain formation through bonding of a number of hard spheres and due to association. A dispersion term is added as a perturbation to the reference fluid. The Carnahan-Starling expression is used for the hard sphere term. Huang and Radoz used a fourth order perturbation term (polynomial) as dispersion term, which has been widely accepted later. This dispersion term is originally based on molecular dynamics simulation data for the square-well. The chain formation term as well as the association term is based on the work of Wertheim: from the first order thermodynamic perturbation theory (TPT)[48, 49].

Later numerous modified versions of SAFT with certain improvements were made by different research groups. Simplified SAFT EOSs have been suggested, such as the hard-sphere SAFT (SAFT-HS) by Jackson et al[50, 51], and the simplified SAFT of Fu and Sandler[52]. More realistic potential models of the reference fluid were adopted to replace the hard-spheres in order to improve the performance of the original SAFT. Examples are SAFT-LJ from Kraska and Gubbins,[53, 54] SAFT-VR from Jackson and co-worker[55, 56] and SAFT1 by Adidharma and Radosz.[57, 58] Recently, Gross and Sadowski [59]present a perturbed-chain SAFT (PC-SAFT) with a hard-chain reference fluid.

Its strong statistical mechanics theoretical basis and the accuracy of SAFT for a number of difficult systems made SAFT a very popular EOS in the academic and industrial communities. Later it has also been extended to systems containing electrolytes. Galindo and coworkers [60] extended their SAFT-VR EOS to aqueous electrolyte systems (1999). Long range Coulombic interactions are calculated with MSA term for the restricted primitive model. Cameretti, Sadowski and Mollerup [61] suggested an electrolyte EOS without counting the association for ions, combining PC-SAFT and the complete Debye-Hückel term. There are two fitting parameters per ion in the PC-SAFT EOS, the ion diameter and the dispersion energy. This EOS is developed mainly for electrolyte systems containing proteins with a relatively narrow targeted temperature range of 278-393 K. The evaluation of the reported correlation results is difficult, for only the results of the fitting of vapour pressure and solution density were shown in the paper. Tan *et al.*[2] (2005) proposed an EOS combining SAFT1 and the MSA term for the restricted primitive model. The EOS contains four fitting parameters, three from SAFT1 (segment volume, segment energy and λ) per ion and one from MSA term (ionic diameter) per salt. Associations for ions are neglected. Beside λ, all of the other three fitting parameters are treated as temperature dependent parameters, which introduces another four parameters. The fitting results of the six aqueous alkali halide solutions are good but slightly worse than the electrolyte EOS from Myers *et al.*[40] Liu *et al.* [62] suggested SAFT with a Lennard-Jones potential combined with the low-density expansion of the MSA closure for the non-primitive model. For binary solutions, the EOS uses two fitting parameters per salt. The remaining three parameters are either calculated by empirical equations (well-depth parameter) or set to some value (such as associate volume, the number of associate site). The relative permittivity of water (or dielectric constant) can be solved from the

non-primitive model. In this EOS there is no need of the empirical equations to calculate the water relative permittivity as in primitive models. Association of ionic species with solvent is also counted for in the Wertheim term. The goodness-of-fit to aqueous alkali halide solutions is very similar to electrolyte SAFT1 from Tan *et al.*.[2]

1.5 *Conclusions*

Some of the above mentioned electrolyte EOSs are summarized in Table 1.1. From Table 1.1, it can be seen that all EOSs are generally composed of two types of terms: non-electrolyte terms which can be one of the commonly used EOS such as SRK, PR or SAFT EOS and electrolyte terms. The electrolyte terms can be divided as Coulombic terms and non-Coulombic terms. Coulombic terms account for the long range electrostatic interaction, such as the different solutions (complete, simplified implicit, and simplified explicit) of OZ equation with MSA closure or different kinds of Debye-Hückel terms (complete or truncated). Non-Coulombic terms include terms like Born, SR2 and association terms. They account for interactions other than the long range electrostatic interaction.

Mean ionic activity coefficients, osmotic coefficients and densities of binary aqueous electrolyte systems are physical properties which have been used to estimate parameters for all electrolyte EOSs. Mixed solvent electrolyte systems have been treated by a few authors. Ternary aqueous electrolyte systems have been considered rarely. Vapour-liquid equilibrium (VLE) calculations containing electrolytes were included by some authors, but solid-liquid equilibrium (SLE) calculations for multi-component electrolyte systems are rarely seen in these papers.

From the literature study it can be concluded that the extension of the EOS to electrolyte systems is feasible and necessary. For electrolyte EOS can be applied to various concentrated electrolyte solutions (up to 6M or higher) at a wide temperature (up to 300 °C) and pressure range (up to 600 Bar). Ion-specific parameters can be obtained for electrolyte EOS to conduct phase equilibrium calculations such as VLE and SLE. It has the potentials of industrial application. The possibility for electrolyte EOS to achieve similar performances as the existing Gibbs free energy model such as the electrolyte NRTL or extended UNIQUAC is quite high.

The goal of this work is to explore the possibility of using an EOS based on ion-specific parameters for multi-component mixtures containing electrolytes and non-electrolytes and the possibility of reproducing SLE phase diagrams with electrolyte EOS. Different short range terms and long range terms were evaluated by applying them to a chosen test system.

Table 1.1 The table of different equations of state in literature.

Author	Applications	Non-electrolyte term	Electrolyte terms	Pure compound parameter	Interaction parameter
Jin and Donohue [44-46] (1988,1991)	1. Mean ionic activity coefficients ($\gamma_{\pm}$) of binary systems of 50 strong electrolytes 2. VLE of binary systems of four weak electrolytes 3. SLE calculation for ternary, quaternary and quinary systems	Perturbed-Anisotropic-Chain theory, PACT [44]	1. perturbation expansion term of long range charge-charge interaction 2. perturbation expansion term of charge-molecule interaction	One adjustable ion-specific parameter	None
Fürst and Renon [28] (1993)	1. Osmotic coefficients (Φ) for 28 binary aqueous alkaline and alkaline-earth halide electrolyte solutions at 25 ºC and 1 bar 2. The representation of experimental Φ for 30 ternary systems without mixing parameters	Modified SRK EOS	1. Simplified Implicit MSA term (primitive model , short as PM) 2. SR2 term	None	One (W_{ij} in the SR2 term, for interactions between cation-anion)
Wu and Prausnitz [39] (1998)	1. Predict the solubility of methane in salt-free water and in an aqueous solution NaCl (1 and 4 molal, 125 °C, 100~600 bar) 2. Correlation results of $\gamma_{\pm}$ and water activity for aqueous NaCl solutions (25 to 300 ºC)	1.PR EOS 2.Wertheim association term of for associating compound	1. Complete MSA (PM). 2. Wertheim association term for ion association 3. Born term	One adjustable ion-specific parameter	None
Myers, Sandler and Wood [40] (2002)	1. Correlations for $\gamma_{\pm}$ for 138 aqueous binary electrolyte solutions (25 ºC, 1 bar) 2. Correlations for $\gamma_{\pm}$, Φ, densities, and free energies of hydration of seven salts at	PR EOS with volume translation parameter	1. Simplified explicit MSA (restricted primitive model, short as RPM) 2. Born term	Three adjustable salt-specific parameters	One (k_{ij} in PR EOS, for salt and water interactions, used only for salts in

	25~300 ºC and 1 to 120 bar 3. The prediction of Φ for ternary systems, NaCl-LiCl-H_2O (25 ºC, 1 bar) and NaCl-$CaCl_2$–H_2O (110 ºC, 1.45 bar)				application 2 and NaCl-$CaCl_2$–H2O in application 3.
Galindo, G-Villegas, Jackson and Burgess [55] (1999)	1. Nine strong aqueous binary electrolyte systems (vapour pressure, density) 2. One aqueous ternary electrolyte system (LiBr + LiI, vapour pressure)	SAFT-VR EOS	1. Simplified explicit MSA (RPM)	One adjustable ion-specific parameter	None
Cameretti, Sadowski and Mollerup [61] (2005)	Vapour pressures and densities of 12 binary electrolyte systems in the temperature range from 5 to 60 °C	PC-SAFT EOS	1. The complete Debye-Hückel term	Two adjustable ion-specific parameters	None
Tan *et al.* [2] (2005)	1. Six aqueous alkali halide solutions ($\gamma_{\pm}$, Φ, vapour pressure and density) at 25 °C 2. One binary system ($\gamma_{\pm}$, Φ and density)at 25, 50 and 100°C	SAFT1 EOS	1. Simplified explicit MSA (RPM) and neglect the associations for ions	Four adjustable ion-specific parameters	None
Liu *et al.* [62]	Fifteen binary aqueous alkali halide solutions ($\gamma_{\pm}$, Φ, density) at 25°C	SAFT EOS with a Lennard-Jones potential	1. The low-density expansion of the MSA closure for the non-primitive model 2. Wertheim term for association of ions and solvent	Two salt-specific parameters	None

Reference

1. Loehe JR, Donohue MD. Recent advances in modelling thermodynamic properties of Aqueous Strong Electrolyte Systems. *AIChE J.* 1997; 43:180-195.

2. Tan SP, Adidharma H, Radosz M. Statistical Associating Fluid Theory Coupled with Restricted Primitive Model To Represent Aqueous Strong Electrolytes. *Ind Eng Chem Res.* 2005; 44: 4442-4452.

3. Hu Y, Jiu G, Xu Y, Tan Z, ed. *Ying Yong Tong Ji Li Xue---Liu Ti Wu Xin De Yan Jiu Ji Su (Statistic Mechanism, foundations for the research of the physical properties of the fluids)*. P. R. China: Hua Xue Gong Ye Chu Ban Se (The Chemical Engineering Industry Publishing House); 1990.

4. Friedman HL. Electrolyte solutions at equilibrium. *Ann Rev Phys Chem.* 1981; 32: 179-204.

5. McQuarrie DA, ed. *Statistical Mechanics*. New York, NY: HARPER & ROW Publishers; 1976.

6. Dimitrios PT, ed. *Applied Chemical Engineering Thermodynamics*. Germany: Springer-Verlag; 1993.

7. Debye P, Hückel E. Zur Theorie der Elektrolyte. I.Gefrierpunktserniedrigung und verwandte Erscheinungen. *Physik Z.* 1923; 24: 185-206.

8. Gronwall TH, La Mer VK, Sandved K. Über den Einfluss der sogenannten höheren Glieder in der Debye-Hückelsen Theorie der Lösungen starker Elektrolyte. *Physik Z.* 1928; 29: 358-393.

9. Barker JA, Henderson D. Perturbation theory and equation of state for fluids. Square-well potential. *J Chem Phys.* 1967; 47(8): 2856-2861.

10. Barker JA, Henderson D. Perturbation theory and equation of state for fluids. II. Successful theory of liquids. *J Chem Phys.* 1967; 47(11): 4714-4721.

11. Leonard PJ, Henderson D, Barker JA. Perturbation theory and liquid mixtures. *Trans Faraday Soc.* 1970; 66(10): 2439-2452.

12. Blum L. Mean Spherical model for asymmetric electrolytes I. Method of solution. *Molecular Physics*. 1975; 30(5): 1529-1535.

13. Blum L, Høye JS. Mean Spherical Model for Asymmetric Electrolytes. 2. Thermodynamic Properties and the pair Correlation Function. *J Phys Chem.* 1977; 81(13): 1311-1316.

14 . Wei D, Blum L. Internal Energy in the Mean Spherical Approximation As Compared to Debye-Hückel Theory. *J Phys Chem.* 1987; 91: 4342-4343.

15. Corti HR, Fernandez Prini R, Blum L. An analytical approximation to the hypernetted chain (HNC) pair correlation functions: the case of 2:2 electrolytes. *J Chem Phys.* 1987; 87(5):3052-3055.

16. Kirkwood JG, Buff FP. The statistical mechanical theory of solutions. I. *J Chem Phys.* 1951; 19: 774-777.

17. Sørensen TS. How wrong is the Debye -Hückel approximation for dilute primitive model electrolytes with moderate Bjerrum parameter? *J Chem Soc Faraday Trans.* 1990; 86(10): 1815-1843.

18. Lu G, Li C, Wang W, Wang Z. Structure of KNO_3 electrolyte solutions: a Monte Carlo study *Fluid Phase Equilib.* 2004; 225: 1-11.

19. Breil MP. *Thermodynamics, Experimental, and Modelling of Aqueous Electrolyte and Amino Acid Solutions.* PhD Thesis. Copenhagen, Denmark: Technical University of Denmark; 2001.

20. Prausnitz JM, Lichtenthaler RN, de Azevedo EG, ed. *Molecular Thermodynamics of Fluid-Phase Equilibria (Third Edition)*. USA: Prentice Hall International Series in the Physical and Chemical Engineering Sciences; 1999.

21. Thomsen K. *Aqueous electrolytes: model parameters and process simulation.* PhD thesis. Copenhagen, Denmark: Technical University of Denmark; 1997.

22. Pitzer KS. Thermodynamics of Electrolytes I. Theoretical Basis and General Equations. *J Phys Chem.* 1973;77:268-277.

23. Thomsen K, ed. *Mixture with Electrolytes*. Copenhagen, Denmark: Technical University of Denmark, IVC-SEP Ph. D. Summer School; 2003.

24. Bromley LA. Thermodynamic Properites of Strong Electrolytes in Aqueous Solutions. *AIChE Journal*. 1973;19:313-320.

25. Abbas Z, Gunnarsson M, Ahlberg E, Nordholm S. Corrected Debye-Hückel Theory of Salt Solutions: Size Asymmetry and Effective Diameters. *J Phys Chem B*. 2002;106:1403-1420.

26. Harvey A, Copeman TW, Prausnitz JM. Explicit approximations to the mean spherical approximation for electrolyte systems with unequal ion sizes. *J Phys Chem.*1988;92:6432–6436.

27. Planche H, Renon H. Mean Spherical Approximation applied to a simple but non-primitive model of interaction for electrolyte solutions and polar substances. *J Phys Chem*. 1981;5:3924-3929.

28. Fürst W, Renon H. Representation of Excess Properties of Electrolyte Solutions Using a New Equation of State. *AIChE J*. 1993; 39: 335-343.

29. Sanchez-Castro C, Blum L. Explicit approximation for the unrestricted mean spherical approximation for ionic solutions. *J Phys Chem.* 1989; 93(21): 7478-7482.

30. Percus JK, Yevick GJ. Hard-Core Insertion in the Many-Body Problem. *Phys Rev.* 1964; 136(1B): 290-296.

31. Chen CC, Britt HI, Boston JF, Evans LB. Local. Composition Model for Excess Gibbs Energy of Electrolyte Systems. *AIChE J.* 1982; 28: 588-596.

32. Chen CC, Evans LB. A Local Composition Model for the Excess Gibbs Energy of Aqueous Electrolyte Systems. *AIChE J.* 1986; 32: 444-454.

33. Sander B, Fredenslund A, Rasmussen P. Calculation of Vapour-Liquid Equilibria in Mixed Solvent/Salt Systems Using an Extended UNIQUAC Equation. *Chem Eng Science.* 1986;41:1171-1183.

34. Thomsen K, Rasmussen P. Modeling of Vapour-liquid-solid equilibrium in gas-aqueous electrolyte systems. *Chem Eng Science.* 1999;54:1787-1802.

35. Iliuta M, Thomsen K, Rasmussen P. Extended UNIQUAC model for correlation and prediction of vapour-liquid-solid equilibrium in aqueous salt systems containing non-electrolytes. Part A. Methanol – Water – Salt systems. *Chem Eng Science.* 2000;55:2673-2686.

36. Haghtalab A, Vera JH. A nonrandom factor model for the excess Gibbs energy of electrolyte solutions. *AIChE J*. 1988; 34(5): 803-813.

37. Haghtalab A, Vera JH. Nonrandom factor model for electrolyte solutions. *AIChE J*. 1991; 37(1): 147-149.

38. Liu Y, Harvey AH, Prausnitz JM. Thermodynamics of concentrated electrolyte solutions. *Chem. Eng. Commun.* 1989; (77): 43-66.

39. Wu J, Prausnitz JM. Phase Equilibirum for systems Containing Hydrocarbons, Water and Salt: An Extended Peng-Robinson Equation of State. *Ind Eng Chem Res.* 1998; 37: 1634-1643.

40. Myers JA, Sandler SI, Wood RH. An Equation of State for Electrolyte Solutions Covering Wide Range of Temperature, Pressure and Composition. *Ind Eng Chem Res.* 2002; 41: 3282-3297.

41. Born M. Volumen und Hydratationswärme der Ionen. Zeitschrift für Physik. 1920; 1: 45-49.

42. Sanchez-Castro C, Blum L. Explicit approxiamtion for the unrestricted mean spherical approximation for ionic solutions. *J Phys Chem.*1989; 93: 7478-7482.

43. Uematsu M, Franck EU. Static dielectric constant of water and steam. *J Phys Chem Ref Data.* 1980; 9(4):1291-1305.

44. Jin G, Donohue MD. An equation of state for electrolyte solutions. 1. Aqueous systems containing strong electrolytes. *Ind Eng Chem Res.* 1988; 27: 1073-1084.

45. Jin G, Donohue MD. An equation of state for electrolyte solutions. 2. Single volatile weak electrolytes in water. *Ind Eng Chem Res.* 1988; 27: 1737-1743.

46. Jin G, Donohue MD. An equation of State for Electrolyte Solutions. 3. Aqueous Solutions Containing Multiple Salts. *Ind Eng Chem Res.* 1991; 30: 240-248.

47. Economou IG. Statistical Associating Fluid Theory: A Successful Model for the Calculation of Thermodynamic and Phase Equilibrium Properties of Complex Fluid Mixtures. *Ind Eng Chem Res.* 2002; 41(5): 953-962.

48. Wertheim MS. Fluids with Highly Directional Attractive Forces. I. Statistical Thermodynamics. *J Stat Phys.* 1984; 35: 19-34.

49. Wertheim MS. Fluids with Highly Directional Attractive Forces. II. Thermodynamic Perturbation Theory and Integral Equations. *J Stat Phys.* 1984; 35:35-47.

50. Green DG, Jackson G. Theory of Phase Equilibria for Model Aqueous Solutions of Chain Molecules: Water + Alkane Mixtures. *J Chem Soc*, *Faraday Trans.* 1992; 88:1395-1409.

51. Garcia-Lisbona MN, Galindo A, Jackson G, Burgess AN. An examination of the cloud curves of liquid-liquid immiscibility in aqueous solutions of alkyl polyoxyethylene surfactants using the SAFT-HS approach with transferable parameters. *J Am Chem Soc.* 1998;120: 4191-4199.

52. Fu YH, Sandler SI. A simplified SAFT equation of state for associating compounds and mixtures. *Ind Eng Chem Res.* 1995;34:1897-1909.

53. Kraska T, Gubbins KE. Phase equilibria calculations with a modified SAFT equation of state. 1. Pure alkanes, alkanols, and water. *Ind Eng Chem Res.* 1996;35:4727-4737.

54. Kraska T, Gubbins KE. Phase equilibria calculations with a modified SAFT equation of state. 2. Binary mixtures of *n*-alkanes, 1-alkanols, and water. *Ind Eng Chem Res.* 1996;35:4738-4746.

55. Gil-Villegas A, Galindo A, Whitehead PJ, Mills SJ, Jackson G, Burgess AN. Statistical associating fluid theory for chain molecules with attractive potentials of variable range. *J Chem Phys.* 1997;106:4168-4186.

56. McCabe C, Gil-Villegas A, Jackson G, Del Rı´o F. The thermodynamics of heteronuclear molecules formed from bonded square-well (BSW) segments using the SAFT-VR approach. *Mol Phys.* 1999; 97(4): 551-558.

57. Adidharma H, Radosz M. Prototype of an engineering equation of state for heterosegmented polymers. *Ind Eng Chem Res.* 1998;37:4453-4462.

58. Adidharma H, Radosz M. A study of square-well statistical associating fluid theory approximations. *Fluid Phase Equilib.* 1999; 161(1): 1-20.

59. Gross J, Sadowski G. Perturbed-Chain SAFT: an equation of state based on a perturbation theory for chain molecules. *Ind Eng Chem Res.* 2001;40:1244-1260.

60. Galindo A, Gil-Villegas A, Jackson G, Burgess AN. SAFT-VRE: phase behaviour of electrolyte solutions with the statistical associating fluid theory for potentials of variable range. *J Phys Chem B.* 1999; 103: 10272-10281.

61 . Cameretti LF, Sadowski G, Mollerup JM. Modeling of aqueous electrolyte solutions with perturbed-chain statistical associated fluid theory. *Ind Eng Chem Res.* 2005;44 (9): 3355-3362

62. Liu Z, Wang W, Li Y. An equation of state for electrolyte solutions by a combination of low-density expansion of nonprimitive mean spherical approximation and statistical associating fluid theory. *Fluid Phase Equilib.* 2005; 227: 147-156.

CHAPTER 2 Thermodynamics and electrolyte EOS

2.1 *Thermodynamics of electrolyte solution*

2.1.1 Activity coefficient

When conducting phase equilibrium calculation for electrolyte systems, a chemical potential is usually needed.

$$\mu_i(T,P,\mathbf{n}) = \mu_i^{\,0}(T,P) + RT\ln a_i(T,P,\mathbf{n}) \tag{2.1}$$

The activity is defined from fugacity in thermodynamic. The ratio of the fugacity of species *i* in a mixture over the corresponding pure component fugacity at the same temperature and pressure defines the activity.

$$a_i(T,P,\mathbf{n}) = \frac{\hat{f}_i(T,P,\mathbf{n})}{f_i(T,P)} \tag{2.2}$$

To account for the non-ideality, an activity coefficient is introduced. The activity coefficient of species *i* is defined as the activity divided by the mole fraction of species *i* in a non-ideal solution. This is the mole-fraction-based activity coefficient. It is also described as the symmetric activity coefficient. It can be calculated as the ratio of the fugacity coefficient of the compound *i* in the solution to the fugacity coefficient of the pure compound *i*.

$$\gamma_i(T,P,\mathbf{n}) \triangleq \frac{a_i(T,P,\mathbf{n})}{x_i} = \frac{\hat{f}_i(T,P,\mathbf{n})}{x_i f_i(T,P)} = \frac{\hat{\varphi}_i(T,P,\mathbf{n})}{\varphi_i(T,P)} \tag{2.3}$$

The symmetric mole-fraction-based activity coefficient of a solvent species in an electrolyte solution can also be calculated using equation (2.3).

$$\gamma_i(T,P,\mathbf{n}) = \frac{\hat{\varphi}_i(T,P,\mathbf{n})}{\hat{\varphi}_i(T,P)} \tag{2.4}$$

The unsymmetric mole-fraction-based activity coefficient of a solute species (ion) in an electrolyte solution is defined as the ratio of the activity coefficient of the ionic compound *i* in the solution to the infinite dilution activity coefficient of the ionic compound *i*:

$$\gamma_i^*(T,P,\mathbf{n}) = \frac{\gamma_i(T,P,\mathbf{n})}{\gamma_i(T,P,\mathbf{n}_0)}, \quad i = ion \tag{2.5}$$

$\mathbf{n}_0$ is a vector of the mole number of each component at infinite dilution. The infinite dilution activity coefficient of the ionic compound *i* is:

$$\gamma_i(T,P,\mathbf{n}_0) = \lim_{n_i \to 0} \gamma_i(T,P,\mathbf{n}), \quad i = \text{ion} \tag{2.6}$$

The unsymmetric mole-fraction-based activity coefficient of a solute species tends towards unity at infinite dilution in the pure solvent. The expression for the unsymmetric activity coefficient calculated from the fugacity coefficients is:

$$\gamma_i^*(T,P,\mathbf{n}) = \frac{\hat{\varphi}_i(T,P,\mathbf{n})}{\hat{\varphi}_i(T,P,\mathbf{n}_0)}, \quad i = ion \tag{2.7}$$

$\hat{\varphi}_i(T,P,\mathbf{n}_0)$ is the infinite dilution fugacity coefficient for solute species.

$$\hat{\varphi}_i(T,P,\mathbf{n}_0)=\lim_{n_i\to 0}\hat{\varphi}_i(T,P,\mathbf{n}),\quad i=\text{solute spieces} \tag{2.8}$$

In order to compare the calculated values with experimental data presented in literature, it is necessary to convert the mole-fraction-based activity coefficient to molality-based activity coefficient. The molality-based activity coefficient of component *i* is calculated as

$$\gamma_i^m(T,P,\mathbf{n})=\left(\sum_{solvent}x_{solvent}\right)\gamma_i^*(T,P,\mathbf{n}) \tag{2.9}$$

Experimental data of activity coefficient are usually presented in the form of molality-based mean activity coefficients in literature. The molality-based mean activity coefficient for a certain dissolved salt is defined as:

$$\gamma_{\pm}^m=\left[\left(\gamma_c^m\right)^{\nu_c}\left(\gamma_a^m\right)^{\nu_a}\right]^{1/\nu} \tag{2.10}$$

where and ν_c and ν_a are the stoichiometric coefficients of cations and anions in the salt. The subscripts *c* and *a* denote cation and anion. The superscript *m* stands for the molality. If a salt is composed by cation A^{m+} and anion B^{n-}, it can fully dissociate into:

$$A_{\nu_c}B_{\nu_a}=\nu_c A^{m+}+\nu_a B^{n-} \tag{2.11}$$

and $\nu=\nu_c+\nu_a$.

2.1.2 Osmotic coefficient

The water activity is an important property of electrolyte solutions. Usually the water activity is expressed as an osmotic coefficient. The osmotic coefficient is defined as follows:

$$\Phi=-\frac{n_{solvent}\ln a_{solvent}}{\nu n_{solute}} \tag{2.12}$$

$n_{solvent}$ is the mole number of the solvent.

2.1.3 Apparent molar volume

Volumetric properties are also important properties of electrolyte solutions. For electrolyte solutions, the apparent molar volume (abbreviated as AMV) of the salt is often measured directly. The apparent molar volume V_Φ of a salt is defined through the following equation

$$nv=n_{solvent}v^0_{solvent}+n_{solute}V_\phi \tag{2.13}$$

where *v* and v^0 are the molar volume of the solution and the molar volume of the pure solvent respectively.

The AMV of a salt is more sensitive to model accuracy than density. Very small deviations in the calculated density against experimental data can lead to a large deviation in the predicted AMV values. Therefore it is more difficult to fit AMV than

density. In other words, using experimental data of AMV in parameter fitting can improve the goodness of fit of density data.

2.1.4 Solubility index

The saturation index of salt can be used for evaluating the accuracy of SLE calculations. It is defined as the activity product of the salt *k* divided by its solubility product.

$$SI_k = \frac{\prod_i a_i^{v_i}}{K_k}, \text{ where } a_i = x_i \gamma_i \tag{2.14}$$

2.2 *Michelsen-Mollerup framework*

2.2.1 General algorithm

Equations of state are often constructed in terms of the Helmholtz free energy. Helmholtz free energy is a function taking system temperature, volume and composition as its natural independent variables. Experimental data of thermodynamic properties are usually measured and reported as functions of system temperature, pressure and composition. All thermodynamic properties of a system can be derived from Helmholtz free energy by standard differentiation with respect to its independent variables. The relationship of different thermodynamic properties and the derivatives of Helmholtz free energy is summarized in the below Michelsen-Mollerup framework[1]. The Michelsen-Mollerup framework[1] is rather convenient to use in engineering applications.

Computation of the thermodynamic properties from Helmholtz free energy EOS is accomplished by first calculating the volume V^* of a single liquid phase in the system from the pressure equation at given temperature, pressure and composition (T, P^*, **n**), as that of experimental data. The pressure equation is given by

$$P^* = f(T, V^*, \mathbf{n}) = -\left(\frac{\partial A(T,V,\mathbf{n})}{\partial V}\right)_{T,\mathbf{n}}\Bigg|_{V=V^*} \tag{2.15}$$

Any equation root-finding algorithm (root solver routine) such as bisection method or Newton-Raphson method can do the job. Secondly substitute the volume V^* into different derivatives of Helmholtz free energy to calculate other thermodynamic properties. Such as the fugacity coefficient of a component in a mixture is calculated through the expression in terms of temperature, volume and composition.

$$\hat{\varphi}_i(T, P^*, \mathbf{n}) = \frac{nRT}{PV} \exp\left(\frac{\partial A^r(T,V,\mathbf{n})}{RT\partial n_i}\right)_{T,V,n_{j\neq i}}\Bigg|_{V=V^*} \tag{2.16}$$

The chemical potential of component *i* in mixture is

$$\mu_i(T,P^*,\mathbf{n}) = \mu_i(T,V^*,\mathbf{n}) = -\left(\frac{\partial A(T,V,\mathbf{n})}{\partial n_i}\right)_{T,V,\mathbf{n}/n_i}\Bigg|_{V=V^*} \tag{2.17}$$

.

Other thermodynamic properties can be calculated this way. The relevant analytic expressions are given in the next section. The algorithm is presented below. Vector and matrix variables are expressed in bold font in the algorithm. The algorithm is written in the Matlab format.

Algorithm 2.1

Function [**fug_coef**, **fug_coef_derivatives**, **thermo_properties**]=EOS(T, P^*, **n**, **parameters**)
Call function [**parameters0**]=EOS_parameter_intialization(T, P^*, **n**, **parameters**)

Call function [V^*]=volume_solver(T, P^*, **n**, **parameters0**)

Call function
[**fug_coef**, **fug_coef_derivatives**, **thermo_properties**] = fugacity_calculator(T, V^*,P^*, **n**, **parameters0**)

End function EOS

Function [V^*]=volume_solver(T, P^*, **n**, **parameters**)

function='Pressure_equation'
set starting value V_0

Call [V^*, **output_information**]=Newton_Raphson(function, V_0, [T, P^*, **n**, **parameters**], **inputsetting**)

End function volume_solver

Function [*f*, *dfdV*]= Pressure_equation (T, V, P*, **n**, **parameters**)

$$f = P^* - \left(\frac{\partial A(T,V,\mathbf{n})}{\partial V}\right)_{T,\mathbf{n}}$$

$$dfdV = -\left(\frac{\partial^2 A(T,V,\mathbf{n})}{\partial V^2}\right)_{T,\mathbf{n}}$$

End function Pressure_equation

2.2.2 Calculation of thermodynamic properties from derivatives of Helmholtz free energy

$A^r(T,V,\mathbf{n})$ is the residual Helmholtz free energy defined as the difference between the total Helmholtz free energy and the ideal gas Helmholtz free energy. Residual Helmholtz free energy by definition is calculated by integration:

$$A^r(T,V,\mathbf{n}) = -\int_{\infty}^{V}(P - \frac{nRT}{V})dV \tag{2.18}$$

Pressure equation can be derived from residual Helmholtz free energy through differentiation:

$$P = P(T,V,\mathbf{n}) = -\left(\frac{\partial A^r}{\partial V}\right)_{T,\mathbf{n}} + \frac{nRT}{V} \tag{2.19}$$

The fugacity coefficient of each component in a mixture is an important quantity for phase equilibrium calculation. Fugacity coefficient can be derived from residual Helmholtz free energy by partial molar differentiation:

$$RT\ln\hat{\varphi}_i = \left(\frac{\partial A^r}{\partial n_i}\right)_{T,V,\mathbf{n}/n_i} - RT\ln Z = -\left(\frac{\partial}{\partial n_i}\left(\int_\infty^V (P - \frac{nRT}{V})dV\right)\right)_{T,V,\mathbf{n}/n_i} - RT\ln Z \tag{2.20}$$

Reduced residual Helmholtz free energy (dimensionless) is defined as

$$F = \frac{A^r(T,V,\mathbf{n})}{RT} \tag{2.21}$$

Pressure equation and the derivatives of pressure in terms of residual Helmholtz free energy[1] can be expressed in the below equation (2.22) to (2.24):

$$P = P(T,V,\mathbf{n}) = -RT\left(\frac{\partial F}{\partial V}\right)_{T,\mathbf{n}} + \frac{nRT}{V}, \qquad Z = \frac{PV}{nRT} \tag{2.22}$$

$$\left(\frac{\partial P}{\partial V}\right)_{T,\mathbf{n}} = -RT\left(\frac{\partial^2 F}{\partial V^2}\right)_{T,\mathbf{n}} - \frac{nRT}{V^2} \tag{2.23}$$

$$\left(\frac{\partial P}{\partial T}\right)_{V,\mathbf{n}} = -RT\left(\frac{\partial^2 F}{\partial T\partial V}\right)_{V,\mathbf{n}} + \frac{P}{T} \qquad \left(\frac{\partial P}{\partial n_i}\right)_{T,V,\mathbf{n}/n_i} = -RT\left(\frac{\partial^2 F}{\partial n_i\partial V}\right)_{T,V,\mathbf{n}/n_i} + \frac{RT}{V} \tag{2.24}$$

Fugacity coefficient and the derivatives of fugacity coefficient in terms of reduced residual Helmholtz free energy can be expressed in the below equation (2.25) to (2.28)

$$\ln\hat{\varphi}_i = \left(\frac{\partial F}{\partial n_i}\right)_{T,V,\mathbf{n}/n_i} - \ln Z, \tag{2.25}$$

$$\left(\frac{\partial \ln\hat{\varphi}_i}{\partial n_i}\right)_{T,P,\mathbf{n}/n_i} = -RT\left(\frac{\partial^2 F}{\partial n_j\partial n_i}\right)_{T,V,\mathbf{n}/n_i} + \frac{1}{n} - \frac{\bar{V}_i}{RT}\left(\frac{\partial P}{\partial n_j}\right)_{T,V,\mathbf{n}/n_i} \tag{2.26}$$

$$\left(\frac{\partial \ln\hat{\varphi}_i}{\partial T}\right)_{P,\mathbf{n}} = -RT\left(\frac{\partial^2 F}{\partial T\partial n_i}\right)_{V,\mathbf{n}} + \frac{1}{T} - \frac{\bar{V}_i}{RT}\left(\frac{\partial P}{\partial T}\right)_{V,\mathbf{n}} \tag{2.27}$$

$$\bar{V}_i = \left(\frac{\partial V}{\partial n_i}\right)_{P,T,\mathbf{n}/n_i} = -\left(\frac{\partial P}{\partial n_i}\right)_{V,T,\mathbf{n}/n_i} \Big/ \left(\frac{\partial P}{\partial V}\right)_{T,\mathbf{n}} \qquad \left(\frac{\partial \ln\varphi_i}{\partial P}\right)_{T,\mathbf{n}} = \frac{\bar{V}_i}{RT} - \frac{1}{P} \tag{2.28}$$

With above equations (2.21) to (2.28) we can obtain majority of the thermodynamic properties needed in this project once Helmholtz free energy is analytically expressed.

2.3 *Cubic equation of state*

2.3.1 General cubic EOS

The general form for cubic EOS can be written in the following way.

$$P = \frac{RT}{v - b_1} - \frac{a(T)}{(v + b_2)(v + b_3)} \tag{2.29}$$

The different values for coefficient b_1, b_2 and b_3 will result in different cubic EOS. For the most commonly seen cubic EOS such as SRK and PR can be obtained by setting the b_i coefficient.

If $b_1 = b_2 = b$ and $b_3 = 0$, we obtained the SRK EOS:

$$P = \frac{RT}{v-b} - \frac{a(T)}{v(v+b)} \tag{2.30}$$

If $b_1 = b, b_2 = (1+\sqrt{2})b, b_3 = (1-\sqrt{2})b$, then we got the PR EOS:

$$P = \frac{RT}{v-b} - \frac{a(T)}{v(v+b)+b(v-b)} \Rightarrow P = \frac{RT}{v-b} - \frac{a(T)}{v^2+2bv-b^2} \tag{2.31}$$

The coefficients $a(T)$, b in SRK and PR EOS are calculated in the following way:

$$a(T) = \frac{\Omega_a T_c^2 R^2 \alpha(T)}{P_c}, \quad b = \frac{\Omega_b T_c R}{P_c} \tag{2.32}$$

Their units in IS are J m^3 and m^3 respectively.

The constant in equation (2.32) Ω_a and Ω_b can be calculated as follows:

$$\Omega_a = \frac{1+\sqrt[3]{2}+\sqrt[3]{4}}{9} \approx 0.42748, \qquad \Omega_b = \frac{\sqrt[3]{2}-1}{3} \approx 0.08664 \tag{2.33}$$

For the sake of computation simplification, it is more advantageous to have dimensionless variables other than to have variables with units (dimensions) in the computation. The above generalized form of the cubic EOS (2.29) can be transformed into the dimensionless form by introducing the compressibility $Z = \frac{Pv}{RT}$ into the EOS.

$$\begin{aligned} P &= \frac{RT}{v-b_1}\frac{P/RT}{P/RT} - \frac{a(T)}{(v+b_2)(v+b_3)}\frac{P^2/R^2T^2}{P^2/R^2T^2} \\ &= \frac{P}{vP/RT - b_1P/RT} - \frac{P(a(T)P/R^2T^2)}{(vP/RT + b_2P/RT)(vP/RT + b_3P/RT)} \\ &= \frac{P}{Z - b_1P/RT} - \frac{P(a(T)P/R^2T^2)}{(Z + b_2P/RT)(Z + b_3P/RT)} \end{aligned} \tag{2.34}$$

Signify the dimensionless coefficients

$$A(T) \triangleq \frac{a(T)P}{R^2T^2} \tag{2.35}$$

and

$$B_i \triangleq \frac{b_iP}{RT}, \quad i = 1,2,3 \tag{2.36}$$

and substitute them into the above equations(2.34), we have:

$$P = \frac{P}{Z-B_1} - \frac{PA(T)}{(Z+B_2)(Z+B_3)} \Rightarrow 1 = \frac{1}{Z-B_1} - \frac{A(T)}{(Z+B_2)(Z+B_3)} \tag{2.37}$$

If $(Z-B_1)(Z+B_2)(Z+B_3) \neq 0$, then we have:

$$(Z+B_2)(Z+B_3)(Z-B_1) - (Z+B_2)(Z+B_3) + A(T)(Z-B_1) = 0 \tag{2.38}$$

Rewrite it in the descent order of Z, we obtained:

$$Z^3 + \left[B_2 + B_3 - (B_1+1)\right]Z^2 + \left[B_2B_3 - (B_2+B_3)(B_1+1) + A(T)\right]Z - \left[(B_1+1)B_2B_3 + A(T)B_1\right] = 0 \tag{2.39}$$

If all the coefficients in the above third order one variable equation (2.39) are determined, solving Z from the above cubic equation and from Z we can calculate P or V if the other one variable is fixed.

2.3.2 The residual Helmholtz free energy A^r of the cubic EOS

The residual Helmholtz free energy can be calculated through the general equation(2.18).

Substitute the generalized cubic EOS into (2.18) and we obtained:

$$\begin{aligned} A^r(T,V,\mathbf{n}) &= -n\int_{\infty}^{v}\left(\frac{RT}{v-b_1}-\frac{a(T)}{(v+b_2)(v+b_3)}-\frac{RT}{v}\right)d\frac{V}{n} \\ &= -n\left(RT\ln(v-b_1)-RT\ln v-\frac{a(T)}{b_3-b_2}\ln\frac{(v+b_2)}{(v+b_3)}\right)\Bigg|_{\infty}^{v} \\ &= -n\left(RT\ln\frac{(v-b_1)}{v}-\frac{a(T)}{b_3-b_2}\ln\frac{(v+b_2)}{(v+b_3)}-0\right) \end{aligned} \tag{2.40}$$

If the total volume V instead of the molar volume v is used in the deduction, we still obtained a similar expression as in (2.40).

$$\begin{aligned} A^r(T,V,\mathbf{n}) &= -\int_{\infty}^{V}\left(\frac{nRT}{V-nb_1}-\frac{a(T)n^2}{(V+nb_2)(V+nb_3)}-\frac{nRT}{V}\right)dV \\ &= -n\left(RT\ln\frac{(V-nb_1)}{V}-\frac{a(T)}{b_3-b_2}\ln\frac{(V+nb_2)}{(V+nb_3)}\right) \end{aligned} \tag{2.41}$$

From the above expression for the residual Helmholtz free energy, the fugacity needed in the phase equilibrium calculation can be calculated easily from the residual Helmholtz free energy. It is often advantageous to do the following substitution for the coefficients $a(T)$ and b_i:

$$\tilde{A}=n^2a,\ \ \tilde{B}_1=nb_1,\ \ \tilde{B}_2=nb_2,\ \ \tilde{B}_3=nb_3 \tag{2.42}$$

.

Mathematically it is simpler to calculate the molar derivatives of the above $\tilde{A}$ and $\tilde{B}_i$ than those for $a(T)$ and b_i . If the conventional quadratic and linear mixing rules are used in the model for mixtures we have

$$\tilde{A}=n^2a=\sum_i\sum_j n_in_ja_{ij},\ \ \tilde{B}_k=nb_k=\sum_i n_ib_{i,k},\ \ k=1,2,3. \tag{2.43}$$

Substitute (2.42) into(2.41), then get:

$$A^r(T,V,n)=-n\left(RT\ln\frac{(V-\tilde{B}_1)}{V}-\frac{\tilde{A}(T)}{\tilde{B}_3-\tilde{B}_2}\ln\frac{(V+\tilde{B}_2)}{(V+\tilde{B}_3)}\right) \tag{2.44}$$

2.3.3 General cubic equation of state with volume translation parameter

A volume translation parameter can be introduced into the EOS to archive improvement of the correlation of density without changing too much of the original EOS. The general form for cubic EOS with volume translation parameter c can be written in the following way.

$$P = \frac{RT}{v - b_1 + c} - \frac{a(T)}{(v + b_2 + c)(v + b_3 + c)} \tag{2.45}$$

As in previous section, if $b_1 = b_2 = b$ and $b_3 = 0$, we obtained the SRK EOS with volume translation parameter.

If $b_1 = b, b_2 = (1+\sqrt{2})b, b_3 = (1-\sqrt{2})b$, then we obtained the PR EOS with volume translation parameter:

$$P = \frac{RT}{v - b + c} - \frac{a(T)}{(v + c)(v + b + c) + b(v - b + c)} \Rightarrow P = \frac{RT}{v - b + c} - \frac{a(T)}{(v + c)^2 + 2b(v + c) - b^2} \tag{2.46}$$

This is the PR EOS with volume translation parameter used by Myers *et al.* in their electrolyte EOS. The coefficients $a(T)$, b in SRK and PR EOS are calculated in the same way as in (2.32).

The above generalized form of the cubic EOS (2.45) can be transformed into the dimensionless form in the same way as in previous section by introducing the compressibility $Z = \frac{Pv}{RT}$ into the EOS. Denote the dimensionless coefficients

$$A(T) \triangleq \frac{a(T)P}{R^2T^2} \tag{2.47}$$

and

$$B_i \triangleq \frac{b_i P}{RT}, \quad i = 1, 2, 3 \tag{2.48}$$

and

$$C \triangleq \frac{cP}{RT} \tag{2.49}$$

we have the dimensionless form of the general cubic EOS with volume translation parameter:

$$1 = \frac{1}{Z - B_1 + C} - \frac{A(T)}{(Z + B_2 + C)(Z + B_3 + C)} \tag{2.50}$$

If $(Z - B_1 + C)(Z + B_2 + C)(Z + B_3 + C) \neq 0$, then we have:

$$(Z + B_2 + C)(Z + B_3 + C)(Z - B_1 + C) - (Z + B_2 + C)(Z + B_3 + C) + A(T)(Z - B_1 + C) = 0 \tag{2.51}$$

Rewrite it in the descent order of Z, we obtained:

$$(Z + C)^3 + \left[B_2 + B_3 - (B_1 + 1)\right](Z + C)^2 + \left[B_2B_3 - (B_2 + B_3)(B_1 + 1) + A(T)\right](Z + C) - \left[(B_1 + 1)B_2B_3 + A(T)B_1\right] = 0 \tag{2.52}$$

We can solve Z from the above cubic equation.

2.3.4 The residual Helmholtz free energy A^r of the cubic EOS with volume translation parameter

The residual Helmholtz free energy can be calculated through equation (2.18):

$$A^r(T,V,\mathbf{n}) = -\int_{\infty}^{V}\left(\frac{nRT}{V-nb_1+nc} - \frac{a(T)n^2}{(V+nb_2+nc)(V+nb_3+nc)} - \frac{nRT}{V}\right)dV$$
$$= -n\left(RT\ln\frac{(V-nb_1+nc)}{V} - \frac{a(T)}{b_3-b_2}\ln\frac{(V+nb_2+nc)}{(V+nb_3+nc)}\right)\Bigg|_{\infty}^{V} \quad (2.53)$$
$$= -n\left(RT\ln\frac{(V-nb_1+nc)}{V} - \frac{a(T)}{b_3-b_2}\ln\frac{(V+nb_2+nc)}{(V+nb_3+nc)}\right)$$

The above residual Helmholtz free energy can be used to construct the electrolyte EOS by adding other contribution terms in terms of Helmholtz free energy. It is mathematically advantageous to do the following substitution for the coefficients *a(T)* and b_i. It is simpler to calculate the molar derivatives.

$$\tilde{A} = n^2 a,\ \ \tilde{\mathrm{B}}_1 = \mathrm{n}b_1,\ \ \tilde{\mathrm{B}}_2 = \mathrm{n}b_2,\ \ \tilde{\mathrm{B}}_3 = \mathrm{n}b_3,\ \tilde{C} = n\mathrm{c} \quad (2.54)$$

.

If the conventional quadratic and linear mixing rules are used in the model we have for mixtures

$$\tilde{A} = n^2 a = \sum_i\sum_j n_i n_j a_{ij},\ \ \tilde{\mathrm{B}}_{\mathrm{k}} = nb_k = \sum_i n_i b_{i,k},\ \ k = 1,2,3,\ \tilde{C} = nc = \sum_i n_i c_i \quad (2.55)$$

Substitute (2.54) into (2.53), then we get:

$$A^r(T,V,\mathbf{n}) = -n\left(RT\ln\frac{(V-\tilde{B}_1+\tilde{C})}{V} - \frac{\tilde{A}(T)}{\tilde{B}_3-\tilde{B}_2}\ln\frac{(V+\tilde{B}_2+\tilde{C})}{(V+\tilde{B}_3+\tilde{C})}\right) \quad (2.56)$$

2.4 *The CPA EOS*

2.4.1 Introduction

The water molecule and many other substances of importance to industrial applications such as alcohols, amines, acids and phenols form hydrogen bonds. The strong attractive interactions of hydrogen bonding between molecules result in molecular cluster formation. In mixtures, hydrogen-bonding interactions may occur between molecules of the same species (self-association) or between molecules of different species (cross-association) [2] . These interactions strongly affect the thermodynamic properties of the fluids, and species forming hydrogen bonds often exhibit unusual thermodynamic behaviour. E.g. in terms of the association, water would be a gas rather than a liquid at room temperature and atmospheric pressure.[3]

EOSs have traditionally been applied to model systems with non-polar and slightly polar compounds. For systems with associating compounds, conventional models like cubic EOS (SRK and PR) are often insufficient, especially for multi-component and multiphase equilibria.[4,5] The cubic EOS, such as the SRK and the PR equations, can describe quantitatively the phase behaviour of aqueous systems using the one fluid van der Waals mixing rules with different interaction parameters for each phase. For the water-rich phase the interaction parameters must be temperature-dependent, since the strong local composition effects caused by hydrogen-bonding interactions are not accounted for explicitly by the conventional van der Waals one-fluid mixing rules.[3]

A variety of models, described as “association models”, have been suggested in literature to account for the effects of association in solutions. In these models, we can

recognize two contribution terms with the following general form in terms of the Helmholtz free energy:

$$A^r(T,V,\mathbf{n}) = \Delta A^{phys} + \Delta A^{assoc} \tag{2.57}$$

A physical term (*phys*) accounts for the deviation due to physical forces and an association term (*assoc*) accounts for the effect of association. The physical term can be either a non-cubic or a cubic EOS. Peschel and Wenzel (1984) showed that whatever expression is used for the physical part (a cubic or a non-cubic EOS) the resulting models yield similar results for non-electrolytes.[2] Thus, the crucial part in describing non-electrolyte associating compounds with an EOS is the association term. Several investigations have confirmed this conclusion.[2]

The Cubic Plus Association (CPA) equation is a thermodynamic model, which combines the well-known cubic SRK EOS and the association term from statistical mechanics suggested by Wertheim, typically applied in models like SAFT. CPA uses a simplified expression for the association strength, which contributes significantly to the computational efficiency of the EOS. For non-polar (non self-associating) compounds CPA reduces to SRK. CPA has been shown in the past to be a successful model for phase equilibria calculations for binary or ternary systems containing water, hydrocarbons and alcohols, glycols.[2-6] Recently its application has been extended to binary and multi-component systems containing aromatic hydrocarbons and glycols, polymers.[4,5,7,8] CPA EOS is under continuous development. It is of our interest to extend the CPA equation to electrolyte systems. Wu and Prausnitz's[9] EOS is an example of electrolyte CPA based on PR EOS. It is interesting to try a SRK based CPA EOS. The association term has a great potential in describing the cross association between the polar non-electrolyte compound in mix-solvent electrolyte systems and it might also help to describe the association between ion-ion and ion-solvent later.

The CPA EOS for pure compounds has the following general form expressed in the Helmholtz free energy:

$$A^r(T,V,\mathbf{n}) = \Delta A^{SRK}(T,V,\mathbf{n}) + \Delta A^{assoc}(T,V,\mathbf{n}) \tag{2.58}$$

$$\frac{\Delta A^{SRK}(T,V,\mathbf{n})}{RT} = \frac{an}{RTb}\ln\left(\frac{V}{V+b}\right) + n\ln\left(\frac{V}{V-b}\right),$$

$$\frac{\Delta A^{assoc}(T,V,\mathbf{n})}{RT} = \sum_i n_i \sum_{A_i} (\ln X_{A_i} + \frac{1-X_{A_i}}{2}), \tag{2.59}$$

ρ is the molar density of the mixture.

x_i is the superficial (apparent) mole fraction of the component i in the mixture.

The classic van der Waals one-fluid mixing rules are typically used for estimating the physical term parameters of EOS for mixtures (a_m, b_m):

$$a_m = \sum_i \sum_j x_i x_j a_{ij}; \qquad b_m = \sum_i x_i b_i \tag{2.60}$$

where the cross energy parameters are estimated by combining rules:

$$a_{ij} = \sqrt{a_i a_j}(1-k_{ij}); \tag{2.61}$$

where $a_i = a_{0i}\left(1 + c_{1i}\left(1-\sqrt{T_r}\right)\right)$, and a_{0i} and c_{1i} are fitting parameters of pure component i . k_{ij} is often the only adjustable interaction parameter of the CPA EOS for a binary mixture.

Mixing rules are often used to improve the goodness-of-fit of the difficult electrolyte systems in the literature and in all of the four previously mentioned electrolyte EOSs, it has been adopted to describe the ion-ion, ion-water and water-hydrocarbons

interactions. However, a bit different than the non-electrolyte multi-component systems, it is not used after the pure component parameters have been fitted: For electrolyte systems, the interaction parameters for ions are often used as an additional degree of freedom in the data fitting: It is often optimized simultaneously with the energy parameter *a* for salts. It will also be used in our electrolyte CPA EOS and the modified MSW EOS in the later section if the system is difficult to fit without interaction parameters.

X_{A_i} is the mole fraction of the molecule *i* not bonded at site A, also known as the monomer mole fraction and is defined as:

$$X_{A_i} = \left(1 + \rho \sum_j \sum_{B_j} x_j X_{B_j} \Delta^{A_i B_j} \right)^{-1} \tag{2.62}$$

and X_{A_i} is calculated by solving equation (2.62) and an examples will be given in the next section.

The association strength parameter is defined as:

$$\Delta^{A_i B_j} = g(\rho) \left[\exp\left(\frac{\varepsilon^{A_i B_j}}{RT}\right) - 1 \right] b_{ij} \beta^{A_i B_j} \tag{2.63}$$

$\Delta^{A_i B_j}$ is the association strength between two association sites belonging in two different molecules, where $\varepsilon^{A_i B_j}$ and $\beta^{A_i B_j}$ are the association energy and the association volume of interaction between site A of the molecule *i* and site B of the molecule *j*, respectively. *g(ρ)* is the radial distribution function. In 1999 Kontogeorgis *et al.* suggested the following simplified hard-sphere radial distribution function and CPA using equation (2.64) is denoted as simplified CPA [6]:

$$g(\rho) = \frac{1}{1 - 1.9y}, \text{ where } y = \frac{b}{4V} \tag{2.64}$$

Combining rules are needed in the association term of CPA for cross-association systems. No combining rules are needed for the association parameters $\varepsilon^{A_i B_j}$ and $\beta^{A_i B_j}$ for the mixtures containing only one associating compound. The conventional combining rules for the association energy, $\varepsilon^{A_i B_j}$ and the association volume, $\beta^{A_i B_j}$ in the association term are either the arithmetic mean combining rule (2.65) or the geometric mean combining rule.

$$x^{A_i B_j} = \frac{x^{A_i B_i} + x^{A_j B_j}}{2}, \quad x = \varepsilon, \beta \tag{2.65}$$

$$x^{A_i B_j} = \sqrt{x^{A_i B_i} x^{A_j B_j}}, \quad x = \varepsilon, \beta \tag{2.66}$$

An alternative simpler way is the Elliott combining rule. Suresh and Elliott suggested a combining rule for the cross-association strength which is actually the property applied in mixtures:

$$\Delta_{12}^{A_i B_j} = \sqrt{\Delta_1^{A_i B_i} \Delta_2^{A_j B_j}} \tag{2.67}$$

Elliott mentioned that equation (2.67) could only be applied to mixtures of alcohols or other associating fluids where compounds have the same or similar associating behaviour or scheme. However, using the Elliott rule gives another advantage. It yields increased computational speed thus it is recommended to use if possible.

For ions, the combining rules may be used if necessary. For the sake of simplicity it is not necessary to consider combining rules and association parameters for ions at the starting stage.

2.4.2 The determination of pure compound parameters for the CPA EOS

As stated in the previous section, the total is five parameters of CPA for pure associating compounds. Three from the SRK EOS: a_0, c_1 in the energy term and the co-volume parameter b. Two parameters in the association term are the association energy, $\varepsilon^{A_iB_j}$ and the association volume, $\beta^{A_iB_j}$. The co-volume parameter b is included in both the physical and the association term, see equation (2.59) and (2.63).
The determination of CPA model's parameters is based on experimental data for pure-compound liquid densities and vapour pressure. The DIPPR database is typically used for this purpose in this case. Note that the DIPPR correlations incorporate both the experimental uncertainty and the errors of the DIPPR's equation. [4,5]

A suggested objective function to be used in the optimization of the five parameters is:

$$f = \sum_{i=1}^{N}\left(\frac{P_i^{Dippr} - P_i^{cal}}{P_i^{Dippr}}\right)^2 + \sum_{i=1}^{N}\left(\frac{\rho_i^{Dippr} - \rho_i^{cal}}{\rho_i^{Dippr}}\right)^2 \qquad (2.68)$$

.
where P^{Dippr} and P^{cal} are the experimental and the calculated vapour pressure respectively, and ρ^{Dippr} and ρ^{cal} are the experimental and calculated liquid densities, respectively.
The following step towards estimating the five parameters of CPA is to assign the association scheme. So far the two-site (2B) and the four-site (4C) association schemes have been employed frequently. Special association schemes may be assigned to special compounds. The monomer fraction X_A using the 4 site scheme is derived as an example. For the four –site association schemes (4C), where we have:

$\Delta^{AA}=\Delta^{AB}=\Delta^{BB}=\Delta^{CC}=\Delta^{CD}=\Delta^{DD}=0$;
$\Delta^{AC}=\Delta^{AD}=\Delta^{BC}=\Delta^{BD}=\Delta\neq 0$ and $X_A=X_B=X_C=X_D$.

According to equation (2.62) above, X_A the fraction of a single associating molecule non-bonded at site A can be calculated in the following way:

$$X_A = \left(1+\rho\sum_B X_B\Delta^{AB}\right)^{-1} \qquad (2.69)$$

For 4C scheme it can be obtained

$$X_A = \left(1+\rho\left(X_A\Delta^{AA} + X_B\Delta^{AB} + X_C\Delta^{AC} + X_D\Delta^{AD}\right)\right)^{-1} \qquad (2.70)$$

Combining (2.69), equation (2.70) can be simplified to:

$$X_A = \left(1+2\rho X_A\Delta\right)^{-1} \qquad \Rightarrow \qquad 2\rho\Delta X_A^{\,2} + X_A - 1 = 0 \qquad (2.71)$$

Solving the second order equation, we get $X_A = \dfrac{-1\pm\sqrt{8\rho\Delta+1}}{4\rho\Delta}$. Bear in mind that $X_A > 0$, we finally reach the following equation:

$$X_A = \frac{-1+\sqrt{8\rho\Delta+1}}{4\rho\Delta} \tag{2.72}$$

The above example is how X_{A_i} is calculated from equation (2.62) after an association scheme is determined.

Further information regarding the phase equilibrium of the tested system is needed for the selection of the best parameter set, and according to Derawi *et al*. [4,5], liquid-liquid equilibrium (LLE) data of binary systems have been used for this purpose. An alternative way of selecting the best parameter set is to consider the second Virial coefficients, however due to lack of reliable experimental data; this method has often difficulties in practical application. The use of binary LLE data could facilitate not only the selection of the physically correct parameter set but also the selection of the suitable association scheme as well, and this appeared to be highly applicable [4,5].

In this project for electrolyte, the complex systems are not considered at present and the only focus is the aqueous electrolyte solutions. Therefore there is only one non-ionic compound which is needed to fit the parameters here, i.e. water. The parameters used in this project for the pure compound water is as follows:

Table 2.1 The pure water parameters used in CPA for calculation of electrolyte solution.

Parameters for water	Optimised Values	unit
a_0	0.122735083	Pa m^6/mol^2
b	1.4515e-05	m^3/mol
c_1	0.673590004	/
ε/R	2003.72998	K
β	0.069200002	/

2.5 *Comparison of Debye-Hückel Helmholtz function with MSA*

In this section, the difference between the Debye-Hückel and the explicit MSA term will be compared analytically using Talyor expansion in the term of the Helmholtz Free energy. The detailed mathematical deductions are presented in Appendix II. Only a brief overview will be given, from which it can be seen that the difference between them is very small. The general and theoretical comparison of the two terms, please refer to Wei and Blum[10].

From previous chapter, the complete solution of the MSA is given (1.31)-(1.36). It can be seen that the explicit form of Γ cannot be obtained from the complete MSA term. Thus the explicit expression of the excess thermodynamic properties are not available either, including the Helmholtz free energy, internal energy, activity coefficients, chemical potentials and osmotic coefficients. However, an explicit expression for the excess Helmholtz function from the MSA term can be achieved. If all ions have the same diameter σ (e.g. using a mixing rule for ion size parameter), we have the following simple expression:

$$\Gamma = \frac{1}{2\sigma}\left[\sqrt{1+2\sigma\kappa}-1\right] \text{ and } \kappa = \left(\frac{e^2 N_A^2}{\varepsilon\varepsilon_0 RTV}\sum_{ions} n_i Z_i^2\right)^{1/2} \tag{2.73}$$

The expression of the excess Helmholtz function from the MSA term turns to be the following simplified expression:

$$A^E = -\frac{2\Gamma^3 RTV}{3\pi N_A}\left\{1+\frac{3}{2}\Gamma\sigma\right\} \tag{2.74}$$

So the expression of the excess Helmholtz function from the MSA term and Debye-Hückel can be compared under this assumption of the same diameters ions.
Rearrange A^E and substitute Γ into the expression for A^E, we have

$$\left(\frac{A^E}{RT}\right)_{MSA} = -\frac{V}{3\pi 2^2\sigma^3 N_A}\left(\left[\sqrt{1+2\sigma\kappa}-1\right]^3+\frac{3}{4}\left[\sqrt{1+2\sigma\kappa}-1\right]^4\right) \tag{2.75}$$

Combine commen terms, $\left(\frac{A^E}{RT}\right)_{MSA}$ can be simplified as:

$$\left(\frac{A^E}{RT}\right)_{MSA} = -\frac{V}{3\pi 2^2\sigma^3 N_A}\left(\frac{3}{4}\left(1+2\sigma\kappa\right)^2-2\left(\sqrt{1+2\sigma\kappa}\right)^3+\frac{3}{2}\left(1+2\sigma\kappa\right)-\frac{1}{4}\right) \tag{2.76}$$

Expand the $\left(1+2\sigma\kappa\right)$ term, we have:

$$\left(\frac{A^E}{RT}\right)_{MSA} = -\frac{V}{4\pi\sigma^3 N_A}\left(\sigma^2\kappa^2+2\sigma\kappa+\frac{2}{3}-\frac{2}{3}\left(1+2\sigma\kappa\right)^{3/2}\right) \tag{2.77}$$

Talyor expand the term $\left(1+2\sigma\kappa\right)^{3/2}$ in the expression of $\left(\frac{A^E}{RT}\right)_{MSA}$, we have:

$$\left(\frac{A^E}{RT}\right)_{MSA} = -\frac{V}{4\pi\sigma^3 N_A}\left(\frac{1}{3}(\sigma\kappa)^3-\frac{1}{4}(\sigma\kappa)^4+\frac{1}{4}(\sigma\kappa)^5-\frac{7}{24}(\sigma\kappa)^6+O\left((\sigma\kappa)^7\right)\right),\ (\ |\sigma\kappa|<1/2\ ) \tag{2.78}$$

From DH equation, we know the excess Helmholtz function derived from DH equation has the following form:

$$\left(\frac{A^E}{RT}\right)_{DH} = -\frac{V}{4\pi N_A\sum x_i z_i^2}\sum\frac{x_i z_i^2}{a_i^3}\left(\frac{3}{2}+\ln\left(1+a_i\kappa\right)-2\left(1+a_i\kappa\right)+\frac{\left(1+a_i\kappa\right)^2}{2}\right) \tag{2.79}$$

where a_i is the closest approach distance and x_i is the mole fraction of species *i*. The rest of the parameters are the same as in MSA term. If we substitute the closest approach distance a_i with the average diameters of the ions σ, we obtain the following expression:

$$\left(\frac{A^E}{RT}\right)_{DH} = -\frac{V}{4\pi N_A\sigma^3}\left(\ln\left(1+\sigma\kappa\right)-\sigma\kappa+\frac{\left(\sigma\kappa\right)^2}{2}\right) \tag{2.80}$$

Talyor expand the term $\ln\left(1+\sigma\kappa\right)$ in the expression of $\frac{A^E}{RT}$, we have:

$$\left(\frac{A^E}{RT}\right)_{DH} = -\frac{V}{4\pi N_A\sigma^3}\left(\frac{1}{3}\left(\sigma\kappa\right)^3-\frac{1}{4}\left(\sigma\kappa\right)^4+\frac{1}{5}\left(\sigma\kappa\right)^5-\frac{1}{6}\left(\sigma\kappa\right)^6+O\left((\sigma\kappa)^7\right)\right),\quad |\sigma\kappa|<1 \tag{2.81}$$

Comparing with the results from explicit MSA term in (2.78), the difference between the excess Helmholtz free energy is

$$\left(\frac{A^E}{RT}\right)_{MSA}-\left(\frac{A^E}{RT}\right)_{DH}=-\frac{V}{4\pi\sigma^3 N_A}\left(\frac{1}{20}(\sigma\kappa)^5-\frac{1}{8}(\sigma\kappa)^6+O\left((\sigma\kappa)^7\right)\right)$$
$$\approx-\frac{V}{4\pi\sigma^3 N_A}\left(\frac{O\left((\sigma\kappa)^5\right)}{20}\right),\ (\ |\sigma\kappa|<1/2\ ) \tag{2.82}$$

The excess Helmholtz free energy from MSA term and DH have very small difference if the σκ is a small quantity. From this mathematic analysis, it also partly validates the literature report that the numerical results from MSA term are very close to that of DH term. In the later part of the establishment of electrolyte EOS, there is no need to investigate with great effort the performance of MSA term or DH term. The difference cannot be too much, as it has been shown in the work of Cameretti comparing with other EOSs using different MSA terms.[11]

2.6 *Expression of the electrolyte EOS established*

2.6.1 The electrolyte EOS

In this section, we summarize how the different terms are combined for constructing the six EOSs investigated in this work. We aim at performing phase equilibrium calculation for complex multi-component electrolyte solutions.

1) **Myers, Sandler and Wood Electrolyte equation of state[12] (MSW EOS)** In this work the MSW EOS is used with ion-specific parameters rather than the salt-specific parameters used by Myers *et al*. The expression for the total change in Helmholtz free energy to form the electrolyte system is:

$$A(T,V,\mathbf{n})-A^{IGM}(T,V,\mathbf{n})=\Delta A^{PR}+\Delta A_{ex}^{sMSA}+\Delta A_{dis}^{Born}+\Delta A_{chg}^{Born} \tag{2.83}$$

The PR EOS with volume translation parameter was used here as the short range term. According to Myers *et al*., the use of a volume translation parameter *c* for ions has no significant effect on the properties tested. This was confirmed by our initial tests. Therefore it was set equal to zero for all ions. In this work the MSW EOS is used with three adjustable ion-specific parameters, the attraction and co-volume parameters, *a* and *b*, the ion diameter σ and one binary interaction parameter for each species pair.

2) Modified Myers, Sandler and Wood Electrolyte EOS (mMSW EOS) This modified EOS is developed simply for the purpose of comparison between the simplified explicit MSA term (1.58) and the simplified implicit MSA term (1.68). The simplified explicit MSA term in MSW EOS is replaced by the simplified implicit MSA term used in Fürst's electrolyte EOS[16] to construct the new modified EOS. The rest of the terms in MSW EOS remain unchanged. The mMSW EOS can be expressed in terms of Helmholtz free energy as follows:

$$A(T,V,\mathbf{n})-A^{IGM}(T,V,\mathbf{n})=\Delta A^{PR}+\Delta A_{im}^{sMSA}+\Delta A_{dis}^{Born}+\Delta A_{chg}^{Born} \tag{2.84}$$

The mMSW EOS is used with the same number of adjustable parameters as the MSW EOS.

3) The Electrolyte CPA EOS (eCPA EOS)

The CPA EOS has been applied successfully to many systems. The CPA EOS is considerably simpler than SAFT and performs as well as SAFT (or even better) for systems containing water. Therefore it would be preferable to extend the SRK based CPA equation to electrolyte systems. Wu and Prausnitz's EOS [9] is an example of an electrolyte CPA EOS based on the PR EOS. Here an SRK based CPA EOS would be tested. In this EOS, the non-electrolyte term (PR EOS) in mMSW EOS (2.84) is just replaced by CPA EOS and the rest terms remain unchanged. The eCPA EOS has the following general form.

$$A(T,V,\mathbf{n}) - A^{IGM}(T,V,\mathbf{n}) = \Delta A^{SRK} + \Delta A^{Assoc} + \Delta A_{im}^{sMSA} + \Delta A_{dis}^{Born} + \Delta A_{chg}^{Born} \qquad (2.85)$$

The eCPA EOS does not have a volume translation parameter. To minimize the number of fitting parameters, the association term is not used for ions and only used to account for the self-association of water. The water-ion cross-association contribution can be accounted for by the hydrated diameters in the MSA term. For the electrolyte systems chosen, the ionic association has been neglected. Thus the eCPA EOS is used with three adjustable ion-specific parameters: the attraction and co-volume parameters, *a* and *b*, the ion diameter σ; and one binary interaction parameter per species pair.

4) Debye-Hückel SRK electrolyte EOS (SRK+DH EOS) It is interesting to examine whether or not the performance of an electrolyte EOS is proportional to its complexity. For this reason, a very simple EOS has been developed. It consists of two terms and the expression for SRK+DH EOS is as follows:

$$\ln\gamma^{*}(T,V,\mathbf{n}) = \ln\gamma^{SRK}(T,V,\mathbf{n}) + \ln\gamma^{sDH}(T,\mathbf{n}) \qquad (2.86)$$

γ^{*} is the mole-fraction-based activity coefficient of a component in a mixture. $ln\gamma^{sDH}$ is the truncated, simplified Debye-Hückel term in (1.22).

$$\ln\gamma_i^{sDH}(T,\mathbf{n}) = -z_i^2 \frac{AI^{½}}{1+bI^{½}} \qquad (2.87)$$

$ln\gamma^{SRK}$ is the activity coefficient contribution from SRK EOS calculated from the fugacity coefficient of SRK EOS using equation (2.7):

$$\ln\gamma^{SRK}(T,V,\mathbf{n}) = \ln\left(\frac{\hat{\varphi}_i^{SRK}(T,V,\mathbf{n})}{\hat{\varphi}_i^{SRK}(T,V,\mathbf{n}_0)}\right) \qquad (2.88)$$

The fugacity coefficient of SRK EOS can be calculated by the generalized cubic EOS (2.29). Since the Debye-Hückel term makes no contribution to the system volume, the volume is calculated from the SRK EOS alone. The computational speed of this EOS is much higher than that of the other three EOSs. The SRK+DH EOS has only two ion-specific parameters: the attraction parameter *a* and the co-volume parameter *b.* This equation has one binary interaction parameter per species pair in SRK term too.

5) Modified MSW Electrolyte EOS and electrolyte CPA EOS with SR2 term (mMSW+SR2 EOS and eCPA+SR2 EOS)

The following two equations of state are developed simply for the purpose of studying the SR2 term (1.66) used in Fürst's electrolyte EOS[16]. The SR2 term used in Fürst's

electrolyte EOS[16] is added to mMSW EOS in (2.84) to construct the mMSW+SR2 EOS. The rest of the terms in mMSW EOS are unchanged. The mMSW+SR2 EOS can be expressed in terms of Helmholtz free energy as follows:

$$A(T,V,\mathbf{n}) - A^{IGM}(T,V,\mathbf{n}) = \Delta A^{PR} + \Delta A_{im}^{sMSA} + \Delta A_{dis}^{Born} + \Delta A_{chg}^{Born} + \Delta A^{SR2} \quad (2.89)$$

The eCPA+SR2 EOS is constructed in the similar way as mMSW+SR2 EOS from eCPA EOS.

$$A(T,V,\mathbf{n}) - A^{IGM}(T,V,\mathbf{n}) = \Delta A^{SRK} + \Delta A^{Assoc} + \Delta A_{im}^{sMSA} + \Delta A_{dis}^{Born} + \Delta A_{chg}^{Born} + \Delta A^{SR2} \quad (2.90)$$

The mMSW+SR2 EOS and the eCPA+SR2 EOS have one additional interaction parameter W_{ij} in SR2 term (1.66) compared with the mMSW EOS and eCPA EOS respectively. The two equations reduced to the mMSW EOS and eCPA EOS respectively when W_{ij} is set to zero.

All of the above-mentioned EOSs are summarized in Table 2.

Table 2.2 The table of different electrolyte equation of states developed in this work.

Electrolyte EOS	Non-electrolyte term	Electrolyte terms	Pure compound parameter	Interaction parameter	Model for water relative permittivity
MSW EOS	1.PR EOS with volume translation parameter	1. Simplified explicit MSA 2. Born term	Three adjustable parameters *a, b,* σ. Volume translation parameter *c* is not used for ions.	One (k_{ij} in PR EOS)	1. Uematsu-Franck model
mMSW EOS	1.PR EOS with volume translation parameter	1. Simplified implicit MSA 2. Born term	Three adjustable parameters *a, b,* σ. Volume translation parameter *c* is not used for ions.	One (k_{ij} in PR EOS)	1. Uematsu-Franck model 2. Pottel model
mMSW+SR2 EOS	1.PR EOS with volume translation parameter	1. Simplified implicit MSA 2. Born term 3. SR2 term	Three adjustable parameters *a, b,* σ. Volume translation parameter *c* is not used for ions.	Two (k_{ij} in PR EOS and W_{ij} in SR2 term)	1. Uematsu-Franck model 2. Pottel model
eCPA EOS	1. SRK EOS 2.Wertheim association term of for associating compound	1. Simplified implicit MSA 2. Born term	Three adjustable parameters *a, b,* σ.	One (k_{ij} in SRK EOS)	1. Uematsu-Franck model 2. Pottel model
eCPA+SR2 EOS	1. SRK EOS 2.Wertheim association term of for associating compound	1. Simplified implicit MSA 2. Born term 3. SR2 term	Three adjustable parameters *a, b,* σ.	Two (k_{ij} in SRK EOS and W_{ij} in SR2 term)	1. Uematsu-Franck model 2. Pottel model
SRK+DH EOS	1. SRK EOS	1.Simplified textbook Debye-Hückel term	Two adjustable parameters *a, b* in SRK EOS.	One (k_{ij} in SRK EOS)	No model needed

2.6.2 Water parameters

Prior to the determination of parameters for electrolytes, the parameters for pure water should be determined. In this way the equations of state can accurately predict the properties of pure water in the limit of infinite dilution concentration of an aqueous salt solution. Myers *et al*.[12] provided a set of best-fit temperature dependent parameters (nine parameters) for the PR EOS with a volume translation parameter, see equation (1.53) to (1.55). This set of parameters results in average relative deviations (abbreviated as ARD) of 0.22% and 0.83%, respectively, for vapour pressure and liquid densities of water over wide temperature (10~374.15 °C) and pressure ranges (up to 250 bar). The same set of parameters for water has been used in the mMSW EOS and mMSW+SR2 EOS. Regarding the CPA EOS, Kontogeorgis *et al.* [6] provided an optimal set of CPA parameters (five parameters) with a 4C association scheme for water by fitting vapour pressure and density data in the range of the reduced temperature of water from 0.5 to 0.95 and the corresponding water vapour pressure range, see Table 2.1. The ARDs of CPA is 0.8% for vapour pressure and 0.5% for liquid densities of water[13]. The SRK term in SRK+DH EOS uses the critical properties of water simply to calculate the attractive parameter *a* and the co-volume parameter *b*.

The PR EOS with volume translation parameter and the CPA EOS give reliable, sufficient representation of pure water as a basis for aqueous electrolyte solutions. SRK EOS gives a less accurate representation of the properties of water than these two EOSs.

2.6.3 The models for relative permittivity of water

The primitive model (PM) for electrolyte needs an additional equation to calculate the water relative permittivity externally. Both the DH term and the simplified MSA terms from the OZ equation in this work belong to the primitive models. The *A* parameter in the DH term is correlated by a temperature dependent equation (1.23), hence no external model for the relative permittivity of water is needed in the SRK+DH EOS.

Several empirical equations are available in the literature for calculating the permittivity of water. Fernandez *et al*.[14] have developed a very accurate 12-parameter model treating the relative permittivity of pure water as a function of temperature (238-873 K) and density over a pressure range up to 1200 MPa. However, Uematsu and Franck[15] have alternatively developed a simpler 10-parameter model valid within 273-1273 K and pressure below 1600 Mpa. The Uematsu and Franck model for water relative permittivity is a function of temperature and water density. Its mathematical expression will be given in Chapter 3 when deriving its derivatives. The pure water density is obtained by an approximation suggested by Myers *et al.*[12]:

$$d_{H_2O} \approx n_{H_2O} \bullet M_{H_2O} / V \tag{2.91}$$

where n_{H_2O} is the number of moles of water in the solution, M_{H_2O} is the molecular mass of water in kg/mol and V is the system volume of the aqueous electrolyte solution, not the pure water volume. This approximation simplifies the electrolyte EOS and improves calculation speed. Under this approximation the water permittivity becomes a function of system temperature T, system volume V and water mole

number n_{H_2O} . Therefore the contribution of partial derivatives of water relative permittivity should be included when deducing the first order and second order derivatives of the Helmholtz free energy with respect to *T, V* and n_{H_2O}. This approach has been used for all electrolyte EOSs in this work when the Uematsu-Franck model is used.

An alternative model for relative permittivity of water used in this work is the Pottel model in (1.69) used by Fürst and Renon.[16] It is simply implemented for the purpose of comparison with the Uematsu-Franck model.

2.6.4 Ion parameters

Models using salt-specific parameters have different sets of parameter values for the common ions contained in different salts. The salt-specific parameters for cation and anion of a certain salt are set equal to the same single value. For example, the values of the attraction, co-volume and the ion size parameters (*a*, *b* and σ) of MSW EOS for Na^+ are not universal in different sodium salts according to Myers *et al*[12] due to their use of salt-specific parameters: The values of the attraction parameter *a* for Na^+ in NaCl and NaBr are 2.4611 and 3.2858 Pa*m^6/mol respectively. The same ion is mathematically treated as different species in different salts. Salt-specific parameters are easier to obtain than the ion-specific parameters. The salt-specific parameters of each salt are obtained by fitting the model to the binary experimental data of that salt only. It is also possible to conduct solid-liquid phase equilibrium computations for multi-component systems containing common ions using salt-specific parameters. However, it requires the use of a specially constructed program to conduct the calculation.

In order to perform the same type of calculation with a general EOS, it is necessary to use ion-specific parameters. Ion-specific parameters require a simultaneous regression of much more sets of different type of experimental data of many binary and ternary systems. If available, it is the best to have the experimental data of all electrolyte systems which are the possible combinations of the targeting ions. The amount of data required is huge and the optimization process is quite time-consuming. But it is still preferable to have ion-specific parameters as the final parameters for EOS in this work, while using salt-specific parameters can speed up and simplify the process of studying the performances of different electrolyte EOSs at the starting stage. The ion-specific parameters determined in this work are valid and optimized for the selected ions in study of the test system.

Reference

1. Michelsen ML, Mollerup JM, ed. *Thermodynamic Model:, Fundamentals and Computational Aspects.* Holte, Denmark: Tie-Line Publication.

2. Kontogeorgis GM, ed. *Association Theories and Model. (Course material of course 28423 in Technical University of Denmark, 2002)*. Lyngby, Denmark: Technical University of Denmark.

3. Kontogeorgis GM, Voutsas EC, Yakoumis IV, Tassios DP. An Equation of State for Associating Fluids. *Ind Eng Chem Res.* 1996; 35(11): 4310-4318.

4. Derawi SO, Michelsen MM, Kontogeorgis GM, Stenby EH. Application of the CPA equation of state to Glycol/hydrocarbons liquid-liquid equilibria. *Fluid Phase Equilibria*. 2003;209(2):163-184.

5. Derawi SO, Michelsen MM, Kontogeorgis GM, Stenby EH. Extension of the CPA Equation of State to Glycol-water Cross_Associating systems*, Ind Eng Chem Res.* 2003;42(7):1440-1477.

6. Kontogeorgis GM, Yakoumis IV, Meijer H, Hendriks E, Moorwood T. Multicomponent phase equilibrium calculations for water-methanol-alkane mixtures. *Fluid Phase Equilib.* 1999; 158-160: 201-209.

7. Yakoumis IV, Kontogeorgis GM, Voutsas EC, Hendriks EM, Tassios DP. Prediction of phase equilibria in binary aqueous systems containing alkanes, cycloalkanes, and alkenes with the cubic-plus-association equation of state*. Ind Eng Chem Res.* 1998; 37(10): 4175-4182.

8. Folas GK, Kontogeorgis GM, Michelsen ML, Stenby EH. Application of the Cubic-Plus-Association (CPA) equation of state to complex mixtures with aromatic hydrocarbons. *Ind Eng Chem Res.* 2006;45: 1527-1538.

9. Wu J, Prausnitz JM. Phase Equilibrium for systems Containing Hydrocarbons, Water and Salt: An Extended Peng-Robinson Equation of State. *Ind Eng Chem Res.* 1998; 37: 1634-1643.

10. Wei D, Blum L. Internal Energy in the Mean Spherical Approximation As Compared to Debye-Hückel Theory. *J Phys Chem.* 1987; 91: 4342-4343.

11. Cameretti LF, Sadowski G, Mollerup JM. Modeling of aqueous electrolyte solutions with perturbed-chain statistical associated fluid theory. *Ind Eng Chem Res.* 2005;44 (9): 3355-3362.

12. Myers JA, Sandler SI, Wood RH. An Equation of State for Electrolyte Solutions Covering Wide Range of Temperature, Pressure and Composition. *Ind Eng Chem Res.* 2002; 41: 3282-3297.

13. Personal communication with Kontogeorgis GM.

14. Fernández DP, Goodwin ARH, Lemmon EW, Levelt Sengers JMH, Williams RC. A Formulation for the static permittivity of water and steam at temperature from 238 to 873 K at pressures up to 1200 MPa, including derivatives and Debye-Hückel Coefficients. *J Phys Chem Ref Data.* 1997; 26:1125-1166.

15. Uematsu M, Franck EU. Static dielectric constant of water and steam. *J Phys Chem Ref Data.* 1980; 9(4):1291-1305.

16. Fürst W, Renon H. Representation of Excess Properties of Electrolyte Solutions Using a New Equation of State. *AIChE J.* 1993; 39: 335-343.

CHAPTER 3 Derivatives of the Helmholtz energy terms for electrolyte EOS

3.1 *General*

The above-mentioned EOSs are expressed in terms of the Helmholtz free energy and contains several terms accounting for the various interactions in solution. The terms differ from each other depending on the forces taken into account. Thermodynamic properties can be derived from the Helmholtz free energy by standard differentiation. In this chapter the mathematical theory (vector analysis) used to simplify the deduction and the analytical form of first and second order derivatives of the electrolyte and non-electrolyte terms will be explained. The detailed deduction of all derivatives of the terms used to construct the electrolyte EOS are given in Appendix IV and V.

3.2 *The general chain rule applies to the vector function (composite function)*

The energy terms used in this work are all complex multi-variable functions. To calculate the first and second order derivatives of these kind of function, we often transform them into the form of a composite function and a chain rule is needed to derive the derivatives of composite function. By introducing composite function, the repetitive work can be avoided and the complex multi variable functions can be transformed into simpler and concise forms[1]. The following is the chain rule for composite scalar function.

If $g(x)$ is differentiable at the point x and $f(x)$ is differentiable at the point $g(x)$, then $f \bullet g$ is differentiable at x. Furthermore, let $y = g(f(x))$ and $u = g(x)$, then

$$\frac{dy}{dx} = \frac{dy}{du} \cdot \frac{du}{dx} \tag{3.1}$$

There are a number of related results that also go under the name of "chain rules." For example, if $z = f(x, y)$, $x = g(t)$, and $y = h(t)$, then

$$\frac{dz}{dt} = \frac{\partial z}{\partial x} \cdot \frac{dx}{dt} + \frac{\partial z}{\partial y} \cdot \frac{dy}{dt} \tag{3.2}$$

Frequently this is not sufficient in this work; we need to use a general chain rule for the composite vector function. Before introducing the general chain rule for composite vector function, it is necessary to define the gradient, Jacobian matrix and Hessian matrix.

Given a vector function $\mathbf{f} : \mathbb{R}^n \to \mathbb{R}^m$ of m function components in n variables, written explicitly as:

$$\mathbf{f}(\mathbf{x}) = \left[f_1(\mathbf{x}),\ f_2(\mathbf{x}), \cdots, f_m(\mathbf{x}) \right]^T . \tag{3.3}$$

We define $\mathbf{J}_f \in \mathbb{R}^{m \times n}$ as the Jacobian matrix, sometimes simply described as "the Jacobian", containing the first partial derivatives of the function components:

$$\left(\mathbf{J}_f(\mathbf{x}) \right)_{ij} = \frac{\partial f_i(\mathbf{x})}{\partial x_j} \tag{3.4}$$

written explicitly as:

$$\mathbf{J}_f(\mathbf{x}) = \left(\frac{\partial f_i}{\partial x_j}\right) = \begin{pmatrix} \frac{\partial f_1}{\partial x_1} & \frac{\partial f_1}{\partial x_2} & \cdots & \frac{\partial f_1}{\partial x_n} \\ \vdots & \vdots & \ddots & \vdots \\ \frac{\partial f_m}{\partial x_1} & \frac{\partial f_m}{\partial x_2} & \cdots & \frac{\partial f_m}{\partial x_n} \end{pmatrix} \tag{3.5}$$

Given a differentiable scalar function of a vector $f : \mathbb{R}^n \to \mathbb{R}$
The gradient $\mathbf{g}$ can be written in a vector function as follows (3.6):

$$\mathbf{g}(\mathbf{x}) \triangleq \mathbf{f}'(\mathbf{x}) = \begin{bmatrix} \frac{\partial f(\mathbf{x})}{\partial x_1} \\ \frac{\partial f(\mathbf{x})}{\partial x_2} \\ \vdots \\ \frac{\partial f(\mathbf{x})}{\partial x_n} \end{bmatrix} \tag{3.6}$$

The Hessian of a scalar function of a vector variable is the matrix of partial second derivatives. Note that when f is in C^2 (i.e. has continuous second derivatives), the Hessian matrix of a function $f : \mathbb{R}^n \to \mathbb{R}$ is:

$$H \triangleq f''(\mathbf{x}) \equiv \left[\frac{\partial^2 f(\mathbf{x})}{\partial x_i \partial x_j}\right] = \begin{bmatrix} \frac{\partial^2 f}{\partial x_1^2} & \frac{\partial^2 f}{\partial x_1 \partial x_2} & \cdots & \frac{\partial^2 f}{\partial x_1 \partial x_n} \\ \frac{\partial^2 f}{\partial x_2 \partial x_1} & \frac{\partial^2 f}{\partial x_2^2} & \cdots & \frac{\partial^2 f}{\partial x_2 \partial x_n} \\ \vdots & \vdots & \ddots & \vdots \\ \frac{\partial^2 f}{\partial x_n \partial x_1} & \frac{\partial^2 f}{\partial x_n \partial x_2} & \cdots & \frac{\partial^2 f}{\partial x_n^2} \end{bmatrix} \tag{3.7}$$

It can be easily seen that the Hessian matrix of the scalar function *f* is actually the Jacobian of the gradient $\mathbf{g}$ of the same scalar function *f*. Note gradient is a vector function and it is also the Jacobian of the scalar function *f*. The Hessian (3.7) is symmetric i.e. of the equality of mixed partials.
The general chain rule for composite vector function applies to two sets of functions

$$\begin{aligned} y_1 &= f_1(u_1, \cdots, u_p) \\ &\vdots \\ y_m &= f_m(u_1, \ldots, u_p) \end{aligned} \tag{3.8}$$

and

$$\begin{aligned} u_1 &= g_1(x_1, \cdots, x_n) \\ &\vdots \\ u_p &= g_p(x_1, \cdots, x_n) \end{aligned} \tag{3.9}$$

The $m \times n$ Jacobian matrix of vector function $\mathbf{y} = \mathbf{f}(\mathbf{u}(\mathbf{x}))$ is

$$\left(\frac{\partial y_i}{\partial x_j}\right)=\begin{pmatrix}\frac{\partial y_1}{\partial x_1} & \frac{\partial y_1}{\partial x_2} & \cdots & \frac{\partial y_1}{\partial x_n}\\ \vdots & \vdots & \ddots & \vdots\\ \frac{\partial y_m}{\partial x_1} & \frac{\partial y_m}{\partial x_2} & \cdots & \frac{\partial y_m}{\partial x_n}\end{pmatrix} \tag{3.10}$$

and similarly for matrixes $\partial y_i/\partial u_j$ and $\partial u_i/\partial x_j$, then it gives

$$\left(\frac{\partial y_i}{\partial x_j}\right)=\left(\frac{\partial y_i}{\partial u_j}\right)\left(\frac{\partial u_i}{\partial x_j}\right) \tag{3.11}$$

In differential form, this becomes

$$dy_1=\left(\frac{\partial y_1}{\partial u_1}\frac{\partial u_1}{\partial x_1}+\cdots+\frac{\partial y_1}{\partial u_p}\frac{\partial u_p}{\partial x_1}\right)dx_1+\left(\frac{\partial y_1}{\partial u_1}\frac{\partial u_1}{\partial x_2}+\cdots+\frac{\partial y_1}{\partial u_p}\frac{\partial u_p}{\partial x_2}\right)dx_2+\cdots \tag{3.12}$$

The general chain rule in (3.11) is used in this work rather frequently. Function **y** can be a vector composite function or a scalar composite function in a simple case. And the expressions of the derivatives were all written in the matrix and vector forms instead of a long summation form.

The reason for choosing vector and matrix forms is as follow. First, it will simplify the deduction of derivatives. A long chain expression of summation for derivatives is decomposed into dot products of two vectors. Instead of deriving all derivatives at one time like in (3.12), it is changed to derive the derivatives of element functions in a vector/matrix function one by one, see (3.10). Secondly, numerical programs are available to check whether a Jacobian matrix is correctly derived from its original vector function. Such program is also able to locate the specific indexes of the erroneous elements in Jacobian matrix, e.g. their locations. That is much easier to find out what element function in the matrix function is wrong with the help of such program. While a long chain of summation expression, if there are some mistakes, the whole expression has to be checked from the beginning to the end manually to locate the erroneous terms and no program can easily locate which terms in the summation are wrong. It is clear that under this condition, it is more convenient to use the vector and matrix forms.

3.3 *The second order derivatives of a composite function in matrix and vector form*

An example is given to illustrate the idea of expressing derivatives of a composite function in matrix and vector forms. In deducting the analytical form of the second order partial molar derivatives of residual Helmholtz function, intermediate variables are introduced to simplify the deduction and numerical calculation rather often. The intermediate variables are often dependent on molar number of each component in the mixture. This forms a composite function and we need to apply the chain rule to conduct the deduction.

The composite function can be generalized as follows:

$$A^r(\mathbf{n})=A^r(n(\mathbf{n}),\tilde{A}(\mathbf{n},T),\tilde{B}_1(\mathbf{n}),\tilde{B}_2(\mathbf{n}),\tilde{B}_3(\mathbf{n}),\cdots,\tilde{B}_i(\mathbf{n})) \tag{3.13}$$

The intermediate variables n, $\tilde{A}$, $\tilde{B}_1$, $\tilde{B}_2$, $\tilde{B}_3$ and $\tilde{B}_i$ are dependent on a molar number of each component in the mixture, n_i. A graph of the relationship between composite

function and the intermediate variables and the variable can be constructed as below figure.

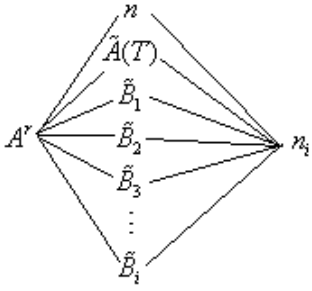

The first and second partial derivative of this type of a composite function can be calculated using chain rules. Sometimes the expressions for the partial derivatives are very complicated if written down in a whole analytical expression in the summation form. It is more clear and convenient to write them in the matrix and vector form.

Introducing a new intermediate vector function

$$\boldsymbol{\eta}(\mathbf{n}) = \left[n(\mathbf{n}), \tilde{A}(\mathbf{n},T), \tilde{B}_1(\mathbf{n}), \tilde{B}_2(\mathbf{n}), \tilde{B}_3(\mathbf{n}), \cdots, \tilde{B}_i(\mathbf{n}) \right]^T \tag{3.14}$$

and (3.13) can be simplified to (3.15)

$$A^r(\mathbf{n}) = A^r(\boldsymbol{\eta}(\mathbf{n})), \text{ where } \boldsymbol{\eta}(\mathbf{n}) = \left[n(\mathbf{n}), \tilde{A}(\mathbf{n},T), \tilde{B}_1(\mathbf{n}), \tilde{B}_2(\mathbf{n}), \tilde{B}_3(\mathbf{n}), \cdots, \tilde{B}_i(\mathbf{n}) \right]^T \tag{3.15}$$

Define the first order partial mole number derivative of a vector function as follows:

$$\boldsymbol{\eta}(\mathbf{n})_{n_i} \triangleq \frac{\partial \boldsymbol{\eta}(\mathbf{n})}{\partial n_i} = \left[\frac{\partial n(\mathbf{n})}{\partial n_i}, \frac{\partial \tilde{A}(\mathbf{n},T)}{\partial n_i}, \frac{\partial \tilde{B}_1(\mathbf{n})}{\partial n_i}, \frac{\partial \tilde{B}_2(\mathbf{n})}{\partial n_i}, \frac{\partial \tilde{B}_3(\mathbf{n})}{\partial n_i}, \cdots, \frac{\partial \tilde{B}_i(\mathbf{n})}{\partial n_i} \right]^T \tag{3.16}$$

Define the second order partial mole number derivative of a vector function as:

$$\boldsymbol{\eta}(\mathbf{n})_{n_i n_j} \triangleq \frac{\partial^2 \boldsymbol{\eta}(\mathbf{n})}{\partial n_i \partial n_j} = \left[\frac{\partial^2 n(\mathbf{n})}{\partial n_i \partial n_j}, \frac{\partial^2 \tilde{A}(\mathbf{n},T)}{\partial n_i \partial n_j}, \frac{\partial^2 \tilde{B}_1(\mathbf{n})}{\partial n_i \partial n_j}, \frac{\partial^2 \tilde{B}_2(\mathbf{n})}{\partial n_i \partial n_j}, \frac{\partial^2 \tilde{B}_3(\mathbf{n})}{\partial n_i \partial n_j}, \cdots, \frac{\partial^2 \tilde{B}_i(\mathbf{n})}{\partial n_i \partial n_j} \right]^T \tag{3.17}$$

According to the definition of the gradient vector and Hessian matrix of a scalar function of a vector variable in (3.6) and (3.7), we can write the gradient and Hessian matrix of the scalar function $A^r(\boldsymbol{\eta})$ of a vector variable $\boldsymbol{\eta}$ as in (3.18) and (3.19).

$$\begin{aligned} \mathbf{A^{r\prime}}(\boldsymbol{\eta}(\mathbf{n})) &= \left[\frac{\partial A^r}{\partial n}, \frac{\partial A^r}{\partial \tilde{A}}, \frac{\partial A^r}{\partial \tilde{B}_1}, \frac{\partial A^r}{\partial \tilde{B}_2}, \frac{\partial A^r}{\partial \tilde{B}_3}, \cdots, \frac{\partial A^r}{\partial \tilde{B}_i} \right]^T \\ &\triangleq \left[A^r{}_n, A^r{}_{\tilde{A}}, A^r{}_{\tilde{B}_1}, A^r{}_{\tilde{B}_2}, A^r{}_{\tilde{B}_3}, \cdots, A^r{}_{\tilde{B}_i} \right]^T \end{aligned} \tag{3.18}$$

Here we adopt a short notation for the partial derivative $\frac{\partial y}{\partial x}$ as y_x for $A^{r\prime}(\boldsymbol{\eta})$ and $\frac{\partial^2 y}{\partial x \partial z}$ as y_{xz} for $A^{r\prime\prime}(\boldsymbol{\eta})$:

$$\mathbf{A^{r''}(\eta)} = \begin{bmatrix} \frac{\partial^2 A^r}{\partial n^2} & \frac{\partial^2 A^r}{\partial \tilde{A}\partial n} & \frac{\partial^2 A^r}{\partial \tilde{B}_1\partial n} & \frac{\partial^2 A^r}{\partial \tilde{B}_2\partial n} & \frac{\partial^2 A^r}{\partial \tilde{B}_3\partial n} & \cdots & \frac{\partial^2 A^r}{\partial \tilde{B}_i\partial n} \\ \frac{\partial^2 A^r}{\partial n\partial \tilde{A}} & \frac{\partial^2 A^r}{\partial \tilde{A}^2} & \frac{\partial^2 A^r}{\partial \tilde{B}_1\partial \tilde{A}} & \frac{\partial^2 A^r}{\partial \tilde{B}_2\partial \tilde{A}} & \frac{\partial^2 A^r}{\partial \tilde{B}_3\partial \tilde{A}} & \cdots & \frac{\partial^2 A^r}{\partial \tilde{B}_i\partial \tilde{A}} \\ \frac{\partial^2 A^r}{\partial n\partial \tilde{B}_1} & \frac{\partial^2 A^r}{\partial \tilde{A}\partial \tilde{B}_1} & \frac{\partial^2 A^r}{\partial \tilde{B}_1^2} & \frac{\partial^2 A^r}{\partial \tilde{B}_2\partial \tilde{B}_1} & \frac{\partial^2 A^r}{\partial \tilde{B}_3\partial \tilde{B}_1} & \cdots & \frac{\partial^2 A^r}{\partial \tilde{B}_i\partial \tilde{B}_1} \\ \frac{\partial^2 A^r}{\partial n\partial \tilde{B}_2} & \frac{\partial^2 A^r}{\partial \tilde{A}\partial \tilde{B}_2} & \frac{\partial^2 A^r}{\partial \tilde{B}_1\partial \tilde{B}_2} & \frac{\partial^2 A^r}{\partial \tilde{B}_2^2} & \frac{\partial^2 A^r}{\partial \tilde{B}_3\partial \tilde{B}_2} & \cdots & \frac{\partial^2 A^r}{\partial \tilde{B}_i\partial \tilde{B}_2} \\ \frac{\partial^2 A^r}{\partial n\partial \tilde{B}_3} & \frac{\partial^2 A^r}{\partial \tilde{A}\partial \tilde{B}_3} & \frac{\partial^2 A^r}{\partial \tilde{B}_1\partial \tilde{B}_3} & \frac{\partial^2 A^r}{\partial \tilde{B}_2\partial \tilde{B}_3} & \frac{\partial^2 A^r}{\partial \tilde{B}_3^2} & \cdots & \frac{\partial^2 A^r}{\partial \tilde{B}_i\partial \tilde{B}_3} \\ \vdots & \vdots & \vdots & \vdots & \vdots & \ddots & \vdots \\ \frac{\partial^2 A^r}{\partial n\partial \tilde{B}_i} & \frac{\partial^2 A^r}{\partial \tilde{A}\partial \tilde{B}_i} & \frac{\partial^2 A^r}{\partial \tilde{B}_1\partial \tilde{B}_i} & \frac{\partial^2 A^r}{\partial \tilde{B}_2\partial \tilde{B}_i} & \frac{\partial^2 A^r}{\partial \tilde{B}_3\partial \tilde{B}_i} & \cdots & \frac{\partial^2 A^r}{\partial \tilde{B}_i^2} \end{bmatrix}$$

$$\triangleq \begin{bmatrix} A^r{}_{nn} & A^r{}_{\tilde{A}n} & A^r{}_{\tilde{B}_1 n} & A^r{}_{\tilde{B}_2 n} & A^r{}_{\tilde{B}_3 n} & \cdots & A^r{}_{\tilde{B}_i n} \\ A^r{}_{n\tilde{A}} & A^r{}_{\tilde{A}\tilde{A}} & A^r{}_{\tilde{B}_1\tilde{A}} & A^r{}_{\tilde{B}_2\tilde{A}} & A^r{}_{\tilde{B}_3\tilde{A}} & \cdots & A^r{}_{\tilde{B}_i\tilde{A}} \\ A^r{}_{n\tilde{B}_1} & A^r{}_{\tilde{A}\tilde{B}_1} & A^r{}_{\tilde{B}_1\tilde{B}_1} & A^r{}_{\tilde{B}_2\tilde{B}_1} & A^r{}_{\tilde{B}_3\tilde{B}_1} & \cdots & A^r{}_{\tilde{B}_i\tilde{B}_1} \\ A^r{}_{n\tilde{B}_2} & A^r{}_{\tilde{A}\tilde{B}_2} & A^r{}_{\tilde{B}_1\tilde{B}_2} & A^r{}_{\tilde{B}_2\tilde{B}_2} & A^r{}_{\tilde{B}_3\tilde{B}_2} & \cdots & A^r{}_{\tilde{B}_i\tilde{B}_2} \\ A^r{}_{n\tilde{B}_3} & A^r{}_{\tilde{A}\tilde{B}_3} & A^r{}_{\tilde{B}_1\tilde{B}_3} & A^r{}_{\tilde{B}_2\tilde{B}_3} & A^r{}_{\tilde{B}_3\tilde{B}_3} & \cdots & A^r{}_{\tilde{B}_i\tilde{B}_3} \\ \vdots & \vdots & \vdots & \vdots & \vdots & \ddots & \vdots \\ A^r{}_{n\tilde{B}_i} & A^r{}_{\tilde{A}\tilde{B}_i} & A^r{}_{\tilde{B}_1\tilde{B}_i} & A^r{}_{\tilde{B}_2\tilde{B}_i} & A^r{}_{\tilde{B}_3\tilde{B}_i} & \cdots & A^r{}_{\tilde{B}_i\tilde{B}_i} \end{bmatrix} \tag{3.19}$$

Introducing the gradient and Hessian matrix of $A^r(\boldsymbol{\eta}(\mathbf{n}))$ and the first and second derivatives of $\boldsymbol{\eta}(\mathbf{n})$, we can express the first order partial derivatives $\frac{\partial A^r(n)}{\partial n_i}$ and the second order partial derivatives $\frac{\partial^2 A^r}{\partial n_i \partial n_j}$ of $A^r(\boldsymbol{\eta}(\mathbf{n}))$ in the dot product form of vector and matrix, which is quite concise and clear.

The first order partial derivatives $\frac{\partial A^r(n)}{\partial n_i}$ can be expressed as:

$$\frac{\partial A^r(n)}{\partial n_i} = \frac{\partial A^r}{\partial n}\cdot\frac{\partial n}{\partial n_i} + \frac{\partial A^r}{\partial \tilde{A}}\cdot\frac{\partial \tilde{A}(\mathbf{n},T)}{\partial n_i} + \frac{\partial A^r}{\partial \tilde{B}_1}\cdot\frac{\partial \tilde{B}_1}{\partial n_i} + \frac{\partial A^r}{\partial \tilde{B}_2}\cdot\frac{\partial \tilde{B}_2}{\partial n_i} + \frac{\partial A^r}{\partial \tilde{B}_3}\cdot\frac{\partial \tilde{B}_3}{\partial n_i} + \cdots + \frac{\partial A^r}{\partial \tilde{B}_i}\cdot\frac{\partial \tilde{B}_i}{\partial n_i}$$

$$= (\boldsymbol{\eta}(\mathbf{n})_{n_i})^T \cdot \mathbf{A^{r'}}(\boldsymbol{\eta}(\mathbf{n})) \tag{3.20}$$

The second order partial derivatives $\frac{\partial^2 A^r}{\partial n_i \partial n_j}$ can be expressed as:

$$\frac{\partial^2 A^r}{\partial n_i \partial n_j} = \left[\begin{array}{l} \frac{\partial^2 A^r}{\partial n^2}\frac{\partial n}{\partial n_i}\frac{\partial n}{\partial n_j} + \frac{\partial^2 A^r}{\partial \tilde{A}\partial n}\frac{\partial \tilde{A}}{\partial n_i}\frac{\partial n}{\partial n_j} + \frac{\partial^2 A^r}{\partial \tilde{B}_1\partial n}\frac{\partial \tilde{B}_1}{\partial n_i}\frac{\partial n}{\partial n_j} + \frac{\partial^2 A^r}{\partial \tilde{B}_2\partial n}\frac{\partial \tilde{B}_2}{\partial n_i}\frac{\partial n}{\partial n_j} + \cdots + \frac{\partial^2 A^r}{\partial \tilde{B}_i\partial n}\frac{\partial \tilde{B}_i}{\partial n_i}\frac{\partial n}{\partial n_j} + \\ \frac{\partial^2 A^r}{\partial n\partial \tilde{A}}\frac{\partial n}{\partial n_i}\frac{\partial \tilde{A}}{\partial n_j} + \frac{\partial^2 A^r}{\partial \tilde{A}^2}\frac{\partial \tilde{A}}{\partial n_i}\frac{\partial \tilde{A}}{\partial n_j} + \frac{\partial^2 A^r}{\partial \tilde{B}_1\partial \tilde{A}}\frac{\partial \tilde{B}_1}{\partial n_i}\frac{\partial \tilde{A}}{\partial n_j} + \frac{\partial^2 A^r}{\partial \tilde{B}_2\partial \tilde{A}}\frac{\partial \tilde{B}_2}{\partial n_i}\frac{\partial \tilde{A}}{\partial n_j} + \cdots + \frac{\partial^2 A^r}{\partial \tilde{B}_i\partial \tilde{A}}\frac{\partial \tilde{B}_i}{\partial n_i}\frac{\partial \tilde{A}}{\partial n_j} + \\ \frac{\partial^2 A^r}{\partial n\partial \tilde{B}_1}\frac{\partial n}{\partial n_i}\frac{\partial \tilde{B}_1}{\partial n_j} + \frac{\partial^2 A^r}{\partial \tilde{A}\partial \tilde{B}_1}\frac{\partial \tilde{A}}{\partial n_i}\frac{\partial \tilde{B}_1}{\partial n_j} + \frac{\partial^2 A^r}{\partial \tilde{B}_1^2}\frac{\partial \tilde{B}_1}{\partial n_i}\frac{\partial \tilde{B}_1}{\partial n_j} + \frac{\partial^2 A^r}{\partial \tilde{B}_2\partial \tilde{B}_1}\frac{\partial \tilde{B}_2}{\partial n_i}\frac{\partial \tilde{B}_1}{\partial n_j} + \cdots + \frac{\partial^2 A^r}{\partial \tilde{B}_i\partial \tilde{B}_1}\frac{\partial \tilde{B}_i}{\partial n_i}\frac{\partial \tilde{B}_1}{\partial n_j} + \\ \frac{\partial^2 A^r}{\partial n\partial \tilde{B}_2}\frac{\partial n}{\partial n_i}\frac{\partial \tilde{B}_2}{\partial n_j} + \frac{\partial^2 A^r}{\partial \tilde{A}\partial \tilde{B}_2}\frac{\partial \tilde{A}}{\partial n_i}\frac{\partial \tilde{B}_2}{\partial n_j} + \frac{\partial^2 A^r}{\partial \tilde{B}_1\partial \tilde{B}_2}\frac{\partial \tilde{B}_1}{\partial n_i}\frac{\partial \tilde{B}_2}{\partial n_j} + \frac{\partial^2 A^r}{\partial \tilde{B}_2^2}\frac{\partial \tilde{B}_2}{\partial n_i}\frac{\partial \tilde{B}_2}{\partial n_j} + \cdots + \frac{\partial^2 A^r}{\partial \tilde{B}_i\partial \tilde{B}_2}\frac{\partial \tilde{B}_i}{\partial n_i}\frac{\partial \tilde{B}_2}{\partial n_j} + \\ \frac{\partial^2 A^r}{\partial n\partial \tilde{B}_3}\frac{\partial n}{\partial n_i}\frac{\partial \tilde{B}_3}{\partial n_j} + \frac{\partial^2 A^r}{\partial \tilde{A}\partial \tilde{B}_3}\frac{\partial \tilde{A}}{\partial n_i}\frac{\partial \tilde{B}_3}{\partial n_j} + \frac{\partial^2 A^r}{\partial \tilde{B}_1\partial \tilde{B}_3}\frac{\partial \tilde{B}_1}{\partial n_i}\frac{\partial \tilde{B}_3}{\partial n_j} + \frac{\partial^2 A^r}{\partial \tilde{B}_2\partial \tilde{B}_3}\frac{\partial \tilde{B}_2}{\partial n_i}\frac{\partial \tilde{B}_3}{\partial n_j} + \cdots + \frac{\partial^2 A^r}{\partial \tilde{B}_i\partial \tilde{B}_3}\frac{\partial \tilde{B}_i}{\partial n_i}\frac{\partial \tilde{B}_3}{\partial n_j} + \\ \cdots \\ \frac{\partial^2 A^r}{\partial n\partial \tilde{B}_i}\frac{\partial n}{\partial n_i}\frac{\partial \tilde{B}_i}{\partial n_j} + \frac{\partial^2 A^r}{\partial \tilde{A}\partial \tilde{B}_i}\frac{\partial \tilde{A}}{\partial n_i}\frac{\partial \tilde{B}_i}{\partial n_j} + \frac{\partial^2 A^r}{\partial \tilde{B}_1\partial \tilde{B}_i}\frac{\partial \tilde{B}_1}{\partial n_i}\frac{\partial \tilde{B}_i}{\partial n_j} + \frac{\partial^2 A^r}{\partial \tilde{B}_2\partial \tilde{B}_i}\frac{\partial \tilde{B}_2}{\partial n_i}\frac{\partial \tilde{B}_i}{\partial n_j} + \cdots + \frac{\partial^2 A^r}{\partial \tilde{B}_i^2}\frac{\partial \tilde{B}_i}{\partial n_i}\frac{\partial \tilde{B}_i}{\partial n_j} \end{array} \right]$$

$$+ \left[\frac{\partial A^r}{\partial n}\frac{\partial^2 n}{\partial n_i \partial n_j} + \frac{\partial A^r}{\partial \tilde{A}}\frac{\partial^2 \tilde{A}(\mathbf{n},T)}{\partial n_i \partial n_j} + \frac{\partial A^r}{\partial \tilde{B}_1}\frac{\partial^2 \tilde{B}_1(\mathbf{n})}{\partial n_i \partial n_j} + \frac{\partial A^r}{\partial \tilde{B}_2}\frac{\partial^2 \tilde{B}_2(\mathbf{n})}{\partial n_i \partial n_j} + \frac{\partial A^r}{\partial \tilde{B}_3}\frac{\partial^2 \tilde{B}_3(\mathbf{n})}{\partial n_i \partial n_j} + \cdots + \frac{\partial A^r}{\partial \tilde{B}_i}\frac{\partial^2 \tilde{B}_i(\mathbf{n})}{\partial n_i \partial n_j} \right]$$

$$= (\boldsymbol{\eta}'(\mathbf{n})_{n_i})^T \cdot \mathbf{A}^{\mathbf{r}''}(\boldsymbol{\eta}) \cdot \boldsymbol{\eta}'(\mathbf{n})_{n_j} + \mathbf{A}^{\mathbf{r}'}(\boldsymbol{\eta})^T \cdot \boldsymbol{\eta}(\mathbf{n})_{n_i n_j} \tag{3.21}$$

The idea of writing derivatives of a function into dot product of vector and matrix function are implemented through this work and also in programming.

3.4 *The algorithm for Fürst and Renon's implicit MSA term*

The simplified implicit MSA of Fürst and Renon[3] can be written in the following way:

$$F_{sMSA\_Furst} = \frac{A^r{}_{sMSA\_Furst}}{RT} = -\frac{\alpha_{sMSA}^2}{4\pi}\sum_i \frac{n_i z_i^2 \Gamma}{1+\Gamma\sigma_i} + \frac{\Gamma^3 V}{3\pi N_A}, \text{ where } \alpha_{sMSA}^2 = \frac{e^2 N_A}{\varepsilon_0 \varepsilon RT} \tag{3.22}$$

and

$$4\Gamma^2 = \alpha_{sMSA}^2 N_A \sum_i \frac{n_i}{V}\left[\frac{z_i}{1+\Gamma\sigma_i}\right]^2 \tag{3.23}$$

The relative permittivity ε is calculated as follows

$$\varepsilon = 1 + (\varepsilon_s - 1)\frac{1-\varepsilon_3}{1+\varepsilon_3/2} \tag{3.24}$$

Where ε_3 is calculated by the same equation as in (1.67): $\varepsilon_3 = \frac{N_A \pi}{6V}\sum_k n_k \sigma_k^3$ and the solvent relative permittivity ε_s can be calculated according to the equation (1.70).
Define the intermediate variables

$$X \triangleq \sum_i \frac{n_i z_i^2 \Gamma}{1+\Gamma\sigma_i} = \sum_i \frac{n_i z_i^2}{\sigma_i}\left(1 - \frac{1}{1+\Gamma\sigma_i}\right) \tag{3.25}$$

and

$$Y = \frac{\Gamma^3 V}{3\pi N_A} \tag{3.26}$$

And then equation (3.22) can be written as

$$F_{sMSA\_Furst} = \frac{A^r{}_{sMSA\_Furst}}{RT} = -\frac{\alpha^2_{sMSA}}{4\pi} X + Y, \text{ where } \alpha^2_{sMSA} = \frac{e^2 N_A}{\varepsilon_0 \varepsilon RT} \tag{3.27}$$

We got the equivalent composite function

$$F_{sMSA\_Furst} = F_{sMSA\_Furst}(\alpha^2_{sMSA}, X, Y) \tag{3.28}$$

This MSW term from Fürst is an implicit expression in term of Γ. Before using it to calculate derivatives, first Γ have to be solved from equation (3.23) and then use it to calculate other derivatives of Helmholtz free energy of this implicit simplified MSA term, the algorithms for program is presented below.

Algorithm 3.1

Function [Γ, A^r_{sMSA}, **d** A^r_{sMSA} **dx, d²** A^r_{sMSA} **dxdy**]=sMSA(T, P, **n**, **parameters**)

Call function [**parameters0**]=EOS_parameter_intialization(T, P, **n**, **parameters**)

Solve Γ at present conditions (T, P, **n**, **parameters0)** from equation $4\Gamma^2 = \alpha^2_{sMSA} N_A \sum_i \frac{n_i}{V}\left[\frac{z_i}{1+\Gamma\sigma_i}\right]^2$ using any equation root slover such as Newton-Raphson method.

Calculate the Helmholtz free energy of sMSA A^r_{sMSA}

Calculate the first order derivatives of Helmholtz free energy of sMSA **d** A^r_{sMSA} **dx**

Calculate the second order derivatives of Helmholtz free energy of sMSA **d²** A^r_{sMSA} **dxdy**

End function sMSA

Due to the complexity of deduction of the derivatives of implicit function, the deduction and final analytical expression of the first and second order derivatives of the simplified implicit MSA will not be presented in this chapter. It is documented in details in Appendix VI.

3.5 *The Uematsu and Franck model for water permittivity*

In electrolyte EOS, if the electrolyte terms accounting for the long range interactions adopted in the EOS belongs to the primitive model, the relative permittivity of solvent ε is needed during calculation. This is provided by an external model of the relative permittivity of the solvent or a simple temperature correlation of the relative

permittivity of the solvent. For aqueous systems the relative permittivity of water ε can be calculated by the equation suggested by Uematsu and Franck[4]. Its expression is:

$$\varepsilon = 1 + (\frac{A_1}{T_r})\rho_r + (\frac{A_2}{T_r} + A_3 + A_4 T_r)\rho_r{}^2 + (\frac{A_5}{T_r} + A_6 T_r + A_7 T_r{}^2)\rho_r{}^3 + (\frac{A_8}{T_r{}^2} + \frac{A_9}{T_r} + A_{10})\rho_r{}^4 \quad (3.29)$$

Where T_r and ρ_r equal:

$$T_r = T/T_0, \qquad \rho_r = \rho/\rho_0. \quad (3.30)$$

And the values of the coefficients are listed in the below table:

Table 3.1 The values of the coefficients for Uematsu-Frank model for the relative permittivity of water.

Coefficient		Value
A_1	=	7.62571
A_2	=	244.003
A_3	=	-140.569
A_4	=	27.7841
A_5	=	-96.2805
A_6	=	41.7909
A_7	=	-10.2099
A_8	=	-45.2059
A_9	=	84.6395
A_{10}	=	-35.8644
T_0	=	298.15 K
ρ_0	=	1000 kg/m^3

We define two auxiliary vectors $\boldsymbol{\rho}_\mathbf{r}$ and $\mathbf{F}(T)$

$$\boldsymbol{\rho}_\mathbf{r} \triangleq \begin{bmatrix} \rho_r \\ \rho_r{}^2 \\ \rho_r{}^3 \\ \rho_r{}^4 \end{bmatrix}, \quad \mathbf{F}(T) \triangleq \begin{bmatrix} \frac{A_1}{T_r} \\ \frac{A_2}{T_r} + A_3 + A_4 T_r \\ \frac{A_5}{T_r} + A_6 T_r + A_7 T_r{}^2 \\ \frac{A_8}{T_r{}^2} + \frac{A_9}{T_r} + A_{10} \end{bmatrix} \quad (3.31)$$

We further assume an approximation for the water density used in Uematsu-Franck model:

$$\rho = \frac{n_{water} M_{water}}{V} \quad (3.32)$$

Define water density ρ and system temperature T as the intermediate variables. Then the structure of the relative water permittivity ε from Uematsu-Franck model can be expressed in a graph as below:

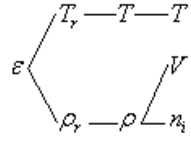

And then the expression of Uematsu-Franck model can be rewritten in the following simple expression:

$$\varepsilon(T, V, \mathbf{n}) = 1 + \boldsymbol{\rho}_\mathbf{r}(V, \mathbf{n}) \bullet \mathbf{F}(T) \quad (3.33)$$

The deduction and final analytical expression of the first and second order derivatives are documented in details in Appendix VI.

Reference

1. Michelsen ML, Mollerup JM, ed. *Thermodynamic Model:, Fundamentals and Computational Aspects.* Holte, Denmark: Tie-Line Publication.

3. Fürst W, Renon H. Representation of Excess Properties of Electrolyte Solutions Using a New Equation of State. *AIChE J*. 1993; 39: 335-343.

4. Uematsu M, Franck EU. Static dielectric constant of water and steam. *J Phys Chem Ref Data*. 1980; 9(4):1291-1305.

CHAPTER 4 Density data collection and databank

4.1 *Introduction*

Volumetric data are of interest in the industrial community. Density of electrolyte is frequently needed in many industrial applications. Volumetric property is also an important property in phase equilibrium calculation. The fugacity coefficients needed in phase equilibrium calculation are derived from Helmholtz free energy, which is a function taking volume as one of its variables. Volumetric data are also essential in parameter estimation for EOS. Information from volumetric measurements is needed for EOS to obtain parameters with physical meanings.

The co-volume parameter b of the cubic EOS is closely related to the microscopic molecular volumes in the mixture according to statistical mechanics, which is macroscopically indirectly related to the system volume. Ion-size parameter σ, if existing in electrolyte EOS, is also a parameter related to the macroscopic property volume. It is also shown in our parameter estimations that experimental data of volumetric properties have a significant effect on the values of b and σ. When volumetric data are included in the parameter estimation it is more likely to help the user to obtain better equilibrium calculations for mixture in the later stage.

Besides, volumetric property also serves as a good judging criterion for proper EOS selection. For non-electrolyte mixtures, it is generally accepted that poor density calculations are most likely due to the usage of an unadaptive EOS while a poor equilibrium calculation is most likely to suggest that the mixing rule is not very well chosen. This empirical rule for non-electrolyte systems is also believed to be constructive for developing electrolyte EOS. An electrolyte EOS which can give good predictions of volumetric properties at a wide temperature and pressure range is more reliable to use and physically sound.

4.2 *IVC-SEP electrolyte databank*

A databank has been developed in IVC-SEP, Department of Chemical Engineering. In 1994 Henrik Nicolaisen described a databank containing experimental activity/osmotic coefficient and SLE data for aqueous electrolytes. This databank has been expanded to contain data on the thermal properties of aqueous electrolyte solution by Thomsen *et al* too. [1] The existing IVC-SEP electrolyte databank for electrolyte systems contains a considerable amount of experimental data for electrolyte systems. More than twenty different types of experimental data for electrolytes are currently included in the databank, such as SLE, VLE and LLE data for electrolytes, osmotic coefficients, activity coefficients, density, AMV, heat of dilution, specific heat and excess heat capacity etc. Details please read Ph. D. thesis of Thomsen[1] and the on-line IVC-SEP electrolyte databank webpage: http://www.ivc-sep.kt.dtu.dk/databank/databank.asp.

The databank is under continuous extension and update. In the existing databank the amount of experimental data for density or AMV is quite rich and large, but still not complete. Density data for the electrolytes composed by the test system (water, Na^+, H^+, Ca^{2+}, Cl^-, OH^-, and SO_4^{2-}) currently studied in this project is limited, especially for binary data at various temperature range, binary data at high pressure and data of

electrolyte mixtures. Therefore, in this Ph. D. project, literature survey and data collection were conducted for volumetric data of the relevant electrolytes.

4.3 *The collected multi-temperature experimental data of volumetric properties*

Multi-temperature volumetric data are of particular interest. Volumetric data of some binary aqueous electrolyte systems are needed too. Unfortunately, a relatively large amount of experimental data for volumetric properties existing in the literature is incomplete. Volumetric data for electrolyte mixtures, such as aqueous ternary or higher systems, mixed-solvent systems are very scarce. Data measured at higher pressures or at temperatures different than room temperature are also limited. Most volumetric experimental data relevant to this study in literature are data of aqueous binary electrolyte systems at room temperature or zero degree Celsius and one atmosphere.

NaCl is the most extensively studied binary systems. Then it follows $CaCl_2$. A three-month literature study was conducted from over 6000 papers in the existing IVC-SEP electrolyte literature database. Besides the volumetric data in the databank, additionally 6815 new volumetric data points were collected. All of them are binary systems. These data can be added to the latest version of the IVC-SEP electrolyte databank later.

The collected experimental data were tabulated in six separate tables according to the electrolytes. The tables are presented in the Appendix VI. They are sodium chloride, calcium chloride, sodium bicarbonate, sodium carbonate, sodium hydroxide and hydrogen chloride. Experimental data for calcium bicarbonate, calcium carbonate and calcium hydroxide were not found in this literature study. This is due to the fact that the solubility of the above-mentioned three calcium electrolytes are so low that the change in the densities of their aqueous solution comparing with pure water is hardly measurable even at saturated concentration. Consequently few experimental data were reported in literature. For other six electrolyte systems, the sodium carbonate and hydrogen chloride aqueous solutions are not very extensively studied. No high pressure data is available. Only three sets of hydrogen chloride data and two sets of sodium carbonate data are measured at temperatures different then 25 °C and 1 atmosphere.

All of the data points collected in this chapter and listed in Appendix VI were digitalized manually and checked with their source. A computer program was used to retrieve data from the databank. The program retrieves the data specified by the user and converts all concentration units to molalities and all temperature units to Kelvin.

Reference

1. Thomsen K. Aqueous electrolytes: model parameters and process simulation, Ph. D. thesis. Technical University of Denmark, Denmark, 1997.

CHAPTER 5 Preliminary study of the implemented electrolyte EOS

5.1 *General*

The ultimate aim is to develop EOS for multi-component electrolyte systems with general ion-specific parameters. As mentioned in previous chapter, the regression of ion-specific parameters needs a huge collection of experimental data and it is a very time-consuming process. Therefore regression of ion-specific parameters is not suitable before it is certain that the program codes were correctly implemented and some basic experiences are obtained with the developed electrolyte EOSs. Consequently, the following preliminary studies of the electrolyte EOSs were done in this chapter. Is thit correcd?

1. Check the codes of the implemented six electrolyte EOSs and correct the errors. Test the electrolyte EOSs in salt-specific parameters.
2. Study how relative permittivity of water influences performance of electrolyte EOS in salt-specific parameters.
3. Study the SR2 term in salt-specific parameters; see whether it is necessary to have this term in the electrolyte EOS.
4. Find possible correlation functions in salt-specific parameters between electrolyte EOS parameters to reduce the number of parameters in the EOS.
5. Preliminary studies of MSW EOS in ion-specific parameters.

After these preliminary studies, it was assured that the codes were correct for the regression of ion-specific parameters in the next stage.

5.1.1 Salt-specific parameters

Regression of salt-specific parameters for one binary system needs much less time and less experimental data than for ion-specific parameters. The optimization is also simpler i.e. salt-specific parameters reduce the number of variables in objective function into half of that of ion-specific parameters for a single binary system.

Another advantage is that it can be used to check the implemented models. From a mathematical point of view, the optimized salt-specific parameters are a special case of the ion-specific parameters: cation parameters equal to anion parameters. The salt-specific parameters are actually the results of constrained optimization of ion-specific parameters. If satisfactory salt-specific parameters are found, i.e. mathematically speaking, it is equivalent to say that the model works at least with special sets of ion-specific parameters. This also indicates that the program code is unlikely to have serious errors and it is more likely to find satisfactory general ion-specific parameters later. On the contrary, no matter whether it is due to programming errors or the model itself, if the program does not work with ion-specific parameters, it will not work when using the salt-specific parameters.

Moreover the experience and knowledge obtained through regression of salt-specific parameters are helpful or even applicable for regression of ion-specific parameters. E.g. after reasonable salt-specific parameters have been obtained during optimization, they can be used as good starting guess when switching to ion-specific parameter optimization. The information obtained from salt-specific parameters is also useful for ion-specific parameter regression (such as the order of the magnitude of parameter

values). For these reasons, it is decided to use salt-specific parameters to conduct the first four preliminary studies in this chapter.

5.1.2 EOSs tested

The six electrolyte EOSs mentioned in section 2.6.1 of chapter 2 were used. They can be divided into two groups. The electrolyte EOSs without SR2 term: MSW EOS, mMSW EOS, eCPA EOS, SRK+DH EOS; and the electrolyte EOSs with SR2 terms: mMSW+SR2 EOS and eCPA+SR2 EOS. Note when using salt-specific parameters, mMSW EOS reduces to MSW EOS, due to the fact that the simplified implicit MSA term reduces to simplified explicit MSA term. The SRK+DH EOS was not tested through salt parameter fitting, and reasons are given in section 5.1.7. The MSW EOS was selected for the preliminary studies using ion-specific parameters for the simple reason that there are sufficient published results for comparison.

5.1.3 Test system

The test system focused on for salt-specific parameters is mainly binary aqueous NaCl at room temperature. It is simply because aqueous NaCl system is a typical strong electrolyte system and the experimental studies of this system were conducted in great details. The physiochemical knowledge of aqueous NaCl system is quite rich and good. The function of the osmotic coefficient or mean ionic activity coefficient versus molality of the aqueous NaCl has a minimum value at concentration interval between 0 and 6 molal. The function curvature follows a tick shape: it decreases from one to a positive minimum value and increases again when molality increases. Usually, any electrolyte EOS has no difficulties to correlate the osmotic coefficient or mean activity coefficient functions if their curvature resembles an exponential-decay function. However, a tick-shaped osmotic coefficient or mean activity coefficient curve could create potential problems in data correlation for an electrolyte EOS. Aqueous NaCl system belongs to this group, thus it is worthy to be used as a test tool. If the EOS works well with this system, it can be continuously used with other systems. Otherwise either the EOS or the parameter schemes have to be changed. To compare our results with those of Myers *et al.*[1], the same activity and osmotic coefficient data generated from Archer's[2] model were used as in the paper. The experimental density data of NaCl used in this chapter are from the paper from Rogers *et al.*[3]

Myers *et al.* published three types of results in their paper [1]:

1. The numerical results (average absolution deviations) of the correlations for 138 aqueous electrolyte solutions at 25 ºC and 1 bar.
2. The numerical and graphical results of the correlations for seven aqueous electrolyte solutions from 0 to 300 ºC and 1 to 120 bar.
3. The graphical results of two aqueous multi-component electrolyte systems.

For the seven aqueous systems at wide temperature and pressure range, the following six out of seven aqueous systems were chosen for reproducing the published slat-specific parameter results and the preliminary study of MSW EOS using ion-specific parameters: NaCl, NaBr, $CaCl_2$, Li_2SO_4, Na_2SO_4, K_2SO_4 and water.

The system of aqueous Cs_2SO_4 was not selected. The test system contained seven ions in total if the H^+, OH^- ions are neglected: Na^+, K^+,Ca^{2+},Li^+, Cl^-, SO_4^{2-}, Br^-. The experimental data from the same source as in the Myers' paper [1] are used in the reproduction of the published results and the preliminary ion-specific parameter

regression. The published MSW EOS results of the six aqueous electrolyte systems were reproduced accurately and successfully. The reproduced graphical results are presented in Appendix VIII.

5.1.4 Thermodynamic properties

With regard to the physical properties to be chosen for parameter fitting, there are several options. Saturated vapour pressure as the experimental input is one choice. However, as found by many authors in the literature, fitting of the vapour pressures alone does not suffice.

Another choice is the osmotic coefficient, which usually is determined from isopietic measurements. It can be directly calculated from the vapour pressure at low pressures too by

$$\Phi = -1000 \frac{\ln\left(P_w / P_w^{\,0}\right)}{\nu m M_w} \tag{5.1}$$

In the logarithm it is the ratio of the partial pressure of water to the vapour pressure of pure water. m is the molality.

The mean ionic activity coefficient has been reported to be another choice. It is related to the osmotic coefficient, it can also be derived independently from electromotive force data[4,5].

The osmotic coefficient can be calculated from the osmotic pressure, which is a directly measurable experimental property, while mean ionic activity coefficient is an indirectly calculated property. Therefore, it is preferable to use the measurable physical properties to retrieve information for the model. Thus the osmotic coefficient will be fitted during the salt-specific parameter optimization instead of mean ionic activity coefficient after section 5.2.2. The differences are not very significant according to the tests done.

Fitting of the salt-specific parameters can produce multiple parameter sets. To obtain an effective set of parameters with physical sense, it is also recommended to either include density data in the parameter fitting process in addition to the mean ionic activity coefficient or the osmotic coefficient data. Or use it as judging criteria for choosing the multiple parameter sets. This is analogous to the fitting of parameters for non-electrolytes to vapour pressure and liquid density data. We use experimental data of osmotic coefficients, mean ionic activity coefficients and densities in parameter regression.

5.1.5 Optimization program

It is a common knowledge that with the increase of the degrees of freedom of the objection function in parameter estimation, the local minima and the computation time to find a local minimum will normally increase consequently. This will create a lot of difficulties for the parameter optimization process. To solve the problem in the case of salt-specific parameters, we adopt a global optimization program for searching all possible local minimum in a predefined space (intervals) and reducing the number of variables in the objective function by constrains.

The numerical tool available for the optimization of salt-specific parameters is a user-friendly Matlab global optimization program. The electrolyte EOSs are made into Fortran dll file called by the Matlab global optimization program. This increased the computational speed significantly.

The numerical tool available for the optimization of ion-specific parameters is a Fortran optimization routine. The Fortran routine is much faster than the Matlab program. It is more suitable for large-scale optimisation such as the simultaneous regression of all ion-specific parameters. A gradient method (Marquardt method) and a direct search method (Nelder-Mead simplex search method) for non-linear least square minimization have been adopted in the Fortran program. It was found that an alteration between the two optimization methods yields good results. Details of the Fortran optimisation program are described in Chapter 6.

5.1.6 The objective function and the numerical criteria of goodness-of-fit

Two most-commonly-used error functions are suggested for salt-specific parameter optimization: the first one is the sum of the square of the errors (residuals) of experimental and calculated points.

$$FF_1(x_i) = \sum_{i=1}^{N} \left(x_i^{\text{experiment}} - x_i^{\text{calculated}} \right)^2 \tag{5.2}$$

The second one is the sum of the square of the relative error between experimental and calculated points.

$$FF_2(x_i) = \sum_{i=1}^{N} \left(\frac{x_i^{\text{experiment}} - x_i^{\text{calculated}}}{x_i^{\text{experiment}}} \right)^2 \tag{5.3}$$

Based on the accomplished tests the above two objective functions perform similarly in optimizing the salt-specific parameters for the electrolyte EOSs. The differences in final parameters obtained are small, so after section 5.2.2 we just use objective function FF_1 (5.2) for our salt-specific parameter optimization. x_i can be mean ionic activity coefficient $\gamma_{\pm}^{m}$ or osmotic coefficient Φ.

The ion-specific parameters were determined through a weighted least squares fit. The sum of the weighted squares of the residuals (i.e. difference between the calculated results and the corresponding values of experimental data) is calculated as follow.

$$f = \sum_{j=1}^{2} \sum_{i=1}^{N_j} \left(w_j \frac{x_{ij}^{\text{exp}} - x_{ij}^{cal}}{x_{ij}^{\text{exp}}} \right)^2 + \sum_{i=1}^{N_{AMV}} \left[w_{AMV} \left(\rho_i^{\text{exp}} - \rho_i^{cal} \right) \right]^2 \tag{5.4}$$

where x_{ij}^{cal} and x_{ij}^{exp} are the calculated value and the corresponding experimental value of osmotic coefficient or molal mean ionic activity coefficient. ρ is the density. w_j is the weight for the data of type *j*.

After the optimization, additional numerical criteria are needed to evaluate the goodness-of-fit of the data points. Two mostly-used numerical criteria for goodness-of-fit are chosen: the Absolute Average Deviation, denoted as AAD (5.5) and the absolute Average Relative Deviation, denoted as ARD (5.6).

$$AAD\% = \frac{\sum_{i=1}^{N} \left| x_i^{\text{experiment}} - x_i^{\text{calculated}} \right|}{N} \times 100\% \tag{5.5}$$

$$ARD\% = \frac{\sum_{i=1}^{N} \left(\left| \frac{x_i^{\text{experiment}} - x_i^{\text{calculated}}}{x_i^{\text{experiment}}} \right| \right)}{N} \times 100\% \tag{5.6}$$

Below, the Absolute Average Deviation (AAD) and the absolute Average Relative Deviation (ARD) are calculated for the physical properties of the salt studied.

5.1.7 The model check

Before the parameter optimization the codes of the electrolyte EOSs have to be correct or it will be a waste of time and energy to do any work. The following four testing methods are applied to check these EOSs:

1. Numerical check of all analytical derivatives. This is done by using a Matlab program "checkgradient", developed by information and mathematic department of DTU[6]. For details of the program please refer to the homepage: http://www2.imm.dtu.dk/courses/02611/. If the program code passed the test, it is guaranteed that the analytical derivatives are mathematically correct. Errors like wrong units or input errors or wrong physical constant cannot be detected by "checkgradient".
2. Consistence test of all implemented EOSs.
3. Apart from the thermodynamic consistence test and the numerical methods to check the derivatives, an alternative way is to test the model using salt-specific parameters:
    - If there are published salt-specific parameters for the model (e.g. MSW EOS), first try to reproduce the published results in the original paper with the published corresponding parameters before go to the second step. If not, directly go to the second step.
    - Try to fit the model to a few typical electrolyte systems using salt-specific parameters and see how it works.

    This step helps to discover units errors or wrong physical constant and such kind of non-mathematic errors.
4. Try to estimate some ion-specific parameters of the electrolyte EOS with a test system and compare the results with salt-specific parameters. (Only done for MSW EOS here due to sufficient published results for comparison.)

The SRK+DH EOS was not undergoing test 3. This EOS only passed the first two tests. Because the code of SRK EOS is the existing one used in IVC-SEP, which has been checked and used for years. The DH term used are checked against the DH model of IVC-SEP and produced the same results. So it is safe to use them.

5.2 *The study of the effect of the relative permittivity in salt-specific parameters*

In Fürst and Renon's paper[7] and Solbraa's Ph.D. thesis[8], Pottel's model is used to calculate the relative permittivity. We would like to study the effect of the relative permittivity and its derivatives on the performances of the electrolyte EOS. According to Fürst, [7] a constant relative permittivity is sufficient. According to Myers *et. al*[1] , it is important to consider the relative permittivity as a function of temperature and density. It is our experiences that a relative permittivity as a function of temperature, density and composition plays an important role in improving the performance of the electrolyte EOS. To study the effects of relative permittivity in salt-specific parameters, the following plan has been made to fit the experimental data. The ion-specific parameters estimation was also carried out following this plan in section 5.6:

1. With a fixed relative permittivity (constant ε) at the desired temperature, for example at 25 °C, ε=78.5. In this case all derivatives of the relative permittivity ε are zero in calculation.
2. Use Pottel model to calculate the relative permittivity and the derivatives at the desired temperature.
3. Use Uematsu-Franck[9] (UF) model to calculate the relative permittivity and the derivatives at the desired temperature.

5.2.1 Constant relative permittivity

5.2.1.1 EOS without SR2 term

To study how relative permittivity influences the performance of electrolyte EOS, we start with a simple case: a constant water relative permittivity at 25°C. The objective functions used were function FF_1 and function FF_2. Both mean ionic coefficient and osmotic coefficient experimental data at 25°C have been tried. It is discovered that with a fixed relative permittivity ε, none of the EOSs without SR2 term was able to fit the experimental data with zero interaction parameter k_{ij}. The graphical results of MSW/mMSW EOS (note now MSW EOS = mMSW EOS) are presented. The results of eCPA EOS look very similar thus omitted. From the Figure 5.1 and Figure 5.2, it can be seen that under this condition the model could not capture the curvature of both osmotic coefficient and the mean ionic activity coefficient functions.

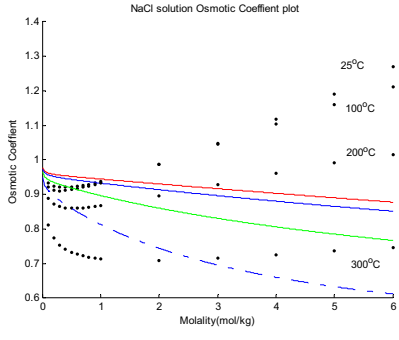

Figure 5.1 The computation results of osmotic coefficient of aqueous NaCl solution by mMSW EOS. The parameters used were optimized by mean ionic activity coefficients at 25°C. The red solid line, blue solid line, green solid line and the blue dashed line are the calculated values at 25°C, 100°C, 200°C, 300°C respectively.

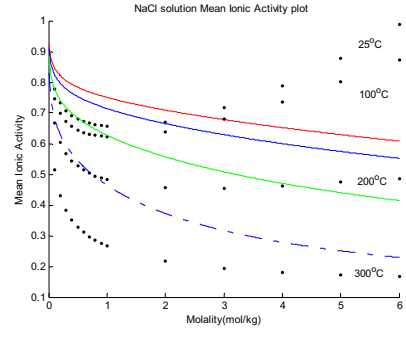

Figure 5.2 The mean activity coefficient of aqueous NaCl solution by mMSW EOS. The parameters used were optimized by mean ionic activity coefficients at 25°C. The red solid line, blue solid line, green solid line and the blue dashed line are the calculated values at 25°C, 100°C, 200°C, 300°C respectively.

The predicted results at other temperatures are also plotted in order to study the temperature predictive ability of the electrolyte EOSs. Note at temperatures other than 25°C, the plotted results are pure predictions based only on the fitted parameters of the experimental data at 25°C. The relative permittivity ε used at 25°C, 100°C, 200°C,

300°C are 78.5, 55.4767, 35.3361, and 20.3776 respectively. They are taken from a physical chemistry handbook.

5.2.1.2 EOSs with SR2 term

According to literature, the solution relative permittivity ε changes along with the solution concentration and temperature. But when SR2 term was used, even with a constant relative permittivity for water, mMSW and eCPA EOS can correlate the data. mMSW+SR2 EOS and eCPA+ SR2 EOS are able to fit the experimental data of mean ionic activity or osmotic coefficients of NaCl at 25°C using a constant ε. SR2 term can improve the correlations. Note there is an additional binary interaction parameter W_{ij} in SR2 term.

If the thermodynamic properties used in the parameter fitting are changed from mean ionic activity coefficient to osmotic coefficient, there is a slight change in the values of the final parameter sets. It is because the mean ionic activity coefficient and the osmotic coefficient impose different weights during parameter optimization when the same objective function is used. But the differences are negligible.

The detailed numerical and graphical results are presented in the later section 5.3.1 when we study the SR2 term. The parameter regression shows that the mMSW+SR2 and eCPA+SR2 EOS work properly and the program source codes seem to be correct.

5.2.2 Pottel model for relative permittivity

In this section, the results shown here are those of the EOSs without SR2 term. For even with a constant relative permittivity, the EOSs with SR2 term could fit the experimental data of NaCl at 25°C. Therefore the EOSs with SR2 term can not directly and clearly exhibit the effects of the Pottel model to the model performances. For EOSs without SR2 term, they can not fit the experimental data with a constant relative permittivity. When switching from constant relative permittivity to Pottel model, if there are any improvement of the data fittings, it is clearly due to the contribution of Pottle model.

5.2.2.1 EOSs without SR2 term

To study the influence of the relative permittivity models further, we start to treat the relative permittivity as a function of temperature and composition. The relative permittivity model used here is the Pottel model.

Table 5.1 The results for parameters optimization for mMSW EOS using relatively permittivity calculated by Pottel model. Parameters are optimized using osmotic coefficient at 25°C.

	x_{opt}					Objective function	γ		Osmotic coefficient	
Number of Local minimum	$a_a=a_c$	$b_a=b_c$	$\sigma_a=\sigma_c$	Wij	K_{ij}	FF_1 (Φ)	AAD	ARD	AAD	ARD
	Pa*m^6/mol	cm^3/mol	Å	cm^3						
1	0.1346	5.7734	4.3039	0	0	1.61E-04	6.84E-03	9.48E-03	2.89E-03	2.84E-03
2	25.7413	89.4963	6.5432	0	0	2.98E-04	2.25E-02	3.10E-02	3.76E-03	3.90E-03
3	18.9578	97.1690	6.7403	0	0	3.50E-04	2.41E-02	3.32E-02	4.08E-03	4.23E-03

Following the scheme to conduct the parameter set optimization, multiple parameter sets have again been discovered in this case. Osmotic coefficients at 25°C have been used here. The optimised parameter sets for mMSW EOS and eCPA EOS are presented in Table 5.1 and Table 5.2 respectively. It is discovered that EOSs without SR2 term were able to fit the experimental data at 25°C satisfactorily after using Pottel model. Predictions at higher temperatures are also conducted and plotted with the fitting results as before.

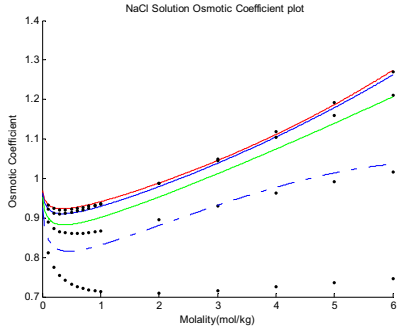

Figure 5.3 The computation results of osmotic coefficient of aqueous NaCl solution for mMSW EOS parameter set No. 1 [0.13462, 5.77344, 4.30393]. The red solid line, blue solid line, green solid line and the blue dashed line are the calculated values at 25°C, 100°C, 200°C, 300°C respectively.

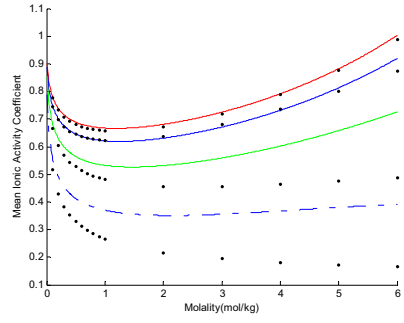

Figure 5.4 The computation results of mean ionic activity coefficient of aqueous NaCl solution for mMSW EOS parameter set No. 1 [0.13462, 5.77344, 4.30393]. The red solid line, blue solid line, green solid line and the blue dashed line are the calculated values at 25°C, 100°C, 200°C, 300°C respectively.

The best three parameter sets of mMSW EOS are presented in Table 5.1 and they were used to calculate the mean ionic activity coefficient, density and osmotic coefficient. Only graphical results of set No.1 are shown. From the Figure 5.3 and Figure 5.4, it can be seen that the model could follow the curvature of both osmotic coefficient and the mean ionic activity coefficient function. Using parameter set number one of mMSW EOS, [0.13462, 5.77344, 4.30393], not only at 25°C does the model give a good correlation, but at 100°C, and 200°C it gives qualitatively correct predictions. However at 300°C, the errors of predictions for mean ionic activity coefficient and osmotic coefficient are large though the predicted trend is still correct. The predicted results of osmotic coefficient are slightly poorer than those of mean ionic activity coefficient at temperatures higher than 25°C, yet still quite good. For density, it gives a qualitatively good prediction at 25°C, 100°C and 200°C. The computational results show a clear trend that follows the experimental data. At 300°C, the trend of the predicted density is wrong: there is a non-existed maximum within the concentration range.

The values of *a* and *b* in parameter set one of the eCPA EOS are smaller than those of modified MSW EOS in Table 5.1. The attraction parameter *a* of eCPA EOS is one order of magnitude smaller than that of the mMSW EOS (around 1/10), while the covolume parameter *b* of eCPA EOS is about half of that in mMSW EOS, yet still at the same order of magnitude. The values of the fitted ionic diameter σ are reasonable.

Table 5.2 The results for parameters optimization for eCPA EOS with Pottel model. Parameters are optimized using osmotic coefficient at 25°C.

Number of Local minimum	x_{opt} $a_a=a_c$ Pa*m^6/mol	$b_a=b_c$ cm^3/mol	$\sigma_a=\sigma_c$ Å	Wij	$\sigma=(3b/(2\pi N_A))^{1/3}$ cm^3	$\sigma=(6b/(\pi N_A))^{1/3}$ Å	γ AAD	γ ARD	Osmotic coefficient AAD	Osmotic coefficient ARD
1	0.0121	2.4418	4.4029	0	1.246	1.979	0.006	0.009	0.004	0.004
2	7.493E-12	6.0729	5.0786	0	1.689	2.681	0.014	0.019	0.009	0.009
3	5.219E-12	16.7149	6.2948	0	2.367	3.757	0.091	0.125	0.075	0.074
4	0.0068	0.0001	2.8273	0	0.039	0.063	0.173	0.222	0.125	0.116
5	3.6495	81.2569	7.7475	0	4.009	6.364	0.343	0.471	0.307	0.307

In Figure 5.7 and Figure 5.6, the activity and osmotic coefficients predicted by eCPA EOS are reasonable when it is below 200°C. The predictability is similar as the mMSW EOS. At 300°C the prediction fails at 4 molal. The predicted densities are positively deviated from the experimental data at 25°C, which is worse than the mMSW EOS. Compared with the correlation results in previous section 5.2.1.1, the Pottel model improves the goodness-of-fit when used in electrolyte EOSs.

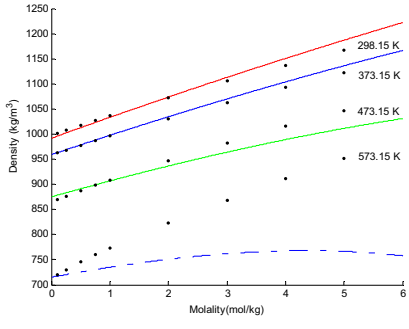

Figure 5.5 The density of aqueous NaCl solution predicted by mMSW EOS using parameter set (1), [0.13462, 5.77344, 4.30393]. The red solid line, blue solid line, green solid line and the blue dashed line are the calculated values at 25°C, 100°C, 200°C, 300°C respectively.

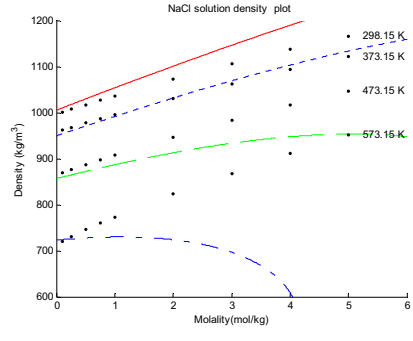

Figure 5.6 The density of aqueous NaCl solution predicted by eCPA EOS using parameter set (1), [0.012167, 2.441844, 4.402929]. The red solid line, blue solid line, green solid line and the blue dashed line are the calculated values at 25°C, 100°C, 200°C, 300°C respectively.

When using parameter set number 2 or number 3 for mMSW and eCPA EOS, the predicted results of $\gamma_{\pm}^{m}$, Φ and density at high temperatures are largely deviated. They are not a physically sound local minimum. This also indicates that some physically incorrect but mathematically sound local minimum can be found if density data are not used in combination with experimental data of the osmotic or mean ionic activity coefficient in parameter optimization. To improve the density prediction, it is necessary to introduce density data into the parameter optimization.

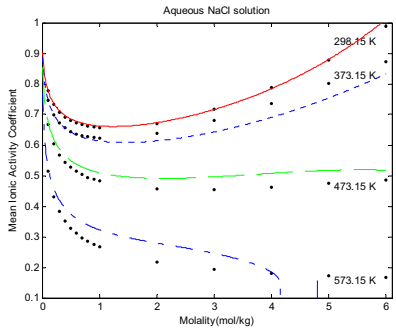

Figure 5.7 The mean ionic activity coefficient plot of aqueous NaCl solution using parameter set (1) of eCPA EOS, [0.012167, 2.441844, 4.402929].

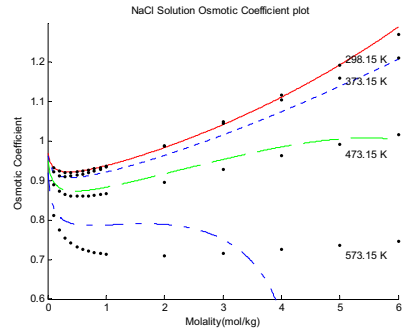

Figure 5.8 The osmotic coefficient plot of aqueous NaCl solution using parameter set (1) of eCPA EOS, [0.012167, 2.441844, 4.402929].

5.2.2.2 EOSs with SR2 term

The electrolyte EOSs with constant relative permittivity can correlate the osmotic coefficients of NaCl at 25 °C fairly well if SR2 term is used. The Pottel model is introduced to see whether it will significantly improve the goodness-of-fit. However, unfortunately the Pottel model improves the fitting very slightly in this circumstance. The correlation results show there are no significant improvements in goodness-of-fit for the electrolyte EOSs with SR2 term. The difference is so small that the graphical results look almost similar. Only the ARDs and AADs show small differences in digits. The similar numerical and graphical results are therefore omitted here.

5.2.3 Uematsu-Franck model for relative permittivity

For EOSs without SR2 term, when switching from constant relative permittivity to UF model, there are improvements in the data fittings. However eCPA EOS still can not fit the experimental data satisfactorily with UF model while MSW EOS can. For EOSs with SR2 term, when switching from constant relative permittivity to UF model, there are little improvements in the data fittings.

5.2.3.1 EOSs without SR2 term

The optimized salt-specific parameters of MSW EOS for NaCl systems at 25 °C were published in the paper of Myers *et al.* [1] The generated experimental data from the same source are used in the parameter optimization (only $\gamma_{\pm}^{m}$) and their parameters were obtained. The results can be reproduced by us here, but more than one local minimum were found. Similar as in previous cases, these local minima are not the best parameter sets. The published parameters [2.4611 34.6464 4.322] for NaCl at 25 °C were used in calculations and predictions, and the results are presented in below Figure 5.9 and Figure 5.10. For MSW EOS, the predictions at other temperatures (above 25 °C) are bad, though using UF model for ε helps the electrolyte EOS to correlate the mean ionic activity or osmotic coefficients. The predicted densities of MSW EOS are worse than that of eCPA EOS and consequently not shown. As

mentioned, mMSW EOS is equivalent to MSW EOS when using salt parameters. The mMSW EOS has been tested with the same parameter sets and exactly the same results as MSW EOS below were obtained.

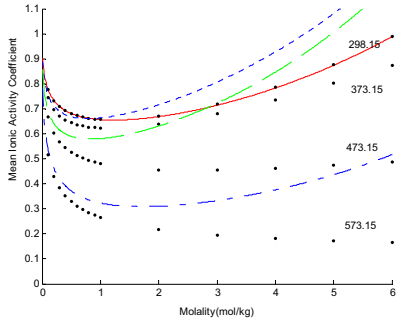

Figure 5.9 The mean ionic activity coefficient plot of aqueous NaCl solution of MSW EOS using parameter [2.4611, 34.6464, 4.3220].

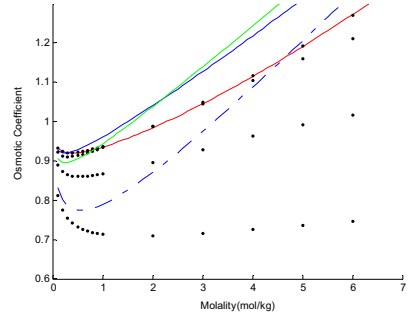

Figure 5.10 The osmotic coefficient plot of aqueous NaCl solution of MSW EOS using parameter [2.4611, 34.6464, 4.3220].

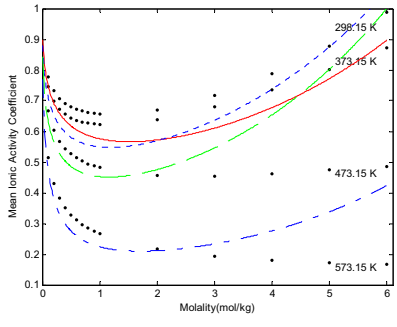

Figure 5.11 The mean ionic activity coefficient plot of aqueous NaCl solution of eCPA EOS using parameter set (1), [0.36757, 20.84411, 2.08644].

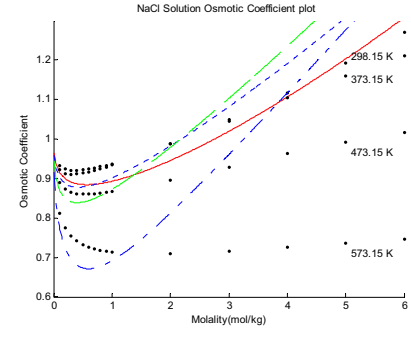

Figure 5.12 The osmotic coefficient plot of aqueous NaCl solution of eCPA EOS using parameter set (1), [0.36757, 20.84411, 2.08644].

Table 5.3 The results for parameters optimization for eCPA EOS using UF model. Parameters are optimized using osmotic coefficient for NaCl at 25°C.

x_{opt}			Wij			Objective function	γ	Osmotic coefficient
$a_a=a_c$	$b_a=b_c$	$\sigma_a=\sigma_c$		$\sigma=(3b/(2\pi N_A))^{1/3}$	$\sigma=(6b/(\pi N_A))^{1/3}$	FF_1 (Φ)	ARD%	ARD%
$Pa*m^6/mol$	cm^3/mol	Å	cm^3	Å	Å			
0.3676	20.8441	2.0864	0	2.547	4.044	0.017	10.248	3.313
0.0129	3.1259	2.1118	0	1.353	2.148	0.631	27.515	14.630

Same procedure was repeated for eCPA EOS. The correlation of osmotic coefficients of eCPA EOS is not as good as MSW EOS. The temperature predictability is also bad. But compared with the results of constant relative permittivity, it is a big improvement.

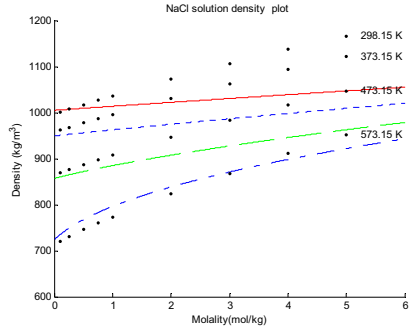

Figure 5.13 The predicted density of aqueous NaCl solution using eCPA EOS parameter set (1), [0.36757, 20.84411, 2.08644].

5.2.3.2 EOSs with SR2 term

Similar as for the electrolyte EOSs with SR2 term using Pottel model in salt-specific parameters, the use of UF model is expected to significantly improve the goodness-of-fit for these EOSs. This was validated by the test results of the EOSs using UF model in this scenario. The correlation results show after using UF model there are no significant improvements in goodness-of-fit for the electrolyte EOSs with SR2 term, just as the case of Pottel model.

To summarise the study of the influence of the relative permittivity for water to electrolyte EOS, it shows that the derivatives of relative permittivity help to improve the performance of electrolyte EOS in salt-specific parameters significantly.

5.3 *The study of SR2 term in salt-specific parameters*

The SR2 terms can improve the performances of electrolyte EOS, especially when the goodness-of-fit is poor. This was validated in the cases of EOSs using constant relative permittivity and eCPA EOS using UF model. When the electrolyte EOS can provide a good correlation without SR2 term, using this term will not improve the goodness-of-fit or predictions significantly. Meanwhile, using SR2 term is at the cost of decreasing the computational speed of the electrolyte EOS and increasing the complexity of the EOS. Therefore, it is preferable not to use SR2 term if not necessary.´

5.3.1 Constant relative permittivity

When SR2 term is used, mMSW+SR2 EOS and eCPA+ SR2 EOS are able to obtain a good fit of the activity coefficients of NaCl at 25°C even with constant relative

permittivity. After using the global optimization algorithm, we locate more than twenty local minimums for mMSW+SR2 EOS and eCPA+SR2 EOS respectively. Only the results of mMSW+SR2 EOS are presented as an example. eCPA+SR2 EOS generally gives the similar results only slightly poorer in density prediction.

Table 5.4 The optimization results for mMSW+SR2 EOS parameters fitting. Parameters are optimized using mean ionic activity coefficient at 25°C.

	x_{opt}					Objective function	γ		Osmotic coefficient	
Number of Local minimum	$a_a=a_c$	$b_a=b_c$	$\sigma_a=\sigma_c$	Wij	K_{ij}	$FF_1(\gamma)$	AAD	ARD	AAD	ARD
	$Pa*m^6/mol$	cm^3/mol	Å	cm^3						
1	0.6711	15.2604	4.5145	-26.7268	0	5.09E-06	4.66E-04	6.47E-04	1.18E-03	1.24E-03
2	66.4860	152.9776	7.6728	40.5424	0	8.30E-04	6.51E-03	8.83E-03	8.92E-03	9.11E-03
3	174.4958	259.7745	9.3486	134.6825	0	1.01E-03	6.55E-03	9.03E-03	9.49E-03	9.91E-03
4	363.6738	377.2406	10.7103	-37.5727	0	1.01E-03	6.40E-03	8.85E-03	9.66E-03	1.02E-02
5	0.1294	5.6875	6.1756	-0.3608	0	1.48E-01	5.91E-02	7.66E-02	6.44E-02	5.88E-02
6	0.8937	17.3449	1.911E+08	-2.4352	0	2.43E-01	9.34E-02	1.20E-01	1.04E-01	9.81E-02
7	2.8193	32.0990	16.7103	0.0322	0	2.90E-01	1.10E-01	1.44E-01	9.95E-02	9.13E-02
8	7.5144	53.4490	11.0771	0.1304	0	3.18E-01	9.65E-02	1.19E-01	1.13E-01	1.03E-01
9	2.1024	27.4909	20.0741	0.0000	0	3.25E-01	1.25E-01	1.67E-01	9.68E-02	8.85E-02
…….										

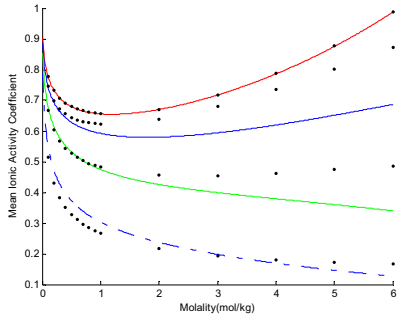

Figure 5.14 The mean ionic activity coefficient of aqueous NaCl solution for mMSW+SR2 EOS using [0.6711, 15.2604, 4.5145, -26.7268]. The red solid line, blue solid line, green solid line and the blue dashed line are the calculated values at 25°C, 100°C, 200°C, 300°C respectively.

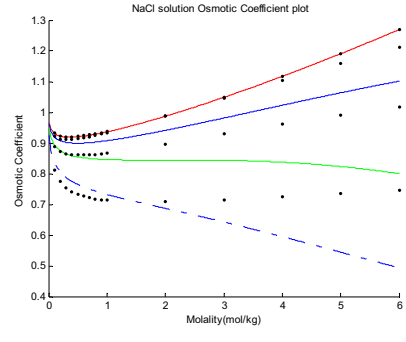

Figure 5.15 The osmotic coefficient of aqueous NaCl solution for mMSW+SR2 EOS using [0.6711, 15.2604, 4.5145, -26.7268]. The red solid line, blue solid line, green solid line and the blue dashed line are the calculated values at 25°C, 100°C, 200°C, 300°C respectively

In the Table 5.4, the first nine best local minimums of mMSW+SR2 EOS are provided. Judging by the ARDs for the calculated mean ionic activity coefficients and osmotic coefficients, local minimum one to four are similarly good. But when we calculated the mean ionic activity coefficient, density, osmotic coefficient versus concentration (molality) at different temperatures, only parameter set one is physically correct. Parameter set one, [0.6711, 15.2604, 4.5145, -26.7268], gives qualitatively good predictions at temperatures other than 25°C. The predicted results

for osmotic coefficient are slightly poorer than those of mean ionic activity coefficient at higher temperatures. The predicted results using parameter set number 2 and number 4 are largely deviated.

For density, using parameter set one of mMSW EOS, it gives a qualitatively good prediction at 25°C and 100°C, but at 200°C or higher, the trend of the calculated density is wrong: it is decreasing with the molality at 300°C. The predicted results of density for set number 2 and number 4 are completely wrong.

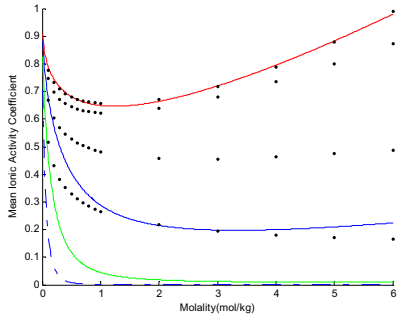

Figure 5.16 The mean ionic activity coefficient of aqueous NaCl solution for mMSW+SR2 EOS using [66.4860, 152.9776, 7.6728, 40.5424].

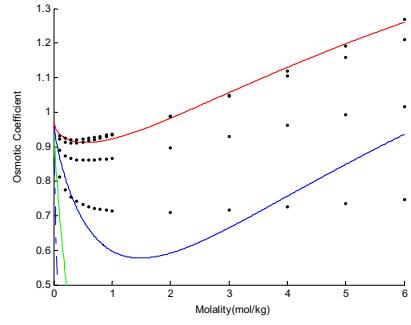

Figure 5.17 The osmotic coefficient of aqueous NaCl solution for mMSW+SR2 EOS using [66.4860, 152.9776, 7.6728, 40.5424]..

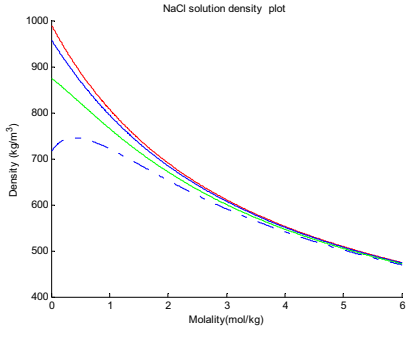

Figure 5.18 The density of aqueous NaCl solution for mMSW+SR2 EOS using [66.4860, 152.9776, 7.6728, 40.5424]. The red solid line, blue solid line, green solid line and the blue dashed line are the calculated values at 25°C, 100°C, 200°C, 300°C respectively.

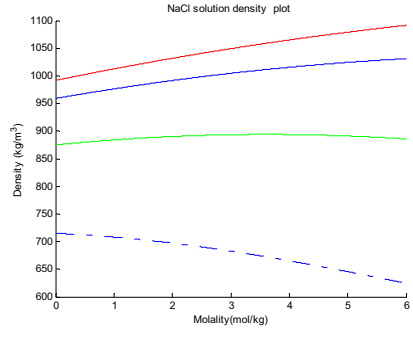

Figure 5.19 The density of aqueous NaCl solution for mMSW+SR2 EOS using [0.6711, 15.2604, 4.5145, -26.7268]. The red solid line, blue solid line, green solid line and the blue dashed line are the calculated values at 25°C, 100°C, 200°C, 300°C respectively.

From this study of the constant relative permittivity with SR2 term, it is known that if the relative permittivity is treated as a constant in EOS, it is relatively difficult to obtain a good fitting of mean ionic activity coefficient or osmotic coefficient without the additional SR2 term.

5.3.2 Pottel model for relative permittivity

The SR2 term can not help to archive better correlation results for any of the EOSs using Pottel model tested in salt-specific parameters. The mMSW and eCPA EOS can correlate the osmotic coefficients of NaCl at 25 °C fairly well if Pottel model is used to calculate the water relative permittivity. Afterwards the SR2 term is introduced to see whether it will significantly improve the goodness-of-fit. Unfortunately it improves the fitting very slightly in these circumstances. The obtained EOS parameters are quite similar to or essentially the same as those without SR2 term. The additional interaction parameter W_{ij} in SR2 term are almost equal to zero in many parameter sets, which suggests there is not much influence from the SR2 term to the goodness-of-fit here. The differences of the results are so small that the graphical results look almost identical with or without SR2 terms. Only the ARDs and AADs show some differences in last few digits. The similar numerical and graphical results are therefore omitted here. This indicates there is not much improvement in data correlation after introducing the SR2 term and the salt-water interaction parameter W_{ij} for the EOSs. This study shows for the electrolyte EOSs with Pottel model no significant improvements in goodness-of-fit are achieved after further introducing SR2 term.

5.3.3 UF model for relative permittivity

There are no significant improvements for mMSW EOS (MSW EOS) using UF model in correlating experimental data when the additional SR2 term is introduced. The reason is simple: they can already provide a fairly good correlation without SR2 term using UF model and there are not much left to be improved. But for eCPA EOS using UF model for relative permittivity, it is different. The eCPA EOS (with UF) can not correlate experimental data equally well as mMSW EOS under this circumstance. With the help of SR2 term, eCPA EOS (with UF) can satisfactorily reproduce experimental data of aqueous NaCl solution at 25 °C.

Table 5.5 The results for parameters optimization for eCPA+SR2 EOS using UF model. Parameters are optimized using osmotic coefficient and density data for NaCl at 25°C.

	x_{opt}						Objective function	γ	Osmotic coefficient	density
	$a_a=a_c$	$b_a=b_c$	$\sigma_a=\sigma_c$	Wij	$\sigma=(3b/(2\pi N_A))^{1/3}$	$\sigma=(6b/(\pi N_A))^{1/3}$	FF_1 (Φ, ρ)	ARD%	ARD%	ARD%
No.	Pa*m^6/mol	cm^3/mol	Å	cm^3	Å	Å				
1	0.0340	4.2550	4.2359	-17.7103	1.5000	2.3811	3.82E-05	0.104	0.122	0.560
2	0.0108	3.5828	4.3351	-15.8158	1.4164	2.2484	4.38E-05	0.110	0.116	0.602
3	0.0080	3.4402	4.3521	-15.6210	1.3974	2.2182	4.89E-05	0.124	0.120	0.612
4	0.0490	4.5186	4.2042	-18.7269	1.5303	2.4292	6.11E-05	0.152	0.149	0.547
5	0.1766	18.4944	3.7113	87.2922	2.4479	3.8858	3.25E-03	0.569	0.300	1.615
…….										

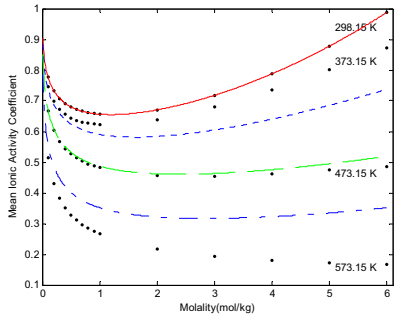

Figure 5.20 The mean ionic activity coefficient plot of aqueous NaCl solution of parameter set (1) of eCPA+SR2 EOS, [0.03103, 4.25983, 4.25436,-17.33781] (Pa*m^6/mol, cm^3/mol, Å, cm^3).

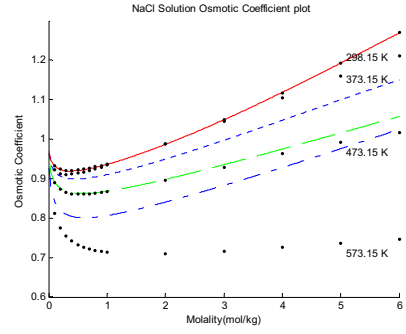

Figure 5.21 The osmotic coefficient plot of aqueous NaCl solution of parameter set (1) of eCPA+SR2 EOS, [0.03103, 4.25983, 4.25436, -17.33781] (Pa*m^6/mol, cm^3/mol, Å, cm^3).

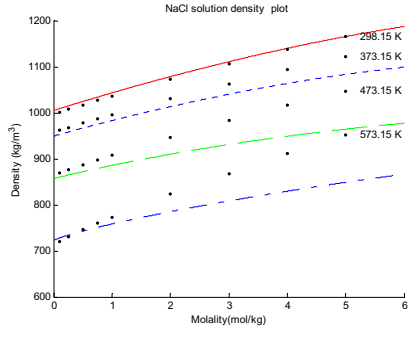

Figure 5.22 The density of aqueous NaCl solution for parameter set (1) of eCPA+SR2 EOS, [0.03103, 4.25983, 4.25436, -17.33781] (Pa*m^6/mol, cm^3/mol, Å, cm^3).

5.4 *Fit osmotic coefficient and density data simultaneously in salt-specific parameters*

It is interesting to see whether the local minimum can be removed when introducing density data in parameter fitting together with osmotic coefficient data. The experimental data for NaCl densities are from Rogers *et al.*[3]. We only tried with eCPA EOS (with Pottel model). The objective function (5.7) will be used to conduct the parameter fitting.

$$FF_1(\Phi_i,\rho_i)=\sum_{i=1}^{N}\left(\Phi_i^{\text{experiment}}-\Phi_i^{\text{calculated}}\right)^2+\sum_{i=1}^{N}\left(\rho_i^{\text{experiment}}-\rho_i^{\text{calculated}}\right)^2 \qquad (5.7)$$

After the optimization, it appears that the old local minima producing wrong density predictions are gone but some new local minima appear. Those new local minima fit both the osmotic coefficient and density data well but only give different objective

function values, see Table 5.6. The multiple sets do not disappear this time. The results are presented in the following table.

Table 5.6 The results for parameters optimization for eCPA EOS using relatively permittivity calculated by Pottel model. Parameters are optimized using osmotic coefficient and density data for NaCl at 25°C.

x_{opt}				σ=	σ=	Objective function	γ		Osmotic coefficient		density	
$a_a=a_c$	$b_a=b_c$	$\sigma_a=\sigma_c$	Wij	$(3b/(2\pi N_A))^{1/3}$	$(6b/(\pi N_A))^{1/3}$	FF_1 (Φ, ρ)	AAD%	ARD%	AAD%	ARD%	AAD	ARD%
$Pa*m^6/mol$	cm^3/mol	Å	cm^3	Å	Å						kg/m^3	
0.0705	5.9968	4.5330	0	1.6817	2.6696	0.0016	0.804	1.143	0.495	0.487	4.37478	0.425
0.0541	5.7008	4.5223	0	1.6536	2.6249	0.0017	0.814	1.165	0.488	0.484	4.48779	0.435
0.0981	6.4088	4.5679	0	1.7194	2.7294	0.0017	0.831	1.161	0.528	0.510	4.24358	0.412
0.0000	3.3357	4.7658	0	1.3831	2.1955	0.0076	1.583	2.081	0.725	0.680	5.94589	0.571
0.3364	8.4086	5.1008	0	1.8823	2.9880	0.0803	2.606	3.186	2.847	2.545	4.17945	0.406
0.5251	9.3823	5.3373	0	1.9523	3.0991	0.2425	6.681	8.947	6.132	5.781	4.36384	0.423

Comparing with the parameters of eCPA fitted without density data in Table 5.2, it can be seen in the best parameter set of the eCPA EOS that *a* parameter and the covolume parameter *b* fitted to both density and osmotic coefficient data become larger than those parameters of the eCPA EOS fitted only to osmotic coefficient data. The fitted attraction parameter *a* of eCPA EOS is still smaller than that of the mMSW EOS (about half of that of mMSW EOS in Table 5.1). The covolume parameter *b* of eCPA becomes slightly larger than the *b* (5.7734) of mMSW EOS. The covolume parameter *b* of the two electrolytes EOSs are almost equal.

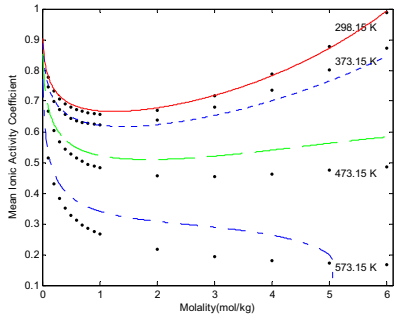

Figure 5.23 The mean ionic activity coefficient plot of aqueous NaCl solution of parameter set (1) of eCPA+SR2 EOS, [0.07053, 5.99675, 4.53304] (Pa*m6/mol, cm3/mol, Å).

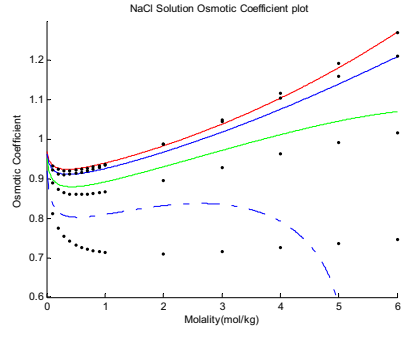

Figure 5.24 The osmotic coefficient plot of aqueous NaCl solution of parameter set (1) of eCPA+SR2 EOS, [0.07053, 5.99675, 4.53304] (Pa*m6/mol, cm3/mol, Å).

The ionic diameter σ is reasonable. The values of NaCl ion diameter σ from all best sets of electrolyte EOSs tested fall in the range of 4.4 ~ 4.9 Å in this work and the reported values of the salt-specific σ parameter from other different EOSs [1,4] in

literature are also within this range. Tan *et al.* [4] gave more values of the ion diameter from some other EOSs falling within this range. The values of the ion diameter obtained in this work are consistent with those obtained from other models.

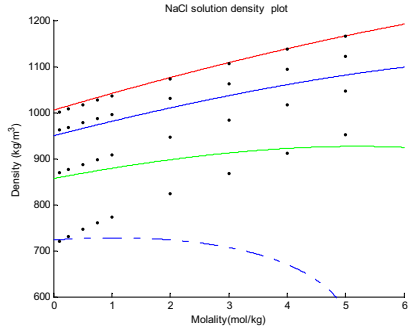

Figure 5.25 The density of aqueous NaCl solution for parameter set (1), [0.07053, 5.99675, 4.53304].

5.5 *The correlation equations for the electrolyte EOS parameter b and σ*

It is preferable to have as few variables as possible to exhibit the good performance of the electrolyte EOS. To reduce the number of fitting parameters in electrolyte EOS, correlation equations between model parameters are suggested, according to the literature. Fürst *et al.* [7] and Wu *et al.* [10] suggested the following two different correlation equations between ion-size parameter σ and covolume parameter b (using ion-specific parameters). These two correlation equations in the parameter optimization were used to calculate ion-size parameter σ from the fitted parameter b. Unfortunately none of the five developed EOSs here could provide satisfactory fitting results. It does not seem to work with salt-specific parameter when equation (5.8) and (5.9) are used. So they are just used to calculate σ from the fitted b values and compare the calculated σ with the fitted σ. In below Table 5.7, the calculated σ and the fitted σ values are presented for mMSW EOS using Pottel model. The fitted parameters are from Table 5.2.

$$\sigma_i = \sqrt[3]{\frac{6b_i}{\pi N_A}} \tag{5.8}$$

$$\sigma_i = \sqrt[3]{\frac{3b_i}{2\pi N_A}} \tag{5.9}$$

When the optimised σ parameter sets are compared with the calculated σ values using equation (5.8) suggested by Fürst *et al.*[7] and (5.9) by Wu [10], it can be seen in Table 5.7 that the fitted values are within the same order of the magnitude of the calculated values. It is interesting to note that equation (5.8) suggested by Fürst *et al.* [7] gives values closer to the fitted values than equation (5.9). It seems that the equation (5.9) from Wu and Prausnitz [10] is somehow less accurate when applied.

Table 5.7 The optimization results of mMSW EOS for ion diameter σ_i using Pottel model and the calculated results for ion diameter σ_i from ionic covolume parameter b_i using equations.

	$a_a=a_c$ Pa*m^6/mol	$b_a=b_c$ cm^3/mol	$\sigma_a=\sigma_c$ Å	Wij cm^3	$\sigma_i = \sqrt[3]{3b_i/2\pi N_A}$ Å	$\sigma_i = \sqrt[3]{6b_i/\pi N_A}$ Å
1	0.1346	5.7734	4.3039	0	1.682	2.636
2	25.7413	89.4963	6.5432	0	1.654	6.573
3	18.9578	97.1690	6.7403	0	1.719	6.755

This kind of calculations for σ parameter was conducted for majority tabulated salt-specific parameter *b* in this chapter and the calculated values were presented in the same table. The only exceptions are Table 5.1 and Table 5.4.

5.6 *The preliminary test of electrolyte EOS using ion-specific parameters at wide temperature range*

In this section, preliminary test runs of MSW EOS in ion-specific parameters at wide temperature and pressure range were conducted. Since the published six aqueous electrolyte systems from Myers *et al.* [1] were reproduced successfully using the published salt-specific parameters, it is natural to use the same electrolytes as the test system for estimation of the ion-specific parameters for MSW EOS. From the studies of the salt-specific parameters for the electrolyte EOSs, we know it is relatively difficult to archive a satisfactory data fitting for the electrolyte EOSs using temperature-independent parameters. Therefore for the test runs of the MSW EOS here with ion-specific parameters, it is decided to use the temperature-dependent parameters similar as Myers *et al.* [1]

5.6.1 Estimate ion-specific parameters without binary interaction parameters

The following simple temperature dependence functions (5.10) and (5.11), were used over the wide temperature range as Myers e*t al.* [1] did. But the pure component parameters were all treated as ion-specific parameters instead.

$$a(T) = a_1 + a_2 / T \tag{5.10}$$

$$\sigma(T) = \sigma_1 + \sigma_2 / T \tag{5.11}$$

Some of the salt-specific parameters from Myers *at el.* [1] were used as the starting guess in the optimization of the ion-specific parameters. Since neither parameters nor results of the H^+ and OH^- ions valid over a wide temperature range were reported in Myers' paper [1], for the sake of simplicity, the dissociation of water (e.g. H^+ and OH^- ions) was not taken into consideration here. The optimization of the ion-specific parameters for MSW EOS started with simple case, i.e. adjusting only the pure component parameters without using binary interaction parameters.

The regressed MSW EOS results for the mean ionic activity and osmotic coefficients in the 0 to 300 ºC temperature range and the 1 to 120 bar pressure range of the NaCl, NaBr and $CaCl_2$ solutions are shown in Figure 5.26 to Figure 5.31. They are slightly better than the results using salt-specific parameters by Myers [1]. The solid lines represent the calculated results using the ion-specific parameters in Table 5.8. The experimental data from the same source as in the Myers' paper [1] are plotted in the figures as solid dots. The regressed densities of the above three electrolyte solutions

are shown in Figure 5.32 to Figure 5.34. The regressed densities have larger error than those published in the original paper, especially at low temperatures.

Table 5.8 The values of the optimized ion-specific parameters for MSW EOS without binary interaction parameters.

	Parameters					
Ion	a_1	a_2	b	σ_1	σ_2	$k_{ion\text{-}water}$
	$Pa*m^6/mol$	$Pa*m^6*K/mol$	cm^3/mol	m^{-10}	$m^{-10}*K$	
Na^+	1.1632	23.320	14.459	5.9103	-1381.90	0.0000
K^+	0.4895	147.48	12.767	5.1555	-1124.80	0.0000
Ca^{2+}	2.6158	0.0000	12.192	4.6118	-970.93	0.0000
Li^+	3.9616	-808.20	21.712	5.1416	-1036.60	0.0000
Cl^-	1.4742	-439.50	16.433	6.4163	-0.6826	0.0000
SO_4^{2-}	0.2208	0.0000	0.0020	2.2981	1578.20	0.0000
Br^-	1.9803	-586.97	20.991	9.2704	0.0000	0.0000
Sum of squared residuals:						115.73245
Root mean square deviation:						0.533249
Number of experimental data:						408

Table 5.9 The values of AADs and ARDs of the MSW EOS calculation using the fitted parameters in Table 5.8.

No	Electrolyte	Density		Activity Coefficient		Osmotic Coefficient	
		AAD (kg/m^3)	ARD%	AAD%	ARD%	AAD%	ARD%
1	NaCl	17.919	1.723	1.322	2.489	1.059	1.210
2	NaBr	18.347	1.569	2.443	3.130	1.801	1.679
3	$CaCl_2$	63.747	7.097	1.588	4.053	1.881	1.576
4	Li_2SO_4	/	/	0.446	1.716	0.985	1.479
5	Na_2SO_4	/	/	0.397	1.773	1.061	1.722
6	K_2SO_4	/	/	0.172	0.815	0.641	1.064

The AADs and ARDs for each property of the six salt solutions are listed in Table 5.9. Compared with the corresponding table 5 in Myers' paper [1], the ARDs of salt 3, 5 and 6 are slightly smaller in this regression except for the densities of $CaCl_2$. The ARD of the regressed densities of $CaCl_2$ is approximately 3.5 times larger than that of Myers[1]. The ARDs of the remaining salts in Table 5.9 are close to those of Myers[1].

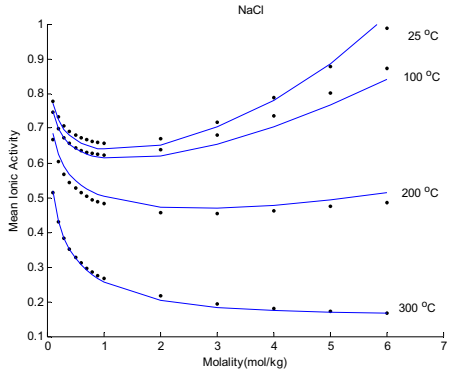

Figure 5.26 Activity coefficient of aqueous NaCl.

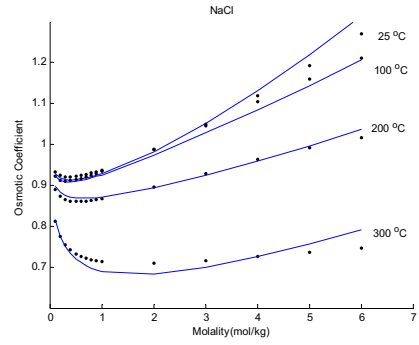

Figure 5.27 Osmotic coefficient of aqueous NaCl.

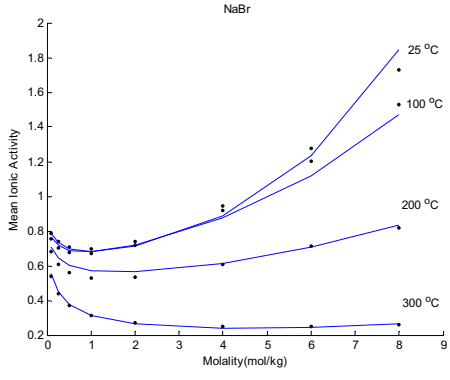

Figure 5.28 Activity coefficient of aqueous NaBr.

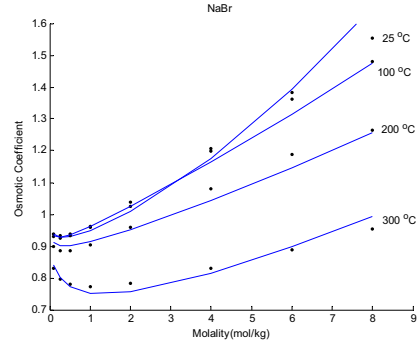

Figure 5.29 Osmotic coefficient of aqueous NaBr.

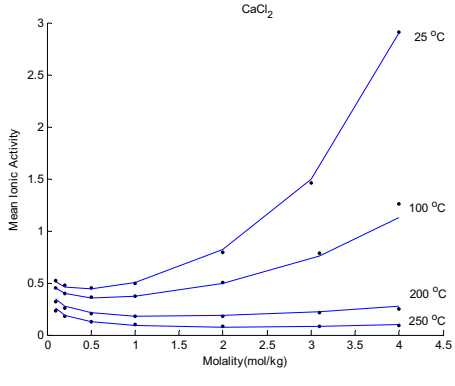

Figure 5.30 Activity coefficient of aqueous $CaCl_2$.

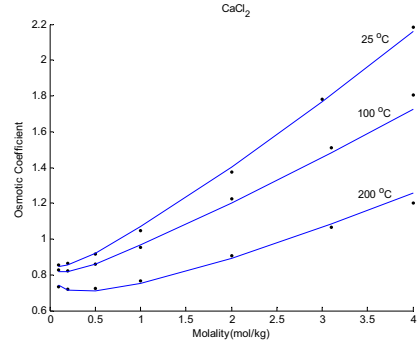

Figure 5.31 Osmotic coefficient of aqueous $CaCl_2$.

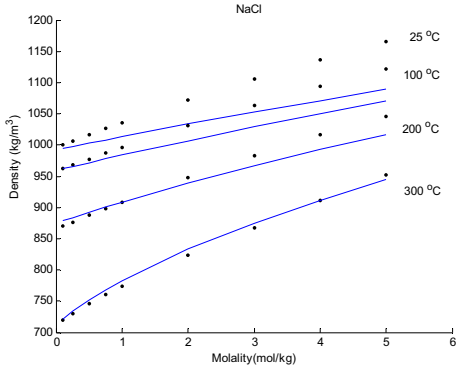

Figure 5.32 Density of aqueous NaCl.

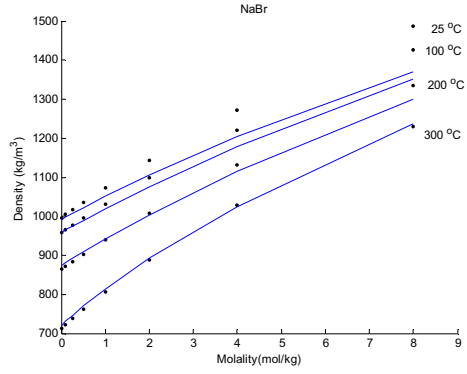

Figure 5.33 Density of aqueous NaBr.

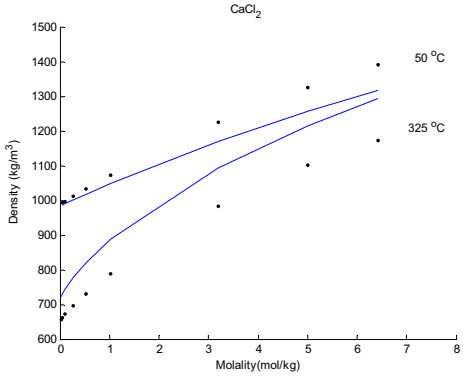

Figure 5.34 Density of aqueous $CaCl_2$.

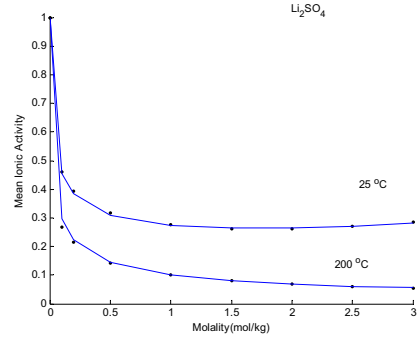

Figure 5.35 Activity coefficient of aqueous Li_2SO_4.

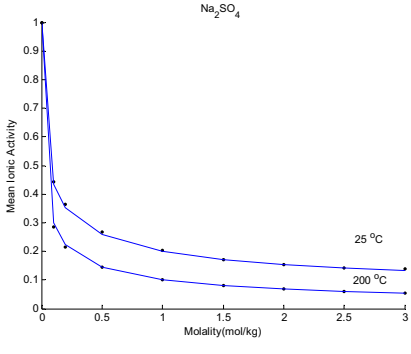

Figure 5.36 Activity coefficient of aqueous Na_2SO_4.

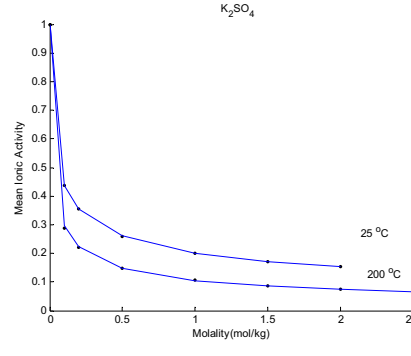

Figure 5.37 Activity coefficient of aqueous K_2SO_4.

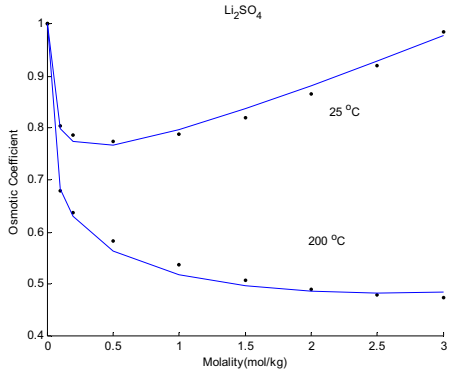

Figure 5.38 Osmotic coefficient of aqueous Li_2SO_4.

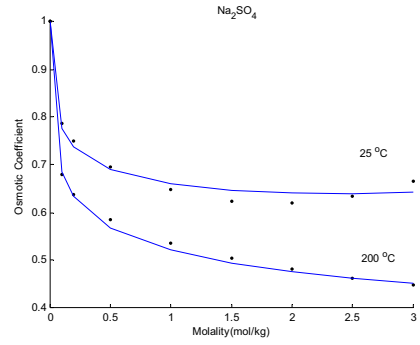

Figure 5.39 Osmotic coefficient of aqueous Na_2SO_4.

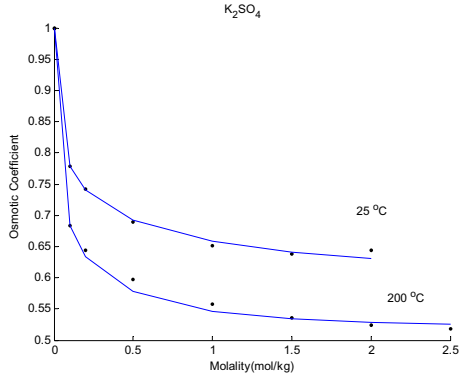

Figure 5.40 Osmotic coefficient of aqueous K_2SO_4.

The graphical results of the calculated mean ionic activity and osmotic coefficients of the Li_2SO_4, Na_2SO_4 and K_2SO_4 aqueous solutions in the range of 0 to 200 ºC and the 1 to 25.6 bar are shown in Figure 5.35 to Figure 5.40. The solid lines stand for the calculated results using the regressed parameters in Table 5.8 and the dots for the experimental data. Note Figure 5.38, the plot of the osmotic coefficient of aqueous Li_2SO_4 solution, is different from the Figure 17 in the Myers' paper [1]. It is because Figure 18 (the osmotic coefficient of aqueous Na_2SO_4 solution) was presented in the Myers' paper [1] twice: Figure 18 for the osmotic coefficient of aqueous Na_2SO_4 solution was by mistake presented as aqueous Li_2SO_4 in Figure 17. Here the correct figure was generated and presented. The densities of aqueous Li_2SO_4, Na_2SO_4 and K_2SO_4 solutions were neither regressed nor calculated in the original paper [1], thus skipped in this section.

5.6.2 The influence of the binary interaction parameters for electrolyte EOS using ion-specific parameters

In this section, the binary interaction parameters are introduced. Here only the water-ion binary interaction parameters are used, which is analogous as Myers *et al.* [1]. They only used the salt-water binary interaction parameters for MSW EOS. The study of the influence of the binary interaction parameters were conducted through study the goodness-of-fit during the regression of the experimental data for the test system. The regression of the binary interaction parameters was done using two different approaches: the classic non-electrolyte EOS approach and the approach of simultaneous regression.

The estimation was first conducted using the classic non-electrolyte EOS approach: keep the pure component parameters for ions obtained in the previous estimation constant (those listed in Table 5.8) and regress only the binary interaction parameters. Seven ion-water binary interaction parameters were consequently obtained for this test system. They are listed in Table 5.10. After introducing seven binary interaction parameters in the optimisation following the classical way, the objective function value could only decrease by approximately 0.9. This does not necessarily indicate that the influence of the ion-water binary interaction parameters is very small or negligible. Instead, it shows that the pure component parameters are optimal for zero binary interaction parameters. The corresponding AADs and ARDs for the parameters in Table 5.11 show the goodness-of-fit of the experimental data is almost unchanged. Only the AADs or ARDs of the activity or osmotic coefficient for salt 2, 3, 5 and 6 improved slightly. The improvement of these fitted properties can hardly be observed visually when plotted, compared with the results in previous section 5.6.1 with no binary interaction parameters. Therefore these similar figures are omitted here.

Table 5.10 The values of the optimized ion-specific parameters and corresponding binary interaction parameters for MSW EOS. The estimation of the ion-water binary interaction parameters k_{ij} was conducted using the classic approach for non-electrolyte EOS.

	Parameters					
Ion	a_1	a_2	b	σ_1	σ_2	$k_{ion\text{-}water}$
	$Pa*m^6/mol$	$Pa*m^6*K/mol$	cm^3/mol	m^{-10}	$m^{-10}*K$	
Na^+	1.1632	23.320	14.459	5.9103	-1381.90	-0.0001
K^+	0.4895	147.48	12.767	5.1555	-1124.80	0.0022
Ca^{2+}	2.6158	0.0000	12.192	4.6118	-970.93	0.0001
Li^+	3.9616	-808.20	21.712	5.1416	-1036.60	0.0009
Cl^-	1.4742	-439.50	16.433	6.4163	-0.6826	0.0002
SO_4^{2-}	0.2208	0.0000	0.0020	2.2981	1578.20	-0.0045
Br^-	1.9803	-586.97	20.991	9.2704	0.0000	-0.0097
Sum of squared residuals:						114.89057
Root mean square deviation:						0.531306
Number of experimental data:						408

Table 5.11 The values of AADs and ARDs of the MSW EOS calculation using the fitted parameters in Table 5.10.

No	Electrolyte	Density		Activity Coefficient		Osmotic Coefficient	
		AAD (kg/m^3)	ARD%	AAD%	ARD%	AAD%	ARD%
1	NaCl	17.919	1.723	1.323	2.489	1.059	1.210
2	NaBr	18.325	1.567	2.332	3.086	1.715	1.611
3	$CaCl_2$	63.747	7.097	1.593	4.054	1.881	1.575
4	Li_2SO_4	/	/	0.446	1.714	0.986	1.479
5	Na_2SO_4	/	/	0.394	1.758	1.070	1.737
6	K_2SO_4	/	/	0.171	0.807	0.636	1.056

The estimation of the ion-water binary interaction parameters was then conducted using the second approach. The five pure component parameters and the water-ion binary interaction parameter were regressed simultaneously. The resulting ion-specific parameters were listed in Table 5.12. If we regressed all parameters simultaneously in the optimisation, the objective function value could decrease from 115.7 to 91.1. This shows the influence of the ion-water binary interaction parameters in the data fitting. The corresponding AADs and ARDs of this test are listed in Table 5.13. The goodness-of-fit of all properties for NaCl, NaBr as well as $CaCl_2$ densities improved considerable. The graphical results of this test are presented in the Appendix IX.

Table 5.12 The values of the optimized ion-specific parameters for MSW EOS obtained from simultaneous regression of all parameters.

	Parameters					
Ion	a_1	a_2	b	σ_1	σ_2	$k_{ion\text{-}water}$
	Pa*m^6/mol	Pa*m^6*K/mol	cm^3/mol	m^{-10}	m^{-10}*K	
Na^+	1.1193	23.004	13.357	6.9857	-1594.90	-0.0884
K^+	0.4305	146.10	12.362	5.6372	-1172.00	-0.0083
Ca^{2+}	2.4581	0.0000	11.534	5.3613	-1091.30	-0.2171
Li^+	3.8606	-809.49	21.250	5.6382	-1085.80	0.0226
Cl^-	1.4743	-439.52	17.231	5.6145	19.9000	0.0561
SO_4^{2-}	0.2922	0.0000	0.0020	1.4406	1649.60	-0.2338
Br^-	1.9967	-586.63	22.312	7.8425	0.0000	0.0000
Sum of squared residuals:						91.144423
Root mean square deviation:						0.473225
Number of experimental data:						408

Table 5.13 The values of AADs and ARDs of the MSW EOS calculation using the fitted parameters in Table 5.12.

No	Electrolyte	Density		Activity Coefficient		Osmotic Coefficient	
		AAD (kg/m^3)	ARD%	AAD%	ARD%	AAD%	ARD%
1	NaCl	17.622	1.689	1.120	2.034	0.872	0.991
2	NaBr	18.572	1.580	1.518	2.250	1.232	1.194
3	$CaCl_2$	60.859	6.755	1.898	3.797	2.084	1.736
4	Li_2SO_4	/	/	0.443	1.785	1.083	1.648

5	Na_2SO_4	/	/	0.417	1.898	1.231	2.047
6	K_2SO_4	/	/	0.180	0.918	0.758	1.278

From the study it can be observed that the introduction of ion-water binary interaction parameters mainly improves the goodness-of-fit of the activity and osmotic coefficients of the test electrolyte system. The influence of ion-water binary interaction parameters to the correlation of the densities of electrolyte solution is small. The accurate correlation of the densities may relay more on the EOS itself or co-volume parameter rather than the binary interaction parameter.

5.6.3 The influence of the models for the relative permittivity

It is advantageous to have some knowledge of how the relative permittivity model for water influences the performances of electrolyte EOS in optimisation of the ion-specific parameters. Here the MSW EOS is following the same methodology in this study as that of salt-specific parameters in section 5.2. The chosen relative permittivity models for this study will be: the constant relative permittivity and the Pottel model. Uematsu-Frank model were already tested in the previous sections.

5.6.3.1 Constant relative permittivity

Here the relative permittivity is set to be temperature-dependent function and independent of the composition. If no ion-water binary interaction parameters were used in this first scenario, it is impossible for MSW EOS to fit the experimental data. After the objective function value reached 3800, it decreased very slowly. The process became very time-consuming. After the value reached 3740, it was almost no improvement in the optimisation. The results of the optimised parameters and the computation results are listed in below Table 5.14 and Table 5.15.

Table 5.14 The values of the optimized ion-specific parameters for MSW EOS obtained from simultaneous regression of all parameters.

	Parameters					
Ion	a_1	a_2	b	σ_1	σ_2	$k_{ion\text{-}water}$
	$Pa*m^6/mol$	$Pa*m^6*K/mol$	cm^3/mol	m^{-10}	$m^{-10}*K$	
Na^+	0.2117	10.190	9.592	6.0391	-1506.10	0.0000
K^+	0.0002	29.35	6.649	5.4056	-1224.70	0.0000
Ca^{2+}	0.1273	0.0000	0.023	4.4529	-1049.10	0.0000
Li^+	1.8476	-487.17	15.000	5.0380	-638.46	0.0000
Cl^-	3.7145	-736.38	24.794	5.7325	645.4600	0.0000
SO_4^{2-}	1.2408	0.0000	5.6919	1.1250	2034.90	0.0000
Br^-	4.4606	-826.91	29.153	12.8260	0.0000	0.0000
Sum of squared residuals:						3729.2654
Root mean square deviation:						3.027014
Number of experimental data:						408

Table 5.15 The values of AADs and ARDs of the MSW EOS calculation using the fitted parameters in Table 5.14.

No	Electrolyte	Density		Activity Coefficient		Osmotic Coefficient	
		AAD (kg/m^3)	ARD%	AAD%	ARD%	AAD%	ARD%
1	NaCl	35.744	3.596	2.889	5.695	10.717	10.755
2	NaBr	35.075	3.001	8.442	11.250	19.988	16.773
3	$CaCl_2$	51.671	5.251	5.418	12.283	41.380	30.056
4	Li_2SO_4	/	/	2.297	11.829	8.850	12.204
5	Na_2SO_4	/	/	0.790	6.105	5.443	9.030
6	K_2SO_4	/	/	0.524	3.587	3.354	5.697

The ion-water binary interaction parameter was first introduced in the classical way as before. The obtained ion-specific parameters are listed in Table 5.16. After introducing the binary interaction parameters, the objective function value could decrease from 3729.2 to 2746.4 in the optimisation. However, the calculation errors are still very significant. The corresponding AADs and ARDs of this test are listed in Table 5.17. The AADs and ARDs of the osmotic coefficients and densities decrease considerablely compared with Table 5.15. The fitting errors of the activity coefficients increase slightly.

Table 5.16 The values of the optimized ion-specific parameters for MSW EOS obtained from simultaneous regression of all parameters.

	Parameters					
Ion	a_1	a_2	b	σ_1	σ_2	$k_{ion\text{-}water}$
	Pa*m^6/mol	Pa*m^6*K/mol	cm^3/mol	m^{-10}	m^{-10}*K	
Na^+	0.2117	10.190	9.592	6.0391	-1506.10	0.6326
K^+	0.0002	29.35	6.649	5.4056	-1224.70	0.9488
Ca^{2+}	0.1273	0.0000	0.023	4.4529	-1049.10	1.7783
Li^+	1.8476	-487.17	15.000	5.0380	-638.46	0.4161
Cl^-	3.7145	-736.38	24.794	5.7325	645.4600	-0.3213
SO_4^{2-}	1.2408	0.0000	5.6919	1.1250	2034.90	-0.5787
Br^-	4.4606	-826.91	29.153	12.8260	0.0000	-0.2638
Sum of squared residuals:						2746.4071
Root mean square deviation:						2.597678
Number of experimental data:						408

Table 5.17 The values of AADs and ARDs of the MSW EOS calculation using the fitted parameters in Table 5.16.

No	Electrolyte	Density		Activity Coefficient		Osmotic Coefficient	
		AAD (kg/m^3)	ARD%	AAD%	ARD%	AAD%	ARD%
1	NaCl	31.897	3.175	3.220	6.483	7.297	7.239
2	NaBr	32.381	2.751	8.149	11.845	15.885	13.184
3	$CaCl_2$	48.418	5.016	7.725	15.288	35.240	25.066

4	Li_2SO_4	/	/	2.476	11.358	5.128	8.689
5	Na_2SO_4	/	/	0.862	6.767	5.019	8.268
6	K_2SO_4	/	/	0.724	5.156	2.212	3.677

If regressing all parameters simultaneously in the optimisation, the objective function value could decrease to 565.4. The corresponding AADs and ARDs of this test are listed in Table 5.13. Though the goodness-of-fit of the properties for the six aqueous electrolyte solutions in some degree improved somehow, the generally results of the correlation is still unsatisfactory for engineering applications compared with those obtained by using UF model. The graphical results of this test are presented in the Appendix IX. Three different regressions suggest that in the later studies simple relative permittivity model, such as a simple temperature correlation, is not sufficient for fitting experimental data of various types of properties over wide temperature and pressure range.

Table 5.18 The values of the optimized ion-specific parameters for MSW EOS obtained from simultaneous regression of all parameters.

	Parameters					
Ion	a_1	a_2	b	σ_1	σ_2	$k_{ion\text{-}water}$
	$Pa*m^6/mol$	$Pa*m^6*K/mol$	cm^3/mol	m^{-10}	$m^{-10}*K$	
Na^+	0.5264	-9.275	7.387	6.9145	-1125.50	-0.3298
K^+	0.2135	25.87	5.282	7.6138	-1458.60	-0.7244
Ca^{2+}	1.1407	0.0000	4.862	8.1788	-1251.70	-0.8325
Li^+	1.9230	-448.76	12.203	5.5931	-684.88	-0.3929
Cl^-	3.0498	-786.45	25.633	3.8486	9.7711	-0.0389
SO_4^{2-}	0.3897	0.0000	3.2393	0.0000	1177.40	-0.1166
Br^-	3.9026	-728.05	37.735	5.9716	0.0000	0.0000
Sum of squared residuals:						565.49151
Root mean square deviation:						1.178734
Number of experimental data:						408

Table 5.19 The values of AADs and ARDs of the MSW EOS calculation using the fitted parameters in Table 5.18.

No	Electrolyte	Density		Activity Coefficient		Osmotic Coefficient	
		AAD (kg/m^3)	ARD%	AAD%	ARD%	AAD%	ARD%
1	NaCl	27.744	2.743	1.917	3.571	3.820	3.964
2	NaBr	43.188	3.632	3.009	3.978	9.228	7.768
3	$CaCl_2$	53.659	5.496	3.718	5.311	10.712	7.691
4	Li_2SO_4	/	/	0.912	4.043	2.455	3.610
5	Na_2SO_4	/	/	0.550	3.568	1.775	2.921
6	K_2SO_4	/	/	0.459	1.879	0.549	0.820

5.6.3.2 Pottel Model

The Pottel model is used for calculating the relative permittivity of water in this section. Pottel model is both temperature and composition dependent. If the ion-water binary interaction parameters were not used, it is possible for MSW EOS (with Pottel model) to fit the experimental data here. However the errors are very significant. When the objective function value reached 865, it decreased very slowly. The process became very time-consuming again. After the value reached 860, there was almost no significant improvement in the optimisation. The results of the optimised parameters using Pottel model with no interaction parameters and the corresponding ARDs and AADs of the computations are listed in below Table 5.20 and Table 5.21.

Table 5.20 The values of the optimized ion-specific parameters for MSW EOS using Pottel model for the relative permittivity of water.

	Parameters					
Ion	a_1	a_2	b	σ_1	σ_2	$k_{ion\text{-}water}$
	$Pa*m^6/mol$	$Pa*m^6*K/mol$	cm^3/mol	m^{-10}	$m^{-10}*K$	
Na^+	1.6257	44.825	14.557	5.9698	-1347.80	0.0000
K^+	0.5560	82.26	6.760	5.3467	-1153.70	0.0000
Ca^{2+}	2.8489	-78.4870	0.002	4.9959	-776.25	0.0000
Li^+	3.9953	-778.97	20.312	5.2216	-1002.00	0.0000
Cl^-	1.6276	-485.26	15.893	3.9338	252.7600	0.0000
SO_4^{2-}	0.2379	25.1650	0.0998	2.1959	1030.80	0.0000
Br^-	3.2035	-777.51	30.798	4.9351	44.6830	0.0000
Sum of squared residuals:						860.01343
Root mean square deviation:						1.453635
Number of experimental data:						408

Table 5.21 The values of AADs and ARDs of the MSW EOS calculation using the fitted parameters in Table 5.20.

No	Electrolyte	Density		Activity Coefficient		Osmotic Coefficient	
		AAD (kg/m^3)	ARD%	AAD%	ARD%	AAD%	ARD%
1	NaCl	25.053	2.488	3.375	6.221	2.655	2.833
2	NaBr	44.125	3.692	5.701	7.062	3.740	3.475
3	$CaCl_2$	30.147	3.661	5.754	13.374	5.007	4.529
4	Li_2SO_4	/	/	1.179	4.811	2.318	3.311
5	Na_2SO_4	/	/	1.205	5.249	2.284	3.832
6	K_2SO_4	/	/	0.955	3.953	1.635	2.637

After adjust the ion-water binary interaction parameters slightly, the objective function value reduced to 765.5. The obtained parameters were listed in Table 5.22. The corresponding AADs and ARDs are listed in Table 5.23. However, the calculation errors are still too large. Adjusting merely the binary interaction

parameters following the classical EOS approach is insufficient to obtain satisfactory results for engineering applications. The second approach, i.e. simultaneous regression, is still needed as in previous study to achieve a satisfactory data fitting.

Table 5.22 The values of the optimized ion-specific parameters for MSW EOS using Pottel model for the relative permittivity of water.

	Parameters					
Ion	a_1	a_2	b	σ_1	σ_2	$k_{ion\text{-}water}$
	$Pa*m^6/mol$	$Pa*m^6*K/mol$	cm^3/mol	m^{-10}	$m^{-10}*K$	
Na^+	1.6257	44.825	14.557	5.9698	-1347.80	0.0092
K^+	0.5560	82.26	6.760	5.3467	-1153.70	0.0136
Ca^{2+}	2.8489	-78.4870	0.002	4.9959	-776.25	0.0003
Li^+	3.9953	-778.97	20.312	5.2216	-1002.00	0.0149
Cl^-	1.6276	-485.26	15.893	3.9338	252.7600	-0.1181
SO_4^{2-}	0.2379	25.1650	0.0998	2.1959	1030.80	-0.0506
Br^-	3.2035	-777.51	30.798	4.9351	44.6830	-0.0218
Sum of squared residuals:						765.53899
Root mean square deviation:						1.37147
Number of experimental data:						408

Table 5.23 The values of AADs and ARDs of the MSW EOS calculation using the fitted parameters in Table 5.22.

No	Electrolyte	Density		Activity Coefficient		Osmotic Coefficient	
		AAD (kg/m^3)	ARD%	AAD%	ARD%	AAD%	ARD%
1	NaCl	23.411	2.308	2.333	4.916	1.722	1.987
2	NaBr	43.803	3.662	5.463	6.877	3.575	3.357
3	$CaCl_2$	30.947	3.789	4.710	12.451	3.810	3.535
4	Li_2SO_4	/	/	1.148	4.514	2.344	3.458
5	Na_2SO_4	/	/	1.187	5.161	2.319	3.881
6	K_2SO_4	/	/	0.949	3.927	1.641	2.644

The objective function value of the simultaneous regression decreased to 227.3 as shown in Table 5.24. The corresponding AADs and ARDs are listed in Table 5.25. Though in some degrees, the goodness-of-fit of the experimental properties improved considerablely, the correlation results are generally still worse than those obtained using UF model. The graphical results of this run are presented in the Appendix IX.

This comparative study of the effects of three different models for the relative permittivity of water suggests that the UF model is the most suitable relative permittivity model. It is the best model for electrolyte EOS to correlate experimental data of various types over wide temperature and pressure range. Secondly the composition derivatives of the relative permittivity of water are very necessary to enhance the model performances of the electrolyte EOS. This is consistent with the study of salt-specific parameters. Therefore in the later study we will focus on UF

model as the best model for the relative permittivity of water in ion-specific parameters regression.

Table 5.24 The values of the optimized ion-specific parameters for MSW EOS using Pottel model for the relative permittivity of water.

	Parameters					
Ion	a_1	a_2	b	σ_1	σ_2	$k_{ion\text{-}water}$
	$Pa*m^6/mol$	$Pa*m^6*K/mol$	cm^3/mol	m^{-10}	$m^{-10}*K$	
Na^+	1.2836	-196.790	9.099	4.4586	-572.13	-0.3150
K^+	0.1776	-44.89	9.450	4.2768	-604.13	0.2947
Ca^{2+}	1.1374	-154.5700	0.003	4.2243	-637.41	-0.9226
Li^+	5.6713	-871.81	33.068	4.0373	-432.53	-0.1725
Cl^-	1.6665	-496.82	15.322	2.9225	413.6800	0.1168
SO_4^{2-}	0.5872	-10.9830	0.1523	1.3372	1121.50	0.6899
Br^-	2.6245	-763.55	24.829	3.1824	654.6700	0.1963
Sum of squared residuals:						227.32218
Root mean square deviation:						0.747349
Number of experimental data:						408

Table 5.25 The values of AADs and ARDs of the MSW EOS calculation using the fitted parameters in Table 5.24.

No	Electrolyte	Density		Activity Coefficient		Osmotic Coefficient	
		AAD (kg/m^3)	ARD%	AAD%	ARD%	AAD%	ARD%
1	NaCl	14.736	1.463	0.894	1.607	1.066	1.218
2	NaBr	28.525	2.425	1.226	2.085	1.442	1.495
3	$CaCl_2$	32.694	3.926	3.252	7.358	3.309	3.368
4	Li_2SO_4	/	/	0.720	2.749	1.821	2.782
5	Na_2SO_4	/	/	0.587	2.776	1.643	2.773
6	K_2SO_4	/	/	0.485	1.950	1.232	1.999

5.7 *Conclusion and future work*

The following points can be concluded from the above numerical experiments with the tested electrolyte EOSs:

1. After numerical check of the derivatives, the consistence test and optimization of salt-specific parameters, we are ensured that the six implemented electrolyte EOSs are running correctly. It is safe to use them in the regression of the ion-specific parameters later. This is also validated by the test run of MSW EOS using ion-specific parameters.

2. The relative permittivity plays an important role in correlating experimental data of mean ionic activity coefficient, osmotic coefficient and density for

electrolytes. When it is treated as a function of temperature, volume and composition rather than a constant, better correlation of the experimental data is obtained without using additional interaction parameters or SR2 term.

3. The Pottel model occasionally gives negative relative permittivity value when the algorithm searches at an ill-conditioned region in parameter space during optimization. This causes the breaking down of the program. Used together with SR2 term, it also tends to have extremely large σ values if bad starting guess is used, see parameter set six in Table 5.4. While such problems are never encountered when using UF model, even though the correlation results for salt-specific parameters are sometimes inferior. For ion-specific parameters, UF model provide the best results for MSW EOS. Overall, it is therefore preferable to use UF model in the later research.

4. The SR2 term from Fürst *et al.*[7] can significantly improve the performances of the EOS by taking into account the interactions between ion and ion or ion and water. But it slows down the computational speed and increases the complexity of the EOS. If the electrolyte EOS could fulfil the needs by using the interaction parameter k_{ij} in the non-electrolyte term or a good relative permittivity model without using the additional SR2 term, it is recommended not to use it. Therefore, SR2 term was not used in the later chapter to make the electrolyte EOS simpler and faster.

5. When mean ionic activity coefficient or osmotic coefficient is used to determine the best-fit parameters for electrolyte EOS, mathematically they do make a difference. However in this work, the differences are not so significant for aqueous NaCl systems in the parameter optimization. Since osmotic coefficient is more directly related to directly measurable experimental property (osmotic pressure), it is preferable to use it as a thermodynamic property in parameter optimization.

6. The covolume parameter b_i and the ion diameter σ_i are well correlated by the equation (5.8) suggested by Fürst. It applies better when b_i values are larger than 10 Å. This can be used as a method to estimate the initial values in parameter fitting.

7. During the parameter optimization process, it is discovered that there are many local minima which result in multiple parameter sets. Some of the parameter sets are only mathematically correct for the objective function; it could go wrong if they are used to calculate other thermodynamic properties. If we only fit the parameters to mean ionic activity coefficient or osmotic coefficient, the parameter sets obtained could give a wrong density prediction. It is necessary to use density data in combination with the osmotic or mean ionic activity coefficient data in parameter optimization.

8. The EOS parameters are temperature dependent. Using temperature independent parameters, none of the electrolyte EOSs tested are able to provide quantitatively correct predictions. Temperature dependence functions have to be adopted when the EOS is used for a wide temperature range.

9. The binary interaction parameter k_{ij} in the non-electrolyte term should be regressed simultaneously with other pure component parameters to obtain the best fittings for electrolyte EOS using ion-specific parameters. If the binary interaction parameter k_{ij} is regressed in the classical way, less accurate correlations will be obtained.

Reference

1. Myers JA, Sandler SI, Wood RH. An Equation of State for Electrolyte Solutions Covering Wide Range of Temperature, Pressure and Composition. *Ind Eng Chem Res.* 2002; 41: 3282-3297.

2. Archer D. Thermodynamic properties of the NaCl + H_2O systems. II. Thermodynamic properties of the NaCl(aq), NaCl-H_2O(cr), and phase equilibria. *J. Phys. Chem. Ref. Data.* 1992;21:793-.

3. Rogers PSZ, Pitzer KS. Volumetric properties of aqueous sodium chloride solutions. *J Phys Chem Ref Data.* 1982; 11(1): 15-81.

4. Liu Z, Wang, W, Li Y. An equation of state for electrolyte solutions by a combination of low-density expansion of nonprimitive mean spherical approximation and statistical associating fluid theory. *Fluid Phase Equilib.* 2005; 227: 147-156.

5. Tan SP, Adidharma H, Radosz M. Statistical Associating Fluid Theory Coupled with Restricted Primitive Model To Represent Aqueous Strong Electrolytes. *Ind Eng Chem Res.* 2005; 44: 4442-4452.

6. Nielsen, HB. *Checking Gradients*. Copenhagen, Denmark: Technical University of Denmark, IMM; 2000.

7. Fürst W, Renon H. Representation of Excess Properties of Electrolyte Solutions Using a New Equation of State. *AIChE J.* 1993; 39: 335-343.

8. Solbraa E. *Equilibrium and Non-Equilibrium Thermodynamics of Natural Gas Processing.* PhD Thesis. Norway: Norwegian University of Science and Technology, Department of Refrigeration and Air Conditioning; December 2002.

9. Uematsu M, Franck EU. Static dielectric constant of water and steam. *J Phys Chem Ref Data.* 1980; 9(4):1291-1305.

10. Wu J, Prausnitz JM. Phase Equilibirum for systems Containing Hydrocarbons, Water and Salt: An Extended Peng-Robinson Equation of State. *Ind Eng Chem Res.* 1998; 37: 1634-1643.

CHAPTER 6 Multi component EOS for electrolytes systems at room temperature

6.1 *General*

This work has been submitted for publication as part of the article titled "A Multi component EOS for electrolytes" in AICHE Journal, 2007 (author Yi Lin, Kaj Thomsen and Jean-Charles de Hemptinne). The goal of this work is to explore the possibility of using an EOS based on ion-specific parameters for multi-component mixtures containing electrolytes and non-electrolytes and the possibility of reproducing SLE phase diagrams with electrolyte EOS. We would like to evaluate different short range terms and long range terms by applying them to a chosen test system.

6.2 *Expression of the electrolyte EOSs*

In this chapter, we only considered four different EOSs listed in Table 6.1. As explained in the previous chapter, SR2 term was not used here to simplify the EOS. We aim at performing phase equilibrium calculation for complex multi-component electrolyte solutions using ion-specific parameters. Ion-specific parameters require a simultaneous regression of experimental data, if available, of all possible combination of ions and the ion-specific parameters determined in this work are valid and optimized for the six ion test systems studied in this work. Since in previous chapter, all EOSs were thoroughly tested and checked and it is safe to use them for ion-specific parameter optimization. The EOSs were explained in brief below.

1) **MSW EOS** [1]

The expression for the total change in Helmholtz free energy to form the electrolyte system is:

$$A(T,V,\mathbf{n}) - A^{IGM}(T,V,\mathbf{n}) = \Delta A^{PR} + \Delta A_{ex}^{sMSA} + \Delta A_{dis}^{Born} + \Delta A_{chg}^{Born} \qquad (5.12)$$

According to Myers *et al.*[1], the use of a volume translation parameter c for ions has no significant effect on the properties tested. This was confirmed by our initial tests. Therefore it was set equal to zero for all ions.

2) Modified MSW EOS (mMSW EOS)

The mMSW EOS can be expressed in terms of Helmholtz free energy as follows:

$$A(T,V,\mathbf{n}) - A^{IGM}(T,V,\mathbf{n}) = \Delta A^{PR} + \Delta A_{im}^{sMSA} + \Delta A_{dis}^{Born} + \Delta A_{chg}^{Born} \qquad (5.13)$$

The mMSW EOS is used with the same number of adjustable parameters as the MSW EOS.

3) The Electrolyte CPA EOS (eCPA EOS)

The eCPA EOS has the following general form:

$$A(T,V,\mathbf{n}) - A^{IGM}(T,V,\mathbf{n}) = \Delta A^{SRK} + \Delta A^{Assoc} + \Delta A_{im}^{sMSA} + \Delta A_{dis}^{Born} + \Delta A_{chg}^{Born} \qquad (5.14)$$

The eCPA EOS does not have a volume translation parameter. To minimize the number of fitting parameters the association term is not used for ions and only used to account for the self-association of water. The water-ion cross-association contribution can be accounted for by the hydrated diameters in the MSA term. For the electrolyte systems chosen the ionic association has been neglected.

4) Debye-Hückel SRK electrolyte EOS (SRK+DH EOS) The expression for SRK+DH EOS is as follows:

$$\ln\gamma^{*}(T,V,\mathbf{n}) = \ln\gamma^{SRK}(T,V,\mathbf{n}) + \ln\gamma^{sDH}(T,\mathbf{n}) \tag{5.15}$$

The MSW, mMSW, and the eCPA EOS are referred to as " three-parameter EOS" in the following sections, due to their three ion-specific parameters. All of the above-mentioned EOSs are summarized in Table 6.1.

Table 6.1 The table of four different electrolyte equations of state applied in this work.

Electrolyte EOS	Non-electrolyte terms	Electrolyte terms	Pure compound parameter	Interaction parameter
MSW EOS	1.PR EOS with volume translation parameter	1. Simplified explicit MSA 2. Born term	Three adjustable ion-specific parameters *a, b, σ*. Volume translation parameter *c* is not used for ions.	One (k_{ij} in PR EOS)
mMSW EOS	1.PR EOS with volume translation parameter	1. Simplified implicit MSA 2. Born term	Three adjustable ion-specific parameters *a, b, σ*. Volume translation parameter *c* is not used for ions.	One (k_{ij} in PR EOS)
eCPA EOS	1. SRK EOS 2.Wertheim association term of for associating compound	1. Simplified implicit MSA 2. Born term	Three adjustable ion-specific parameters *a, b, σ*.	One (k_{ij} in SRK EOS)
SRK+DH EOS	1. SRK EOS	1.Simplified textbook Debye-Hückel term	Two adjustable ion-specific parameters *a, b* in SRK EOS.	One (k_{ij} in SRK EOS)

Water parameters

Prior to the determination of parameters for electrolytes, the parameters for pure water should be determined. In this way the equations of state can accurately predict the properties of pure water in the limit of infinite dilution concentration of an aqueous salt solution. Myers *et al*.[1] provided a set of best-fit temperature dependent parameters (nine parameters) for the PR EOS with a volume translation parameter, see (1.53) to (1.55). The same set of parameters for water has also been used in the mMSW EOS. Regarding the CPA EOS, Kontogeorgis *et al.*[2] provided an optimal set of CPA parameters (five parameters) with a 4C association scheme for water, see Table 2.1.

The ARDs of CPA is 0.8% for vapour pressure and 0.5% for liquid densities of water. The SRK EOS simply use the critical properties of water to calculate the attractive parameter *a* and the co-volume parameter *b*. SRK EOS gives a less accurate representation of the properties of water than these two EOSs.

For this study, we use the Uematsu and Franck[3] model to calculate the relative permittivity of water. Pottel model for relative permittivity was not used in later chapters as mentioned in last chapter. This also makes the later comparison of different electrostatic terms easier. The Uematsu and Franck model for water relative permittivity is a function of temperature and water density. The pure water density is obtained by an approximation suggested by Myers *et al.* [1]:

$$d_{H_2O} \approx n_{H_2O} \bullet M_{H_2O} / V \tag{5.16}$$

This approach was used for all the three-parameter EOSs in this work.

6.3 *The parameter determination for the electrolyte EOS*

In order to determine the model parameters, an objective function was defined. This objective function is presented in equation (5.17). The parameters were determined through a weighted least squares fit. The chosen electrolyte EOS is first used for calculating the selected thermodynamic properties. Then the sum of the squares of the residuals (i.e. difference between the calculated results and the corresponding values of experimental data) is calculated.

$$f = \sum_{j=1}^{2}\sum_{i=1}^{N_j}\left(w_j \frac{x_{ij}^{\exp} - x_{ij}^{cal}}{x_{ij}^{\exp}} \right)^2 + \sum_{i=1}^{N_{AMV}} \left[w_{AMV} \left(V_{\phi,i}^{\exp} - V_{\phi,i}^{cal} \right) \right]^2 + \sum_{i=1}^{N_{SLE}} \left[w_{SLE} \ln(SI_i) \right]^2 \tag{5.17}$$

where x_{ij}^{cal} and $x_{ij}^{\exp}$ are the calculated value and the corresponding experimental value of osmotic coefficient or molal mean ionic activity coefficient. V_ϕ is the AMV. SI_i is the saturation index of SLE data point *i*. w_j is the weight for the data of type *j*.

The parameter optimization can be unweighted optimization (conventional equal weight optimization) or weighted optimization (put more weight on residuals of one property of interests than others) based on the requirements and experiences. The data used for the parameter estimation are all from the IVC-SEP electrolyte databank[4].

A gradient method (Marquardt method) and a direct search method (Nelder-Mead simplex search method) for non-linear least square minimization have been adopted. It was found that an alteration between the two optimization methods yields good results. The algorithm is written in the Matlab format below. The variable in bold font refers to vector or matrix.

Algorithm 6.1

Function [$\mathbf{x_{optimised}}$, Obj_f_{min}]=Combined Optimization($\mathbf{x_0}$, T, P, **n**, **parameters**)

Call function [**parameters0**]=EOS_parameter_intialization(T, P, **n**, **parameters**)

While ($\left|Obj\_f - Obj\_f_{min}\right| > tolerance$)

Call function [$\mathbf{x_0}$, Obj_f] = Simplex($\mathbf{x_0}$, 'Obj_func ', T, P, **n**, **parameters**)

Call function [$\mathbf{x_0}$, Obj_f] = Marquardt($\mathbf{x_0}$, 'Obj_func ', T, P, **n**, **parameters**)

Obj_f_{min} = Obj_f

End %While loop

$\mathbf{x}_{optimised} = \mathbf{x}_0$

End function Combined Optimization

Function [*Obj_f*, **dObj_fdx**]= Obj_func (**x**, T, V, P*, **n**, **parameters**)

$$Obj\_f(\mathbf{x}) = \sum_{j=1}^{2}\sum_{i=1}^{N_j}\left(w_j \frac{x_{ij}^{\exp} - x_{ij}^{cal}(\mathbf{x})}{x_{ij}^{\exp}} \right)^2 + \sum_{i=1}^{N_{AMV}}\left[w_{AMV}\left(V_{\phi,i}^{\exp} - V_{\phi,i}^{cal}(\mathbf{x}) \right) \right]^2 + \sum_{i=1}^{N_{SLE}}\left[w_{SLE} \ln(SI_i(\mathbf{x})) \right]^2$$

$$\mathbf{dObj\_fdx} = -\frac{\partial f}{\partial \mathbf{x}}$$

End function Obj_func

The Marquardt method has a high convergence speed but often stops at a local minimum when the norm of the gradient becomes zero. The simplex method can help to jump out of the local minimum: it can find another point where the objective function gives a lower value than the previous local minimum, as long as the previous local minimum is not the global minimum. Therefore, the combined algorithm often finds a better minimum than when separately running any of the two methods alone.
The parameter regression was performed in three stages using various amounts and types of data:

1) Stage a and stage b.
   a. AMV data alone.
   b. Data for mean ionic activity coefficient plus osmotic coefficient ($\gamma_{\pm} + \Phi$ data).
2) AMV data and data for mean ionic activity coefficient plus osmotic coefficient (short as AMV + $\gamma_{\pm} + \Phi$),
3) AMV data, data for mean ionic activity coefficient, osmotic coefficient, and binary and ternary SLE data.

6.4 *Aqueous electrolyte solution at 25 °C and 0.101325 MPa*

6.4.1 Test system

The four electrolyte equations of state were tested by determining the optimal model parameters for the multi-component system consisting of water, Na^+, H^+, Ca^{2+}, Cl^-, OH^-, and SO_4^{2-} ions. This multi-component system has been chosen as the test system. In all cases, it was attempted to minimize the number of parameters required for a satisfactory prediction of the test system. This was achieved via trial and error.

6.4.2 Stage I)

All of the above mentioned four EOSs can easily represent either a) the AMV data or b) the mean ionic activity coefficient and the osmotic coefficient data exclusively (short as $\gamma_{\pm} + \Phi$). In the above two cases, no interaction parameters were needed for

any of the three-parameter EOSs. At least three interaction parameters were needed for the SRK+DH EOS.

6.4.3 Stage II) Binary systems at 25°C and 0.101325 MPa

When any one of the three-parameter EOSs is simultaneously fitted to the combined three types of data, i.e. AMV + $\gamma_{\pm}$ + Φ, it appears to be very difficult to achieve good results without interaction parameters. It is observed that the AMV causes more difficulties for the EOS than $\gamma_{\pm}$ + Φ during the simultaneous data fitting. The EOS can often give a better representation of the mean ionic activity coefficient and osmotic coefficient than of the AMV data. This is expected, for AMV is a rather sensitive and strict property. After dozens of careful trials, all four EOSs can represent these three types of data when interaction parameters are introduced. The results of the fitted parameters and their ARDs for AMV and mean ionic activity coefficient, osmotic coefficient experimental data are presented in Table 6.2.

Table 6.2 The values of the optimized electrolyte EOS parameter for six ions in the test system based on AMV, mean ionic activity coefficient, and osmotic coefficient experimental data. The AAD and ARD values of the calculated properties are also given.

		Parameters			
EOS	Ion	a	b	σ	k_{ij}*
		Pa*m^6/mol	cm^3/mol	m^{-10}	(water-ion)
	Na^+	0.87012	7.36070	5.08140	
	Ca^{2+}	0.10938	0.78196	2.46610	
MSW	H^+	0.20929	5.68740	2.79430	
	Cl^-	3.57920	19.15500	5.95770	-0.56019
	SO_4^{2-}	16.38100	30.32000	22.44100	-0.72530
	OH^-	0.29526	1.93110	8.95210	-4.21910
	Na^+	1.31000	8.43310	15.38800	
	Ca^{2+}	0.04246	0.44287	5.39270	
mMSW	H^+	0.38680	6.49010	8.66720	
	Cl^-	3.22090	18.75200	1.81550	-0.59243
	SO_4^{2-}	13.89000	28.73500	11.41300	-0.81505
	OH^-	0.11306	0.96579	3.05520	-6.79020
	Na^+	0.92684	8.61080	16.04700	
	Ca^{2+}	0.02000	0.65312	6.13720	
eCPA	H^+	0.02000	4.16140	8.73400	
	Cl^-	0.72390	19.86300	0.87696	-0.82185
	SO_4^{2-}	3.68970	32.66000	3.02240	-1.17450
	OH^-	0.02007	5.95860	0.66376	-9.50000
	Na^+	0.02668	1.88010		
	Ca^{2+}	0.02034	2.19980		
SRK+DH	H^+	0.02000	2.03540		

(V)	Cl^-	0.03623	1.55880		-1.00030
	SO_4^{2-}	0.11775	2.07130		-1.05010
	OH^-	0.02000	0.40576		-2.48120
	Na^+	0.02000	1.25980		
	Ca^{2+}	0.06820	2.82150		
SRK+DH	H^+	0.03585	2.20420		
	Cl^-	0.02000	1.15640		-1.57330
	SO_4^{2-}	0.88127	13.82500		-0.19110
	OH^-	0.31351	8.38990		-0.21427

		Apparent Molar Volume		Activity Coefficient		Osmotic Coefficient	
EOS	Salt	AAD* cm^3/mol	ARD%*	AAD%	%ARD	AAD%	%ARD
MSW	$CaCl_2$	0.44	1.84	/	/	3.57	1.78
	NaOH	0.38	14.38	0.99	1.28	1.13	1.11
	Na_2SO_4	0.73	3.97	/	/	0.75	1.14
	NaCl	0.27	1.44	0.23	0.31	0.44	0.42
	HCl	0.30	4.33	0.92	0.60	0.65	0.46
mMSW	$CaCl_2$	0.48	1.99	/	/	3.95	2.23
	NaOH	0.35	12.74	1.29	1.67	1.33	1.31
	Na_2SO_4	0.62	3.41	/	/	0.82	1.24
	NaCl	0.45	2.4	0.99	1.31	1.24	1.15
	HCl	0.83	4.29	0.56	0.40	0.35	0.27
eCPA	$CaCl_2$	0.56	2.21	/	/	4.25	2.16
	NaOH	0.85	50.28	1.03	1.34	1.28	1.27
	Na_2SO_4	0.25	1.23	/	/	0.29	0.43
	NaCl	0.64	3.47	1.1	1.43	1.37	1.25
	HCl	0.55	2.80	0.75	0.47	0.50	0.34
SRK+DH	$CaCl_2$	1.62	6.66	/	/	7.08	3.73
(V)	NaOH	2.15	151.32	5.78	7.80	5.60	5.16
	Na_2SO_4	0.68	3.91	/	/	0.77	1.17
	NaCl	2.01	10.96	1.44	1.99	1.90	1.66
	HCl	2.03	10.30	1	0.62	0.51	0.36
SRK+DH	$CaCl_2$	4.87	22.84	/	/	3.71	1.95
	NaOH	70.05	3740.40	0.78	0.92	1.20	1.10
	Na_2SO_4	92.02	461.79	/	/	0.90	1.33
	NaCl	10.88	57.35	1.79	2.50	1.91	1.68
	HCl	2.23	11.77	1.51	1.26	1.22	0.94

*** In the column of water-ion interaction parameters, the interaction parameter values are presented according to the corresponding ion in the ion column.**

*** Average absolute deviation is fined by following equation:** $AAD = \frac{1}{N}\sum_{i=1}^{N}\left(\left|x_i^{\text{experiment}} - x_i^{\text{calculated}}\right|\right)$

*** Average relative deviation is fined by following equation:** $ARD\% = \frac{1}{N}\sum_{i=1}^{N}\left(\left|\frac{x_i^{\text{experiment}} - x_i^{\text{calculated}}}{x_i^{\text{experiment}}}\right|\right)\times 100\%$

Due to its simplicity, even with interaction parameters the SRK+DH EOS cannot reproduce AMV experimental data as accurate as the other three EOSs. The reason is that the DH term does not contribute to the volume. However, SRK+DH EOS is able to provide very accurate results when exclusively fitted to $\gamma_{\pm} + \Phi$ data. Therefore, in the third optimization stage, SRK+DH EOS parameters were not fitted to AMV. For comparison of the performance of SRK+DH EOS, the results of fitting only $\gamma_{\pm} + \Phi$ data have been presented both numerically and graphically together with the results of fitting AMV+$\gamma_{\pm} + \Phi$ data. Note in the figure legends "SRK+DH (V)" means the results of the simultaneous fitting AMV+$\gamma_{\pm} + \Phi$ data while "SRK+DH" refers to the results of fitting $\gamma_{\pm} + \Phi$ data.

Interestingly, it is observed that not all interaction parameters have the same effect on the data fitting. The anion-water interaction parameters appear to be more influential than other interaction parameters. Even though other interaction parameters such as the ion-ion or cation–water interaction parameters can improve the goodness of fit, they are not as efficient as anion-water interaction parameters. Consequently, all three anion-water interaction parameters have been chosen in the second stage for binary systems and no other interaction parameters are needed. It is an optimal outcome to achieve both the minimum number of interaction parameters and the best goodness-of-fit based on trial and error approach. The number of interaction parameters can be further reduced to one; however the goodness-of-fit of experimental data deteriorates correspondingly (mainly for AMV). Even with three anion-water interaction parameters, the AMV of certain binary system still appears to be burdensome for the EOS to fit during the fitting of AMV+$\gamma_{\pm} + \Phi$ data, especially for SRK+DH EOS.

The results are presented in Table 6.2. From the table, it can be observed for the three complicated three-parameter EOSs (MSW, mMSW, eCPA) the co-volume parameters b are very close to each other. For Na^+, b is around 8 cm^3/mol for the three EOSs. b values of three-parameter EOSs for Ca^{2+}, H^+, Cl^-, SO_4^{2-} are all very close to each other. Except for OH^-, there are large differences in co-volume parameter values. It can also be observed that the values of interaction parameter k_{ij} for OH^- and water are also significantly different, even though they are all negative.

For attractive parameter a, MSW and mMSW EOS use the same short range term (the PR EOS) and correspondingly their values are similar, except for Ca^{2+}. The mMSW and eCPA EOS, they use the same electrostatic terms: (simplified implicit MSA term + Born term), in which contain the ion diameter, σ. Thus the σ values of the mMSW and eCPA are very close to each other, except for SO_4^{2-} and OH^- ions. Since all four electrolyte EOSs are just engineering models instead of theoretical models, the fitted ion diameters are not expected to have clear physical meanings. Comparison of the fitted ion-diameters and the corresponding Pauling or Stokes diameters of that ion are not so meaningful. No clear relation between them has been observed.

The large absolute values of the interaction parameters for OH^- and water in all of the four EOSs are caused by fitting the AMV of sodium hydroxide. If the AMVs of the hydroxide alkaline are removed in the objective function, the absolute value of k_{ij} for OH^- and water interaction parameter will decrease. This has been shown clearly in the

case of SRK+DH EOS. If AMV is not fitted (in case of SRK+DH), OH^- -water k_{ij} increases from -2.48950 to -0.21427, see Table 6.2.

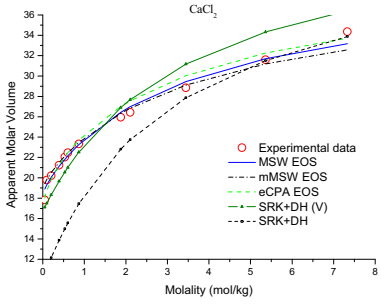

Figure 6.1 Apparent molar volume of aqueous $CaCl_2$ at 25°C. The SRK+DH (V) refers to the fitting to AMV + $\gamma_\pm$ + Φ data. The SRK+DH refers to the fitting only to $\gamma_\pm$ + Φ data.

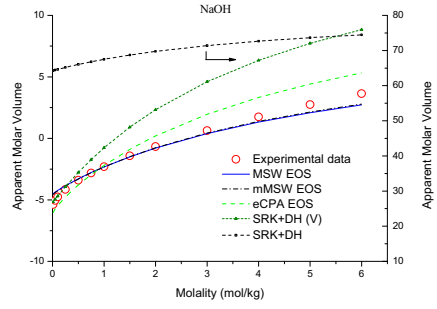

Figure 6.2 AMV of aqueous NaOH at 25°C and 1 atmosphere. The SRK+DH (V) refers to the fitting to AMV + $\gamma_\pm$ + Φ data. The SRK+DH refers to the fitting only to $\gamma_\pm$ + Φ data, see the right vertical axis.

The four EOSs accurately reproduced the mean ionic activity and osmotic coefficient of all solutions over the entire range of concentration. For the simultaneous fitting of AMV + $\gamma_\pm$ + Φ data, the three complicated three-parameter EOSs behave almost similarly well in describing the test systems. The differences in their performances are small. The MSW EOS is slightly better than the mMSW EOS overall and the mMSW EOS is slightly better than the eCPA EOS.

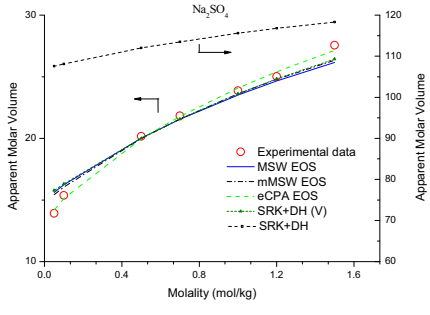

Figure 6.3 AMV of aqueous Na_2SO_4 at 25°C. The SRK+DH (V) refers to the fitting to AMV + $\gamma_\pm$ + Φ data. The SRK+DH refers to the fitting only to $\gamma_\pm$ + Φ data, using the right vertical axis.

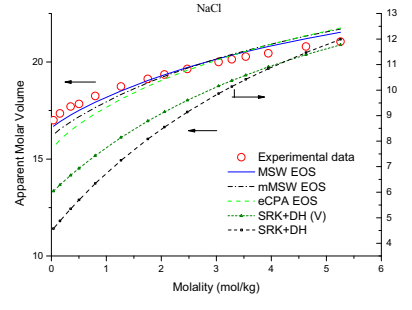

Figure 6.4 AMV of aqueous NaCl at 25°C. The SRK+DH (V) refers to the fitting to AMV + $\gamma_\pm$ + Φ data. The SRK+DH refers to the fitting only to $\gamma_\pm$ + Φ data, see the right vertical axis.

With regard to computational time, the differences are quite large. Generally, the computational speed of eCPA EOS is the slowest due to its Wertheim association term and the implicit MSA term. Its computation time is approximately 4 times as much as that of MSW EOS. The mMSW EOS needs computation time approximately 2 to 2.5 times that of MSW EOS. The computational speed of SRK+DH EOS is highest. The computation speed of MSW EOS and SRK+DH EOS is very similar, but the ability of SRK+DH EOS to reproduce experimental data (especially for AMV) is the worst of the four EOSs. From Figure 6.2 to Figure 6.4 it can be seen that the

goodness-of-fit of SRK+DH(v) is noticeably worse than the other three EOSs. This can clearly be observed numerically in Table 6.2.

In the case of simultaneous fitting of AMV + $\gamma_{\pm}$ + Φ data, SRK+DH EOS can reproduce the $\gamma_{\pm}$ + Φ experimental data of NaCl and HCl aqueous solutions very well. For $CaCl_2$, NaOH and Na_2SO_4, the ARDs are several times higher than the ARDs of the other three complicated EOSs. The SRK+DH EOS could only reproduce the AMV of $CaCl_2$ and Na_2SO_4 solutions. The AMV of the rest three solutions cannot be reproduced by it. However, if SRK+DH EOS is only fitted to $\gamma_{\pm}$ + Φ data, the reproduced results are as good as other three EOSs, see Table 6.2. From Figure 6.6 to Figure 6.13, it can be seen that the calculated lines of four EOSs are very close to each other. This suggests that the simple SRK+DH EOS can describe thermodynamic properties ($\gamma_{\pm}$ and Φ) satisfactorily but not AMV. If the volumetric properties need to be reproduced with high accuracy, SRK+DH EOS cannot fulfil the demand and more sophisticated electrolyte EOSs have to be used. Generally speaking, cubic EOS cannot accurately predict volumetric properties, therefore this is not the unique disadvantage of this simple EOS. Overall, it can be seen in Table 6.2 the AADs of predicted AMV are large for all four EOSs. The ARDs of predicted $\gamma_{\pm}$ + Φ is smaller than 1.5% in general, except for SRK + DH (v).

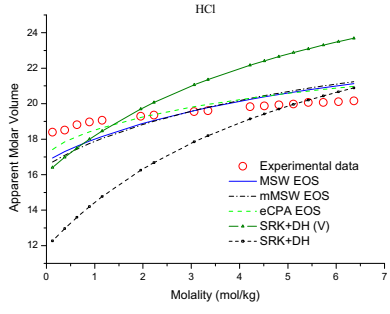

Figure 6.5 AMV of aqueous HCl at 25°C. The SRK+DH (V) refers to the fitting to AMV + $\gamma_{\pm}$ + Φ data.

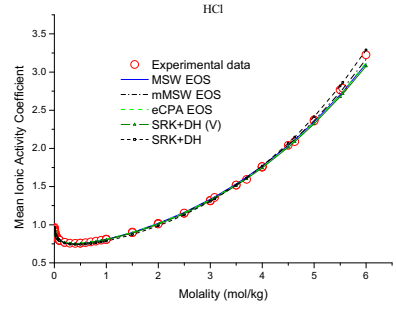

Figure 6.6 Mean ionic activity coefficient of aqueous HCl at 25 °C. The SRK+DH (V) refers to the fitting to AMV + $\gamma_{\pm}$ + Φ data..

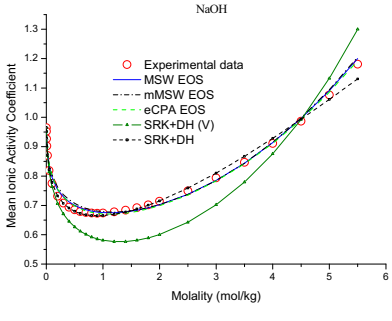

Figure 6.7 Mean ionic activity coefficient of aqueous NaOH at 25°C. The SRK+DH (V) refers to the fitting to AMV + $\gamma_{\pm}$ + Φ data. The SRK+DH refers to the fitting only to $\gamma_{\pm}$ + Φ data.

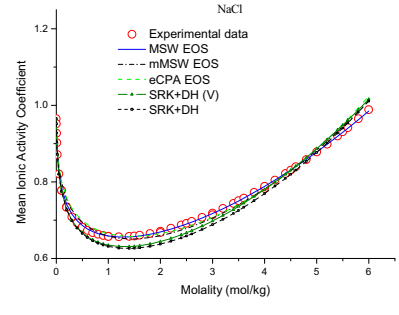

Figure 6.8 Mean ionic activity coefficient of aqueous NaCl at 25 °C. The SRK+DH (V) refers to the fitting to AMV + $\gamma_{\pm}$ + Φ data. The SRK+DH refers to the fitting only to $\gamma_{\pm}$ + Φ data.

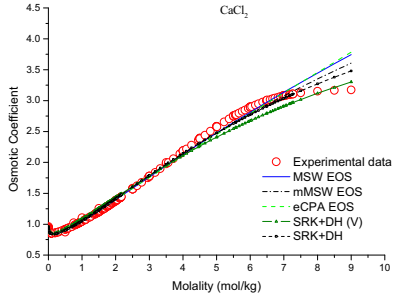

Figure 6.9 Osmotic coefficient of aqueous $CaCl_2$ at 25°C. The SRK+DH (V) refers to the fitting to AMV + $\gamma_{\pm}$ + Φ data. The SRK+DH refers to the fitting only to $\gamma_{\pm}$ + Φ data.

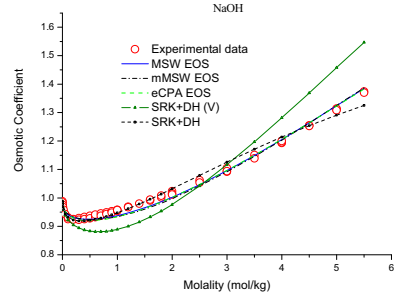

Figure 6.10 Osmotic coefficient of aqueous NaOH at 25°C. The SRK+DH (V) refers to the fitting to AMV + $\gamma_{\pm}$ + Φ data. The SRK+DH refers to the fitting only to $\gamma_{\pm}$ + Φ data.

Still, all EOSs can capture the correct curvatures and trend of AMV. In five electrolyte solutions, the AMV data of aqueous NaOH solution appear to be the most difficult to fit due to its negative AMV values. The AADs of predicted AMV of sodium hydroxide are all larger than 10% for all four EOSs. In the case of eCPA EOS, the AADs are even 50 %. This is also the reason for the very negative k_{ij} of OH^- and water.

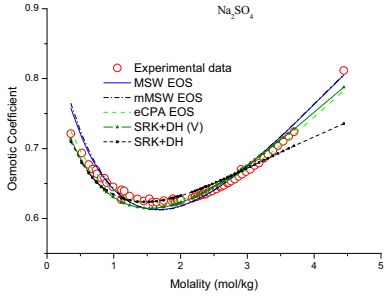

Figure 6.11 Osmotic coefficient of aqueous Na_2SO_4 at 25°C. The SRK+DH (V) refers to the fitting to AMV + $\gamma_{\pm}$ + Φ data. The SRK+DH refers to the fitting only to $\gamma_{\pm}$ + Φ data.

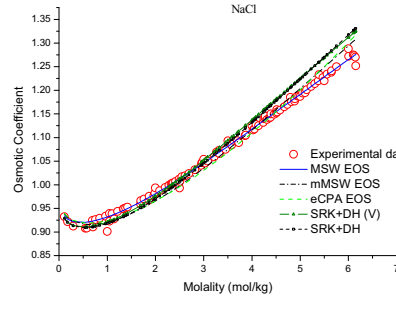

Figure 6.12 Osmotic coefficient of aqueous NaCl at 25°C. The SRK+DH (V) refers to the fitting to AMV + $\gamma_{\pm}$ + Φ data. The SRK+DH refers to the fitting only to $\gamma_{\pm}$ + Φ data.

The second difficult system is the hydrochloric acid solution. In case of $\gamma_{\pm}$ + Φ data, $CaCl_2$ solution has the highest AADs in predicted results of the five electrolyte solutions. This is because of the unique concave curvature of the osmotic coefficient curve of calcium chloride solution at high concentration. The largest deviation occurs at the concentration higher than 7 molal where the curve starts to bend down when concentration increases. In this range, ion complex starts to form in $CaCl_2$ solution and this changes the thermal properties of the solution. Apart from this, all $\gamma_{\pm}$ + Φ data are reproduced with satisfactory accuracy. HCl solutions appear to be the easiest system during parameter estimation. Good fittings of HCl $\gamma_{\pm}$ + Φ data can always first be achieved even when other solutions are relatively poorly represented, see SRK+DH(v) case in Table 6.2.

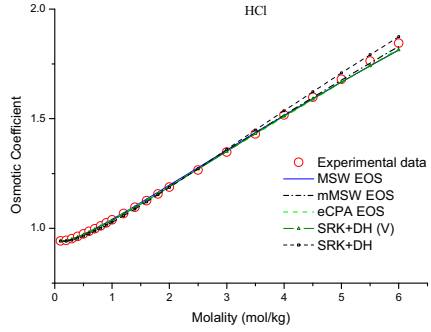

Figure 6.13 Osmotic coefficient of aqueous HCl at 25°C. The SRK+DH (V) refers to the fitting to AMV + $\gamma_{\pm} + \Phi$ data. The SRK+DH refers to the fitting only to $\gamma_{\pm} + \Phi$ data.

6.4.4 Stage III) Binary and ternary systems at 25°C and 0.101325 MPa

In addition to AMV + $\gamma_{\pm} + \Phi$ data, binary and ternary SLE data are included in parameter determination. In this stage, the anion-water interaction parameters alone seem to be insufficient for all EOSs to fulfil the task. With eight interaction parameters (six ion-water interaction parameters and two ion-ion interaction parameters) the goal could be achieved without much difficulty.

The results of the fitted parameters and their ARDs for AMV and mean ionic activity coefficient, osmotic coefficient experimental data are presented in Table 6.3. If a certain inaccuracy of density data or AMV can be accepted, the number of interaction parameters can be further reduced without influencing the calculation accuracy of the other three types of experimental data.

Table 6.3 The optimized electrolyte EOS parameter values for six ions in the test system based on AMV, mean ionic activity coefficient, osmotic coefficient, and SLE experimental data. The AAD and ARD values of the calculated properties are also given.

		Parameters						AAD*	%ARD*	%ARD*
									Activity	Osmotic
EOS	Ion	a	b	σ	k_{ij}*	k_{ij}*	Salt	AMV	Coefficient	Coefficient
		Pa*m^6/mol	cm^3/mol	m^{-10}	(water-ion)	(ion-ion)		cm^3/mol		
						Na^+, OH^-				
	Na^+	1.28860	8.95430	5.21920	0.15705	1.36990	$CaCl_2$	1.63	/	4.29
	Ca^{2+}	0.52778	4.25860	5.43320	1.46570	Ca^{2+}, Cl^-	NaOH	2.20	1.67	0.92
MSW	H^+	0.31489	8.11380	4.19940	0.53501	0.76425	Na_2SO_4	1.69	/	3.79
	Cl^-	2.32510	15.66000	3.05450	-0.81023		NaCl	1.91	3.23	1.12
	SO_4^{2-}	7.46540	22.42500	4.48380	-0.86462		HCl	0.47	1.04	0.65
	OH^-	1.29990	0.02015	4.28390	-0.87093					
						Na^+, OH^-				

	Na^+	0.61611	4.24450	3.14280	-0.96137	1.95720	$CaCl_2$	1.51	/	4.92
	Ca^{2+}	1.16000	0.02366	5.43760	-1.71680	Ca^{2+} , Cl^-	NaOH	1.72	1.54	0.78
mMSW	H^+	0.09110	3.24410	2.51440	-2.58990	0.26958	Na_2SO_4	2.49	/	1.38
	Cl^-	2.82900	19.96600	5.17690	-0.06265		NaCl	0.85	1.14	0.79
	SO_4^{2-}	6.42600	26.26900	4.29670	0.05702		HCl	0.36	0.92	0.68
	OH^-	0.55749	0.16348	4.57400	0.15437					
						Na^+ , OH^-				
	Na^+	0.72975	9.34160	2.59090	0.44503	1.72450	$CaCl_2$	0.84	/	4.79
	Ca^{2+}	0.20587	0.02303	3.25740	3.42320	Ca^{2+} , Cl^-	NaOH	0.41	0.85	0.72
eCPA	H^+	0.02190	4.79750	2.78590	2.71640	1.32550	Na_2SO_4	1.06	/	3.06
	Cl^-	1.05920	19.54100	4.82610	-1.54680		NaCl	0.99	1.56	1.29
	SO_4^{2-}	2.99870	27.05000	5.11120	-1.47080		HCl	0.98	1.08	1.08
	OH^-	0.84542	0.02185	7.15380	-1.07990					
						Na^+ , OH^-				
	Na^+	0.02225	1.37270		0.10808	1.01930	$CaCl_2$	/	/	4.76
	Ca^{2+}	0.02302	0.86771		0.27824	Ca^{2+} , Cl^-	NaOH	/	1.03	0.79
SRK+DH	H^+	0.02002	1.29900		-0.30135	0.31392	Na_2SO_4	/	/	5.86
	Cl^-	0.04277	2.17850		-0.93610		NaCl	/	2.11	0.86
	SO_4^{2-}	0.12454	2.99330		-1.01860		HCl	/	2.00	1.55
	OH^-	0.02000	0.28546		-1.09550					

*** In the column of water-ion interaction parameters, the interaction parameter values are presented according to the corresponding ion in the ion column. In the column of ion-ion interaction parameters, above each value the corresponding ion pairs are given.**

*** Average absolute deviation is fined by following equation:** $AAD = \frac{1}{N}\sum_{i=1}^{N}\left(\left|x_i^{\text{experiment}} - x_i^{\text{calculated}}\right|\right)$

*** Average relative deviation is fined by following equation:** $ARD\% = \frac{1}{N}\sum_{i=1}^{N}\left(\left|\frac{x_i^{\text{experiment}} - x_i^{\text{calculated}}}{x_i^{\text{experiment}}}\right|\right)\times 100\%$

In Table 6.3, it can be seen that the three three-parameter electrolyte EOSs behave similarly well in reproducing AMV + $\gamma_\pm$ + Φ data. Generally speaking, the mMSW EOS reproduces the $\gamma_\pm$ + Φ data most accurately while eCPA EOS gives the best calculated results of AMV. Combining the AMV and $\gamma_\pm$ + Φ data, the eCPA EOS performs slightly better, see Table 6.3. The mMSW EOS is better than MSW EOS but not as good as the eCPA EOS. The SRK+DH EOS gives excellent results. Even though it is a simple EOS, it can still correlate three types of data ($\gamma_\pm$ + Φ +SLE) well with fewer parameters than the other EOSs. Especially with mean ionic activity coefficient and osmotic coefficient, it is as good as the three-parameter EOS. For some electrolytes, it performs even better than the three-parameter EOS, such as the osmotic coefficient of NaCl. Considering its fast computational speed and its simplicity of implementation, this simple electrolyte EOS is outstanding.

The inclusion of AMV data complicates the parameter fitting and the reproduced AMV results are not as good as other fitted properties. Fitting to AMV data helps to improve the accuracy of the calculated density significantly even when the AMV

itself is poorly reproduced. This is illustrated in Figure 6.14 and Figure 6.15. The same parameters were used for calculating the two graphs. In Figure 6.14, the calculated AMV data were plotted together with the experimentally measured AMV data. In Figure 6.15, the same data were converted to density and plotted as such.

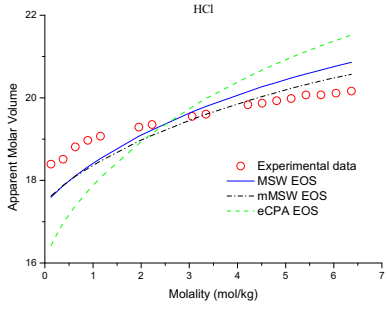

Figure 6.14 Apparent molar volume (cm^3/mol) of aqueous HCl at 25 °C.

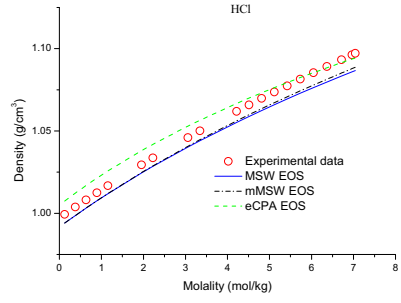

Figure 6.15 Density of aqueous HCl at 25 °C.

From Figure 6.18 to Figure 6.20, it can be seen that the calculated mean ionic activity coefficients and osmotic coefficients of the four EOSs are very close to each other. The same is the case with the remaining systems not shown here.

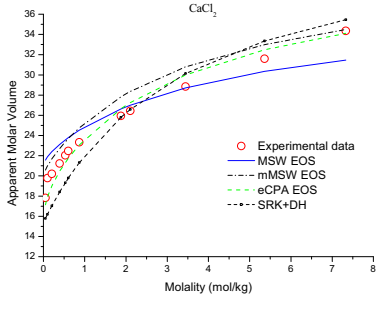

Figure 6.16 Apparent molar volume (cm^3/mol) of aqueous $CaCl_2$ at 25°C.

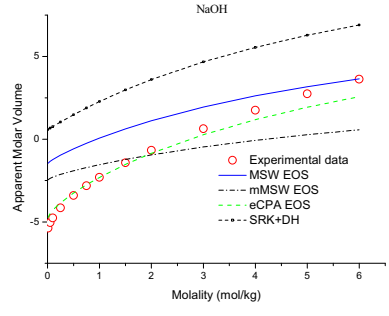

Figure 6.17 Apparent molar volume (cm^3/mol) of aqueous NaOH at 25°C and 1 atmosphere.

Overall, it can be seen in Table 6.3 that the ARDs of the calculated mean ionic activity coefficient and osmotic coefficient are less than 1.6% in general, except for $CaCl_2$ and Na_2SO_4. In contrast, half of the average absolute deviations (AADs) of the calculated AMV are larger than 1.0 cm^3/mol. An AAD value of AMV below 0.8 cm^3/mol indicates a good fitting. It is acceptable if between 1.0 to 1.5 cm^3/mol and it is a poor fitting if concentration is higher than 1.8 cm^3/mol. All three-parameter EOSs can capture the correct curvatures and trend of AMV and consequently give reasonable solution density. However, it is not recommended to use an electrolyte EOS if a high precision of the AMV is required.

Of the five electrolyte solutions for which such data were available, the AMV data of aqueous NaOH and Na_2SO_4 solutions appear to be the most difficult to fit. The AADs

of calculated AMV of sodium sulphate are large for all three-parameter EOSs. The large absolute values of the interaction parameters k_{ij} for OH^--Na^+ in all of the three EOSs result from fitting the AMV of sodium hydroxide. If the AMV data of the hydroxide salts are removed in the objective function, the absolute value of k_{ij} for the OH^--Na^+ interaction parameter will decrease.

It was found that the interaction parameters influence the activity coefficient and osmotic coefficient most. In this context, the large interaction parameters suggest that the mixing rule may not be adaptive for the fittings of activity and osmotic coefficient in the simultaneous fitting. Using a better mixing rule might result in reduced numerical values of the interaction parameters.

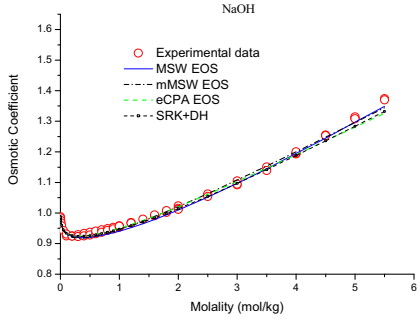

Figure 6.18 Osmotic coefficient of aqueous NaOH at 25°C.

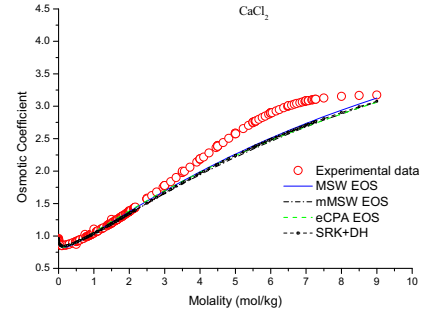

Figure 6.19 Osmotic coefficient of aqueous $CaCl_2$ at 25°C.

Comparing the ARDs of the calculated mean ionic activity coefficient and osmotic coefficient data (Table 6.3) and the graphical results, we find that the osmotic coefficients of the various solutions are calculated with great accuracy except for sodium sulphate (Figure 6.20). The solubility of sodium sulphate is approximately 2 molal at room temperature. When the concentration is higher than 2 molal, the aqueous sodium sulphate solution becomes super-saturated. Figure 6.20 shows that the ability of electrolyte EOS to represent osmotic coefficient over the super-saturated concentration range (2 to 5 molal).

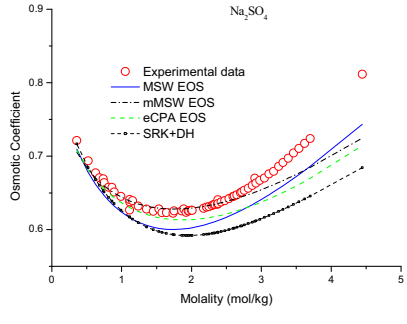

Figure 6.20 Osmotic coefficient of aqueous Na_2SO_4 at 25 °C.

$CaCl_2$ solutions have the highest ARDs of the mean ionic activity coefficient and osmotic coefficient of the test systems. It is probably caused by the unique, concave curvature of the osmotic coefficient curve of calcium chloride solution at high concentration (Figure 6.19). The largest deviation occurs at concentrations higher than 7 molal where the curve starts to bend down when concentration increases. In this concentration range, complex formation starts in $CaCl_2$ solutions[5] and the properties of the solution are changed. SLE data also contribute to the large ARDs of calcium chloride solutions. In order to obtain accurate predictions of SLE data, the osmotic coefficients at saturation concentration have to be accurately fitted. Therefore, the calculated osmotic coefficient curves are forced to pass the point of the osmotic coefficient at saturation concentration (last point in the osmotic coefficient plots) and sacrifice the goodness of fit of the data points from 3 to 9 molal.

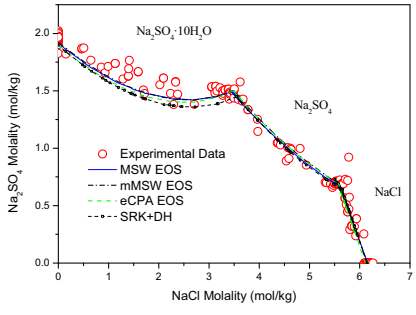

Figure 6.21 Phase diagram for the ternary aqueous system NaCl and Na_2SO_4 at 25°C and 1 atmosphere.

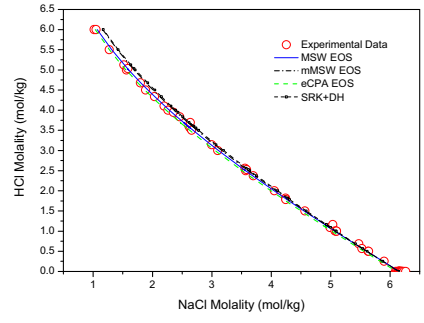

Figure 6.22 Phase diagram for the ternary aqueous system NaCl and HCl at 25°C and 1 atmosphere

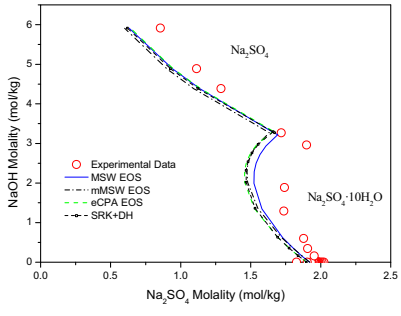

Figure 6.23 Phase diagram for the ternary aqueous system NaOH and Na_2SO_4 at 25°C and 1 atmosphere.

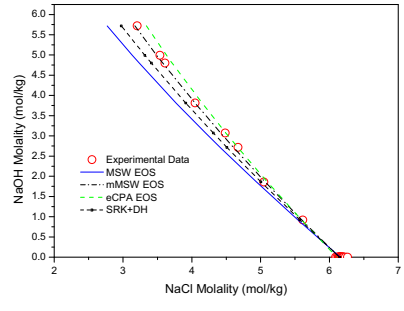

Figure 6.24 Phase diagram for the ternary aqueous system NaOH and NaCl at 25°C and 1 atmosphere.

The solubilities of $CaCl_2$, $Ca(OH)_2$, Na_2SO_4, NaCl, and $CaSO_4$ at 25°C are all very well reproduced, see the solubility at saturation concentration on the axes of the SLE plots in Figure 6.21 to Figure 6.30. Most SLE data of ternary systems are accurately reproduced, such as the aqueous Na_2SO_4-NaCl, NaCl-HCl, NaOH-NaCl, NaCl-$CaCl_2$, $CaSO_4$-$CaCl_2$, $Ca(OH)_2$-$CaCl_2$.

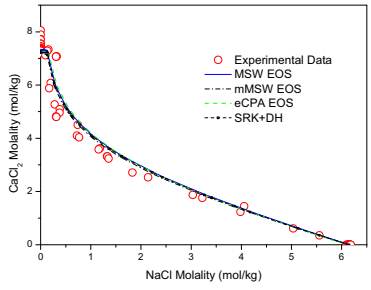

Figure 6.25 Phase diagram for the ternary aqueous system $CaCl_2$ and NaCl at 25°C.

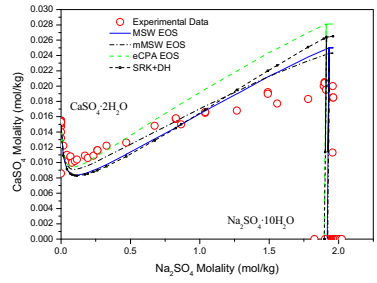

Figure 6.26 Phase diagram for the ternary aqueous system $CaSO_4$ and Na_2SO_4 at 25°C.

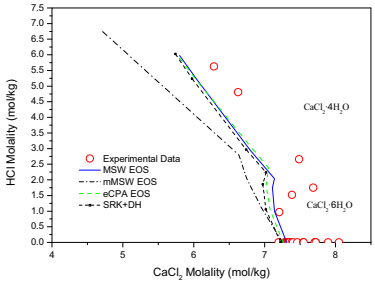

Figure 6.27 Phase diagram for the ternary aqueous system $CaCl_2$ and HCl at 25°C.

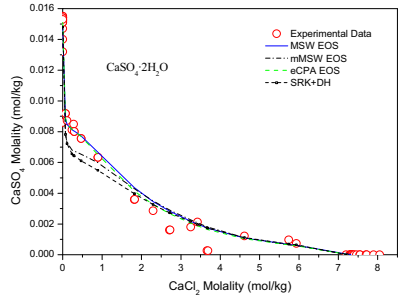

Figure 6.28 Phase diagram for the ternary aqueous system $CaSO_4$ and $CaCl_2$ at 25°C.

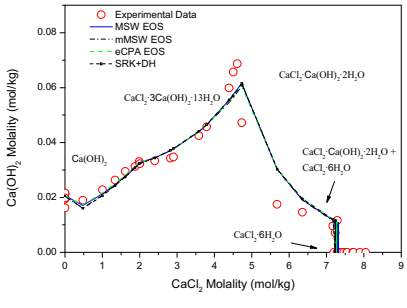

Figure 6.29 Phase diagram for the ternary aqueous system $CaCl_2$ and $Ca(OH)_2$ at 25°C.

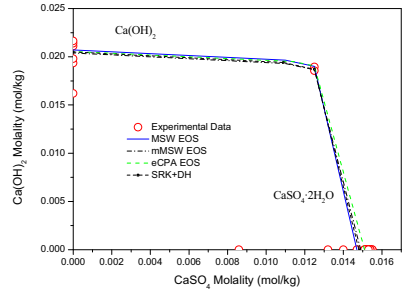

Figure 6.30 Phase diagram for the ternary aqueous system $CaSO_4$ and $Ca(OH)_2$ at 25°C and 1 atmosphere.

For ternary systems containing electrolytes whose mean ionic activity coefficient and osmotic coefficient data of binary system are poorly fitted (such as calcium chloride and sodium sulphate) or containing electrolytes of low solubility whose mean ionic activity coefficient and osmotic coefficient data are unavailable in the literature due to the difficulties of measurement (such as calcium sulphate and calcium hydroxide),

these ternary SLE data are not very well reproduced. Aqueous Na_2SO_4-$CaSO_4$ and $CaCl_2$-HCl belong to these ternary systems, see Figure 6.26 and Figure 6.27.
Generally speaking all four EOSs reproduce the ternary SLE data satisfactorily. For some difficult ternary systems, the three-parameter EOSs perform slightly better than the SRK+DH EOS. In most cases, the calculated saturation curves overlap with each other and the difference is hardly perceptible.

6.5 *Conclusion*

1. The equations of state for electrolytes considered in this work can be applied to multi-component systems using ion-specific parameters. AMV, mean ionic activity coefficient or osmotic coefficient, and solid-liquid equilibrium experimental data can be simultaneously fitted and represented with a small number of interaction parameters. The AMV of aqueous electrolyte solution is only fitted well by the EOS representing water density accurately and containing an electrostatic term contributing to the volume.

2. The interaction parameter k_{ij} plays an important role in simultaneous fittings of volumetric data and thermodynamic data. Especially when AMV is included in the parameter fitting, it can improve the goodness of fit of activity and osmotic coefficient significantly. When the EOS is exclusively fitted to AMV or exclusively fitted to activity and osmotic coefficient data, the number of interaction parameters can be reduced even to zero.

3. There is no significant difference in the performances of complicated electrolyte terms and simple electrolyte terms according to our studies. The explicit MSA term performs as well as the implicit MSA terms or sometimes even better. However, the simplified explicit MSA term needs only one third or one fourth of the computational time required by the implicit MSA term. The simple, truncated Debye-Hückel term with no parameters performs equally well in reproducing activity coefficients and osmotic coefficients as MSA terms in most cases. Apparent molar volumes are not reproduced well by SRK+DH EOS as the electrostatic term does not contribute to the volume of the solution. Considerable work load in programming can be reduced and the computational speed can be increased significantly when the truncated Debye-Hückel term is applied.

4. The difference in performances of the non-electrolyte terms, i.e. the short range terms of SRK, PR, CPA EOS, is small in general when only applied to the single solvent aqueous electrolyte systems at 25°C and 0.101325 MPa. The CPA EOS consumes two or three times more computation time due to its Wertheim association term compared with other EOS. The performance of these short range terms can only be evaluated later when extended to multi-solvent electrolyte systems.

5. It is expected that models based on physical foundations are more likely to present predictive features. In order to evaluate an engineering model for its physical foundations, it is important to compare the resulting optimized parameters with the related physical property. This comparison requires a very critical view, since it is clear that the parameters of such engineering models are not directly related to a measurable, physical property. Yet, some trends may be expected. When looking

closely at the results of this work, we must conclude that we cannot find any such relationship. Hence, even though the properties could be correctly modelled, we would be very cautious in extrapolating outside the fitting region. More work should be performed on electrolyte EOS in order to improve their physical backgrounds.

Reference

1. Myers JA, Sandler SI, Wood RH. An Equation of State for Electrolyte Solutions Covering Wide Range of Temperature, Pressure and Composition. *Ind Eng Chem Res.* 2002; 41: 3282-3297.

2. Kontogeorgis GM, Yakoumis IV, Meijer H, Hendriks E, Moorwood T. Multicomponent phase equilibrium calculations for water-methanol-alkane mixtures. *Fluid Phase Equilib.* 1999; 158-160: 201-209.

3. Uematsu M, Franck EU. Static Dielectric Constant of Water and Steam. *J Phys Chem Ref Data.* 1980; 9(4): 1291-1305.

4. http://www.ivc-sep.kt.dtu.dk/databank/help.htm

5. Rard JA, Clegg SL. Critical evaluation of the thermodynamic properties of $CaCl_2$ 1. Osmotic and activity coefficients of 0-10.77 $mol*kg^{-1}$ aqueous calcium chloride solutions at 298.15 K and correlation with extended Pitzer ion-interaction models. *J Chem Eng Data.* 1997; 42: 819-849.

CHAPTER 7 Multi component EOS for electrolyte systems at a wide temperature range

7.1 *General*

The excess Gibbs free energy models have been applied successfully to numerous geochemical systems and systems of interest in the chemical industry at a wide variety of system condition, including multi-component mixed-solvent electrolytes.

Chen's electrolyte NRTL model using salt-specific parameters was shown to be able to represent SLE of multi-component mixed-solvent electrolytes systems at a wide temperature range [1-4]. It has been used in the Aspen simulator and has received wide acceptance in Industrial practice of thermodynamic modelling of electrolyte systems.

The Extended UNIQUAC model slightly modified by Thomsen *et al*. [5-7] has proven itself applicable for calculations of vapour-liquid-liquid-solid equilibria and calculations of thermal properties in multi-component aqueous solutions of electrolytes and non-electrolytes at wide temperature and pressure range.

In the study of prediction of mineral scale formation in geothermal and oilfield operations using the Extended UNIQUAC model [8,9], the results show that with the added pressure parameters, the Extended UNIQUAC model using ion-specific parameters is able to represent binary, ternary and quaternary solubility data of scaling minerals consist of Na^+, Ca^{2+}, Ba^{2+}, Sr^{2+}, Cl^-, SO_4^{2-}, CO_3^{2-} ions within the experimental accuracy in the range of temperature and pressures from -20 to 250°C and from 1 to 1000 bar, respectively.

Compared with activity coefficient models, the application of electrolyte EOS are rather limited with respect to the types of phase equilibrium calculation, systems studied and the temperature range. The applications of most electrolyte EOSs in literature are summarized in Table 7.1. From this table, it can be seen that applications of electrolyte EOS are mostly correlating thermodynamic properties of binary systems such as density, vapour pressure, mean ionic activity coefficient and osmotic coefficient at varieties of conditions (including room temperature and pressure). Only half of the electrolyte EOSs mentioned in Table 7.1 have been applied to multi-component electrolyte systems (mostly ternary systems). Only one third of the EOSs have been used to correlate or predict vapour pressure or osmotic coefficient of ternary systems. Mixed solvent electrolyte systems have only been treated by Fürst's group[14, 15]. VLE calculations containing electrolytes were conducted by two authors [12,14] .Only methane and argon gas solubility in aqueous NaCl solution have been calculated and reported so far [11, 17]. Merely two EOSs were applied to SLE of multi-component electrolyte systems: one to ternary, quaternary and quinary systems at 25~70 °C [13] and one to two ternary systems at 25°C [22] . Solubility phase diagrams constructed by an EOS for binary systems have not been shown in these papers.

The SLE calculation of multi-component electrolyte systems is a fundamental problem in the design and operation of many industrial processes involving electrolytes [4]. Since relatively little work has been conducted for electrolyte EOS on this subject so far, we have examined the possibility of using electrolyte EOS based on ion-specific parameters to reproduce experimental SLE phase diagrams at a wide range of temperatures besides the conventional correlation of density, mean ionic activity coefficient and osmotic coefficient. As a continuation of the previous chapter, we would like to evaluate different short range terms and long range terms by

applying them to a chosen multi-component system of aqueous electrolytes in a wide temperature range.

7.2 *The electrolyte EOSs*

In this work, we aim at performing phase equilibrium calculation for complex multi-component electrolyte solutions at a wide range temperature range. The equation parameters should be ion-specific as in the previous chapter. The above-mentioned four electrolyte EOSs in Table 6.1 were all used here:

1) Myers, Sandler and Wood Electrolyte EOS[18],
2) Modified Myers, Sandler and Wood Electrolyte EOS,
3) The Electrolyte CPA EOS (eCPA EOS),
4) Debye-Hückel SRK electrolyte EOS (SRK+DH EOS).

The same sets of pure compound parameters for water as in previous chapter were also used for the corresponding electrolyte EOS. The SRK EOS simply use the critical properties of water to calculate the attractive parameter *a* and the co-volume parameter *b*.

The 10 parameter Uematsu and Franck[24] model is used to calculate the relative permittivity of water for MSA and Born terms. The pure water density approximation suggested by Myers *et al.* [18] was used for all the three-parameter EOSs to calculate pure water density in this work.

The parameters were determined through a weighted least squares fit as before with the same objective function.

$$f = \sum_{j=1}^{2}\sum_{i=1}^{N_j}\left(w_j \frac{x_{ij}^{\exp} - x_{ij}^{cal}}{x_{ij}^{\exp}} \right)^2 + \sum_{i=1}^{N_{AMV}} \left[w_{AMV} \left(V_{\phi,i}^{\exp} - V_{\phi,i}^{cal} \right) \right]^2 + \sum_{i=1}^{N_{SLE}} \left[w_{SLE} \ln(SI_i) \right]^2 \qquad (7.1)$$

where x_{ij}^{cal} and $x_{ij}^{\exp}$ are the calculated value and the corresponding experimental value. SI_i is the saturation index of SLE data point *i*. w_j is the weight for the data of type *j*. V_ϕ is the AMV. The multi-temperature data used for the parameter estimation are all from the IVC-SEP electrolyte databank[25]. The combined algorithm alternating between a gradient method (Marquardt method) and a direct search method (Nelder-Mead simplex method) for non-linear least square minimization have been adopted as before. The four electrolyte equations of state were tested by determining the optimal multi-temperature model parameters for the multi-component system consisting of water, Na^+, H^+, Ca^{2+}, Cl^-, OH^-, and SO_4^{2-} ions. A penalty was used for the interaction parameters to prevent their absolute values from becoming to large.

Table 7.1 The table of applications of different equation of states in literature.

Author	Non-electrolyte term	Electrolyte terms	Applications	Temperature range	Pressure range	Electrolyte system	Solvent
Jin and Donohue [11-13] (1988,1991)	Perturbed-Anisotropic-Chain theory, PACT [11]	1. Perturbation expansion term of long range charge-charge interaction 2. Perturbation expansion term of charge-molecule interaction	1. $\gamma_{\pm}$ Specific Volumes of NaCl Solubility (K-factor) of gas in NaCl solution [11] 2. VLE calculation [12] 3. SLE calculation [13]	1. 25 °C 0~100 °C Ar (5~75 °C) [11] 2. 0~150 °C [12] 3. 25 °C 25 °C, 70 °C 28 °C, 50 °C [13]	1. 1.0 bar 1~1000 bar CH_4 (100~600 bar) [11] 2. 0.007~37.48 bar [12] 3. 1 bar [13]	1. 50 strong electrolyte binary systems; NaCl (0~100 °C, 1~1000 bar) Ar-Na-Cl-H_2O and CH_4 -Na-Cl-H_2O 2. four weak electrolytes binary systems [12] 3. ternary systems, quaternary and a quinary system [13]	Aqueous solution
Fürst and Renon [14] (1993)	Modified SRK EOS	1. Simplified Implicit MSA term 2. SR2 term	1. Osmotic coefficients (Φ) correlation 2. Prediction of Φ for ternary systems	25 °C	1 bar	1. 28 electrolyte binary systems 2. 30 ternary systems without mixing parameters	Aqueous solution
Fürst *et al.* [15,16] (1997-2000)	Modified SRK EOS	1. Simplified Implicit MSA term 2. SR2 term 3.Born term (for LLE only)	1. $\gamma_{\pm}$ and VLE of mixed solvent systems 2. LLE of mixed sovent systems	1. .25, 30, 75°C (VLE) 2. 20-40 °C (LLE)	1. 0.55 and 1.1013 Bar (VLE)	1. $\gamma_{\pm}$ of 8 water-alcohol-salt systems; VLE of 26 water-alcohol-salt systems and 12 other nonalcohol mixed-solvent electrolyte systems 2. LLE of 13 ternary systems of water + organic solvent + salt	Mixed solvent
Wu and Prausnitz [17] (1998)	1.PR EOS (PR) 2.Wertheim association term	1.Complete MSA 2. Wertheim association term for ion association 3. Born term	1. Predicted solubility of CH_4 2. $\gamma_{\pm}$ and water activity correlation	1. 125 °C, 2. 25 to 300 °C	1. 100~600 bar 2. Corresponding Saturated Pressure	1. CH_4 -Na-Cl-H_2O 2. NaCl binary solutions	Aqueous solution
Myers, Sandler and Wood [18] (2002)	PR EOS with volume translation	1. Simplified explicit MSA (restricted primitive model, short as RPM)	1. $\gamma_{\pm}$ correlation 2. $\gamma_{\pm}$, Φ, densities (ρ), free energies of hydration	1. 25 °C 2. 25~300 °C 3. 25 °C	1. 1 bar 2. 1 ~ 120 bar 3. 1 bar	1. 138 binary electrolyte solutions 2. Seven binary electrolyte solutions 3. Ternary systems: NaCl-LiCl-H_2O	Aqueous solution

	parameter	2. Born term	correlation 3. Predicted Φ	110 ºC	1.45 bar	and NaCl-$CaCl_2$–H_2O	
Galindo, G-Villegas, Jackson and Burgess [0] (1999)	SAFT-VR EOS	1. Simplified explicit MSA (RPM)	1. Vapour pressure (P_v), ρ correlation 2. P_v correlation	1. 0~100 °C, constant system temperature 2. 40~70 °C	1. Corresponding P_v, 2. Corresponding P_v	1. 9 strong binary electrolyte systems 2. One ternary electrolyte system (LiBr + LiI)	Aqueous solution
Cameretti, Sadowski and Mollerup [20] (2005)	PC-SAFT EOS	1. The complete Debye-Hückel term	P_v and ρ correlation	5 to 60 °C	Corresponding P_v	12 binary electrolyte systems	Aqueous solution
Tan *et al.* [21] (2005)	SAFT1 EOS	1. Simplified explicit MSA (RPM) and neglect the associations for ions	1. $\gamma_{\pm}$ and ρ correlation, predicted P_v 2. $\gamma_{\pm}$ and ρ correlation	1. 25 °C 2. 25, 50, 100°C		1. Six binary alkali halide electrolyte solutions 2. One binary system: NaCl	Aqueous solution
Ji and Tan *et al.* [22] (2006)	SAFT2 EOS	1. Simplified explicit MSA (RPM) and neglect the associations for ions	1. $\gamma_{\pm}$ and ρ correlation, predicted P_v 2. $\gamma_{\pm}$ and ρ correlation	1. 25 °C 2. 25, 50, 100°C		1. Six binary alkali halide electrolyte solutions 2. One binary system: NaCl	Aqueous solution
Liu *et al.* [23]	SAFT EOS with a LJ potential	1. The low-density expansion of the MSA closure for the non-primitive model 2. Wertheim term for association of ions and solvent	$\gamma_{\pm}$,Φ, ρ correlation	25 °C	1 bar	Fifteen binary alkali halide solutions ()	Aqueous solution

7.3 *Determination of temperature function for the attractive parameter a and the ion size parameter σ*

Before conducting the parameter optimization, we determined suitable temperature dependence functions for the attractive parameter *a(T)* and for the ion-size parameter *σ (T)*. Five different temperature functions for the attractive parameter *a(T)* (I to V) and four different temperature functions for the ion-size parameter *σ (T)* (I to IV) were tested. The different temperature functions tested are listed in Table 7.2. The temperature functions include a constant function, a linear temperature dependence, a reciprocal temperature dependence, and second and third order polynomials in temperature.

Table 7.2 Temperature dependence functions tested.

No.	attractive parameter $a(T)$	ion-size parameter $\sigma(T)$
I	$a(T) = a_0$	$\sigma(T) = \sigma_0$
II	$a(T) = a_0 - a_1 / T$	$\sigma(T) = \sigma_0 - \sigma_1 / T$
III	$a(T) = a_0 + a_1 \Delta T$	$\sigma(T) = \sigma_0 + \sigma_1 \Delta T$
IV	$a(T) = a_0 + a_1 \Delta T + a_2 \Delta T^2$	$\sigma(T) = \sigma_0 + \sigma_1 \Delta T + \sigma_2 \Delta T^2$
V	$a(T) = a_0 + a_1 \Delta T + a_2 \Delta T^2 + a_3 \Delta T^3$	/
	$\Delta T = T - 298.15\ \mathrm{K}$	

By combining different terms for the temperature dependence of *a(T)* and *σ (T)* from Table 7.3, seven different temperature dependence functions are established. They are described in Table 7.3, denoted as FT1 to FT7 respectively.

Based on the previous work, it is known that the three-parameter EOSs perform equally well at 25°C and 1.01325 bar and the SRK+DH EOS performs only slightly different from the three-parameter EOSs when AMV data are excluded from parameter optimization. The computation speed of MSW EOS was found to be the highest among the three-parameter EOSs. Consequently, we chose MSW EOS for determining the best temperature dependency functions to reproduce all experimental data by testing all seven functions one by one. After the most suitable temperature dependence functions were found, they were implemented into the other three EOSs and the parameter optimization was performed.

We found it better to perform the parameter optimization in progressive stages than in an all-in-one-step manner with all experimental data points. It helps the optimization routine to find the optimal parameter set more quickly and smoothly. We followed this methodology to determine the best temperature dependence function for EOS parameters. The parameter regressions were performed in four progressive stages using various amounts and types of data:

1) Multi temperature water activity, mean ionic activity coefficient and osmotic coefficient data, short as $\gamma_{\pm} + \Phi$ data.
2) Multi temperature binary and ternary SLE data.
3) Multi temperature binary and ternary SLE data, multi-temperature water activity, mean ionic activity coefficient data and osmotic coefficient data, short as SLE + $\gamma_{\pm} + \Phi$.
4) AMV data at 25 °C plus all multi-temperature data of 3), short as AMV+SLE + $\gamma_{\pm} + \Phi$.

The seven temperature dependence functions for electrolyte EOS (FT1 to FT7) were tested step by step through stage 1 to 4 to screen out the best one. Bad temperature dependence functions for the parameters of electrolyte EOS can only work in certain stage such as in stage 1 or 2. Good temperature dependence functions in contrast can satisfactorily fit all types of experimental data with a minimum number of parameters. After a few preliminary attempts it was discovered that only using the eight temperature-independent interaction parameters as in previous chapter were insufficient to handle the multi-temperature data. However, it is discovered by trial or error that with twelve temperature independent interaction parameters (six ion-water interaction parameters and six ion-ion interaction parameters) it is possible to accomplish the tasks in stage 1 to 4.
The other possibility is to use temperature dependent interaction parameters, but this requires changing the source code of the non-electrolyte terms and a systematic study of the temperature dependent functions for interaction parameters and for the corresponding ionic parameters. Needless to say, it is a comprehensive amount of work thus preserved for the future study. Therefore, twelve temperature independent interaction parameters to be used in data fitting are the main focus.

Table 7.3 The seven temperature dependence functions for the attractive parameter *a(T)* and the ion-size parameter $\sigma(T)$ and their performance.

Temperature dependence function for electrolyte EOS	Expression of temperature dependence *a(T)* and $\sigma(T)$	Optimization stage			
		Stage 1)	Stage 2)	Stage 3)	Stage 4)
		$\gamma_{\pm} + \Phi$ data	SLE data	SLE + $\gamma_{\pm} + \Phi$	AMV + data in stage 3
FT1	$a(T) = a_0$, $\sigma(T) = \sigma_0$	Fail			
FT2	$a(T) = a_0 - a_1/T$, $\sigma(T) = \sigma_0 - \sigma_1/T$	Average	Not Good	Fail	
FT3	$a(T) = a_0 + a_1\Delta T$, $\sigma(T) = \sigma_0 + \sigma_1\Delta T$	Good	Bad	Fail	
FT4	$a(T) = a_0 - a_1/T$, $\sigma(T) = \sigma_0 + \sigma_1\Delta T$	Good	Bad	Fail	
FT5	$a(T) = a_0 + a_1\Delta T + a_2\Delta T^2$ $\sigma(T) = \sigma_0 + \sigma_1\Delta T$	Very Good	Good	Very Good	Considerably Good
FT6	$a(T) = a_0 + a_1\Delta T + a_2\Delta T^2$ $\sigma(T) = \sigma_0 + \sigma_1\Delta T + \sigma_2\Delta T^2$	/	Good, slow [b]	Good, slow [b]	/
FT7	$a(T) = a_0 + a_1\Delta T + a_2\Delta T^2 + a_3\Delta T^3$ $\sigma(T) = \sigma_0 + \sigma_1\Delta T$	/	Good, slow [b]	Good, slow [b]	/

a. The expression of the functions for $a(T)$ and $\sigma(T)$ are summarized in Table 7.2.
b. Optimization process is significantly slowed down when using this function compared to FT5. No significant improvement in the goodness of fit comparing with that of function FT5 when the number of the fitting parameters increased.
c. "/" stand for not chosen for this optimization test.

In stage 1, the constant temperature dependence FT1 failed. Using the temperature dependence FT2 to FT5, the MSW EOS can easily represent both the multi-temperature mean ionic activity coefficient and osmotic coefficient data. FT6 and FT7 have one additional degree of freedom compared with FT5: parameter a_3 in $a(T)$ of FT7 and parameter σ_2 in $\sigma(T)$ of FT6. They should be applied only when FT5 fails or they can significantly improve the fitting results compared to FT5. Since function FT5 is a special case of FT6 and FT7 mathematically ($a_3 = \sigma_2 = 0$), there is no need to test FT6 and FT7 when FT5 gives very good results.

The multi-temperature SLE data are much more difficult to fit then $\gamma_{\pm} + \Phi$ data in stage 1. The optimization process was prolonged significantly in stage 2 (10 times longer than that in stage 1. The reciprocal temperature dependence FT2 of Myers *et al*. [18], see Table 7.3), the linear temperature dependence FT3 and the hybrid temperature dependence of FT4 did not satisfactorily represent multi-temperature SLE data, though they are not a total failure. The temperature dependence of Myers *et al*. [18] is the best of the three, but still not very satisfactory. When using the dependence function FT5, satisfactory results were achieved. FT6 and FT7 were also tested to see whether they could significantly improve the fitting results of FT5. The test shows that the improvements are insignificant, instead the additional parameters in $a(T)$ or $\sigma(T)$ significantly slow down the optimization process.

In stage 3, multi-temperature $\gamma_{\pm} + \Phi$ data are included in the parameter optimization for the MSW EOS. All three two-parameter temperature dependence functions (FT2 to FT4) completely failed to reproduce the experimental data. Only when the number of parameters of $a(T)$ is increased from two to three, it was possible to fit the $\gamma_{\pm} + \Phi$ +SLE data. Interestingly enough, for temperature dependence function FT5, the including of multi-temperature $\gamma_{\pm} + \Phi$ data improved the fitting results of multi-temperature SLE. The objective function value (for the same sets of multi-temperature SLE data) reduced more than 10% of that in stage 2. The objective function value (for multi-temperature $\gamma_{\pm} + \Phi$ data) almost unchanged compared to stage 1. Similarly as in stage 2, FT6 and FT7 did not significantly improve the fitting results of FT5. It seems function FT6 and FT7 are more than necessary if FT5 is sufficient. Consequently, temperature dependence function FT6 and FT7 are not adopted later in this work. Apparently, now FT5 proves to be the best of all temperature dependence functions, with relatively high computational speed and minimum number of parameters required.

The aim of the final stage 4 is not to select the existing temperature dependence functions. It is rather only to see whether FT5 is able to simultaneously reproduce AMV experimental data with the data of stage 3. The calculated AMV values are very sensitive functions of the EOS parameters. The reproduced AMV data are often not as good as other fitted thermodynamic properties. AMV data complicate the parameter fitting significantly, however AMV data helps to achieve parameters with more physical meaning besides its significant improvement of the accuracy of the calculated density. For the sake of simplicity, we only fit the AMV at 25 °C in this work not all temperature range. The reasons are as follows. First, it will speed up the optimization process. Secondly the EOS is well known for its incapability of handling

volumetric properties and this will decrease the difficulties of the parameter estimation. This time, unlike in stage 3, the goodness-of-fit of other properties has been deteriorated slightly rather than improved when AMV was fitted together with them. The duration of the optimization process were significantly prolonged. Overall, FT5 still performs quite well in stage 4, which suggests that it is highly possible that all four types of data in stage 4 can be simultaneously fitted by other EOSs with FT5 as temperature dependence function. The tested temperature dependence functions and their performances are summarized in Table 7.3. The results are satisfactory.

7.4 *Multi-component aqueous electrolyte solution at a wide temperature range (-30 to 130 ℃) and 0.101325 MPa (Binary and ternary systems)*

In the previous section, FT5 was shown to be the best temperature dependence function for the MSW EOS. Due to the similarity of the EOSs tested here, it was assumed that FT5 is also the best temperature function for the other EOSs. The SRK+DH EOS has no adjustable ion-size parameter σ, therefore only the second order polynomial of *a(T)* in FT5 was implemented for this EOS. Besides, AMV data were not used in the SRK+DH EOS parameter optimization. The parameters for this EOS will be determined from the data used in stage 3. For the mMSW EOS and eCPA EOS, the FT5 temperature dependence was used in a manner similar as with the MSW EOS. When determining parameters for the mMSW EOS and the eCPA EOS, the stage 1 and stage 2 were skipped and the data of stage 3 were directly used to determine the parameters. The resulting parameter sets from stage 3 were used as the starting guess in the next stage 4. Note, as before, SRK+DH EOS was not fitted to AMV and thus were not tried in stage 4.

The duration of the parameter optimization of mMSW and eCPA EOS is three times longer than that of MSW EOS because of the implicit MSA term and the association term. Good results were obtained for both of these EOSs in stage 4. The mMSW EOS performs not as good as the MSW EOS while the eCPA EOS performs slightly better than MSW EOS in stage 4. The final objective function value of eCPA is 8% smaller than MSW EOS while that of mMSW is 2.4% larger than MSW EOS. The values of the fitted parameters of the four EOSs and their ARDs for AMV and mean ionic activity coefficient, osmotic coefficient are presented in Table 7.4. Graphical results are also presented in Figure 7.2 to Figure 7.40. Note the isotherms of mean ionic activity coefficient, osmotic coefficient or ternary SLE data at some temperatures have been shifted a distance away from their original place along the x or y axes in the figures. The exact values of the distance for each shifted isotherms (denoted as *a* here) are indicated in the figures as $y \pm a$ or $x \pm a$, meaning that the constant value *a* has been added to or subtracted from the y or x values of the isotherms. In this way the isotherms plotted in the figure can be differentiated clearly. Otherwise most isotherms will overlap or intersect with each other in the figure, making it impossible to distinguish them from one another.

Table 7.4 The values of the optimized electrolyte EOS parameters for six ions in the test system based on AMV, mean ionic activity coefficient, osmotic coefficient, and solid-liquid equilibrium experimental data. The AAD and ARD values of the calculated properties are also given.

EOS	Ions	a_0	a_1*10^2	a_2*10^3	b	σ_0	σ_1	k_{ij}

		Pa*m^6/mol	Pa*m^6/K/mol	Pa*m^6/mol/K^2	cm^3/mol	m^{-10}	m^{-10}/K	component	H_2O	Na^+	Ca^{2+}	H^+	Cl^-	SO_4^{2-}	OH^-
								H_2O	0.0000	0.9243	2.0350	-0.3659	-0.5087	-0.3974	-0.5560
	Na^+	1.6788	-1.3769	0.0709	6.2825	4.5700	0.0417	Na^+	0.9243	0.0000	0.0000	0.0000	0.9885	1.0825	1.8507
	Ca^{2+}	1.5116	-0.6691	0.3556	1.2564	4.9289	0.0539	Ca^{2+}	2.0350	0.0000	0.0000	0.0000	1.7044	1.5886	1.2833
MSW	H^+	0.7122	-1.8273	0.1632	8.6534	12.5070	-0.1166	H^+	-0.3659	0.0000	0.0000	0.0000	0.0000	0.0000	0.0000
	Cl^-	4.1451	1.6762	-0.1437	18.6850	3.2407	0.0252	Cl^-	-0.5087	0.9885	1.7044	0.0000	0.0000	0.0000	0.0000
	SO_4^{2-}	11.9840	8.4689	-0.4345	24.9650	2.5353	0.0261	SO_4^{2-}	-0.3974	1.0825	1.5886	0.0000	0.0000	0.0000	0.0000
	OH^-	1.7498	1.5846	-0.0628	0.0027	3.8783	0.0255	OH^-	-0.5560	1.8507	1.2833	0.0000	0.0000	0.0000	0.0000
								H_2O	0.0000	0.8380	1.9001	-0.4290	-0.5101	-0.4128	-0.5051
	Na^+	1.8638	-1.5675	0.0930	7.6420	4.2002	0.0374	Na^+	0.8380	0.0000	0.0000	0.0000	0.9841	1.0843	1.7653
	Ca^{2+}	1.7012	-1.1221	0.4123	4.1848	4.0657	0.0442	Ca^{2+}	1.9001	0.0000	0.0000	0.0000	1.6303	1.5570	1.3486
mMSW	H^+	0.5953	-1.6200	0.1784	10.1270	9.7188	-0.1526	H^+	-0.4290	0.0000	0.0000	0.0000	0.0000	0.0000	0.0000
	Cl^-	4.3985	1.5424	-0.1623	17.1770	5.1053	0.0498	Cl^-	-0.5101	0.9841	1.6303	0.0000	0.0000	0.0000	0.0000
	SO_4^{2-}	13.9740	7.6710	-0.5652	24.2560	3.6380	0.0203	SO_4^{2-}	-0.4128	1.0843	1.5570	0.0000	0.0000	0.0000	0.0000
	OH^-	2.1306	1.6234	-0.0484	0.0057	4.9924	-0.0093	OH^-	-0.5051	1.7653	1.3486	0.0000	0.0000	0.0000	0.0000
								H_2O	0.0000	1.4602	2.2548	0.0148	-1.0279	-0.8674	-1.1245
	Na^+	1.3392	-0.8371	0.0480	6.0604	3.0787	0.0273	Na^+	1.4602	0.0000	0.0000	0.0000	1.2713	1.3489	1.9862
	Ca^{2+}	2.1072	-0.0072	0.2769	1.0678	3.9298	0.0432	Ca^{2+}	2.2548	0.0000	0.0000	0.0000	1.6918	1.5999	1.2601
eCPA	H^+	0.1689	-0.3560	0.0350	11.6420	5.0429	-0.0446	H^+	0.0148	0.0000	0.0000	0.0000	0.0000	0.0000	0.0000
	Cl^-	2.9032	1.5864	-0.1270	21.7830	5.0655	0.0516	Cl^-	-1.0279	1.2713	1.6918	0.0000	0.0000	0.0000	0.0000
	SO_4^{2-}	9.2420	5.5963	-0.1959	30.6420	3.7853	0.0194	SO_4^{2-}	-0.8674	1.3489	1.5999	0.0000	0.0000	0.0000	0.0000
	OH^-	1.3315	1.3167	-0.0219	0.5259	6.3302	0.0131	OH^-	-1.1245	1.9862	1.2601	0.0000	0.0000	0.0000	0.0000
								H_2O	0.0000	1.6377	2.7408	0.6466	-0.7794	-1.8268	-0.6866
	Na^+	7.1901	-2.3682	0.0544	27.1890			Na^+	1.6377	0.0000	0.0000	0.0000	1.1420	0.2010	1.2999
	Ca^{2+}	6.1910	-2.6696	0.2107	36.8000			Ca^{2+}	2.7408	0.0000	0.0000	0.0000	1.2958	-0.7694	1.1922
SRK+DH	H^+	2.3199	-1.4072	0.1242	33.2760			H^+	0.6466	0.0000	0.0000	0.0000	0.0000	0.0000	0.0000
	Cl^-	20.4090	-0.5772	-0.9203	29.4010			Cl^-	-0.7794	1.1420	1.2958	0.0000	0.0000	0.0000	0.0000
	SO_4^{2-}	50.4190	-43.7090	3.4434	61.0020			SO_4^{2-}	-1.8268	0.2010	-0.7694	0.0000	0.0000	0.0000	0.0000
	OH^-	15.2460	5.8743	-0.7404	24.2220			OH^-	-0.6866	1.2999	1.1922	0.0000	0.0000	0.0000	0.0000

For SRK+DH EOS, the reproduced mean ionic activity coefficient and osmotic coefficient are not as accurate as the results of three-parameter EOSs for most systems. SRK+DH EOS only partly succeeded in fitting experimental data in stage 3. For some difficult systems such as the osmotic coefficient of Na_2SO_4, $CaSO_4$ and mean ionic activity coefficient of $CaCl_2$, $CaSO_4$ and NaOH, the reproduced results are largely deviated. SRK+DH EOS is only able to capture the trend of the curvature of these difficult systems, see corresponding figures. The largely deviated isotherms

calculated with the SRK+DH EOS are therefore not plotted in the figures with the graphical results of other EOSs.

None of the three parameter EOSs can reproduce the mean ionic activity coefficient and osmotic coefficient data with high accuracy in stage 4, at temperatures higher than 100 °C. The S-shaped curves of the osmotic coefficient of aqueous $CaCl_2$ are still impossible for all four EOSs to capture even after the twelve interaction parameters and temperature dependent functions were adopted. The curvatures caused by ion complex formation at high concentration are still underestimated as it was in chapter six. All predicted curves are forced to pass the end point of each isotherm at saturation concentration due to fitting of the SLE data. This problem might be solved by using a proper association scheme for ions as has been shown by Herzog *et al.*[26]. The electrolyte PC-SAFT EOS of Herzog *et al.*[26] could fit an "S-shape" osmotic coefficient of LiCl over the full solubility concentration range, see below figure. This shines light for solving the ion-complex problem like in aqueous $CaCl_2$ solution.

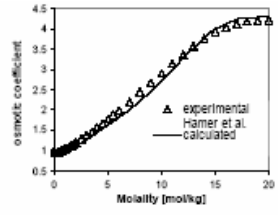

Figure 7.1. Osmotic coefficient at 25°C for the system water + LiBr over the full solubility range from Herzog *et al.*[26]

The deviation of mean ionic activity coefficient and osmotic coefficient of aqueous calcium sulphate solution, see Figure 7.7 and Figure 7.12, is large compared with other electrolyte systems.

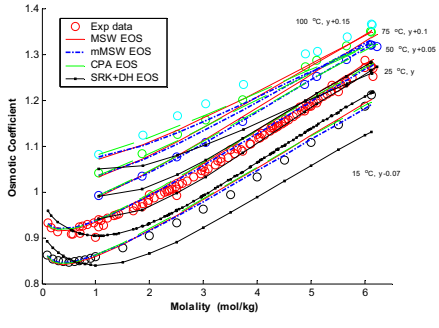

Figure 7.2. Osmotic coefficient of aqueous NaCl at different temperatures. A constant is added to some data at different temperatures to separate them from each other.

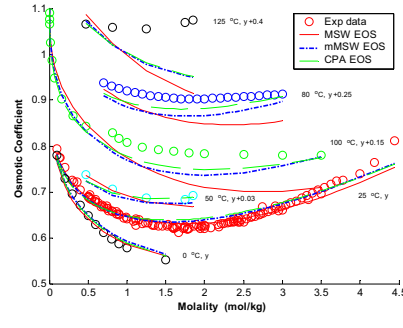

Figure 7.3. Osmotic coefficient of aqueous Na_2SO_4 at different temperatures. Values calculated with the SRK+DH EOS are not shown. A constant is added to some data at different temperatures to separate them from each other.

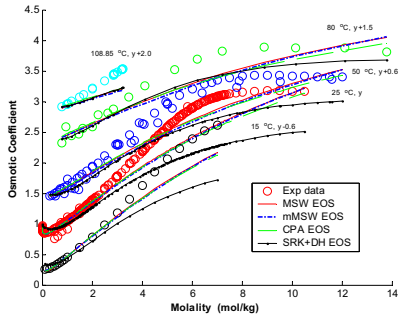

Figure 7.4. Osmotic coefficient of aqueous $CaCl_2$ at different temperatures. A constant is added to some data at different temperatures to separate them from each other.

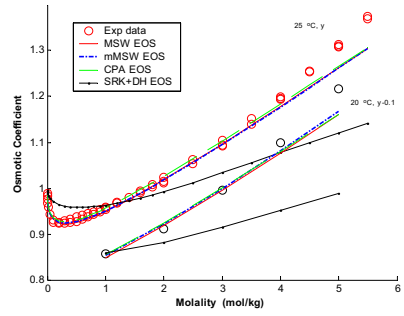

Figure 7.5. Osmotic coefficient of aqueous NaOH at different temperatures. A constant is added to some data at different temperatures to separate them from each other.

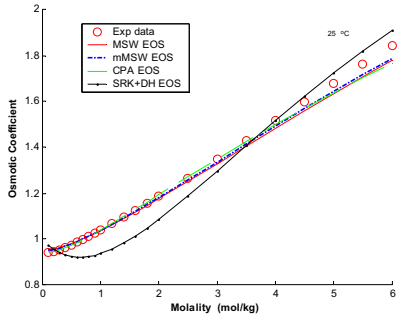

Figure 7.6. Osmotic coefficient of aqueous HCl at 25°C.

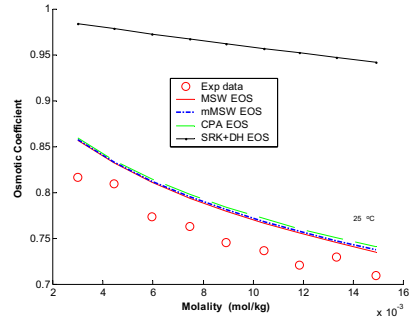

Figure 7.7. Osmotic coefficient of aqueous $CaSO_4$ at 25°C.

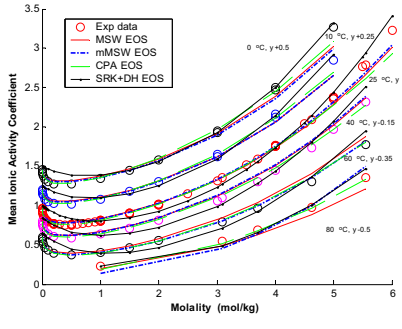

Figure 7.8. Mean ionic activity coefficient of aqueous HCl at different temperatures. A constant is added to some data at different temperatures to separate them from each other.

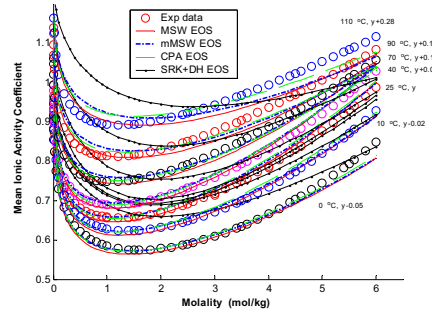

Figure 7.9. Mean ionic activity coefficient of aqueous NaCl at different temperatures. A constant is added to some data at different temperatures to separate them from each other. Only the correlation results of SRK+DH EOS at 0, 25, 70 and 110°C are shown.

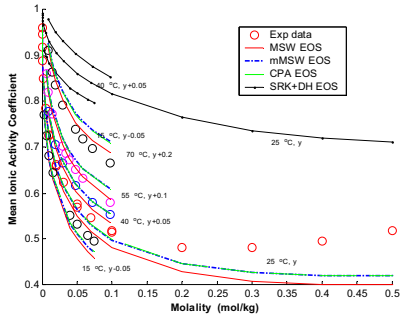

Figure 7.10. Mean ionic activity coefficient of aqueous $CaCl_2$ at different temperatures. A constant is added to some data at different temperatures to separate them from each other. Only three correlation results of SRK+DH EOS at different temperatures are shown.

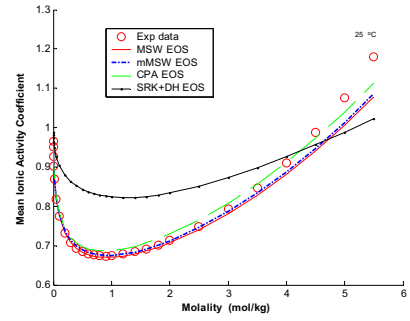

Figure 7.11. Mean ionic activity coefficient of aqueous NaOH at 25°C.

The reproduced AMVs by three-parameter EOSs are not as accurate as in previous chapter, but they are still acceptable.

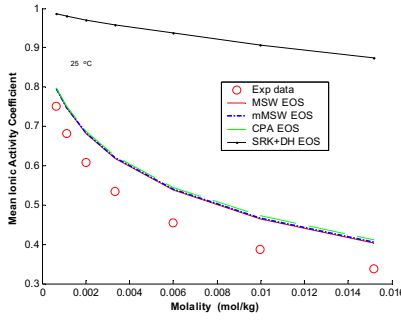

Figure 7.12. Mean ionic activity coefficient of aqueous $CaSO_4$ at 25°C.

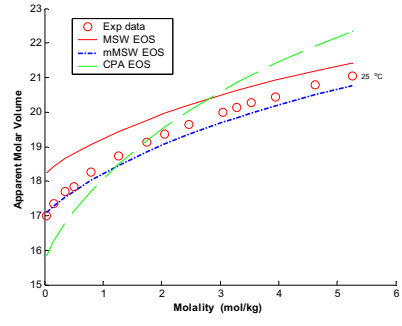

Figure 7.13. Apparent molar volume (cm^3/mol) of aqueous NaCl at 25°C and 1 atmosphere.

The solubility diagrams of binary systems are very well reproduced except at high or low temperatures. For calcium chloride aqueous solution, the predicted results at temperature over 125°C or below -50°C, the deviations of the three-parameter EOS start to increase, see Figure 7.20. The goodness of fitting of binary systems of $CaSO_4$ and $Ca(OH)_2$ are acceptable for SRK+DH EOS. For Na_2SO_4 and $CaCl_2$ systems, we only partly succeeded in fitting certain branch with SRK+DH EOS. The solubility of binary systems is better reproduced by SRK+DH EOS than the mean ionic activity coefficient or osmotic coefficient.

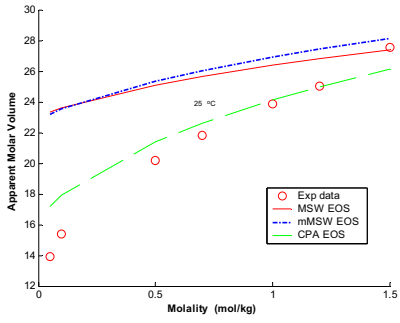

Figure 7.14. Apparent molar volume (cm^3/mol) of aqueous Na_2SO_4 at 25°C and 1 atmosphere.

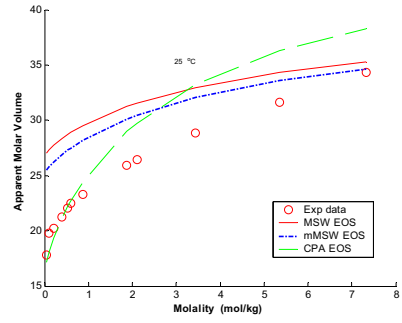

Figure 7.15. Apparent molar volume (cm^3/mol) of aqueous $CaCl_2$ at 25°C and 1 atmosphere.

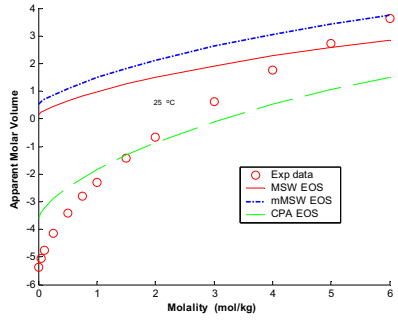

Figure 7.16. Apparent molar volume (cm^3/mol) of aqueous NaOH at 25°C and 1 atmosphere.

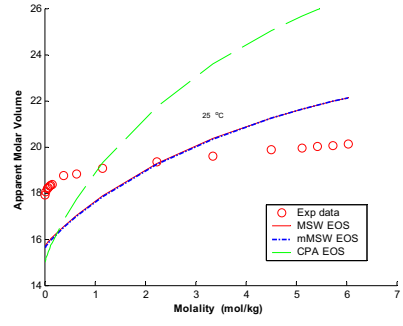

Figure 7.17. Apparent molar volume (cm^3/mol) of aqueous HCl at 25°C and 1 atmosphere.

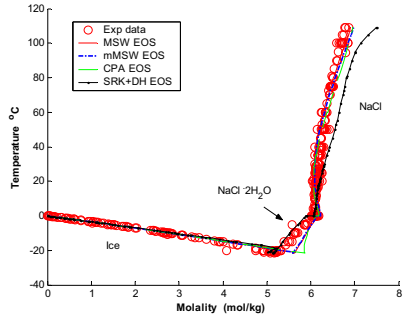

Figure 7.18. Solubility phase diagram of aqueous NaCl system.

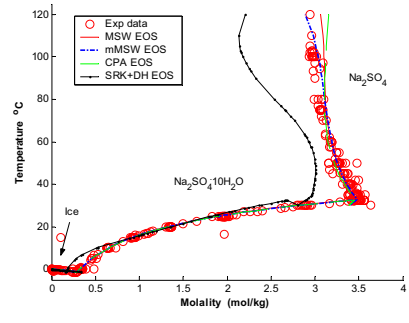

Figure 7.19. Solubility phase diagram of aqueous Na_2SO_4 system.

We failed to reproduce most ternary SLE systems with the SRK+DH EOS but reproduced most ternary SLE system with the three-parameter EOSs. The multi-temperature ternary SLE data are the most difficult to reproduce for SRK+DH EOS. Only the two ternary systems NaCl+HCl, NaCl+NaOH systems could be fitted reasonably well, see corresponding figures. Within the temperature interval [-20, 100]°C, the saturation curves for ice, ice and salt mixture, salt with crystal water or pure salt are all very well represented. Errors become significant at the region of the

two ends of the temperature intervals for experimental data, i.e. below -20°C or above 100°C. See the isotherms at -45°C and 100°C for NaCl+$CaCl_2$ in Figure 7.24, Figure 7.26, isotherms at -20°C for NaCl+Na_2SO_4 in Figure 7.31.

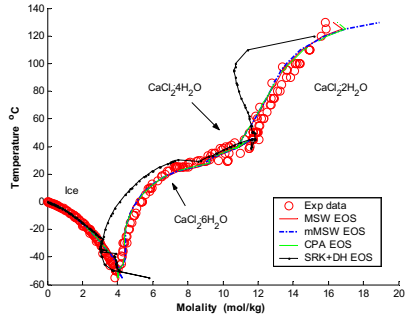

Figure 7.20. Solubility phase diagram of aqueous $CaCl_2$ system.

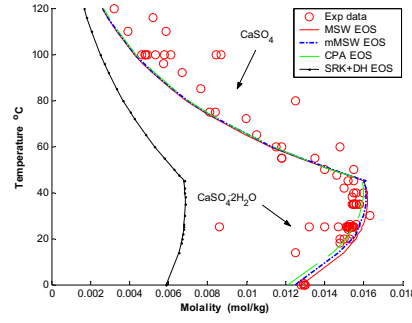

Figure 7.21. Solubility phase diagram of aqueous $CaSO_4$ system.

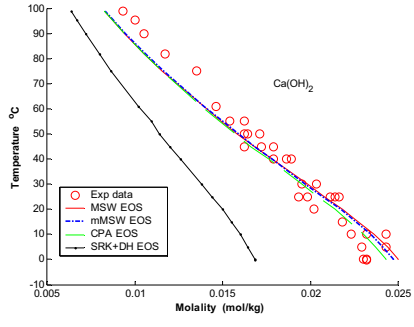

Figure 7.22. Solubility phase diagram of aqueous $Ca(OH)_2$ system.

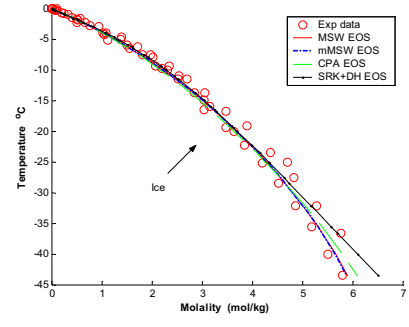

Figure 7.23. Solubility phase diagram of aqueous HCl system.

It is the same case for mean ionic activity coefficient, osmotic coefficient and binary solubility. This suggests that the temperature dependence function FT5 is still not very adaptive at too high or too low temperatures. It is still necessary to find better temperature dependence function for attraction parameter and ion-size parameter. The other possible explanation is that the interaction parameter k_{ij} might be temperature dependent. It should be investigated in the future.

The three-parameter EOS could not provide satisfactory correlation of ternary system $CaCl_2$ + HCl at 25°C. The calculated results agree only qualitatively with the experimental data.

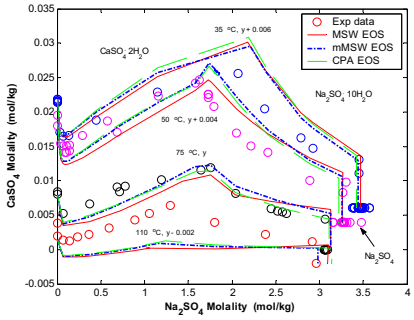

Figure 7.24. Phase diagram of the ternary aqueous system Na_2SO_4 and $CaSO_4$ system at high temperature. A constant is added to some data at different temperatures to separate them from each other.

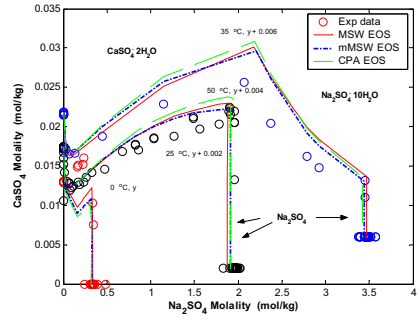

Figure 7.25. Phase diagram of the ternary aqueous system Na_2SO_4 and $CaSO_4$ system at low temperature. A constant is added to some data at different temperatures to separate them from each other.

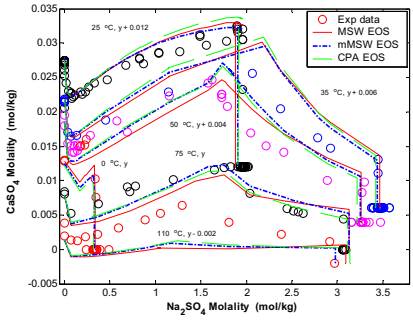

Figure 7.26. Phase diagram of the ternary aqueous system Na_2SO_4 and $CaSO_4$ system A constant is added to some data at different temperatures to separate them from each other.

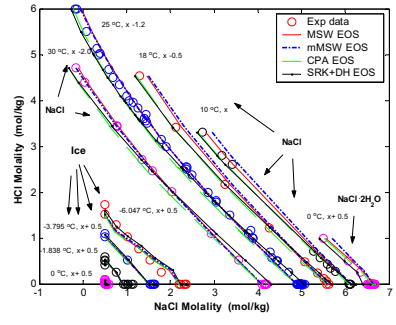

Figure 7.27. Phase diagram of the ternary aqueous system NaCl and HCl at 0.101325 MPa. Note at 0°C, there are two solid phases in the system: ice and NaCl·2H_2O. Above 0°C, there is only one solid phase NaCl.

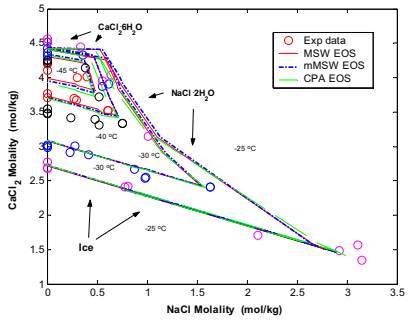

Figure 7.28. Phase diagram of the ternary aqueous system NaCl and $CaCl_2$ from -45°C to -25°C. A constant is added to some data at different temperatures to separate them from each other.

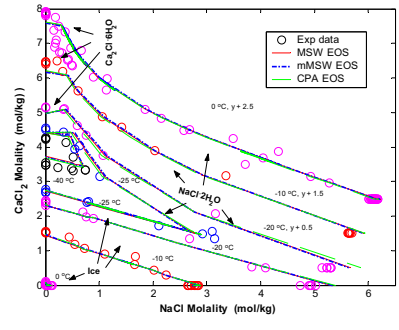

Figure 7.29. Phase diagram of the ternary aqueous system NaCl and $CaCl_2$ from -25°C to 0 °C. A constant is added to some data at different temperatures to separate them from each other.

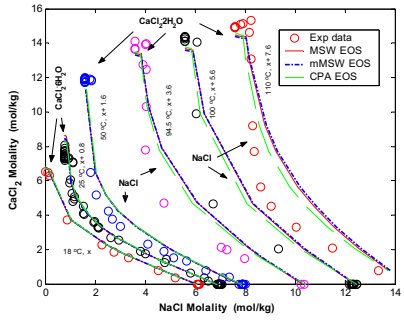

Figure 7.30. Phase diagram of the ternary aqueous system NaCl and $CaCl_2$ from 18°C to 110°C. A constant is added to some data at different temperatures to separate them from each other.

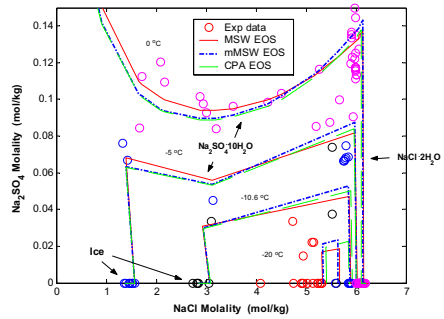

Figure 7.31. Phase diagram of the ternary aqueous system NaCl and Na_2SO_4 from -20°C to 0°C at 0.101325 MPa. A constant is added to some data at different temperatures to separate them from each other.

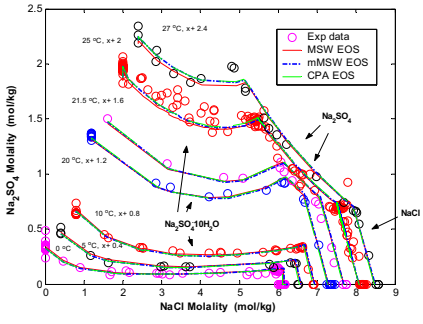

Figure 7.32. Phase diagram of the ternary aqueous system NaCl and Na_2SO_4 from 0°C to 27 °C at 0.101325 MPa. A constant is added to some data at different temperatures to separate them from each other.

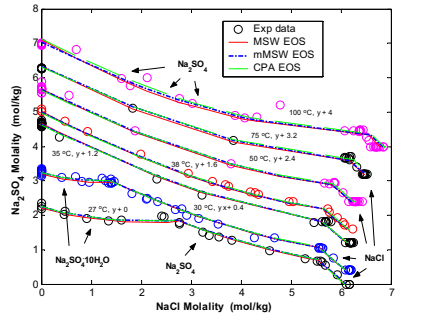

Figure 7.33. Phase diagram of the ternary aqueous system NaCl and Na_2SO_4 from 27°C to 100°C at 0.101325 MPa. A constant is added to some data at different temperatures to separate them from each other.

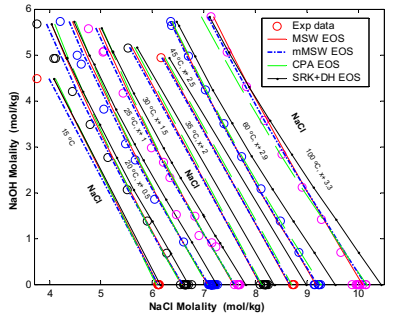

Figure 7.34. Phase diagram of the ternary aqueous system NaCl and NaOH from 15°C to 27°C at 0.101325 MPa. A constant is added to some data at different temperatures to separate them from each other.

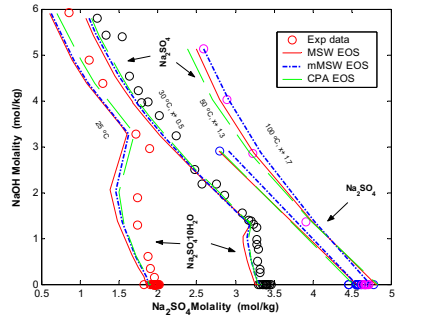

Figure 7.35. Phase diagram of the ternary aqueous system NaOH and Na_2SO_4 from 25°C to 100°C at 0.101325 MPa. A constant is added to some data at different temperatures to separate them from each other.

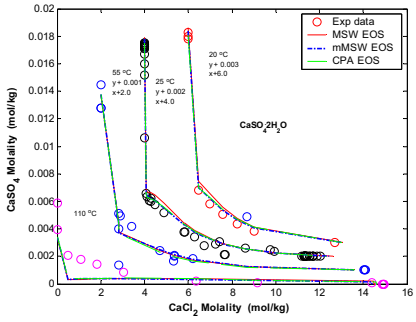

Figure 7.36. Phase diagram of the ternary aqueous system $CaCl_2$ and $CaSO_4$ from 0°C to 27 °C at 0.101325 MPa. A constant is added to some data at different temperatures to separate them from each other.

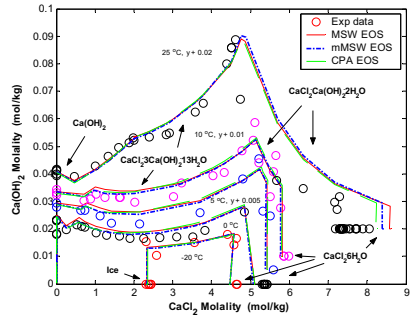

Figure 7.37. The predicted phase diagram of the ternary aqueous system $CaCl_2$ and $Ca(OH)_2$ from -20°C to 25°C at 0.101325 MPa. A constant is added to some data at different temperatures to separate them from each other.

Data for the ternary system H_2O + $CaCl_2$ + $Ca(OH)_2$ were not used in the parameter estimation. Instead, it is preserved to test the predictability of the parameter sets obtained from stage 4. This is a difficult ternary system due to the low solubility of $Ca(OH)_2$. The predicted results are shown graphically in Figures Figure 7.37 and Figure 7.39. The predicted results agree well with the experimental data within temperature range of [-20, 90]°C. Isotherms at various temperatures for ice, $CaCl_2·6H_2O$, $Ca(OH)_2$, $CaCl_2·Ca(OH)_2·2H_2O$ and $CaCl_2·Ca(OH)_2·13H_2O$ are all well predicted. Beyond this temperature range, the errors start to grow. However, the prediction should be carefully conducted within the temperature range of the fitted data [-50, 130]°C and extrapolation beyond this temperature range should be prohibited due to the second order polynomials of *a(T)*.

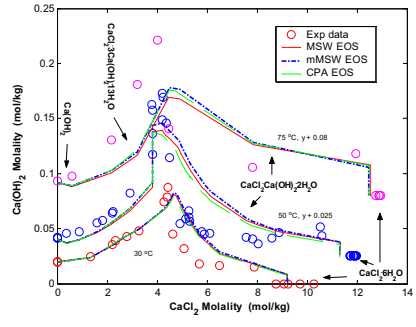

Figure 7.38. The predicted phase diagram of the ternary aqueous system $CaCl_2$ and $Ca(OH)_2$ from 30°C to 75°C at 0.101325 MPa. A constant is added to some data at different temperatures to separate them from each other.

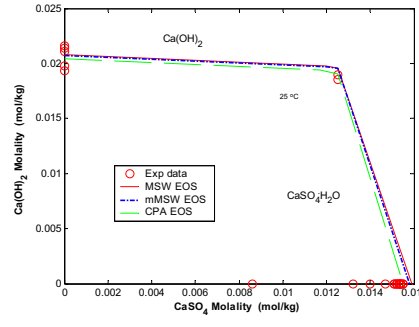

Figure 7.39. Phase diagram of the ternary aqueous system $Ca(OH)_2$ and $CaSO_4$ at 25°C , 0.101325 MPa.

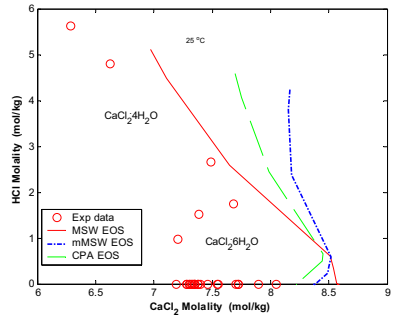

Figure 7.40. Phase diagram of the ternary aqueous system $CaCl_2$ and $CaSO_4$ at 25°C 0.101325 MPa.

From all the results presented above, together with the results in previous chapters, it can be seen that there is no big difference between the complete and the simplified MSA terms in the study. Similar results were obtained using either the simplified implicit or the simplified explicit MSA term in MSW EOS. In future work, eCPA EOS can be updated with the simplified explicit MSA term to enhance computational speed and simplify the EOS. Blum[27] also suggested a new and more theoretically based mixing rule (7.2) for simplified explicit MSA term, which significantly reduced the error between the simplified explicit MSA term and the complete MSW term.

$$\sigma = \frac{\sum_i \rho_i \sigma_i z_i^2}{\sum_i \rho_i z_i^2} \tag{7.2}$$

ρ_i is the number density. This new mixing rule is worthwhile to be implemented. An association term should be studied to see whether it helps to improve the goodness of fit of EOS in the high concentration range where ion complex starts to form. Comparing the short range term of PR EOS and CPA EOS, it seems that CPA EOS provides slightly better results in aqueous systems. For the future mixed solvent systems containing associating compounds, CPA EOS is believed to be more advantageous. The SRK+DH EOS should be further improved in its temperature dependence function to improve its correlation results of multi-temperature multi-component SLE data.

Table 7.5 The AAD and ARD values of the calculated properties at different temperature range using the optimized electrolyte EOS parameter values for six ions in the test system. The optimized electrolyte EOS parameters are from Table 7.4.

Component	Temperature	No. of data	MSW	mMSW	eCPA	SRK+DH
	°C			Apparent Molar Volume		
			AAD	AAD	AAD	AAD
NaCl	25	15	0.680	0.236	0.724	17.548
Na_2SO_4	25	7	4.411	4.696	1.367	20.020
$CaCl_2$	25	12	5.748	4.513	2.012	22.182
NaOH	25	13	3.004	3.434	1.099	3.079
HCl	25	18	1.847	1.883	3.404	17.287

			Osmotic Coefficient			
			ARD%	ARD%	ARD%	ARD%
$CaSO_4$	25	9	4.0113	4.2236	4.5881	27.572
NaCl	10 - 15	21	0.92055	0.68673	0.9308	2.9418
	20 - 25	109	1.2695	0.88451	1.2581	4.3729
	35 - 40	6	1.7917	0.96882	1.1079	4.5578
	40 - 45	7	1.0125	0.42328	0.64729	5.833
	45 - 50	11	0.86008	0.17401	0.3057	5.5684
	60 - 65	5	0.458	0.77698	0.88692	6.2522
	70 - 75	10	0.71557	1.5592	1.5182	6.6198
	85 - 90	6	1.3626	2.5576	2.4335	7.2817
	95 - 100	10	2.0063	3.0894	2.5116	7.9806
Na_2SO_4	-5 - 0	20	1.2546	1.2008	1.0508	16.843
	20 - 25	120	1.0625	1.4776	1.839	21.316
	25 - 30	6	0.69076	1.4043	1.9877	21.77
	35 - 40	11	1.9556	1.2516	0.9976	9.4027
	45 - 50	5	1.5379	1.8711	0.91754	28.839
	70 - 75	5	5.6947	5.7056	4.1981	28.249
	75 - 80	24	7.0267	4.8879	2.9166	22.784
	95 - 100	24	6.6231	4.6346	3.7949	17.945
	120 - 125	5	13.712	10.996	10.532	33.009
$CaCl_2$	-5 - 0	18	4.3028	4.3067	4.2593	10.103
	10 - 15	22	5.7131	5.8116	5.9359	11.15
	20 - 25	331	6.6928	7.0564	6.9715	12.953
	25 - 30	12	10.467	11.165	11.206	18.438
	30 - 35	4	12.71	13.875	13.12	19.025
	35 - 40	24	10.591	11.114	10.964	13.286
	40 - 45	5	13.115	14.555	13.599	17.895
	45 - 50	70	9.1646	9.8203	9.1338	13.318
	50 - 55	2	15.994	17.252	16.986	20.684
	55 - 60	24	12.072	13.309	12.15	14.897
	60 - 65	4	16.033	17.432	16.67	18.688
	65 - 70	30	12.367	13.539	12.697	14.547
	70 - 75	4	18.283	19.834	18.296	18.904
	75 - 80	21	11.104	12.082	11.5	10.774
	80 - 85	4	19.088	20.097	18.125	19.912
	90 - 95	2	23.396	24.829	22.883	22.799
	95 - 100	11	5.7806	6.8693	6.4469	11.676
	100 - 105	3	23.564	25.228	23.309	22.584
	105 - 110	31	14.771	15.89	13.629	14.336
	110 - 115	3	22.982	24.783	22.67	23.276
	115 - 120	4	22.96	24.332	22.471	23.781
	120 - 125	3	28.398	30.832	28.866	32.42
	125 - 130	2	31.381	34.23	32.34	39.973
NaOH	15 - 20	5	1.5155	1.39	1.5248	8.0507
	20 - 25	55	0.96222	0.92165	0.84829	4.6186
HCl	20 - 25	46	1.2317	0.88428	0.71604	5.5058

$NaCl+CaCl_2$	25	36	3.6154	3.7894	3.8565	11.863
$NaCl+Na_2SO_4$	25	119	0.77927	0.73719	1.0889	9.9822
			Mean Ionic Activty Coefficient			
			ARD%	ARD%	ARD%	ARD%
$CaSO_4$	25	7	14.528	14.792	15.678	87.523
NaCl	-5 - 0	46	1.6304	1.0564	1.0187	9.8121
	0 - 5	46	1.1346	0.79176	0.94329	8.7776
	5 - 10	46	0.91293	0.70437	1.087	7.665
	10 - 15	46	0.90291	0.74137	1.2725	6.5381
	15 - 20	46	0.99642	0.84661	1.3387	5.5702
	20 - 25	53	1.0538	0.93252	1.288	5.419
	25 - 30	46	0.99682	1.0162	1.1438	5.0245
	35 - 40	46	0.80014	0.99312	0.67762	5.8485
	45 - 50	46	0.63383	0.77552	0.21342	6.6692
	55 - 60	46	0.82502	0.79182	0.73735	7.1848
	65 - 70	46	1.3818	1.4432	1.3453	7.3824
	75 - 80	46	1.9722	2.11	1.8474	7.3855
	85 - 90	46	2.5285	2.7462	2.2248	7.4801
	95 - 100	46	2.9998	3.3269	2.4943	8.1165
	105 - 110	46	3.369	3.8365	2.7545	9.5954
$CaCl_2$	10 - 15	8	3.6049	2.4438	2.0585	37.819
	20 - 25	25	11.563	9.5521	9.3861	30.857
	30 - 35	7	2.1036	0.62237	0.56805	36.992
	35 - 40	6	1.8449	0.50485	0.59455	45.837
	50 - 55	9	0.60089	3.1035	2.9846	45.221
	65 - 70	8	2.5329	5.7488	5.3599	50.439
NaOH	20 - 25	28	1.2909	1.1043	1.6559	14.654
HCl	-5 - 0	16	3.195	3.0019	1.6549	7.4537
	5 - 10	16	2.6772	2.2427	1.2637	7.7516
	15 - 20	3	2.4019	1.9433	2.2932	2.4784
	20 - 25	138	2.2778	1.8598	0.95119	8.735
	25 - 30	8	2.2657	2.6043	2.0516	3.4337
	35 - 40	19	3.0274	3.0275	1.1536	8.1378
	45 - 50	23	2.6439	1.986	0.81188	7.4288
	55 - 60	16	2.4818	0.83924	0.96065	9.4248
	65 - 70	5	0.85096	4.548	1.4326	4.164
	75 - 80	5	5.8135	6.8092	2.3221	3.4535
			Water Activity Coefficient			
			ARD%	ARD%	ARD%	ARD%
Na_2SO_4	20 - 25	8	0.033906	0.049743	0.059023	0.67986
$CaCl_2$	-5 - 0	2	2.8974	2.8636	2.8419	2.5152
	20 - 25	2	33.234	33.484	34.017	39.965
	110 - 115	19	10.655	10.058	10.504	10.617

NaOH	-5 - 0	4	1.7997	1.4373	1.9598	6.0732
	25 - 30	2	1.5271	1.6287	1.3943	3.5434
	45 - 50	2	0.76179	0.86706	0.6471	0.8596
	55 - 60	3	0.9921	1.4077	0.62477	0.94931
	70 - 75	2	0.59356	0.97866	0.29695	0.33119
	85 - 90	2	0.60305	0.85033	0.3683	0.43104
	95 - 100	2	0.22879	0.49137	0.52627	0.63375
$NaCl+CaCl_2$	100 - 105	19	4.6527	4.2541	4.8326	3.5862
	110 - 115	123	4.4738	4.2208	4.5011	3.8218

*** Average absolute deviation is fined by following equation:** $AAD = \frac{1}{N}\sum_{i=1}^{N}\left(\left|x_i^{\text{experiment}} - x_i^{\text{calculated}}\right|\right)$

*** Average relative deviation is fined by following equation:** $ARD\% = \frac{1}{N}\sum_{i=1}^{N}\left(\left|\frac{x_i^{\text{experiment}} - x_i^{\text{calculated}}}{x_i^{\text{experiment}}}\right|\right)\times 100\%$

7.5 *Conclusion*

1. The equations of state for electrolytes considered in this work (MSW, mMSW and eCPA EOS) can be applied to multi-component systems at a wide temperature range using ion-specific parameters with a proper temperature dependence function for attraction parameter a and ion-size parameter σ. The experimental data could not be well reproduced using the SRK+DH EOS.

2. There is no big difference between the simplified explicit and simplified implicit MSA terms based on this work. It is recommended to use the most simple MSA term: the explicit MSA term.

3. The ion-specific parameter sets obtained in this work (see Table 4) are not merely meaningless mathematical numbers from optimization routines. However, the prediction should be carefully conducted within the temperature range of the fitted data [-50, 130] °C and extrapolation beyond this temperature range should be strictly prohibited, since the second order polynomials of $a(T)$ cannot be used for extrapolation.

4. The temperature dependence function FT5 has limited applicability and fails at very high and very low temperatures. It is still necessary to find better temperature dependence function for attraction parameter and ion-size parameter. The temperature dependence of the interaction parameter k_{ij} should be investigated in the future work.

Reference

1. Chen CC, Britt HI, Boston JF, Evans LB. Local. Composition Model for Excess Gibbs Energy of Electrolyte Systems. *AIChE J.* 1982; 28: 588-596.

2. Chen CC, Evans LB. A Local Composition Model for the Excess Gibbs Energy of Aqueous Electrolyte Systems. *AIChE J.* 1986; 32: 444-454.

3. Chen CC, Song YH. Generalized electrolyte-NRTL model for mixed-solvent electrolyte systems. *AIChE J.* 2004; 50(8): 1928-1941.

4. Chen CC. Representation of solid-liquid equilibrium of aqueous electrolyte systems with the electrolyte NRTL model. *Fluid Phase Equilib.* 1986; (27): 457-74.

5. Thomsen K. *Aqueous electrolytes: model parameters and process simulation.* PhD thesis. Copenhagen, Denmark: Technical University of Denmark; 1997.

6. Thomsen K, Rasmussen P. Modeling of Vapour-liquid-solid equilibrium in gas-aqueous electrolyte systems. *Chem Eng Science.* 1999; 54:1787-1802.

7. Iliuta M, Thomsen K, Rasmussen P. Extended UNIQUAC model for correlation and prediction of vapour-liquid-solid equilibrium in aqueous salt systems containing non-electrolytes. Part A. Methanol – Water – Salt systems. *Chem Eng Science.* 2000; 55:2673-2686.

8. Garcia AV, Thomsen K, Stenby EH. Prediction of mineral scale formation in geothermal and oilfield operations using the Extended UNIQUAC model. Part I Sulfate scaling minerals. *Geothermics.* 2005; 34(1): 61-97.

9. Garcia AV, Thomsen K, Stenby EH. Prediction of mineral scale formation in geothermal and oilfield operations using the Extended UNIQUAC model. *Geothermics.* 2006; 35(3): 239-284.

10. Planche H, Renon H. Mean Spherical Approximation applied to a simple but non-primitive model of interaction for electrolyte solutions and polar substances. *J Phys Chem*. 1981; 5: 3924-3929.

11. Jin G, Donohue MD. An equation of state for electrolyte solutions. 1. Aqueous systems containing strong electrolytes. *Ind Eng Chem Res.* 1988; 27: 1073-1084.

12. Jin G, Donohue MD. An equation of state for electrolyte solutions. 2. Single volatile weak electrolytes in water. *Ind Eng Chem Res.* 1988; 27: 1737-1743,

13. Jin G, Donohue MD. An Equaiton of State for Electrolyte Solutions. 3. Aqueous Solutions Containing Multiple Salts. *Ind Eng Chem Res.* 1991; 30: 240-248.

14. Fürst W, Renon H. Representation of Excess Properties of Electrolyte Solutions Using a New Equation of State. *AIChE J*. 1993; 39: 335-343.

15. Zuo JY, Zhang D, Fürst W. Predicting LLE in Mixed-Solvent Electrolyte Systems by an Eletrolyte EOS. *AIChE J*. 2000; 46: 2318-2328.

16. Vu VQ, Suchaux PD, Furst W. Use of a predictive electrolyte equation of state for the calculation of the gas hydrate formation temperature in the case of systems with methanol and salts. Fluid Phase Equilib. 2002; 194-197: 361-370.

17. Wu J, Prausnitz JM. Phase Equilibirum for systems Containing Hydrocarbons, Water and Salt: An Extended Peng-Robinson Equation of State. *Ind Eng Chem Res.* 1998; 37: 1634-1643.

18. Myers JA, Sandler SI, Wood RH. An Equation of State for Electrolyte Solutions Covering Wide Range of Temperature, Pressure and Composition. *Ind Eng Chem Res.* 2002; 41: 3282-3297.

19. Galindo A, Gil-Villegas A, Jackson G, Burgess AN. SAFT-VRE: Phase Behavior of Electrolyte Solutions with the Statistical Associating Fluid Theory for Potentials of Variable Range. *J Phys Chem B.* 1999; 103: 10272-10281.

20. Cameretti LF, Sadowski G, Mollerup JM. Modeling of aqueous electrolyte solutions with perturbed-chain statistical associated fluid theory. *Ind Eng Chem Res.* 2005;44 (9): 3355-3362.

21. Tan SP, Adidharma H, Radosz M. Statistical Associating Fluid Theory Coupled with Restricted Primitive Model To Represent Aqueous Strong Electrolytes. *Ind Eng Chem Res.* 2005; 44: 4442-4452.

22. Ji XY, Tan SP, Adidharma H, Radosz M. Statistical Associating Fluid Theory Coupled with Restricted Primitive Model to Represent Aqueous Strong Electrolytes: Multiple-Salt Solutions. *Ind Eng Chem Res.* 2005; 44(19): 7584 - 7590.

23. Liu Z, Wang W, Li Y. An equation of state for electrolyte solutions by a combination of low-density expansion of nonprimitive mean spherical approximation and statistical associating fluid theory. *Fluid Phase Equilib.* 2005; 227: 147-156.

24. Uematsu M, Franck EU. Static Dielectric Constant of Water and Steam. *J Phys Chem Ref Data.* 1980; 9(4): 1291-1305.

25. http://www.ivc-sep.kt.dtu.dk/databank/

26. Herzog S, Arlt W, Gross J. Modeling of electrolyte solution with the non-primitive mean spherical approximation. *ESAT 2006, 22nd European Symposium on Applied Thermodynamics*. Nørhaven Book A/S, Denmark; 2006.

27. Sanchez-Castro C, Blum L. Explicit approxiamtion for the unrestricted mean spherical approximation for ionic solutions. *J Phys Chem.*1989; 93: 7478-7482.

CHAPTER 8 Conclusion

1. The electrolyte EOSs implemented in this work were thoroughly checked. Six implemented electrolyte EOSs were tested through 1) the numerical check of the derivatives, 2) the consistence test both in salt and ion-specific parameters, 3) the correlation of strong electrolyte using salt-specific parameters. Later four out of the six electrolyte EOSs were applied to multi-component aqueous systems (strong electrolytes) using ion-specific parameters both at room temperature and at a wide temperature range. The program of these electrolyte EOSs are running smoothly. It is safe to use them in the future studies.

2. It is shown in this work that the electrolyte equations of state can be applied to multi-component systems over full concentration range using ion-specific parameters. When electrolyte EOSs are applied to multi-component systems at a wide temperature range using ion-specific parameters, proper temperature dependence functions are needed for the adjustable parameters of the EOSs. AMV, mean ionic activity coefficient or osmotic coefficient, and solid-liquid equilibrium experimental data can be simultaneously fitted and represented with certain number of interaction parameters. The AMV of aqueous electrolyte solution is only fitted well by the EOSs representing water density accurately and containing an electrostatic term contributing to the volume.

   Problems will be encountered by the electrolyte EOSs considered in this work when applied to strong electrolytes forming ion complex. The osmotic and mean ionic activity coefficients at high concentration range cannot be captured by any EOSs in this work. MSW, mMSW, eCPA and SRK+DH EOS give all good performances at room temperature or at a wide temperature range. The multi-temperature experimental data could not be well reproduced when using the SRK+DH EOS. The failure of SRK+DH EOS at a wide temperature range needs to be further explored in the future work

3. The interaction parameter plays an important role in simultaneous fittings of volumetric data and thermodynamic data. When using salt parameters the interaction parameter k_{ij} in cubic EOS and the interaction parameter W_{ij} in SR2 term can both improve the goodness-of-fit. Especially when AMV is included in the parameter fitting (ion-specific), the interaction parameter k_{ij} can improve the goodness of fit of activity and osmotic coefficient significantly. When the EOS is exclusively fitted to AMV or exclusively fitted to activity and osmotic coefficient data at constant temperature using ion-specific parameters, the number of interaction parameters can be reduced even to zero.

4. The SR2 term from Fürst *et al.*[1] can significantly improve the performances of the EOS by taking into account the interactions between ion and ion or ion and water. But it slows down the computational speed and increases the complexity of the EOS. If the electrolyte EOS could fulfil the needs by using the interaction parameter k_{ij} in the non-electrolyte term (cubic EOS) without using the additional SR2 term, it is recommended not to use it.

5. There is no significant difference in the performances of complicated electrolyte terms and simple electrolyte terms according to our studies at either constant temperature or at wide temperature range. The simplified explicit MSA term performs as well as the complicated simplified implicit MSA terms or sometimes even better. However, the simplified explicit MSA term needs only one third or one fourth of the computational time required by the implicit MSA term. Thus eCPA EOS can be further simplified and upgraded by using the simplified explicit MSA term. The simple, truncated Debye-Hückel term with no parameters performs equally well in reproducing activity coefficients and osmotic coefficients as MSA terms in most cases at constant temperature. Apparent molar volumes are not reproduced well by SRK+DH EOS as the electrostatic term does not contribute to the volume of the solution. Considerable work load in programming can be reduced and the computational speed can be increased significantly when the truncated Debye-Hückel term is applied.

6. The difference in performances of the non-electrolyte terms, i.e. the short range terms of SRK, PR, CPA EOS, is small in general when only applied to the single solvent aqueous electrolyte systems at 0.101325 MPa. The CPA EOS consumes two or three times more computation time due to its Wertheim association term compared with other EOSs. The performance of these short range terms can only be evaluated later when extended to multi-solvent electrolyte systems.

7. It is expected that models based on physical foundations are more likely to present predictive features. In order to evaluate an engineering model for its physical foundations, it is important to compare the resulting optimized parameters with the related physical property. This comparison requires a very critical view, since it is clear that the parameters of such engineering models are not directly related to a measurable, physical property. Yet, some trends may be expected. When looking closely at the results of this work, we must conclude that we cannot find any such relationship. Hence, even though the properties could be correctly modelled, we would be very cautious in extrapolating outside the fitting region. More work should be performed on electrolyte EOS in order to improve their physical backgrounds.

8. The temperature dependence function FT5 has limited applicability and fails at very high and very low temperatures. The ion-specific parameter sets obtained in this work are not merely meaningless mathematical numbers from optimization routines rather it can be used to predict other systems. However, the prediction of multi-temperature data should be carefully conducted within the parameter fitting temperature range [-50, 130] °C. The extrapolation beyond this temperature range should be prohibited, since the temperature dependence of $a(T)$ are second order polynomials, which cannot be used in extrapolation.

9. It is still necessary to find better temperature dependence function for ion-specific parameters. The temperature dependence of the interaction parameter k_{ij} should be investigated in the future work, to see whether it can improve the performances of the EOSs tested. The Wertheim association term should be

studied in the future, as it is shown by Herzog *et al.*[2] that the association term can help to describe ion-association and fit the thermodynamic properties at the full concentration range of strong electrolytes that form ion complex. New mixing rules suggested by Blum[3] for explicit MSA term should also be implemented in the future to improve the accuracy of the explicit MSA term. Multi component electrolyte systems with mixed solvent and weak electrolytes should also be modelled.

Reference

1. Fürst W, Renon H. Representation of Excess Properties of Electrolyte Solutions Using a New Equation of State. *AIChE J*. 1993; 39: 335-343.

2. Herzog S, Arlt W, Gross J. Modeling of electrolyte solution with the non-primitive mean spherical approximation. *ESAT 2006, 22nd European Symposium on Applied Thermodynamics*. Nørhaven Book A/S, Denmark; 2006.

3 . Sanchez-Castro C, Blum L. Explicit approxiamtion for the unrestricted mean spherical approximation for ionic solutions. *J Phys Chem.*1989; 93: 7478-7482.

APPENDIX I The deduction of the complete solution of the Debye-Hückel theory

Poisson-Boltzmann equation theory

Many models are derived from the approximate solution of Poisson-Boltzmann equation, such as Debye-Hückel equation and the Pitzer model etc. In this theory the radial distribution function can be expressed in the following form:

$$g_{ij}(r) = e^{-\beta w_{ij}(r)} \tag{1-1}$$

where w_{ij} is the potential of mean force (PMF). of the t is assumed that the electrostatic potential energy of a given ion is equal to the PMF, i.e. $w_{ij} = z_j \varepsilon \psi_i(r)$. Note in Appendixes the equation number format is changed compared with that of previous chapters. In Appendixes, the separator in the equation number is "-" instead of ".". Equation (1-1)becomes:

$$g_{ij}(r) = \exp\left[-\beta z_i e \psi_i(r)\right] \tag{1-2}$$

where z_j is the number of charges on ion j, r is the distance from central ion i to another ion j. $\psi_i(r)$ is the average electrostatic potential of the ion i as a function of distance from it. ε is the charge of electron and $\beta = 1/k_B T$, where k_B is the Boltzmann's constant. Equation (1-2) has a form of Boltzmann distribution.
If equation (1-2) is substituted into Poisson equation

$$\nabla^2 \psi_i(r) = -\frac{1}{\varepsilon \varepsilon_0} \rho_i(r) = -\frac{1}{\varepsilon \varepsilon_0} \sum_j z_j e \rho_j g_{ij}(r) \tag{1-3}$$

then we obtained the Poisson-Boltzmann equation

$$\nabla^2 \psi_i(r) = -\frac{1}{\varepsilon \varepsilon_0} \sum_j z_j e \rho_j \exp\left[-\beta z_j e \psi_j(r)\right] \tag{1-4}$$

for calculating the electrostatic potential $\psi_i(r)$.
The $\rho_i(r)$ in equation (1-3) is the charge density at the distance r from the central ion. ρ_i is the number of ions i per unit volume. Taylor expand the radial distribution function, i.e. the exponential term in the left hand side of the equation (4),

$$g_{ij}(r) = \exp\left[-\frac{z_j e \psi_i(r)}{kT}\right] = 1 - \frac{z_j e \psi_i(r)}{kT} + \frac{1}{2}\left[\frac{z_j e \psi_i(r)}{kT}\right]^2 - \cdots \tag{1-5}$$

and maintains different terms according to the accuracy requirement to solve equation (1-4), then different approximate models are obtained.

Debye-Hückel theory

The detailed derivation of the Debye-Hückel theory will be given below.
In Debye-Hückel theory, the radial distribution function has the form of

$$g_{ij}(r) = \exp\left[-\frac{z_j e \psi_i(r)}{kT}\right] \approx 1 - \frac{z_j e \psi_i(r)}{kT} \tag{1-6}$$

and after Taylor expand the exponential function, drop the higher order terms, substitute it into the Poisson-Boltzmann equation and it becomes

$$\nabla^2\psi_i(r)=\frac{1}{\varepsilon\varepsilon_0}\sum_j z_j^2e^2\rho_j\frac{\psi_i(r)}{kT} \tag{1-7}$$

Assume that the ions are spherical and are symmetrically charged, the above Laplacian equation can be simplified into

$$\frac{d^2\left[r\psi_i(r)\right]}{dr^2}=\frac{e^2}{\varepsilon\varepsilon_0 kT}\sum_j z_j^2\rho_j r\psi_i(r)\equiv\kappa^2 r\psi_i(r),\ \text{where}\ \kappa^2=\frac{e^2}{\varepsilon\varepsilon_0 kT}\sum_j z_j^2\rho_j \tag{1-8}$$

with the boundary condition

$$\frac{d\psi_i(a_i)}{dr}=\frac{e\,z_i}{\varepsilon\varepsilon_0 a_i^2},\ \text{where}\ a_i\ \text{is the closest approach and}\ \lim_{r\to\infty}\psi_i(r)=0$$

Solve the second order ordinary differential equation, we get the analytically expression for the electrical potential at distant *r*:

$$\psi_i(r)=\frac{e\,z_i}{4\pi\varepsilon\varepsilon_0(1+\kappa a_i)}\frac{e^{\kappa a-\kappa r}}{r} \tag{1-9}$$

Here Debye and Hückel assume that the electrical potential of any point in the solution $\psi_i(r)$ is the sum of the electrical potential ϕ_i of the ion *i* at this point and the electrical potential of the ion atmosphere $\phi(r)$:

$$\psi_i(r)=\phi_i+\phi(r)=\frac{e\,z_i}{4\pi\varepsilon\varepsilon_0 r}+\phi(r)=\frac{e\,z_i}{4\pi\varepsilon\varepsilon_0(1+\kappa a_i)}\frac{e^{\kappa a-\kappa r}}{r} \tag{1-10}$$

if $r=a_i$, and we get $\phi(a_i)=-\dfrac{e\,z_i\kappa}{4\pi\varepsilon\varepsilon_0(1+\kappa a_i)}$

and the charge of electric potential energy of a single ion is $u=-\dfrac{e^2\,z_i^2\kappa}{8\pi\varepsilon\varepsilon_0(1+\kappa a_i)}$

The way Debye and Hückel deduced their excess Helmholtz free energy function is as follows. From the change of electric potential energy of a single ion $u=-\dfrac{e^2\,z_i^2\kappa}{8\pi\varepsilon\varepsilon_0(1+\kappa a_i)}$, they calculate the total electric potential energy of the electrolyte solution with various ion species as:

$$U_e=-\sum\frac{N_i e^2\,z_i^2\kappa}{8\pi\varepsilon\varepsilon_0(1+\kappa a_i)},\ \text{where}\ N_i=n_iN_A \tag{1-11}$$

From $-\dfrac{A}{T}=S-\dfrac{U}{T}$, we have $\left[\dfrac{\partial(A/T)}{\partial(1/T)}\right]_V=U$, thus

$$-\frac{A^E}{T}=\int\frac{U_e}{T^2}dT \tag{1-12}$$

Differentiate on both sides of $\kappa^2=\dfrac{e^2}{\varepsilon\varepsilon_0 kT}\sum_j z_j^2\rho_j$, we have

$$2\kappa d\kappa=-\frac{e^2}{\varepsilon\varepsilon_0 k}\sum_j z_j^2\rho_j\frac{dT}{T^2} \tag{1-13}$$

Substitute equation (1-11) and (1-13) into equation (1-12), we arrive at

$$-\frac{A^E}{T}=\int\frac{U_e}{T^2}dT=\frac{kV}{4\pi N_A\sum x_i z_i^2}\sum\int\frac{x_i z_i^2\kappa^2 d\kappa}{(1+\kappa a_i)}$$
$$=\frac{kV}{4\pi N_A\sum x_i z_i^2}\sum\frac{x_i z_i^2}{a_i^3}\left(\frac{3}{2}+\ln\left(1+a_i\kappa\right)-2\left(1+a_i\kappa\right)+\frac{\left(1+a_i\kappa\right)^2}{2}\right) \quad (1\text{-}14)$$

Equation (1-14) is the original expression deduced by Debye and Hückel, if we differentiate equation (1-14) with respect to mole composition, we will get the complete expression for activity coefficient.

APPENDIX II The deduction of simplified explicit MSA term from the complete MSA term

The Mean Spherical Approximation (MSA)

The MSA term is based on the following closure of the OZ equation:

$$g_{ij} = 0 \qquad r_{ij} < \sigma_{ij}$$

$$c_{ij} = -\beta u_{ij}(r) = -\frac{\beta z_i z_j e^2}{4\pi\varepsilon\varepsilon_0 r_{ij}} \qquad r_{ij} > \sigma_{ij}$$

The complete solution of the MSA yields the following equations:

$$\Omega = 1 + \frac{\pi}{2\Theta}\sum_{ions}\frac{\rho_i\sigma_i^3}{1+\Gamma\sigma_i},\ P_n = \frac{1}{\Omega}\sum_{ions}\frac{\rho_i\sigma_i z_i}{1+\Gamma\sigma_i},\ \text{where}\ \Theta = 1 - \frac{\pi}{6}\sum_{ions}\rho_i\sigma_i^3,$$

$$\Gamma = \frac{e}{2\sqrt{\varepsilon_0\varepsilon kT}}\left\{\sum_i \rho_i\left[\frac{z_i - \frac{\pi\sigma_i^2 P_n}{2\Theta}}{1+\Gamma\sigma_i}\right]^2\right\}^{1/2}, \text{where}\ \rho_i = \frac{N_i}{V}\ (\text{number density of species } i)$$

The only restriction imposed is the electro-neutrality condition:

$$\sum_j \rho_j z_j = 0$$

Γ is the MSA screening parameter and κ is the Debye screening length ($\Gamma \to \kappa/2$ at infinite dilution). e is the electronic charge, k is the Boltzmann's constant, ε is the relative permittivity of the medium, ε_0 is the vacuum permittivity, z_i is the valence and σ_i is the the diameter of species i, and the closest distance of the approach in MSA is $\sigma_{ij} = (\sigma_i + \sigma_j)/2$. T is the absolute temperature, ρ_i is the number density of species i. From the expression of the MSA screening parameter Γ, it can be seen that the explicit form of Γ cannot obtained from the complete MSA.

Explicit approximations of the excess Helmholtz energy, the excess internal energy and the osmotic coefficient from the MSA term are presented below.

$$A^E = -\frac{Ve^2}{4\pi\varepsilon_0\varepsilon}\left\{\Gamma\sum_{ions}\frac{\rho_i z_i^2}{1+\Gamma\sigma_i} + \frac{\pi}{2\Theta}\Omega P_n^2\right\} + \frac{V\Gamma}{3\pi}kT,$$

$$U^E = -\frac{Ve^2}{4\pi\varepsilon_0\varepsilon}\left\{\Gamma\sum_{ions}\frac{\rho_i z_i^2}{1+\Gamma\sigma_i} + \frac{\pi}{2\Theta}\Omega P_n^2\right\},$$

$$\Phi^E = -\frac{\Gamma^3}{3\pi\rho} - \frac{1}{8\rho}\left(\frac{4\pi e^2 P_n^2}{DkT\Theta^2}\right), \text{where}\ \rho = \sum_{ions}\rho_i$$

If all ions have the same diameter σ, we have the following simplified expression:

$$P_n = \frac{1}{\Omega}\sum_{ions}\frac{\rho_i\sigma_i z_i}{1+\Gamma\sigma_i} = \frac{1}{\Omega}\frac{\sigma}{1+\Gamma\sigma}\sum_{ions}\rho_i z_i = 0,$$ (from the electroneutriality condition $\sum_j \rho_j z_j = 0$).

Then we can simplify the MSA screening parameter Γ into explicit form:

$$\Gamma = \frac{e}{2\sqrt{\varepsilon_0 \varepsilon kT}} \left\{ \sum_i \rho_i \left[\frac{z_i - \frac{\pi \sigma_i^2 P_n}{2\Theta}}{1 + \Gamma \sigma_i} \right]^2 \right\}^{1/2} = \frac{e}{2\sqrt{\varepsilon_0 \varepsilon kT}} \frac{1}{1 + \Gamma \sigma} \left\{ \sum_i \rho_i [z_i - 0]^2 \right\}^{1/2}$$

$$= \frac{e}{2\sqrt{\varepsilon_0 \varepsilon kT}} \frac{\left\{ \sum_i \rho_i z_i^{\,2} \right\}^{1/2}}{1 + \Gamma \sigma} \quad \Rightarrow \quad 2\Gamma(+\Gamma\sigma) = e\sqrt{\frac{\sum_i \rho_i z_i^{\,2}}{\varepsilon_0 \varepsilon kT}} = \kappa \quad \Rightarrow$$

$$\Gamma = \frac{1}{2\sigma} \left[\sqrt{1 + 2\sigma\kappa} - 1 \right] \quad \text{and} \quad \kappa = \left(\frac{e^2 N_A^2}{\varepsilon \varepsilon_0 RTV} \sum_{ions} n_i Z_i^2 \right)^{1/2}$$

The expressions of the excess Helmholtz energy, the excess internal energy and the osmotic coefficient from the MSA term turn to be the following simplified explicit expressions:

$$A^E = -\frac{2\Gamma^3 RTV}{3\pi N_A} \left\{ 1 + \frac{3}{2} \Gamma\sigma \right\},$$

$$U^E = -\frac{\Gamma^3 (1 + \Gamma\sigma) RTV}{\pi N_A},$$

$$\Phi^E = -\frac{\Gamma^3}{3\pi\rho}, \text{ where } \rho = \sum_{ions} \rho_i$$

APPENDIX III The analytical comparison between the simplified explicit MSA term and the DH term

From previous Appendix II, the complete solution of the MSA yields the following equations:

$$\Omega = 1 + \frac{\pi}{2\Theta}\sum_{ions}\frac{\rho_i\sigma_i^3}{1+\Gamma\sigma_i},\ P_n = \frac{1}{\Omega}\sum_{ions}\frac{\rho_i\sigma_i z_i}{1+\Gamma\sigma_i},\ \text{where}\ \Theta = 1 - \frac{\pi}{6}\sum_{ions}\rho_i\sigma_i^3,$$

$$\Gamma = \frac{e}{2\sqrt{\varepsilon_0\varepsilon kT}}\left\{\sum_i \rho_i\left[\frac{z_i - \frac{\pi\sigma_i^2 P_n}{2\Theta}}{1+\Gamma\sigma_i}\right]^2\right\}^{1/2},\ \text{where}\ \rho_i = \frac{N_i}{V}\ (\text{number density of species } i)$$

In the above expression of the MSA screening parameter Γ, it can be seen that the explicit form of Γ cannot be obtained from the complete MSA term. Thus the explicit expressions of the excess thermodynamic properties are not available either, including the Helmholtz free energy, internal energy, activity coefficients, chemical potentials and osmotic coefficients. However, an explicit expression for the excess Helmholtz function from the MSA term can be achieved if all the ions have the same diameters. Therefore the expressions of the excess Helmholtz function from the MSA and Debye-Hückel can be compared under this common ion size assumption.

If all ions have the same diameter σ (e.g. using the mixing rule $\sigma = \frac{\sum_{ions} n_i\sigma_i}{\sum_{ions} n_i}$), we have the following explicit expression:

$$\Gamma = \frac{1}{2\sigma}\left[\sqrt{1+2\sigma\kappa}-1\right] \text{and}\ \kappa = \left(\frac{e^2N_A^2}{\varepsilon\varepsilon_0 RTV}\sum_{ions} n_i Z_i^2\right)^{1/2}$$

The expression of the excess Helmholtz function from the MSA term turns to be the following simplified expression:

$$A^E = -\frac{2\Gamma^3 RTV}{3\pi N_A}\left\{1+\frac{3}{2}\Gamma\sigma\right\}$$

Rearrange A^E and substitute Γ into the expression of A^E, we have

$$\frac{A^E}{RT} = -\frac{2V}{3\pi N_A}\left(1+\frac{3}{2}\Gamma\sigma\right)\Gamma^3 = -\frac{2V}{3\pi N_A}\left(1+\frac{3}{4}\left[\sqrt{1+2\sigma\kappa}-1\right]\right)\frac{1}{2^3\sigma^3}\left[\sqrt{1+2\sigma\kappa}-1\right]^3$$

$$= -\frac{V}{3\pi 2^2\sigma^3 N_A}\left(1+\frac{3}{4}\left[\sqrt{1+2\sigma\kappa}-1\right]\right)\left[\sqrt{1+2\sigma\kappa}-1\right]^3$$

$$\frac{A^E}{RT} = -\frac{V}{3\pi 2^2\sigma^3 N_A}\left(\left[\sqrt{1+2\sigma\kappa}-1\right]^3 + \frac{3}{4}\left[\sqrt{1+2\sigma\kappa}-1\right]^4\right)$$

Knowing that $\left(\left[x-1\right]^3 + \frac{3}{4}\left[x-1\right]^4\right) = \frac{3}{4}x^4 - 2x^3 + \frac{3}{2}x^2 - \frac{1}{4}$, $\frac{A^E}{RT}$ can be simplified as:

$$\frac{A^E}{RT} = -\frac{V}{3\pi 2^2\sigma^3 N_A}\left(\frac{3}{4}\left(\sqrt{1+2\sigma\kappa}\right)^4 - 2\left(\sqrt{1+2\sigma\kappa}\right)^3 + \frac{3}{2}\left(\sqrt{1+2\sigma\kappa}\right)^2 - \frac{1}{4}\right)$$

$$= -\frac{V}{3\pi 2^2\sigma^3 N_A}\left(\frac{3}{4}(1+2\sigma\kappa)^2 - 2\left(\sqrt{1+2\sigma\kappa}\right)^3 + \frac{3}{2}(1+2\sigma\kappa) - \frac{1}{4}\right)$$

Expand the $(1+2\sigma\kappa)$ term, we have:

$$\frac{A^E}{RT} = -\frac{V}{3\pi 2^2\sigma^3 N_A}\left(3\sigma^2\kappa^2 + 6\sigma\kappa + 2 - 2\left(\sqrt{1+2\sigma\kappa}\right)^3\right)$$

$$\frac{A^E}{RT} = -\frac{V}{4\pi\sigma^3 N_A}\left(\sigma^2\kappa^2 + 2\sigma\kappa + \frac{2}{3} - \frac{2}{3}(1+2\sigma\kappa)^{3/2}\right)$$

Bare in mind the Taylor expansion for (1 + x)[a], we know that

$$(1+x)^a = 1 + ax + \frac{a(a-1)}{2!}x^2 + \cdots + \frac{a(a-1)(a-2)\cdots(a-n+1)}{n!}x^n + \cdots, \quad |x| < 1.$$

Talyor expand the term $(1+2\sigma\kappa)^{3/2}$ in the expression $\frac{A^E}{RT}$, we have:

$$\frac{A^E}{RT} = -\frac{V}{4\pi\sigma^3 N_A}\left(\sigma^2\kappa^2 + 2\sigma\kappa + \frac{2}{3} - \frac{2}{3}\left(1 + \frac{3}{2}2\sigma\kappa + \frac{\frac{3}{2}(\frac{3}{2}-1)}{2!}(2\sigma\kappa)^2 + \frac{\frac{3}{2}(\frac{3}{2}-1)(\frac{3}{2}-2)}{3!}(2\sigma\kappa)^3 + \right.\right.$$

$$\left.\left.\frac{\frac{3}{2}(\frac{1}{2})(-\frac{1}{2})(-\frac{3}{2})}{4!}(2\sigma\kappa)^4 + \frac{\frac{3}{2}(\frac{1}{2})(-\frac{1}{2})(-\frac{3}{2})(-\frac{5}{2})}{5!}(2\sigma\kappa)^5 + \frac{\frac{3}{2}(\frac{1}{2})(-\frac{1}{2})(-\frac{3}{2})(-\frac{5}{2})(-\frac{7}{2})}{6!}(2\sigma\kappa)^6 + O((\sigma\kappa)^7)\right)\right)$$

$$= -\frac{V}{4\pi\sigma^3 N_A}\left(\sigma^2\kappa^2 + 2\sigma\kappa + \frac{2}{3} - \frac{2}{3}\left(1 + 3\sigma\kappa + \frac{3\times 1}{2!}(\sigma\kappa)^2 + \frac{3\times 1\times(-1)}{3!}(\sigma\kappa)^3 + \frac{3\times 1\times(-1)\times(-3)}{4!}(\sigma\kappa)^4\right.\right.$$

$$\left.\left. + \frac{3\times 1\times(-1)\times(-3)\times(-5)}{5!}(\sigma\kappa)^5 + \frac{3\times 1\times(-1)\times(-3)\times(-5)\times(-7)}{6!}(\sigma\kappa)^6 + O((\sigma\kappa)^7)\right)\right)$$

$$\frac{A^E}{RT} = -\frac{V}{4\pi\sigma^3 N_A}\left(\sigma^2\kappa^2 + 2\sigma\kappa + \frac{2}{3} - \frac{2}{3}\left(1 + 3\sigma\kappa + \frac{3}{2}(\sigma\kappa)^2 - \frac{1}{2}(\sigma\kappa)^3 + \frac{3}{4\times 2}(\sigma\kappa)^4 - \frac{3}{8}(\sigma\kappa)^5 + \frac{3\times 7}{6\times 4\times 2}(\sigma\kappa)^6 + O\left((\sigma\kappa)^7\right)\right)\right)$$

$$\frac{A^E}{RT} = -\frac{V}{4\pi\sigma^3 N_A}\left(\frac{1}{3}(\sigma\kappa)^3 - \frac{1}{4}(\sigma\kappa)^4 + \frac{1}{4}(\sigma\kappa)^5 - \frac{7}{24}(\sigma\kappa)^6 + O\left((\sigma\kappa)^7\right)\right), (|\sigma\kappa| < 1/2)$$

From the Debye-Hückel equation it is know that the excess Helmholtz function derived from Debye-Hückel equation has the following form:

$$\frac{A^E}{RT} = -\frac{V}{4\pi N_A\sum x_i z_i^2}\sum\frac{x_i z_i^2}{a_i^3}\left(\frac{3}{2} + \ln(1+a_i\kappa) - 2(1+a_i\kappa) + \frac{(1+a_i\kappa)^2}{2}\right)$$

where a_i is the closest approach distance and x_i is the mole fraction of species *i*. The rest of the parameters are the same as in MSA term. If the closest approach distance a_i is substituted with the average diameters of the ions σ, the following expression is obtained:

$$\frac{A^E}{RT}=-\frac{V}{4\pi N_A\sum x_i z_i^2}\sum\frac{x_i z_i^2}{\sigma^3}\left(\frac{3}{2}+\ln(1+\sigma\kappa)-2(1+\sigma\kappa)+\frac{(1+\sigma\kappa)^2}{2}\right)$$

$$=-\frac{V}{4\pi N_A\sigma^3}\left(\frac{3}{2}+\ln(1+\sigma\kappa)-2(1+\sigma\kappa)+\frac{(1+\sigma\kappa)^2}{2}\right)\frac{\sum x_i z_i^2}{\sum x_i z_i^2}$$

$$=-\frac{V}{4\pi N_A\sigma^3}\left(\ln(1+\sigma\kappa)-\sigma\kappa+\frac{(\sigma\kappa)^2}{2}\right)$$

Bearing in mind the Taylor expansion for $ln(1 + x)$ it is known that

$$\ln(1+x)=x-\frac{1}{2}x^2+\frac{1}{3}x^3-\cdots+(-1)^n\frac{x^n}{n!}+\cdots,\quad |x|<1.$$

Talyor expands the term $\ln(1+\sigma\kappa)$ in the expression $\frac{A^E}{RT}$:

$$\frac{A^E}{RT}=-\frac{V}{4\pi N_A\sigma^3}\left(\sigma\kappa-\frac{1}{2}(\sigma\kappa)^2+\frac{1}{3}(\sigma\kappa)^3-\frac{1}{4}(\sigma\kappa)^4+\frac{1}{5}(\sigma\kappa)^5-\frac{1}{6}(\sigma\kappa)^6+O((\sigma\kappa)^7)-\sigma\kappa+\frac{(\sigma\kappa)^2}{2}\right)$$

$$\frac{A^E}{RT}=-\frac{V}{4\pi N_A\sigma^3}\left(\frac{1}{3}(\sigma\kappa)^3-\frac{1}{4}(\sigma\kappa)^4+\frac{1}{5}(\sigma\kappa)^5-\frac{1}{6}(\sigma\kappa)^6+O((\sigma\kappa)^7)\right),\ |\sigma\kappa|<1$$

Comparing with the results from MSA term,

$$\frac{A^E}{RT}=-\frac{V}{4\pi\sigma^3 N_A}\left(\frac{1}{3}(\sigma\kappa)^3-\frac{1}{4}(\sigma\kappa)^4+\frac{1}{4}(\sigma\kappa)^5-\frac{7}{24}(\sigma\kappa)^6+O((\sigma\kappa)^7)\right),\ (|\sigma\kappa|<1/2)$$

the difference between the excess Helmholtz free energy is

$$\left(\frac{A^E}{RT}\right)_{MSA}-\left(\frac{A^E}{RT}\right)_{D-H}=-\frac{V}{4\pi\sigma^3 N_A}\left(\frac{1}{20}(\sigma\kappa)^5-\frac{1}{8}(\sigma\kappa)^6+O((\sigma\kappa)^7)\right)\approx-\frac{V}{4\pi\sigma^3 N_A}\left(\frac{O((\sigma\kappa)^5)}{20}\right),\ (|\sigma\kappa|<1/2)$$

APPENDIX IV The derivatives of the non-electrolyte term

1.1 Derivatives of Helmholtz free energy A^r of the general cubic equation of state with volume translation parameter

If the volume translation parameter in the cubic EOS is set to zero, the EOS with volume translation parameter is reduced to the conventional EOS without volume translation parameter. The same applies to the derivatives of the cubic EOS with volume translation parameter. For this reason only the derivatives of the general cubic EOS with volume translation parameter are presented. Note in Appendixes, the separator in the equation number is changed to "-" instead of "." in previous chapters. This is will prevent readers from confusion.

1.1.1 First order partial molar derivatives

The first order partial molar derivative of the residual Helmholtz free energy for the general cubic EOS with volume translation parameter is presented below if the expression in equation (2.56) and the chain rule are used. After some simplification and rewriting the equation in terms of the partial molar derivatives of total molar number n, the coefficients a and b_i, we have:

$$\left(\frac{\partial A^r}{\partial n_i}\right)_{T,V,n_{j\neq i}} = -RT\ln\frac{(V-nb_1+nc)}{V}\frac{\partial n}{\partial n_i}+\frac{1}{b_3-b_2}\ln\frac{(V+nb_2+nc)}{(V+nb_3+nc)}\left(n\frac{\partial a(T)}{\partial n_i}+a(T)\right)+$$

$$\frac{nRT}{V-nb_1+nc}\left(b_1+n\frac{\partial b_1}{\partial n_i}\right)+\frac{na(T)}{b_3-b_2}\left[\frac{b_2+n\frac{\partial b_2}{\partial n_i}}{(V+nb_2+nc)}-\frac{b_3+n\frac{\partial b_3}{\partial n_i}}{(V+nb_3+nc)}\right]+$$

$$\frac{na(T)}{(b_3-b_2)^2}\ln\frac{(V+nb_2+nc)}{(V+nb_3+nc)}\left(\frac{\partial b_2}{\partial n_i}-\frac{\partial b_3}{\partial n_i}\right)+$$

$$\left(\frac{n^2a(T)}{(V+nb_2+nc)(V+nb_3+nc)}-\frac{nRT}{V-nb_1+nc}\right)\left(c+n\frac{\partial c}{\partial n_i}\right) \tag{4-1}$$

The partial molar derivatives of the coefficients *a(T)* and b_i are determined by the mixing rules used in the model. If the conventional quadratic and linear mixing rules are used in the model, for mixtures we can introduce new variables n, $\tilde{A}(T)$, $\tilde{B}_1$, $\tilde{B}_2$ and $\tilde{B}_3$ in (4-1) and get:

$$\left(\frac{\partial A^r}{\partial n_i}\right)_{T,V,n_{j\neq i}} = -RT\ln\frac{(V-\tilde{B}_1+\tilde{C})}{V}\left(\frac{\partial n}{\partial n_i}\right)+\frac{1}{\tilde{B}_3-\tilde{B}_2}\ln\frac{(V+n\tilde{B}_2+\tilde{C})}{(V+n\tilde{B}_3+\tilde{C})}\left(\frac{\partial \tilde{A}(T)}{\partial n_i}\right)+$$

$$\frac{nRT}{V-\tilde{B}_1+\tilde{C}}\left(\frac{\partial \tilde{B}_1}{\partial n_i}\right)+\frac{\tilde{A}(T)}{\tilde{B}_3-\tilde{B}_2}\left[\frac{\dfrac{\partial \tilde{B}_2}{\partial n_i}}{(V+\tilde{B}_2+\tilde{C})}-\frac{\dfrac{\partial \tilde{B}_3}{\partial n_i}}{(V+\tilde{B}_3+\tilde{C})}\right]$$

$$+\frac{\tilde{A}(T)}{\left(\tilde{B}_3-\tilde{B}_2\right)^2}\ln\frac{(V+\tilde{B}_2+\tilde{C})}{(V+\tilde{B}_3+\tilde{C})}\left(\frac{\partial \tilde{B}_2}{\partial n_i}-\frac{\partial \tilde{B}_3}{\partial n_i}\right)+\left(\frac{\tilde{A}(T)}{(V+\tilde{B}_2+\tilde{C})(V+\tilde{B}_3+\tilde{C})}-\frac{nRT}{V-\tilde{B}_1+\tilde{C}}\right)\left(\frac{\partial \tilde{C}}{\partial n_i}\right)$$

(4-2)

The first order partial molar derivative of the residual Helmholtz free energy can be expressed in a vector form to simplify the programming and calculation:

$$\frac{\partial A^r(n)}{\partial n_i} = (\boldsymbol{\eta}(\mathbf{n})_{n_i})^T \cdot \mathbf{A^{r\prime}}(\boldsymbol{\eta}(\mathbf{n}))$$

$$= \frac{\partial A^r}{\partial n}\cdot\frac{\partial n}{\partial n_i}+\frac{\partial A^r}{\partial \tilde{A}}\cdot\frac{\partial \tilde{A}(\mathbf{n},T)}{\partial n_i}+\frac{\partial A^r}{\partial \tilde{B}_1}\cdot\frac{\partial \tilde{B}_1}{\partial n_i}+\frac{\partial A^r}{\partial \tilde{B}_2}\cdot\frac{\partial \tilde{B}_2}{\partial n_i}+\frac{\partial A^r}{\partial \tilde{B}_3}\cdot\frac{\partial \tilde{B}_3}{\partial n_i}+\frac{\partial A^r}{\partial \tilde{C}}\cdot\frac{\partial \tilde{C}}{\partial n_i}, \quad (4\text{-}3)$$

where $\mathbf{A^{r\prime}}(\boldsymbol{\eta}(\mathbf{n}))$ and $(\boldsymbol{\eta}(\mathbf{n})_{n_i})$ are explicitly written below:

$$\mathbf{A^{r\prime}}(\boldsymbol{\eta}(\mathbf{n})) = \begin{bmatrix} \dfrac{\partial A^r}{\partial n} \\ \dfrac{\partial A^r}{\partial \tilde{A}} \\ \dfrac{\partial A^r}{\partial \tilde{B}_1} \\ \dfrac{\partial A^r}{\partial \tilde{B}_2} \\ \dfrac{\partial A^r}{\partial \tilde{B}_3} \\ \dfrac{\partial A^r}{\partial \tilde{C}} \end{bmatrix} = \begin{bmatrix} -RT\ln\dfrac{(V-\tilde{B}_1+\tilde{C})}{V} \\ \dfrac{1}{\tilde{B}_3-\tilde{B}_2}\ln\dfrac{(V+\tilde{B}_2+\tilde{C})}{(V+\tilde{B}_3+\tilde{C})} \\ \dfrac{nRT}{V-\tilde{B}_1+\tilde{C}} \\ \dfrac{\tilde{A}(T)}{\left(\tilde{B}_3-\tilde{B}_2\right)^2}\ln\dfrac{(V+\tilde{B}_2+\tilde{C})}{(V+\tilde{B}_3+\tilde{C})}+\dfrac{\tilde{A}(T)}{(\tilde{B}_3-\tilde{B}_2)(V+\tilde{B}_2+\tilde{C})} \\ -\dfrac{\tilde{A}(T)}{\left(\tilde{B}_3-\tilde{B}_2\right)^2}\ln\dfrac{(V+\tilde{B}_2+\tilde{C})}{(V+\tilde{B}_3+\tilde{C})}-\dfrac{\tilde{A}(T)}{(\tilde{B}_3-\tilde{B}_2)(V+\tilde{B}_3+\tilde{C})} \\ \dfrac{\tilde{A}(T)}{(V+\tilde{B}_2+\tilde{C})(V+\tilde{B}_3+\tilde{C})}-\dfrac{nRT}{V-\tilde{B}_1+\tilde{C}} \end{bmatrix} \quad (4\text{-}4)$$

The first and second order derivatives of the vector function $\boldsymbol{\eta}(\mathbf{n})$ are specifically related to the mixing rules used and its deduction is neither very complicated nor cumbersome. Consequently, only the vector function $\boldsymbol{\eta}(\mathbf{n})$ of PR EOS with volume translation parameter is presented. The mixing rule used is the conventional quadratic and linear mixing rules for the energy parameter and the covolume parameter, see (2.55). We have:

$$\begin{aligned}\boldsymbol{\eta}(\mathbf{n})_{n_i} &\triangleq \frac{\partial \boldsymbol{\eta}(\mathbf{n})}{\partial n_i} = \left[\frac{\partial n(\mathbf{n})}{\partial n_i}, \frac{\partial \tilde{A}(\mathbf{n},T)}{\partial n_i}, \frac{\partial \tilde{B}_1(\mathbf{n})}{\partial n_i}, \frac{\partial \tilde{B}_2(\mathbf{n})}{\partial n_i}, \frac{\partial \tilde{B}_3(\mathbf{n})}{\partial n_i}, \frac{\partial \tilde{C}(\mathbf{n})}{\partial n_i}\right]^T \\ &= \left[1, \quad 2\sum_j n_j \sqrt{a_i a_j}(1-k_{ij}), \quad b_i, \quad (1+\sqrt{2})b_i, \quad (1-\sqrt{2})b_i, \quad c_i\right]^T\end{aligned} \tag{4-5}$$

1.1.2 Second order partial molar derivatives

The second order partial molar derivative of the residual Helmholtz free energy for the Cubic EOS will be very long and complicated, if it is presented in a full scalar form. And it is very easy to make mistakes if the long and cumbersome scalar expression of the second order partial molar derivative is adopted in programming. So it is recommended to use a vector and matrix form instead. Each partial derivative is written as an element in the vector or matrix. It is clear and concise.

The general form of a vector and matrix form and their deduction is presented in CHAPTER 3. The results from CHAPTER 3 are directly used.

$$\frac{\partial^2 A^r}{\partial n_i \partial n_j} = (\boldsymbol{\eta}'(\mathbf{n})_{n_i})^T \cdot \mathbf{A}^{\mathbf{r}''}(\boldsymbol{\eta}) \cdot \boldsymbol{\eta}'(\mathbf{n})_{n_j} + \mathbf{A}^{\mathbf{r}'}(\boldsymbol{\eta})^T \cdot \boldsymbol{\eta}(\mathbf{n})_{n_i n_j}, \tag{4-6}$$

where the gradient $\mathbf{A}^{\mathbf{r}'}(\boldsymbol{\eta})$ and $\boldsymbol{\eta}'(\mathbf{n})_{n_i}$, the first derivative of the vector function $\boldsymbol{\eta}(\mathbf{n})$, are as in equation (4-4) and (4-5). The Hessian of A^r and the second derivative of the vector function $\boldsymbol{\eta}(\mathbf{n})$ are presented below. Note in the symmetric matrix (4-9) the following notation (4-7) is adopted to simplify the expression of the high order partial derivatives:

$$\frac{\partial^2 f(u,v)}{\partial u \partial v} = f_{uv}(u,v) \tag{4-7}$$

$$\begin{aligned}\boldsymbol{\eta}(\mathbf{n})_{n_i n_j} &\triangleq \frac{\partial^2 \boldsymbol{\eta}(\mathbf{n})}{\partial n_i \partial n_j} = \left[\frac{\partial^2 n(\mathbf{n})}{\partial n_i \partial n_j}, \frac{\partial^2 \tilde{A}(\mathbf{n},T)}{\partial n_i \partial n_j}, \frac{\partial^2 \tilde{B}_1(\mathbf{n})}{\partial n_i \partial n_j}, \frac{\partial^2 \tilde{B}_2(\mathbf{n})}{\partial n_i \partial n_j}, \frac{\partial^2 \tilde{B}_3(\mathbf{n})}{\partial n_i \partial n_j}, \frac{\partial^2 \tilde{C}(\mathbf{n})}{\partial n_i \partial n_j}\right]^T \\ &= \left[0, \quad 2\sqrt{a_i a_j}(1-k_{ij}), \quad 0, \quad 0, \quad 0, \quad 0\right]^T\end{aligned} \tag{4-8}$$

and

$$\mathbf{A}^{\mathbf{r}''}(\boldsymbol{\eta}) = \begin{bmatrix} A^r_{nn} & A^r_{\tilde{A}n} & A^r_{\tilde{B}_1 n} & A^r_{\tilde{B}_2 n} & A^r_{\tilde{B}_3 n} & A^r_{\tilde{C}n} \\ A^r_{n\tilde{A}} & A^r_{\tilde{A}\tilde{A}} & A^r_{\tilde{B}_1\tilde{A}} & A^r_{\tilde{B}_2\tilde{A}} & A^r_{\tilde{B}_3\tilde{A}} & A^r_{\tilde{C}\tilde{A}} \\ A^r_{n\tilde{B}_1} & A^r_{\tilde{A}\tilde{B}_1} & A^r_{\tilde{B}_1\tilde{B}_1} & A^r_{\tilde{B}_2\tilde{B}_1} & A^r_{\tilde{B}_3\tilde{B}_1} & A^r_{\tilde{C}\tilde{B}_1} \\ A^r_{n\tilde{B}_2} & A^r_{\tilde{A}\tilde{B}_2} & A^r_{\tilde{B}_1\tilde{B}_2} & A^r_{\tilde{B}_2\tilde{B}_2} & A^r_{\tilde{B}_3\tilde{B}_2} & A^r_{\tilde{C}\tilde{B}_2} \\ A^r_{n\tilde{B}_3} & A^r_{\tilde{A}\tilde{B}_3} & A^r_{\tilde{B}_1\tilde{B}_3} & A^r_{\tilde{B}_2\tilde{B}_3} & A^r_{\tilde{B}_3\tilde{B}_3} & A^r_{\tilde{C}\tilde{B}_3} \\ A^r_{n\tilde{C}} & A^r_{\tilde{A}\tilde{C}} & A^r_{\tilde{B}_1\tilde{C}} & A^r_{\tilde{B}_2\tilde{C}} & A^r_{\tilde{B}_3\tilde{C}} & A^r_{\tilde{C}\tilde{C}} \end{bmatrix} \quad (4\text{-}9)$$

$$= \begin{bmatrix} 0 & 0 & A^r_{\tilde{B}_1 n} & 0 & 0 & A^r_{\tilde{C}n} \\ 0 & 0 & 0 & A^r_{\tilde{B}_2\tilde{A}} & A^r_{\tilde{B}_3\tilde{A}} & A^r_{\tilde{C}\tilde{A}} \\ A^r_{n\tilde{B}_1} & 0 & A^r_{\tilde{B}_1\tilde{B}_1} & 0 & 0 & A^r_{\tilde{C}\tilde{B}_1} \\ 0 & A^r_{\tilde{A}\tilde{B}_2} & 0 & A^r_{\tilde{B}_2\tilde{B}_2} & A^r_{\tilde{B}_3\tilde{B}_2} & A^r_{\tilde{C}\tilde{B}_2} \\ 0 & A^r_{\tilde{A}\tilde{B}_3} & 0 & A^r_{\tilde{B}_2\tilde{B}_3} & A^r_{\tilde{B}_3\tilde{B}_3} & A^r_{\tilde{C}\tilde{B}_3} \\ A^r_{n\tilde{C}} & A^r_{\tilde{A}\tilde{C}} & A^r_{\tilde{B}_1\tilde{C}} & A^r_{\tilde{B}_2\tilde{C}} & A^r_{\tilde{B}_3\tilde{C}} & A^r_{\tilde{C}\tilde{C}} \end{bmatrix}.$$

The non-zero second order derivatives in (4-9) are as follows:

$$A^r_{n\tilde{B}_1} = A^r_{\tilde{B}_1 n} = \frac{RT}{V - \tilde{B}_1 + \tilde{C}}, \qquad A^r_{\tilde{C}n} = A^r_{n\tilde{C}} = \frac{-RT}{V - \tilde{B}_1 + \tilde{C}}$$

$$A^r_{\tilde{A}\tilde{B}_2} = A^r_{\tilde{B}_2\tilde{A}} = \frac{1}{\left(\tilde{B}_3 - \tilde{B}_2\right)^2}\ln\frac{(V + \tilde{B}_2 + \tilde{C})}{(V + \tilde{B}_3 + \tilde{C})} + \frac{1}{(\tilde{B}_3 - \tilde{B}_2)(V + \tilde{B}_2 + \tilde{C})} \quad (4\text{-}10)$$

$$A^r_{\tilde{A}\tilde{B}_3} = A^r_{\tilde{B}_3\tilde{A}} = -\frac{1}{\left(\tilde{B}_3 - \tilde{B}_2\right)^2}\ln\frac{(V + \tilde{B}_2 + \tilde{C})}{(V + \tilde{B}_3 + \tilde{C})} - \frac{1}{(\tilde{B}_3 - \tilde{B}_2)(V + \tilde{B}_3 + \tilde{C})}$$

$$A^r_{\tilde{A}\tilde{C}} = A^r_{\tilde{C}\tilde{A}} = \frac{1}{(V + \tilde{B}_2 + \tilde{C})(V + \tilde{B}_3 + \tilde{C})}$$

$$A^r_{\tilde{B}_1\tilde{B}_1} = \frac{nRT}{\left(V - \tilde{B}_1 + \tilde{C}\right)^2} \qquad A^r_{\tilde{B}_1\tilde{C}} = A^r_{\tilde{C}\tilde{B}_1} = \frac{-nRT}{\left(V - \tilde{B}_1 + \tilde{C}\right)^2} = -A^r_{\tilde{B}_1\tilde{B}_1}$$

$$A^r_{\tilde{B}_2\tilde{B}_2} = \frac{2\tilde{A}}{\left(\tilde{B}_3 - \tilde{B}_2\right)^3}\ln\frac{(V + \tilde{B}_2 + \tilde{C})}{(V + \tilde{B}_3 + \tilde{C})} + \frac{2\tilde{A}}{(\tilde{B}_3 - \tilde{B}_2)^2(V + \tilde{B}_2 + \tilde{C})} + \frac{\tilde{A}}{(\tilde{B}_3 - \tilde{B}_2)(V + \tilde{B}_2 + \tilde{C})^2}$$

$$A^r_{\tilde{B}_2\tilde{B}_3} = A^r_{\tilde{B}_3\tilde{B}_2} = -\frac{2\tilde{A}}{\left(\tilde{B}_3 - \tilde{B}_2\right)^3}\ln\frac{(V + \tilde{B}_2 + \tilde{C})}{(V + \tilde{B}_3 + \tilde{C})} - \frac{\tilde{A}}{(\tilde{B}_3 - \tilde{B}_2)^2}\left(\frac{1}{V + \tilde{B}_3 + \tilde{C}} + \frac{1}{V + \tilde{B}_2 + \tilde{C}}\right)$$

$$A^r_{\tilde{B}_2\tilde{C}} = A^r_{\tilde{C}\tilde{B}_2} = \frac{-\tilde{A}}{(V + \tilde{B}_2 + \tilde{C})^2(V + \tilde{B}_3 + \tilde{C})}$$

$$A^r_{\tilde{B}_3\tilde{B}_3} = \frac{2\tilde{A}}{\left(\tilde{B}_3 - \tilde{B}_2\right)^3}\ln\frac{(V + \tilde{B}_2 + \tilde{C})}{(V + \tilde{B}_3 + \tilde{C})} + \frac{2\tilde{A}}{(\tilde{B}_3 - \tilde{B}_2)^2(V + \tilde{B}_3 + \tilde{C})} - \frac{\tilde{A}}{(\tilde{B}_3 - \tilde{B}_2)(V + \tilde{B}_3 + \tilde{C})^2}$$

$$A^r_{\tilde{B}_3\tilde{C}} = A^r_{\tilde{C}\tilde{B}_2} = \frac{-\tilde{A}}{(V + \tilde{B}_2 + \tilde{C})(V + \tilde{B}_3 + \tilde{C})^2}$$

$$A^r_{\tilde{C}\tilde{C}} = -\frac{\tilde{A}}{(V + \tilde{B}_2 + \tilde{C})(V + \tilde{B}_3 + \tilde{C})^2} - \frac{\tilde{A}}{(V + \tilde{B}_2 + \tilde{C})^2(V + \tilde{B}_3 + \tilde{C})} + \frac{nRT}{\left(V - \tilde{B}_1 + \tilde{C}\right)^2} = A^r_{\tilde{B}_2\tilde{C}} + A^r_{\tilde{B}_3\tilde{C}} + A^r_{\tilde{B}_1\tilde{B}_1}$$

(4-11)

The first and second order derivatives of the vector function **η**(**n**) are specifically related to the mixing rules used and its deduction is not very complicated nor difficult. Consequently they are not presented.

1.2 Fugacity coefficient

1.2.1 Pure compound

The fugacity coefficient for pure compound can be calculated from the residual Helmholtz free energy according to below equation

$$\ln\varphi = \frac{A^r(T,V,n)}{RT} + Z - 1 - \ln Z \tag{4-12}$$

Substitute the expression of the residual Helmholtz free energy from the Cubic EOS (4-1) to the above (4-12), the following is obtained:

$$\ln\varphi = \frac{-n}{RT}\left(RT\ln\frac{(v-b_1+c)}{v} - \frac{a(T)}{b_3-b_2}\ln\frac{(v+b_2+c)}{(v+b_3+c)}\right) + Z - 1 - \ln Z \tag{4-13}$$

After some simplification, we reach to:

$$\ln\varphi = -n\ln\frac{(v-b_1+c)}{v} + \frac{a(T)n}{b_3-b_2}\ln\frac{(v+b_2+c)}{(v+b_3+c)} + Z - 1 - \ln Z \tag{4-14}$$

Let the molar number n = 1, we have:

$$\ln\varphi = -\ln\frac{(v-b_1+c)}{v} + \frac{a(T)}{b_3-b_2}\ln\frac{(v+b_2+c)}{(v+b_3+c)} + Z - 1 - \ln Z \tag{4-15}$$

The above equation (4-15) can also be transformed into the dimensionless form by introducing the compressibility factor Z and the dimensionless coefficients in equation (2.47), (2.48) and (2.49), we have:

$$\ln\varphi = -\ln(Z - B_1 + C) + \frac{A(T)}{B_3 - B_2}\ln\frac{(Z+B_2+C)}{(Z+B_3+C)} + Z - 1 \tag{4-16}$$

1.2.2 Component in a mixture

The fugacity of the component *i* in the mixture can be calculated according to the below equation (4-17):

$$RT\ln\hat{\varphi}_i = \left(\frac{\partial A^r}{\partial n_i}\right)_{T,V,n_{j\neq i}} - RT\ln Z \tag{4-17}$$

Substitute equation (4-1) into the fugacity of the component *i* in the a mixture in (4-17), the complete equation of fugacity of the component *i* in the a mixture can be obtained.

$$\ln\hat{\varphi}_i =$$

$$\left\{-\ln\frac{(V-nb_1+nc)}{V}\frac{\partial n}{\partial n_i}+\frac{1}{RT(b_3-b_2)}\ln\frac{(V+nb_2+nc)}{(V+nb_3+nc)}\left(n\frac{\partial a(T)}{\partial n_i}+a(T)\right)+\frac{n}{V-nb_1+nc}\left(b_1+n\frac{\partial b_1}{\partial n_i}\right)\right.$$

$$+\frac{na(T)}{RT(b_3-b_2)}\left[\frac{b_2+n\dfrac{\partial b_2}{\partial n_i}}{(V+nb_2+nc)}-\frac{b_3+n\dfrac{\partial b_3}{\partial n_i}}{(V+nb_3+nc)}\right]+\frac{na(T)}{RT\left(b_3-b_2\right)^2}\ln\frac{(V+nb_2+nc)}{(V+nb_3+nc)}\left(\frac{\partial b_2}{\partial n_i}-\frac{\partial b_3}{\partial n_i}\right)+$$

$$\left.\left(\frac{n^2a(T)}{(V+nb_2+nc)(V+nb_3+nc)}-\frac{nRT}{V-nb_1+nc}\right)\left(c+n\frac{\partial c}{\partial n_i}\right)\right\}-\ln Z$$

(4-18)

If new variables $n, \tilde{A}(T), \tilde{B}_1, \tilde{B}_2$ and $\tilde{B}_3$ are introduced and expressed the partial molar derivatives of the residual Helmholtz free energy in the above mentioned new variables as in (4-2), we will get:

$$\ln\hat{\varphi}_{ii} =$$

$$\left\{-\ln\frac{(V-\tilde{B}_1+\tilde{C})}{V}\left(\frac{\partial n}{\partial n_i}\right)+\frac{1}{RT(\tilde{B}_3-\tilde{B}_2)}\ln\frac{(V+n\tilde{B}_2+\tilde{C})}{(V+n\tilde{B}_3+\tilde{C})}\left(\frac{\partial\tilde{A}(T)}{\partial n_i}\right)+\frac{nRT}{V-\tilde{B}_1+\tilde{C}}\left(\frac{\partial\tilde{B}_1}{\partial n_i}\right)+\right.$$

$$\frac{\tilde{A}(T)}{\tilde{B}_3-\tilde{B}_2}\left[\frac{1}{(V+\tilde{B}_2+\tilde{C})}\frac{\partial\tilde{B}_2}{\partial n_i}-\frac{1}{(V+\tilde{B}_3+\tilde{C})}\frac{\partial\tilde{B}_3}{\partial n_i}\right]+\frac{\tilde{A}(T)}{RT\left(\tilde{B}_3-\tilde{B}_2\right)^2}\ln\frac{(V+\tilde{B}_2+\tilde{C})}{(V+\tilde{B}_3+\tilde{C})}\left(\frac{\partial\tilde{B}_2}{\partial n_i}-\frac{\partial\tilde{B}_3}{\partial n_i}\right)$$

$$\left.+\left(\frac{\tilde{A}(T)}{(V+\tilde{B}_2+\tilde{C})(V+\tilde{B}_3+\tilde{C})}-\frac{nRT}{V-\tilde{B}_1+\tilde{C}}\right)\left(\frac{\partial\tilde{C}}{\partial n_i}\right)\right\}-\ln Z$$

(4-19)

The above equation (4-19) is used in the program code.

APPENDIX V The derivatives of the electrolyte term

1.1 Fürst and Renon's ionic short range term (SR2 term)

The short range ionic term SR2 is given as

$$F_{SR2} = \frac{A_{SR2} - A^0}{RT} = -\sum_k \sum_l \frac{n_k n_l W_{kl}}{V(1-\varepsilon_3)} \triangleq \frac{W}{V(1-\varepsilon_3)} \tag{4-20}$$

where the function is defined as

$$W = -\sum_k \sum_l n_k n_l W_{kl} \tag{4-21}$$

and

$$\varepsilon_3 = \frac{N_A \pi}{6} \sum_k \frac{n_k \sigma_k^3}{V} \tag{4-22}$$

The composite function is obtained

$$F_{SR2} = F_{SR2}(W(n_i), \varepsilon_3(n_i, V), V) \tag{4-23}$$

1.1.1 First order partial derivatives of SR2 term

Define

$$\boldsymbol{\eta}(\mathbf{x})_F = \begin{bmatrix} W \\ \varepsilon_3 \\ V \end{bmatrix} = \begin{bmatrix} -\sum_k \sum_l n_k n_l W_{kl} \\ \frac{N_A \pi}{6} \sum_k \frac{n_k \sigma_k^3}{V} \\ V \end{bmatrix} \tag{4-24}$$

Then we have:

$$\frac{\partial F(\boldsymbol{\eta})}{\partial \boldsymbol{\eta}_F} = \begin{bmatrix} \frac{\partial F}{\partial W} \\ \frac{\partial F}{\partial \varepsilon_3} \\ \frac{\partial F}{\partial V} \end{bmatrix} = \begin{bmatrix} \frac{1}{V(1-\varepsilon_3)} \\ \frac{W}{V(1-\varepsilon_3)^2} \\ \frac{-W}{V^2(1-\varepsilon_3)} \end{bmatrix} \tag{4-25}$$

$$\frac{\partial \boldsymbol{\eta}_F}{\partial n_k} = \frac{\partial}{\partial n_k} \begin{bmatrix} W \\ \varepsilon_3 \\ V \end{bmatrix} = \begin{bmatrix} -2\sum_l n_l W_{kl} \\ \frac{N_A \pi}{6} \frac{\sigma_k^3}{V} \\ 0 \end{bmatrix} \tag{4-26}$$

$$\frac{\partial \boldsymbol{\eta}_F}{\partial V}=\frac{\partial}{\partial V}\begin{bmatrix} W \\ \varepsilon_3 \\ V \end{bmatrix}=\begin{bmatrix} 0 \\ -\dfrac{N_A\pi}{6V^2}\sum_k n_k\sigma_k^3 \\ 1 \end{bmatrix}=\begin{bmatrix} 0 \\ -\dfrac{\varepsilon_3}{V} \\ 1 \end{bmatrix} \tag{4-27}$$

$$\frac{\partial \boldsymbol{\eta}_F}{\partial T}=\frac{\partial}{\partial T}\begin{bmatrix} W \\ \varepsilon_3 \\ V \end{bmatrix}=[0] \tag{4-28}$$

The first order differentials of this function are:

$$\frac{\partial F}{\partial n_k}=\left(\frac{\partial F}{\partial \boldsymbol{\eta}_F}\right)^T\cdot\frac{\partial \boldsymbol{\eta}_F}{\partial n_k}=\begin{bmatrix} \dfrac{1}{V(1-\varepsilon_3)} & \dfrac{W}{V(1-\varepsilon_3)^2} & \dfrac{-W}{V^2(1-\varepsilon_3)} \end{bmatrix}\cdot\begin{bmatrix} -2\sum_l n_l W_{kl} \\ \dfrac{N_A\pi}{6}\dfrac{\sigma_k^3}{V} \\ 0 \end{bmatrix} \tag{4-29}$$

$$\frac{\partial F}{\partial V}=\left(\frac{\partial F}{\partial \boldsymbol{\eta}_F}\right)^T\cdot\frac{\partial \boldsymbol{\eta}_F}{\partial V}=\begin{bmatrix} \dfrac{1}{V(1-\varepsilon_3)} & \dfrac{W}{V(1-\varepsilon_3)^2} & \dfrac{-W}{V^2(1-\varepsilon_3)} \end{bmatrix}\cdot\begin{bmatrix} 0 \\ -\dfrac{\varepsilon_3}{V} \\ 1 \end{bmatrix}=\frac{-W\varepsilon_3}{V^2(1-\varepsilon_3)^2} \tag{4-30}$$

$$\frac{\partial F}{\partial T}=\left(\frac{\partial F}{\partial \boldsymbol{\eta}_F}\right)^T\cdot\frac{\partial \boldsymbol{\eta}_F}{\partial T}=\left(\frac{\partial F}{\partial \boldsymbol{\eta}_F}\right)^T\cdot\mathbf{0}=0 \tag{4-31}$$

1.1.2 Second order partial derivatives of SR2 term

Denote

$$\mathbf{F}''(\boldsymbol{\eta}_F)=\begin{bmatrix} F_{WW} & F_{W\varepsilon_3} & F_{WV} \\ F_{\varepsilon_3 W} & F_{\varepsilon_3\varepsilon_3} & F_{\varepsilon_3 V} \\ F_{VW} & F_{V\varepsilon_3} & F_{VV} \end{bmatrix}=\begin{bmatrix} 0 & F_{W\varepsilon_3} & F_{WV} \\ F_{\varepsilon_3 W} & F_{\varepsilon_3\varepsilon_3} & F_{\varepsilon_3 V} \\ F_{VW} & F_{V\varepsilon_3} & F_{VV} \end{bmatrix}$$

$$=\begin{bmatrix} 0 & \dfrac{1}{W}\dfrac{\partial F}{\partial \varepsilon_3} & \dfrac{1}{W}\dfrac{\partial F}{\partial V} \\ \dfrac{1}{W}\dfrac{\partial F}{\partial \varepsilon_3} & \dfrac{2}{1-\varepsilon_3}\dfrac{\partial F}{\partial \varepsilon_3} & \dfrac{1}{1-\varepsilon_3}\dfrac{\partial F}{\partial V} \\ \dfrac{1}{W}\dfrac{\partial F}{\partial V} & \dfrac{1}{1-\varepsilon_3}\dfrac{\partial F}{\partial V} & -\dfrac{2}{V}\dfrac{\partial F}{\partial V} \end{bmatrix}=\begin{bmatrix} 0 & \dfrac{1}{V(1-\varepsilon_3)^2} & \dfrac{-1}{V^2(1-\varepsilon_3)} \\ \dfrac{1}{V(1-\varepsilon_3)^2} & \dfrac{2W}{V(1-\varepsilon_3)^3} & \dfrac{-W}{V^2(1-\varepsilon_3)^2} \\ \dfrac{-1}{V^2(1-\varepsilon_3)} & \dfrac{-W}{V^2(1-\varepsilon_3)^2} & \dfrac{2W}{V^3(1-\varepsilon_3)} \end{bmatrix} \tag{4-32}$$

We have:

$$\frac{\partial^2 \boldsymbol{\eta}_F}{\partial n_k\partial n_l}=\frac{\partial^2}{\partial n_k\partial n_l}\begin{bmatrix} W \\ \varepsilon_3 \\ V \end{bmatrix}=\begin{bmatrix} -2W_{kl} \\ 0 \\ 0 \end{bmatrix} \tag{4-33}$$

$$\frac{\partial^2 \boldsymbol{\eta}_F}{\partial V^2} = \frac{\partial}{\partial V^2}\begin{bmatrix} W \\ \varepsilon_3 \\ V \end{bmatrix} = \begin{bmatrix} 0 \\ \dfrac{N_A \pi}{3V^3}\sum_k n_k \sigma_k^3 \\ 0 \end{bmatrix} = \begin{bmatrix} 0 \\ \dfrac{2\varepsilon_3}{V^2} \\ 0 \end{bmatrix} \tag{4-34}$$

$$\frac{\partial^2 \boldsymbol{\eta}_F}{\partial V \partial n_k} = \frac{\partial^2}{\partial V \partial n_k}\begin{bmatrix} W \\ \varepsilon_3 \\ V \end{bmatrix} = \begin{bmatrix} 0 \\ -\dfrac{N_A \pi}{6}\dfrac{\sigma_k^3}{V^2} \\ 0 \end{bmatrix} = \begin{bmatrix} 0 \\ \dfrac{-1}{V}\left(\dfrac{\partial \varepsilon_3}{\partial n_k}\right)_{T,V,\mathbf{n}/n_k} \\ 0 \end{bmatrix} \tag{4-35}$$

The second order differentials are given as :

$$\frac{\partial^2 F}{\partial n_k \partial n_l} = \left(\frac{\partial \boldsymbol{\eta}_F}{\partial n_l}\right)^T \mathbf{F}''(\boldsymbol{\eta}_F)\frac{\partial \boldsymbol{\eta}_F}{\partial n_k} + \left(\frac{\partial F}{\partial \boldsymbol{\eta}_F}\right)^T \cdot \frac{\partial^2 \boldsymbol{\eta}_F}{\partial n_k \partial n_l} \tag{4-36}$$

$$\boxed{\frac{\partial^2 F}{\partial n_k \partial n_l} = F_{\varepsilon_3\varepsilon_3}\frac{\partial \varepsilon_3}{\partial n_l}\frac{\partial \varepsilon_3}{\partial n_k} + F_{W\varepsilon_3}\left(\frac{\partial W}{\partial n_l}\frac{\partial \varepsilon_3}{\partial n_k} + \frac{\partial \varepsilon_3}{\partial n_l}\frac{\partial W}{\partial n_k}\right) + \left(\frac{\partial F}{\partial W}\right)\cdot\frac{\partial^2 W}{\partial n_k \partial n_l}} \tag{4-37}$$

$$\frac{\partial^2 F}{\partial V^2} = \left(\frac{\partial \boldsymbol{\eta}_F}{\partial V}\right)^T \mathbf{F}''(\boldsymbol{\eta}_F)\frac{\partial \boldsymbol{\eta}_F}{\partial V} + \left(\frac{\partial F}{\partial \boldsymbol{\eta}_F}\right)^T \frac{\partial^2 \boldsymbol{\eta}_F}{\partial V^2} \tag{4-38}$$

$$\boxed{\frac{\partial^2 F}{\partial V^2} = F_{\varepsilon_3\varepsilon_3}\left(\frac{\partial \varepsilon_3}{\partial V}\right)^2 + 2F_{\varepsilon_3 V}\left(\frac{\partial \varepsilon_3}{\partial V}\right) + F_{VV} + \left(\frac{\partial F}{\partial V}\right)\frac{\partial^2 \varepsilon_3}{\partial V^2}} \tag{4-39}$$

$$\frac{\partial^2 F}{\partial V \partial n_k} = \left(\frac{\partial \boldsymbol{\eta}_F}{\partial V}\right)^T \mathbf{F}''(\boldsymbol{\eta}_F)\frac{\partial \boldsymbol{\eta}_F}{\partial n_k} + \left(\frac{\partial F}{\partial \boldsymbol{\eta}_F}\right)^T \cdot \frac{\partial^2 \boldsymbol{\eta}_F}{\partial V \partial n_k} \tag{4-40}$$

$$\boxed{\frac{\partial^2 F}{\partial V \partial n_k} = F_{\varepsilon_3\varepsilon_3}\frac{\partial \varepsilon_3}{\partial V}\frac{\partial \varepsilon_3}{\partial n_k} + F_{W\varepsilon_3}\frac{\partial \varepsilon_3}{\partial V}\frac{\partial W}{\partial n_k} + F_{V\varepsilon_3}\frac{\partial \varepsilon_3}{\partial n_k} + F_{VW}\frac{\partial W}{\partial n_k} + \left(\frac{\partial F}{\partial \varepsilon_3}\right)\cdot\frac{\partial^2 \varepsilon_3}{\partial V \partial n_k}} \tag{4-41}$$

$$\frac{\partial^2 F}{\partial T \partial V} = 0, \quad \frac{\partial^2 F}{\partial T \partial n_k} = 0 \tag{4-42}$$

1.2 The derivatives of simplified explicit MSA (sMSA) term

The expression of the Helmholtz free energy for the simplified explicit MSA term is:

$$A^r{}_{sMSA}(T,V,n) = -\frac{2\Gamma^3 V}{3\pi N_A}RT\left(1+\frac{3}{2}\sigma\Gamma\right) \tag{4-43}$$

where

$$\Gamma = \frac{1}{2\sigma}\left(\sqrt{1+2\sigma\kappa}-1\right) \tag{4-44}$$

and

$$\sigma = \frac{\sum_i n_i \sigma_i}{\sum_i n_i}, \quad \kappa = \sqrt{\frac{e^2 {N_A}^2 \sum_i n_i {z_i}^2}{\varepsilon_0 \varepsilon RTV}} \tag{4-45}$$

The relative permittivity of water ε is calculated by a certain model, i.e. like the Uematsu-Franck model etc.

Substitute Γ into (4-43) and divide both sides of the equation with RT we have,

$$F_{sMSA} = \frac{A^r{}_{sMSA}}{RT} = -\frac{V}{4\pi N_A}\frac{1}{\sigma^3}\left(\sigma^2\kappa^2 + 2\sigma\kappa + \frac{2}{3} - \frac{2}{3}(1+2\sigma\kappa)^{3/2}\right) \tag{4-46}$$

Define the intermediate variables:

$$c(V) = -\frac{V}{4\pi N_A} \tag{4-47}$$

$$f(\sigma) = \frac{1}{\sigma^3} \tag{4-48}$$

and

$$g(\sigma\kappa) = \sigma^2\kappa^2 + 2\sigma\kappa + \frac{2}{3} - \frac{2}{3}(1+2\sigma\kappa)^{3/2} \tag{4-49}$$

Then equation (4-46) can be written as

$$F_{sMSA} = \frac{A^r{}_{sMSA}}{RT} \triangleq c(V)f(\sigma)g(\sigma\kappa) \tag{4-50}$$

We got the function

$$F_{sMSA} = F_{sMSA}(c(V), f(\sigma), g(\sigma\kappa)) \tag{4-51}$$

The structure of the composite function $F_{sMSA} = F_{sMSA}(c(V), f(\sigma), g(\sigma\kappa))$ can be expressed in a graph as below:

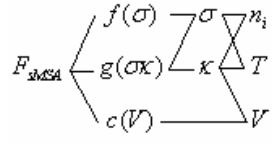

1.2.1 First order partial derivatives

Define vector function:

$$\boldsymbol{\eta}(\mathbf{x})_{F_{sMSA}} = \begin{bmatrix} f(\sigma) \\ g(\sigma\kappa) \\ c(V) \end{bmatrix} = \begin{bmatrix} \dfrac{1}{\sigma^3} \\ \sigma^2\kappa^2 + 2\sigma\kappa + \dfrac{2}{3} - \dfrac{2}{3}(1+2\sigma\kappa)^{3/2} \\ -\dfrac{V}{4\pi N_A} \end{bmatrix} \tag{4-52}$$

Then we have:

$$\frac{\partial F_{sMSA}(\boldsymbol{\eta}_{F_{sMSA}})}{\partial \boldsymbol{\eta}_{F_{sMSA}}} = \begin{bmatrix} c(V)g(\sigma\kappa) \\ c(V)f(\sigma) \\ f(\sigma)g(\sigma\kappa) \end{bmatrix} = \begin{bmatrix} -\frac{V}{4\pi N_A}\left(\sigma^2\kappa^2 + 2\sigma\kappa + \frac{2}{3} - \frac{2}{3}(1+2\sigma\kappa)^{3/2}\right) \\ -\frac{V}{4\pi N_A}\frac{1}{\sigma^3} \\ \frac{1}{\sigma^3}\left(\sigma^2\kappa^2 + 2\sigma\kappa + \frac{2}{3} - \frac{2}{3}(1+2\sigma\kappa)^{3/2}\right) \end{bmatrix} \tag{4-53}$$

Note

$$\frac{df}{d\sigma} = -\frac{3}{\sigma^4} \quad \text{and} \quad \frac{dg}{d(\sigma\kappa)} = 2\sigma\kappa + 2 - 2(1+2\sigma\kappa)^{1/2} \tag{4-54}$$

and we have:

$$\left(\frac{\partial \boldsymbol{\eta}_{F_{sMSA}}}{\partial n_i}\right)_{T,V,\mathbf{n}/n_i} = \left(\frac{\partial}{\partial n_i}\begin{bmatrix} f(\sigma) \\ g(\sigma\kappa) \\ c(V) \end{bmatrix}\right)_{T,V,\mathbf{n}/n_i} = \begin{bmatrix} \left(\frac{\partial f(\sigma)}{\partial n_i}\right)_{T,V,\mathbf{n}/n_i} \\ \left(\frac{\partial g(\sigma\kappa)}{\partial n_i}\right)_{T,V,\mathbf{n}/n_i} \\ 0 \end{bmatrix} \tag{4-55}$$

$$\left(\frac{\partial \boldsymbol{\eta}_{F_{sMSA}}}{\partial n_i}\right)_{T,V,\mathbf{n}/n_i} = \begin{bmatrix} \frac{df}{d\sigma}\left(\frac{\partial \sigma}{\partial n_i}\right)_{T,V,\mathbf{n}/n_i} \\ \frac{dg}{d(\sigma\kappa)}\left(\kappa\left(\frac{\partial \sigma}{\partial n_i}\right)_{T,V,\mathbf{n}/n_i} + \sigma\left(\frac{\partial \kappa}{\partial n_i}\right)_{T,V,\mathbf{n}/n_i}\right) \\ 0 \end{bmatrix} \tag{4-56}$$

To calculate $\left(\frac{\partial \boldsymbol{\eta}_{F_{sMSA}}}{\partial n_i}\right)_{T,V,\mathbf{n}/n_i}$, we have to calculate $\left(\frac{\partial \sigma}{\partial n_i}\right)_{T,V,\mathbf{n}/n_i}$ and $\left(\frac{\partial \kappa}{\partial n_i}\right)_{T,V,\mathbf{n}/n_i}$:

$$\left(\frac{\partial \sigma}{\partial n_i}\right)_{T,V,\mathbf{n}/n_i} = \frac{\sigma_i - \sigma}{\sum_i n_i} = \frac{\sigma_i - \sum_i n_i\sigma_i \Big/ \sum_i n_i}{\sum_i n_i} \tag{4-57}$$

$$\kappa = \sqrt{\frac{e^2 N_A{}^2 \sum_i n_i z_i{}^2}{\varepsilon_0 \varepsilon RTV}} \Rightarrow \kappa^2 = \frac{e^2 N_A{}^2 \sum_i n_i z_i{}^2}{\varepsilon_0 \varepsilon RTV} \tag{4-58}$$

$$\varepsilon\kappa^2 = \frac{e^2 N_A{}^2}{\varepsilon_0 RTV}\sum_i n_i z_i{}^2 \triangleq k\sum_i n_i z_i{}^2 \tag{4-59}$$

Take mole number derivatives on both sides of (4-59), we have:

$$\kappa^2\left(\frac{\partial \varepsilon}{\partial n_i}\right)_{T,V,\mathbf{n}/n_i} + \varepsilon 2\kappa\left(\frac{\partial \kappa}{\partial n_i}\right)_{T,V,\mathbf{n}/n_i} = kz_i{}^2 \tag{4-60}$$

and we have $\left(\frac{\partial \kappa}{\partial n_i}\right)_{T,V,\mathbf{n}/n_i}$:

$$\boxed{\left(\frac{\partial \kappa}{\partial n_i}\right)_{T,V,\mathbf{n}/n_i} = \frac{kz_i^2 - \kappa^2\left(\frac{\partial \varepsilon}{\partial n_i}\right)_{T,V,\mathbf{n}/n_i}}{2\varepsilon\kappa},\quad k = \frac{e^2 N_A^2}{\varepsilon_0 RTV}} \tag{4-61}$$

$\left(\frac{\partial \varepsilon}{\partial n_i}\right)_{T,V,\mathbf{n}/n_i}$, $\left(\frac{\partial \varepsilon}{\partial V}\right)_{\mathbf{n},T}$ and $\left(\frac{\partial \varepsilon}{\partial T}\right)_{\mathbf{n},V}$ can be derived from the specific water relativity model, such as the Uematsu-Franck or the Pottel models.

From (4-53) and (4-56), it is easy to get the first order composition derivatives:

$$\boxed{\begin{aligned}&\left(\frac{\partial F_{sMSA}}{\partial n_i}\right)_{T,V,\mathbf{n}/n_i} = \left(\frac{\partial F_{sMSA}}{\partial \boldsymbol{\eta}_{F_{sMSA}}}\right)\left(\frac{\partial \boldsymbol{\eta}_{F_{sMSA}}}{\partial n_i}\right)_{T,V,\mathbf{n}/n_i}\\ &= c(V)\left(g(\sigma\kappa)\frac{df}{d\sigma}\left(\frac{\partial \sigma}{\partial n_i}\right)_{T,V,\mathbf{n}/n_i} + f(\sigma)\frac{dg}{d(\sigma\kappa)}\left(\kappa\left(\frac{\partial \sigma}{\partial n_i}\right)_{T,V,\mathbf{n}/n_i} + \sigma\left(\frac{\partial \kappa}{\partial n_i}\right)_{T,V,\mathbf{n}/n_i}\right)\right)\end{aligned}} \tag{4-62}$$

$$\begin{aligned}\left(\frac{\partial F_{sMSA}}{\partial n_i}\right)_{T,V,\mathbf{n}/n_i} &= -\frac{V}{4\pi N_A}\left(-\frac{3}{\sigma^4}\left(\sigma^2\kappa^2 + 2\sigma\kappa + \frac{2}{3} - \frac{2}{3}(1+2\sigma\kappa)^{3/2}\right)\left(\frac{\partial \sigma}{\partial n_i}\right)_{T,V,\mathbf{n}/n_i}\right.\\ &\left. + \frac{2}{\sigma^3}\left(\sigma\kappa + 1 - (1+2\sigma\kappa)^{1/2}\right)\left(\kappa\left(\frac{\partial \sigma}{\partial n_i}\right)_{T,V,\mathbf{n}/n_i} + \sigma\left(\frac{\partial \kappa}{\partial n_i}\right)_{T,V,\mathbf{n}/n_i}\right)\right)\end{aligned} \tag{4-63}$$

For volume derivatives, first we need to derive:

$$\left(\frac{\partial \boldsymbol{\eta}_{A_{Born}}}{\partial V}\right)_{\mathbf{n},T} = \left(\frac{\partial}{\partial V}\begin{bmatrix} f(\sigma) \\ g(\sigma\kappa) \\ c(V) \end{bmatrix}\right)_{\mathbf{n},T} = \begin{bmatrix} 0 \\ \frac{dg(\sigma\kappa)}{d(\sigma\kappa)}\sigma\left(\frac{\partial \kappa}{\partial V}\right)_{\mathbf{n},T} \\ \left(\frac{\partial c(V)}{\partial V}\right)_{\mathbf{n},T} \end{bmatrix} = \begin{bmatrix} 0 \\ \sigma\frac{dg(\sigma\kappa)}{d(\sigma\kappa)}\left(\frac{\partial \kappa}{\partial V}\right)_{\mathbf{n},T} \\ -\frac{1}{4\pi N_A} \end{bmatrix} \tag{4-64}$$

$$\kappa^2 = \frac{e^2 N_A^2 \sum_i n_i z_i^2}{\varepsilon_0 \varepsilon RTV} \Rightarrow V\varepsilon\kappa^2 = \frac{e^2 N_A^2}{\varepsilon_0 RT}\sum_i n_i z_i^2 \tag{4-65}$$

Take volume derivatives on both sides of (4-65):

$$\kappa^2 V\left(\frac{\partial \varepsilon}{\partial V}\right)_{\mathbf{n},T} + \varepsilon V 2\kappa\left(\frac{\partial \kappa}{\partial V}\right)_{\mathbf{n},T} + \kappa^2\varepsilon = 0 \tag{4-66}$$

Finally we have:

$$\boxed{\left(\frac{\partial \kappa}{\partial V}\right)_{\mathbf{n},T} = -\frac{\kappa}{2V} - \frac{\kappa}{2\varepsilon}\left(\frac{\partial \varepsilon}{\partial V}\right)_{\mathbf{n},T}} \tag{4-67}$$

Combine (4-53) and (4-56), and the volume derivative can be calculated:

$$\boxed{\begin{aligned}\left(\frac{\partial F_{sMSA}}{\partial V}\right)_{T,\mathbf{n}} &= \left(\frac{\partial F_{sMSA}}{\partial \boldsymbol{\eta}_{F_{sMSA}}}\right)^{T}\cdot\left(\frac{\partial \boldsymbol{\eta}_{F_{sMSA}}}{\partial V}\right)_{T,\mathbf{n}} \\ &= -\frac{V}{4\pi N_A} f(\sigma)\sigma\frac{dg(\sigma\kappa)}{d(\sigma\kappa)}\left(\frac{\partial \kappa}{\partial V}\right)_{\mathbf{n},T} - \frac{1}{4\pi N_A} f(\sigma)g(\sigma\kappa)\end{aligned}} \tag{4-68}$$

For temperature derivatives:

$$\left(\frac{\partial \boldsymbol{\eta}_{A_{Born}}}{\partial T}\right)_{\mathbf{n},V} = \left(\frac{\partial}{\partial T}\begin{bmatrix} f(\sigma) \\ g(\sigma\kappa) \\ c(V)\end{bmatrix}\right)_{\mathbf{n},V} = \begin{bmatrix} \dfrac{df}{d\sigma}\left(\dfrac{\partial \sigma}{\partial T}\right)_{\mathbf{n},V} \\ \dfrac{dg}{d(\sigma\kappa)}\left(\kappa\left(\dfrac{\partial \sigma}{\partial T}\right)_{\mathbf{n},V} + \sigma\left(\dfrac{\partial \kappa}{\partial T}\right)_{\mathbf{n},V}\right) \\ 0\end{bmatrix} \tag{4-69}$$

Note that

$$\left(\frac{\partial(\sigma\kappa)}{\partial T}\right)_{\mathbf{n},V} = \kappa\left(\frac{\partial \sigma}{\partial T}\right)_{\mathbf{n},V} + \sigma\left(\frac{\partial \kappa}{\partial T}\right)_{\mathbf{n},V} \tag{4-70}$$

$$\left(\frac{\partial \sigma}{\partial T}\right)_{V,\mathbf{n}} = \frac{\sum_i n_i\left(\dfrac{\partial \sigma_i}{\partial T}\right)_{V,\mathbf{n}}}{\sum_i n_i} \tag{4-71}$$

$$\kappa^2 = \frac{e^2 {N_A}^2 \sum_i n_i z_i^2}{\varepsilon_0 \varepsilon RTV} \Rightarrow T\varepsilon\kappa^2 = \frac{e^2 {N_A}^2}{\varepsilon_0 RV}\sum_i n_i z_i^2 \tag{4-72}$$

Take volume derivatives on both sides of (4-65):

$$\kappa^2 T\left(\frac{\partial \varepsilon}{\partial T}\right)_{V,\mathbf{n}} + 2\varepsilon T\kappa\left(\frac{\partial \kappa}{\partial T}\right)_{V,\mathbf{n}} + \kappa^2\varepsilon = 0 \tag{4-73}$$

Finally we have:

$$\boxed{\left(\frac{\partial \kappa}{\partial T}\right)_{V,\mathbf{n}} = -\frac{\kappa}{2T} - \frac{\kappa}{2\varepsilon}\left(\frac{\partial \varepsilon}{\partial T}\right)_{V,\mathbf{n}}} \tag{4-74}$$

The first order temperature derivative is

$$\begin{aligned}\left(\frac{\partial F_{sMSA}}{\partial T}\right)_{V,\mathbf{n}} &= \left(\frac{\partial F_{sMSA}}{\partial \boldsymbol{\eta}_{F_{sMSA}}}\right)^{T}\cdot\left(\frac{\partial \boldsymbol{\eta}_{F_{sMSA}}}{\partial T}\right)_{V,\mathbf{n}} \\ &= -\frac{V}{4\pi N_A}\left(g(\sigma\kappa)\frac{df}{d\sigma}\left(\frac{\partial \sigma}{\partial T}\right)_{\mathbf{n},V} + f(\sigma)\frac{dg}{d(\sigma\kappa)}\left(\kappa\left(\frac{\partial \sigma}{\partial T}\right)_{\mathbf{n},V} + \sigma\left(\frac{\partial \kappa}{\partial T}\right)_{\mathbf{n},V}\right)\right) \\ &= -\frac{V}{4\pi N_A}\left(-\frac{3g(\sigma\kappa)}{\sigma^4}\frac{\sum_i n_i\left(\dfrac{\partial \sigma_i}{\partial T}\right)_{V,\mathbf{n}}}{\sum_i n_i} + \frac{1}{\sigma^3}\frac{dg}{d(\sigma\kappa)}\left(\frac{\kappa\sum_i n_i\left(\dfrac{\partial \sigma_i}{\partial T}\right)_{V,\mathbf{n}}}{\sum_i n_i} + \sigma\left(-\frac{\kappa}{2T} - \frac{\kappa}{2\varepsilon}\left(\frac{\partial \varepsilon}{\partial T}\right)_{V,\mathbf{n}}\right)\right)\right)\end{aligned} \tag{4-75}$$

1.2.2 Second order partial derivatives

Denote

$$\mathbf{F_{sMSA}}''(\boldsymbol{\eta}_{F_{sMSA}})=\begin{bmatrix}\frac{\partial^2 F_{sMSA}}{\partial f^2} & \frac{\partial^2 F_{sMSA}}{\partial f\partial g} & \frac{\partial^2 F_{sMSA}}{\partial f\partial c}\\ \frac{\partial^2 F_{sMSA}}{\partial g\partial f} & \frac{\partial^2 F_{sMSA}}{\partial g^2} & \frac{\partial^2 F_{sMSA}}{\partial g\partial c}\\ \frac{\partial^2 F_{sMSA}}{\partial c\partial f} & \frac{\partial^2 F_{sMSA}}{\partial c\partial g} & \frac{\partial^2 F_{sMSA}}{\partial c^2}\end{bmatrix}=\begin{bmatrix}0 & c(V) & g(\sigma\kappa)\\ c(V) & 0 & f(\sigma)\\ g(\sigma\kappa) & f(\sigma) & 0\end{bmatrix} \quad (4\text{-}76)$$

We have

$$\mathbf{F_{sMSA}}''(\boldsymbol{\eta}_{F_{sMSA}})==\begin{bmatrix}0 & -\frac{V}{4\pi N_A} & \sigma^2\kappa^2+2\sigma\kappa+\frac{2}{3}-\frac{2}{3}(1+2\sigma\kappa)^{3/2}\\ -\frac{V}{4\pi N_A} & 0 & \frac{1}{\sigma^3}\\ \sigma^2\kappa^2+2\sigma\kappa+\frac{2}{3}-\frac{2}{3}(1+2\sigma\kappa)^{3/2} & \frac{1}{\sigma^3} & 0\end{bmatrix} \quad (4\text{-}77)$$

1. $\left(\frac{\partial^2 F_{sMSA}(\boldsymbol{\eta}_{F_{sMSA}})}{\partial n_i\partial n_j}\right)_{T,V,\mathbf{n}/n_i}$

$$\left(\frac{\partial^2\boldsymbol{\eta}_{F_{sMSA}}}{\partial n_i\partial n_j}\right)_{T,V,\mathbf{n}/n_i}=\left(\frac{\partial^2}{\partial n_i\partial n_j}\begin{bmatrix}f(\sigma)\\ g(\sigma\kappa)\\ c(V)\end{bmatrix}\right)_{T,V,\mathbf{n}/n_i}=\begin{bmatrix}\left(\frac{\partial^2 f(\sigma)}{\partial n_i\partial n_j}\right)_{T,V,\mathbf{n}/n_i} & \left(\frac{\partial^2 g(\sigma\kappa)}{\partial n_i\partial n_j}\right)_{T,V,\mathbf{n}/n_i} & 0\end{bmatrix}^T \quad (4\text{-}78)$$

$$\frac{d^2 f}{d\sigma^2}=\frac{12}{\sigma^5},\quad \frac{d^2 g}{d(\sigma\kappa)^2}=2-2(1+2\sigma\kappa)^{-1/2} \quad (4\text{-}79)$$

From equation (4-57), we have:

$$\left(\frac{\partial\sigma}{\partial n_i}\right)_{T,V,\mathbf{n}/n_i}\sum_i n_i=\sigma_i-\sigma\Rightarrow\left(\frac{\partial^2\sigma}{\partial n_i\partial n_j}\right)_{T,V,\mathbf{n}/n_i}\sum_i n_i+\left(\frac{\partial\sigma}{\partial n_i}\right)_{T,V,\mathbf{n}/n_i}=0-\left(\frac{\partial\sigma}{\partial n_j}\right)_{T,V,\mathbf{n}/n_j} \quad (4\text{-}80)$$

Thus:

$$\left(\frac{\partial^2\sigma}{\partial n_i\partial n_j}\right)_{T,V,\mathbf{n}/n_i}=-\frac{\left(\frac{\partial\sigma}{\partial n_i}\right)_{T,V,\mathbf{n}/n_i}+\left(\frac{\partial\sigma}{\partial n_j}\right)_{T,V,\mathbf{n}/n_j}}{\sum_i n_i}=-\frac{1}{\sum_i n_i}\left(\frac{\sigma_i-\sigma}{\sum_i n_i}+\frac{\sigma_j-\sigma}{\sum_j n_j}\right)=-\frac{\sigma_i+\sigma_j-2\sigma}{\left(\sum_i n_i\right)^2} \quad (4\text{-}81)$$

Take mole number derivatives on both sides of equation (4-60), we have:

$$\kappa^2\left(\frac{\partial^2\varepsilon}{\partial n_i\partial n_j}\right)_{T,V,\mathbf{n}/n_i}+2\kappa\left(\frac{\partial\varepsilon}{\partial n_i}\right)_{T,V,\mathbf{n}/n_i}\left(\frac{\partial\kappa}{\partial n_j}\right)_{T,V,\mathbf{n}/n_j}$$
$$+2\left(\frac{\partial\kappa}{\partial n_i}\right)_{T,V,\mathbf{n}/n_i}\left(\kappa\left(\frac{\partial\varepsilon}{\partial n_j}\right)_{T,V,\mathbf{n}/n_j}+\varepsilon\left(\frac{\partial\kappa}{\partial n_j}\right)_{T,V,\mathbf{n}/n_j}\right)+2\varepsilon\kappa\left(\frac{\partial^2\kappa}{\partial n_i\partial n_j}\right)_{T,V,\mathbf{n}/n_i}=0 \tag{4-82}$$

and $\left(\frac{\partial^2\kappa}{\partial n_i\partial n_j}\right)_{T,V,\mathbf{n}/n_i}$ is:

$$\left(\frac{\partial^2\kappa}{\partial n_i\partial n_j}\right)_{T,V,\mathbf{n}/n_i}=-\frac{\kappa}{2\varepsilon}\left(\frac{\partial^2\varepsilon}{\partial n_i\partial n_j}\right)_{T,V,\mathbf{n}/n_i}-\frac{1}{\varepsilon}\left(\frac{\partial\varepsilon}{\partial n_i}\right)_{T,V,\mathbf{n}/n_i}\left(\frac{\partial\kappa}{\partial n_j}\right)_{T,V,\mathbf{n}/n_j}$$
$$-\left(\frac{\partial\kappa}{\partial n_i}\right)_{T,V,\mathbf{n}/n_i}\left(\frac{1}{\varepsilon}\left(\frac{\partial\varepsilon}{\partial n_j}\right)_{T,V,\mathbf{n}/n_j}+\frac{1}{\kappa}\left(\frac{\partial\kappa}{\partial n_j}\right)_{T,V,\mathbf{n}/n_j}\right) \tag{4-83}$$

Substitute $\left(\frac{\partial\kappa}{\partial n_i}\right)_{T,V,\mathbf{n}/n_i}$ from (4-60) into (4-83)and we expand the expression:

$$\left(\frac{\partial^2\kappa}{\partial n_i\partial n_j}\right)_{T,V,\mathbf{n}/n_i}=\frac{\kappa}{2\varepsilon}\left[-\frac{z_i^2}{\varepsilon^2}\left(\frac{\partial\varepsilon}{\partial n_j}\right)_{T,V,\mathbf{n}/n_j}-\frac{z_j^2}{\varepsilon^2}\left(\frac{\partial\varepsilon}{\partial n_i}\right)_{T,V,\mathbf{n}/n_i}-\frac{\sum_i n_i z_i^2}{\varepsilon^2}\left(\frac{\partial^2\varepsilon}{\partial n_i\partial n_j}\right)_{T,V,\mathbf{n}/n_i}\right.$$
$$\left.+\frac{2\sum_i n_i z_i^2}{\varepsilon^3}\left(\frac{\partial\varepsilon}{\partial n_j}\right)_{T,V,\mathbf{n}/n_j}\left(\frac{\partial\varepsilon}{\partial n_i}\right)_{T,V,\mathbf{n}/n_i}\right]-\frac{1}{\kappa}\left(\frac{\partial\kappa}{\partial n_j}\right)_{T,V,\mathbf{n}/n_j}\left(\frac{\partial\kappa}{\partial n_i}\right)_{T,V,\mathbf{n}/n_i} \tag{4-84}$$

To calculate (4-78), we need:

$$\left(\frac{\partial^2 f}{\partial n_i\partial n_j}\right)_{T,V,\mathbf{n}/n_i}=\frac{d^2 f}{d\sigma^2}\left(\frac{\partial\sigma}{\partial n_i}\right)_{T,V,\mathbf{n}/n_i}\left(\frac{\partial\sigma}{\partial n_j}\right)_{T,V,\mathbf{n}/n_j}+\frac{df}{d\sigma}\left(\frac{\partial^2\sigma}{\partial n_i\partial n_j}\right)_{T,V,\mathbf{n}/n_i}$$
$$=\frac{12}{\sigma^5}\left(\frac{\partial\sigma}{\partial n_i}\right)_{T,V,\mathbf{n}/n_i}\left(\frac{\partial\sigma}{\partial n_j}\right)_{T,V,\mathbf{n}/n_j}-\frac{3}{\sigma^4}\left(\frac{\partial^2\sigma}{\partial n_i\partial n_j}\right)_{T,V,\mathbf{n}/n_i} \tag{4-85}$$

$$\left(\frac{\partial^2 g(\sigma\kappa)}{\partial n_i\partial n_j}\right)_{T,V,\mathbf{n}/n_i}=\frac{d^2 g(\sigma\kappa)}{d(\sigma\kappa)^2}\left(\frac{\partial(\sigma\kappa)}{\partial n_i}\right)_{T,V,\mathbf{n}/n_i}\left(\frac{\partial(\sigma\kappa)}{\partial n_j}\right)_{T,V,\mathbf{n}/n_j}+\frac{dg(\sigma\kappa)}{d(\sigma\kappa)}\left(\frac{\partial^2(\sigma\kappa)}{\partial n_i\partial n_j}\right)_{T,V,\mathbf{n}/n_i}$$
$$=2\left(1-\left(1+2\sigma\kappa\right)^{-½}\right)\left(\frac{\partial(\sigma\kappa)}{\partial n_i}\right)_{T,V,\mathbf{n}/n_i}\left(\frac{\partial(\sigma\kappa)}{\partial n_j}\right)_{T,V,\mathbf{n}/n_j}-2\left(\sigma\kappa+1-(1+2\sigma\kappa)^{½}\right)\left(\frac{\partial^2(\sigma\kappa)}{\partial n_i\partial n_j}\right)_{T,V,\mathbf{n}/n_i} \tag{4-86}$$

$$\left(\frac{\partial(\sigma\kappa)}{\partial n_i}\right)_{T,V,\mathbf{n}/n_i}=\kappa\left(\frac{\partial\sigma}{\partial n_i}\right)_{T,V,\mathbf{n}/n_i}+\sigma\left(\frac{\partial\kappa}{\partial n_i}\right)_{T,V,\mathbf{n}/n_i} \tag{4-87}$$

$$\left(\frac{\partial^2(\sigma\kappa)}{\partial n_i\partial n_j}\right)_{T,V,\mathbf{n}/n_i} = \left(\frac{\partial\sigma}{\partial n_i}\right)_{T,V,\mathbf{n}/n_i}\left(\frac{\partial\kappa}{\partial n_j}\right)_{T,V,\mathbf{n}/n_j} + \left(\frac{\partial\sigma}{\partial n_j}\right)_{T,V,\mathbf{n}/n_j}\left(\frac{\partial\kappa}{\partial n_i}\right)_{T,V,\mathbf{n}/n_i} + \kappa\left(\frac{\partial^2(\sigma)}{\partial n_i\partial n_j}\right)_{T,V,\mathbf{n}/n_i} + \sigma\left(\frac{\partial^2(\kappa)}{\partial n_i\partial n_j}\right)_{T,V,\mathbf{n}/n_i} \tag{4-88}$$

Finally:

$$\begin{aligned}&\left(\frac{\partial^2 F_{sMSA}(\boldsymbol{\eta}_{F_{sMSA}})}{\partial n_i\partial n_j}\right)_{T,V,\mathbf{n}/n_i}\\ &= \left(\left(\frac{\partial\boldsymbol{\eta}_{F_{sMSA}}}{\partial n_i}\right)_{T,V,\mathbf{n}/n_i}\right)^T \mathbf{F}''_{sMSA}(\boldsymbol{\eta}_{F_{sMSA}})\left(\frac{\partial\boldsymbol{\eta}_{F_{sMSA}}}{\partial n_j}\right)_{T,V,\mathbf{n}/n_j} + \left(\frac{\partial F_{sMSA}}{\partial\boldsymbol{\eta}_{F_{sMSA}}}\right)^T\cdot\left(\frac{\partial^2\boldsymbol{\eta}_{F_{sMSA}}}{\partial n_i\partial n_j}\right)_{T,V,\mathbf{n}/n_i}\\ &= c(V)\left[\left(\frac{\partial f(\sigma)}{\partial n_i}\right)_{T,V,\mathbf{n}/n_i}\left(\frac{\partial g(\sigma\kappa)}{\partial n_j}\right)_{T,V,\mathbf{n}/n_j} + \left(\frac{\partial g(\sigma\kappa)}{\partial n_i}\right)_{T,V,\mathbf{n}/n_i}\left(\frac{\partial f(\sigma)}{\partial n_j}\right)_{T,V,\mathbf{n}/n_j}\right.\\ &\left. + g(\sigma\kappa)\left(\frac{\partial^2 f(\sigma)}{\partial n_i\partial n_j}\right)_{T,V,\mathbf{n}/n_i} + f(\sigma)\left(\frac{\partial^2 g(\sigma\kappa)}{\partial n_i\partial n_j}\right)_{T,V,\mathbf{n}/n_i}\right]\end{aligned} \tag{4-89}$$

$$\begin{aligned}\left(\frac{\partial^2 F_{sMSA}(\boldsymbol{\eta}_{F_{sMSA}})}{\partial n_i\partial n_j}\right)_{T,V,\mathbf{n}/n_i} &= -\frac{V}{4\pi N_A}\left[\left(\frac{\partial f(\sigma)}{\partial n_i}\right)_{T,V,\mathbf{n}/n_i}\left(\frac{\partial g(\sigma\kappa)}{\partial n_j}\right)_{T,V,\mathbf{n}/n_j}\right.\\ &\left. + \left(\frac{\partial g(\sigma\kappa)}{\partial n_i}\right)_{T,V,\mathbf{n}/n_i}\left(\frac{\partial f(\sigma)}{\partial n_j}\right)_{T,V,\mathbf{n}/n_j} + g(\sigma\kappa)\left(\frac{\partial^2 f(\sigma)}{\partial n_i\partial n_j}\right)_{T,V,\mathbf{n}/n_i} + f(\sigma)\left(\frac{\partial^2 g(\sigma\kappa)}{\partial n_i\partial n_j}\right)_{T,V,\mathbf{n}/n_i}\right]\end{aligned} \tag{4-90}$$

2. $\left(\frac{\partial^2 F_{sMSA}}{\partial V^2}\right)_{T,\mathbf{n}}$

$$\left(\frac{\partial^2\boldsymbol{\eta}_{A_{Born}}}{\partial V^2}\right)_{T,\mathbf{n}} = \left(\frac{\partial^2}{\partial V^2}\begin{bmatrix} f(\sigma)\\ g(\sigma\kappa)\\ c(V)\end{bmatrix}\right)_{T,\mathbf{n}} = \begin{bmatrix} 0\\ \left(\frac{\partial^2 g(\sigma\kappa)}{\partial V^2}\right)_{T,\mathbf{n}}\\ 0\end{bmatrix} \tag{4-91}$$

$$\begin{aligned}\left(\frac{\partial^2 g(\sigma\kappa)}{\partial V^2}\right)_{T,\mathbf{n}} &= \frac{d^2 g(\sigma\kappa)}{d(\sigma\kappa)^2}\left(\frac{\partial(\sigma\kappa)}{\partial V}\right)_{T,\mathbf{n}}^2 + \frac{dg(\sigma\kappa)}{d(\sigma\kappa)}\left(\frac{\partial^2(\sigma\kappa)}{\partial V^2}\right)_{T,\mathbf{n}}\\ &= \frac{d^2 g(\sigma\kappa)}{d(\sigma\kappa)^2}\sigma^2\left(\frac{\partial\kappa}{\partial V}\right)_{T,\mathbf{n}}^2 + \frac{dg(\sigma\kappa)}{d(\sigma\kappa)}\sigma\left(\frac{\partial^2\kappa}{\partial V^2}\right)_{T,\mathbf{n}}\end{aligned} \tag{4-92}$$

To calculate $\left(\frac{\partial^2\kappa}{\partial V^2}\right)_{T,\mathbf{n}}$, we take volume derivatives on both sides of (4-66)

$$2\varepsilon\left(\frac{\partial\kappa}{\partial V}\right)_{\mathbf{n},T}+2V\left(\frac{\partial\varepsilon}{\partial V}\right)_{\mathbf{n},T}\left(\frac{\partial\kappa}{\partial V}\right)_{\mathbf{n},T}+2V\varepsilon\left(\frac{\partial^2\kappa}{\partial V^2}\right)_{\mathbf{n},T}=-\varepsilon\left(\frac{\partial\kappa}{\partial V}\right)_{\mathbf{n},T}$$
$$-2\kappa\left(\frac{\partial\varepsilon}{\partial V}\right)_{\mathbf{n},T}-V\left(\frac{\partial\kappa}{\partial V}\right)_{\mathbf{n},T}\left(\frac{\partial\varepsilon}{\partial V}\right)_{\mathbf{n},T}-\kappa V\left(\frac{\partial^2\varepsilon}{\partial V^2}\right)_{\mathbf{n},T}\Rightarrow \tag{4-93}$$
$$2V\varepsilon\left(\frac{\partial^2\kappa}{\partial V^2}\right)_{\mathbf{n},T}=-3\left(\frac{\partial\kappa}{\partial V}\right)_{\mathbf{n},T}\left(\varepsilon+V\left(\frac{\partial\varepsilon}{\partial V}\right)_{\mathbf{n},T}\right)-2\kappa\left(\frac{\partial\varepsilon}{\partial V}\right)_{\mathbf{n},T}-\kappa V\left(\frac{\partial^2\varepsilon}{\partial V^2}\right)_{\mathbf{n},T}$$

Combined the common terms, we get:

$$\boxed{\left(\frac{\partial^2\kappa}{\partial V^2}\right)_{T,\mathbf{n}}=-\frac{3}{2}\left(\frac{\partial\kappa}{\partial V}\right)_{\mathbf{n},T}\left(\frac{1}{V}+\frac{1}{\varepsilon}\left(\frac{\partial\varepsilon}{\partial V}\right)_{\mathbf{n},T}\right)-\frac{\kappa}{V\varepsilon}\left(\frac{\partial\varepsilon}{\partial V}\right)_{\mathbf{n},T}-\frac{\kappa}{2\varepsilon}\left(\frac{\partial^2\varepsilon}{\partial V^2}\right)_{\mathbf{n},T}} \tag{4-94}$$

And finally we have:

$$\left(\frac{\partial^2F_{sMSA}}{\partial V^2}\right)_{T,\mathbf{n}}=\left(\left(\frac{\partial\boldsymbol{\eta}_{F_{sMSA}}}{\partial V}\right)_{T,\mathbf{n}}\right)^T\mathbf{F}_{sMSA}{}''(\boldsymbol{\eta}_{F_{sMSA}})\left(\frac{\partial\boldsymbol{\eta}_{F_{sMSA}}}{\partial V}\right)_{T,\mathbf{n}}+\left(\frac{\partial F_{sMSA}}{\partial\boldsymbol{\eta}_{F_{sMSA}}}\right)^T\cdot\left(\frac{\partial^2\boldsymbol{\eta}_{F_{sMSA}}}{\partial V^2}\right)_{T,\mathbf{n}}$$
$$=2f(\sigma)\left(\frac{\partial g(\sigma\kappa)}{\partial V}\right)_{\mathbf{n},T}\left(\frac{\partial c(V)}{\partial V}\right)_{\mathbf{n},T}+c(V)f(\sigma)\left(\frac{\partial^2g(\sigma\kappa)}{\partial V^2}\right)_{T,\mathbf{n}} \tag{4-95}$$
$$=-\frac{1}{4\pi N_A}\frac{1}{\sigma^3}\left(2\left(\frac{\partial g(\sigma\kappa)}{\partial V}\right)_{T,\mathbf{n}}{}^2+V\left(\frac{\partial^2g(\sigma\kappa)}{\partial V^2}\right)_{T,\mathbf{n}}\right)$$

3. $\left(\frac{\partial^2F_{sMSA}}{\partial V\partial n_i}\right)_{T,\mathbf{n}}$

$$\left(\frac{\partial^2\boldsymbol{\eta}_{A_{Born}}}{\partial V\partial n_i}\right)_{T,\mathbf{n}}=\left(\frac{\partial^2}{\partial V\partial n_i}\begin{bmatrix}f(\sigma)\\g(\sigma\kappa)\\c(V)\end{bmatrix}\right)_{T,\mathbf{n}}=\begin{bmatrix}0\\\left(\frac{\partial^2g(\sigma\kappa)}{\partial V\partial n_i}\right)_{T,\mathbf{n}}\\0\end{bmatrix} \tag{4-96}$$

$$\left(\frac{\partial^2g(\sigma\kappa)}{\partial V\partial n_i}\right)_{T,\mathbf{n}}=\frac{d^2g(\sigma\kappa)}{d(\sigma\kappa)^2}\left(\frac{\partial(\sigma\kappa)}{\partial V}\right)_{T,\mathbf{n}}\left(\frac{\partial(\sigma\kappa)}{\partial n_i}\right)_{T,V,\mathbf{n}/n_i}+\frac{dg(\sigma\kappa)}{d(\sigma\kappa)}\left(\frac{\partial^2(\sigma\kappa)}{\partial V\partial n_i}\right)_{T,\mathbf{n}} \tag{4-97}$$

$$\left(\frac{\partial^2\sigma\kappa}{\partial V\partial n_i}\right)_{T,\mathbf{n}}=\left(\frac{\partial\sigma}{\partial V}\right)_{T,\mathbf{n}}\left(\frac{\partial\kappa}{\partial n_i}\right)_{T,V,\mathbf{n}/n_i}+\left(\frac{\partial\kappa}{\partial V}\right)_{T,\mathbf{n}}\left(\frac{\partial\sigma}{\partial n_i}\right)_{T,V,\mathbf{n}/n_i}+\sigma\left(\frac{\partial^2\kappa}{\partial V\partial n_i}\right)_{T,\mathbf{n}}+\kappa\left(\frac{\partial^2\sigma}{\partial V\partial n_i}\right)_{T,\mathbf{n}}$$

(4-98)

$$\left(\frac{\partial^2(\sigma\kappa)}{\partial V\partial n_i}\right)_{T,\mathbf{n}}==\left(\frac{\partial\kappa}{\partial V}\right)_{T,\mathbf{n}}\left(\frac{\partial\sigma}{\partial n_i}\right)_{T,V,\mathbf{n}/n_i}+\sigma\left(\frac{\partial^2\kappa}{\partial V\partial n_i}\right)_{T,\mathbf{n}} \tag{4-99}$$

To calculate $\left(\frac{\partial^2\kappa}{\partial V\partial n_i}\right)_{T,\mathbf{n}}$, we take volume derivatives on both sides of (4-67)

$$\left(\frac{\partial^2\kappa}{\partial V\partial n_i}\right)_{\mathbf{n},T}=\left(\frac{\partial}{\partial n_i}\left(\frac{\partial\kappa}{\partial V}\right)_{\mathbf{n},T}\right)_{T,V,\mathbf{n}/n_i}=-\left(\frac{\partial}{\partial n_i}\left(\frac{\kappa}{2V}+\frac{\kappa}{2\varepsilon}\left(\frac{\partial\varepsilon}{\partial V}\right)_{\mathbf{n},T}\right)\right)_{T,V,\mathbf{n}/n_i}$$
$$=-\left(\frac{\partial\kappa}{\partial n_i}\right)_{T,V,\mathbf{n}/n_i}\left(\frac{1}{2V}+\frac{1}{2\varepsilon}\left(\frac{\partial\varepsilon}{\partial V}\right)_{\mathbf{n},T}\right)-\kappa\left(\frac{\partial}{\partial n_i}\left(\frac{1}{2\varepsilon}\left(\frac{\partial\varepsilon}{\partial V}\right)_{\mathbf{n},T}\right)\right)_{T,V,\mathbf{n}/n_i} \quad (4\text{-}100)$$

Finally we reach:

$$\boxed{\left(\frac{\partial^2\kappa}{\partial V\partial n_i}\right)_{\mathbf{n},T}=-\frac{1}{\kappa}\left(\frac{\partial\kappa}{\partial V}\right)_{\mathbf{n},T}\left(\frac{\partial\kappa}{\partial n_i}\right)_{T,V,\mathbf{n}/n_i}+\frac{\kappa}{2\varepsilon}\left(\frac{1}{\varepsilon}\left(\frac{\partial\varepsilon}{\partial n_i}\right)_{T,V,\mathbf{n}/n_i}\left(\frac{\partial\varepsilon}{\partial V}\right)_{\mathbf{n},T}-\left(\frac{\partial^2\varepsilon}{\partial V\partial n_i}\right)_{\mathbf{n},T}\right)} \quad (4\text{-}101)$$

And

$$\left(\frac{\partial^2 F_{sMSA}}{\partial V\partial n_i}\right)_{T,\mathbf{n}}=\left(\left(\frac{\partial\boldsymbol{\eta}_{F_{sMSA}}}{\partial V}\right)_{T,\mathbf{n}}\right)^T\mathbf{F}_{sMSA}''(\boldsymbol{\eta}_{F_{sMSA}})\left(\frac{\partial\boldsymbol{\eta}_{F_{sMSA}}}{\partial n_i}\right)_{T,V,\mathbf{n}/n_i}+\left(\frac{\partial F_{sMSA}}{\partial\boldsymbol{\eta}_{F_{sMSA}}}\right)^T\cdot\left(\frac{\partial^2\boldsymbol{\eta}_{F_{sMSA}}}{\partial V\partial n_i}\right)_{T,\mathbf{n}}$$
$$=2f(\sigma)\left(\frac{\partial g(\sigma\kappa)}{\partial V}\right)_{\mathbf{n},T}\left(\frac{\partial c(V)}{\partial V}\right)_{\mathbf{n},T}+c(V)f(\sigma)\left(\frac{\partial^2 g(\sigma\kappa)}{\partial V\partial n_i}\right)_{T,\mathbf{n}}$$
$$=-\frac{1}{4\pi N_A}\frac{1}{\sigma^3}\left(2\left(\frac{\partial g(\sigma\kappa)}{\partial V}\right)_{T,\mathbf{n}}^2+V\left(\frac{\partial^2 g(\sigma\kappa)}{\partial V\partial n_i}\right)_{T,\mathbf{n}}\right)$$

(4-102)

4. $\left(\frac{\partial^2 F_{sMSA}}{\partial T^2}\right)_{V,\mathbf{n}}$

$$\left(\frac{\partial^2\boldsymbol{\eta}_{A_{Born}}}{\partial T^2}\right)_{V,\mathbf{n}}=\left(\frac{\partial^2}{\partial T^2}\begin{bmatrix}f(\sigma)\\g(\sigma\kappa)\\c(V)\end{bmatrix}\right)_{V,\mathbf{n}}=\begin{bmatrix}\left(\frac{\partial^2 f(\sigma)}{\partial T^2}\right)_{V,\mathbf{n}}\\\left(\frac{\partial^2 g(\sigma\kappa)}{\partial T^2}\right)_{V,\mathbf{n}}\\0\end{bmatrix} \quad (4\text{-}103)$$

$$\left(\frac{\partial^2 f(\sigma)}{\partial T^2}\right)_{V,\mathbf{n}}=\frac{d^2 f(\sigma)}{d\sigma^2}\left(\frac{\partial\sigma}{\partial T}\right)_{V,\mathbf{n}}^2+\frac{df(\sigma)}{d\sigma}\left(\frac{\partial^2\sigma}{\partial T^2}\right)_{V,\mathbf{n}} \quad (4\text{-}104)$$

$$\left(\frac{\partial^2 g(\sigma\kappa)}{\partial T^2}\right)_{V,\mathbf{n}}=\frac{d^2 g(\sigma\kappa)}{d(\sigma\kappa)^2}\left(\frac{\partial(\sigma\kappa)}{\partial T}\right)_{V,\mathbf{n}}^2+\frac{dg(\sigma\kappa)}{d(\sigma\kappa)}\left(\frac{\partial^2(\sigma\kappa)}{\partial T^2}\right)_{V,\mathbf{n}}$$

(4-105)

Note that

$$\left(\frac{\partial^2(\sigma\kappa)}{\partial T^2}\right)_{V,\mathbf{n}}=\left(\frac{\partial}{\partial T}\left(\frac{\partial(\sigma\kappa)}{\partial T}\right)_{\mathbf{n},V}\right)_{\mathbf{n},V}=\left(\frac{\partial}{\partial T}\left(\kappa\left(\frac{\partial\sigma}{\partial T}\right)_{\mathbf{n},V}+\sigma\left(\frac{\partial\kappa}{\partial T}\right)_{\mathbf{n},V}\right)\right)_{\mathbf{n},V}$$
$$=2\left(\frac{\partial\sigma}{\partial T}\right)_{V,\mathbf{n}}\left(\frac{\partial\kappa}{\partial T}\right)_{V,\mathbf{n}}+\kappa\left(\frac{\partial^2\sigma}{\partial T^2}\right)_{\mathbf{n},V}+\sigma\left(\frac{\partial^2\kappa}{\partial T^2}\right)_{\mathbf{n},V} \quad (4\text{-}106)$$

To calculate $\left(\frac{\partial^2 \kappa}{\partial T^2}\right)_{\mathbf{n},V}$, we take temperature derivatives on both sides of (4-74):

$$\left(\frac{\partial^2 \kappa}{\partial T^2}\right)_{\mathbf{n},V} = \left(\frac{\partial}{\partial T}\left(\frac{\partial \kappa}{\partial T}\right)_{V,\mathbf{n}}\right)_{V,\mathbf{n}} = -\left(\frac{\partial}{\partial T}\left(\frac{\kappa}{2T} + \frac{\kappa}{2\varepsilon}\left(\frac{\partial \varepsilon}{\partial T}\right)_{V,\mathbf{n}}\right)\right)_{V,\mathbf{n}} \tag{4-107}$$

Combined the common terms, we get:

$$\boxed{\left(\frac{\partial^2 \kappa}{\partial T^2}\right)_{\mathbf{n},V} = -\left(\frac{\partial \kappa}{\partial T}\right)_{V,\mathbf{n}}\left(\frac{1}{2T} + \frac{1}{2\varepsilon}\left(\frac{\partial \varepsilon}{\partial T}\right)_{V,\mathbf{n}}\right) + \kappa\left(\frac{1}{2T^2} + \frac{1}{2\varepsilon^2}\left(\frac{\partial \varepsilon}{\partial T}\right)_{V,\mathbf{n}}^{\ 2} + \frac{1}{2\varepsilon}\left(\frac{\partial^2 \varepsilon}{\partial T^2}\right)_{\mathbf{n},V}\right)} \tag{4-108}$$

And we have

$$\begin{aligned}\left(\frac{\partial^2 F_{sMSA}}{\partial T^2}\right)_{V,\mathbf{n}} &= \left(\left(\frac{\partial \boldsymbol{\eta}_{F_{sMSA}}}{\partial T}\right)_{V,\mathbf{n}}\right)^T \mathbf{F}_{sMSA}''(\boldsymbol{\eta}_{F_{sMSA}})\left(\frac{\partial \boldsymbol{\eta}_{F_{sMSA}}}{\partial T}\right)_{V,\mathbf{n}} + \left(\frac{\partial F_{sMSA}}{\partial \boldsymbol{\eta}_{F_{sMSA}}}\right)^T \cdot \left(\frac{\partial^2 \boldsymbol{\eta}_{F_{sMSA}}}{\partial T^2}\right)_{V,\mathbf{n}} \\ &= c(V)\left(2\left(\frac{\partial g(\sigma\kappa)}{\partial T}\right)_{V,\mathbf{n}}\left(\frac{\partial f(\sigma)}{\partial T}\right)_{V,\mathbf{n}} + f(\sigma)\left(\frac{\partial^2 g(\sigma\kappa)}{\partial T^2}\right)_{V,\mathbf{n}} + g(\sigma\kappa)\left(\frac{\partial^2 f(\sigma)}{\partial T^2}\right)_{V,\mathbf{n}}\right) \\ &= -\frac{1}{4\pi N_A}\left(2\left(\frac{\partial g(\sigma\kappa)}{\partial T}\right)_{V,\mathbf{n}}\left(\frac{\partial f(\sigma)}{\partial T}\right)_{V,\mathbf{n}} + \frac{1}{\sigma^3}\left(\frac{\partial^2 g(\sigma\kappa)}{\partial T^2}\right)_{V,\mathbf{n}} + g(\sigma\kappa)\left(\frac{\partial^2 f(\sigma)}{\partial T^2}\right)_{V,\mathbf{n}}\right)\end{aligned} \tag{4-109}$$

5. $\left(\frac{\partial^2 F_{sMSA}}{\partial T \partial n_i}\right)_{V,\mathbf{n}}$

$$\left(\frac{\partial^2 \boldsymbol{\eta}_{A_{Born}}}{\partial T \partial n_i}\right)_{V,\mathbf{n}} = \left(\frac{\partial^2}{\partial T \partial n_i}\begin{bmatrix} f(\sigma) \\ g(\sigma\kappa) \\ c(V) \end{bmatrix}\right)_{V,\mathbf{n}} = \begin{bmatrix} \left(\frac{\partial^2 f(\sigma)}{\partial T \partial n_i}\right)_{V,\mathbf{n}} \\ \left(\frac{\partial^2 g(\sigma\kappa)}{\partial T \partial n_i}\right)_{V,\mathbf{n}} \\ 0 \end{bmatrix} \tag{4-110}$$

$$\left(\frac{\partial^2 f(\sigma)}{\partial T \partial n_i}\right)_{V,\mathbf{n}} = \frac{d^2 f(\sigma)}{d\sigma^2}\left(\frac{\partial \sigma}{\partial T}\right)_{V,\mathbf{n}}\left(\frac{\partial \sigma}{\partial n_i}\right)_{T,V,\mathbf{n}/n_i} + \frac{df}{d\sigma}\left(\frac{\partial^2 \sigma}{\partial T \partial n_i}\right)_{V,\mathbf{n}} \tag{4-111}$$

$$\text{where } \left(\frac{\partial^2 \sigma}{\partial T \partial n_i}\right)_{V,\mathbf{n}} = \frac{\left(\frac{\partial \sigma_i}{\partial T}\right)_{V,\mathbf{n}} - \left(\frac{\partial \sigma}{\partial T}\right)_{V,\mathbf{n}}}{\sum_i n_i} \tag{4-112}$$

$$\left(\frac{\partial^2 g(\sigma\kappa)}{\partial T \partial n_i}\right)_{V,\mathbf{n}} = \frac{d^2 g(\sigma\kappa)}{d(\sigma\kappa)^2}\left(\frac{\partial(\sigma\kappa)}{\partial T}\right)_{V,\mathbf{n}}\left(\frac{\partial(\sigma\kappa)}{\partial n_i}\right)_{T,V,\mathbf{n}/n_i} + \frac{dg(\sigma\kappa)}{d(\sigma\kappa)}\left(\frac{\partial^2(\sigma\kappa)}{\partial T \partial n_i}\right)_{V,\mathbf{n}} \tag{4-113}$$

$$\left(\frac{\partial^2(\sigma\kappa)}{\partial T \partial n_i}\right)_{V,\mathbf{n}} = \left(\frac{\partial \sigma}{\partial T}\right)_{V,\mathbf{n}}\left(\frac{\partial \kappa}{\partial n_i}\right)_{T,V,\mathbf{n}/n_i} + \left(\frac{\partial \kappa}{\partial T}\right)_{V,\mathbf{n}}\left(\frac{\partial \sigma}{\partial n_i}\right)_{T,V,\mathbf{n}/n_i} + \sigma\left(\frac{\partial^2 \kappa}{\partial T \partial n_i}\right)_{V,\mathbf{n}} + \kappa\left(\frac{\partial^2 \sigma}{\partial T \partial n_i}\right)_{V,\mathbf{n}} \tag{4-114}$$

To calculate $\left(\frac{\partial^2\kappa}{\partial T\partial n_i}\right)_{V,\mathbf{n}}$, we take volume derivatives on both sides of (4-67)

$$\left(\frac{\partial^2\kappa}{\partial T\partial n_i}\right)_{V,\mathbf{n}}=\left(\frac{\partial}{\partial n_i}\left(\frac{\partial\kappa}{\partial T}\right)_{V,\mathbf{n}}\right)_{T,V,\mathbf{n}/n_i}=-\left(\frac{\partial}{\partial n_i}\left(\frac{\kappa}{2T}+\frac{\kappa}{2\varepsilon}\left(\frac{\partial\varepsilon}{\partial T}\right)_{V,\mathbf{n}}\right)\right)_{T,V,\mathbf{n}/n_i}$$

$$=-\frac{\kappa}{2}\left[\left(\frac{\partial\kappa}{\partial n_i}\right)_{T,V,\mathbf{n}/n_i}\left(\frac{1}{T}+\frac{1}{\varepsilon}\left(\frac{\partial\varepsilon}{\partial T}\right)_{V,\mathbf{n}}\right)+\left(-\frac{1}{\varepsilon^2}\left(\frac{\partial\varepsilon}{\partial n_i}\right)_{T,V,\mathbf{n}/n_i}\left(\frac{\partial\varepsilon}{\partial T}\right)_{V,\mathbf{n}}+\frac{1}{\varepsilon}\left(\frac{\partial^2\varepsilon}{\partial T\partial n_i}\right)_{V,\mathbf{n}}\right)_{T,V,\mathbf{n}/n_i}\right]$$

(4-115)

$$\boxed{\left(\frac{\partial^2\kappa}{\partial T\partial n_i}\right)_{V,\mathbf{n}}=\frac{1}{\kappa}\left(\frac{\partial\kappa}{\partial n_i}\right)_{T,V,\mathbf{n}/n_i}\left(\frac{\partial\kappa}{\partial T}\right)_{V,\mathbf{n}}+\frac{\kappa}{2\varepsilon^2}\left(\frac{\partial\varepsilon}{\partial n_i}\right)_{T,V,\mathbf{n}/n_i}\left(\frac{\partial\varepsilon}{\partial T}\right)_{V,\mathbf{n}}-\frac{\kappa}{2\varepsilon}\left(\frac{\partial^2\varepsilon}{\partial T\partial n_i}\right)_{V,\mathbf{n}}}\quad(4\text{-}116)$$

Finally we reach:

$$\left(\frac{\partial^2 F_{sMSA}}{\partial T\partial n_i}\right)_{V,\mathbf{n}}=\left(\left(\frac{\partial\boldsymbol{\eta}_{F_{sMSA}}}{\partial T}\right)_{V,\mathbf{n}}\right)^T\mathbf{F}_{sMSA}''(\boldsymbol{\eta}_{F_{sMSA}})\left(\frac{\partial\boldsymbol{\eta}_{F_{sMSA}}}{\partial T}\right)_{V,\mathbf{n}}+\left(\frac{\partial F_{sMSA}}{\partial\boldsymbol{\eta}_{F_{sMSA}}}\right)^T\cdot\left(\frac{\partial^2\boldsymbol{\eta}_{F_{sMSA}}}{\partial T\partial n_i}\right)_{V,\mathbf{n}}$$

$$=c(V)\left[\left(\frac{\partial f(\sigma)}{\partial T}\right)_{V,\mathbf{n}}\left(\frac{\partial g(\sigma\kappa)}{\partial n_i}\right)_{T,V,\mathbf{n}/n_i}+\left(\frac{\partial g(\sigma\kappa)}{\partial T}\right)_{V,\mathbf{n}}\left(\frac{\partial f(\sigma)}{\partial n_i}\right)_{T,V,\mathbf{n}/n_i}\right]$$

$$+c(V)\left[f(\sigma)\left(\frac{\partial^2 g(\sigma\kappa)}{\partial T\partial n_i}\right)_{V,\mathbf{n}}+g(\sigma\kappa)\left(\frac{\partial^2 f(\sigma)}{\partial T\partial n_i}\right)_{V,\mathbf{n}}\right]$$

(4-117)

6. $\left(\frac{\partial^2 F_{sMSA}}{\partial T\partial V}\right)_{V,\mathbf{n}}$

$$\left(\frac{\partial^2\boldsymbol{\eta}_{A_{Born}}}{\partial T\partial V}\right)_{V,\mathbf{n}}=\left(\frac{\partial^2}{\partial T\partial V}\begin{bmatrix}f(\sigma)\\g(\sigma\kappa)\\c(V)\end{bmatrix}\right)_{V,\mathbf{n}}=\begin{bmatrix}0\\\left(\frac{\partial^2 g(\sigma\kappa)}{\partial T\partial V}\right)_{V,\mathbf{n}}\\0\end{bmatrix}\quad(4\text{-}118)$$

$$\left(\frac{\partial^2 g(\sigma\kappa)}{\partial T\partial V}\right)_{V,\mathbf{n}}=\frac{d^2 g(\sigma\kappa)}{d(\sigma\kappa)^2}\left(\frac{\partial(\sigma\kappa)}{\partial T}\right)_{V,\mathbf{n}}\left(\frac{\partial(\sigma\kappa)}{\partial V}\right)_{\mathbf{n},T}+\frac{dg(\sigma\kappa)}{d(\sigma\kappa)}\left(\frac{\partial^2(\sigma\kappa)}{\partial T\partial V}\right)_{V,\mathbf{n}}\quad(4\text{-}119)$$

Note that

$$\left(\frac{\partial^2(\sigma\kappa)}{\partial T\partial V}\right)_{V,\mathbf{n}}=\left(\frac{\partial}{\partial T}\left(\frac{\partial(\sigma\kappa)}{\partial V}\right)_{\mathbf{n},T}\right)_{\mathbf{n},V}=\left(\frac{\partial}{\partial T}\left(\sigma\left(\frac{\partial\kappa}{\partial V}\right)_{T,\mathbf{n}}\right)\right)_{\mathbf{n},V}$$

$$=\left(\frac{\partial\sigma}{\partial T}\right)_{V,\mathbf{n}}\left(\frac{\partial\kappa}{\partial V}\right)_{T,\mathbf{n}}+\sigma\left(\frac{\partial^2\kappa}{\partial T\partial V}\right)_{\mathbf{n},V}\quad(4\text{-}120)$$

To calculate $\left(\frac{\partial^2\kappa}{\partial T\partial V}\right)_{\mathbf{n},V}$, we take temperature derivatives on both sides of (4-67):

$$\begin{aligned}\left(\frac{\partial^2\kappa}{\partial T\partial V}\right)_{V,\mathbf{n}} &= \left(\frac{\partial}{\partial T}\left(\frac{\partial\kappa}{\partial V}\right)_{T,\mathbf{n}}\right)_{V,\mathbf{n}} = -\left(\frac{\partial}{\partial T}\left(\frac{\kappa}{2V}+\frac{\kappa}{2\varepsilon}\left(\frac{\partial\varepsilon}{\partial V}\right)_{T,\mathbf{n}}\right)\right)_{V,\mathbf{n}} \\ &= -\frac{1}{2V}\left(\frac{\partial\kappa}{\partial T}\right)_{V,\mathbf{n}} - \frac{\kappa}{2\varepsilon}\left(\frac{\partial^2\varepsilon}{\partial T\partial V}\right)_{V,\mathbf{n}} - \left(\frac{\partial\varepsilon}{\partial V}\right)_{T,\mathbf{n}}\left(\frac{\partial}{\partial T}\frac{\kappa}{2\varepsilon}\right)_{V,\mathbf{n}}\end{aligned} \tag{4-121}$$

Finally, we get:

$$\boxed{\left(\frac{\partial^2\kappa}{\partial T\partial V}\right)_{V,\mathbf{n}} = -\frac{1}{2V}\left(\frac{\partial\kappa}{\partial T}\right)_{V,\mathbf{n}} - \frac{\kappa}{2\varepsilon}\left(\frac{\partial^2\varepsilon}{\partial T\partial V}\right)_{V,\mathbf{n}} - \frac{1}{2\varepsilon^2}\left[\varepsilon\left(\frac{\partial\kappa}{\partial T}\right)_{V,\mathbf{n}} - \kappa\left(\frac{\partial\varepsilon}{\partial T}\right)_{V,\mathbf{n}}\right]\left(\frac{\partial\varepsilon}{\partial V}\right)_{T,\mathbf{n}}} \tag{4-122}$$

$$\begin{aligned}&\left(\frac{\partial^2 F_{sMSA}}{\partial T\partial V}\right)_{V,\mathbf{n}} = \left(\left(\frac{\partial\boldsymbol{\eta}_{F_{sMSA}}}{\partial T}\right)_{V,\mathbf{n}}\right)^T \mathbf{F}_{sMSA}''(\boldsymbol{\eta}_{F_{sMSA}})\left(\frac{\partial\boldsymbol{\eta}_{F_{sMSA}}}{\partial V}\right)_{T,\mathbf{n}} + \left(\frac{\partial F_{sMSA}}{\partial\boldsymbol{\eta}_{F_{sMSA}}}\right)^T \cdot \left(\frac{\partial^2\boldsymbol{\eta}_{F_{sMSA}}}{\partial T\partial V}\right)_{V,\mathbf{n}} \\ &= c(V)\left(\frac{\partial f(\sigma)}{\partial T}\right)_{V,\mathbf{n}}\left(\frac{\partial g(\sigma\kappa)}{\partial V}\right)_{T,\mathbf{n}} + g(\sigma\kappa)\left(\frac{\partial f(\sigma)}{\partial T}\right)_{V,\mathbf{n}}\left(\frac{\partial c(V)}{\partial V}\right)_{T,\mathbf{n}} \\ &+ f(\sigma)\left(\frac{\partial g(\sigma\kappa)}{\partial T}\right)_{V,\mathbf{n}}\left(\frac{\partial c(V)}{\partial V}\right)_{T,\mathbf{n}} + c(V)f(\sigma)\left(\frac{\partial^2 g(\sigma\kappa)}{\partial T\partial V}\right)_{V,\mathbf{n}}\end{aligned} \tag{4-123}$$

And

$$\begin{aligned}&\left(\frac{\partial^2 F_{sMSA}}{\partial T\partial V}\right)_{V,\mathbf{n}} = \\ &c(V)\left[\left(\frac{\partial f(\sigma)}{\partial T}\right)_{V,\mathbf{n}}\left(\frac{\partial g(\sigma\kappa)}{\partial V}\right)_{T,\mathbf{n}} + f(\sigma)\left(\frac{\partial^2 g(\sigma\kappa)}{\partial T\partial V}\right)_{V,\mathbf{n}}\right] + \left(\frac{\partial c(V)}{\partial V}\right)_{T,\mathbf{n}}\left[g(\sigma\kappa)\left(\frac{\partial f(\sigma)}{\partial T}\right)_{V,\mathbf{n}} + f(\sigma)\left(\frac{\partial g(\sigma\kappa)}{\partial T}\right)_{V,\mathbf{n}}\right]\end{aligned} \tag{4-124}$$

1.3 The derivatives of Born term

The Helmholtz free energy required to charge all ions in a medium with relative permittivity of ε is calculated by the equation suggested by Born. Its expression is:

$$\Delta A^r_{Born}(T,V,\mathbf{n}) = -\frac{N_A e^2}{4\pi\varepsilon_0}\left(1-\frac{1}{\varepsilon}\right)\sum_{ions}\frac{n_i Z_i^2}{\sigma_i(T)},\ i\text{=ion} \tag{4-125}$$

Define the intermediate functions

$$f(\varepsilon(T,V,\mathbf{n})) \triangleq \left(1-\frac{1}{\varepsilon(T,V,\mathbf{n})}\right) \tag{4-126}$$

and

$$g(T,\mathbf{n}) \triangleq \sum_i \frac{n_i Z_i^2}{\sigma_i(T)},\ i\text{=ion} \tag{4-127}$$

and the constant

$$k = \frac{N_A e^2}{4\pi\varepsilon_0} \tag{4-128}$$

And then equation (4-125) can be written as

$$\Delta A^r_{Born}(T,V,\mathbf{n}) = -k \bullet f(T,V,\mathbf{n}) g(T,\mathbf{n}),\ i\text{=ion} \tag{4-129}$$

We got the function

$$A_{Born} = A^r{}_{Born}(f(T,V,\mathbf{n}), g(T,\mathbf{n})) \tag{4-130}$$

The structure of the composite function A_{Born} can be expressed in a graph as below:

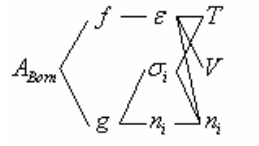

1.3.1 First order partial derivatives

Define

$$\boldsymbol{\eta}(\mathbf{x})_{A_{Born}} = \begin{bmatrix} f & g \end{bmatrix}^T = \begin{bmatrix} \left(1-\frac{1}{\varepsilon}\right) & \sum_i \frac{n_i Z_i^2}{\sigma_i(T)} \end{bmatrix}^T \tag{4-131}$$

Then we have:

$$\frac{\partial A_{Born}(\boldsymbol{\eta}_{A_{Born}})}{\partial \boldsymbol{\eta}_{A_{Born}}} = \begin{bmatrix} \frac{\partial A_{Born}}{\partial f} \\ \frac{\partial A_{Born}}{\partial g} \end{bmatrix} = \begin{bmatrix} -kg \\ -kf \end{bmatrix} = \begin{bmatrix} -\frac{N_A e^2}{4\pi\varepsilon_0}\left(1-\frac{1}{\varepsilon}\right) \\ -\frac{N_A e^2}{4\pi\varepsilon_0}\sum_i \frac{n_i Z_i^2}{\sigma_i(T)} \end{bmatrix} \tag{4-132}$$

Note

$$\frac{df}{d\varepsilon} = \frac{1}{\varepsilon^2} \tag{4-133}$$

and we have:

$$\left(\frac{\partial \boldsymbol{\eta}_{A_{Born}}}{\partial n_i}\right)_{T,V,\mathbf{n}/n_i} = \left(\frac{\partial}{\partial n_i}\begin{bmatrix} f \\ g \end{bmatrix}\right)_{T,V,\mathbf{n}/n_i} = \begin{bmatrix} \frac{df}{d\varepsilon}\left(\frac{\partial \varepsilon}{\partial n_i}\right)_{T,V,\mathbf{n}/n_i} \\ \left(\frac{\partial g}{\partial n_i}\right)_{T,V,\mathbf{n}/n_i} \end{bmatrix} = \begin{bmatrix} \frac{1}{\varepsilon^2}\left(\frac{\partial \varepsilon}{\partial n_i}\right)_{T,V,\mathbf{n}/n_i} \\ \left(\frac{\partial g}{\partial n_i}\right)_{T,V,\mathbf{n}/n_i} \end{bmatrix} \tag{4-134}$$

To calculate $\left(\frac{\partial \boldsymbol{\eta}_{A_{Born}}}{\partial n_i}\right)_{T,V,\mathbf{n}/n_i}$, we have to calculate:

$$\left(\frac{\partial g}{\partial n_i}\right)_{T,V,\mathbf{n}/n_i} = \begin{cases} \frac{Z_i^2}{\sigma_i(T)} & ,\ i\text{=ion} \\ 0 & ,\ i \neq \text{ion} \end{cases} \tag{4-135}$$

$\left(\frac{\partial \varepsilon}{\partial n_i}\right)_{T,V,\mathbf{n}/n_i}$, $\left(\frac{\partial \varepsilon}{\partial V}\right)_{\mathbf{n},T}$ and $\left(\frac{\partial \varepsilon}{\partial T}\right)_{\mathbf{n},V}$ can be derived from the specific water relativity model, such as the Uematsu-Franck or the Pottel models.

From (4-132) and (4-134), it is easy to get the first order composition derivatives:

$$\left(\frac{\partial A_{Born}}{\partial n_i}\right)_{T,V,\mathbf{n}/n_i} = \left(\frac{\partial A_{Born}}{\partial \boldsymbol{\eta}_{A_{Born}}}\right)\left(\frac{\partial \boldsymbol{\eta}_{A_{Born}}}{\partial n_i}\right)_{T,V,\mathbf{n}/n_i} \tag{4-136}$$

For volume derivatives it is necessary to derive:

$$\left(\frac{\partial \boldsymbol{\eta}_{A_{Born}}}{\partial V}\right)_{\mathbf{n},T} = \left(\frac{\partial}{\partial V}\begin{bmatrix} f & g \end{bmatrix}^T\right)_{\mathbf{n},T} = \begin{bmatrix} \frac{df}{d\varepsilon}\left(\frac{\partial \varepsilon}{\partial V}\right)_{\mathbf{n},T} & 0 \end{bmatrix}^T = \begin{bmatrix} \frac{1}{\varepsilon^2}\left(\frac{\partial \varepsilon}{\partial V}\right)_{\mathbf{n},T} & 0 \end{bmatrix}^T \tag{4-137}$$

Combine (4-132) and (4-183), we can calculate the volume derivative:

$$\left(\frac{\partial A_{Born}}{\partial V}\right)_{T,\mathbf{n}} = \left(\frac{\partial A_{Born}}{\partial \boldsymbol{\eta}_{A_{Born}}}\right)^T \cdot \left(\frac{\partial \boldsymbol{\eta}_{A_{Born}}}{\partial V}\right)_{T,\mathbf{n}} = -\frac{N_A e^2}{4\pi\varepsilon_0}\left(\sum_i \frac{n_i Z_i^2}{\sigma_i(T)}\right)\frac{1}{\varepsilon^2}\left(\frac{\partial \varepsilon}{\partial V}\right)_{\mathbf{n},T} \tag{4-138}$$

For temperature derivatives:

$$\left(\frac{\partial \boldsymbol{\eta}_{A_{Born}}}{\partial T}\right)_{\mathbf{n},V} = \left(\frac{\partial}{\partial T}\begin{bmatrix} f & g \end{bmatrix}^T\right)_{\mathbf{n},V} = \begin{bmatrix} \frac{df}{d\varepsilon}\left(\frac{\partial \varepsilon}{\partial T}\right)_{\mathbf{n},V} \\ \left(\frac{\partial g}{\partial T}\right)_{\mathbf{n},V} \end{bmatrix} = \begin{bmatrix} \frac{1}{\varepsilon^2}\left(\frac{\partial \varepsilon}{\partial T}\right)_{\mathbf{n},V} \\ -\sum_i\left(\frac{n_i Z_i^2}{\sigma_i^2}\left(\frac{\partial \sigma_i(T)}{\partial T}\right)\right)_{\mathbf{n},V} \end{bmatrix} \tag{4-139}$$

The first order temperature derivative is

$$\begin{aligned}\left(\frac{\partial A_{Born}}{\partial T}\right)_{V,\mathbf{n}} &= \left(\frac{\partial A_{Born}}{\partial \boldsymbol{\eta}_{A_{Born}}}\right)^T \cdot \left(\frac{\partial \boldsymbol{\eta}_{A_{Born}}}{\partial T}\right)_{V,\mathbf{n}} \\ &= -\frac{N_A e^2}{4\pi\varepsilon_0}\left(\sum_i \frac{n_i Z_i^2}{\sigma_i(T)}\right)\frac{1}{\varepsilon^2}\left(\frac{\partial \varepsilon}{\partial T}\right)_{\mathbf{n},V} + \frac{N_A e^2}{4\pi\varepsilon_0}\left(1-\frac{1}{\varepsilon}\right)\sum_i\left(\frac{n_i Z_i^2}{\sigma_i^2}\left(\frac{\partial \sigma_i(T)}{\partial T}\right)\right)_{\mathbf{n},V}\end{aligned} \tag{4-140}$$

1.3.2 Second order partial derivatives

Denote

$$\mathbf{A}''_{Born}(\boldsymbol{\eta}_{A_{Born}}) = \begin{bmatrix} \frac{\partial^2 A_{Born}}{\partial f^2} & \frac{\partial^2 A_{Born}}{\partial f \partial g} \\ \frac{\partial^2 A_{Born}}{\partial g \partial f} & \frac{\partial^2 A_{Born}}{\partial g^2} \end{bmatrix} = \begin{bmatrix} 0 & -k \\ -k & 0 \end{bmatrix} = \begin{bmatrix} 0 & -\frac{N_A e^2}{4\pi\varepsilon_0} \\ -\frac{N_A e^2}{4\pi\varepsilon_0} & 0 \end{bmatrix} \tag{4-141}$$

1. The composition derivatives

$$\left(\frac{\partial^2 \boldsymbol{\eta}_{A_{Born}}}{\partial n_i \partial n_j}\right)_{T,V,\mathbf{n}/n_i} = \left(\frac{\partial^2}{\partial n_i \partial n_j}\begin{bmatrix} f & g \end{bmatrix}^T\right)_{T,V,\mathbf{n}/n_i}$$
$$= \left[\left(\frac{\partial^2 f}{\partial n_i \partial n_j}\right)_{T,V,\mathbf{n}/n_i} \quad \left(\frac{\partial^2 g}{\partial n_i \partial n_j}\right)_{T,V,\mathbf{n}/n_i}\right]^T = \left[\left(\frac{\partial^2 f}{\partial n_i \partial n_j}\right)_{T,V,\mathbf{n}/n_i} \quad 0\right]^T \tag{4-142}$$

$$\frac{d^2 f}{d\varepsilon^2} = -\frac{2}{\varepsilon^3} \tag{4-143}$$

$$\left(\frac{\partial^2 f}{\partial n_i \partial n_j}\right)_{T,V,\mathbf{n}/n_i} = \frac{d^2 f}{d\varepsilon^2}\left(\frac{\partial \varepsilon}{\partial n_i}\right)_{T,V,\mathbf{n}/n_i}\left(\frac{\partial \varepsilon}{\partial n_j}\right)_{T,V,\mathbf{n}/n_j} + \frac{df}{d\varepsilon}\left(\frac{\partial^2 \varepsilon}{\partial n_i \partial n_j}\right)_{T,V,\mathbf{n}/n_i}$$
$$= \frac{-2}{\varepsilon^3}\left(\frac{\partial \varepsilon}{\partial n_i}\right)_{T,V,\mathbf{n}/n_i}\left(\frac{\partial \varepsilon}{\partial n_j}\right)_{T,V,\mathbf{n}/n_j} + \frac{1}{\varepsilon^2}\left(\frac{\partial^2 \varepsilon}{\partial n_i \partial n_j}\right)_{T,V,\mathbf{n}/n_i} \tag{4-144}$$

$$\left(\frac{\partial^2 A_{Born}(\boldsymbol{\eta}_{A_{Born}})}{\partial n_i \partial n_j}\right)_{T,V,\mathbf{n}/n_i}$$
$$= \left(\left(\frac{\partial \boldsymbol{\eta}_{A_{Born}}}{\partial n_i}\right)_{T,V,\mathbf{n}/n_i}\right)^T \mathbf{A}_{Born}''(\boldsymbol{\eta}_{A_{Born}})\left(\frac{\partial \boldsymbol{\eta}_{A_{Born}}}{\partial n_j}\right)_{T,V,\mathbf{n}/n_j} + \left(\frac{\partial A_{Born}}{\partial \boldsymbol{\eta}_{A_{Born}}}\right)^T \cdot \left(\frac{\partial^2 \boldsymbol{\eta}_{A_{Born}}}{\partial n_i \partial n_j}\right)_{T,V,\mathbf{n}/n_i} \tag{4-145}$$
$$= 0 + \frac{\partial A_{Born}}{\partial f}\left(\frac{\partial^2 f}{\partial n_i \partial n_j}\right)_{T,V,\mathbf{n}/n_i} = -\frac{N_A e^2}{4\pi\varepsilon_0}\left(1 - \frac{1}{\varepsilon}\right)\left(\frac{\partial^2 f}{\partial n_i \partial n_j}\right)_{T,V,\mathbf{n}/n_i}$$

2. The volume derivatives

$$\left(\frac{\partial^2 \boldsymbol{\eta}_{A_{Born}}}{\partial V^2}\right)_{T,\mathbf{n}} = \left(\frac{\partial^2}{\partial V^2}\begin{bmatrix} f & g \end{bmatrix}^T\right)_{T,\mathbf{n}} = \left[\left(\frac{\partial^2 f}{\partial V^2}\right)_{T,\mathbf{n}} \quad \left(\frac{\partial^2 g}{\partial V^2}\right)_{T,\mathbf{n}}\right]^T$$
$$= \left[\left(\frac{\partial^2 f}{\partial V^2}\right)_{T,\mathbf{n}} \quad 0\right]^T = \begin{bmatrix} \frac{d^2 f}{d\varepsilon^2}\left(\frac{\partial \varepsilon}{\partial V}\right)_{T,\mathbf{n}}^2 + \frac{df}{d\varepsilon}\left(\frac{\partial^2 \varepsilon}{\partial V^2}\right)_{T,\mathbf{n}} \\ 0 \end{bmatrix} \tag{4-146}$$

$$\left(\frac{\partial^2 A_{Born}}{\partial V^2}\right)_{T,\mathbf{n}} = \left(\left(\frac{\partial \boldsymbol{\eta}_{A_{Born}}}{\partial V}\right)_{T,\mathbf{n}}\right)^T \mathbf{A}_{Born}''(\boldsymbol{\eta}_{A_{Born}})\left(\frac{\partial \boldsymbol{\eta}_{A_{Born}}}{\partial V}\right)_{T,\mathbf{n}} + \left(\frac{\partial A_{Born}}{\partial \boldsymbol{\eta}_{A_{Born}}}\right)^T \cdot \left(\frac{\partial^2 \boldsymbol{\eta}_{A_{Born}}}{\partial V^2}\right)_{T,\mathbf{n}} \tag{4-147}$$
$$= -kg\left(\frac{\partial^2 f}{\partial V^2}\right)_{T,\mathbf{n}} = -kg\left(-\frac{2}{\varepsilon^3}\left(\frac{\partial \varepsilon}{\partial V}\right)_{T,\mathbf{n}}^2 + \frac{1}{\varepsilon^2}\left(\frac{\partial^2 \varepsilon}{\partial V^2}\right)_{T,\mathbf{n}}\right)$$

$$\left(\frac{\partial^2 \boldsymbol{\eta}_{A_{Born}}}{\partial V \partial n_i}\right)_{T,\mathbf{n}} = \left(\frac{\partial^2}{\partial V \partial n_i}\begin{bmatrix} f & g \end{bmatrix}^T\right)_{T,\mathbf{n}} = \begin{bmatrix} \left(\frac{\partial^2 f}{\partial V \partial n_i}\right)_{T,\mathbf{n}} & \left(\frac{\partial^2 g}{\partial V \partial n_i}\right)_{T,\mathbf{n}} \end{bmatrix}^T$$
$$= \begin{bmatrix} \left(\frac{\partial^2 f}{\partial V \partial n_i}\right)_{T,\mathbf{n}} \\ 0 \end{bmatrix} = \begin{bmatrix} \frac{d^2 f}{d\varepsilon^2}\left(\frac{\partial \varepsilon}{\partial V}\right)_{T,\mathbf{n}}\left(\frac{\partial \varepsilon}{\partial n_i}\right)_{T,V,\mathbf{n}/n_i} + \frac{df}{d\varepsilon}\left(\frac{\partial^2 \varepsilon}{\partial V \partial n_i}\right)_{T,\mathbf{n}} \\ 0 \end{bmatrix} \quad (4\text{-}148)$$

$$\left(\frac{\partial^2 A_{Born}}{\partial V \partial n_i}\right)_{T,\mathbf{n}} = \left(\left(\frac{\partial \boldsymbol{\eta}_{A_{Born}}}{\partial V}\right)_{T,\mathbf{n}}\right)^T \mathbf{A}_{Born}''(\boldsymbol{\eta}_{A_{Born}})\left(\frac{\partial \boldsymbol{\eta}_{A_{Born}}}{\partial n_i}\right)_{T,V,\mathbf{n}/n_i} + \left(\frac{\partial A_{Born}}{\partial \boldsymbol{\eta}_{A_{Born}}}\right)^T \cdot \left(\frac{\partial^2 \boldsymbol{\eta}_{A_{Born}}}{\partial V \partial n_i}\right)_{T,\mathbf{n}}$$
$$= -k\left(\frac{\partial f}{\partial V}\right)_{T,\mathbf{n}}\left(\frac{\partial g}{\partial n_i}\right)_{T,V,\mathbf{n}/n_i} - kg\left(\frac{\partial^2 f}{\partial V \partial n_i}\right)_{T,\mathbf{n}} \quad (4\text{-}149)$$

2. The temperature derivatives

$$\left(\frac{\partial^2 \boldsymbol{\eta}_{A_{Born}}}{\partial T^2}\right)_{V,\mathbf{n}} = \left(\frac{\partial^2}{\partial T^2}\begin{bmatrix} f & g \end{bmatrix}^T\right)_{V,\mathbf{n}} = \begin{bmatrix} \left(\frac{\partial^2 f}{\partial T^2}\right)_{V,\mathbf{n}} & \left(\frac{\partial^2 g}{\partial T^2}\right)_{V,\mathbf{n}} \end{bmatrix}^T$$
$$= \begin{bmatrix} \frac{d^2 f}{d\varepsilon^2}\left(\frac{\partial \varepsilon}{\partial T}\right)_{V,\mathbf{n}}^2 + \frac{df}{d\varepsilon}\left(\frac{\partial^2 \varepsilon}{\partial T^2}\right)_{V,\mathbf{n}} \\ \frac{\partial^2 g}{\partial \sigma_i^2}\left(\frac{\partial \sigma_i}{\partial T}\right)_{V,\mathbf{n}}^2 + \frac{\partial g}{\partial \sigma_i}\left(\frac{\partial^2 \sigma_i}{\partial T^2}\right)_{V,\mathbf{n}} \end{bmatrix} \quad (4\text{-}150)$$

$$\left(\frac{\partial^2 A_{Born}}{\partial T^2}\right)_{V,\mathbf{n}} = \left(\left(\frac{\partial \boldsymbol{\eta}_{A_{Born}}}{\partial T}\right)_{V,\mathbf{n}}\right)^T \mathbf{A}_{Born}''(\boldsymbol{\eta}_{A_{Born}})\left(\frac{\partial \boldsymbol{\eta}_{A_{Born}}}{\partial T}\right)_{V,\mathbf{n}} + \left(\frac{\partial A_{Born}}{\partial \boldsymbol{\eta}_{A_{Born}}}\right)^T \cdot \left(\frac{\partial^2 \boldsymbol{\eta}_{A_{Born}}}{\partial T^2}\right)_{V,\mathbf{n}} \quad (4\text{-}151)$$

$$\left(\frac{\partial^2 \boldsymbol{\eta}_{A_{Born}}}{\partial T \partial n_i}\right)_{V,\mathbf{n}} = \left(\frac{\partial^2}{\partial T \partial n_i}\begin{bmatrix} f & g \end{bmatrix}^T\right)_{V,\mathbf{n}} = \begin{bmatrix} \left(\frac{\partial^2 f}{\partial T \partial n_i}\right)_{V,\mathbf{n}} & \left(\frac{\partial^2 g}{\partial T \partial n_i}\right)_{V,\mathbf{n}} \end{bmatrix}^T$$
$$= \begin{bmatrix} \frac{d^2 f}{d\varepsilon^2}\left(\frac{\partial \varepsilon}{\partial T}\right)_{V,\mathbf{n}}\left(\frac{\partial \varepsilon}{\partial n_i}\right)_{T,V,\mathbf{n}/n_i} + \frac{df}{d\varepsilon}\left(\frac{\partial^2 \varepsilon}{\partial T \partial n_i}\right)_{V,\mathbf{n}} \\ \left(\frac{\partial^2 g}{\partial T \partial n_i}\right)_{V,\mathbf{n}} \end{bmatrix} \quad (4\text{-}152)$$

$\left(\frac{\partial^2 g}{\partial T \partial n_i}\right)_{V,\mathbf{n}}$ can be calculated by (4-153):

$$\left(\frac{\partial^2 g}{\partial T \partial n_i}\right)_{V,\mathbf{n}} = \begin{cases} -\frac{Z_i^2}{\sigma_i(T)^2}\left(\left(\frac{\partial \sigma_i(T)}{\partial T}\right)_{V,\mathbf{n}}\right) & , \ i\text{=ion} \\ 0 & , \ i \neq \text{ion} \end{cases} \quad (4\text{-}153)$$

Finally:

$$\left(\frac{\partial^2 A_{Born}}{\partial T\partial n_i}\right)_{V,\mathbf{n}} = \left(\left(\frac{\partial \boldsymbol{\eta}_{A_{Born}}}{\partial T}\right)_{V,\mathbf{n}}\right)^T \mathbf{A}_{Born}''(\boldsymbol{\eta}_{A_{Born}})\left(\frac{\partial \boldsymbol{\eta}_{A_{Born}}}{\partial n_i}\right)_{T,V,\mathbf{n}/n_i} + \left(\frac{\partial A_{Born}}{\partial \boldsymbol{\eta}_{A_{Born}}}\right)^T \cdot \left(\frac{\partial^2 \boldsymbol{\eta}_{A_{Born}}}{\partial T\partial n_i}\right)_{V,\mathbf{n}} \quad (4\text{-}154)$$

$$= -k\left(\frac{\partial f}{\partial T}\right)_{V,\mathbf{n}}\left(\frac{\partial g}{\partial n_i}\right)_{T,V,\mathbf{n}/n_i} - k\left(\frac{\partial g}{\partial T}\right)_{V,\mathbf{n}}\left(\frac{\partial f}{\partial n_i}\right)_{T,V,\mathbf{n}/n_i} - kg\left(\frac{\partial^2 f}{\partial T\partial n_i}\right)_{V,\mathbf{n}} - kf\left(\frac{\partial^2 g}{\partial T\partial n_i}\right)_{V,\mathbf{n}}$$

$$\left(\frac{\partial^2 \boldsymbol{\eta}_{A_{Born}}}{\partial T\partial V}\right)_{V,\mathbf{n}} = \left[\left(\frac{\partial^2 f}{\partial T\partial V}\right)_{V,\mathbf{n}} \quad \left(\frac{\partial^2 g}{\partial T\partial V}\right)_{V,\mathbf{n}}\right]^T$$
$$= \begin{bmatrix} \dfrac{d^2 f}{d\varepsilon^2}\left(\dfrac{\partial \varepsilon}{\partial T}\right)_{V,\mathbf{n}}\left(\dfrac{\partial \varepsilon}{\partial V}\right)_{T,\mathbf{n}} + \dfrac{df}{d\varepsilon}\left(\dfrac{\partial^2 \varepsilon}{\partial T\partial V}\right)_{V,\mathbf{n}} \\ 0 \end{bmatrix} \quad (4\text{-}155)$$

Finally:

$$\left(\frac{\partial^2 A_{Born}}{\partial T\partial V}\right)_{V,\mathbf{n}} = \left(\left(\frac{\partial \boldsymbol{\eta}_{A_{Born}}}{\partial T}\right)_{V,\mathbf{n}}\right)^T \mathbf{A}_{Born}''(\boldsymbol{\eta}_{A_{Born}})\left(\frac{\partial \boldsymbol{\eta}_{A_{Born}}}{\partial V}\right)_{T,\mathbf{n}} + \left(\frac{\partial A_{Born}}{\partial \boldsymbol{\eta}_{A_{Born}}}\right)^T \cdot \left(\frac{\partial^2 \boldsymbol{\eta}_{A_{Born}}}{\partial T\partial V}\right)_{V,\mathbf{n}}$$

$$= -k\left(\frac{\partial g}{\partial T}\right)_{V,\mathbf{n}}\left(\frac{\partial f}{\partial V}\right)_{T,\mathbf{n}} - kg\left(\frac{\partial^2 f}{\partial T\partial V}\right)_{V,\mathbf{n}} \quad (4\text{-}156)$$

$$= -k\left(\frac{\partial g}{\partial T}\right)_{V,\mathbf{n}}\left(\frac{\partial f}{\partial V}\right)_{T,\mathbf{n}} - kg\left(\frac{d^2 f}{d\varepsilon^2}\left(\frac{\partial \varepsilon}{\partial T}\right)_{V,\mathbf{n}}\left(\frac{\partial \varepsilon}{\partial V}\right)_{T,\mathbf{n}} + \frac{df}{d\varepsilon}\left(\frac{\partial^2 \varepsilon}{\partial T\partial V}\right)_{V,\mathbf{n}}\right)$$

1.4 The derivatives from Fürst and Renon's sMSA term

From Fürst and Renon we have the simplified implicit MSA term in (4-157).

$$F_{sMSA\_Furst} = \frac{A^r{}_{sMSA\_Furst}}{RT} = -\frac{\alpha_{sMSA}^2}{4\pi}\sum_i \frac{n_i z_i^2 \Gamma}{1+\Gamma\sigma_i} + \frac{\Gamma^3 V}{3\pi N_A}, \text{ where } \alpha_{sMSA}^2 = \frac{e^2 N_A}{\varepsilon_0 \varepsilon RT} \quad (4\text{-}157)$$

and

$$4\Gamma^2 = \alpha_{sMSA}^2 N_A \sum_i \frac{n_i}{V}\left[\frac{z_i}{1+\Gamma\sigma_i}\right]^2 \quad (4\text{-}158)$$

The relative permittivity ε is calculated as follows

$$\varepsilon = 1 + (\varepsilon_s - 1)\frac{1-\varepsilon_3}{1+\varepsilon_3/2} \quad (4\text{-}159)$$

Where ε_3 is calculated by the same equation as in (4-22): $\varepsilon_3 = \frac{N_A\pi}{6V}\sum_k n_k\sigma_k^3$ and the solvent relative permittivity ε_s can be calculated according to the following equation:

$$\varepsilon_s = \frac{\sum_i n_i\varepsilon_i}{\sum_i n_i} \quad (4\text{-}160)$$

Define the intermediate functions

$$X \triangleq \sum_i \frac{n_i z_i^2 \Gamma}{1+\Gamma\sigma_i} = \sum_i \frac{n_i z_i^2}{\sigma_i}\left(1-\frac{1}{1+\Gamma\sigma_i}\right) \tag{4-161}$$

and

$$Y = \frac{\Gamma^3 V}{3\pi N_A} \tag{4-162}$$

And then equation (4-157) can be written as

$$F_{sMSA\_Furst} = \frac{A^r{}_{sMSA\_Furst}}{RT} = -\frac{\alpha_{sMSA}^2}{4\pi}X + Y, \text{ where } \alpha_{sMSA}^2 = \frac{e^2 N_A}{\varepsilon_0 \varepsilon RT} \tag{4-163}$$

We got the function

$$F_{sMSA\_Furst} = F_{sMSA\_Furst}(\alpha_{sMSA}^2, X, Y) \tag{4-164}$$

The structure of the composite function $F_{sMSA\_Furst} = F_{sMSA\_Furst}(\alpha_{sMSA}^2, X, Y)$ can be expressed in a graph as below:

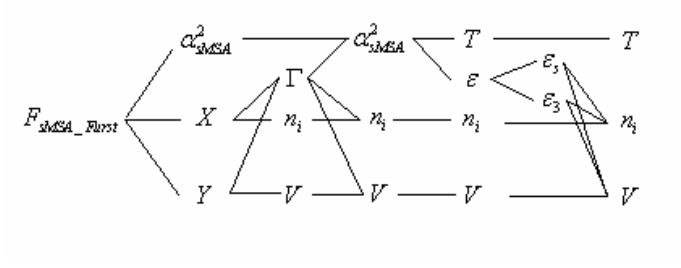

1.4.1 First order partial derivatives

Define

$$\boldsymbol{\eta}(\mathbf{x})_{F_{sMSA}} = \left[\alpha_{sMSA}^2 \quad X \quad Y\right]^T = \left[\frac{e^2 N_A}{\varepsilon_0 \varepsilon RT} \quad \sum_i \frac{n_i z_i^2 \Gamma}{1+\Gamma\sigma_i} \quad \frac{\Gamma^3 V}{3\pi N_A}\right]^T \tag{4-165}$$

Then

$$\frac{\partial F_{sMSA\_Furst}(\boldsymbol{\eta})}{\partial \boldsymbol{\eta}_{F_{sMSA}}} = \left[\frac{\partial F}{\partial \alpha_{sMSA}^2} \quad \frac{\partial F}{\partial X} \quad \frac{\partial F}{\partial Y}\right]^T = \left[-\frac{X}{4\pi} \quad -\frac{\alpha_{sMSA}^2}{4\pi} \quad 1\right]^T \tag{4-166}$$

$$\left(\frac{\partial \boldsymbol{\eta}_{F_{sMSA}}}{\partial n_i}\right)_{T,V,\mathbf{n}/n_i} = \left(\frac{\partial}{\partial n_i}\begin{bmatrix}\alpha_{sMSA}^2 \\ X \\ Y\end{bmatrix}\right)_{T,V,\mathbf{n}/n_i} = \begin{bmatrix} 2\alpha_{sMSA}\left(\frac{\partial \alpha_{sMSA}}{\partial n_i}\right)_{T,V,\mathbf{n}/n_i} \\ \left(\frac{\partial X}{\partial n_i}\right)_{T,V,\mathbf{n}/n_i} \\ \left(\frac{\partial Y}{\partial n_i}\right)_{T,V,\mathbf{n}/n_i} \end{bmatrix} \tag{4-167}$$

To calculate $\left(\frac{\partial X}{\partial n_i}\right)_{T,V,\mathbf{n}/n_i}$, we define

$$\boldsymbol{\eta}_X = \begin{bmatrix} n_i & n_j & \Gamma \end{bmatrix}^T \tag{4-168}$$

Then we have

$$\frac{\partial X(n_i,T,V)}{\partial \boldsymbol{\eta}_X} = \begin{bmatrix} \frac{\partial X}{\partial n_i} & \frac{\partial X}{\partial n_j} & \frac{\partial X}{\partial \Gamma} \end{bmatrix}^T = \begin{bmatrix} \frac{z_i^2\Gamma}{1+\Gamma\sigma_i} & \frac{z_j^2\Gamma}{1+\Gamma\sigma_j} & \sum_i \frac{n_i z_i^2}{(1+\Gamma\sigma_i)^2} \end{bmatrix}^T \tag{4-169}$$

$$\left(\frac{\partial \boldsymbol{\eta}_X}{\partial n_i}\right)_{T,V,\mathbf{n}/n_i} = \begin{bmatrix} 1 & 0 & \left(\frac{\partial \Gamma}{\partial n_i}\right)_{T,V,\mathbf{n}/n_i} \end{bmatrix}^T \tag{4-170}$$

It is easy to get

$$\left(\frac{\partial X}{\partial n_i}\right)_{T,V,\mathbf{n}/n_i} = \left(\frac{\partial X(n_i,T,V)}{\partial \boldsymbol{\eta}_X}\right)^T \left(\frac{\partial \boldsymbol{\eta}_X}{\partial n_i}\right)_{T,V,\mathbf{n}/n_i} = \frac{z_i^2\Gamma}{1+\Gamma\sigma_i} + \left(\sum_i \frac{n_i z_i^2}{(1+\Gamma\sigma_i)^2}\right)\left(\frac{\partial \Gamma}{\partial n_i}\right)_{T,V,\mathbf{n}/n_i} \tag{4-171}$$

To calculate $\frac{\partial \Gamma}{\partial n_i}$, we define

$$\boldsymbol{\eta}_\Gamma = \begin{bmatrix} \alpha_{sMSA}^2 & n_i & n_j & V \end{bmatrix}^T \tag{4-172}$$

Define

$$\begin{aligned} &\mathrm{F}_1\left(\boldsymbol{\eta}_{\mathrm{F}_1}\right) = \mathrm{F}_1\left(\left[\Gamma, \alpha_{sMSA}^2, V, \mathbf{n}\right]^T\right) \\ &= 4\Gamma^2 - \alpha_{sMSA}^2 \sum_i \frac{n_i z_i^{\,2}}{V(1+\Gamma\sigma_i)^2} = = 4\Gamma^2 - \alpha_{sMSA}^2 S(\boldsymbol{\eta}_S) = 0 \end{aligned} \tag{4-173}$$

where

$$S(\boldsymbol{\eta}_S) = S\left(\left[\Gamma, V, \mathbf{n}\right]^T\right) = \sum_i \frac{n_i z_i^{\,2}}{V(1+\Gamma\sigma_i)^2} \tag{4-174}$$

Then from (4-284) in section 1.5.1 in this Appendix V, we have:

$$\frac{\partial \Gamma(\mathbf{n},T,V)}{\partial \boldsymbol{\eta}_\Gamma} = \begin{bmatrix} \left(\frac{\partial \Gamma}{\partial \alpha_{sMSA}^2}\right)_{\mathbf{n},V} & \left(\frac{\partial \Gamma}{\partial n_i}\right)_{\alpha_{sMSA}^2,V,\mathbf{n}/n_i} & \left(\frac{\partial \Gamma}{\partial n_j}\right)_{\alpha_{sMSA}^2,V,\mathbf{n}/n_j} & \left(\frac{\partial \Gamma}{\partial V}\right)_{\alpha_{sMSA}^2,\mathbf{n}} \end{bmatrix}^T =$$

$$N_A(8V\Gamma + 2\alpha_{sMSA}^2 \sum_i \frac{\sigma_i n_i z_i^2}{(1+\Gamma\sigma_i)^3})^{-1} \begin{bmatrix} \sum_i \frac{n_i z_i^2}{(1+\Gamma\sigma_i)^2} & \frac{\alpha_{sMSA}^2 z_i^2}{(1+\Gamma\sigma_i)^2} & \frac{\alpha_{sMSA}^2 z_j^2}{(1+\Gamma\sigma_j)^2} & \frac{-\alpha_{sMSA}^2}{V}\sum_i \frac{n_i z_i^2}{(1+\Gamma\sigma_i)^2} \end{bmatrix}^T \tag{4-175}$$

$$\left(\frac{\partial \boldsymbol{\eta}_\Gamma}{\partial n_i}\right)_{T,V,\mathbf{n}/n_i} = \begin{bmatrix} \left(\frac{\partial \alpha_{sMSA}^2}{\partial n_i}\right)_{T,V,\mathbf{n}/n_i} & 1 & 0 & 0 \end{bmatrix}^T = \begin{bmatrix} 2\alpha_{sMSA}\left(\frac{\partial \alpha_{sMSA}}{\partial n_i}\right)_{T,V,\mathbf{n}/n_i} & 1 & 0 & 0 \end{bmatrix}^T \tag{4-176}$$

From (4-157):

$$\alpha_{sMSA}^2 = \frac{e^2 N_A}{\varepsilon_0 \varepsilon(n_i,V) RT} \qquad \Rightarrow \qquad \alpha_{sMSA}^2 \varepsilon = \frac{e^2 N_A}{\varepsilon_0 RT}, \tag{4-177}$$

take first order derivatives with respect to mole number on both sides of equation (4-177), we have

$$\boxed{\left(\frac{\partial \alpha_{sMSA}}{\partial n_i}\right)_{T,V} = -\frac{\alpha_{sMSA}}{2\varepsilon}\left(\frac{\partial \varepsilon}{\partial n_i}\right)_{T,V,\mathbf{n}/n_i}} \tag{4-178}$$

Combine (4-178) and (4-176):

$$\begin{aligned}\left(\frac{\partial \boldsymbol{\eta}_\Gamma}{\partial n_i}\right)_{T,V,\mathbf{n}/n_i} &= \left[2\alpha_{sMSA}\left(\frac{\partial \alpha_{sMSA}}{\partial n_i}\right)_{T,V,\mathbf{n}/n_i} \quad 1 \quad 0 \quad 0\right]^T \\ &= \left[2\alpha_{sMSA}\left(-\frac{\alpha_{sMSA}}{2\varepsilon}\left(\frac{\partial \varepsilon}{\partial n_i}\right)_{T,V,\mathbf{n}/n_i}\right) \quad 1 \quad 0 \quad 0\right]^T = \left[-\frac{\alpha_{sMSA}^2}{\varepsilon}\left(\frac{\partial \varepsilon}{\partial n_i}\right)_{T,V,\mathbf{n}/n_i} \quad 1 \quad 0 \quad 0\right]^T\end{aligned} \tag{4-179}$$

From (4-284) in section 1.5.1, it is easy to get

$$\begin{aligned}\left(\frac{\partial \Gamma}{\partial n_i}\right)_{T,V,\mathbf{n}/n_i} &= \left(\frac{\partial \Gamma(n_i,T,V)}{\partial \boldsymbol{\eta}_\Gamma}\right)^T\left(\frac{\partial \boldsymbol{\eta}_\Gamma}{\partial n_i}\right)_{T,V,\mathbf{n}/n_i} = \left(\frac{\partial \Gamma}{\partial \alpha_{sMSA}^2}\right)_{\mathbf{n},V}\left(\frac{\partial \alpha_{sMSA}^2}{\partial n_i}\right)_{T,V,\mathbf{n}/n_i} + \left(\frac{\partial \Gamma}{\partial n_i}\right)_{\mathbf{n}/n_i,V,\alpha_{sMSA}^2}\left(\frac{\partial n_i}{\partial n_i}\right)_{T,V,\mathbf{n}/n_i} \\ &= -\left(\frac{\partial\, \mathrm{F}_1}{\partial \alpha_{sMSA}^2}\right)_{\boldsymbol{\eta}_{\mathrm{F}_1}/\alpha_{sMSA}^2} \Bigg/ \left(\frac{\partial\, \mathrm{F}_1}{\partial \Gamma}\right)_{\boldsymbol{\eta}_{\mathrm{F}_1}/\Gamma}\left(\frac{\partial \alpha_{sMSA}^2}{\partial n_i}\right)_{T,V,\mathbf{n}/n_i} - \left(\frac{\partial\, \mathrm{F}_1}{\partial n_i}\right)_{\boldsymbol{\eta}_{\mathrm{F}_1}/n_i} \Bigg/ \left(\frac{\partial\, \mathrm{F}_1}{\partial \Gamma}\right)_{\boldsymbol{\eta}_{\mathrm{F}_1}/\Gamma} \cdot 1\end{aligned} \tag{4-180}$$

Combine equation, (4-281) and (4-282) in section 1.5.1 and (4-180), and calculate $\left(\frac{\partial \Gamma}{\partial n_i}\right)_{T,V,\mathbf{n}/n_i}$.

$$\boxed{\left(\frac{\partial \Gamma}{\partial n_i}\right)_{T,V,\mathbf{n}/n_i} = \frac{S}{8\Gamma - \alpha_{sMSA}^2\left(\frac{\partial S}{\partial \Gamma}\right)_{\boldsymbol{\eta}_S/\Gamma}}\left(\frac{\partial \alpha_{sMSA}^2}{\partial n_i}\right)_{T,V,\mathbf{n}/n_i} + \frac{\alpha_{sMSA}^2\left(\frac{\partial S}{\partial n_i}\right)_{\boldsymbol{\eta}_S/n_i}}{8\Gamma - \alpha_{sMSA}^2\left(\frac{\partial S}{\partial \Gamma}\right)_{\boldsymbol{\eta}_S/\Gamma}}} \tag{4-181}$$

$$\boxed{\begin{aligned}\left(\frac{\partial \Gamma}{\partial n_i}\right)_{T,V,\mathbf{n}/n_i} &= \left(2\alpha_{sMSA}\frac{\partial \alpha_{sMSA}}{\partial n_i}\sum_i \frac{n_i z_i^2}{\left(1+\Gamma\sigma_i\right)^2} + \frac{\alpha_{sMSA}^2 z_i^2}{\left(1+\Gamma\sigma_i\right)^2} + 0\right) \Bigg/ \left(8V\Gamma + 2\alpha_{sMSA}^2\sum_i \frac{\sigma_i n_i z_i^2}{\left(1+\Gamma\sigma_i\right)^3}\right) \\ &= \left(-\frac{\alpha_{sMSA}^2}{\varepsilon}\frac{\partial \varepsilon}{\partial n_i}\sum_i \frac{n_i z_i^2}{\left(1+\Gamma\sigma_i\right)^2} + \frac{\alpha_{sMSA}^2 z_i^2}{\left(1+\Gamma\sigma_i\right)^2} + 0\right) \Bigg/ \left(8V\Gamma + 2\alpha_{sMSA}^2\sum_i \frac{\sigma_i n_i z_i^2}{\left(1+\Gamma\sigma_i\right)^3}\right)\end{aligned}} \tag{4-182}$$

Combine equation(4-331),(4-340), (4-330) and (4-182) and we can calculate $\left(\frac{\partial \Gamma}{\partial n_i}\right)_{T,V,\mathbf{n}/n_i}$.

$$\left(\frac{\partial \boldsymbol{\eta}_\Gamma}{\partial V}\right)_{\mathbf{n},T} = \left(\frac{\partial}{\partial V}\left[\alpha_{sMSA}^2 \quad n_i \quad V\right]^T\right)_{\mathbf{n},T} = \left[2\alpha_{sMSA}\left(\frac{\partial \alpha_{sMSA}}{\partial V}\right)_{\mathbf{n},T} \quad 0 \quad 1\right]^T \tag{4-183}$$

Take first order derivatives with respect to volume V on both sides of equation (4-177):

$$2\varepsilon\alpha_{sMSA}\left(\frac{\partial\alpha_{sMSA}}{\partial V}\right)_{\mathbf{n},T}+\alpha_{sMSA}^2\left(\frac{\partial\varepsilon}{\partial V}\right)_{\mathbf{n},T}=0 \qquad \Rightarrow \boxed{\left(\frac{\partial\alpha_{sMSA}}{\partial V}\right)_{\mathbf{n},T}=-\frac{\alpha_{sMSA}}{2\varepsilon}\left(\frac{\partial\varepsilon}{\partial V}\right)_{\mathbf{n},T}} \quad .(4\text{-}184)$$

Combine (4-183) and (4-184), we have

$$\left(\frac{\partial\boldsymbol{\eta}_\Gamma}{\partial V}\right)_{\mathbf{n},T}=\left(\frac{\partial}{\partial V}\left[\alpha_{sMSA}^2 \quad n_i \quad V\right]^T\right)_{\mathbf{n},T}=\left[2\alpha_{sMSA}\left(\frac{\partial\alpha_{sMSA}}{\partial V}\right)_{\mathbf{n},T} \quad 0 \quad 1\right]^T=\left[-\frac{\alpha_{sMSA}^2}{\varepsilon}\left(\frac{\partial\varepsilon}{\partial V}\right)_{\mathbf{n},T} \quad 0 \quad 1\right]^T \tag{4-185}$$

Combine (4-175) and (4-185):

$$\left(\frac{\partial\Gamma}{\partial V}\right)_{T,\mathbf{n}}=\left(\frac{\partial\Gamma}{\partial\boldsymbol{\eta}_\Gamma}\right)^T\cdot\left(\frac{\partial\boldsymbol{\eta}_\Gamma}{\partial V}\right)_{T,\mathbf{n}}=N_A\left(8V\Gamma+2\alpha_{sMSA}^2\sum_i\frac{\sigma_i n_i z_i^2}{\left(1+\Gamma\sigma_i\right)^3}\right)^{-1}\cdot \left[\sum_i\frac{n_i z_i^2}{\left(1+\Gamma\sigma_i\right)^2} \quad \frac{\alpha_{sMSA}^2 z_i^2}{\left(1+\Gamma\sigma_i\right)^2} \quad \frac{-\alpha_{sMSA}^2}{V}\sum_i\frac{n_i z_i^2}{\left(1+\Gamma\sigma_i\right)^2}\right]\cdot\left[-\frac{\alpha_{sMSA}^2}{\varepsilon}\left(\frac{\partial\varepsilon}{\partial V}\right)_{T,\mathbf{n}} \quad 0 \quad 1\right]^T \tag{4-186}$$

$$\boxed{\left(\frac{\partial\Gamma}{\partial V}\right)_{\mathbf{n},T}=-\left(\frac{1}{\varepsilon}\left(\frac{\partial\varepsilon}{\partial V}\right)_{\mathbf{n},T}+\frac{1}{V}\right)\left(\sum_i\frac{N_A\alpha_{sMSA}^2 n_i z_i^2}{\left(1+\Gamma\sigma_i\right)^2}\right)\Bigg/\left(8V\Gamma+2\alpha_{sMSA}^2\sum_i\frac{\sigma_i n_i z_i^2}{\left(1+\Gamma\sigma_i\right)^3}\right)} \tag{4-187}$$

For temperature derivatives:

$$\left(\frac{\partial\boldsymbol{\eta}_\Gamma}{\partial T}\right)_{\mathbf{n},V}=\left(\frac{\partial}{\partial T}\left[\alpha_{sMSA}^2 \quad n_i \quad V\right]^T\right)_{\mathbf{n},V}=\left[2\alpha_{sMSA}\left(\frac{\partial\alpha_{sMSA}}{\partial T}\right)_{\mathbf{n},V} \quad 0 \quad 0\right]^T \tag{4-188}$$

For a more general case i.e. the relative permittivity is a function of temperature:

$$\alpha_{sMSA}^2=\frac{e^2N_A}{\varepsilon_0\varepsilon(T,V,\mathbf{n})RT} \qquad \Rightarrow \qquad \alpha_{sMSA}^2T\varepsilon=\frac{e^2N_A}{\varepsilon_0R}, \tag{4-189}$$

take first order derivatives with respect to temperature on both sides of equation (4-189):

.

$$\boxed{\left(\frac{\partial\alpha_{sMSA}^2}{\partial T}\right)_{\mathbf{n},V}=2\alpha_{sMSA}\left(\frac{\partial\alpha_{sMSA}}{\partial T}\right)_{\mathbf{n},V}=-\frac{\alpha_{sMSA}^2}{T}-\frac{\alpha_{sMSA}^2}{\varepsilon}\left(\frac{\partial\varepsilon}{\partial T}\right)_{\mathbf{n},V}} \tag{4-190}$$

If the relative permittivity is not a function of temperature, we have:

$$\boxed{\left(\frac{\partial\alpha_{sMSA}^2}{\partial T}\right)_{\mathbf{n},V}=2\alpha_{sMSA}\left(\frac{\partial\alpha_{sMSA}}{\partial T}\right)_{\mathbf{n},V}=-\frac{\alpha_{sMSA}^2}{T}} \tag{4-191}$$

$$\boxed{\left(\frac{\partial^2\alpha_{sMSA}^2}{\partial T^2}\right)_{\mathbf{n},V}=\frac{1}{\alpha_{sMSA}^2}\left(\frac{\partial\alpha_{sMSA}^2}{\partial T}\right)^2+\frac{\alpha_{sMSA}^2}{T^2}+\frac{\alpha_{sMSA}^2}{\varepsilon^2}\left(\frac{\partial\varepsilon}{\partial T}\right)_{\mathbf{n},V}^2-\frac{\alpha_{sMSA}^2}{\varepsilon}\left(\frac{\partial^2\varepsilon}{\partial T^2}\right)_{\mathbf{n},V}} \tag{4-192}$$

$$\boxed{\left(\frac{\partial^2\alpha_{sMSA}^2}{\partial T\partial n_i}\right)_{\mathbf{n},V}=-\left(\frac{\partial}{\partial n_i}\frac{\alpha_{sMSA}^2}{T}\right)_{\mathbf{n}/n_i,T,V}=\frac{\alpha_{sMSA}^2}{T\varepsilon}\left(\frac{\partial\varepsilon}{\partial n_i}\right)_{\mathbf{n}/n_i,T,V}} \tag{4-193}$$

$$\boxed{\left(\frac{\partial^2\alpha_{sMSA}^2}{\partial T\partial V}\right)_{\mathbf{n},V}=-\left(\frac{\partial}{\partial V}\frac{\alpha_{sMSA}^2}{T}\right)_{\mathbf{n},T}=\frac{\alpha_{sMSA}^2}{T\varepsilon}\left(\frac{\partial\varepsilon}{\partial V}\right)_{\mathbf{n},T}} \tag{4-194}$$

If the relative permittivity is not a function of temperature, we have

$$\boxed{\left(\frac{\partial^2\alpha_{sMSA}^2}{\partial T^2}\right)_{\mathbf{n},V}=\frac{2\alpha_{sMSA}^2}{T^2}} \tag{4-195}$$

$$\boxed{\left(\frac{\partial^2\alpha_{sMSA}^2}{\partial T\partial n_i}\right)_{\mathbf{n},V}=-\left(\frac{\partial}{\partial n_i}\frac{\alpha_{sMSA}^2}{T}\right)_{\mathbf{n}/n_i,T,V}=\frac{\alpha_{sMSA}^2}{T\varepsilon}\left(\frac{\partial\varepsilon}{\partial n_i}\right)_{\mathbf{n}/n_i,T,V}} \tag{4-196}$$

$$\boxed{\left(\frac{\partial^2\alpha_{sMSA}^2}{\partial T\partial V}\right)_{\mathbf{n},V}=-\left(\frac{\partial}{\partial V}\frac{\alpha_{sMSA}^2}{T}\right)_{\mathbf{n},T}=\frac{\alpha_{sMSA}^2}{T\varepsilon}\left(\frac{\partial\varepsilon}{\partial V}\right)_{\mathbf{n},T}} \tag{4-197}$$

Combine (4-188) and (4-191):

$$\left(\frac{\partial\boldsymbol{\eta}_\Gamma}{\partial T}\right)_{\mathbf{n},V}=\left(\frac{\partial}{\partial T}\begin{bmatrix}\alpha_{sMSA}^2 & n_i & V\end{bmatrix}^T\right)_{\mathbf{n},V}=\begin{bmatrix}-\dfrac{\alpha_{sMSA}^2}{T}-\dfrac{\alpha_{sMSA}^2}{\varepsilon}\left(\dfrac{\partial\varepsilon}{\partial T}\right)_{\mathbf{n},V} & 0 & 0\end{bmatrix}^T \tag{4-198}$$

Combine (4-175) and (4-198):

$$\boxed{\left(\frac{\partial\Gamma}{\partial T}\right)_{\mathbf{n},V}=\left(\frac{\partial\Gamma}{\partial\boldsymbol{\eta}_\Gamma}\right)^T\cdot\left(\frac{\partial\boldsymbol{\eta}_\Gamma}{\partial T}\right)_{\mathbf{n},V}=\frac{\left(-\dfrac{\alpha_{sMSA}^2}{T}-\dfrac{\alpha_{sMSA}^2}{\varepsilon}\left(\dfrac{\partial\varepsilon}{\partial T}\right)_{\mathbf{n},V}\right)\sum_i\dfrac{n_iz_i^2}{\left(1+\Gamma\sigma_i\right)^2}}{\left(8V\Gamma+2\alpha_{sMSA}^2\sum_i\dfrac{\sigma_in_iz_i^2}{\left(1+\Gamma\sigma_i\right)^3}\right)}} \tag{4-199}$$

Other first order derivatives of X with respect to V and T, are calculated in the following way.

To calculate $\left(\frac{\partial X}{\partial V}\right)_{T,n_i}$, we have

$$\left(\frac{\partial\boldsymbol{\eta}_X}{\partial V}\right)_{T,\mathbf{n}}=\begin{bmatrix}0 & 0 & \left(\dfrac{\partial\Gamma}{\partial V}\right)_{T,\mathbf{n}}\end{bmatrix}^T$$

$$\frac{\partial X(n_i,T,V)}{\partial\boldsymbol{\eta}_X}=\begin{bmatrix}\dfrac{\partial X}{\partial n_i} & \dfrac{\partial X}{\partial n_j} & \dfrac{\partial X}{\partial\Gamma}\end{bmatrix}^T=\begin{bmatrix}\dfrac{z_i^2\Gamma}{1+\Gamma\sigma_i} & \dfrac{z_j^2\Gamma}{1+\Gamma\sigma_j} & \displaystyle\sum_i\dfrac{n_iz_i^2}{\left(1+\Gamma\sigma_i\right)^2}\end{bmatrix}^T$$

thus

$$\boxed{\begin{aligned}\left(\frac{\partial X}{\partial V}\right)_{T,n_i}&=\left(\frac{\partial X(n_i,T,V)}{\partial\boldsymbol{\eta}_X}\right)^T\cdot\left(\frac{\partial\boldsymbol{\eta}_X}{\partial V}\right)_{T,n_i}\\&=\begin{bmatrix}\dfrac{z_i^2\Gamma}{1+\Gamma\sigma_i} & \displaystyle\sum_i\dfrac{n_iz_i^2}{\left(1+\Gamma\sigma_i\right)^2}\end{bmatrix}\cdot\begin{bmatrix}0 & \dfrac{\partial\Gamma}{\partial V}\end{bmatrix}^T=\sum_i\frac{n_iz_i^2}{\left(1+\Gamma\sigma_i\right)^2}\left(\frac{\partial\Gamma}{\partial V}\right)_{T,n_i}\end{aligned}} \tag{4-200}$$

$$\left(\frac{\partial X}{\partial V}\right)_{T,n_i}=-\left(\frac{1}{\varepsilon}\frac{\partial\varepsilon}{\partial V}+\frac{1}{V}\right)\left(\sum_i\frac{N_A\alpha_{sMSA}n_iz_i^2}{\left(1+\Gamma\sigma_i\right)^2}\right)^2\Bigg/\left(8V\Gamma+2\alpha_{sMSA}^2\sum_i\frac{\sigma_in_iz_i^2}{\left(1+\Gamma\sigma_i\right)^3}\right) \tag{4-201}$$

To calculate $\left(\frac{\partial\Gamma}{\partial T}\right)_{n_i,V}$, we have:

$$\left(\frac{\partial\boldsymbol{\eta}_X}{\partial T}\right)_{\mathbf{n},V}=\begin{bmatrix}0 & 0 & \left(\dfrac{\partial\Gamma}{\partial T}\right)_{V,\mathbf{n}}\end{bmatrix}^T \tag{4-202}$$

$$\boxed{\begin{aligned}\left(\frac{\partial X}{\partial T}\right)_{n_i,V} &= \left(\frac{\partial X(n_i,T,V)}{\partial \boldsymbol{\eta}_X}\right)^T \cdot \left(\frac{\partial \boldsymbol{\eta}_X}{\partial T}\right)_{n_i,V} \\ &= \left[\frac{z_i^2\Gamma}{1+\Gamma\sigma_i} \quad \sum_i \frac{n_i z_i^2}{\left(1+\Gamma\sigma_i\right)^2}\right] \cdot \left[0 \quad 0 \quad \left(\frac{\partial \Gamma}{\partial T}\right)_{V,\mathbf{n}}\right]^T = \sum_i \frac{n_i z_i^2}{\left(1+\Gamma\sigma_i\right)^2}\left(\frac{\partial \Gamma}{\partial T}\right)_{n_i,V}\end{aligned}} \tag{4-203}$$

$$\left(\frac{\partial X}{\partial T}\right)_{n_i,V} = -\left(\sum_i \frac{\alpha_{sMSA} n_i z_i^2}{\left(1+\Gamma\sigma_i\right)^2}\right)^2 \Bigg/ T\left(8V\Gamma + 2\alpha_{sMSA}^2 \sum_i \frac{\sigma_i n_i z_i^2}{\left(1+\Gamma\sigma_i\right)^3}\right) \tag{4-204}$$

The first order differential of $Y = \dfrac{\Gamma^3 V}{3\pi N_A}$ is calculated in the following way.

To calculate $\dfrac{\partial Y}{\partial n_i}$, we define:

$$\boldsymbol{\eta}_Y = \begin{bmatrix}\Gamma & V\end{bmatrix}^T \tag{4-205}$$

Then we have

$$\frac{\partial Y(n_i,T,V)}{\partial \boldsymbol{\eta}_Y} = \begin{bmatrix}\dfrac{\partial Y}{\partial \Gamma} & \dfrac{\partial Y}{\partial V}\end{bmatrix}^T = \begin{bmatrix}\dfrac{\Gamma^2 V}{\pi N_A} & \dfrac{\Gamma^3}{3\pi N_A}\end{bmatrix}^T \tag{4-206}$$

$$\left(\frac{\partial \boldsymbol{\eta}_Y}{\partial n_i}\right)_{T,V,\mathbf{n}/n_i} = \begin{bmatrix}\left(\dfrac{\partial \Gamma}{\partial n_i}\right)_{T,V,\mathbf{n}/n_i} & 0\end{bmatrix}^T \tag{4-207}$$

$$\boxed{\left(\frac{\partial Y}{\partial n_i}\right)_{T,V,\mathbf{n}/n_i} = \left(\frac{\partial Y(n_i,T,V)}{\partial \boldsymbol{\eta}_Y}\right)^T \cdot \left(\frac{\partial \boldsymbol{\eta}_Y}{\partial n_i}\right)_{T,V,\mathbf{n}/n_i} = \frac{\Gamma^2 V}{\pi N_A}\left(\frac{\partial \Gamma}{\partial n_i}\right)_{T,V,\mathbf{n}/n_i}} \tag{4-208}$$

$$\left(\frac{\partial \boldsymbol{\eta}_Y}{\partial T}\right)_{n_i,V} = \begin{bmatrix}\dfrac{\partial \Gamma}{\partial T} & 0\end{bmatrix}^T \tag{4-209}$$

$$\boxed{\left(\frac{\partial Y}{\partial T}\right)_{n_i,V} = \left(\frac{\partial Y(n_i,T,V)}{\partial \boldsymbol{\eta}_Y}\right)^T \cdot \left(\frac{\partial \boldsymbol{\eta}_Y}{\partial T}\right)_{n_i,V} = \frac{\Gamma^2 V}{\pi N_A}\left(\frac{\partial \Gamma}{\partial T}\right)_{n_i,V}} \tag{4-210}$$

$$\left(\frac{\partial Y}{\partial T}\right)_{n_i,V} = -\frac{\Gamma^2 V \alpha_{sMSA}^2 \sum_i \dfrac{n_i z_i^2}{\left(1+\Gamma\sigma_i\right)^2}}{T\pi N_A\left(8V\Gamma + 2\alpha_{sMSA}^2 \sum_i \dfrac{\sigma_i n_i z_i^2}{\left(1+\Gamma\sigma_i\right)^3}\right)} \tag{4-211}$$

$$\left(\frac{\partial \boldsymbol{\eta}_Y}{\partial V}\right)_{n_i,T} = \begin{bmatrix}\dfrac{\partial \Gamma}{\partial V} & 1\end{bmatrix}^T \tag{4-212}$$

$$\boxed{\left(\frac{\partial Y}{\partial V}\right)_{T,n_i} = \left(\frac{\partial Y(n_i,T,V)}{\partial \boldsymbol{\eta}_Y}\right)^T \cdot \left(\frac{\partial \boldsymbol{\eta}_Y}{\partial V}\right)_{T,n_i} = \frac{\Gamma^2 V}{\pi N_A}\left(\frac{\partial \Gamma}{\partial V}\right)_{T,n_i} + \frac{\Gamma^3}{3\pi N_A}} \tag{4-213}$$

The first order differential of the vector function is

$$\left(\frac{\partial \boldsymbol{\eta}_{F_{sMSA}}}{\partial n_i}\right)_{T,V,\mathbf{n}/n_i}=\left(\frac{\partial}{\partial n_i}\begin{bmatrix}\alpha_{sMSA}^2\\ X\\ Y\end{bmatrix}\right)_{T,V,\mathbf{n}/n_i}=\begin{bmatrix}2\alpha_{sMSA}\left(\dfrac{\partial \alpha_{sMSA}}{\partial n_i}\right)_{T,V,\mathbf{n}/n_i}\\ \dfrac{z_i^2\Gamma}{1+\Gamma\sigma_i}+\left(\sum_i \dfrac{n_i z_i^2}{\left(1+\Gamma\sigma_i\right)^2}\right)\left(\dfrac{\partial \Gamma}{\partial n_i}\right)_{T,V,\mathbf{n}/n_i}\\ \dfrac{\Gamma^2 V}{\pi N_A}\left(\dfrac{\partial \Gamma}{\partial n_i}\right)_{T,V,\mathbf{n}/n_i}\end{bmatrix} \tag{4-214}$$

$$\begin{aligned}\left(\frac{\partial \boldsymbol{\eta}_{F_{sMSA}}}{\partial V}\right)_{n_i,T}&=\left(\frac{\partial}{\partial V}\left[\alpha_{sMSA}^2 \quad X \quad Y\right]^T\right)_{n_i,T}\\&=\left[2\alpha_{sMSA}\left(\frac{\partial \alpha_{sMSA}}{\partial V}\right)_{n_i,T} \quad \left(\frac{\partial X}{\partial V}\right)_{n_i,T} \quad \left(\frac{\partial Y}{\partial V}\right)_{n_i,T}\right]^T\end{aligned} \tag{4-215}$$

$$\boxed{\left(\frac{\partial \boldsymbol{\eta}_{F_{sMSA}}}{\partial V}\right)_{n_i,T}=\left[-\frac{\alpha_{sMSA}^2}{\varepsilon}\left(\frac{\partial \varepsilon}{\partial V}\right)_{n_i,T} \quad \left(\frac{\partial X}{\partial V}\right)_{n_i,T} \quad \left(\frac{\partial Y}{\partial V}\right)_{n_i,T}\right]^T} \tag{4-216}$$

$$\begin{aligned}\left(\frac{\partial \boldsymbol{\eta}_{F_{sMSA}}}{\partial T}\right)_{n_i,V}&=\left(\frac{\partial}{\partial T}\left[\alpha_{sMSA}^2 \quad X \quad Y\right]^T\right)_{n_i,V}\\&=\left[2\alpha_{sMSA}\left(\frac{\partial \alpha_{sMSA}}{\partial T}\right)_{n_i,V} \quad \left(\frac{\partial X}{\partial T}\right)_{n_i,V} \quad \left(\frac{\partial Y}{\partial T}\right)_{n_i,V}\right]^T\end{aligned} \tag{4-217}$$

$$\boxed{\left(\frac{\partial \boldsymbol{\eta}_{F_{sMSA}}}{\partial T}\right)_{n_i,V}=\left[\left(\frac{\partial \alpha^2{}_{sMSA}}{\partial T}\right)_{n_i,V} \quad \left(\frac{\partial X}{\partial T}\right)_{n_i,V} \quad \left(\frac{\partial Y}{\partial T}\right)_{n_i,V}\right]^T} \tag{4-218}$$

The first order differential of this function is

$$\begin{aligned}\left(\frac{\partial F_{sMSA\_Furst}}{\partial n_i}\right)_{T,V,\mathbf{n}/n_i}&=\left(\frac{\partial F}{\partial \boldsymbol{\eta}_{F_{sMSA}}}\right)^T\cdot\left(\frac{\partial \boldsymbol{\eta}_{F_{sMSA}}}{\partial n_i}\right)_{T,V,\mathbf{n}/n_i}\\&=\left[\frac{\partial F}{\partial \alpha_{sMSA}^2} \quad \frac{\partial F}{\partial X} \quad \frac{\partial F}{\partial Y}\right]\cdot\left(\frac{\partial \boldsymbol{\eta}_{F_{sMSA}}}{\partial n_i}\right)_{T,V,\mathbf{n}/n_i}=\left[-\frac{X}{4\pi} \quad -\frac{\alpha_{sMSA}^2}{4\pi} \quad 1\right]\cdot\left(\frac{\partial \boldsymbol{\eta}_{F_{sMSA}}}{\partial n_i}\right)_{T,V,\mathbf{n}/n_i}\end{aligned} \tag{4-219}$$

$$\boxed{\begin{aligned}\left(\frac{\partial F_{sMSA\_Furst}}{\partial n_i}\right)_{T,V,\mathbf{n}/n_i}&=-\frac{1}{4\pi}\left(\frac{\partial \alpha_{sMSA}^2}{\partial n_i}\right)_{T,V,\mathbf{n}/n_i}\sum_i \frac{n_i z_i^2\Gamma}{1+\Gamma\sigma_i}\\&-\frac{\alpha_{sMSA}^2}{4\pi}\left(\frac{z_i^2\Gamma}{1+\Gamma\sigma_i}+\left(\sum_i \frac{n_i z_i^2}{\left(1+\Gamma\sigma_i\right)^2}\right)\left(\frac{\partial \Gamma}{\partial n_i}\right)_{T,V,\mathbf{n}/n_i}\right)+\frac{\Gamma^2 V}{\pi N_A}\left(\frac{\partial \Gamma}{\partial n_i}\right)_{T,V,\mathbf{n}/n_i}\end{aligned}} \tag{4-220}$$

And $\left(\dfrac{\partial \Gamma}{\partial n_i}\right)_{T,V,\mathbf{n}/n_i}$ can be found in (4-181) and (4-182).

$$\left(\frac{\partial F_{sMSA\_Furst}(\boldsymbol{\eta})}{\partial V}\right)_{n_i,T}=\left(\frac{\partial F_{sMSA\_Furst}}{\partial \boldsymbol{\eta}_{F_{sMSA}}}\right)^T\cdot\left(\frac{\partial \boldsymbol{\eta}_{F_{sMSA}}}{\partial V}\right)_{n_i,T}$$

$$=\left[-\frac{X}{4\pi}\quad -\frac{\alpha_{sMSA}^2}{4\pi}\quad 1\right]\cdot\left[\frac{\alpha_{sMSA}^2}{\varepsilon}\left(\frac{\partial\varepsilon}{\partial V}\right)_{n_i,T}\quad \left(\frac{\partial X}{\partial V}\right)_{n_i,T}\quad \left(\frac{\partial Y}{\partial V}\right)_{n_i,T}\right]^T \tag{4-221}$$

$$=-\frac{X}{4\pi}\frac{\alpha_{sMSA}^2}{\varepsilon}\left(\frac{\partial\varepsilon}{\partial V}\right)_{T,V}-\frac{\alpha_{sMSA}^2}{4\pi}\left(\frac{\partial X}{\partial V}\right)_{n_i,T}+\left(\frac{\partial Y}{\partial V}\right)_{n_i,T}$$

$$\left(\frac{\partial F_{sMSA\_Furst}(\boldsymbol{\eta})}{\partial T}\right)_{n_i,V}=\left(\frac{\partial F_{sMSA\_Furst}}{\partial \boldsymbol{\eta}_{F_{sMSA}}}\right)^T\cdot\left(\frac{\partial \boldsymbol{\eta}_{F_{sMSA}}}{\partial T}\right)_{n_i,V}$$

$$=\left(\frac{\partial F_{sMSA\_Furst}}{\partial \boldsymbol{\eta}_{F_{sMSA}}}\right)^T\cdot\left[-\frac{\alpha_{sMSA}^2}{T}\quad \left(\frac{\partial X}{\partial T}\right)_{n_i,V}\quad \left(\frac{\partial Y}{\partial T}\right)_{n_i,V}\right]^T \tag{4-222}$$

$$=\frac{X}{4\pi}\frac{\alpha_{sMSA}^2}{T}+\frac{\alpha_{sMSA}^2}{4\pi}\left(\frac{\partial X}{\partial T}\right)_{n_i,V}+\left(\frac{\partial Y}{\partial T}\right)_{n_i,V}$$

1.4.2 Second order partial derivatives

Denote

$$\mathbf{F}''(\boldsymbol{\eta}_{F_{sMSA}})=\begin{bmatrix}F_{\alpha_{sMSA}^2\alpha_{sMSA}^2} & F_{\alpha_{sMSA}^2X} & F_{\alpha_{sMSA}^2V}\\ F_{X\alpha_{sMSA}^2} & F_{XX} & F_{XY}\\ F_{Y\alpha_{sMSA}^2} & F_{YX} & F_{YY}\end{bmatrix}=\begin{bmatrix}0 & -\frac{1}{4\pi} & 0\\ -\frac{1}{4\pi} & 0 & 0\\ 0 & 0 & 0\end{bmatrix} \tag{4-223}$$

$$\left(\frac{\partial^2\boldsymbol{\eta}_{F_{sMSA}}}{\partial n_i\partial n_j}\right)_{T,V,\mathbf{n}/n_i}=\left(\frac{\partial^2}{\partial n_i\partial n_j}\left[\alpha_{sMSA}^2\quad X\quad Y\right]^T\right)_{T,V,\mathbf{n}/n_i}=\left[2\left(\frac{\partial\alpha_{sMSA}}{\partial n_i}\right)_{T,V,\mathbf{n}/n_i}\left(\frac{\partial\alpha_{sMSA}}{\partial n_j}\right)_{T,V,\mathbf{n}/n_i}\right.$$

$$\left.+2\alpha_{sMSA}\left(\frac{\partial^2\alpha_{sMSA}}{\partial n_i\partial n_j}\right)_{T,V,\mathbf{n}/n_i}\left(\frac{\partial^2X}{\partial n_i\partial n_j}\right)_{T,V,\mathbf{n}/n_i}\quad \left(\frac{\partial^2Y}{\partial n_i\partial n_j}\right)_{T,V,\mathbf{n}/n_i}\right]^T \tag{4-224}$$

$$\left(\frac{\partial\alpha_{sMSA}}{\partial n_i}\right)_{T,V}=-\frac{\alpha_{sMSA}}{2\varepsilon}\left(\frac{\partial\varepsilon}{\partial n_i}\right)_{T,V,\mathbf{n}/n_i} \tag{4-225}$$

$$\left(\frac{\partial^2\alpha_{sMSA}}{\partial n_i\partial n_j}\right)_{T,V,\mathbf{n}/n_i} =$$

$$-\frac{1}{2\varepsilon}\left(\left(\frac{\partial\alpha_{sMSA}}{\partial n_j}\right)_{T,V,\mathbf{n}/n_j}\left(\frac{\partial\varepsilon}{\partial n_i}\right)_{T,V,\mathbf{n}/n_i} - \frac{\alpha_{sMSA}}{\varepsilon}\left(\frac{\partial\varepsilon}{\partial n_i}\right)_{T,V,\mathbf{n}/n_i}\left(\frac{\partial\varepsilon}{\partial n_j}\right)_{T,V,\mathbf{n}/n_j} + \alpha_{sMSA}\left(\frac{\partial^2\varepsilon}{\partial n_i\partial n_j}\right)_{T,V,\mathbf{n}/n_i}\right)$$

(4-226)

$$\left(\frac{\partial^2\alpha^2_{sMSA}}{\partial n_i\partial n_j}\right)_{T,V,\mathbf{n}/n_i} = -\frac{1}{\varepsilon}\left(\left(\frac{\partial\alpha^2_{sMSA}}{\partial n_j}\right)_{T,V,\mathbf{n}/n_j}\left(\frac{\partial\varepsilon}{\partial n_i}\right)_{T,V,\mathbf{n}/n_i} + \left(\frac{\partial\alpha^2_{sMSA}}{\partial n_i}\right)_{T,V,\mathbf{n}/n_i}\left(\frac{\partial\varepsilon}{\partial n_j}\right)_{T,V,\mathbf{n}/n_j} + \alpha^2_{sMSA}\left(\frac{\partial^2\varepsilon}{\partial n_i\partial n_j}\right)_{T,V,\mathbf{n}/n_i}\right)$$

(4-227)

$$\left(\frac{\partial^2\boldsymbol{\eta}_X}{\partial n_i\partial n_j}\right)_{T,V} = \begin{bmatrix} 0 & 0 & \left(\frac{\partial^2\Gamma}{\partial n_i\partial n_j}\right)_{T,V} \end{bmatrix} \qquad (4\text{-}228)$$

$\left(\frac{\partial^2\Gamma}{\partial n_i\partial n_j}\right)_{T,V,\mathbf{n}/n_i}$ can be calculated according to (4-312).

$$\left(\frac{\partial^2 X}{\partial n_i\partial n_j}\right)_{T,V,\mathbf{n}/n_i} = \left(\left(\frac{\partial\boldsymbol{\eta}_X}{\partial n_i}\right)_{T,V}\right)^T \mathbf{X}''(\boldsymbol{\eta}_X)\left(\frac{\partial\boldsymbol{\eta}_X}{\partial n_j}\right)_{T,V} + \left(\frac{\partial X}{\partial\boldsymbol{\eta}_X}\right)^T\cdot\left(\frac{\partial^2\boldsymbol{\eta}_X}{\partial n_i\partial n_j}\right)_{T,V} \qquad (4\text{-}229)$$

$$\mathbf{X}''(\boldsymbol{\eta}_X) = \begin{bmatrix} \left(\frac{\partial^2 X}{\partial n_i^2}\right)_{\Gamma,\mathbf{n}/n_i} & \left(\frac{\partial^2 X}{\partial n_i\partial n_j}\right)_{\Gamma,\mathbf{n}/n_i} & \left(\frac{\partial^2 X}{\partial n_i\partial\Gamma}\right)_{\Gamma,\mathbf{n}/n_i} \\ \left(\frac{\partial^2 X}{\partial n_j\partial n_i}\right)_{\Gamma,\mathbf{n}/n_i} & \left(\frac{\partial^2 X}{\partial n_j^2}\right)_{\Gamma,\mathbf{n}/n_i} & \left(\frac{\partial^2 X}{\partial n_j\partial\Gamma}\right)_{\Gamma,\mathbf{n}/n_j} \\ \left(\frac{\partial^2 X}{\partial\Gamma\partial n_i}\right)_{\mathbf{n}} & \left(\frac{\partial^2 X}{\partial\Gamma\partial n_j}\right)_{\Gamma,\mathbf{n}/n_j} & \left(\frac{\partial^2 X}{\partial\Gamma^2}\right)_{\mathbf{n}} \end{bmatrix} = \begin{bmatrix} 0 & 0 & \left(\frac{\partial^2 X}{\partial n_i\partial\Gamma}\right)_{\Gamma,\mathbf{n}/n_i} \\ 0 & 0 & \left(\frac{\partial^2 X}{\partial n_j\partial\Gamma}\right)_{\Gamma,\mathbf{n}/n_j} \\ \left(\frac{\partial^2 X}{\partial\Gamma\partial n_i}\right)_{\mathbf{n}} & \left(\frac{\partial^2 X}{\partial\Gamma\partial n_j}\right)_{\Gamma,\mathbf{n}/n_j} & \left(\frac{\partial^2 X}{\partial\Gamma^2}\right)_{\mathbf{n}} \end{bmatrix}$$

(4-230)

From (4-169) we get

$$\left(\frac{\partial X}{\partial n_i}\right)_{\Gamma} = \frac{z_i^2\Gamma}{1+\Gamma\sigma_i} \qquad \Rightarrow \qquad \left(\frac{\partial X}{\partial n_i}\right)_{\Gamma}\left(1+\Gamma\sigma_i\right) = z_i^2\Gamma$$

$$\left(\frac{\partial^2 X}{\partial n_i\partial\Gamma}\right)_{\Gamma,\mathbf{n}/n_i}\left(1+\Gamma\sigma_i\right) = z_i^2 - \frac{z_i^2\Gamma}{1+\Gamma\sigma_i}\sigma_i = \frac{z_i^2+z_i^2\Gamma\sigma_i-z_i^2\Gamma\sigma_i}{1+\Gamma\sigma_i} = \frac{z_i^2}{1+\Gamma\sigma_i}$$

$$\left(\frac{\partial^2 X}{\partial n_i\partial\Gamma}\right)_{\Gamma,\mathbf{n}/n_i} = \left(\frac{\partial^2 X}{\partial\Gamma\partial n_i}\right)_{\mathbf{n}} = \frac{z_i^2}{\left(1+\Gamma\sigma_i\right)^2} \qquad (4\text{-}231)$$

$$\left(\frac{\partial^2 X}{\partial\Gamma^2}\right)_{\mathbf{n}} = \sum_i\frac{-2n_iz_i^2\sigma_i}{\left(1+\Gamma\sigma_i\right)^3} \qquad (4\text{-}232)$$

$$\left(\frac{\partial^2 X}{\partial n_i \partial n_j}\right)_{T,V,\mathbf{n}/n_i} = \left(\frac{\partial^2 X}{\partial n_i \partial \Gamma}\right)_{\Gamma,\mathbf{n}/n_i}\left(\frac{\partial n_i}{\partial n_i}\right)_{T,V,\mathbf{n}/n_i}\left(\frac{\partial \Gamma}{\partial n_j}\right)_{T,V,\mathbf{n}/n_i} + \left(\frac{\partial^2 X}{\partial n_j \partial \Gamma}\right)_{\Gamma,\mathbf{n}/n_j}\left(\frac{\partial n_j}{\partial n_j}\right)_{T,V,\mathbf{n}/n_j}\left(\frac{\partial \Gamma}{\partial n_i}\right)_{T,V,\mathbf{n}/n_i}$$
$$+\left(\frac{\partial^2 X}{\partial \Gamma^2}\right)_{\mathbf{n}}\left(\frac{\partial \Gamma}{\partial n_j}\right)_{T,V,\mathbf{n}/n_i}\left(\frac{\partial \Gamma}{\partial n_i}\right)_{T,V,\mathbf{n}/n_i} + \left(\frac{\partial X}{\partial \Gamma}\right)_{\mathbf{n}} \cdot \left(\frac{\partial^2 \Gamma}{\partial n_i \partial n_j}\right)_{T,V,\mathbf{n}/n_i} \tag{4-233}$$

$\left(\frac{\partial^2 \Gamma}{\partial n_i \partial n_j}\right)_{T,V,\mathbf{n}/n_i}$ can be calculated according to (4-312).

$$\left(\frac{\partial^2 X}{\partial V^2}\right)_{T,\mathbf{n}} = \left(\left(\frac{\partial \boldsymbol{\eta}_X}{\partial V}\right)_{T,\mathbf{n}}\right)^T \mathbf{X}''(\boldsymbol{\eta}_X)\left(\frac{\partial \boldsymbol{\eta}_X}{\partial V}\right)_{T,\mathbf{n}} + \left(\frac{\partial X}{\partial \boldsymbol{\eta}_X}\right)^T \cdot \left(\frac{\partial^2 \boldsymbol{\eta}_X}{\partial V^2}\right)_{T,\mathbf{n}} \tag{4-234}$$

$$\left(\frac{\partial^2 X}{\partial V^2}\right)_{T,\mathbf{n}} = \left(\frac{\partial^2 X}{\partial \Gamma^2}\right)_{\boldsymbol{\eta}_X/\Gamma} \cdot \left(\frac{\partial \Gamma}{\partial V}\right)^2_{T,\mathbf{n}} + \left(\frac{\partial X}{\partial \Gamma}\right)_{\boldsymbol{\eta}_X/\Gamma} \cdot \left(\frac{\partial^2 \Gamma}{\partial V^2}\right)_{T,\mathbf{n}} \tag{4-235}$$

$$\left(\frac{\partial^2 X}{\partial V \partial n_i}\right)_{T,\mathbf{n}} = \left(\left(\frac{\partial \boldsymbol{\eta}_X}{\partial n_i}\right)_{T,V}\right)^T \mathbf{X}''(\boldsymbol{\eta}_X)\left(\frac{\partial \boldsymbol{\eta}_X}{\partial V}\right)_{T,\mathbf{n}} + \left(\frac{\partial X}{\partial \boldsymbol{\eta}_X}\right)^T \cdot \left(\frac{\partial^2 \boldsymbol{\eta}_X}{\partial n_i \partial V}\right)_{T,V,\mathbf{n}/n_i} \tag{4-236}$$

$$\left(\frac{\partial^2 X}{\partial V \partial n_i}\right)_{T,\mathbf{n}} = \left(\frac{\partial^2 X}{\partial \Gamma^2}\right)_{\boldsymbol{\eta}_X/\Gamma} \cdot \left(\frac{\partial \Gamma}{\partial V}\right)_{T,\mathbf{n}} \left(\frac{\partial \Gamma}{\partial n_i}\right)_{T,V,\mathbf{n}/n_i} +$$
$$\left(\frac{\partial^2 X}{\partial n_i \partial \Gamma}\right)_{\Gamma,\mathbf{n}/n_i}\left(\frac{\partial n_i}{\partial n_i}\right)_{T,V,\mathbf{n}/n_i}\left(\frac{\partial \Gamma}{\partial V}\right)_{T,\mathbf{n}} + \left(\frac{\partial X}{\partial \Gamma}\right)_{\boldsymbol{\eta}_X/\Gamma} \cdot \left(\frac{\partial^2 \Gamma}{\partial n_i \partial V}\right)_{T,V,\mathbf{n}/n_i} \tag{4-237}$$

$\left(\frac{\partial^2 \Gamma}{\partial V^2}\right)_{T,\mathbf{n}}$, $\left(\frac{\partial^2 \Gamma}{\partial n_i \partial V}\right)_{T,V,\mathbf{n}/n_i}$ can be calculated by (4-319) and (4-317)

$$\left(\frac{\partial^2 X}{\partial T^2}\right)_{V,\mathbf{n}} = \left(\left(\frac{\partial \boldsymbol{\eta}_X}{\partial T}\right)_{V,\mathbf{n}}\right)^T \mathbf{X}''(\boldsymbol{\eta}_X)\left(\frac{\partial \boldsymbol{\eta}_X}{\partial T}\right)_{V,\mathbf{n}} + \left(\frac{\partial X}{\partial \boldsymbol{\eta}_X}\right)^T \cdot \left(\frac{\partial^2 \boldsymbol{\eta}_X}{\partial T^2}\right)_{V,\mathbf{n}} \tag{4-238}$$

$$\left(\frac{\partial^2 X}{\partial T^2}\right)_{V,\mathbf{n}} = \left(\frac{\partial^2 X}{\partial \Gamma^2}\right)_{\boldsymbol{\eta}_X/\Gamma} \cdot \left(\frac{\partial \Gamma}{\partial T}\right)^2_{V,\mathbf{n}} + \left(\frac{\partial X}{\partial \Gamma}\right)_{\boldsymbol{\eta}_X/\Gamma} \cdot \left(\frac{\partial^2 \Gamma}{\partial T^2}\right)_{V,\mathbf{n}} \tag{4-239}$$

$$\left(\frac{\partial^2 X}{\partial T \partial n_i}\right)_{V,\mathbf{n}} = \left(\left(\frac{\partial \boldsymbol{\eta}_X}{\partial n_i}\right)_{T,V}\right)^T \mathbf{X}''(\boldsymbol{\eta}_X)\left(\frac{\partial \boldsymbol{\eta}_X}{\partial T}\right)_{V,\mathbf{n}} + \left(\frac{\partial X}{\partial \boldsymbol{\eta}_X}\right)^T \cdot \left(\frac{\partial^2 \boldsymbol{\eta}_X}{\partial n_i \partial T}\right)_{T,V,\mathbf{n}/n_i} \tag{4-240}$$

$$\left(\frac{\partial^2 X}{\partial T \partial n_i}\right)_{V,\mathbf{n}} = \left(\frac{\partial^2 X}{\partial \Gamma^2}\right)_{\boldsymbol{\eta}_X/\Gamma} \cdot \left(\frac{\partial \Gamma}{\partial T}\right)_{V,\mathbf{n}} \left(\frac{\partial \Gamma}{\partial n_i}\right)_{T,V,\mathbf{n}/n_i} +$$
$$\left(\frac{\partial^2 X}{\partial n_i \partial \Gamma}\right)_{\Gamma,\mathbf{n}/n_i}\left(\frac{\partial n_i}{\partial n_i}\right)_{T,V,\mathbf{n}/n_i}\left(\frac{\partial \Gamma}{\partial T}\right)_{V,\mathbf{n}} + \left(\frac{\partial X}{\partial \Gamma}\right)_{\boldsymbol{\eta}_X/\Gamma} \cdot \left(\frac{\partial^2 \Gamma}{\partial n_i \partial T}\right)_{T,V,\mathbf{n}/n_i} \tag{4-241}$$

$$\left(\frac{\partial^2 X}{\partial V \partial T}\right)_{T,\mathbf{n}} = \left(\left(\frac{\partial \boldsymbol{\eta}_X}{\partial T}\right)_{V,\mathbf{n}}\right)^T \mathbf{X}''(\boldsymbol{\eta}_X)\left(\frac{\partial \boldsymbol{\eta}_X}{\partial V}\right)_{T,\mathbf{n}} + \left(\frac{\partial X}{\partial \boldsymbol{\eta}_X}\right)^T \cdot \left(\frac{\partial^2 \boldsymbol{\eta}_X}{\partial T \partial V}\right)_{V,\mathbf{n}} \tag{4-242}$$

$$\boxed{\left(\frac{\partial^2 X}{\partial V \partial T}\right)_{T,\mathbf{n}} = \left(\frac{\partial^2 X}{\partial \Gamma^2}\right)_{\boldsymbol{\eta}_X/\Gamma} \cdot \left(\frac{\partial \Gamma}{\partial V}\right)_{T,\mathbf{n}} \left(\frac{\partial \Gamma}{\partial T}\right)_{V,\mathbf{n}} + \left(\frac{\partial X}{\partial \Gamma}\right)_{\boldsymbol{\eta}_X/\Gamma} \cdot \left(\frac{\partial^2 \Gamma}{\partial T \partial V}\right)_{V,\mathbf{n}}} \tag{4-243}$$

$\left(\frac{\partial^2 \Gamma}{\partial T^2}\right)_{V,\mathbf{n}}$, $\left(\frac{\partial^2 \Gamma}{\partial n_i \partial T}\right)_{T,V,\mathbf{n}/n_i}$ and $\left(\frac{\partial^2 \Gamma}{\partial T \partial V}\right)_{V,\mathbf{n}}$ can be calculated by (4-319) and (4-317)

$$\left(\frac{\partial^2 Y}{\partial n_i \partial n_j}\right)_{T,V,\mathbf{n}/n_i} = \left(\left(\frac{\partial \boldsymbol{\eta}_Y}{\partial n_i}\right)_{T,V}\right)^T \mathbf{Y}''(\boldsymbol{\eta}_Y)\left(\frac{\partial \boldsymbol{\eta}_Y}{\partial n_j}\right)_{T,V} + \left(\frac{\partial Y}{\partial \boldsymbol{\eta}_Y}\right)^T \cdot \left(\frac{\partial^2 \boldsymbol{\eta}_Y}{\partial n_i \partial n_j}\right)_{T,V} \tag{4-244}$$

$$\left(\frac{\partial^2 \boldsymbol{\eta}_Y}{\partial n_i \partial n_j}\right)_{T,V} = \begin{bmatrix} \left(\frac{\partial^2 \Gamma}{\partial n_i \partial n_j}\right)_{T,V} & 0 \end{bmatrix} \tag{4-245}$$

$$\mathbf{Y}''(\boldsymbol{\eta}_Y) = \begin{bmatrix} \left(\frac{\partial^2 Y}{\partial \Gamma^2}\right)_V & \left(\frac{\partial^2 Y}{\partial V \partial \Gamma}\right)_\Gamma \\ \left(\frac{\partial^2 Y}{\partial V \partial \Gamma}\right)_V & \left(\frac{\partial^2 Y}{\partial V^2}\right)_\Gamma \end{bmatrix} = \begin{bmatrix} \frac{2\Gamma V}{\pi N_A} & \frac{\Gamma^2}{\pi N_A} \\ \frac{\Gamma^2}{\pi N_A} & 0 \end{bmatrix} \tag{4-246}$$

$$\left(\frac{\partial^2 Y}{\partial n_i \partial n_j}\right)_{T,V,\mathbf{n}/n_i} = \left(\frac{\partial^2 Y}{\partial \Gamma^2}\right)_V \left(\frac{\partial \Gamma}{\partial n_j}\right)_{T,V,\mathbf{n}/n_j} \left(\frac{\partial \Gamma}{\partial n_i}\right)_{T,V,\mathbf{n}/n_i} + \left(\frac{\partial Y}{\partial \Gamma}\right)_V \cdot \left(\frac{\partial^2 \Gamma}{\partial n_i \partial n_j}\right)_{T,V,\mathbf{n}/n_i} \tag{4-247}$$

$$\left(\frac{\partial^2 Y}{\partial V^2}\right)_{T,\mathbf{n}} = \left(\left(\frac{\partial \boldsymbol{\eta}_Y}{\partial V}\right)_{T,\mathbf{n}}\right)^T \mathbf{Y}''(\boldsymbol{\eta}_Y)\left(\frac{\partial \boldsymbol{\eta}_Y}{\partial V}\right)_{T,\mathbf{n}} + \left(\frac{\partial Y}{\partial \boldsymbol{\eta}_Y}\right)^T \cdot \left(\frac{\partial^2 \boldsymbol{\eta}_Y}{\partial V^2}\right)_{T,\mathbf{n}} \tag{4-248}$$

$$\boxed{\begin{aligned} \left(\frac{\partial^2 Y}{\partial V^2}\right)_{T,\mathbf{n}} &= \left(\frac{\partial^2 Y}{\partial \Gamma^2}\right)_{\boldsymbol{\eta}_Y/\Gamma} \cdot \left(\frac{\partial \Gamma}{\partial V}\right)^2_{T,\mathbf{n}} + \left(\frac{\partial^2 Y}{\partial \Gamma \partial V}\right)_{\boldsymbol{\eta}_Y/\Gamma} \cdot \left(2\frac{\partial \Gamma}{\partial V}\right)_{T,\mathbf{n}} + \\ &\left(\frac{\partial^2 Y}{\partial V^2}\right)_{\boldsymbol{\eta}_Y/V} \cdot \left(\frac{\partial V}{\partial V}\right)^2_{T,\mathbf{n}} + \left(\frac{\partial Y}{\partial \Gamma}\right)_{\boldsymbol{\eta}_Y/\Gamma} \cdot \left(\frac{\partial^2 \Gamma}{\partial V^2}\right)_{T,\mathbf{n}} \end{aligned}} \tag{4-249}$$

$$\left(\frac{\partial^2 Y}{\partial V \partial n_i}\right)_{T,\mathbf{n}} = \left(\left(\frac{\partial \boldsymbol{\eta}_Y}{\partial n_i}\right)_{T,V,\mathbf{n}/n_i}\right)^T \mathbf{Y}''(\boldsymbol{\eta}_Y)\left(\frac{\partial \boldsymbol{\eta}_Y}{\partial V}\right)_{T,\mathbf{n}} + \left(\frac{\partial Y}{\partial \boldsymbol{\eta}_Y}\right)^T \cdot \left(\frac{\partial^2 \boldsymbol{\eta}_Y}{\partial n_i \partial V}\right)_{T,V,\mathbf{n}/n_i} \tag{4-250}$$

$$\boxed{\begin{aligned} \left(\frac{\partial^2 Y}{\partial V \partial n_i}\right)_{T,\mathbf{n}} &= \left(\frac{\partial^2 Y}{\partial \Gamma^2}\right)_{\boldsymbol{\eta}_X/\Gamma} \cdot \left(\frac{\partial \Gamma}{\partial V}\right)_{T,\mathbf{n}} \left(\frac{\partial \Gamma}{\partial n_i}\right)_{T,V,\mathbf{n}/n_i} + \\ &\left(\frac{\partial^2 Y}{\partial \Gamma \partial V}\right)_{\boldsymbol{\eta}_Y/\Gamma} \left(\frac{\partial \Gamma}{\partial n_i}\right)_{T,V,\mathbf{n}/n_i} \left(\frac{\partial V}{\partial V}\right)_{T,\mathbf{n}} + \left(\frac{\partial Y}{\partial \Gamma}\right)_{\boldsymbol{\eta}_Y/\Gamma} \cdot \left(\frac{\partial^2 \Gamma}{\partial n_i \partial V}\right)_{T,V,\mathbf{n}/n_i} \end{aligned}} \tag{4-251}$$

$\left(\frac{\partial^2 \Gamma}{\partial V^2}\right)_{T,\mathbf{n}}$, $\left(\frac{\partial^2 \Gamma}{\partial n_i \partial V}\right)_{T,V,\mathbf{n}/n_i}$ can be calculated by (4-319) and (4-317)

$$\left(\frac{\partial^2 Y}{\partial T^2}\right)_{V,\mathbf{n}} = \left(\left(\frac{\partial \boldsymbol{\eta}_Y}{\partial T}\right)_{V,\mathbf{n}}\right)^T \mathbf{Y}''(\boldsymbol{\eta}_Y)\left(\frac{\partial \boldsymbol{\eta}_Y}{\partial T}\right)_{V,\mathbf{n}} + \left(\frac{\partial Y}{\partial \boldsymbol{\eta}_Y}\right)^T \cdot \left(\frac{\partial^2 \boldsymbol{\eta}_Y}{\partial T^2}\right)_{V,\mathbf{n}} \tag{4-252}$$

$$\boxed{\left(\frac{\partial^2 Y}{\partial T^2}\right)_{V,\mathbf{n}} = \left(\frac{\partial^2 Y}{\partial \Gamma^2}\right)_{\boldsymbol{\eta}_Y/\Gamma} \cdot \left(\frac{\partial \Gamma}{\partial T}\right)^2_{V,\mathbf{n}} + \left(\frac{\partial Y}{\partial \Gamma}\right)_{\boldsymbol{\eta}_Y/\Gamma} \cdot \left(\frac{\partial^2 \Gamma}{\partial T^2}\right)_{V,\mathbf{n}}} \tag{4-253}$$

$$\left(\frac{\partial^2 Y}{\partial T \partial n_i}\right)_{V,\mathbf{n}} = \left(\left(\frac{\partial \boldsymbol{\eta}_Y}{\partial n_i}\right)_{T,V}\right)^T \mathbf{Y}''(\boldsymbol{\eta}_Y)\left(\frac{\partial \boldsymbol{\eta}_Y}{\partial T}\right)_{V,\mathbf{n}} + \left(\frac{\partial Y}{\partial \boldsymbol{\eta}_Y}\right)^T \cdot \left(\frac{\partial^2 \boldsymbol{\eta}_Y}{\partial n_i \partial T}\right)_{T,V,\mathbf{n}/n_i} \tag{4-254}$$

$$\boxed{\left(\frac{\partial^2 Y}{\partial T \partial n_i}\right)_{V,\mathbf{n}} = \left(\frac{\partial^2 Y}{\partial \Gamma^2}\right)_{\boldsymbol{\eta}_Y/\Gamma} \cdot \left(\frac{\partial \Gamma}{\partial T}\right)_{V,\mathbf{n}} \left(\frac{\partial \Gamma}{\partial n_i}\right)_{T,V,\mathbf{n}/n_i} + \left(\frac{\partial Y}{\partial \Gamma}\right)_{\boldsymbol{\eta}_Y/\Gamma} \cdot \left(\frac{\partial^2 \Gamma}{\partial n_i \partial T}\right)_{T,V,\mathbf{n}/n_i}} \tag{4-255}$$

$$\left(\frac{\partial^2 Y}{\partial V \partial T}\right)_{T,\mathbf{n}} = \left(\left(\frac{\partial \boldsymbol{\eta}_Y}{\partial T}\right)_{V,\mathbf{n}}\right)^T \mathbf{Y}''(\boldsymbol{\eta}_Y)\left(\frac{\partial \boldsymbol{\eta}_Y}{\partial V}\right)_{T,\mathbf{n}} + \left(\frac{\partial Y}{\partial \boldsymbol{\eta}_Y}\right)^T \cdot \left(\frac{\partial^2 \boldsymbol{\eta}_Y}{\partial T \partial V}\right)_{V,\mathbf{n}} \tag{4-256}$$

$$\boxed{\begin{aligned}\left(\frac{\partial^2 Y}{\partial V \partial T}\right)_{T,\mathbf{n}} &= \left(\frac{\partial^2 Y}{\partial \Gamma^2}\right)_{\boldsymbol{\eta}_Y/\Gamma} \cdot \left(\frac{\partial \Gamma}{\partial V}\right)_{T,\mathbf{n}} \left(\frac{\partial \Gamma}{\partial T}\right)_{V,\mathbf{n}} \\ &+ \left(\frac{\partial^2 Y}{\partial \Gamma \partial V}\right)_{\boldsymbol{\eta}_Y/\Gamma} \left(\frac{\partial V}{\partial V}\right)_{T,\mathbf{n}} \left(\frac{\partial \Gamma}{\partial T}\right)_{V,\mathbf{n}} + \left(\frac{\partial Y}{\partial \Gamma}\right)_{\boldsymbol{\eta}_Y/\Gamma} \cdot \left(\frac{\partial^2 \Gamma}{\partial T \partial V}\right)_{V,\mathbf{n}}\end{aligned}} \tag{4-257}$$

$\left(\frac{\partial^2 \Gamma}{\partial T^2}\right)_{V,\mathbf{n}}$, $\left(\frac{\partial^2 \Gamma}{\partial n_i \partial T}\right)_{T,V,\mathbf{n}/n_i}$ and $\left(\frac{\partial^2 \Gamma}{\partial T \partial V}\right)_{V,\mathbf{n}}$ can be calculated by (4-319) and (4-317)

$$\left(\frac{\partial^2 \boldsymbol{\eta}_{F_{sMSA}}}{\partial V^2}\right)_{\mathbf{n},T} = \left(\frac{\partial^2}{\partial V^2}\left[\alpha^2_{sMSA} \quad X \quad Y\right]^T\right)_{\mathbf{n},T} = \left[\left(\frac{\partial^2 \alpha^2_{sMSA}}{\partial V^2}\right)_{\mathbf{n},T} \quad \left(\frac{\partial^2 X}{\partial V^2}\right)_{\mathbf{n},T} \quad \left(\frac{\partial^2 Y}{\partial V^2}\right)_{\mathbf{n},T}\right]^T \tag{4-258}$$

From $\left(\frac{\partial \alpha^2_{sMSA}}{\partial V}\right)_{\mathbf{n},T} = -\frac{\alpha^2_{sMSA}}{\varepsilon}\left(\frac{\partial \varepsilon}{\partial V}\right)_{\mathbf{n},T}$ we have:

$$\boxed{\left(\frac{\partial^2 \alpha^2_{sMSA}}{\partial V^2}\right)_{\mathbf{n},T} = -\frac{1}{\varepsilon}\left(\left(\frac{\partial \varepsilon}{\partial V}\right)_{\mathbf{n},T}\left(\frac{\partial \alpha^2_{sMSA}}{\partial V}\right)_{\mathbf{n},T} + \alpha^2_{sMSA}\left(\left(\frac{\partial^2 \varepsilon}{\partial V^2}\right)_{\mathbf{n},T} - \frac{1}{\varepsilon}\left(\frac{\partial \varepsilon}{\partial V}\right)^2_{\mathbf{n},T}\right)\right)} \tag{4-259}$$

$$\left(\frac{\partial^2 \boldsymbol{\eta}_{F_{sMSA}}}{\partial V \partial n_i}\right)_{\mathbf{n},T} = \left(\frac{\partial^2}{\partial V \partial n_i}\left[\alpha^2_{sMSA} \quad X \quad Y\right]^T\right)_{\mathbf{n},T} = \left[\left(\frac{\partial^2 \alpha^2_{sMSA}}{\partial V \partial n_i}\right)_{\mathbf{n},T} \quad \left(\frac{\partial^2 X}{\partial V \partial n_i}\right)_{\mathbf{n},T} \quad \left(\frac{\partial^2 Y}{\partial V \partial n_i}\right)_{\mathbf{n},T}\right]^T \tag{4-260}$$

$$\boxed{\left(\frac{\partial^2 \alpha^2_{sMSA}}{\partial V \partial n_i}\right)_{\mathbf{n},T} = -\frac{1}{\varepsilon}\left(\left(\frac{\partial \alpha^2_{sMSA}}{\partial n_i}\right)_{\mathbf{n}/n_i,T,V}\left(\frac{\partial \varepsilon}{\partial V}\right)_{\mathbf{n},T} + \alpha^2_{sMSA}\left(\left(\frac{\partial^2 \varepsilon}{\partial V \partial n_i}\right)_{\mathbf{n},T} - \frac{1}{\varepsilon}\left(\frac{\partial \varepsilon}{\partial V}\right)_{\mathbf{n},T}\left(\frac{\partial \varepsilon}{\partial n_i}\right)_{\mathbf{n}/n_i,T,V}\right)\right)} \tag{4-261}$$

$$\mathbf{F}''(\boldsymbol{\eta}_{F_{sMSA}}) = \begin{bmatrix} 0 & -1/4\pi & 0 \\ -1/4\pi & 0 & 0 \\ 0 & 0 & 0 \end{bmatrix} \tag{4-262}$$

The second order differentials is given as :

$$\frac{\partial^2 F_{sMSA\_Furst}(\boldsymbol{\eta})}{\partial n_i \partial n_j} = \left(\left(\frac{\partial \boldsymbol{\eta}_{F_{sMSA}}}{\partial n_i} \right)_{T,V} \right)^T \mathbf{F}''(\boldsymbol{\eta}_{F_{sMSA}}) \left(\frac{\partial \boldsymbol{\eta}_{F_{sMSA}}}{\partial n_j} \right)_{T,V} + \left(\frac{\partial F}{\partial \boldsymbol{\eta}_{F_{sMSA}}} \right)^T \cdot \left(\frac{\partial^2 \boldsymbol{\eta}_{F_{sMSA}}}{\partial n_i \partial n_j} \right)_{T,V} \tag{4-263}$$

$$\frac{\partial^2 F_{sMSA\_Furst}(\boldsymbol{\eta})}{\partial n_i \partial n_j} = -\frac{1}{4\pi} \left(\left(\frac{\partial \alpha_{sMSA}^2}{\partial n_i} \right)_{T,V,\mathbf{n}/n_i} \left(\frac{\partial X}{\partial n_j} \right)_{T,V,\mathbf{n}/n_j} + \left(\frac{\partial X}{\partial n_i} \right)_{T,V,\mathbf{n}/n_i} \left(\frac{\partial \alpha_{sMSA}^2}{\partial n_j} \right)_{T,V,\mathbf{n}/n_j} \right)$$
$$+ \left[\left(\frac{\partial F}{\partial \alpha_{sMSA}^2} \right)_{\boldsymbol{\eta}_F / \alpha_{sMSA}^2} \left(\frac{\partial^2 \alpha_{sMSA}^2}{\partial n_i \partial n_j} \right)_{T,V,\mathbf{n}/n_i} + \left(\frac{\partial F}{\partial X} \right)_{\boldsymbol{\eta}_F / X} \left(\frac{\partial^2 X}{\partial n_i \partial n_j} \right)_{T,V,\mathbf{n}/n_i} + \left(\frac{\partial F}{\partial Y} \right)_{\boldsymbol{\eta}_F / Y} \left(\frac{\partial^2 Y}{\partial n_i \partial n_j} \right)_{T,V,\mathbf{n}/n_i} \right] \tag{4-264}$$

$$\frac{\partial^2 F_{sMSA\_Furst}}{\partial V^2} = \left(\left(\frac{\partial \boldsymbol{\eta}_{F_{sMSA}}}{\partial V} \right)_{\mathbf{n},T} \right)^T \mathbf{F}''(\boldsymbol{\eta}_{F_{sMSA}}) \left(\frac{\partial \boldsymbol{\eta}_{F_{sMSA}}}{\partial V} \right)_{\mathbf{n},T} + \left(\frac{\partial F}{\partial \boldsymbol{\eta}_{F_{sMSA}}} \right)^T \left(\frac{\partial^2 \boldsymbol{\eta}_{F_{sMSA}}}{\partial V^2} \right)_{\mathbf{n},T}$$
$$= \left(\frac{\partial^2 F}{\partial \alpha_{sMSA}^2 \partial X} \right)_{\boldsymbol{\eta}_F / \alpha_{sMSA}^2} \left(2 \left(\frac{\partial \alpha_{sMSA}^2}{\partial V} \right)_{\mathbf{n},T} \left(\frac{\partial X}{\partial V} \right)_{\mathbf{n},T} \right) + \tag{4-265}$$
$$\left[\left(\frac{\partial F}{\partial \alpha_{sMSA}^2} \right)_{\boldsymbol{\eta}_F / \alpha_{sMSA}^2} \left(\frac{\partial^2 \alpha_{sMSA}^2}{\partial V^2} \right)_{\mathbf{n},T} + \left(\frac{\partial F}{\partial X} \right)_{\boldsymbol{\eta}_F / X} \left(\frac{\partial^2 X}{\partial V^2} \right)_{\mathbf{n},T} + \left(\frac{\partial F}{\partial Y} \right)_{\boldsymbol{\eta}_F / Y} \left(\frac{\partial^2 Y}{\partial V^2} \right)_{\mathbf{n},T} \right]$$

$$\boxed{\frac{\partial^2 F_{sMSA\_Furst}}{\partial V^2} = -\frac{1}{2\pi} \left(\frac{\partial \alpha_{sMSA}^2}{\partial V} \right)_{\mathbf{n},T} \left(\frac{\partial X}{\partial V} \right)_{\mathbf{n},T} + \left[\left(\frac{\partial F}{\partial \alpha_{sMSA}^2} \right)_{\boldsymbol{\eta}_F / \alpha_{sMSA}^2} \left(\frac{\partial^2 \alpha_{sMSA}^2}{\partial V^2} \right)_{\mathbf{n},T} + \left(\frac{\partial F}{\partial X} \right)_{\boldsymbol{\eta}_F / X} \left(\frac{\partial^2 X}{\partial V^2} \right)_{\mathbf{n},T} + \left(\frac{\partial F}{\partial Y} \right)_{\boldsymbol{\eta}_F / Y} \left(\frac{\partial^2 Y}{\partial V^2} \right)_{\mathbf{n},T} \right]} \tag{4-266}$$

$$\left(\frac{\partial^2 F_{sMSA\_Furst}(\boldsymbol{\eta}_{F_{sMSA}})}{\partial V \partial n_i} \right)_{\mathbf{n},T} = \left(\left(\frac{\partial \boldsymbol{\eta}_{F_{sMSA}}}{\partial V} \right)_{\mathbf{n},T} \right)^T \mathbf{F}''(\boldsymbol{\eta}_{F_{sMSA}}) \left(\frac{\partial \boldsymbol{\eta}_{F_{sMSA}}}{\partial n_i} \right)_{T,V} + \left(\frac{\partial F}{\partial \boldsymbol{\eta}_{F_{sMSA}}} \right)^T \cdot \left(\frac{\partial^2 \boldsymbol{\eta}_{F_{sMSA}}}{\partial V \partial n_i} \right)_{\mathbf{n},T}$$
$$= \left(\frac{\partial^2 F}{\partial \alpha_{sMSA}^2 \partial X} \right)_{\boldsymbol{\eta}_F / \alpha_{sMSA}^2} \left(\left(\frac{\partial \alpha_{sMSA}^2}{\partial V} \right)_{\mathbf{n},T} \left(\frac{\partial X}{\partial n_i} \right)_{T,V,\mathbf{n}/n_i} + \left(\frac{\partial \alpha_{sMSA}^2}{\partial n_i} \right)_{T,V,\mathbf{n}/n_i} \left(\frac{\partial X}{\partial V} \right)_{\mathbf{n},T} \right) +$$
$$\left[\left(\frac{\partial F}{\partial \alpha_{sMSA}^2} \right)_{\boldsymbol{\eta}_F / \alpha_{sMSA}^2} \left(\frac{\partial^2 \alpha_{sMSA}^2}{\partial V \partial n_i} \right)_{\mathbf{n},T} + \left(\frac{\partial F}{\partial X} \right)_{\boldsymbol{\eta}_F / X} \left(\frac{\partial^2 X}{\partial V \partial n_i} \right)_{\mathbf{n},T} + \left(\frac{\partial F}{\partial Y} \right)_{\boldsymbol{\eta}_F / Y} \left(\frac{\partial^2 Y}{\partial V \partial n_i} \right)_{\mathbf{n},T} \right] \tag{4-267}$$

$$\left(\frac{\partial^2 F_{sMSA\_Furst}(\boldsymbol{\eta}_{F_{sMSA}})}{\partial V \partial n_i}\right)_{\mathbf{n},T} = -\frac{1}{4\pi}\left(\left(\frac{\partial \alpha^2_{sMSA}}{\partial V}\right)_{\mathbf{n},T}\left(\frac{\partial X}{\partial n_i}\right)_{T,V,\mathbf{n}/n_i} + \left(\frac{\partial \alpha^2_{sMSA}}{\partial n_i}\right)_{T,V,\mathbf{n}/n_i}\left(\frac{\partial X}{\partial V}\right)_{\mathbf{n},T}\right) + \left[\left(\frac{\partial F}{\partial \alpha^2_{sMSA}}\right)_{\boldsymbol{\eta}_F/\alpha^2_{sMSA}}\left(\frac{\partial^2 \alpha^2_{sMSA}}{\partial V \partial n_i}\right)_{\mathbf{n},T} + \left(\frac{\partial F}{\partial X}\right)_{\boldsymbol{\eta}_F/X}\left(\frac{\partial^2 X}{\partial V \partial n_i}\right)_{\mathbf{n},T} + \left(\frac{\partial F}{\partial Y}\right)_{\boldsymbol{\eta}_F/Y}\left(\frac{\partial^2 Y}{\partial V \partial n_i}\right)_{\mathbf{n},T}\right] \quad (4\text{-}268)$$

$$\left(\frac{\partial^2 F_{sMSA\_Furst}}{\partial T^2}\right)_{\mathbf{n},V} = \left(\frac{\partial^2 F}{\partial \alpha^2_{sMSA}\partial X}\right)_{\boldsymbol{\eta}_F/\alpha^2_{sMSA}}\left(2\cdot\left(\frac{\partial \alpha^2_{sMSA}}{\partial T}\right)_{V,\mathbf{n}}\left(\frac{\partial X}{\partial T}\right)_{V,\mathbf{n}}\right) + \left[\left(\frac{\partial F}{\partial \alpha^2_{sMSA}}\right)_{\boldsymbol{\eta}_F/\alpha^2_{sMSA}}\left(\frac{\partial^2 \alpha^2_{sMSA}}{\partial T^2}\right)_{V,\mathbf{n}} + \left(\frac{\partial F}{\partial X}\right)_{\boldsymbol{\eta}_F/X}\left(\frac{\partial^2 X}{\partial T^2}\right)_{V,\mathbf{n}} + \left(\frac{\partial F}{\partial Y}\right)_{\boldsymbol{\eta}_F/Y}\left(\frac{\partial^2 Y}{\partial T^2}\right)_{V,\mathbf{n}}\right] \quad (4\text{-}269)$$

$$\left(\frac{\partial^2 F_{sMSA\_Furst}}{\partial T^2}\right)_{\mathbf{n},V} = -\frac{1}{2\pi}\cdot\left(\frac{\partial \alpha^2_{sMSA}}{\partial T}\right)_{V,\mathbf{n}}\left(\frac{\partial X}{\partial T}\right)_{V,\mathbf{n}} + \left[\left(\frac{\partial F}{\partial \alpha^2_{sMSA}}\right)_{\boldsymbol{\eta}_F/\alpha^2_{sMSA}}\left(\frac{\partial^2 \alpha^2_{sMSA}}{\partial T^2}\right)_{V,\mathbf{n}} + \left(\frac{\partial F}{\partial X}\right)_{\boldsymbol{\eta}_F/X}\left(\frac{\partial^2 X}{\partial T^2}\right)_{V,\mathbf{n}} + \left(\frac{\partial F}{\partial Y}\right)_{\boldsymbol{\eta}_F/Y}\left(\frac{\partial^2 Y}{\partial T^2}\right)_{V,\mathbf{n}}\right] \quad (4\text{-}270)$$

$$\left(\frac{\partial^2 F_{sMSA\_Furst}}{\partial T \partial V}\right)_{\mathbf{n},V} = \left(\frac{\partial^2 F}{\partial \alpha^2_{sMSA}\partial X}\right)_{\boldsymbol{\eta}_F/\alpha^2_{sMSA}}\left(\left(\frac{\partial \alpha^2_{sMSA}}{\partial T}\right)_{V,\mathbf{n}}\left(\frac{\partial X}{\partial V}\right)_{\mathbf{n},T} + \left(\frac{\partial \alpha^2_{sMSA}}{\partial V}\right)_{\mathbf{n},T}\left(\frac{\partial X}{\partial T}\right)_{V,\mathbf{n}}\right) + \left[\left(\frac{\partial F}{\partial \alpha^2_{sMSA}}\right)_{\boldsymbol{\eta}_F/\alpha^2_{sMSA}}\left(\frac{\partial^2 \alpha^2_{sMSA}}{\partial V \partial T}\right)_{\mathbf{n},T} + \left(\frac{\partial F}{\partial X}\right)_{\boldsymbol{\eta}_F/X}\left(\frac{\partial^2 X}{\partial V \partial T}\right)_{\mathbf{n},T} + \left(\frac{\partial F}{\partial Y}\right)_{\boldsymbol{\eta}_F/Y}\left(\frac{\partial^2 Y}{\partial V \partial T}\right)_{\mathbf{n},T}\right] \quad (4\text{-}271)$$

$$\left(\frac{\partial^2 F_{sMSA\_Furst}}{\partial T \partial V}\right)_{\mathbf{n},V} = -\frac{1}{4\pi}\left(\left(\frac{\partial \alpha^2_{sMSA}}{\partial T}\right)_{V,\mathbf{n}}\left(\frac{\partial X}{\partial V}\right)_{\mathbf{n},T} + \left(\frac{\partial \alpha^2_{sMSA}}{\partial V}\right)_{\mathbf{n},T}\left(\frac{\partial X}{\partial T}\right)_{V,\mathbf{n}}\right) + \left[\left(\frac{\partial F}{\partial \alpha^2_{sMSA}}\right)_{\boldsymbol{\eta}_F/\alpha^2_{sMSA}}\left(\frac{\partial^2 \alpha^2_{sMSA}}{\partial V \partial T}\right)_{\mathbf{n},T} + \left(\frac{\partial F}{\partial X}\right)_{\boldsymbol{\eta}_F/X}\left(\frac{\partial^2 X}{\partial V \partial T}\right)_{\mathbf{n},T} + \left(\frac{\partial F}{\partial Y}\right)_{\boldsymbol{\eta}_F/Y}\left(\frac{\partial^2 Y}{\partial V \partial T}\right)_{\mathbf{n},T}\right] \quad (4\text{-}272)$$

$$\left(\frac{\partial^2 F_{sMSA\_Furst}}{\partial T \partial n_i}\right)_{\mathbf{n},V} = \left(\frac{\partial^2 F}{\partial \alpha^2_{sMSA}\partial X}\right)_{\boldsymbol{\eta}_F/\alpha^2_{sMSA}}\left(\left(\frac{\partial \alpha^2_{sMSA}}{\partial T}\right)_{V,\mathbf{n}}\left(\frac{\partial X}{\partial n_i}\right)_{T,V,\mathbf{n}/n_i} + \left(\frac{\partial \alpha^2_{sMSA}}{\partial n_i}\right)_{T,V,\mathbf{n}/n_i}\left(\frac{\partial X}{\partial T}\right)_{V,\mathbf{n}}\right) + \left[\left(\frac{\partial F}{\partial \alpha^2_{sMSA}}\right)_{\boldsymbol{\eta}_F/\alpha^2_{sMSA}}\left(\frac{\partial^2 \alpha^2_{sMSA}}{\partial T \partial n_i}\right)_{V,\mathbf{n}} + \left(\frac{\partial F}{\partial X}\right)_{\boldsymbol{\eta}_F/X}\left(\frac{\partial^2 X}{\partial T \partial n_i}\right)_{V,\mathbf{n}} + \left(\frac{\partial F}{\partial Y}\right)_{\boldsymbol{\eta}_F/Y}\left(\frac{\partial^2 Y}{\partial T \partial n_i}\right)_{V,\mathbf{n}}\right] \quad (4\text{-}273)$$

$$\left(\frac{\partial^2 F_{sMSA\_Furst}}{\partial T\partial n_i}\right)_{\mathbf{n},V} = -\frac{1}{4\pi}\left(\left(\frac{\partial\alpha_{sMSA}^2}{\partial T}\right)_{V,\mathbf{n}}\left(\frac{\partial X}{\partial n_i}\right)_{T,V,\mathbf{n}/n_i} + \left(\frac{\partial\alpha_{sMSA}^2}{\partial n_i}\right)_{T,V,\mathbf{n}/n_i}\left(\frac{\partial X}{\partial T}\right)_{V,\mathbf{n}}\right) + \left[\left(\frac{\partial F}{\partial\alpha_{sMSA}^2}\right)_{\boldsymbol{\eta}_F/\alpha_{sMSA}^2}\left(\frac{\partial^2\alpha_{sMSA}^2}{\partial T\partial n_i}\right)_{V,\mathbf{n}} + \left(\frac{\partial F}{\partial X}\right)_{\boldsymbol{\eta}_F/X}\left(\frac{\partial^2 X}{\partial T\partial n_i}\right)_{V,\mathbf{n}} + \left(\frac{\partial F}{\partial Y}\right)_{\boldsymbol{\eta}_F/Y}\left(\frac{\partial^2 Y}{\partial T\partial n_i}\right)_{V,\mathbf{n}}\right] \tag{4-274}$$

1.5 Implicit differentiation of the screening parameter Γ in the MSA term

1.5.1 First order partial derivatives

$$4\Gamma^2 = \alpha_{sMSA}^2 N_A \sum_i \frac{n_i z_i^{\,2}}{V\left(1+\Gamma\sigma_i\right)^2} \tag{4-275}$$

Define

$$\begin{aligned} &\mathrm{F_1}\left(\boldsymbol{\eta}_{\mathrm{F_1}}\right) = \mathrm{F_1}\left(\left[\Gamma, \alpha_{sMSA}^2, V, \mathbf{n}\right]^T\right) \\ &= 4\Gamma^2 - \alpha_{sMSA}^2 N_A \sum_i \frac{n_i z_i^{\,2}}{V\left(1+\Gamma\sigma_i\right)^2} = \; = 4\Gamma^2 - \alpha_{sMSA}^2 S\left(\boldsymbol{\eta}_S\right) = 0 \end{aligned} \tag{4-276}$$

where

$$S\left(\boldsymbol{\eta}_S\right) = S\left(\left[\Gamma, V, \mathbf{n}\right]^T\right) = N_A \sum_i \frac{n_i z_i^{\,2}}{V\left(1+\Gamma\sigma_i\right)^2} \tag{4-277}$$

$$\begin{aligned} \frac{\partial S}{\partial \boldsymbol{\eta}_S} &= \left[\left(\frac{\partial S}{\partial\Gamma}\right)_{\boldsymbol{\eta}_S/\Gamma} \quad \left(\frac{\partial S}{\partial V}\right)_{\boldsymbol{\eta}_S/V} \quad \left(\frac{\partial S}{\partial n_i}\right)_{\boldsymbol{\eta}_S/n_i}\right]^T \\ &= \left[-2N_A\sum_i \frac{n_i z_i^{\,2}\sigma_i}{V\left(1+\Gamma\sigma_i\right)^3} \quad -\sum_i \frac{N_A n_i z_i^{\,2}}{V^2\left(1+\Gamma\sigma_i\right)^2} \quad \frac{N_A z_i^{\,2}}{V\left(1+\Gamma\sigma_i\right)^2}\right]^T \end{aligned} \tag{4-278}$$

$$\mathbf{v}_\Gamma = \left[\alpha_{sMSA}^2 \quad \mathbf{n} \quad V\right]^T \tag{4-279}$$

The structure of the composite function expressed in a graph is as below:

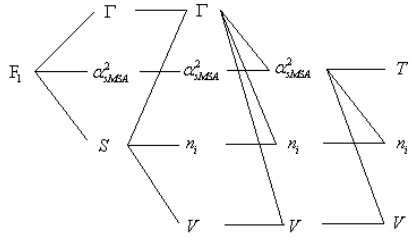

Use the equation of implicit differentiation:

$$\left(\frac{\partial\Gamma}{\partial V}\right)_{\mathbf{n},\alpha_{sMSA}^2}=-\left(\frac{\partial\,\mathrm{F}_1}{\partial V}\right)_{\boldsymbol{\eta}_{\mathrm{F}_1}/V}\Bigg/\left(\frac{\partial\,\mathrm{F}_1}{\partial\Gamma}\right)_{\boldsymbol{\eta}_{\mathrm{F}_1}/\Gamma}=\frac{\alpha_{sMSA}^2\left(\frac{\partial S}{\partial V}\right)_{\boldsymbol{\eta}_S/V}}{8\Gamma-\alpha_{sMSA}^2\left(\frac{\partial S}{\partial\Gamma}\right)_{\boldsymbol{\eta}_S/\Gamma}} \tag{4-280}$$

$$\left(\frac{\partial\Gamma}{\partial\alpha_{sMSA}^2}\right)_{\mathbf{n},V}=-\left(\frac{\partial\,\mathrm{F}_1}{\partial\alpha_{sMSA}^2}\right)_{\boldsymbol{\eta}_{\mathrm{F}_1}/\alpha_{sMSA}^2}\Bigg/\left(\frac{\partial\,\mathrm{F}_1}{\partial\Gamma}\right)_{\boldsymbol{\eta}_{\mathrm{F}_1}/\Gamma}=\frac{S}{8\Gamma-\alpha_{sMSA}^2\left(\frac{\partial S}{\partial\Gamma}\right)_{\boldsymbol{\eta}_S/\Gamma}} \tag{4-281}$$

$$\left(\frac{\partial\Gamma}{\partial n_i}\right)_{\mathbf{n}/n_i,V,\alpha_{sMSA}^2}=-\left(\frac{\partial\,\mathrm{F}_1}{\partial n_i}\right)_{\boldsymbol{\eta}_{\mathrm{F}_1}/n_i}\Bigg/\left(\frac{\partial\,\mathrm{F}_1}{\partial\Gamma}\right)_{\boldsymbol{\eta}_{\mathrm{F}_1}/\Gamma}=\frac{\alpha_{sMSA}^2\left(\frac{\partial S}{\partial n_i}\right)_{\boldsymbol{\eta}_S/n_i}}{8\Gamma-\alpha_{sMSA}^2\left(\frac{\partial S}{\partial\Gamma}\right)_{\boldsymbol{\eta}_S/\Gamma}} \tag{4-282}$$

$$\left(\frac{\partial\Gamma}{\partial n_j}\right)_{\mathbf{n}/n_j,V,\alpha_{sMSA}^2}=-\left(\frac{\partial\,\mathrm{F}_1}{\partial n_j}\right)_{\boldsymbol{\eta}_{\mathrm{F}_1}/n_j}\Bigg/\left(\frac{\partial\,\mathrm{F}_1}{\partial\Gamma}\right)_{\boldsymbol{\eta}_{\mathrm{F}_1}/\Gamma}=\frac{\alpha_{sMSA}^2\left(\frac{\partial S}{\partial n_j}\right)_{\boldsymbol{\eta}_S/n_j}}{8\Gamma-\alpha_{sMSA}^2\left(\frac{\partial S}{\partial\Gamma}\right)_{\boldsymbol{\eta}_S/\Gamma}} \tag{4-283}$$

Then we have

$$\frac{\partial\Gamma(n_i,T,V)}{\partial\boldsymbol{\eta}_\Gamma}=\left[\left(\frac{\partial\Gamma}{\partial\alpha_{sMSA}^2}\right)_{\mathbf{n},V}\quad\left(\frac{\partial\Gamma}{\partial n_i}\right)_{\mathbf{n}/n_i,\alpha_{sMSA}^2,V}\quad\left(\frac{\partial\Gamma}{\partial n_j}\right)_{\mathbf{n}/n_j,V,\alpha_{sMSA}^2}\left(\frac{\partial\Gamma}{\partial V}\right)_{\alpha_{sMSA}^2,\mathbf{n}}\right]^T=$$

$$(8V\Gamma+2\alpha_{sMSA}^2\sum_i\frac{\sigma_i n_i z_i^2}{\left(1+\Gamma\sigma_i\right)^3})^{-1}\left[\sum_i\frac{N_A n_i z_i^2}{\left(1+\Gamma\sigma_i\right)^2}\quad\frac{N_A\alpha_{sMSA}^2 z_i^2}{\left(1+\Gamma\sigma_i\right)^2}\quad\frac{N_A\alpha_{sMSA}^2 z_j^2}{\left(1+\Gamma\sigma_j\right)^2}\quad\frac{-\alpha_{sMSA}^2}{V}\sum_i\frac{N_A n_i z_i^2}{\left(1+\Gamma\sigma_i\right)^2}\right]^T \tag{4-284}$$

1.5.2 Second order partial derivatives

Note

$$y=\frac{u}{v}\quad\Rightarrow\qquad y'=\frac{u'v-uv'}{v^2}\quad\Rightarrow\qquad y'=\frac{u'-yv'}{v} \tag{4-285}$$

$$\begin{bmatrix} \left(\frac{\partial^2 S}{\partial \Gamma^2}\right)_{\boldsymbol{\eta}_S/\Gamma} \\ \left(\frac{\partial^2 S}{\partial n_i \partial \Gamma}\right)_{\boldsymbol{\eta}_S/n_i} \\ \left(\frac{\partial^2 S}{\partial \Gamma \partial V}\right)_{\boldsymbol{\eta}_S/\Gamma} \\ \left(\frac{\partial^2 S}{\partial n_i \partial n_j}\right)_{\boldsymbol{\eta}_S/n_i} \\ \left(\frac{\partial^2 S}{\partial V^2}\right)_{\boldsymbol{\eta}_S/V} \\ \left(\frac{\partial^2 S}{\partial n_i \partial V}\right)_{\boldsymbol{\eta}_S/n_i} \end{bmatrix} = \begin{bmatrix} 6\sum_i \left(\frac{\partial S}{\partial \Gamma}\right)_i \frac{\sigma_i}{1+\Gamma\sigma_i} \\ \frac{1}{n_i}\left(\frac{\partial S}{\partial \Gamma}\right)_i \\ -\frac{1}{V}\left(\frac{\partial S}{\partial \Gamma}\right)_{\boldsymbol{\eta}_S/\Gamma} \\ 0 \\ -\frac{2}{V}\left(\frac{\partial S}{\partial V}\right)_{\boldsymbol{\eta}_S/V} \\ \frac{1}{V}\left(\frac{\partial S}{\partial n_i}\right)_{\boldsymbol{\eta}_S/n_i} \end{bmatrix} = \begin{bmatrix} 6\sum_i \frac{N_A n_i {z_i}^2 {\sigma_i}^2}{V\left(1+\Gamma\sigma_i\right)^4} \\ \frac{-2\sigma_i {z_i}^2 N_A}{V\left(1+\Gamma\sigma_i\right)^3} \\ \sum_i \frac{2N_A n_i {z_i}^2 \sigma_i}{V^2\left(1+\Gamma\sigma_i\right)^3} \\ 0 \\ 2\sum_i \frac{N_A n_i {z_i}^2}{V^3\left(1+\Gamma\sigma_i\right)^2} \\ \frac{-{z_i}^2 N_A}{V^2\left(1+\Gamma\sigma_i\right)^2} \end{bmatrix}$$

(4-286)

$$\left(\frac{\partial^2 \Gamma}{\left(\partial \alpha_{sMSA}^2\right)^2}\right)_{\mathbf{n},V} = \left(\frac{\partial}{\partial \alpha_{sMSA}^2}\left(\frac{\partial \Gamma}{\partial \alpha_{sMSA}^2}\right)_{\mathbf{n},V}\right)_{\mathbf{n},V} = \left(\frac{\partial}{\partial \alpha_{sMSA}^2}\left(\frac{\partial \Gamma}{\partial \alpha_{sMSA}^2}\right)_{\boldsymbol{\eta}_\Gamma/\alpha_{sMSA}^2}\right)_{\boldsymbol{\eta}_\Gamma/\alpha_{sMSA}^2}$$

$$= \left(\frac{\partial}{\partial \alpha_{sMSA}^2}\left[-\left(\frac{\partial \mathrm{F}_1}{\partial \alpha_{sMSA}^2}\right)_{\boldsymbol{\eta}_{\mathrm{F}_1}} \Bigg/ \left(\frac{\partial \mathrm{F}_1}{\partial \Gamma}\right)_{\boldsymbol{\eta}_{\mathrm{F}_1}}\right]\right)_{\boldsymbol{\eta}_\Gamma/\alpha_{sMSA}^2}$$

(4-287)

$$\boxed{\left(\frac{\partial^2 \Gamma}{\left(\partial \alpha_{sMSA}^2\right)^2}\right)_{\mathbf{n},V} = \left[-\left(\frac{\partial^2 \mathrm{F}_1}{\partial\left(\alpha_{sMSA}^2\right)^2}\right)_{\boldsymbol{\eta}_\Gamma/\alpha_{sMSA}^2} - \left(\frac{\partial \Gamma}{\partial \alpha_{sMSA}^2}\right)_{\boldsymbol{\eta}_\Gamma/\alpha_{sMSA}^2}\left(\frac{\partial^2 \mathrm{F}_1}{\partial \alpha_{sMSA}^2 \partial \Gamma}\right)_{\boldsymbol{\eta}_\Gamma/\alpha_{sMSA}^2}\right] \Bigg/ \left(\frac{\partial \mathrm{F}_1}{\partial \Gamma}\right)_{\boldsymbol{\eta}_{\mathrm{F}_1}}}$$

(4-288)

$$\left(\frac{\partial}{\partial \alpha_{sMSA}^2}\left(\frac{\partial \mathrm{F}_1}{\partial \alpha_{sMSA}^2}\right)_{\boldsymbol{\eta}_{\mathrm{F}_1}}\right)_{\mathbf{n},V} = \left(\frac{\partial(-S)}{\partial \alpha_{sMSA}^2}\right)_{\mathbf{n},V} = \left(\frac{\partial(-S)}{\partial \alpha_{sMSA}^2}\right)_{\boldsymbol{\eta}_\Gamma/\alpha_{sMSA}^2} = -\left(\frac{\partial S}{\partial \Gamma}\right)_{\boldsymbol{\eta}_S/\Gamma}\left(\frac{\partial \Gamma}{\partial \alpha_{sMSA}^2}\right)_{\boldsymbol{\eta}_\Gamma/\alpha_{sMSA}^2}$$

(4-289)

$$\left(\frac{\partial}{\partial \alpha_{sMSA}^2}\left(\frac{\partial \mathrm{F}_1}{\partial \Gamma}\right)_{\boldsymbol{\eta}_{\mathrm{F}_1}}\right)_{\mathbf{n},V} = \left(\frac{\partial}{\partial \alpha_{sMSA}^2}\left(8\Gamma - \alpha_{sMSA}^2\left(\frac{\partial S}{\partial \Gamma}\right)_{\boldsymbol{\eta}_S/\Gamma}\right)\right)_{\boldsymbol{\eta}_\Gamma/\alpha_{sMSA}^2}$$

$$= 8\left(\frac{\partial \Gamma}{\partial \alpha_{sMSA}^2}\right)_{\boldsymbol{\eta}_\Gamma/\alpha_{sMSA}^2} - \left(\frac{\partial S}{\partial \Gamma}\right)_{\boldsymbol{\eta}_S/\Gamma} - \alpha_{sMSA}^2\left(\frac{\partial^2 S}{\partial \Gamma^2}\right)_{\boldsymbol{\eta}_S/\Gamma} \bullet \left(\frac{\partial \Gamma}{\partial \alpha_{sMSA}^2}\right)_{\boldsymbol{\eta}_\Gamma/\alpha_{sMSA}^2} \tag{4-290}$$

$$\left(\frac{\partial}{\partial n_i}\left(\frac{\partial\Gamma}{\partial\alpha_{sMSA}^2}\right)_{\mathbf{n},V}\right)_{\mathbf{n}/n_i,V,\alpha_{sMSA}^2}=\left(\frac{\partial}{\partial n_i}\left(\frac{\partial\Gamma}{\partial\alpha_{sMSA}^2}\right)_{\mathbf{n},V}\right)_{\boldsymbol{\eta}_\Gamma/n_i}$$
$$=\left(\frac{\partial}{\partial n_i}\left[-\left(\frac{\partial\,\mathrm{F}_1}{\partial\alpha_{sMSA}^2}\right)_{\boldsymbol{\eta}_{\mathrm{F}_1}}\Big/\left(\frac{\partial\,\mathrm{F}_1}{\partial\Gamma}\right)_{\boldsymbol{\eta}_{\mathrm{F}_1}}\right]\right)_{\boldsymbol{\eta}_\Gamma/n_i} \quad (4\text{-}291)$$

$$\boxed{\left(\frac{\partial}{\partial n_i}\left(\frac{\partial\Gamma}{\partial\alpha_{sMSA}^2}\right)_{\mathbf{n},V}\right)_{\boldsymbol{\eta}_\Gamma/n_i}=\left[-\left(\frac{\partial^2\mathrm{F}_1}{\partial n_i\partial\alpha_{sMSA}^2}\right)_{\boldsymbol{\eta}_\Gamma/n_i}-\left(\frac{\partial\Gamma}{\partial\alpha_{sMSA}^2}\right)_{\mathbf{n},V}\left(\frac{\partial^2\mathrm{F}_1}{\partial n_i\partial\Gamma}\right)_{\boldsymbol{\eta}_\Gamma/n_i}\right]\Big/\left(\frac{\partial\,\mathrm{F}_1}{\partial\Gamma}\right)_{\boldsymbol{\eta}_{\mathrm{F}_1}}} \quad (4\text{-}292)$$

$$\left(\frac{\partial}{\partial n_i}\left(\frac{\partial\,\mathrm{F}_1}{\partial\alpha_{sMSA}^2}\right)_{\boldsymbol{\eta}_{\mathrm{F}_1}}\right)_{\mathbf{n}/n_i,V,\alpha_{sMSA}^2}=\left(-\frac{\partial}{\partial n_i}S\right)_{\boldsymbol{\eta}_\Gamma/n_i}=-\left(\frac{\partial S}{\partial n_i}\right)_{\boldsymbol{\eta}_S/n_i}\bullet 1-\left(\frac{\partial S}{\partial\Gamma}\right)_{\boldsymbol{\eta}_S/\Gamma}\left(\frac{\partial\Gamma}{\partial n_i}\right)_{\boldsymbol{\eta}_\Gamma/n_i} \quad (4\text{-}293)$$

$$\left(\frac{\partial}{\partial n_i}\left(\frac{\partial\,\mathrm{F}_1}{\partial\Gamma}\right)_{\boldsymbol{\eta}_{\mathrm{F}_1}}\right)_{\mathbf{n}/n_i,V,\alpha_{sMSA}^2}=8\left(\frac{\partial\Gamma}{\partial n_i}\right)_{\boldsymbol{\eta}_\Gamma/n_i}-\alpha_{sMSA}^2\left(\left(\frac{\partial^2 S}{\partial n_i\partial\Gamma}\right)_{\boldsymbol{\eta}_S/n_i}\bullet 1+\left(\frac{\partial^2 S}{\partial\Gamma^2}\right)_{\boldsymbol{\eta}_S/\Gamma}\bullet\left(\frac{\partial\Gamma}{\partial n_i}\right)_{\boldsymbol{\eta}_\Gamma/n_i}\right)$$
(4-294)

$$\left(\frac{\partial}{\partial V}\left(\frac{\partial\Gamma}{\partial\alpha_{sMSA}^2}\right)_{\mathbf{n},V}\right)_{\mathbf{n},\alpha_{sMSA}^2}=\left(\frac{\partial}{\partial V}\left[-\left(\frac{\partial\,\mathrm{F}_1}{\partial\alpha_{sMSA}^2}\right)_{\boldsymbol{\eta}_{\mathrm{F}_1}}\Big/\left(\frac{\partial\,\mathrm{F}_1}{\partial\Gamma}\right)_{\boldsymbol{\eta}_{\mathrm{F}_1}}\right]\right)_{\boldsymbol{\eta}_\Gamma/V} \quad (4\text{-}295)$$

$$\boxed{\left(\frac{\partial^2\Gamma}{\partial V\partial\alpha_{sMSA}^2}\right)_{\mathbf{n},\alpha_{sMSA}^2}=\left[-\left(\frac{\partial^2\mathrm{F}_1}{\partial V\partial\alpha_{sMSA}^2}\right)_{\boldsymbol{\eta}_\Gamma/V}-\left(\frac{\partial\Gamma}{\partial\alpha_{sMSA}^2}\right)_{\mathbf{n},V}\left(\frac{\partial^2\mathrm{F}_1}{\partial V\partial\Gamma}\right)_{\boldsymbol{\eta}_\Gamma/V}\right]\Big/\left(\frac{\partial\,\mathrm{F}_1}{\partial\Gamma}\right)_{\boldsymbol{\eta}_{\mathrm{F}_1}}} \quad (4\text{-}296)$$

$$\left(\frac{\partial}{\partial V}\left(\frac{\partial\,\mathrm{F}_1}{\partial\alpha_{sMSA}^2}\right)_{\boldsymbol{\eta}_{\mathrm{F}_1}}\right)_{\boldsymbol{\eta}_\Gamma/V}=\left(-\frac{\partial S}{\partial V}\right)_{\boldsymbol{\eta}_\Gamma/V}=-\left(\frac{\partial S}{\partial V}\right)_{\boldsymbol{\eta}_S/V}\left(\frac{\partial V}{\partial V}\right)_{\boldsymbol{\eta}_\Gamma/V}-\left(\frac{\partial S}{\partial\Gamma}\right)_{\boldsymbol{\eta}_S/\Gamma}\left(\frac{\partial\Gamma}{\partial V}\right)_{\boldsymbol{\eta}_\Gamma/V} \quad (4\text{-}297)$$

$$\left(\frac{\partial}{\partial V}\left(\frac{\partial\,\mathrm{F}_1}{\partial\Gamma}\right)_{\boldsymbol{\eta}_{\mathrm{F}_1}}\right)_{\mathbf{n},\alpha_{sMSA}^2}=\left(\frac{\partial}{\partial V}\left(\frac{\partial\,\mathrm{F}_1}{\partial\Gamma}\right)_{\boldsymbol{\eta}_{\mathrm{F}_1}}\right)_{\boldsymbol{\eta}_\Gamma/V}=\left(\frac{\partial}{\partial V}\left(8\Gamma-\alpha_{sMSA}^2\left(\frac{\partial S}{\partial\Gamma}\right)_{\boldsymbol{\eta}_S/\Gamma}\right)\right)_{\boldsymbol{\eta}_\Gamma/V}$$
$$=8\left(\frac{\partial\Gamma}{\partial V}\right)_{\boldsymbol{\eta}_\Gamma/V}-\alpha_{sMSA}^2\left(\left(\frac{\partial^2 S}{\partial V\partial\Gamma}\right)_{\boldsymbol{\eta}_S/V}\left(\frac{\partial V}{\partial V}\right)_{\boldsymbol{\eta}_\Gamma/V}+\left(\frac{\partial^2 S}{\partial\Gamma^2}\right)_{\boldsymbol{\eta}_S/\Gamma}\left(\frac{\partial\Gamma}{\partial V}\right)_{\boldsymbol{\eta}_\Gamma/V}\right) \quad (4\text{-}298)$$

$$\left(\frac{\partial}{\partial n_i}\left(\frac{\partial\Gamma}{\partial n_j}\right)_{\mathbf{n}/n_j,V,\alpha_{sMSA}^2}\right)_{\mathbf{n}/n_i,V,\alpha_{sMSA}^2}=\left(\frac{\partial}{\partial n_i}\left(\frac{\partial\Gamma}{\partial n_j}\right)_{\boldsymbol{\eta}_\Gamma/n_j}\right)_{\boldsymbol{\eta}_\Gamma/n_i}=\left(\frac{\partial}{\partial n_i}\left[-\left(\frac{\partial\,\mathrm{F}_1}{\partial n_j}\right)_{\boldsymbol{\eta}_{\mathrm{F}_1}/n_j}\Big/\left(\frac{\partial\,\mathrm{F}_1}{\partial\Gamma}\right)_{\boldsymbol{\eta}_{\mathrm{F}_1}/\Gamma}\right]\right)_{\boldsymbol{\eta}_\Gamma/n_i}$$
(4-299)

$$\boxed{\left(\frac{\partial}{\partial n_i}\left(\frac{\partial\Gamma}{\partial n_j}\right)_{\boldsymbol{\eta}_\Gamma/n_j}\right)_{\boldsymbol{\eta}_\Gamma/n_i}=\left[-\left(\frac{\partial^2\mathrm{F}_1}{\partial n_i\partial n_j}\right)_{\boldsymbol{\eta}_{\mathrm{F}_1}/n_j}-\left(\frac{\partial\Gamma}{\partial n_j}\right)_{\boldsymbol{\eta}_\Gamma/n_j}\left(\frac{\partial^2\mathrm{F}_1}{\partial n_i\partial\Gamma}\right)_{\boldsymbol{\eta}_\Gamma/n_i}\right]\Big/\left(\frac{\partial\,\mathrm{F}_1}{\partial\Gamma}\right)_{\boldsymbol{\eta}_{\mathrm{F}_1}/\Gamma}} \quad (4\text{-}300)$$

$$\left(\frac{\partial}{\partial n_i}\left(\frac{\partial \mathrm{F}_1}{\partial n_j}\right)_{\boldsymbol{\eta}_{\mathrm{F}_1}/n_j}\right)_{\boldsymbol{\eta}_\Gamma/n_i}=\left(-\alpha_{sMSA}^2\frac{\partial}{\partial n_i}\left(\frac{\partial S}{\partial n_j}\right)_{\boldsymbol{\eta}_S/n_j}\right)_{\boldsymbol{\eta}_\Gamma/n_i}$$

$$=-\alpha_{sMSA}^2\left[\left(\frac{\partial^2 S}{\partial n_i\partial n_j}\right)_{\boldsymbol{\eta}_S/n_i}\left(\frac{\partial n_j}{\partial n_i}\right)_{\boldsymbol{\eta}_\Gamma/n_i}+\left(\frac{\partial^2 S}{\partial\Gamma\partial n_j}\right)_{\boldsymbol{\eta}_S/\Gamma}\left(\frac{\partial\Gamma}{\partial n_i}\right)_{\boldsymbol{\eta}_\Gamma/n_i}\right]=-\alpha_{sMSA}^2\left(\frac{\partial^2 S}{\partial\Gamma\partial n_j}\right)_{\boldsymbol{\eta}_S/\Gamma}\left(\frac{\partial\Gamma}{\partial n_i}\right)_{\boldsymbol{\eta}_\Gamma/n_i}$$

(4-301)

From (4-294) we have:

$$\left(\frac{\partial}{\partial n_i}\left(\frac{\partial \mathrm{F}_1}{\partial\Gamma}\right)_{\boldsymbol{\eta}_{\mathrm{F}_1}}\right)_{\mathbf{n}/n_i,V,\alpha_{sMSA}^2}=8\left(\frac{\partial\Gamma}{\partial n_i}\right)_{\boldsymbol{\eta}_\Gamma/n_i}-\alpha_{sMSA}^2\left(\left(\frac{\partial^2 S}{\partial n_i\partial\Gamma}\right)_{\boldsymbol{\eta}_S/n_i}\bullet 1+\left(\frac{\partial^2 S}{\partial\Gamma^2}\right)_{\boldsymbol{\eta}_S/\Gamma}\bullet\left(\frac{\partial\Gamma}{\partial n_i}\right)_{\boldsymbol{\eta}_\Gamma/n_i}\right)$$

$$\left(\frac{\partial}{\partial n_i}\left(\frac{\partial\Gamma}{\partial V}\right)_{\mathbf{n},\alpha_{sMSA}^2}\right)_{\mathbf{n}/n_i,V,\alpha_{sMSA}^2}=\left(\frac{\partial}{\partial n_i}\left(\frac{\partial\Gamma}{\partial V}\right)_{\boldsymbol{\eta}_\Gamma/V}\right)_{\boldsymbol{\eta}_\Gamma/n_i}=\left(\frac{\partial}{\partial n_i}\left[-\left(\frac{\partial \mathrm{F}_1}{\partial V}\right)_{\boldsymbol{\eta}_{\mathrm{F}_1}/V}\Big/\left(\frac{\partial \mathrm{F}_1}{\partial\Gamma}\right)_{\boldsymbol{\eta}_{\mathrm{F}_1}/\Gamma}\right]\right)_{\boldsymbol{\eta}_\Gamma/n_i}\quad(4\text{-}302)$$

$$\boxed{\left(\frac{\partial}{\partial n_i}\left(\frac{\partial\Gamma}{\partial V}\right)_{\mathbf{n},\alpha_{sMSA}^2}\right)_{\mathbf{n}/n_i,V,\alpha_{sMSA}^2}=\left[-\left(\frac{\partial}{\partial n_i}\left(\frac{\partial \mathrm{F}_1}{\partial V}\right)_{\boldsymbol{\eta}_{\mathrm{F}_1}/V}\right)_{\boldsymbol{\eta}_\Gamma/n_i}-\left(\frac{\partial\Gamma}{\partial V}\right)_{\boldsymbol{\eta}_\Gamma/V}\left(\frac{\partial}{\partial n_i}\left(\frac{\partial \mathrm{F}_1}{\partial\Gamma}\right)_{\boldsymbol{\eta}_{\mathrm{F}_1}}\right)_{\boldsymbol{\eta}_\Gamma/n_i}\right]\Big/\left(\frac{\partial \mathrm{F}_1}{\partial\Gamma}\right)_{\boldsymbol{\eta}_{\mathrm{F}_1}/\Gamma}}$$

(4-303)

$$\left(\frac{\partial}{\partial n_i}\left(\frac{\partial \mathrm{F}_1}{\partial V}\right)_{\boldsymbol{\eta}_{\mathrm{F}_1}/V}\right)_{\boldsymbol{\eta}_\Gamma/n_i}=\left(-\alpha_{sMSA}^2\frac{\partial}{\partial n_i}\left(\frac{\partial S}{\partial V}\right)_{\boldsymbol{\eta}_S/V}\right)_{\boldsymbol{\eta}_\Gamma/n_i}$$

$$=-\alpha_{sMSA}^2\left[\left(\frac{\partial^2 S}{\partial n_i\partial V}\right)_{\boldsymbol{\eta}_S/n_i}\left(\frac{\partial n_j}{\partial n_i}\right)_{\boldsymbol{\eta}_\Gamma/n_i}+\left(\frac{\partial^2 S}{\partial\Gamma\partial V}\right)_{\boldsymbol{\eta}_S/\Gamma}\left(\frac{\partial\Gamma}{\partial n_i}\right)_{\boldsymbol{\eta}_\Gamma/n_i}\right]\quad(4\text{-}304)$$

From (4-294) we have:

$$\left(\frac{\partial}{\partial n_i}\left(\frac{\partial \mathrm{F}_1}{\partial\Gamma}\right)_{\boldsymbol{\eta}_{\mathrm{F}_1}}\right)_{\mathbf{n}/n_i,V,\alpha_{sMSA}^2}=8\left(\frac{\partial\Gamma}{\partial n_i}\right)_{\boldsymbol{\eta}_\Gamma/n_i}-\alpha_{sMSA}^2\left(\left(\frac{\partial^2 S}{\partial n_i\partial\Gamma}\right)_{\boldsymbol{\eta}_S/n_i}\bullet 1+\left(\frac{\partial^2 S}{\partial\Gamma^2}\right)_{\boldsymbol{\eta}_S/\Gamma}\bullet\left(\frac{\partial\Gamma}{\partial n_i}\right)_{\boldsymbol{\eta}_\Gamma/n_i}\right)$$

$$\left(\frac{\partial}{\partial V}\left(\frac{\partial\Gamma}{\partial V}\right)_{\mathbf{n},\alpha_{sMSA}^2}\right)_{\mathbf{n},\alpha_{sMSA}^2}=\left(\frac{\partial}{\partial V}\left(\frac{\partial\Gamma}{\partial V}\right)_{\boldsymbol{\eta}_\Gamma/V}\right)_{\boldsymbol{\eta}_\Gamma/V}=\left(\frac{\partial}{\partial V}\left[-\left(\frac{\partial \mathrm{F}_1}{\partial V}\right)_{\boldsymbol{\eta}_{\mathrm{F}_1}/V}\Big/\left(\frac{\partial \mathrm{F}_1}{\partial\Gamma}\right)_{\boldsymbol{\eta}_{\mathrm{F}_1}/\Gamma}\right]\right)_{\boldsymbol{\eta}_\Gamma/V}\quad(4\text{-}305)$$

$$\boxed{\left(\frac{\partial}{\partial V}\left(\frac{\partial\Gamma}{\partial V}\right)_{\mathbf{n},\alpha_{sMSA}^2}\right)_{\mathbf{n},\alpha_{sMSA}^2}=\left[-\left(\frac{\partial}{\partial V}\left(\frac{\partial \mathrm{F}_1}{\partial V}\right)_{\boldsymbol{\eta}_{\mathrm{F}_1}/V}\right)_{\boldsymbol{\eta}_\Gamma/V}-\left(\frac{\partial\Gamma}{\partial V}\right)_{\boldsymbol{\eta}_\Gamma/V}\left(\frac{\partial}{\partial V}\left(\frac{\partial \mathrm{F}_1}{\partial\Gamma}\right)_{\boldsymbol{\eta}_{\mathrm{F}_1}}\right)_{\boldsymbol{\eta}_\Gamma/V}\right]\Big/\left(\frac{\partial \mathrm{F}_1}{\partial\Gamma}\right)_{\boldsymbol{\eta}_{\mathrm{F}_1}/\Gamma}}$$

(4-306)

$$\left(\frac{\partial}{\partial V}\left(\frac{\partial \mathrm{F}_1}{\partial V}\right)_{\boldsymbol{\eta}_{\mathrm{F}_1}/V}\right)_{\boldsymbol{\eta}_\Gamma/V}=-\alpha_{sMSA}^2\left(\frac{\partial}{\partial V}\left(\frac{\partial S}{\partial V}\right)_{\boldsymbol{\eta}_S/V}\right)_{\boldsymbol{\eta}_\Gamma/V}$$

$$=-\alpha_{sMSA}^2\left[\left(\frac{\partial^2 S}{\partial V^2}\right)_{\boldsymbol{\eta}_S/V}\left(\frac{\partial V}{\partial V}\right)_{\boldsymbol{\eta}_\Gamma/V}+\left(\frac{\partial^2 S}{\partial\Gamma\partial V}\right)_{\boldsymbol{\eta}_S/\Gamma}\left(\frac{\partial\Gamma}{\partial V}\right)_{\boldsymbol{\eta}_\Gamma/V}\right]\quad(4\text{-}307)$$

From (4-298) we have:

$$\left(\frac{\partial}{\partial V}\left(\frac{\partial \mathrm{F}_1}{\partial \Gamma}\right)_{\boldsymbol{\eta}_{\mathrm{F}_1}}\right)_{\mathbf{n},\alpha^2_{sMSA}} = \left(\frac{\partial}{\partial V}\left(\frac{\partial \mathrm{F}_1}{\partial \Gamma}\right)_{\boldsymbol{\eta}_{\mathrm{F}_1}}\right)_{\boldsymbol{\eta}_\Gamma/V} =$$

$$= 8\left(\frac{\partial \Gamma}{\partial V}\right)_{\boldsymbol{\eta}_\Gamma/V} - \alpha^2_{sMSA}\left(\left(\frac{\partial^2 S}{\partial V \partial \Gamma}\right)_{\boldsymbol{\eta}_S/V}\left(\frac{\partial V}{\partial V}\right)_{\boldsymbol{\eta}_\Gamma/V} + \left(\frac{\partial^2 S}{\partial \Gamma^2}\right)_{\boldsymbol{\eta}_S/\Gamma}\left(\frac{\partial \Gamma}{\partial V}\right)_{\boldsymbol{\eta}_\Gamma/V}\right)$$

$$\boldsymbol{\Gamma}''(\boldsymbol{\eta}_\Gamma) = \begin{bmatrix} \Gamma_{\alpha^2_{sMSA}\alpha^2_{sMSA}} & \Gamma_{\alpha^2_{sMSA}n_i} & \Gamma_{\alpha^2_{sMSA}n_j} & \Gamma_{\alpha^2_{sMSA}V} \\ \Gamma_{n_i\alpha^2_{sMSA}} & \Gamma_{n_in_i} & \Gamma_{n_in_j} & \Gamma_{n_iV} \\ \Gamma_{n_j\alpha^2_{sMSA}} & \Gamma_{n_jn_i} & \Gamma_{n_jn_j} & \Gamma_{n_jV} \\ \Gamma_{V\alpha^2_{sMSA}} & \Gamma_{Vn_i} & \Gamma_{Vn_j} & \Gamma_{VV} \end{bmatrix} \tag{4-308}$$

$$\frac{\partial \Gamma(n_i,T,V)}{\partial \boldsymbol{\eta}_\Gamma} = \left[\left(\frac{\partial \Gamma}{\partial \alpha^2_{sMSA}}\right)_{\mathbf{n},V} \quad \left(\frac{\partial \Gamma}{\partial n_i}\right)_{\mathbf{n}/n_i,\alpha^2_{sMSA},V} \quad \left(\frac{\partial \Gamma}{\partial n_j}\right)_{\mathbf{n}/n_j,V,\alpha^2_{sMSA}} \left(\frac{\partial \Gamma}{\partial V}\right)_{\alpha^2_{sMSA},\mathbf{n}}\right]^T \tag{4-309}$$

$$= \left[\left(\frac{\partial \Gamma}{\partial \alpha^2_{sMSA}}\right)_{\boldsymbol{\eta}_\Gamma/\alpha^2_{sMSA}} \quad \left(\frac{\partial \Gamma}{\partial n_i}\right)_{\boldsymbol{\eta}_\Gamma/n_i} \quad \left(\frac{\partial \Gamma}{\partial n_j}\right)_{\boldsymbol{\eta}_\Gamma/n_j}\left(\frac{\partial \Gamma}{\partial V}\right)_{\boldsymbol{\eta}_\Gamma/V}\right]^T$$

$$\left(\frac{\partial \boldsymbol{\eta}_\Gamma}{\partial n_i}\right)_{T,V,\mathbf{n}/n_i} = \left[\left(\frac{\partial \alpha^2_{sMSA}}{\partial n_i}\right)_{T,V,\mathbf{n}/n_i} \quad \left(\frac{\partial n_i}{\partial n_i}\right)_{T,V,\mathbf{n}/n_i} \quad \left(\frac{\partial n_j}{\partial n_i}\right)_{T,V,\mathbf{n}/n_i} \quad \left(\frac{\partial V}{\partial n_i}\right)_{T,V,\mathbf{n}/n_i}\right]^T \tag{4-310}$$

$$= \left[\left(\frac{\partial \alpha^2_{sMSA}}{\partial n_i}\right)_{T,V,\mathbf{n}/n_i} \quad 1 \quad 0 \quad 0\right]^T$$

$$\left(\frac{\partial^2 \Gamma}{\partial n_i \partial n_j}\right)_{T,V,\mathbf{n}/n_i} = \left(\left(\frac{\partial \boldsymbol{\eta}_\Gamma}{\partial n_i}\right)_{T,V,\mathbf{n}/n_i}\right)^T \boldsymbol{\Gamma}''(\boldsymbol{\eta}_\Gamma)\left(\frac{\partial \boldsymbol{\eta}_\Gamma}{\partial n_j}\right)_{T,V,\mathbf{n}/n_j} + \left(\frac{\partial \Gamma}{\partial \boldsymbol{\eta}_\Gamma}\right)^T \cdot \left(\frac{\partial^2 \boldsymbol{\eta}_\Gamma}{\partial n_i \partial n_j}\right)_{T,V,\mathbf{n}/n_i} \tag{4-311}$$

$$\begin{aligned}
\left(\frac{\partial^2 \Gamma}{\partial n_i \partial n_j}\right)_{T,V,\mathbf{n}/n_i} &= \left(\frac{\partial^2 \Gamma}{\left(\partial \alpha^2_{sMSA}\right)^2}\right)_{\boldsymbol{\eta}_\Gamma/\alpha^2_{sMSA}} \left(\frac{\partial \alpha^2_{sMSA}}{\partial n_i}\right)_{T,V,\mathbf{n}/n_i}\left(\frac{\partial \alpha^2_{sMSA}}{\partial n_j}\right)_{T,V,\mathbf{n}/n_j} \\
&+ \left(\frac{\partial}{\partial n_i}\left(\frac{\partial \Gamma}{\partial \alpha^2_{sMSA}}\right)_{\mathbf{n},V}\right)_{\boldsymbol{\eta}_\Gamma/n_i}\left(\frac{\partial n_i}{\partial n_i}\right)_{T,V,\mathbf{n}/n_i}\left(\frac{\partial \alpha^2_{sMSA}}{\partial n_j}\right)_{T,V,\mathbf{n}/n_j} + \left(\frac{\partial^2 \Gamma}{\partial n_i \partial n_j}\right)_{\boldsymbol{\eta}_\Gamma/n_i}\left(\frac{\partial n_j}{\partial n_j}\right)_{T,V,\mathbf{n}/n_j}\left(\frac{\partial n_i}{\partial n_i}\right)_{T,V,\mathbf{n}/n_i} \\
&+ \left(\frac{\partial^2 \Gamma}{\partial n_i \partial \alpha^2_{sMSA}}\right)_{\boldsymbol{\eta}_\Gamma/n_i}\left(\frac{\partial n_i}{\partial n_i}\right)_{T,V,\mathbf{n}/n_i}\left(\frac{\partial \alpha^2_{sMSA}}{\partial n_j}\right)_{T,V,\mathbf{n}/n_j} + \left(\frac{\partial \Gamma}{\partial \alpha^2_{sMSA}}\right)_{\boldsymbol{\eta}_\Gamma/\alpha^2_{sMSA}}\left(\frac{\partial^2 \alpha^2_{sMSA}}{\partial n_i \partial n_j}\right)_{T,V,\mathbf{n}/n_i}
\end{aligned} \tag{4-312}$$

$$\left(\frac{\partial \boldsymbol{\eta}_\Gamma}{\partial V}\right)_{\mathbf{n},T} = \left[\left(\frac{\partial \alpha^2_{sMSA}}{\partial V}\right)_{\mathbf{n},T} \quad \left(\frac{\partial n_i}{\partial V}\right)_{\mathbf{n},T} \quad \left(\frac{\partial n_j}{\partial V}\right)_{\mathbf{n},T} \quad \left(\frac{\partial V}{\partial V}\right)_{\mathbf{n},T}\right]^T = \left[\left(\frac{\partial \alpha^2_{sMSA}}{\partial V}\right)_{\mathbf{n},T} \quad 0 \quad 0 \quad 1\right]^T \tag{4-313}$$

$$\left(\frac{\partial^2 \boldsymbol{\eta}_\Gamma}{\partial V \partial n_i}\right)_{\mathbf{n},T} = \left[\left(\frac{\partial^2 \alpha_{sMSA}^2}{\partial V \partial n_i}\right)_{\mathbf{n},T} \quad 0 \quad 0 \quad 0\right]^T \tag{4-314}$$

$$\left(\frac{\partial^2 \boldsymbol{\eta}_\Gamma}{\partial V^2}\right)_{\mathbf{n},T} = \left[\left(\frac{\partial^2 \alpha_{sMSA}^2}{\partial V^2}\right)_{\mathbf{n},T} \quad 0 \quad 0 \quad 0\right]^T \tag{4-315}$$

$$\left(\frac{\partial^2 \Gamma}{\partial n_i \partial V}\right)_{T,V,\mathbf{n}/n_i} = \left(\left(\frac{\partial \boldsymbol{\eta}_\Gamma}{\partial n_i}\right)_{T,V,\mathbf{n}/n_i}\right)^T \boldsymbol{\Gamma}''(\boldsymbol{\eta}_\Gamma)\left(\frac{\partial \boldsymbol{\eta}_\Gamma}{\partial V}\right)_{T,\mathbf{n}} + \left(\frac{\partial \Gamma}{\partial \boldsymbol{\eta}_\Gamma}\right)^T \cdot \left(\frac{\partial^2 \boldsymbol{\eta}_\Gamma}{\partial n_i \partial V}\right)_{T,\mathbf{n}} \tag{4-316}$$

$$\begin{aligned}\left(\frac{\partial^2 \Gamma}{\partial n_i \partial V}\right)_{T,V,\mathbf{n}/n_i} &= \left(\frac{\partial^2 \Gamma}{\left(\partial \alpha_{sMSA}^2\right)^2}\right)_{\boldsymbol{\eta}_\Gamma/\alpha_{sMSA}^2} \left(\frac{\partial \alpha_{sMSA}^2}{\partial n_i}\right)_{T,V,\mathbf{n}/n_i} \left(\frac{\partial \alpha_{sMSA}^2}{\partial V}\right)_{T,\mathbf{n}} \\ &+ \left(\frac{\partial^2 \Gamma}{\partial n_i \partial \alpha_{sMSA}^2}\right)_{\boldsymbol{\eta}_\Gamma/n_i} \left(\frac{\partial n_i}{\partial n_i}\right)_{T,V,\mathbf{n}/n_i} \left(\frac{\partial \alpha_{sMSA}^2}{\partial V}\right)_{\mathbf{n},T} + \left(\frac{\partial^2 \Gamma}{\partial n_i \partial V}\right)_{\boldsymbol{\eta}_\Gamma/n_i} \left(\frac{\partial V}{\partial V}\right)_{T,\mathbf{n}} \left(\frac{\partial n_i}{\partial n_i}\right)_{T,V,\mathbf{n}/n_i} \\ &+ \left(\frac{\partial^2 \Gamma}{\partial \alpha_{sMSA}^2 \partial V}\right)_{\boldsymbol{\eta}_\Gamma/\alpha_{sMSA}^2} \left(\frac{\partial \alpha_{sMSA}^2}{\partial n_i}\right)_{T,V,\mathbf{n}/n_i} \left(\frac{\partial V}{\partial V}\right)_{T,\mathbf{n}} + \left(\frac{\partial \Gamma}{\partial \alpha_{sMSA}^2}\right)_{\boldsymbol{\eta}_\Gamma/\alpha_{sMSA}^2} \cdot \left(\frac{\partial^2 \alpha_{sMSA}^2}{\partial V \partial n_i}\right)_{\mathbf{n},T}\end{aligned} \tag{4-317}$$

$$\left(\frac{\partial^2 \Gamma}{\partial V^2}\right)_{T,V,\mathbf{n}/n_i} = \left(\left(\frac{\partial \boldsymbol{\eta}_\Gamma}{\partial V}\right)_{T,\mathbf{n}}\right)^T \boldsymbol{\Gamma}''(\boldsymbol{\eta}_\Gamma)\left(\frac{\partial \boldsymbol{\eta}_\Gamma}{\partial V}\right)_{T,\mathbf{n}} + \left(\frac{\partial \Gamma}{\partial \boldsymbol{\eta}_\Gamma}\right)^T \cdot \left(\frac{\partial^2 \boldsymbol{\eta}_\Gamma}{\partial V^2}\right)_{T,\mathbf{n}} \tag{4-318}$$

$$\begin{aligned}\left(\frac{\partial^2 \Gamma}{\partial V^2}\right)_{T,\mathbf{n}} &= \left(\frac{\partial^2 \Gamma}{\left(\partial \alpha_{sMSA}^2\right)^2}\right)_{\boldsymbol{\eta}_\Gamma/\alpha_{sMSA}^2} \left(\frac{\partial \alpha_{sMSA}^2}{\partial V}\right)_{T,\mathbf{n}}^2 + \left(\frac{\partial^2 \Gamma}{\partial V^2}\right)_{\boldsymbol{\eta}_\Gamma/V} \left(\frac{\partial V}{\partial V}\right)_{T,\mathbf{n}}^2 \\ &+ 2 \cdot \left(\frac{\partial^2 \Gamma}{\partial \alpha_{sMSA}^2 \partial V}\right)_{\boldsymbol{\eta}_\Gamma/\alpha_{sMSA}^2} \left(\frac{\partial V}{\partial V}\right)_{T,\mathbf{n}} \left(\frac{\partial \alpha_{sMSA}^2}{\partial V}\right)_{\mathbf{n},T} + \left(\frac{\partial \Gamma}{\partial \alpha_{sMSA}^2}\right)_{\boldsymbol{\eta}_\Gamma/\alpha_{sMSA}^2} \cdot \left(\frac{\partial^2 \alpha_{sMSA}^2}{\partial V^2}\right)_{T,\mathbf{n}}\end{aligned} \tag{4-319}$$

$$\left(\frac{\partial^2 \boldsymbol{\eta}_\Gamma}{\partial T \partial n_i}\right)_{V,\mathbf{n}} = \left[\left(\frac{\partial^2 \alpha_{sMSA}^2}{\partial T \partial n_i}\right)_{V,\mathbf{n}} \quad 0 \quad 0 \quad 0\right]^T \tag{4-320}$$

$$\left(\frac{\partial^2 \boldsymbol{\eta}_\Gamma}{\partial V \partial T}\right)_{\mathbf{n},T} = \left[\left(\frac{\partial^2 \alpha_{sMSA}^2}{\partial V \partial T}\right)_{\mathbf{n},T} \quad 0 \quad 0 \quad 0\right]^T \tag{4-321}$$

$$\left(\frac{\partial^2 \boldsymbol{\eta}_\Gamma}{\partial T^2}\right)_{V,\mathbf{n}} = \left[\left(\frac{\partial^2 \alpha_{sMSA}^2}{\partial T^2}\right)_{V,\mathbf{n}} \quad 0 \quad 0 \quad 0\right]^T \tag{4-322}$$

$$\left(\frac{\partial^2 \Gamma}{\partial T^2}\right)_{T,V,\mathbf{n}/n_i} = \left(\left(\frac{\partial \boldsymbol{\eta}_\Gamma}{\partial T}\right)_{T,\mathbf{n}}\right)^T \boldsymbol{\Gamma}''(\boldsymbol{\eta}_\Gamma)\left(\frac{\partial \boldsymbol{\eta}_\Gamma}{\partial T}\right)_{T,\mathbf{n}} + \left(\frac{\partial \Gamma}{\partial \boldsymbol{\eta}_\Gamma}\right)^T \cdot \left(\frac{\partial^2 \boldsymbol{\eta}_\Gamma}{\partial T^2}\right)_{T,\mathbf{n}} \tag{4-323}$$

$$\left(\frac{\partial^2 \Gamma}{\partial T^2}\right)_{V,\mathbf{n}} = \left(\frac{\partial^2 \Gamma}{\left(\partial \alpha_{sMSA}^2\right)^2}\right)_{\boldsymbol{\eta}_\Gamma/\alpha_{sMSA}^2} \left(\frac{\partial \alpha_{sMSA}^2}{\partial T}\right)_{V,\mathbf{n}}^2 + \left(\frac{\partial \Gamma}{\partial \alpha_{sMSA}^2}\right)_{\boldsymbol{\eta}_\Gamma/\alpha_{sMSA}^2} \cdot \left(\frac{\partial^2 \alpha_{sMSA}^2}{\partial T^2}\right)_{V,\mathbf{n}} \tag{4-324}$$

$$\left(\frac{\partial^2\Gamma}{\partial n_i\partial T}\right)_{T,V,\mathbf{n}/n_i}=\left(\left(\frac{\partial\boldsymbol{\eta}_\Gamma}{\partial n_i}\right)_{T,V,\mathbf{n}/n_i}\right)^T\boldsymbol{\Gamma}''(\boldsymbol{\eta}_\Gamma)\left(\frac{\partial\boldsymbol{\eta}_\Gamma}{\partial T}\right)_{V,\mathbf{n}}+\left(\frac{\partial\Gamma}{\partial\boldsymbol{\eta}_\Gamma}\right)^T\cdot\left(\frac{\partial^2\boldsymbol{\eta}_\Gamma}{\partial n_i\partial T}\right)_{T,\mathbf{n}} \tag{4-325}$$

$$\begin{aligned}\left(\frac{\partial^2\Gamma}{\partial n_i\partial T}\right)_{T,V,\mathbf{n}/n_i}&=\left(\frac{\partial^2\Gamma}{\left(\partial\alpha^2_{sMSA}\right)^2}\right)_{\boldsymbol{\eta}_\Gamma/\alpha^2_{sMSA}}\left(\frac{\partial\alpha^2_{sMSA}}{\partial n_i}\right)_{T,V,\mathbf{n}/n_i}\left(\frac{\partial\alpha^2_{sMSA}}{\partial T}\right)_{V,\mathbf{n}}\\&+\left(\frac{\partial^2\Gamma}{\partial n_i\partial\alpha^2_{sMSA}}\right)_{\boldsymbol{\eta}_\Gamma/n_i}\left(\frac{\partial n_i}{\partial n_i}\right)_{T,V,\mathbf{n}/n_i}\left(\frac{\partial\alpha^2_{sMSA}}{\partial T}\right)_{V,\mathbf{n}}+\left(\frac{\partial\Gamma}{\partial\alpha^2_{sMSA}}\right)_{\boldsymbol{\eta}_\Gamma/\alpha^2_{sMSA}}\cdot\left(\frac{\partial^2\alpha^2_{sMSA}}{\partial T\partial n_i}\right)_{V,\mathbf{n}}\end{aligned} \tag{4-326}$$

$$\left(\frac{\partial^2\Gamma}{\partial V\partial T}\right)_{T,V,\mathbf{n}/n_i}=\left(\left(\frac{\partial\boldsymbol{\eta}_\Gamma}{\partial V}\right)_{T,\mathbf{n}}\right)^T\boldsymbol{\Gamma}''(\boldsymbol{\eta}_\Gamma)\left(\frac{\partial\boldsymbol{\eta}_\Gamma}{\partial T}\right)_{V,\mathbf{n}}+\left(\frac{\partial\Gamma}{\partial\boldsymbol{\eta}_\Gamma}\right)^T\cdot\left(\frac{\partial^2\boldsymbol{\eta}_\Gamma}{\partial V\partial T}\right)_{T,\mathbf{n}} \tag{4-327}$$

$$\begin{aligned}\left(\frac{\partial^2\Gamma}{\partial V\partial T}\right)_{T,\mathbf{n}}&=\left(\frac{\partial^2\Gamma}{\left(\partial\alpha^2_{sMSA}\right)^2}\right)_{\boldsymbol{\eta}_\Gamma/\alpha^2_{sMSA}}\left(\frac{\partial\alpha^2_{sMSA}}{\partial V}\right)_{T,\mathbf{n}}\left(\frac{\partial\alpha^2_{sMSA}}{\partial T}\right)_{V,\mathbf{n}}+\\&+\left(\frac{\partial^2\Gamma}{\partial\alpha^2_{sMSA}\partial V}\right)_{\boldsymbol{\eta}_\Gamma/\alpha^2_{sMSA}}\left(\frac{\partial V}{\partial V}\right)_{T,\mathbf{n}}\left(\frac{\partial\alpha^2_{sMSA}}{\partial T}\right)_{V,\mathbf{n}}+\left(\frac{\partial\Gamma}{\partial\alpha^2_{sMSA}}\right)_{\boldsymbol{\eta}_\Gamma/\alpha^2_{sMSA}}\cdot\left(\frac{\partial^2\alpha^2_{sMSA}}{\partial V\partial T}\right)_{T,\mathbf{n}}\end{aligned} \tag{4-328}$$

APPENDIX VI The derivatives of relative permittivity model

1.1 The derivatives of Pottel model

1.1.1 First order partial derivatives

From (4-159) we have:

$$\varepsilon = 1 + (\varepsilon_s - 1)\frac{1-\varepsilon_3}{1+\varepsilon_3/2} \Rightarrow \qquad \varepsilon(1+\frac{\varepsilon_3}{2}) = (1+\frac{\varepsilon_3}{2}) + (\varepsilon_s - 1)(1-\varepsilon_3) \tag{4-329}$$

Take first order derivatives with respect to mole number on both sides of equation (4-329):

$$\boxed{\left(\frac{\partial \varepsilon}{\partial n_i}\right)_{T,V,\mathbf{n}/n_i} = \frac{2-2\varepsilon_3}{2+\varepsilon_3}\left(\frac{\partial \varepsilon_s}{\partial n_i}\right)_{T,V,\mathbf{n}/n_i} + \frac{3-2\varepsilon_s-\varepsilon}{2+\varepsilon_3}\left(\frac{\partial \varepsilon_3}{\partial n_i}\right)_{T,V,\mathbf{n}/n_i}} \tag{4-330}$$

From equation (4-22) we have:

$$\varepsilon_3 = \frac{N_A\pi}{6V}\sum_k n_k\sigma_k^3, \qquad \boxed{\left(\frac{\partial \varepsilon_3}{\partial n_i}\right)_{T,V,\mathbf{n}/n_i} = \frac{N_A\pi}{6V}\sigma_i^3} \tag{4-331}$$

$$\left(\frac{\partial^2 \varepsilon_3}{\partial n_i \partial n_j}\right)_{T,V,\mathbf{n}/n_i} = 0 \tag{4-332}$$

$$\varepsilon_3 V = \frac{N_A\pi}{6}\sum_k n_k\sigma_k^3, \qquad \varepsilon_3 + V\left(\frac{\partial \varepsilon_3}{\partial V}\right)_{n_i,T} = 0 \tag{4-333}$$

k is the ionic species.

$$\boxed{\left(\frac{\partial \varepsilon_3}{\partial V}\right)_{n_i,T} = \frac{-\varepsilon_3}{V}} \tag{4-334}$$

From(4-333)

$$2\left(\frac{\partial \varepsilon_3}{\partial V}\right)_{n_i,T} + V\left(\frac{\partial^2 \varepsilon_3}{\partial V^2}\right)_{n_i,T} = 0 \tag{4-335}$$

$$\boxed{\left(\frac{\partial^2 \varepsilon_3}{\partial V^2}\right)_{n_i,T} = \frac{-2}{V}\left(\frac{\partial \varepsilon_3}{\partial V}\right)_{n_i,T}} \tag{4-336}$$

$$\boxed{\left(\frac{\partial \varepsilon_3}{\partial T}\right)_{n_i,V} = 0, \text{ if } \sigma_i \text{ is temperature independent}} \tag{4-337}$$

$$\boxed{\left(\frac{\partial \varepsilon_3}{\partial T}\right)_{n_i,V} = -\frac{N_A\pi}{3V}\sum_k n_k\sigma_k^2\left(\frac{\partial \sigma_k}{\partial T}\right)_{V,n_i}, \text{ if } \sigma_k(\mathrm{T}) \text{ is temperature dependent}} \tag{4-338}$$

$$\left(\frac{\partial^2\varepsilon_3}{\partial T^2}\right)_{n_i,V} = -\frac{N_A\pi}{3V}\sum_k n_k\left(\sigma_k^2\left(\frac{\partial^2\sigma_k}{\partial T^2}\right)_{V,n_i} + 2\sigma_k\left(\frac{\partial\sigma_k}{\partial T}\right)^2_{V,n_i}\right), \quad \text{(4-339)}$$

if σ_k(T) is temperature dependent

We have:

$$\varepsilon_s = \frac{\sum_i n_i\varepsilon_i}{\sum_i n_i} \quad \Rightarrow \quad \left(\frac{\partial\varepsilon_s}{\partial n_i}\right)_{T,V} = \frac{\varepsilon_i - \varepsilon_s + n_i\left(\frac{\partial\varepsilon_i}{\partial n_i}\right)_{T,V}}{\sum_i n_i} \quad \text{(4-340)}$$

i is the non-ionic solute species and

$$\left(\frac{\partial^2\varepsilon_s}{\partial n_i\partial n_j}\right)_{T,V,\mathbf{n}/n_i} = \frac{2\varepsilon_s - \varepsilon_i - \varepsilon_j}{\left(\sum_i n_i\right)^2} \quad \text{(4-341)}$$

For temperature and volume derivatives, we have:

$$\left(\frac{\partial\varepsilon_s}{\partial T}\right)_{n_i,T} = \frac{\sum_i n_i\left(\frac{\partial\varepsilon_i}{\partial T}\right)_{n_i,V}}{\sum_i n_i} \quad \text{(4-342)}$$

$$\left(\frac{\partial\varepsilon_s}{\partial V}\right)_{n_i,T} = \frac{\sum_i n_i\left(\frac{\partial\varepsilon_i}{\partial V}\right)_{n_i,T}}{\sum_i n_i} \quad \text{(4-343)}$$

Take the first order derivatives with respect to volume *V* on both sides of equation (4-329)

$$\left(\frac{\partial\varepsilon}{\partial V}\right)_{\mathbf{n},T} = \frac{3-2\varepsilon_s-\varepsilon}{2+\varepsilon_3}\left(\frac{\partial\varepsilon_3}{\partial V}\right)_{\mathbf{n},T} + \frac{2-2\varepsilon_3}{2+\varepsilon_3}\left(\frac{\partial\varepsilon_s}{\partial V}\right)_{\mathbf{n},T} \quad \text{(4-344)}$$

The first order temperature derivatives

$$\left(\frac{\partial\varepsilon}{\partial T}\right)_{\mathbf{n},V} = \frac{3-2\varepsilon_s-\varepsilon}{2+\varepsilon_3}\left(\frac{\partial\varepsilon_3}{\partial T}\right)_{\mathbf{n},V} + \frac{2-2\varepsilon_3}{2+\varepsilon_3}\left(\frac{\partial\varepsilon_s}{\partial T}\right)_{\mathbf{n},V} \quad \text{(4-345)}$$

1.1.2 Second order partial derivatives

From (4-330) we have:

$$\left(\frac{\partial^2\varepsilon}{\partial n_i\partial n_j}\right)_{T,V,\mathbf{n}/n_i} = \frac{2-2\varepsilon_3}{2+\varepsilon_3}\left(\frac{\partial^2\varepsilon_s}{\partial n_i\partial n_j}\right)_{T,V,\mathbf{n}/n_i} + \frac{3-2\varepsilon_s-\varepsilon}{2+\varepsilon_3}\left(\frac{\partial^2\varepsilon_3}{\partial n_i\partial n_j}\right)_{T,V,\mathbf{n}/n_i} - \frac{1}{2+\varepsilon_3}\times$$
$$\left[\left(\left(\frac{\partial\varepsilon}{\partial n_j}\right)_{T,V,\mathbf{n}/n_j} + 2\left(\frac{\partial\varepsilon_s}{\partial n_j}\right)_{T,V,\mathbf{n}/n_j}\right)\left(\frac{\partial\varepsilon_3}{\partial n_i}\right)_{T,V,\mathbf{n}/n_i} + \left(\left(\frac{\partial\varepsilon}{\partial n_i}\right)_{T,V,\mathbf{n}/n_i} + 2\left(\frac{\partial\varepsilon_s}{\partial n_i}\right)_{T,V,\mathbf{n}/n_i}\right)\left(\frac{\partial\varepsilon_3}{\partial n_j}\right)_{T,V,\mathbf{n}/n_j}\right]$$

(4-346)

From (4-346),(4-332) and (4-341) we have:

$$\left(\frac{\partial^2\varepsilon}{\partial n_i\partial n_j}\right)_{T,V,\mathbf{n}/n_i}=\frac{2-2\varepsilon_3}{2+\varepsilon_3}\left(\frac{\partial^2\varepsilon_s}{\partial n_i\partial n_j}\right)_{T,V,\mathbf{n}/n_i}+\frac{3-2\varepsilon_s-\varepsilon}{2+\varepsilon_3}\left(\frac{\partial^2\varepsilon_3}{\partial n_i\partial n_j}\right)_{T,V,\mathbf{n}/n_i}-\frac{1}{2+\varepsilon_3}\times$$

$$\left[\left(\left(\frac{\partial\varepsilon}{\partial n_j}\right)_{T,V,\mathbf{n}/n_j}-2\left(\frac{\partial\varepsilon_s}{\partial n_j}\right)_{T,V,\mathbf{n}/n_j}\right)\left(\frac{\partial\varepsilon_3}{\partial n_i}\right)_{T,V,\mathbf{n}/n_i}+\left(\left(\frac{\partial\varepsilon}{\partial n_i}\right)_{T,V,\mathbf{n}/n_i}-2\left(\frac{\partial\varepsilon_s}{\partial n_i}\right)_{T,V,\mathbf{n}/n_i}\right)\left(\frac{\partial\varepsilon_3}{\partial n_j}\right)_{T,V,\mathbf{n}/n_j}\right]$$

$$=\frac{2-2\varepsilon_3}{2+\varepsilon_3}\times\frac{2\varepsilon_s-\varepsilon_i-\varepsilon_j}{\left(\sum_i n_i\right)^2}+\frac{3-2\varepsilon_s-\varepsilon}{2+\varepsilon_3}\times 0+\frac{1}{2+\varepsilon_3}\left[\left(\left(\frac{\partial\varepsilon}{\partial n_j}\right)_{T,V,\mathbf{n}/n_j}-2\left(\frac{\partial\varepsilon_s}{\partial n_j}\right)_{T,V,\mathbf{n}/n_j}\right)\times\right.$$

$$\left.\left(\frac{\partial\varepsilon_3}{\partial n_i}\right)_{T,V,\mathbf{n}/n_i}+\left(\left(\frac{\partial\varepsilon}{\partial n_i}\right)_{T,V,\mathbf{n}/n_i}-2\left(\frac{\partial\varepsilon_s}{\partial n_i}\right)_{T,V,\mathbf{n}/n_i}\right)\left(\frac{\partial\varepsilon_3}{\partial n_j}\right)_{T,V,\mathbf{n}/n_j}\right] \tag{4-347}$$

1.2 The derivatives of Uematsu and Franck model for water permittivity

The expression of the Uematsu-Franck model can be rewritten in the following simple expression, see Chapter three. This form is used to calculate the derivatives:

$$\varepsilon(T,V,\mathbf{n})=1+\boldsymbol{\rho}_{\mathbf{r}}(V,\mathbf{n})\bullet\mathbf{F}(T) \tag{4-348}$$

Note that the approximation for the water density used in the Uematsu-Franck mode isl:

$$\rho=\frac{n_{water}M_{water}}{V} \tag{4-349}$$

Then the structure of the relative water permittivity ε from the Uematsu-Frack model can be expressed in a graph as below:

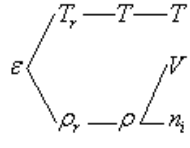

1.2.1 First order partial derivatives

Define

$$\boldsymbol{\eta}(\mathbf{x})_{\varepsilon}=\begin{bmatrix}\rho & T\end{bmatrix}^T \tag{4-350}$$

To calculate $\frac{\partial\varepsilon}{\partial\rho}$ and $\frac{\partial\varepsilon}{\partial T}$, it is necessary to calculate the derivatives of the two auxiliary vectors $\frac{\partial\boldsymbol{\rho}_{\mathbf{r}}}{\partial\rho}$ and $\frac{\partial\mathbf{F}(T)}{\partial T}$:

$$\frac{\partial \boldsymbol{\rho}_{\mathbf{r}}}{\partial \rho}=\frac{1}{\rho_0}\begin{bmatrix}1\\ 2\rho_r\\ 3{\rho_r}^2\\ 4{\rho_r}^3\end{bmatrix},\quad \frac{\partial \mathbf{F}(T)}{\partial T}=\frac{1}{T_0}\begin{bmatrix}-\frac{A_1}{{T_r}^2}\\ -\frac{A_2}{{T_r}^2}+A_4\\ -\frac{A_5}{{T_r}^2}+A_6+2A_7T_r\\ -\frac{2A_8}{{T_r}^3}-\frac{A_9}{{T_r}^2}\end{bmatrix} \tag{4-351}$$

Then we have:

$$\frac{\partial \varepsilon(\boldsymbol{\eta}_\varepsilon)}{\partial \boldsymbol{\eta}_\varepsilon}=\begin{bmatrix}\frac{\partial \varepsilon}{\partial \rho}\\ \frac{\partial \varepsilon}{\partial T}\end{bmatrix}=\begin{bmatrix}\left(\frac{\partial \boldsymbol{\rho}_{\mathbf{r}}}{\partial \rho}\right)^T\bullet\mathbf{F}(T)\\ {\boldsymbol{\rho}_{\mathbf{r}}}^T\bullet\frac{\partial \mathbf{F}(T)}{\partial T}\end{bmatrix} \tag{4-352}$$

Note

$$\left(\frac{\partial \boldsymbol{\eta}_\varepsilon}{\partial n_i}\right)_{T,V,\mathbf{n}/n_i}=\left(\frac{\partial}{\partial n_i}\begin{bmatrix}\rho\\ T\end{bmatrix}\right)_{T,V,\mathbf{n}/n_i}=\begin{bmatrix}\left(\frac{\partial \rho}{\partial n_i}\right)_{T,V,\mathbf{n}/n_i}\\ \left(\frac{\partial T}{\partial n_i}\right)_{T,V,\mathbf{n}/n_i}\end{bmatrix}=\begin{bmatrix}\left(\frac{\partial \rho}{\partial n_i}\right)_{T,V,\mathbf{n}/n_i}\\ 0\end{bmatrix}, \tag{4-353}$$

$$\text{where}\ \left(\frac{\partial \rho}{\partial n_i}\right)_{T,V,\mathbf{n}/n_i}=\begin{cases}\frac{M_{water}}{V} & i=water\\ 0 & i\neq water\end{cases}$$

From (4-132) and (4-134) it is easy to get the first order composition derivatives:

$$\left(\frac{\partial \varepsilon}{\partial n_i}\right)_{T,V,\mathbf{n}/n_i}=\left(\frac{\partial \varepsilon}{\partial \boldsymbol{\eta}_\varepsilon}\right)\left(\frac{\partial \boldsymbol{\eta}_\varepsilon}{\partial n_i}\right)_{T,V,\mathbf{n}/n_i}=\left(\frac{\partial \varepsilon}{\partial \rho}\right)\left(\frac{\partial \rho}{\partial n_i}\right)_{T,V,\mathbf{n}/n_i}=\left(\frac{\partial \boldsymbol{\rho}_{\mathbf{r}}}{\partial \rho}\right)^T\bullet\mathbf{F}(T)\left(\frac{\partial \rho}{\partial n_i}\right)_{T,V,\mathbf{n}/n_i} \tag{4-354}$$

For volume derivatives it is necessary first to derive:

$$\left(\frac{\partial \boldsymbol{\eta}_\varepsilon}{\partial V}\right)_{\mathbf{n},T}=\left(\frac{\partial}{\partial V}\begin{bmatrix}\rho & T\end{bmatrix}^T\right)_{\mathbf{n},T}=\begin{bmatrix}\left(\frac{\partial \rho}{\partial V}\right)_{\mathbf{n},T} & \left(\frac{\partial T}{\partial V}\right)_{T,\mathbf{n}}\end{bmatrix}^T=\begin{bmatrix}-\frac{1}{\rho_0}\frac{n_{water}M_{water}}{V^2} & 0\end{bmatrix}^T \tag{4-355}$$

Combine (4-132) and (4-183) and calculate the volume derivative:

$$\left(\frac{\partial \varepsilon}{\partial V}\right)_{T,\mathbf{n}}=\left(\frac{\partial \varepsilon}{\partial \boldsymbol{\eta}_\varepsilon}\right)^T\cdot\left(\frac{\partial \boldsymbol{\eta}_\varepsilon}{\partial V}\right)_{T,\mathbf{n}}=\left(\frac{\partial \boldsymbol{\rho}_{\mathbf{r}}}{\partial \rho}\right)^T\bullet\mathbf{F}(T)\left(\frac{\partial \rho}{\partial V}\right)_{T,\mathbf{n}}=-\frac{1}{\rho_0}\frac{n_{water}M_{water}}{V^2}\left(\frac{\partial \boldsymbol{\rho}_{\mathbf{r}}}{\partial \rho}\right)^T\bullet\mathbf{F}(T) \tag{4-356}$$

For temperature derivatives:

$$\left(\frac{\partial \boldsymbol{\eta}_\varepsilon}{\partial T}\right)_{\mathbf{n},V}=\left(\frac{\partial}{\partial T}\begin{bmatrix}\rho\\ T\end{bmatrix}\right)_{\mathbf{n},V}=\begin{bmatrix}0\\ 1\end{bmatrix} \tag{4-357}$$

The first order temperature derivative is:

$$\left(\frac{\partial \varepsilon}{\partial T}\right)_{\mathbf{n},V}=\left(\frac{\partial \varepsilon}{\partial \boldsymbol{\eta}_\varepsilon}\right)^T\cdot\left(\frac{\partial \boldsymbol{\eta}_\varepsilon}{\partial T}\right)_{\mathbf{n},V}={\boldsymbol{\rho}_{\mathbf{r}}}^T\bullet\frac{\partial \mathbf{F}(T)}{\partial T}\left(\frac{\partial T}{\partial T}\right)_{\mathbf{n},V}={\boldsymbol{\rho}_{\mathbf{r}}}^T\bullet\frac{\partial \mathbf{F}(T)}{\partial T} \tag{4-358}$$

1.2.2 Second order partial derivatives

Denote

$$\boldsymbol{\varepsilon}''(\boldsymbol{\eta}_\varepsilon)=\begin{bmatrix}\dfrac{\partial^2\varepsilon}{\partial\rho^2} & \dfrac{\partial^2\varepsilon}{\partial\rho\partial T}\\ \dfrac{\partial^2\varepsilon}{\partial T\partial\rho} & \dfrac{\partial^2\varepsilon}{\partial T^2}\end{bmatrix}=\begin{bmatrix}\left(\dfrac{\partial^2\boldsymbol{\rho}_\mathbf{r}}{\partial\rho^2}\right)^T\bullet\mathbf{F}(T) & \left(\dfrac{\partial\boldsymbol{\rho}_\mathbf{r}}{\partial\rho}\right)^T\bullet\dfrac{\partial\mathbf{F}(T)}{\partial T}\\ \left(\dfrac{\partial\boldsymbol{\rho}_\mathbf{r}}{\partial\rho}\right)^T\bullet\dfrac{\partial\mathbf{F}(T)}{\partial T} & \boldsymbol{\rho}_\mathbf{r}{}^T\bullet\dfrac{\partial^2\mathbf{F}(T)}{\partial T^2}\end{bmatrix}$$

(4-359)

where

$$\frac{\partial^2\boldsymbol{\rho}_\mathbf{r}}{\partial\rho^2}=\frac{1}{\rho_0{}^2}\begin{bmatrix}0\\2\\6\rho_r\\12\rho_r{}^2\end{bmatrix},\quad \frac{\partial^2\mathbf{F}(T)}{\partial T^2}=\frac{1}{T_0{}^2}\begin{bmatrix}\frac{2A_1}{T_r^3}\\-\frac{2A_2}{T_r^3}\\-\frac{2A_5}{T_r^3}+2A_7\\-\frac{6A_8}{T_r^2}-\frac{2A_9}{T_r^3}\end{bmatrix} \tag{4-360}$$

$$\left(\frac{\partial^2\boldsymbol{\eta}_\varepsilon}{\partial T^2}\right)_{V,\mathbf{n}}=\left(\frac{\partial^2\boldsymbol{\eta}_\varepsilon}{\partial T\partial n_i}\right)_{V,\mathbf{n}}=\left(\frac{\partial^2\boldsymbol{\eta}_\varepsilon}{\partial T\partial V}\right)_{V,\mathbf{n}}=\left(\frac{\partial^2\boldsymbol{\eta}_\varepsilon}{\partial n_i\partial n_j}\right)_{T,V,\mathbf{n}/n_i}=\begin{bmatrix}0\\0\end{bmatrix} \tag{4-361}$$

$$\left(\frac{\partial^2\varepsilon}{\partial n_i\partial n_j}\right)_{T,V,\mathbf{n}/n_i}=\left(\left(\frac{\partial\boldsymbol{\eta}_\varepsilon}{\partial n_i}\right)_{T,V,\mathbf{n}/n_i}\right)^T\boldsymbol{\varepsilon}''(\boldsymbol{\eta}_\varepsilon)\left(\frac{\partial\boldsymbol{\eta}_\varepsilon}{\partial n_j}\right)_{T,V,\mathbf{n}/n_j}+\left(\frac{\partial\varepsilon}{\partial\boldsymbol{\eta}_\varepsilon}\right)^T\cdot\left(\frac{\partial^2\boldsymbol{\eta}_\varepsilon}{\partial n_i\partial n_j}\right)_{T,V,\mathbf{n}/n_i}$$

$$=\begin{cases}\left(\dfrac{\partial^2\boldsymbol{\rho}_\mathbf{r}}{\partial\rho^2}\right)^T\bullet\mathbf{F}(T)\left(\dfrac{M_{water}}{V}\right)^2 & i,j=water\\ 0 & i,j\neq water\end{cases} \tag{4-362}$$

$$\left(\frac{\partial^2\boldsymbol{\eta}_\varepsilon}{\partial V^2}\right)_{T,\mathbf{n}}=\begin{bmatrix}\left(\dfrac{\partial^2\rho}{\partial V^2}\right)_{T,\mathbf{n}}\\ \left(\dfrac{\partial^2T}{\partial V^2}\right)_{T,\mathbf{n}}\end{bmatrix}=\begin{bmatrix}\dfrac{2n_{water}M_{water}}{\rho_0V^3}\\0\end{bmatrix} \tag{4-363}$$

$$\left(\frac{\partial^2\varepsilon}{\partial V^2}\right)_{T,\mathbf{n}}=\left(\left(\frac{\partial\boldsymbol{\eta}_\varepsilon}{\partial V}\right)_{T,\mathbf{n}}\right)^T\boldsymbol{\varepsilon}''(\boldsymbol{\eta}_\varepsilon)\left(\frac{\partial\boldsymbol{\eta}_\varepsilon}{\partial V}\right)_{T,\mathbf{n}}+\left(\frac{\partial\varepsilon}{\partial\boldsymbol{\eta}_\varepsilon}\right)^T\cdot\left(\frac{\partial^2\boldsymbol{\eta}_\varepsilon}{\partial V^2}\right)_{T,\mathbf{n}}$$

$$=\left(\frac{\partial^2\varepsilon}{\partial\rho^2}\right)\left(\frac{\partial\rho}{\partial V}\right)_{T,\mathbf{n}}{}^2+\left(\frac{\partial\varepsilon}{\partial\rho}\right)\left(\frac{\partial^2\rho}{\partial V^2}\right)_{T,\mathbf{n}} \tag{4-364}$$

$$=\left(\frac{\partial^2\boldsymbol{\rho}_\mathbf{r}}{\partial\rho^2}\right)^T\bullet\mathbf{F}(T)\left(\frac{n_{water}M_{water}}{\rho_0V^2}\right)^2+\frac{2n_{water}M_{water}}{\rho_0V^3}\left(\frac{\partial\boldsymbol{\rho}_\mathbf{r}}{\partial\rho}\right)^T\bullet\mathbf{F}(T)$$

$$\left(\frac{\partial^2 \boldsymbol{\eta}_{\varepsilon}}{\partial V \partial n_i}\right)_{T,\mathbf{n}} = \left(\frac{\partial^2}{\partial V \partial n_i}\begin{bmatrix}\rho & T\end{bmatrix}^T\right)_{T,\mathbf{n}} = \begin{bmatrix}\left(\frac{\partial^2 \rho}{\partial V \partial n_i}\right)_{T,\mathbf{n}} & \left(\frac{\partial^2 T}{\partial V \partial n_i}\right)_{T,\mathbf{n}}\end{bmatrix}^T$$
$$= \begin{bmatrix}\left(\frac{\partial^2 \rho}{\partial V \partial n_i}\right)_{T,\mathbf{n}} \\ 0\end{bmatrix}, \quad \text{where}\left(\frac{\partial^2 \rho}{\partial V \partial n_i}\right)_{T,\mathbf{n}} = \begin{cases} -\frac{M_{water}}{\rho_0 V^2} & i, j = water \\ 0 & i, j \neq water \end{cases} \tag{4-365}$$

$$\left(\frac{\partial^2 \varepsilon}{\partial V \partial n_i}\right)_{T,\mathbf{n}} = \left(\left(\frac{\partial \boldsymbol{\eta}_{\varepsilon}}{\partial V}\right)_{T,\mathbf{n}}\right)^T \boldsymbol{\varepsilon}''(\boldsymbol{\eta}_{\varepsilon})\left(\frac{\partial \boldsymbol{\eta}_{\varepsilon}}{\partial n_i}\right)_{T,V,\mathbf{n}/n_i} + \left(\frac{\partial \varepsilon}{\partial \boldsymbol{\eta}_{\varepsilon}}\right)^T \cdot \left(\frac{\partial^2 \boldsymbol{\eta}_{\varepsilon}}{\partial V \partial n_i}\right)_{T,\mathbf{n}}$$
$$= \left(\frac{\partial^2 \varepsilon}{\partial \rho^2}\right)\left(\frac{\partial \rho}{\partial V}\right)_{T,\mathbf{n}}\left(\frac{\partial \rho}{\partial n_i}\right)_{T,V,\mathbf{n}/n_i} + \left(\frac{\partial \varepsilon}{\partial \rho}\right)\left(\frac{\partial^2 \rho}{\partial V \partial n_i}\right)_{T,\mathbf{n}}$$
$$= \begin{cases} \left(\frac{\partial^2 \boldsymbol{\rho}_{\mathbf{r}}}{\partial \rho^2}\right)^T \bullet \mathbf{F}(T)\left(\frac{M_{water}}{\rho_0 V^2}\right)\left(\frac{2n_{water}M_{water}}{\rho_0 V^3}\right)^2 + \frac{M_{water}}{\rho_0 V^2}\left(\frac{\partial \boldsymbol{\rho}_{\mathbf{r}}}{\partial \rho}\right)^T \bullet \mathbf{F}(T) & i, j = water \\ 0 & i, j \neq water \end{cases}$$

(4-366)

$$\left(\frac{\partial^2 \boldsymbol{\eta}_{\varepsilon}}{\partial T^2}\right)_{V,\mathbf{n}} = \begin{bmatrix}0 \\ 0\end{bmatrix} \tag{4-367}$$

$$\left(\frac{\partial^2 \varepsilon}{\partial T^2}\right)_{V,\mathbf{n}} = \left(\left(\frac{\partial \boldsymbol{\eta}_{\varepsilon}}{\partial T}\right)_{V,\mathbf{n}}\right)^T \boldsymbol{\varepsilon}''(\boldsymbol{\eta}_{\varepsilon})\left(\frac{\partial \boldsymbol{\eta}_{\varepsilon}}{\partial T}\right)_{V,\mathbf{n}} + \left(\frac{\partial \boldsymbol{\varepsilon}}{\partial \boldsymbol{\eta}_{\varepsilon}}\right)^T \cdot \left(\frac{\partial^2 \boldsymbol{\eta}_{\varepsilon}}{\partial T^2}\right)_{V,\mathbf{n}} \tag{4-368}$$
$$= \frac{\partial^2 \varepsilon}{\partial T^2}(1)^2 + 0 = \boldsymbol{\rho}_{\mathbf{r}}{}^T \bullet \frac{\partial^2 \mathbf{F}(T)}{\partial T^2}$$

$$\left(\frac{\partial^2 \boldsymbol{\eta}_{\varepsilon}}{\partial T \partial n_i}\right)_{V,\mathbf{n}} = \begin{bmatrix}0 \\ 0\end{bmatrix} \tag{4-369}$$

Finally:

$$\left(\frac{\partial^2 \varepsilon}{\partial T \partial n_i}\right)_{V,\mathbf{n}} = \left(\left(\frac{\partial \boldsymbol{\eta}_{\varepsilon}}{\partial T}\right)_{V,\mathbf{n}}\right)^T \boldsymbol{\varepsilon}''(\boldsymbol{\eta}_{\varepsilon})\left(\frac{\partial \boldsymbol{\eta}_{\varepsilon}}{\partial n_i}\right)_{T,V,\mathbf{n}/n_i} + \left(\frac{\partial \varepsilon}{\partial \boldsymbol{\eta}_{\varepsilon}}\right)^T \cdot \left(\frac{\partial^2 \boldsymbol{\eta}_{\varepsilon}}{\partial T \partial n_i}\right)_{V,\mathbf{n}}$$
$$= \frac{\partial^2 \varepsilon}{\partial T \partial \rho}\left(\frac{\partial T}{\partial T}\right)_{V,\mathbf{n}}\left(\frac{\partial \rho}{\partial n_i}\right)_{T,V,\mathbf{n}/n_i} + 0 = \left(\frac{\partial \boldsymbol{\rho}_{\mathbf{r}}}{\partial \rho}\right)^T \bullet \frac{\partial \mathbf{F}(T)}{\partial T}\left(\frac{\partial \rho}{\partial n_i}\right)_{T,V,\mathbf{n}/n_i} \tag{4-370}$$
$$= \begin{cases} \frac{M_{water}}{V}\left(\frac{\partial \boldsymbol{\rho}_{\mathbf{r}}}{\partial \rho}\right)^T \bullet \frac{\partial \mathbf{F}(T)}{\partial T} & i, j = water \\ 0 & i, j \neq water \end{cases}$$

$$\left(\frac{\partial^2 \boldsymbol{\eta}_{\varepsilon}}{\partial T \partial V}\right)_{V,\mathbf{n}} = \begin{bmatrix}0 \\ 0\end{bmatrix} \tag{4-371}$$

Finally:

$$\left(\frac{\partial^2\varepsilon}{\partial T\partial V}\right)_{V,\mathbf{n}}=\left(\left(\frac{\partial\boldsymbol{\eta}_{\varepsilon}}{\partial T}\right)_{V,\mathbf{n}}\right)^{T}\boldsymbol{\varepsilon}''(\boldsymbol{\eta}_{\varepsilon})\left(\frac{\partial\boldsymbol{\eta}_{\varepsilon}}{\partial V}\right)_{T,\mathbf{n}}+\left(\frac{\partial\varepsilon}{\partial\boldsymbol{\eta}_{\varepsilon}}\right)^{T}\cdot\left(\frac{\partial^2\boldsymbol{\eta}_{\varepsilon}}{\partial T\partial V}\right)_{V,\mathbf{n}}$$

$$=\frac{\partial^2\varepsilon}{\partial T\partial V}\left(\frac{\partial T}{\partial T}\right)_{V,\mathbf{n}}\left(\frac{\partial\rho}{\partial V}\right)_{T,\mathbf{n}}+0=\left(\frac{\partial\boldsymbol{\rho}_{\mathbf{r}}}{\partial\rho}\right)^{T}\bullet\frac{\partial\mathbf{F}(T)}{\partial T}\left(\frac{\partial\rho}{\partial V}\right)_{T,\mathbf{n}}=-\frac{n_{water}M_{water}}{\rho_0V^2}\left(\frac{\partial\boldsymbol{\rho}_{\mathbf{r}}}{\partial\rho}\right)^{T}\bullet\frac{\partial\mathbf{F}(T)}{\partial T}$$

(4-372)

APPENDIX VII The collected multi-temperature experimental data of volumetric properties for electrolytes

The data sets are tabulated according to its source. The following relevant information for the data sets are all given in the table in a separate column: the author of the source paper for the experimental data set, the serial number of the source paper in IVC-SEP electrolyte literature database, the reference number, number of data points of each set in the source paper and the ranges of volumetric properties, its temperature, pressure and concentration. Temperature ranges reported in the source paper are all converted into Kelvin. Pressure, aqueous solution concentration and volumetric properties are tabulated in their original units in accordance with their source paper and not converted. Pressure units are mostly atmosphere. Other pressure units such as bar, mmHg and MPa etc. are also used.

The concentrations of the solution are reported in various ways in literature. Apart from the molality (mol/kg H_2O) and molarity (mol/l) concentration, concentrations such as weight percent salt concentration, mol percent concentration weight concentration (g/l) etc. are all used. The units of each concentration are all given in the table. Volumetric properties are mostly reported as density, relative density or AMV. Densities are mostly reported in kg/m^3 or g/cm^3 in literature. AMV is in cm^3/mol.

Table 0.1 The experimental volumetric data of the aqueous NaCl solution collected for the IVC-SEP electrolyte databank.

Data Set	Temperature (K)	Pressure range		Concentration range		Density range		Number of data	IVC-SEP electrolyte literature database no.	Reference	Author
1	348.15 - 473.15	20.27 - 20.27	bar	0.053 - 4.3933	molality	867.67 - 1121.9	g/cm^3	48	04550L	1	Rogers PSZ, Bradley DJ, Pitzer KS
2	573.15 - 873.15	100 - 3000	bar	6 - 20	weight percent salt	0.440529 - 1.03734	g/cm^3	237	05379L	2	Gehrig M, Lentz H,Franck EU
3	313.15 - 553.15	101.325 - 101.325	bar	0.001 - 1.5	molality	0.755744 - 1.05787	g/cm^3	65	07309L	3	Gorbachev SV,Kondrat'ev VP, Androsonov VI, Kolupaev VG
4	293.15 - 671.35	100 - 4000	bar	0.1 - 101	weight percent salt	0.7737 - 1.2359	SV cm^3/g	884	01331L	4	Hilbert R
5	298.15 - 473.15	20.265 - 20.265	bar	0.1 - 1	molality	869.95 - 1037.17	kg/m^3	32	06030L	5	Ellis AJ
6	446.18 - 627.38	200 - 200	bar	0.1 - 4	molality	610.6 - 1042.1	kg/m^3	68	06035L	6	Grant-Taylor DF
7	298.15 - 298.15	1 - 1	atm	0.087 - 4.2899	molality	1001 - 1173.58	kg/m^3	7	06061L	7	Guetachew T, Ye S, Mokbel I, Jose J, Xans P
8	373.15 - 690.65	0.9807 - 327.248	bar	1 - 5	weight percent salt	370 - 992	kg/m^3	39	06034L	8	Khaibullin IKh, Novikov BE
9	298.15 - 623.15	98.0665 - 980.665	bar	2 - 24	weight percent salt	630 - 1209	kg/m^3	276	06010L	9	Zarembo VI and Fedorov MK
10	373.15 - 713.15	0.001 - 999	kgf/cm^3	1 - 25	weight percent salt	370 - 1138	kg/m^3	300	06033L	10	Khaibullin IKh, Borisov NM
11	298.15 - 298.15	1 - 1	atm	0.5011 - 4.5052	molality	1017.1 - 1150.28	kg/m^3	9	05377L	11	Stakhanova MS,

12	298.15 - 298.15	1 - 1	atm	0.295378 - 1.00076	molality	1009 - 1036.18	kg/m^3	4	05382L	12	Kawaizumi F, Nakao F, Nomura H
13	298.226 - 308.124	1 - 1	atm	0.0844 - 6.0398	molality	997.446 - 1195.285	kg/m^3	23	05342L	13	Oakes CS, Simonson JM, Bodnar RJ
14	298.15 - 298.15	1 - 1	atm	0.01252 - 0.48824	molality	997.56 - 1017.22	kg/m^3	7	05394L	14	Schmelzer N, Einfeldt J
15	293.15 - 298.15	1 - 1	atm	0.487 - 19.93	weight percent salt	1001.55 – 1144	kg/m^3	7	06024L	15	Celeda J, Skramovsky S
16	278.252 - 318.212	1 - 1	atm	4 - 4	molality	1126.29 - 1145.384	kg/m^3	8	06011L	16	Wirth HE, Losurdo A
17	298.15 - 298.15	1 - 1	atm	0.002557 - 0.740175	weight percent salt	997.1772 - 1026.874	kg/m^3	15	06058L	17	Kruis A
18	293.15 - 298.15	1 - 1	atm	0.1 - 2	weight percent salt	998.9 - 1075.39	kg/m^3	1	06038L	18	Lengyel S, Fezler G
19	293.15 - 293.15	1 - 1	atm	0.1 - 20	weight percent salt	998.9 - 1147.82	kg/m^3	13	06026L	19	Jelinek RM, Leopold H
20	298.15 - 298.15	1 - 1	atm	0.02265 - 0.6409	weight percent salt	998.2 - 1022.4	kg/m^3	5	06025L	20	Werblan L
21	288.15 - 328.15	1 - 1	atm	0.05 - 5	molality	987.63 - 1171.05	kg/m^3	56	05341L	21	Isono T
22	298.15 - 298.15	1 - 1	atm	0.02037 - 0.1142	molality	997.975 - 1001.76	kg/m^3	3	06027L	22	Gopal R, Singh K
23	298.15 - 298.15	1 - 1	atm	0.0234 - 6.0216	molality	998 - 1194.9	kg/m^3	54	06012L	23	Zhang HL, Han SJ
24	298.15 - 323.15	1 - 1	atm	0.00784 - 5.82267	molality	988.68 - 1188.88	kg/m^3	44	05365L	24	Goncalves FA, Kestin J
25	308.15 - 308.15	1 - 1	atm	0.11518 - 1.91974	weight percent salt	998.4 - 10067.8	kg/m^3	11	06070L	25	Singh NP, Tikoo PK
26	298.15 - 298.15	1 - 1	atm	1.25 - 5	weight percent salt	1045.4 - 1183.1	kg/m^3	4	06057L	26	Herz W
27	298.15 - 298.15	1 - 1	atm	0.2787 - 5.1053	molality	1008.362 - 1169.198	kg/m^3	10	06039L	27	Alary JF, Simard MA, Dumont J, Jolicoeur C
28	298.15 - 298.15	1 - 1	atm	0.02011 - 3.2652	molality	997.861 - 1114.254	kg/m^3	33	06040L	28	Lankford JI, Criss CM
29	298.15 - 328.15	1 - 1	atm	0.088598 - 0.345501	molality	989.181 - 1011.02	kg/m^3	12	06062L	29	Patel SG, Kishore N
30	298.15 - 298.15	1 - 1	atm	0.01126 - 5.325	molality	997.516 - 1175.395	kg/m^3	22	06028L	30	Simard MA, Fortier JL
31	286.35 - 303.35	1 - 1	atm	0.9995 - 5.0003	molality	1037.5 - 1164.3	kg/m^3	5	06069L	31	Nagasaka Y, Okada H, Suzuki J, Nagashima A
32	298.15 - 298.15	1 - 1	atm	1.092 - 6.156	molality	1039.63 - 1198.1	kg/m^3	11	06037L	32	Zdanovskii AB
33	313.15 - 313.15	1 - 1	atm	0.2 - 3	weight percent salt	1000.4 – 1107	kg/m^3	15	06066L	33	Baabor J, Gilchrist MA, Delgado EJ
34	298.15 - 298.15	1 - 1	atm	0.0001 - 1.99962	weight percent salt	997.078 - 1075.294	kg/m^3	14	06016L	34	Jones G, Ray WA
35	293.15 - 293.15	1 - 1	atm	0.201 - 5.541	molality	1006.75 - 1194.7	kg/m^3	8	06017L	35	Harkins WD, McLaughlin HM
36	293.15 - 293.15	1 - 1	atm	0.01 - 0.4	weight percent salt	998.6 - 1014.6	kg/m^3	5	06063L	36	Kidokoro M
37	277.15 - 343.15	1 - 1	atm	0.1 - 1	molality	981.69 - 1041.75	kg/m^3	201	06023L	37	Apelblat A, Manzurola E
38	293.15 - 313.15	1 - 1	atm	0 - 4	molality	992.2 - 1139.2	kg/m^3	27	06013L	38	Comesana JF, Otero JJ, Garcia E, Correa A
39	253 - 293	1 - 1	atm	0.00858 - 6.0141	molality	996.91 - 1207.46	kg/m^3	135	06019L	39	Mironenko MV,

											Boitnott GE, Grant SA, Sletten RS
40	298.15 - 298.15	1 - 1	atm	0.1 - 6.144	molality	1001.17 - 1197.8	kg/m^3	11	06036L	40	Heyrovska R
41	298.15 - 318.15	1 - 1	atm	1.6689 - 5.4186	molality	1052.06 - 1178.13	kg/m^3	15	06059L	41	Hoelemann P, Kohner H
42	298.15 - 318.15	1 - 1	atm	1 - 6.1	molality	1028.24 - 1196.59	kg/m^3	40	05343L	42	Romankiw LA, Chou IM
43	298.15 - 298.15	1 - 1	atm	0.20913 - 0.80891	weight percent salt	1005.644 - 1029.591	kg/m^3	2	06068L	43	Dunn LA
44	298.15 - 448.15	1 - 1	atm	0.1 - 2.5	molality	897.9 - 1089.2	kg/m^3	32	05346L	44	Fabuss BM, Korosi A, Huq A
45	298.15 - 298.15	1 - 1	atm	0.0021 - 0.0806	molality	997.1 - 1000.7	kg/m^3	7	06056L	45	Jozwiak M
46	298.15 - 298.15	1 - 1	atm	0.00301 - 0.6409	weight percent salt	997.5 - 1022.4	kg/m^3	7	06029L	46	Werblan L, Rotowska A, Minc S
47	298.15 - 298.15	1 - 1	atm	1.81 - 9.17	mol percent	1037.1 - 1184.4	kg/m^3	5	06021L	47	Ostroff AG, Snowden BS, Woessner DE
48	298.15 - 423.15	1 - 1	atm	0.0999 - 3.6024	molality	922.1 - 1122.6	kg/m^3	28	05345L	48	Korosi A, Fabuss BM
49	298.15 - 298.15	1 - 1	atm	0.1 - 4	molality	1001.2 - 1137.5	kg/m^3	7	06018L	49	Ruby CE, Kawai J
50	298.15 - 298.15	1 - 1	atm	0.164569 - 4.534427	weight percent salt	1003.788 - 1167.427	kg/m^3	11	06031L	50	Gucker FT, Stubley D, Hill DJ
51	448.15 - 623.15	1 - 1	atm	0.5 - 3	molality	628 - 1002	kg/m^3	32	01464L	51	Ellis AJ, Golding RM
52	293.15 - 293.15	1 - 1	atm	0.0996 - 2.9718	molality	1002.35 - 1107.02	kg/m^3	14	06032L	52	Khimenko MT
53	283.15 - 313.15	1 - 1	atm	0.02705 - 2.8986	molality	15.13 - 19.94	AMV cm^3/mol	55	00771L	53	Allred GC, Woolley EM
54	298.15 - 298.15	1 - 1	atm	0.03994 - 3.0234	molality	0.998697 - 1.106506	1000(d-d0) g/cm3	21	00779L	54	Fortier JL, Leduc PA, Desnoyers JE
55	298.15 - 298.15	1 - 1	atm	0.05 - 3.5	molality	17.032 - 20.267	AMV cm^3/mol	19	06096L	55	Vaslow F
56	604.41 - 725.51	18.36 - 38.04	mPa	0.002503 - 3.0955	molality	0.41 - 495	1000(d-d$_0$) g/cm^3	490	06121L	56	Majer V , Lu Hui, Crovetto R , Wood RH
57	393.4 - 393.4	1 - 37.4	mPa	0.05145 - 3.09	molality	2.08 - 108.73	1000(d-d$_0$) g/cm^3	8	06120L	57	Majer V , Crovetto R , Wood RH
58	278.15 - 318.15	1 - 1	atm	0.37131 - 5.99684	molality	994.4032 - 1005.261	kg/m^3	46	06114L	58	Lo Surdo A, Alzola EM, Millero FJ
59	273.15 - 308.15	1 - 1	atm	0.00992 - 1.49986	molality	995.7019 - 1060.683	kg/m^3	57	05347L	59	Chen C-TA, Chen JH, Millero FJ
60	273.15 - 323.15	99.9 - 1001.2	bar	0.03027 - 2.008	molality	14.871 - 31.133	AMV cm^3/mol	179	06112L	60	Chen C T, Emmet R T, Millero F J
61	321.57 - 597.45	0.1 - 40.16	mPa	0.002585 - 5.0464	molality	0.076 - 248.85	1000(d-d$_0$) g/cm^3	443	06118L	61	Majer V, Gates JA, Inglese A, Wood RH
62	298.15 - 298.15	1 - 1	atm	0.295378 - 1.000761	molality	1.009 - 1.03618	g/cm^3	4	05382L	62	Kawaizumi F, Nakao F,Nomura H
63	623.15 - 623.15	200 - 500	bar	2 - 4	molality	0.781 - 0.895	g/cm^3	10	05831L	63	Fournier RO
64	298.15 - 298.15	0.1013 - 40.78	mPa	0.0582 - 4.991	molality	2.35 - 169.022	1000(d-d$_0$) g/cm^3	40	01324L	64	Gates JA, Wood RH
65	278.15 - 318.15	1 - 1	atm	0.78747 - 5.9518	molality	30.189 - 202.893	1000(d-d$_0$) g/cm^3	53	02782L	65	Perron G, Roux A, Desnoyers JE
66	274.15 - 274.15	1 - 1	atm	0.11425 - 0.11425	molality	16.864 - 18.513	AMV cm^3/mol	21	01098LE	66	Out DJP, Los JM

67	278.15 - 368.15	1 - 1	atm	0.96584 - 1.04919	molality	0.1 - 1.2	g/cm^3	60	05363LE	67	Millero FJ and Drost-Hansen W
68	302.1 - 318.9	1 - 1	atm	1 - 2.96	g/100g H_2O	1006.42 - 1166.47	kg/m^3	40	02269L	68	Redman T P, Rohani S
						total data points		4475			

Molality: mol/kg H_2O.

Table 0.2 The experimental volumetric data of the aqueous $CaCl_2$ solution collected for the IVC-SEP electrolyte databank.

Data Set	Temperature (K)	Pressure range		Concentration range		Density range		Number of data	IVC-SEP electrolyte literature database no.	Reference	Author
1	273.15 - 273.15	1 - 1	atm	0.01 - 1	g/l	1.000982 - 1.08744	g/cm^3	9	00944LE	69	Jones HC, Pearce JN
2	293.15 - 343.15	1 - 1	atm	0.098 - 5.988	molality	986.9 - 1392.3	kg/m^3	70	06117Le	70	Tashima Y, Arai Y
3	288.15 - 328.15	1 - 1	atm	0.05 - 6	molality	990.19 - 1391.93	kg/m^3	56	07302LE	71	Toshiaki I
4	298.15 - 298.15	1 - 1	atm	0.00045 - 0.77465	weight percent salt	18 - 23.19	AMV cm^3/mol	10	01774L	72	Dunn LA
5	298.153 - 308.154	1 - 1	atm	0.282 - 19.2372	molality	1002.475 - 1408.609	kg/m^3	38	05342L	73	Oakes CS, Simonson JM, Bodnar RJ
6	323.15 - 473.15	20 - 20	atm	0.05 - 1	molality	870.7 - 1072.52	kg/m^3	35	06082L	74	Ellis AJ
7	283.15 - 373.15	1 - 1	atm	30 - 45	weight percent salt	1240 - 1448	kg/m^3	116	06081L	75	Bogatykh SA, Evnovich ID
8	323.15 - 473.15	20.27 - 20.27	bar	0.5039 - 6.4389	molality	917.01 - 1376.88	kg/m^3	63	06083L	76	Kumar A
9	293.15 - 323.15	1 - 1	atm	0.266 - 5.099	molality	1011.38 - 1349.69	kg/m^3	87	06110LE	77	Goncalves FA, Kestin J
10	293.15 - 303.15	1 - 1	atm	0.05 - 0.05	molality	1000.1 - 1002.7	kg/m^3	3	06084L	78	Nowicka B, Kacperska A, Barczynska J, Bald A, TaniewskaOsinska S
11	298.15 - 298.15	1 - 1	atm	0.022 - 7.8783	molality	999.1 - 1465	kg/m^3	97	05378Le	79	Zhang HL, Chen GH, Han SJ
12	298.15 - 298.15	1 - 1	atm	0.5177 - 5.6803	molality	1040.206 - 1374.387	kg/m^3	7	00904L	80	Vasil'ev VA, Fedyainov NV, Kurenkov VV
13	298.15 - 298.15	1 - 1	atm	0.0397645 - 0.1272975	weight percent salt	1000.7 - 1008.68	kg/m^3	4	06079LE	81	Shedlovsky T, Brown AS
14	298.15 - 298.15	1 - 1	atm	0.0174 - 0.1492	weight percent salt	999.1 - 1011	kg/m^3	16	06130LE	82	Barczynska J, Bald A, Szejgis A
15	298.15 - 303.15	1 - 1	atm	0.1 - 7	molality	1005.02 - 1431.6	kg/m^3	13	06080L	83	Harkins WD, Gilbert EC
16	298.15 - 298.15	1 - 1	atm	1.28655 - 6.72	molality	1104.449 - 1420.94	kg/m^3	6	06109LE	84	Pesce G
17	293.15 - 323.15	1 - 1	atm	3.55 - 48.34	weight percent salt	1017.29 - 1487.72	kg/m^3	54	06134L	85	Brandani V, Del Re G, Di Giacomo G
18	313.15 - 353.15	11.1 - 352.1	mm Hg	19.8 - 957	g/l	994 - 1583	kg/m^3	98	02783LE	86	Harrison WR, Perman EP
19	313.15 - 353.15	1 - 1	atm	3.23 - 58.01	weight percent salt	1002 - 1586	kg/m^3	44	02783LE	87	Harrison WR, Perman EP

20	298.15 - 298.15	1 - 1	atm	7.698812 - 44.92	weight percent salt	1.453 - 1.463	g/cm^3	1	00454L	87	Ehret, WmF
21	293 - 298.15	1 - 1	atm	6.799 - 7.698812	molality	1.4145 - 1.463	g/cm^3	1	04017L	88	Benrath A
22	293 - 323	1 - 1	atm	6.799 - 11.845	mol/1000 mol H_2O	1.4145 - 1.5455	g/cm^3	4	06124L	89	Trypuc M, Kielkowska U
23	298.15 - 298.15	1 - 1	atm	0.02 - 0.5	weight percent salt	999 - 1041.3	kg/m^3	9	06111L	90	Emara MM, Farid NA
24	298.15 - 318.15	1 - 1	atm	0.46 - 5.05	molality	1030.69 - 1366.88	kg/m^3	65	05343L	91	Romankiw LA, Chou IM
25	298.05 - 363.27	1 - 1	atm	9.87 - 51.32	weight percent salt	1065.7 - 1514.2	kg/m^3	51	06075L	92	Wimby JM and Berntsson TS
26	297.19 - 371.96	6 - 6	bar	0.02976 - 0.98452	molality	0.962271 - 1.072038	g/cm^3	33	00750L	93	Saluja PPS, LeBlanc JC
27	298.15 - 298.15	1 - 1	atm	0.1 - 1	weight percent salt	1207.2 - 1389.1	kg/m^3	10	06133L	94	Sood ML
28	291.55 - 343.14	1 - 1	atm	9.87 - 51.32	weight percent salt	1065.99 - 1516.43	kg/m^3	60	06075L	95	Wimby JM and Berntsson TS
29	298.15 - 298.15	1 - 1	atm	0.555 - 2.252	molality	1045.4 - 1175.3	kg/m^3	9	06037L	96	Zdanovskii AB
30	298.15 - 298.15	1 - 1	atm	0.0953 - 2.016	weight percent salt	1.2072 - 1.4577	g/cm^3	11	06077L	97	Lyons PA, Riley JF
31	298.15 - 298.15	0.1013 - 40.71	mPa	0.0505 - 4.98	molality	4.505 - 344.431	1000(d-d$_0$) g/cm^3	39	01324L	98	Gates JA, Wood RH
32	298.15 - 298.15	1 - 1	atm	0.05001 - 6.4644	molality	4.568 - 413.788	1000(d-d$_0$) g/cm^3	14	02782L	99	Perron G, Roux A, Desnoyers JE
33	298.15 - 298.15	1 - 1	atm	19.1 - 45.5	weight percent salt	1.165 - 1.465	g/cm^3	4	03479L	100	Mead D J, Fuoss R M
34	298.15 - 298.15	1 - 1	atm	0.0334 - 7.4	molality	3.01 - 456.15	1000(d-d$_0$) g/cm^3	19	05399L	101	Kumar A, Atkinson G, Howell RD
						total data points		1156			

Molality: mol/kg H_2O.

Table 0.3 The experimental volumetric data of the aqueous $NaHCO_3$ solution collected for the IVC-SEP electrolyte databank.

Data Set	Temperature (K)	Pressure range		Concentration range		Density range		Number of data	IVC-SEP electrolyte literature database no.	Reference	Author
1	288.15 - 288.15	1 - 1	atm	8.1 - 8.1	weight percent salt	1.058 - 1.058	g/cm^3	1	06065L	102	Mazunin SA, Panasenko VA, Zubarev MP, Mazunina EL
2	273.15 - 318.15	1 - 1	atm	0.00298 - 1.00844	molality	993.6402 - 1058.7398	kg/m^3	73	06116LE	103	Hershey JP, Sotolongo S, Millero FJ
3	293.15 - 373.15	1 - 1	atm	1 - 14.1	weight percent salt	0.9819 - 1.10211	g/cm^3	177	05356LE	104	Rashkovskaya E.A, Chernen'kaya EI
						total data points		251			

Molality: mol/kg H_2O.

Table 0.4 The experimental volumetric data of the aqueous HCl solution collected for the IVC-SEP electrolyte databank.

Data Set	Temperature (K)	Pressure range	Concentration range	Density range	Number of data	IVC-SEP electrolyte literature	Reference	Author

										IVC-SEP electrolyte literature database no.		
1	283.15 - 313.15	1 - 1	atm	0.02239 - 0.39197	molality	17.53 - 18.89	AMV cm^3/mol	38	00771L	105	Allred GC, Woolley EM
2	288.15 - 328.15	1 - 1	atm	0.01005 - 0.2303	molality	0.183 - 4.228	1000(d-d_0) g/cm^3	45	00770L	106	Pogue R and Atkinson G
3	298.15 - 298.15	1 - 1	atm	0.05765 - 0.7932	molality	0.998 - 1.011	g/cm^3	14	00779L	107	Fortier J.L, Leduc PA, Desnoyers J.E
4	278.15 - 398.15	1 - 1	bar	0.05152 - 1.27612	molality	940.80 - 1015.77	kg/m^3	49	01773L	108	Hershey J.P, Damesceno R, Millero FJ
5	298.15 - 298.15	1 - 1	atm	0.000879 - 0.83624	weight percent salt	17.88 - 18.9	AMV cm^3/mol	8	01774L	109	Dunn LA
6	298.15 - 298.15	1 - 1	atm	0.58 - 10.744	weight percent salt	18.86 - 21.027	AMV cm^3/mol	10	00210L	110	Geffcken W
						total data points		164			

Molality: mol/kg H_2O.

Table 0.5 The experimental volumetric data of the aqueous Na_2CO_3 solution collected for the IVC-SEP electrolyte databank.

Data Set	Temperature (K)	Pressure range		Concentration range		Density range		Number of data	IVC-SEP electrolyte literature database no.	Reference	Author
1	298.15 - 298.15	1 - 1	atm	0.1925 - 1.5359	molality	1.0176 - 1.1442	g/cm^3	8	06037L	111	Hershey JP, Sotolongo S, Millero FJ.
2	293.15 - 293.15	1 - 1	atm	2.15 - 5.06	weight percent salt	1.0196 - 1.0502	g/cm^3	2	06024L	112	Pesce G
3	298.15 - 298.15	1 - 1	atm	0.4759 - 1.32925	molality	1046.68 - 1126.87	kg/m^3	3	06109LE	113	Zdanovskii AB
4	273.15 - 318.15	1 - 1	atm	0.004 - 1.0079	molality	994.86 - 1101.72	kg/m^3	105	06116LE	114	Celeda J, kramovsky S
						total data points		118			

Molality: mol/kg H_2O.

Table 0.6 The experimental volumetric data of the aqueous NaOH solution collected for the IVC-SEP electrolyte databank.

Data Set	Temperature (K)	Pressure range		Concentration range		Density range		Number of data	IVC-SEP electrolyte literature database no.	Reference	Author
1	298.15 - 313.15	1 - 1	atm	0.05 - 1	weight percent salt	994.8 - 1039.4	kg/m^3	24	01337L	115	Vazquez G, Alvarez E, Varela R, Cancela A, Navaza J
2	298.15 - 348.15	1 - 1	atm	0.5038 - 3.0094	molality	0.99541 - 1.11514	g/cm^3	66	06087L	116	Herrington TM, Pethybridge AD, Roffey MGJ
3	278.15 - 368.15	0.35 - 0.35	mPa	0.07496 - 0.50002	molality	-8.3 - -1.774	AMV cm^3/mol	50	07264L	117	Patterson BA, Call TG, Jardine JJ, Origlia-Luster ML, and Woolley EM
4	273.15 - 343.15	1 - 1	atm	1.0089 - 25.74	molality	-5.205 - 12.973	AMV cm^3/mol	120	06085L	118	Åkerlöf G and Kegeles G
5	273.15 - 523.15	1 - 1	atm	0 - 6		-55.64 - 4.48	AMV cm^3/mol	112	00854L	119	Simonson JM, Mesmer RE, Rogers

PSZ

					molality						
6	273.15 - 313.15	1 - 1	atm	0.03595 - 0.37323		-7.23 - -2.77	AMV cm^3/mol	39	00771L	120	Allred GC, Woolley EM
7	278.15 - 325.15	1 - 1	bar	0.05109 - 1.0036	molality	998.362 - 1044.815	kg/m^3	49	01773L	121	Hershey JP, Damesceno R, Millero FJ
8	303.15 - 353.15	1 - 1	atm	8.99 - 66.18	$g/100g\ H_2O$	1.0804 - 1.6214	g/cm^3	51	01032L	122	Hayward AM, Perman EP
9	277.73 - 317.48	0.68 - 4.47	mPa	0.0601 - 25.0202	molality	-8.539 - 12.73	AMV cm^3/mol	55	06100L	123	Simonson JM, Ryther, RJ
10	298.15 - 298.15	1 - 1	atm	0.999 - 25.292	molality	1.039028 - 1.519337	g/cm^3	23	06098L	124	Sipos PM, Hefter G, May PM
11	373.15 - 523.15	0.4 - 4.8	mPa	0.2944 - 3.1265	molality	0.8174 - 1.0685	g/cm^3	26	06119LE	125	Corti HR, Fernandez Prini R, Svarc F
12	290.75 - 343.15	1 - 1	atm	12.6 - 72.8	weight percent salt	1.111 - 1.689	g/cm^3	37	06088L	126	Krings W
						total data points		652			

Molality: mol/kg H_2O.

Reference

1. Rogers PSZ, Bradley DJ, Pitzer KS. Densities of aqueous sodium chloride solutions from 75 to 200°C at 20 bar. *J Chem Eng Data.* 1982;27:47-50.

2. Gehrig M; Lentz H, Franck EU. Concentrated aqueous sodium chloride solutions from 200 to 600 C and to 3000 bar phase equilibria and pvt-data. *Ber Bunsen-Ges Phys Chem.* 1983;87:597-600.

3. Gorbachev SV, Kondrat'ev VP, Androsonov VI, Kolupaev VG. Specific volumes of aqueous solutions of alkali-metal chlorides. *Russ J Phys Chem.* 1974;48:1641-1642

4. Hilbert R . pVT-Daten von Wasser und von wässrigen Natriumchlorid-Lösungen Dissertation (ISBN 3-8107-2053-4). Karlsruhe, 1979.

5. Ellis AJ. Partial molal volumes of alkali chlorides in aqueous solutions 200°C. *J Chem Soc A.* 1966;11:1579-1584.

6. Grant-Taylor DF. Partial molar volumes of sodium chloride solutions at 200 bar and temperatures from 175 to 350°C. *J Sol Chem.* 1981;10(9):621-630.

7. Guetachew T, Ye S, Mokbel I, Jose J, Xans P. Study of NaCl solutions in a mixed solvent H_2O - CH_3OH: Experimental densities and comparison with calculated values obtained with a modified Pitzer's model. *J Sol Chem.* 1996;25(9):895-903.

8. Khaibullin IKh, Novikov BE. A Thermodynamic study of aqueous and steam solutions of sodi sulfate at high temperatures. *High Temp.* 1973;11(2):276-282.

9. Zarembo VI and Fedorov MK. Density of sodium chloride solutions in the temperature range 25-350 °C at pressures up to 1000 kg/cm^2. *J Appl Chem.* 1975;48(9):2021-2024.

10. Khaibullin IKh, Borisov NM. Experimental investigation of the thermal properties of aque and vapour solutions of sodium and potassium chlorides at phase equilibrium. *High Temp.* 1966;4 (4):489-494.

11. Stakhanova MS;Vasilev VA. volume and heat capacity changes in aqueous salt solutions I The systems CsCl - LiCl - H_2O and CsCl - NaCl - H_2O. *Russ J Phys Chem.* 1963;37(7):839-843.

12. Kawaizumi F, Nakao F, Nomura H. Partial molar volumes and compressibilities of 1-1 type chlorides, bromides, (Ph_4P)Cl, and Na(Ph_4B) in water - acetone mixtures. *J Chem Eng Data.* 1988;33:204-211.

13. Oakes CS, Simonson JM, Bodnar RJ. The system sodium chloride-calcium chloride-water 2 Densities for ionic strengths 0.1-19.2 molúkg-1 at 298.15 and 308.15 and at 0.1 MPa. *J Chem Eng Data.* 1990;35:304-309.

14. Schmelzer N, Einfeldt J. Density measurements in some aqueous and non-aqueous electrolyte solutions at 25°C. *Wiss Z Univ Rostock Naturw Reihe.* 1989;38(6):81-82.

15. Celeda J, Skramovsky S. The metachor as a characteristic of the association of electrolytes in aqueous solutions. *Collect Czech Chem Commun.* 1984;49:1061-1078.

16. Wirth HE, Losurdo A. Temperature dependence of volume changes on mixing electrolyte solutions. *J Chem Eng Data.* 1968;13(2):226-231.

17. Kruis A. Über die Konzentrationsabhängigkeit des scheinbaren Molvolumens einiger starker Elektrolyte. *Z Phys Chem Abt B.* 1936;34(1-2):1-12.

18. Lengyel S, Fezler G. Studies on the structure of aqueous solutions containing two electrolytes by density determinations. *Acta Chim Acad Sci Hung.* 1963;37:319-327.

19. Jelinek RM, Leopold H. Precision measurements of the density of some organic liquid according to the oscillator method. *Monatsh Chem.* 1978;109:387-393.

20. Werblan L. Viscous flow mechanisms in water - methanol solutions of alk metal halides I. *Bull Acad Pol Sci Ser Sci Chim.* 1979;27(11):873-890.

21. Isono Toshiaki. Measurements of density, viscosity and electrolyte conductivity of concentrated aqueous electrolyte solutions. *Rikagaku Kenkyusho Hokoku.* 1980;56:103-114 (5/6).

22. Gopal R, Singh K. A study of the application of the debye-hueckel theory in di-tetraalkylammonium salts solutions in formamide from apparent molal volume data. *Z Phys Chem NF.* 1970;69(5-6):81-87.

23. Zhang HL, Han SJ. Viscosity and density of water + sodium chloride + potassium chloride solutions at 298.15 K. *J Chem Eng Data.* 1996;41(3):516-520.

24. Goncalves FA; Kestin J. The viscosity of nacl and kcl in the range 25-50°C. *Ber Bunsenges Phys Chem.* 1977;81:1156.

25. Singh NP, Tikoo PK. The viscosity of concentrated electrolyte solutions. *J Electrochem Soc India.* 1980;29(4):219-224.

26. Herz W. Die innere Reibung von Salzlosungen (The internal friction of salt solutions). *Z Anorg Allgem Chem.* 1914;89(4):393-396.

27. Alary JF, Simard MA, Dumont J, Jolicoeur C. Simultaneous flow measurement of specific heats and thermal expansion coefficients of liquids: aqueous t-buoh mixtures and neat alkanols and alkanediols at 25°C. *J Solution Chem.* 1982;11(11):755-776.

28. Lankford JI, Criss CM. Partial molar heat capacities of selected electrolytes and benzene in methanol and dimethylsulfoxide at 25, 40, and 80°C. *J Solution Chem.* 1987;16(11):885-905.

29. Patel SG, Kishore N. Thermodynamics of nucleic acid bases and nucleosides in wate from 25 to 55 °C. *J Solution Chem.* 1995;24(1):25-38.

30. Simard MA, Fortier JL. Heat capacity measurements of liquids with a picker mixing f microcalorimeter. *Can J Chem.* 1981;59:3208-3211.

31. Nagasaka Y, Okada H, Suzuki J, Nagashima A. Absolute measurements of the thermal conductivity of aqueous nacl solutions at pressures up to 40 MPa. *Ber Bunsenges Phys Chem.* 1983;87:859-866.

32. Zdanovskii AB. Partial heats of dilution for aqueous solutions of salts. *Russ J Phys Chem.* 1994;68(4):556-561.

33. Baabor J, Gilchrist MA, Delgado EJ. Irreversible thermodynamics of electrolyte solutions IV. Aqueous LiCl and NaCl solutions at 40°C. *Bol Soc Chil Quim.* 1993;38(2):113-118.

34. Jones G, Ray WA. The surface tension of solutions of electrolytes as a functi of the concentration III sodium chloride. *J Am Chem Soc.* 1941;63(12):3262-3263.

35. Harkins WD, McLaughlin HM. The structure of films of water on salt solutions I Surface tension and adsorption for aqueous solutions of sodium chloride. *J Am Chem Soc.* 1925;47:2083-2088.

36. Kidokoro M. The interfacial tensions between hexane and aqueous salt solutions. *Bull Chem Soc Jpn.* 1932;:280-286.

37. Apelblat A, Manzurola E. Volumetric properties of water, and solutions of sodium chlo and potassium chloride at temperatures from T=277.15 K to T=343.15 K. *J Chem Thermodyn.* 1999;31(7):869-893.

38. Comesana JF, Otero JJ, Garcia E, Correa A. Densities and viscosities of ternary systems of water - gluc - sodium chloride at several temperatures. *J Chem Eng Data.* 2003;48(2):362-366.

39. Mironenko MV, Boitnott GE, Grant SA, Sletten RS. Experimental determination of the volumetric properties of n solutions to 253 K. *J Phys Chem B.* 2001;105(41):910-912.

40. Heyrovska R. Physical electrochemistry of strong electrolytes based on partial dissociation and hydration Quantitative interpretation of the thermodynamic properties of NaCl(aq) from zero to saturation. *J Electrochem Soc.* 1996;143(6):1789-1793.

41. Hoelemann P, Kohner H. On the temperature dependence of equivalent refractive index strong electrolytes 1. *Z Phys Chem Abt B.* 1931;13(6):338-346.

42. Romankiw LA, Chou IM. Densities of aqueous sodium chloride, potassium chloride, magnesium chloride, and calcium chloride binary solutions in the concentration range 0.5-6.1 m at 25, 30, 35, 40, and 45°C. *J Chem Eng Data.* 1983;28:300-305.

43. Dunn LA. Apparent molar volumes of electrolytes 2 some 1-1 electrol in aqueous solution at 25 °C. *J Chem Soc Faraday trans.* 1968;64:1898-1903.

44. Fabuss BM; Korosi A; Huq A. Densities of binary and ternary aqueous solutions of NaCl, $NaSO_4$ and $MgSO_4$, of seawaters, and seawater concentrations. *J Chem Eng Data.* 1966;11:325-331.

45. Jozwiak M. Viscosimetric investigations of NaCl and NaBr in hexamethylphosphoramide - water mixtures at 298.15 K. *Acta Univ Lodz Folia Chim.* 1991;9(9):3-18.

46. Werblan L, Rotowska A, Minc S. Viscosity of water - methanol solutions of $LiClO_4$, $NaClO_4$ an NaCl. *Electrochim Acta.* 1971;16:41-59.

47. Ostroff AG, Snowden BS, Woessner DE. Viscosities of protonated and deuterated water solutions of alkali metal chlorides. *J Phys Chem*. 1969;73(8):2784-2785.

48. Korosi A; Fabuss BM. Viscosities of binary aqueous solutions of NaCl, KCl, $Na_2SO_4$and $MgSO_4$ at concentrations amd temperatures of interest in delalination processes. *J Chem Eng Data*. 1968;13:548.

49. Ruby CE, Kawai J. The densities, equivalent conductances and relative viscosity at 25°C, of solutions of hydrochloric acid, potassium chloride and sodium chloride, and of their binary and ternary mixtures of constant chloride-ion-constituent content. *J Am Chem Soc*. 1926;48(5):1119-1128.

50. Gucker FT, Stubley D, Hill DJ. The isotropic compressibilities of aqueous solutions of some alkali halides at 298.15 K. *J Chem Thermodyn*. 1975;7:865-873.

51. Ellis AJ, Golding RM . The solubility of CO_2 above 100°C in water and in NaCl solutions. *American Journal of Science.* 1963;261:47-60

52. Khimenko MT. The use of refractometric data for the calculation of the polarisabilities and radii of species in solution. *Russ J Phys Chem.* 1969;43(7):1043-1046

53. Allred GC, Woolley EM. Heat capacities of aqueous HCl, NaOH, and NaCl at 283.15, 298.15 and 313.15K: delta Cp for ionization of water. *J Chem Thermodyn.* 1981;13:147-154

54. Fortier JL, Leduc PA, Desnoyers JE. Thermodynamic properties of alkali halides II Enthalpies of dilution and heat capacities in water at 25°C. *J Sol Chem.* 1974;3:323-349

55. Vaslow F. The Apparent molal volumes of the alkali metal chlorides in aqueous solution and evidence for salt-induced structure transitions. *J Phys Chem.* 1966;70(7):2286 – 2294

56. Majer V, Lu Hui, Crovetto R , Wood RH. Volumetric properties of aqueous 1-1 electrolyte solutions near and above the critical temperature of water I Densities and apparent molar volumes of NaCl(aq) from 0.0025 to 3.1 mol*kg-1, 604.4 K to 725.5 K, and 18.5 MPa to 38.0 MPa. *J Chem Thermodyn*. 1991;23:213-229.

57. Majer V , Crovetto R , Wood RH. A new version of vibrating-tube flow densitometer for measurements at temperatures up to 730 K. *J Chem Thermodyn*. 1991;23:333-344.

58. Lo Surdo A, Alzola EM, Millero FJ. The (p,V,T) properties of concentrated aqueous electrolytes I Densities and apparent molar volumes of NaCl, Na_2SO_4, MgCl2, and $MgSO_4$ solutions from 0.1mol*kg-1 to saturation and from 273.15 to 323.15 K. *J Chem Thermodyn.* 1982;14:649-662.

59. Chen CT; Chen JH; Millero FJ. Densities of NaCl, MgCl2, Na_2SO_4 and Mg SO_4. Aqueous solutions at 1 atm from 0 to 50°C and from 0.001 to 1.5m. *J Chem Eng Data.* 1980;25:307-310.

60. Chen CT, Emmet R T; Millero FJ. The apparent molal volumes of aqueous solutions of NaCl, KCl, $MgCl_2$, Na_2SO_4, and $MgSO_4$ from 0 to 1000 bars at 0, 25, and 50°C. *J Chem Eng Data.* 1977; 22:201-207.

61. Majer V, Gates JA, Inglese A, Wood RH. Volumetric properties of aqueous NaCl solutions from 0.0025 to 5.0 mol*kg^{-1}, 323 to 600 K, and 0.1 to 40 MPa. *J Chem Thermodyn.* 1988;20:949-968.

62. Kawaizumi F, Nakao F, Nomura H. Partial molar volumes and compressibilities of 1-1 type chlorides, bromides, (Ph4P)Cl, and Na(Ph4B) in water - acetone mixtures. *J Chem Eng Data.* 1988;33:204-211.

63. Fournier RO. A method of calculating quartz solubilities in aqueous sodium chloride solutions. *Geochimica et Cosmochimica Acta.* 1983;47:579-586.

64. Gates JA, Wood RH. Densities of aqueous solutions of NaCl, $MgCl_2$, KCl, NaBr *J Chem Eng Data.* 1985;30:44-49

65. Perron G, Roux A, Desnoyers JE. Heat capacities and volumes of NaCl, $MgCl_2$, $CaCl_2$, $NiCl_2$ up to 6 molal in water. *Can J Chem.* 1981;59:3049-54.

66. Out DJP; Los JM. Viscosity of aqueous solutions of univalent electrolyes from 5 to 95°C. *J Sol Chem.* 1980;9:19-35.

67. Millero FJ and Drost-Hansen W. Apparent molal volumes of aqueous monovalent salt solutions at various temperatures. *J Chem Eng Data.* 1968;13:330-333.

68. Redman T P, Rohani S. On-line determination of supersaturation of a KCl-NaCl aqueous solution based on density measurement. *Can J Chem Eng.* 1994;72:64-71.

69. Jones HC, Pearce JN. Dissociation as measured by freezing point lowering and by conductivity - bearing on the hydrate theory. *Am Chem J.* 1907;38:683-743.

70. Tashima Y, Arai Y. Densities of some alcohols and water containing calcium chloride in the region 20-70°C. Relation with salt effect on vapour-liquid equilibria. *Mem Fac Eng Kyushu Univ.* 1981;41(3):217-232.

71. Toshiaki Isono. Density, viscosity, and electrolytic conductivity of concentrated aqueous electrolyte solutions at several temperatures Alkaline-earth chlorides, lanthanum chloride, sodium sulfate, sodium nitrate, sodium bromide, potassium nitrate, potassium bromide, and cadmium nitrate. *J Chem Eng Data.* 1984;29(1):45-52.

72. Dunn LA. Apparent molar volumes of electrolytes. *Faraday society, FS Transactions.* 1966;62:2348-2354.

73. Oakes CS, Simonson JM, Bodnar RJ. The system sodium chloride-calcium chloride-water. 2 Densities for ionic strengths 01-19.2 mol*kg^{-1} at 298.15 and 308.15 and at 0.1 MPa. *J Chem Eng Data.* 1990;35:304-309.

74. Ellis AJ. Partial Molal Volumes of Magnesium Chloride, Calcium Chloride, Strontium Chloride, and Barium Chloride in Aqueous Solutions to 200°C. *J Chem Soc A.* 1967;35(4):660-664.

75. Bogatykh SA, Evnovich ID. Investigation of Densities of Aqueous LiBr, LiCl, and $CaCl_2$ Solutions in Relation to Conditions of Gas Drying. *J Appl Chem USSR.* 1965;38(4):932-933.

76. Kumar A. Densities and apparent molal volumes of aqueous concentrated calcium chloride solutions from 50 to 200°C at 20.27 Bar. *J Sol Chem* 1986;15(5):409-412.

77. Goncalves FA, Kestin J. The viscosity of calcium chloride solutions in the range 20 to 50°C. *Ber Bunsen-Ges Phys Chem.* 1979;83(1): 24-27

78. Nowicka B, Kacperska A, Barczynska J, Bald A, Taniewska-Osinska S. Viscosity of solution of NaI and $CaCl_2$ in water –ethanol and of NaI in water - tetrahydrofuran mixtures. *J Chem Soc Faraday Trans I* . 1988;84(11):3877-3884.

79. Zhang H-L; Chen G-H; Han S-J. Viscosity and density of H_2O + NaCl + $CaCl_2$ and H_2O + KCl + $CaCl_2$ at 298.15 K. *J Chem Eng Data.* 1997;42:526-530.

80. Vasil'ev VA, Fedyainov NV, Kurenkov VV. Specific heats and specific volumes of isopiestic aqueous solutions of beryllium-subgroup metal chlorides. *Russ J Phys Chem.* 1973;47:1570-3.

81. Shedlovsky T, Brown AS. The electrolytic conductivity of alkaline earth chlorides in water at 25 °C . *J Am Chem Soc.* 1934;56(5):1066-1071.

82. Barczynska J, Bald A, Szejgis A. Viscometric and conductometric studies for $CaCl_2$ solutions in water - propan-1-ol mixtures at 25°C . *J Chem Soc Faraday Trans I.* 1990;86(19):2887-2890.

83. Harkins WD, Gilbert EC. The structure of films of water on salt solutions II. The surface tension of calcium chloride solutions at 25°C. *J Am Chem Soc.* 1926;48(3):604 – 607.

84. Pesce G. Variation with concentration of equivalent refraction of dissolved electrolytes. *Z Phys Chem Abt A.* 1932;160(2-3):295-300.

85. Brandani V, Del Re G, Di Giacomo G. Vapour-Liquid Equilibrium of Water - Calcium Chloride and Ethanol - Calcium Chloride, from 30 to 95 °C. *Chim Ind Milan.* 1985;67(7-8):392-399.

86. Harrison WR, Perman EP. Vapour pressure and heat of dilution of aqueous solutions. Trans *Faraday Soc.* 1927;23:1-22.

87. Ehret WmF. Ternary Systems. *J Am Chem Soc.* 1932;54:3126-34.

88. Benrath A. Über die Systeme $CoCl_2$-MeCl oder $MeCl_2$-H_2O. *Z Anorg Allgem Chem.* 1927;163:396-404.

89. Trypuc M, Kielkowska U. Studies of ammonium chloride - calcium chloride - water system. *Pol J Appl Chem.* 1992;36(3-4):269-276.

90. Emara MM, Farid NA. Thermodynamic molar properties of aqueous solutions of Ca and Mg salts using sound velocity measurements. *J Indian Chem Soc.* 1981;58:474-478.

91. Romankiw LA, Chou IM. Densities of aqueous sodium chloride, potassium chloride, magnesium chloride, and calcium chloride binary solutions in the concentration range 0.5-6.1 m at 25, 30, 35, 40, and 45°C. *J Chem Eng Data.* 1983;28:300-305.

92. Wimby JM and Berntsson TS. Viscosity and density of aqueous solutions of lithium bromide, lithium chloride, zinc bromide, calcium chloride and lithium nitrate 1 Single salt solutions. *J Chem Eng Data.* 1994; 39(1):68 – 72.

93. Saluja PPS, J C LeBlanc. Apparent molar heat capacities and volumes of aqueous solutions of $MgCl_2$, $CaCl_2$ and $SrCl_2$ at elevated temperature. *J Chem Eng Data.* 1987;32:72-76.

94. Sood ML. A new correlation for improving diffusion coefficients. *Acta Cienc Indica.* 1976;2(2):110-114.

95. Wimby JM and Berntsson TS. Viscosity and density of aqueous solutions of lithium bromide, lithium chloride, zinc bromide, calcium chloride and lithium nitrate 1 Single salt solutions. *J Chem Eng Data.* 1994;39(1):68 – 72.

96. Zdanovskii AB. Partial heats of dilution for aqueous solutions of salts. *Russ J Phys Chem*. 1994;68(4):556-561.

97. Lyons PA, Riley JF. Diffusion coefficients for aqueous solutions of calcium chloride and cesium chloride at 25°. *J Am Chem Soc.* 1954;76(20):5216 – 5220.

98. Gates JA, Wood RH. "Densities of aqueous solutions of NaCl, $MgCl_2$, KCl, NaBr. *J Chem Eng Data.* 1985;30:44-49.

99. Perron G, Roux A, Desnoyers JE. Heat capacities and volumes of NaCl, $MgCl_2$, $CaCl_2$, $NiCl_2$ up to 6 molal in water. *Can J Chem.* 1981;59:3049-54.

100. Mead D J, Fuoss R M. Conductance and viscosity of concentrated solutions of calcium and zinc chlorides. *J Phys Chem.* 1949;49:480-482.

101. Kumar A; Atkinson G; Howell RD. Thermodynamics of concentrated electrolyte mixtures II Densities and compressibilities of aqueous sodium chloride-calcium chloride at 25°C. *J Sol Chem*. 1982;11:857-870.

102. Mazunin SA, Panasenko VA, Zubarev MP, Mazunina EL. Examination of the solubility in the system Na^+, NH_4^+ // HCO Cl^-, H_2O at 15, 20, 25, 30 °C. *Z Neorg Khim*. 1999;44(6):999-1007.

103. Hershey JP, Sotolongo S, Millero FJ. Densities and compressibilities of aqueous sodium carbonate and bicarbonate from 0 to 45 °C. *J Sol Chem*. 1983;2:233–254.

104. Rashkovskaya EA, Chernen'kaya EI. Densities of ammonium bicarbonate, sodium bicarbonate, and ammonium chloride and ammonia salt solutions at 20-100°. *Zhurnal Prikladnoi Khimii.* 1967;40:301.

105. Allred GC, Woolley EM. Heat capacities of aqueous HCl, NaOH, and NaCl at 283.15, 298.15 and 313.15K: delta Cp for ionization of water. *J Chem Thermodyn*. 1981;13:147-154.

106. Pogue R and G Atkinson. "Aparent molal volumes and heat capacities of aqueous HCl and $HClO_4$ at 15-55°C. *J Chem Eng Data.* 1988;33:495-499.

107. Fortier JL, Leduc PA, Desnoyers JE. Thermodynamic properties of alkali halides II Enthalpies of dilution and heat capacities in water at 25°C. *J Sol Chemistry*. 1974;3:323-349.

108. Hershey JP, Damesceno R, Millero FJ. Densities and compressibilities of aqueous HCl and NaOH from 0 to 45°C. The effect of pressure on the ionization. *J Sol Chemistry*. 1984;13: 825-848.

109. Dunn LA. Apparent molar volumes of electrolytes. *Faraday society, FS Transactions.* 1966;62:2348-2354.

110. Geffcken W. Über die scheinbaren Molvolumina gel"ster Elektrolyte I. *Z phys Chem Abt A.* 1931;155:1-28.

111. Hershey JP, Sotolongo S, Millero FJ. Densities and compressibilities of aqueous sodium carbonate and bicarbonate from 0 to 45 °C. *J Sol Chem.* 1983;12:233–254.

112. Pesce G. Variation with concentration of equivalent refraction of dissolved electrolytes. *Z Phys Chem Abt A.* 1932;160(2-3):295-300.

113. Zdanovskii AB. Partial heats of dilution for aqueous solutions of salts. *Russ J Phys Chem.* 1994;68(4):556-561.

114. Celeda J, Skramovsky S. The metachor as a characteristic of the association of electrolytes in aqueous solutions. *Collect Czech Chem Commun.* 1984;49:1061-1078.

115. Vazquez G, Alvarez E, Varela R, Cancela A, Navaza J. Density and viscosity of aqueous solutions of sodium dithionitef sodium hydroxide, sodium dithionite + sucrose, and sodium dithionite + sodium hydroxide + sucrose from 25 °C to 40 °C. *J Chem Eng Data.* 1996;41:244-248.

116. Herrington TM, Pethybridge AD, Roffey MGJ. Densities of aqueous lithium, sodium and potassium hydroxides from 25 to 75 °C at 1 atm. *J Chem Eng Data.* 1986;31(1):31–34.

117. Patterson BA, Call TG, Jardine JJ, Origlia-Luster ML, and Woolley EM. Thermodynamics for ionization of water at temperatures from 278.15 K to 393.15 K and at the pressure 0.35 MPa: apparent molar volumes of aqueous KCl, KOH, and NaOH and apparent molar heat capacities of aqueous HCl, KCl, KOH, and NaOH. *J Chem Thermodyn*. 2001;33:1237-1262.

118. Åkerlöf G and Kegeles G. The density of aqueous solutions of sodium hydroxide. *J Am Chem Soc.* 1939;61(5):1027 – 1032.

119. Simonson JM, Mesmer RE, Rogers PSZ. The enthalpy of dilution and apparent molar heat capacity of NaOH(aq) to 523K and 40 MPa. *J Chem Thermodyn*. 1989;21:561-584.

120. Allred GC, Woolley EM. Heat capacities of aqueous HCl, NaOH, and NaCl at 283.15, 298.15 and 313.15K: delta Cp for ionization of water. *J Chem Thermodyn*. 1981;13:147-154.

121. Hershey JP, Damesceno R, Millero FJ. Densities and compressibilities of aqueous HCl and NaOH from 0 to 45°C The effect of pressure on the ionization. *J Sol Chem*. 1984;13: 825-848

122. Hayward AM, Perman EP. Vapour pressure and heat of dilution -part VII Vapour pressures of aqueous solutions of sodium hydroxide and of alcoholic solutions of calcium chloride. *TransFaraday Soc.* 1931;27:59-69.

123. Simonson J M; Ryther R J. Volumetric properties of aqueous sodium hydroxide from 273.15 to 348.15 K. *J Chem Eng Data.* 1989;34(1):57-63.

124. Sipos PM, Hefter G, May PM. Viscosities and densities of highly concentrated aqueous MOH solutions (M^+) Na^+, K^+, Li^+, Cs^+, $(CH_3)_4N^+$) at 250 °C. *J Chem Eng Data.* 2000;45(4):613-617.

125. Corti HR, Fernandez Prini R, Svarc F. Densities and partial molar volumes of lithium, sodium and potassium hydroxides up to 250 °C. *J Sol Chem.* 1990;19:793-809.

126. Krings W. Die Viskosität und die Dichte von Natronlaugen bis zu hohen Konzehtrationen und bei höheren Temperature. *Z Anorg Chem.* 1948;255:294-298.

APPENDIX VIII The reproduced results of MSW EOS at wide temperature range

Myers *et al.* published three types of results in their paper [1]: the numerical results (average absolution deviations) of the correlations for 138 aqueous electrolyte solutions at 25 ºC and 1 bar, the numerical and graphical results of the correlations for seven aqueous electrolyte solutions from 0 to 300 ºC and 1 to 120 bar and graphical results of two aqueous multi-component electrolyte systems.

We selected some of the first two types of the published results and reproduced them. For the aqueous electrolyte solutions at 25 ºC and 1 bar, we chose the common electrolytes like NaCl, $CaCl_2$, KCl, Na_2SO_4 using the published parameters by Myers *et al.* [1] and calculated the mean ionic activity coefficients. (See table one in their paper: % AADs in mean ionic activity coefficients at 25 ºC) In the paper, the authors only reported the average absolution deviations of the fittings without any figures, besides no other information of the experimental data used in the regressions are given (e.g. number of data points used in the regression), apart from the literature source of the data. It is therefore not very easy to compare the reproduced results with those published in details. Qualitative comparison was conducted: the average absolute deviations of the aforementioned four salts were calculated using the experimental data from the same literature as in the original paper. The values are very close but not exactly equal to those published by Myers *et al.*[1]. The generated mean ionic activity coefficients agreed satisfactorily with the experimental data when plotted.

For the seven aqueous systems at wide temperature range, sufficient information was provided by the authors to compare the reproduced results with the original ones. The following six out of seven systems were chosen for the test. Cs_2SO_4 was not selected. The parameters from original paper[1] were listed in below Table 1 and used in the reproduction of the results. The following simple temperature dependence functions (8-1) and (8-2), according to the authors, should be used if the computation is over a wide temperature range.

$$a(T) = a_0 + a_1 / T \tag{8-1}$$

$$\sigma(T) = \sigma_0 + \sigma_1 / T \tag{8-2}$$

Table 1 The best-fit parameter values for electrolytes according to Myers[1].

No	Electrolyte	a_1	a_2	b (cm3/mol)	k_{sw}	σ_1	σ_2
1	NaCl	0.932	-207.9	9.90	-0.2540	5.695	-551.3
2	NaBr	1.360	-280.3	14.3	-0.1888	8.114	-1242
3	$CaCl_2$	1.694	-326.7	13.4	-0.4461	6.871	-897.7
4	Li_2SO_4	1.619	-352.7	9.46	-0.1167	4.835	-358.1
5	Na_2SO_4	2.737	-661.3	15.5	0.1670	4.850	-432.2
6	K_2SO_4	1.520	-392.2	10.6	0.2020	4.566	-388.7

The reproduced MSW EOS results for the mean ionic activity and osmotic coefficients in the 0-300 C temperature range and the 1 to 120 bar range of the NaCl, NaBr and $CaCl_2$ solutions are shown in Figure 1-6. The solid lines are the calculated results with the parameters in Table 1. The experimental data from the same source as

in the Myers' paper [1] are plotted in the figures as dots. The reproduced densities of the above three electrolyte solutions are shown in Figure 7-9. These twelve figures exactly agree with those published in the original paper.

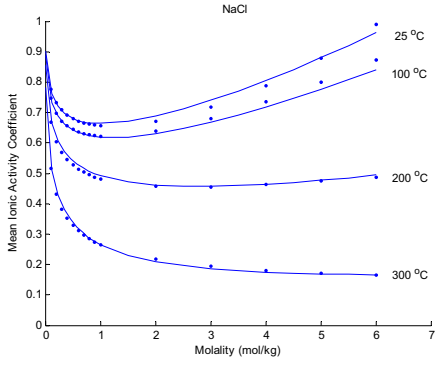

Figure 1. Activity coefficient of aqueous NaCl.

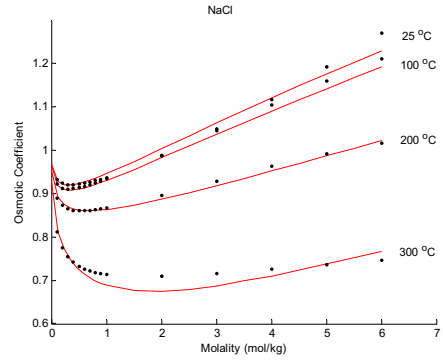

Figure 4. Osmotic coefficient of aqueous NaCl.

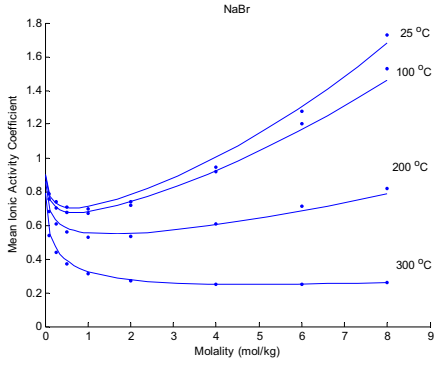

Figure 2. Activity coefficient of aqueous NaBr.

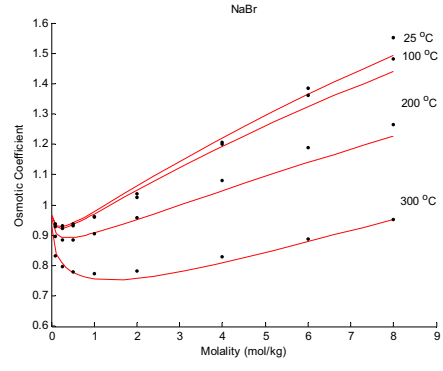

Figure 5. Osmotic coefficient of aqueous NaBr.

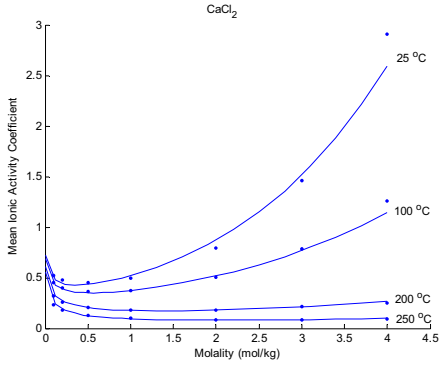

Figure 3. Activity coefficient of aqueous $CaCl_2$.

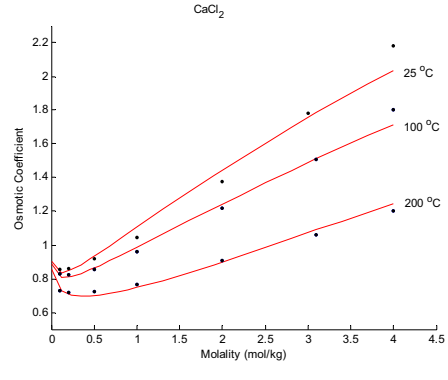

Figure 6. Osmotic coefficient of aqueous $CaCl_2$.

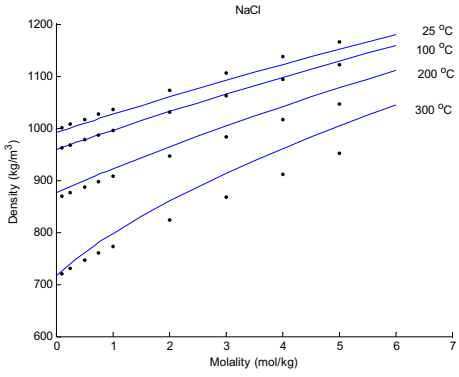

Figure 7. Density of aqueous NaCl.

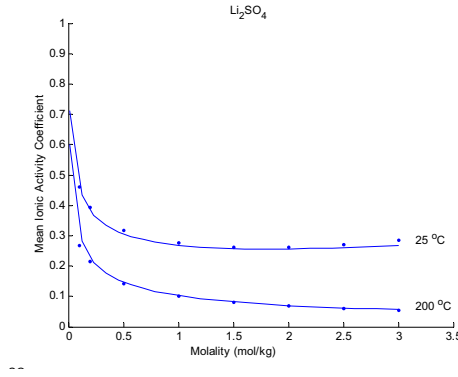

Figure 10. Activity coefficient of aqueous Li_2SO_4.

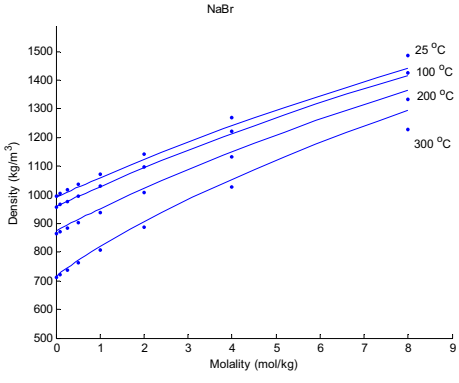

Figure 8. Density of aqueous NaBr.

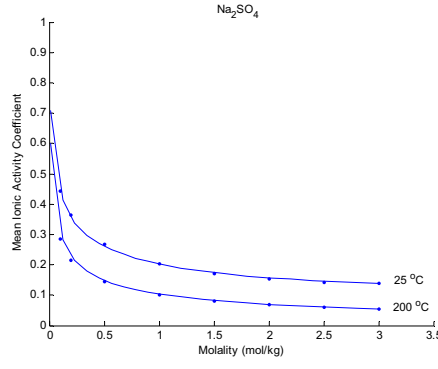

Figure 11. Activity coefficient of aqueous Na_2SO_4.

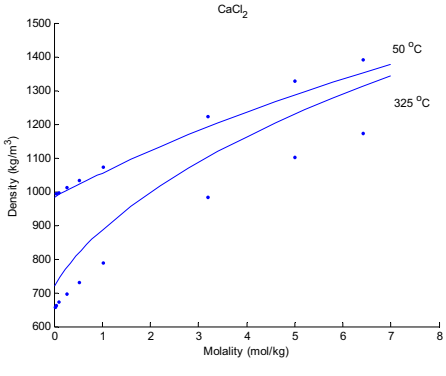

Figure 9. Density of aqueous $CaCl_2$.

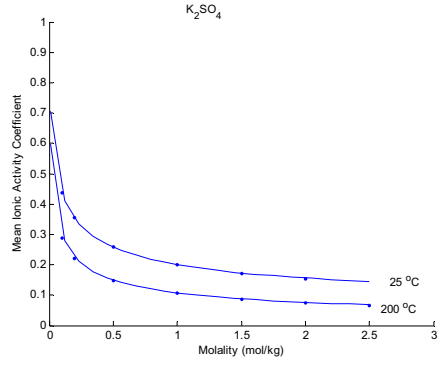

Figure 12. Activity coefficient of aqueous K_2SO_4.

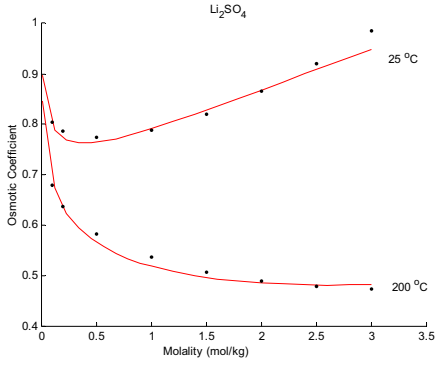

Figure 13. Osmotic coefficient of aqueous Li_2SO_4.

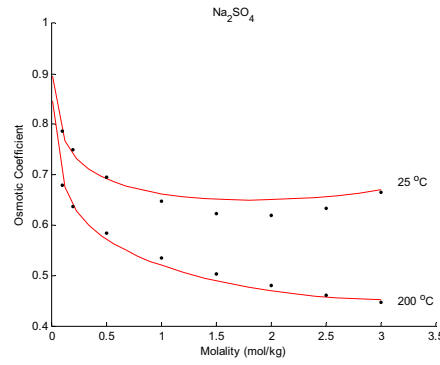

Figure 14. Osmotic coefficient of aqueous Na_2SO_4.

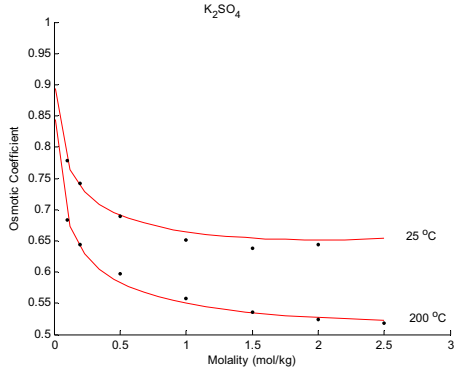

Figure 15. Osmotic coefficient of aqueous K_2SO_4.

The reproduced graphical results of the mean ionic activity and osmotic coefficients of the Li_2SO_4, Na_2SO_4 and K_2SO_4 solutions in the 0-200 ºC temperature range and the 1 to 25.6 bar range are shown in Figure 10-15. The solid lines stand for the calculated results using the parameters in Table 1 and the dots for experimental data. Note that Figure 13, the plot of the osmotic coefficient of aqueous Li_2SO_4 solution version concentration, is different from the Figure 17 in the Myers' paper [1]. It is because the same Figure 18 of the osmotic coefficient of aqueous Na_2SO_4 solution was presented in the Myers' paper [1] twice: the figure for the osmotic coefficient of aqueous Na_2SO_4 solution was by mistake presented as Li_2SO_4 in Figure 17. In this thesis, the correct figure were generated and presented. The calculations of the densities of aqueous Li_2SO_4, Na_2SO_4 and K_2SO_4 solutions were not published in the original paper. They are not presented here consequently.

From the above test to reproduce the published results, it is safe to say that MSW EOS was correctly implemented in FORTRAN and the reported results by Myers [1] are reproducible.

Reference

1. Myers JA, Sandler SI, Wood RH. An Equation of State for Electrolyte Solutions Covering Wide Range of Temperature, Pressure and Composition. *Ind Eng Chem Res.* 2002; 41: 3282-3297.

APPENDIX IX The graphical results of MSW EOS at wide temperature range using ion-specific parameters

1. The results of simutanous regression of all parameters (including binary interaction parameters) in section 5.6.2

The graphical results for the mean ionic activity and osmotic coefficients in the 0-300 C temperature range and the 1 to 120 bar range of the NaCl, NaBr and $CaCl_2$ solutions are shown in Figure 1-6. The solid lines are the calculated results with the parameters in Table 5.12 in section 5.6.2. The experimental data are plotted in the figures as dots. The calculated densities of the above three electrolyte solutions are shown in Figure 7-9. The graphical results of the mean ionic activity and osmotic coefficients of the Li_2SO_4, Na_2SO_4 and K_2SO_4 solutions in the 0-200 ºC temperature range and the 1 to 25.6 bar range are shown in Figure 10-15. These fifteen figures show a better agreement between the calculated values and experimental data than those graphical results in tests in previous section 5.6.1 and 5.6.2 .

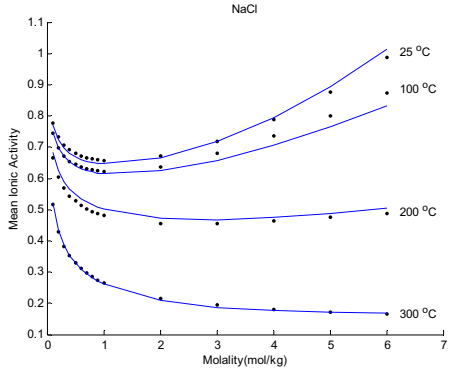

Figure 1. Activity coefficient of aqueous NaCl.

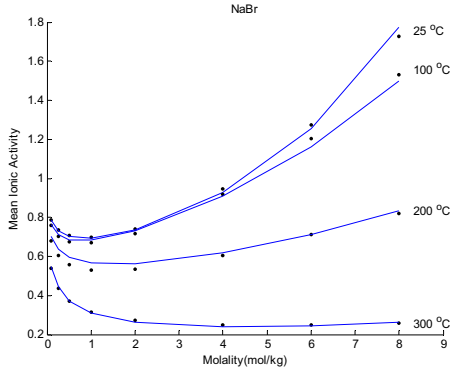

Figure 2. Activity coefficient of aqueous NaBr.

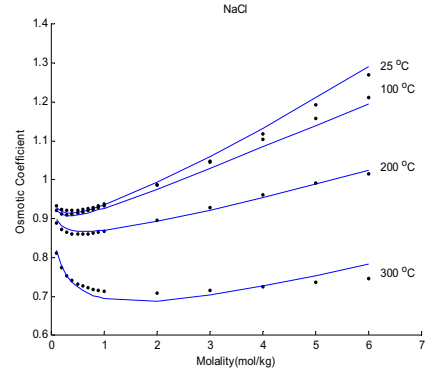

Figure 4. Osmotic coefficient of aqueous NaCl.

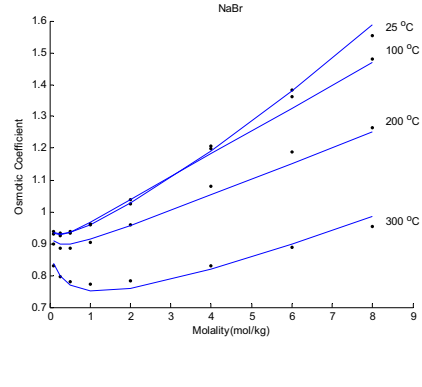

Figure 5. Osmotic coefficient of aqueous NaBr.

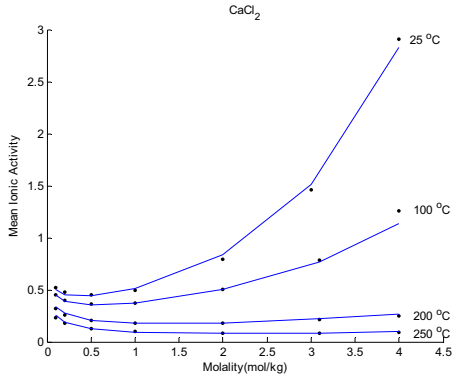

Figure 3. Activity coefficient of aqueous $CaCl_2$.

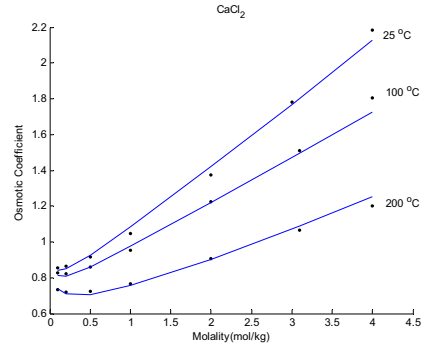

Figure 6. Osmotic coefficient of aqueous $CaCl_2$.

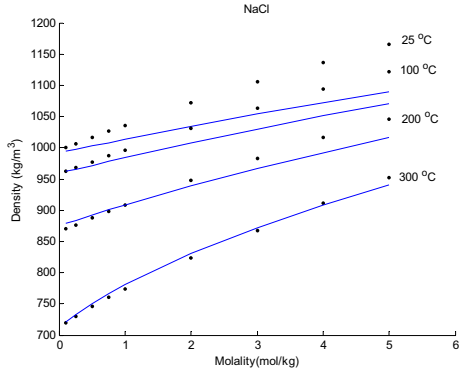

Figure 7. Density of aqueous NaCl.

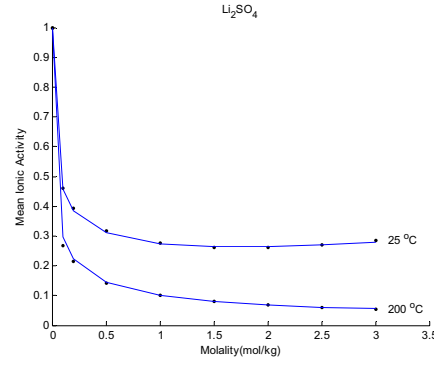

Figure 10. Activity coefficient of aqueous Li_2SO_4.

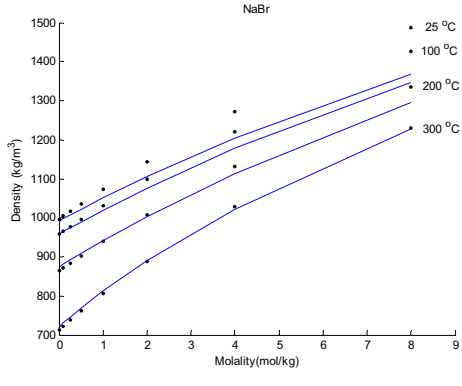

Figure 8. Density of aqueous NaBr.

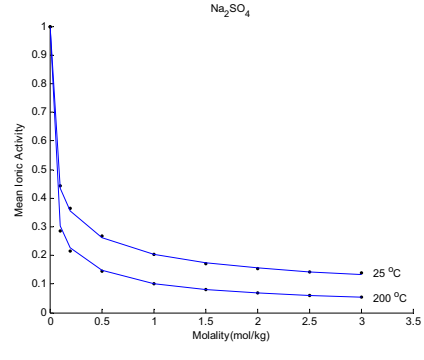

Figure 11. Activity coefficient of aqueous Na_2SO_4.

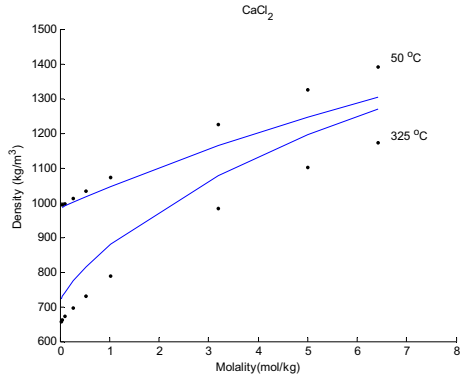

Figure 9. Density of aqueous $CaCl_2$.

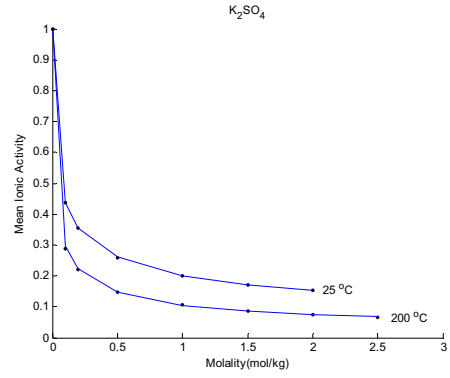

Figure 12. Activity coefficient of aqueous K_2SO_4.

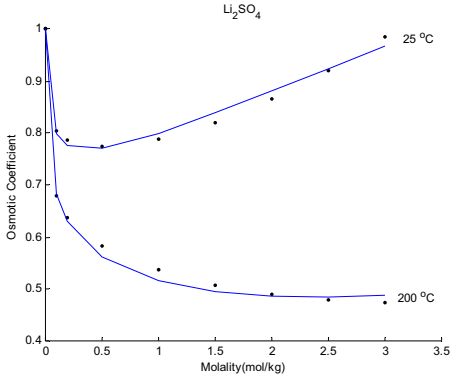

Figure 13. Osmotic coefficient of aqueous Li_2SO_4.

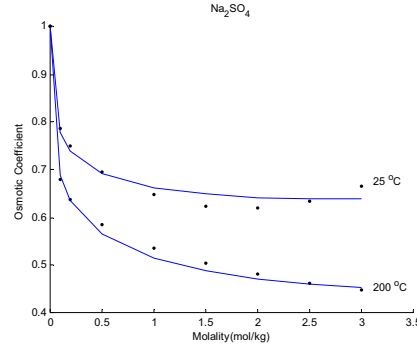

Figure 14. Osmotic coefficient of aqueous Na_2SO_4.

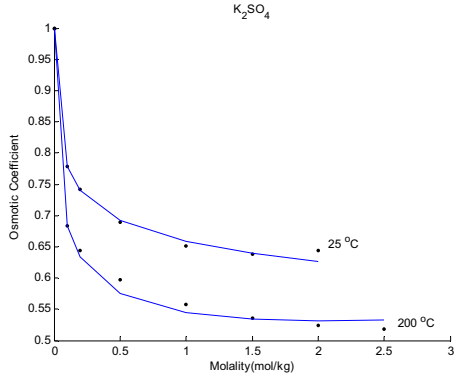

Figure 15. Osmotic coefficient of aqueous K_2SO_4.

2. The results of simutanous regression of all parameters (including binary interaction parameters) using fixed relative permittivity in section 5.6.3.1

The graphical results for the mean ionic activity and osmotic coefficients in the 0-300 C temperature range and the 1 to 120 bar range of the NaCl, NaBr and $CaCl_2$ solutions are shown in Figure 1-6. The solid lines are the calculated results with the parameters in Table 5.12 in section 5.6.3.1. The experimental data are plotted in the figures as dots. The calculated densities of the above three electrolyte solutions are shown in Figure 7-9. The graphical results of the mean ionic activity and osmotic coefficients of the Li_2SO_4, Na_2SO_4 and K_2SO_4 solutions in the 0-200 ºC temperature range and the 1 to 25.6 bar range are shown in Figure 10-15.

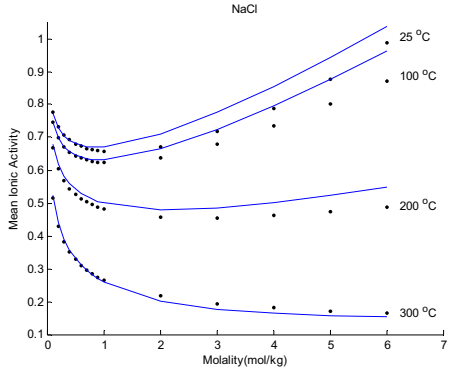

Figure 1. Activity coefficient of aqueous NaCl.

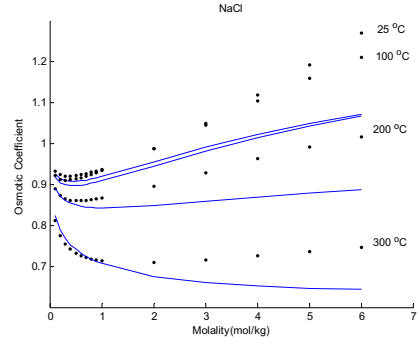

Figure 4. Osmotic coefficient of aqueous NaCl.

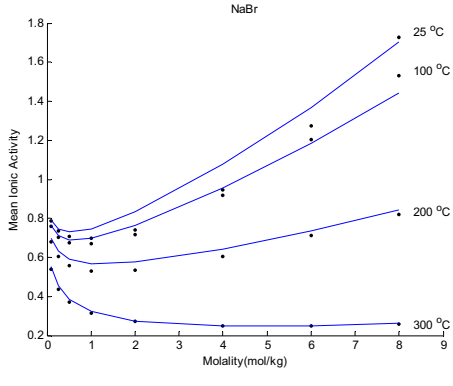

Figure 2. Activity coefficient of aqueous NaBr.

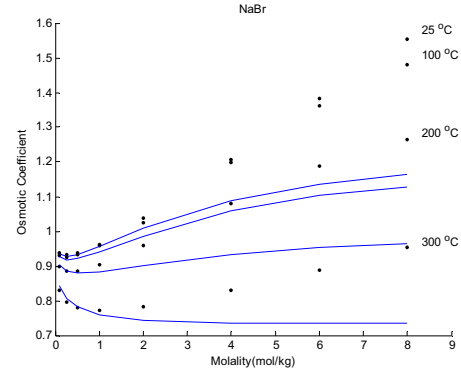

Figure 5. Osmotic coefficient of aqueous NaBr.

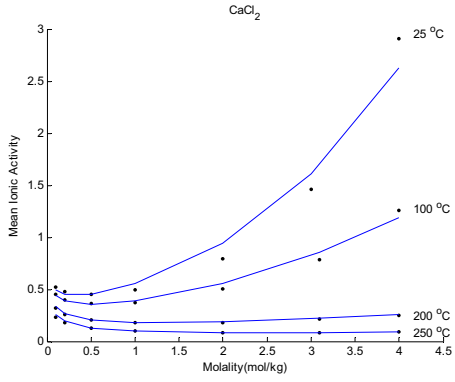

Figure 3. Activity coefficient of aqueous $CaCl_2$.

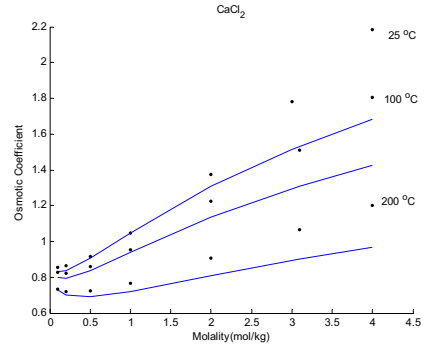

Figure 6. Osmotic coefficient of aqueous $CaCl_2$.

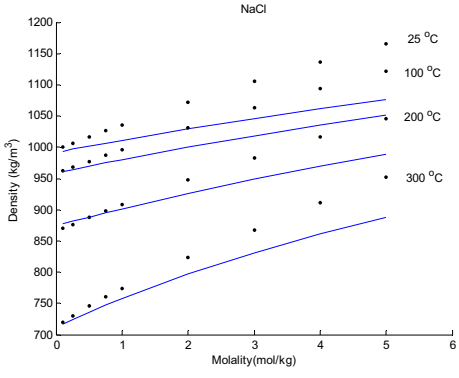

Figure 7. Density of aqueous NaCl.

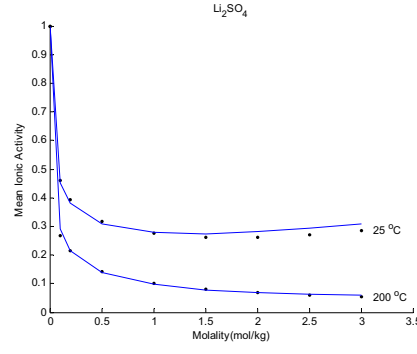

Figure 10. Activity coefficient of aqueous Li_2SO_4.

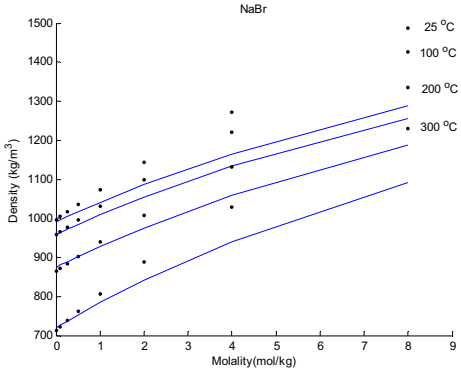

Figure 8. Density of aqueous NaBr.

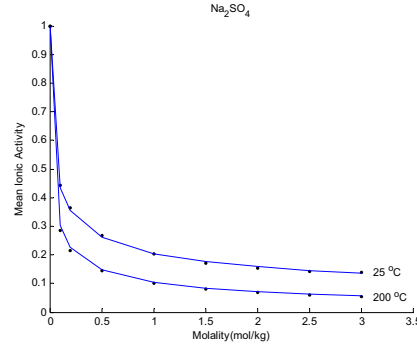

Figure 11. Activity coefficient of aqueous Na_2SO_4.

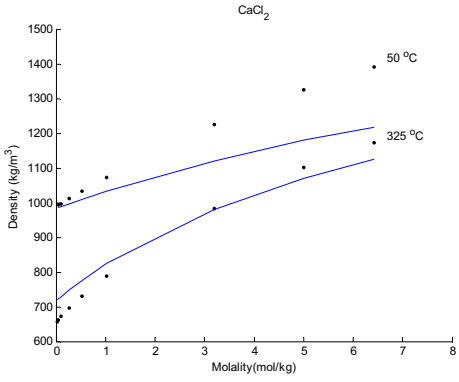

Figure 9. Density of aqueous $CaCl_2$.

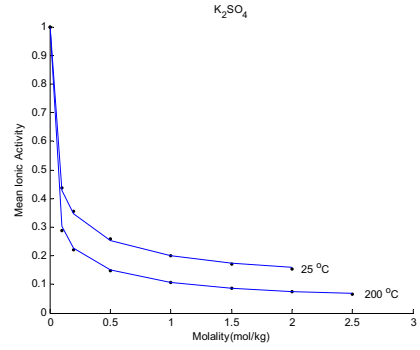

Figure 12. Activity coefficient of aqueous K_2SO_4.

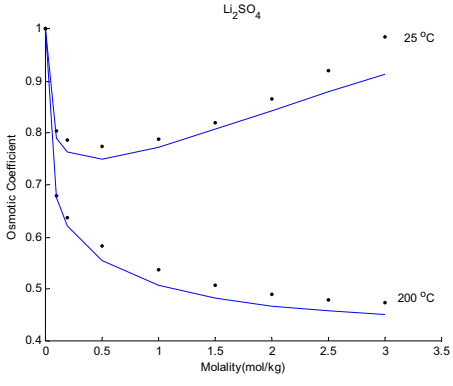

Figure 13. Osmotic coefficient of aqueous Li_2SO_4.

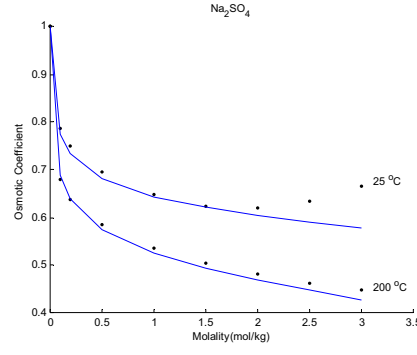

Figure 14. Osmotic coefficient of aqueous Na_2SO_4.

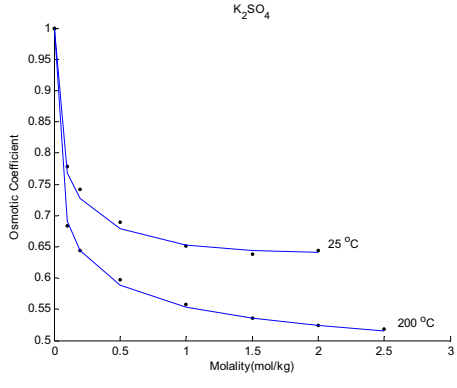

Figure 15. Osmotic coefficient of aqueous K_2SO_4.

3. The results of simutanous regression of all parameters (including binary interaction parameters) using Pottel model in section 5.6.3.2

The graphical results for the mean ionic activity and osmotic coefficients in the 0-300 C temperature range and the 1 to 120 bar range of the NaCl, NaBr and $CaCl_2$ solutions are shown in Figure 1-6. The solid lines are the calculated results using Pottel model and the parameters in Table 5.12 in section 5.6.3.2. The experimental data are plotted in the figures as dots. The calculated densities of the above three electrolyte solutions are shown in Figure 7-9. The graphical results of the mean ionic activity and osmotic coefficients of the Li_2SO_4, Na_2SO_4 and K_2SO_4 solutions in the 0-200 ºC temperature range and the 1 to 25.6 bar range are shown in Figure 10-15.

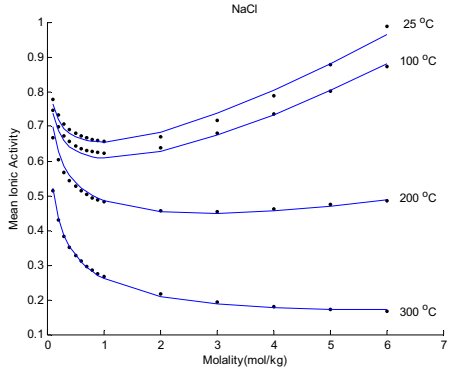

Figure 1. Activity coefficient of aqueous NaCl.

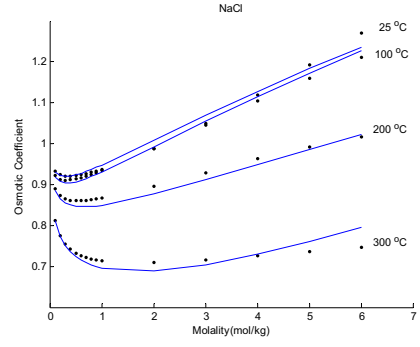

Figure 4. Osmotic coefficient of aqueous NaCl.

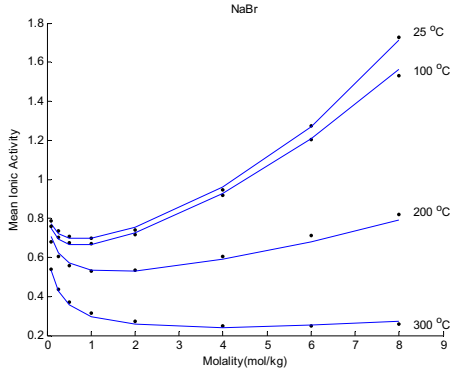

Figure 2. Activity coefficient of aqueous NaBr.

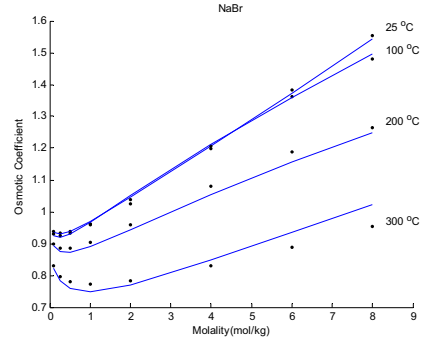

Figure 5. Osmotic coefficient of aqueous NaBr.

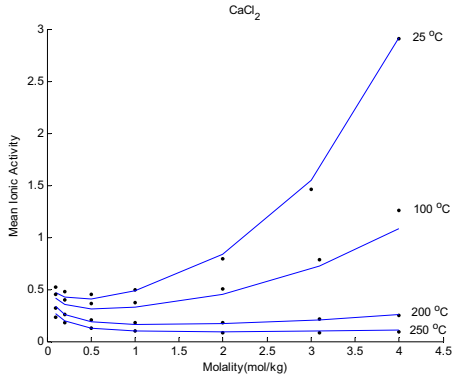

Figure 3. Activity coefficient of aqueous $CaCl_2$.

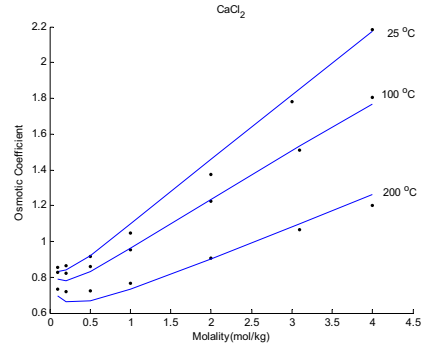

Figure 6. Osmotic coefficient of aqueous $CaCl_2$.

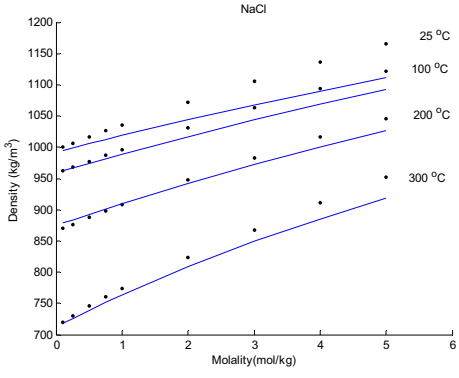

Figure 7. Density of aqueous NaCl.

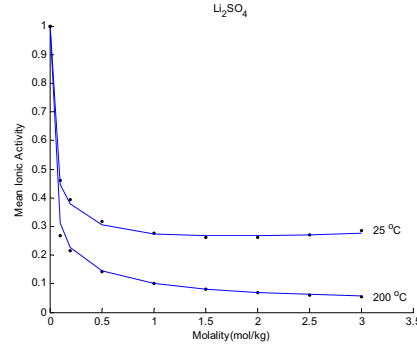

Figure 10. Activity coefficient of aqueous Li_2SO_4.

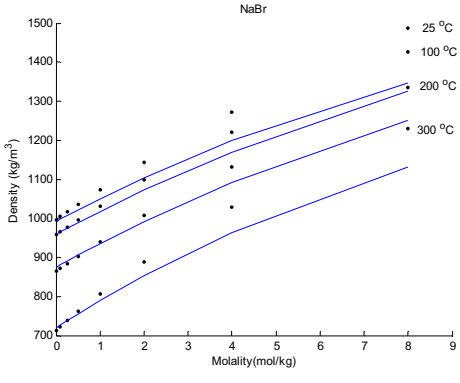

Figure 8. Density of aqueous NaBr.

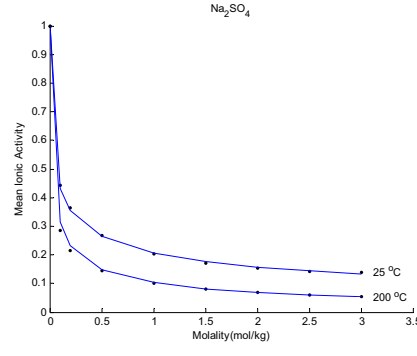

Figure 11. Activity coefficient of aqueous Na_2SO_4.

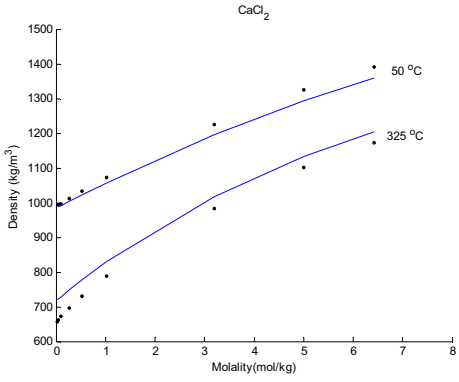

Figure 9. Density of aqueous $CaCl_2$.

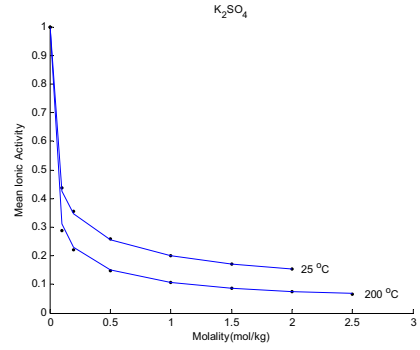

Figure 12. Activity coefficient of aqueous K_2SO_4.

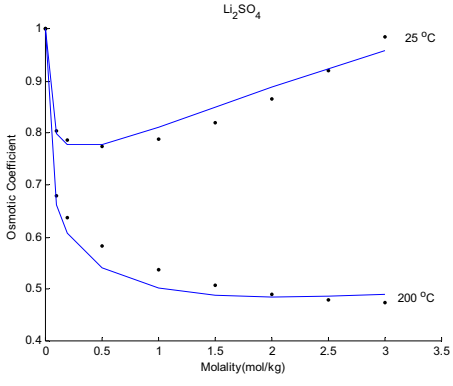

Figure 13. Osmotic coefficient of aqueous Li_2SO_4.

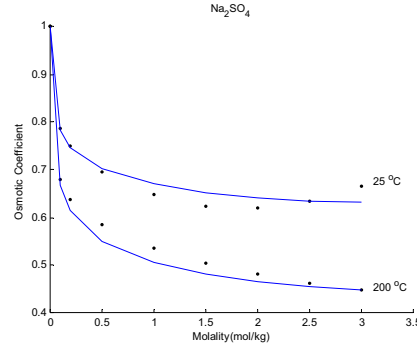

Figure 14. Osmotic coefficient of aqueous Na_2SO_4.

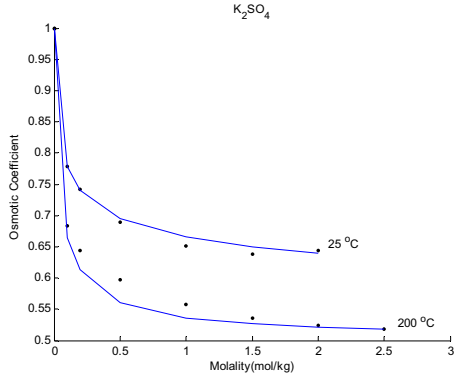

Figure 15. Osmotic coefficient of aqueous K_2SO_4.

Department of Chemical
and Biochemical Engineering
DTU Building 229
Søltofts Plads
DK-2800 Kgs. Lyngby
www.kt.dtu.dk